The impact of ageing on the human haematopoietic stem cell and memory T cell compartments through the lens of single cell transcriptome analysis



Grigore-Aristide Gafencu
Wolfson College
University of Oxford

A thesis submitted for the degree of
Doctor of Philosophy
Trinity 2022

This thesis is dedicated to my family

“Great things are not done by impulse, but by a series of small things brought together.”

Vincent Van Gogh

Acknowledgements

I would like to start by thanking my supervisors, Paresh Vyas and Claus Nerlov for their guidance and support during my journey that my DPhil has been.
I am grateful to Paresh for challenging me to develop critical and independent thinking, to always think from first principles, to ask the right questions and for his patience. To Claus, especially I would like to thank for his guidance in understanding the fascinating and at times confusing biology of haematopoietic stem cells, for his patience and trust in my newly found abilities as a computational biologist.

I would also like to thank all the members of the Vyas and Nerlov laboratories (past and present) who have helped me to learn techniques, provided helpful feedback on my work and been there to listen, help and at times provide nuggets of humour to when things went in every conceivable direction but not ahead. In particular to Batchimeg Usukhbayar, Marlen Metzner, Alison Kennedy, Mirian Angulo Salazar, David Cruz Hernandez, Catherine Garnett, Asger Jakobsen, Connor Sweeney, Catherine Porcher, Bilyana Stoilova, Naser Ansari-Pour, Vasiliki Symeonidou, Susann Rahmig, Sven Turkalj, Gerda Mickute, Mario Buono and Merve Aksöz.

I have benefited immensely during my DPhil from the mentorship of Persephone Borrow, who helped me start to understand T cell biology, and of Supat Thongjuea, who helped me navigate my first steps into bioinformatics and I thank them for their help. A thank you for Daniele Biasci who offered his time to review some of my conceptual approaches when using machine learning methodologies in my work.
I would like to acknowledge Adam Mead, Irene Roberts and Jim Hughes for their advice and support in the capacity of my thesis committee as well as Tom Milne and Andrea Pellagatti for their support in the confirmation of status examination. A thank you to Marella De Bruijn and the staff of the University of Oxford Medical Sciences Division Graduate Schools for their support. Moreover, I would like to thank all the core facilities of the WIMM, particularly the MRC WIMM Centre for Computational Biology for their support and expertise.
My work would have not been possible without the generous funding offered by The Medical Research Council and the MRC Molecular Haematology unit for which I am incredibly grateful.

My work at the WIMM as well as my life in Oxford would not have been the same without the graduate student community at the WIMM (Caitlin Murnane, Alexandra Preston, Spencer Tong, David Grainger, just to name a few) and at Wolfson College (Ryan Walker, Tom Walshe, Andrew Hyslop, Andrew Kirkpatrick and Jonathan Connolly) who really made a positive impact on my DPhil journey. A special thank you to Antara, who made the last year of my DPhil an incredibly enriching experience, from whom I have so much to learn and I can only repay her kindness with my affection.
Finally, I would like to thank my family. My parents, Cezarina and Marius who have provided me so much support and affection over the years and always believed in my goals. To my brother, Mihai, who always had an encouragement to say. This thesis is dedicated to you, my family.

Abstract

Human biological ageing comprises the molecular and physiological changes that negatively affect homeostasis with age and are strongly associated with susceptibility to disease and ultimately death.

This thesis utilises single cell transcriptomics to study the haematopoietic stem and memory T cell compartments in humans and how ageing impacts on their potential functionality in the context of health and disease.

Firstly, we have studied the human haematopoietic stem cell (HSC) compartment utilising single cell transcriptomic datasets from young and old males to address the existence in humans HSCs expressing a gene signature indicative of an output biased towards platelet generation and the inflation of this population with age. Secondly, we have studied how ageing shapes the transcriptome of the memory T cell compartment utilising publicly available single cell transcriptomic datasets with a view to investigate if recovering from a severe case of COVID-19 shares biological processes with ageing in the context of the memory T cell compartment of a healthy donor cohort.

Our study of the HSC compartment has shown that a computationally defined HSC populations exhibiting the gene expression patterns associated with platelet bias in murine HSCs can be identified in healthy human males. The previously identified HSC population is enriched in old individuals. Moreover, this population exhibited the transcriptomic features associated with previously documented HSC populations with high self-renewal capacity and quiescence. With ageing there were no major shifts in which pathways were upregulated or downregulated, but more of an accentuation of the transcriptomic programmes already present at younger ages.

An ageing-associated inflammatory gene expression signature was identified at the level of the memory T cell compartment of the studied healthy human cohort. Known signalling pathways and gene families associated with ageing in the T cell compartment such as IL-10 signalling were associated with this signature as well as novel ones such as the aminoacyl-tRNA synthetases. By leveraging a machine learning-based methodology, it was shown that at the level of the memory T cell compartment, the most important biological processes that are shared between ageing and recovering from COVID-19 are IL-10 signalling and BAX-mediated apoptosis.

The potential functional implications of the ageing associated observations made in the human HSC and memory T cell compartments remain open questions that could potentially allow us to understand what are the signals that determine fate specifications in HSCs and the long-term deleterious effects of experiencing a respiratory viral infection on the functionality of the adaptive immune system.

Table of Contents

Acknowledgements 2

Abstract 3

Chapter I. Introduction 7

The importance of studying the biology of ageing 7

Ageing theories and the role of molecular damage in biological ageing 10

The impact of ageing on the structure and functionality of the haematopoietic stem cell compartment and haematopoiesis at large 16

The impact of ageing on the structure and functionality of the murine and human immune system 27

The impact of ageing on the structure and functionality of the T cell compartment of the murine and human immune system 35

The impact of ageing on the immune system in the context of the coronavirus disease 2019 (COVID-19) 43

The benefits and challenges of utilising single cell transcriptomics in the study of ageing 51

Summary and aims 62

Chapter II. Materials and methods 64

Datasets 64

Methods 70

Alignment and transcript quantitation 70

Data importing and quality control 70

Data normalisation, highly variable gene selection and batch effect correction 73

Dimensionality reduction, clustering and cluster – cell type identity assignation 76

T cell data extraction from peripheral blood mononuclear cell single cell RNA-seq datasets and preparation for downstream analysis 82

Differential gene expression, gene set enrichment and gene signature intersection analysis 83

Trajectory inference and trajectory-informed differential gene expression analysis 89

Machine learning-based methodology for establishing the importance of ageing-associated gene signatures to the severity stratification of the COVID-19 cohort 91

Ageing memory T cell gene score computation 92

Chapter III. The impact of ageing on the heterogeneity and transcriptome of the human haematopoietic stem cell compartment using single cell transcriptome analysis 93

Quality control 93

Young donor dataset analysis – transcriptomic data clustering and cluster characterisation 95

Old donor dataset analysis – transcriptomic data clustering and cluster characterisation 100

Age-associated HSC subpopulation frequency fluctuation and transcriptomic phenomena **103**
Meta-analysis of the young and old HSC datasets 103
Integrative analysis of the young and old HSC datasets 109

Chapter IV. The ageing-associated transcriptomic features of the memory T cell compartment in the context of post COVID-19 recovery ***119***

A description of the age-related transcriptomic changes in the memory T cell compartment of a healthy cohort **119**
Initial quality control of the healthy cohort scRNA-seq datasets 119
Healthy donor cohort scRNA-seq datasets integrated analysis – transcriptomic data clustering and cluster characterisation 121
Age-associated T cell population size fluctuation and gene expression patterns recorded in the healthy donor cohort 127

Determining the common transcriptomic features between the ageing memory T cell compartment phenomenon and the recovery from COVID-19. ..... **130**
Extraction of the memory T cell data from the convalescent COVID-19 cohort dataset 130
Probing the association between age group, gender and comorbidities and the acute phase COVID-19 severity or respiratory PACS in the convalescent COVID-19 cohort 136

Genes associated with the ageing of the memory T cell compartment in healthy cohort are capable of stratifying a convalescent COVID-19 one based on the severity of the acute disease starting from scRNA-seq data collected months after symptoms onset. **144**

Chapter V. Discussion ***147***

HSCs exhibiting the transcriptomic features of platelet lineage bias can be identified in human HSC single cell RNA sequencing datasets **147**

Human HSCs exhibiting the transcriptomic features of platelet lineage bias increase in frequency with age, but to a lesser extent than in mice **150**

The transcriptomic differences between the computationally inferred platelet biased and multilineage HSCs populations present in young donors are exacerbated by ageing **154**

Ageing of the memory T cell compartment is characterised by an inflammatory gene signature and a heterogenous effect on the size fluctuations of its subpopulations **157**

At the level of the memory T cell compartment, recovering from a COVID-19 -related hospitalisation and ageing share common biological processes **161**

Future studies **167**

Conclusions **170**

Appendices ***173***

Appendix figures **173**
Appendix figure 1 173
Appendix figure 2 176
Appendix figure 3 177
Appendix figure 4 179

Appendix figure 5 180
Appendix figure 6 181
Appendix figure 7 182
Appendix figure 8 183
Appendix figure 9 184
Appendix figure 10 185
Appendix figure 11 187

Appendix tables 188
Appendix table 1 188
Appendix table 2 190
Appendix table 3 211
Appendix table 4 281
Appendix table 5 284
Appendix table 6 293
Appendix table 7 315
Appendix methods table 1 316
Appendix methods table 2 343

References 354

Chapter I. Introduction

The importance of studying the biology of ageing

Though still lacking a fully accepted complete paradigm, human biological ageing comprises the molecular and physiological changes that negatively affect homeostasis with age and are strongly associated with susceptibility to disease and ultimately death (1–7).

The definition of human biological ageing clearly indicates the impact of this phenomenon on human lifespan and Finch et al. have shown that the probability of dying of an individual doubles every 8 years lived past the age of 30 (8). There is an association between old age and increased susceptibility to disease and with the average life expectancy in the developed countries doubling in the past 200 years and likely continuing on the same trend (9,10) it is projected that it will lead to an increase in global burden of late-life disease (11). Thus, there is a societal and economic rationale for advancing the state of knowledge in the field of biological ageing. Utilising insights obtained from studies of the biological processes behind aging has started to yield interventions aiming at reducing the disease burden associated with old age. One such intervention with the potential of reducing disease burden associated with old age are dietary restrictions (12), such as ones low in calories, sugars, and proteins but high in unsaturated fats that can improve blood pressure and IGF-1 levels, thus impacting on factors known to affect cardiovascular and cancer-related morbidity, particularly in

the most vulnerable demographics (13). By extrapolating on the predicted economic impact of healthier diets that could align with the dietary restrictions previously mentioned (14), such interventions could be beneficial in alleviating the societal and economical pressure that the increase in ageing-related morbidity puts on healthcare systems (14,15).

Studying the biology of ageing has the potential for helping us understand the pathophysiology and the therapeutic opportunities of pathologies, ranging from cancer to COVID-19, in which old age can be seen as a negative prognostic factor (16,17). At the core of the interface between the biology of ageing and the pathophysiology of a wide range of diseases lies the process of senescence, an irreversible cell cycle arrest state, often under the control of DNA response pathways, characterised by a specific secretory phenotype and associated with resistance to apoptosis, lysosomal and mitochondrial expansion and accumulation of β-galactosidase (18). Senescence has been shown to be a process responsible for both tumour suppression, as during oncogene activation, DNA damage is induced and this in turn leads to the activation of the p53 pathway leading to senescence or cell death (19). Moreover, senescence is involved in tumour progression as well, by inducing an immunosurveillance disfunction via the cytokines part of the senescence-associated secretory phenotype (SASP) (16,20,21). In the case of the pathophysiology of COVID-19, disease severity has been linked with immunosenescence (22–24), a phenomenon in which the components of SASP secreted by the accumulating senescent cells in an ageing organism generate a proinflammatory milieu which in turn contributes to dysfunctional antigen

presentation, naive T cell priming and CD8+ T cell cytotoxic function, a myeloid biased haemopoiesis, altered type I interferon (IFN) responses, diminished phagocytic function for innate immune cell types, a restricted naive T cell and B cell repertoire and impaired production of high-avidity antibodies (17,25). In the case of both cancer and COVID-19 therapeutic agents aimed at the elimination of senescent cells, senolytics, have been proposed as therapeutical options with various degrees of success and deployment in clinical practice: navitoclax, a pro-apoptotic agent acting as a BCL-2, BCL- XL and BCL-W inhibitor (26) has been used in conjunction with rituximab, an anti-CD20 monoclonal antibody and a senescence inducer (27) as a therapy for chronic lymphocytic leukaemia with positive results in a phase II clinical trial (28) and the combination of dasatinib and quercetin, acting as inhibitors of PI3K–AKT signalling (29), was shown to eliminate senescent cells and reduce the titre of SASP cytokines in a murine model of SARS-CoV2 infection as well as improving the survival of the infected mice in the treated versus the placebo control groups (30).

An effort to better understand the biology of ageing has the potential to revolutionise how we understand the pathophysiology of many diseases and, in the process alleviate societal pressures. In their review, Partridge et al. elaborate the concept of compression of morbidity, which represents the reduction in the length and severity of late-life morbidity, a goal that societies should strive for in an age where we are faced with an ageing population in the developed economies (11). Thus the study of the biological underpinnings of ageing is a necessity and arguably a prerequisite for avoiding an ageing population induced healthcare crisis (11).

Ageing theories and the role of molecular damage in biological ageing

In an effort to summarise the general biological processes known to be associated or causally linked to ageing, one has to address the fundamental question of why ageing as a phenomenon exists. This question has been the subject of ample debates that have yet to yield a conclusive answer and the debate in the past century has been revolving around the evolutionary theories of ageing (31,32). These theories of ageing posit that the features of ageing are not determined by evolutionary selective pressures as the impact of natural selection diminishes with age due to extrinsic mortality factors in the wild, but this implied that features of ageing have to be ascribed to evolutionary processes to account for their existence (33). In 1951, Medawar elaborated the mutation accumulation theory, postulating that mutations accumulate in the germline over generations and these mutations manifest themselves as detrimental in the post-reproductive period (34). Building to an extent on Medawar's theory, in 1957 William emitted the antagonistic pleiotropy theory, in which physiological processes that could prove deleterious later in ontogeny are selected due to their beneficial impact earlier in the development of an organism, giving the example of calcification which can be deleterious later in life, i.e. calcification of the connective tissues of arteries, but it is fundamental for the development of the skeleton in mammals (35). Diverging from a purely genetic theory of ageing, in 1977 Kirkwood elaborated the theory of disposable soma in which he posits that an organism shifts the allocation of its own resources to either reproduction or to processes that maintain the soma (growth and homeostasis) and ageing is a physiological trade-off, ensuring that the germline is propagated (36).

These 3 theories have constituted the main theoretical foundations for the development of a biological understanding of ageing.

While the determinants of longevity are distinct from those that influence the rate at which an organism ages (37), lifespan can be seen as the result of the integration of the rates of ageing at multiple levels of an organism (33). Human tissues do not age at the same rate thought the life of one individual as evidence from epigenetic and transcriptomic studies, such as tracking genome-wide methylation and gene expression changes at the level of peripheral blood (38) and skin (39) suggests. Moreover, multiomics analysis of a variety of ageing biomarkers in a cohort of individuals has pointed out the existence of ageotypes, according to the types of molecular pathways that changed over time in a given individual (3). How these observations relate with the evolutionary theories of ageing is actively debated, but they hint at the asynchronous nature of the process of ageing (33).

Existing theories of ageing do not always agree on the nature of ageing, but they all find a common denominator in considering that the accumulation of molecular damage, constituted from metabolic by-products, mutations, epimutations and errors in transcription and translation, denominated as the deleteriome (40) is the cornerstone for the biology of ageing (41). Next, we'll discuss the major categories of molecular damage and relate them to observations related to the biology of ageing.

DNA damage as represented by mutations in the nuclear and mitochondrial DNA, accumulates with age and is caused by DNA replication and transcription (42–44). The

role of DNA damage in ageing is supported by the conserved DNA repair mechanisms that evolved to protect the integrity of genomic DNA, the aged phenotype that is associated with DNA-damage-repair-deficient progeroid diseases such as xeroderma pigmentosum and Cockayne syndrome (45) and the fact that genotoxic therapies are known to accelerate the onset of age-related diseases, in which DNA damage is a potent driver of cellular senescence which in turn has a role in both ageing and the genesis of age-related diseases (41,46,47). Evidence of increased genomic DNA damage with age is provided by the accumulation of oxidative DNA lesions, single strand breaks and increased expression of elements of the DNA damage response (DDR) machinery, such as p53, p21 or GADD45, modified histones (γH2AX) as well as activation of the DDR (phospho-p53, phospho-ATM and 53BP1 nuclear foci) (41,48,49). In the case of mitochondrial DNA damage in humans, the increase of heteroplasmy at locus m.3243 A>G has been a phenomenon associated with poorer cognitive performance, decreased grip strength and increased risk of mortality, features that are all associated with ageing in humans (50).

Changes in the epigenetic state of the genome have been summarised by the Shannon methylation entropy. This is a metric that in the context of epigenetics quantifies the magnitude of the change in methylation of a set of CpG sites. Shannon methylation entropy is minimal when all the CpG sites analysed are either demethylated or methylated and maximal when only some of them are methylated (51). Studies in both humans (51) and in mice (52) have shown that with age there is an increase in the Shannon methylation entropy for a set of CpG sites.

Integration of the increasing level of variation in methylation profiles of hundreds of methylation sites with the chronological age of the individuals from whom the samples have been acquired for profiling has generated “clocks” of organismal ageing, that can be pan- or tissue-specific and have been used to account for mortality risks and are now used to quantify the effect of longevity interventions in mice (53–55).Thus, this class of damage has been used as a tool for quantifying the phenomenon of age acceleration, which is consistently associated with morbidity in human cohort studies and is represented numerically by the difference between the chronological age and the epigenetic age inferred by an epigenetic clock (55,56).

Chemical modifications, transcriptional errors, cross-links, strand breaks of RNA molecules, as well as errors in splicing, can be considered as part of the contribution of the RNA to the deleteriome (41). Another source of RNA damage are colliding ribosomes and nonsense-mediated decay defects (57,58). Age-correlated splicing alterations have been detected in humans as well as in *C. elegans*, in which the lifespan expanding effects of caloric restriction have been linked with the activity of the *sfa-1* splicing factor (59,60). RNA sequencing (RNA-seq) has been a popular genomic technique used in studies aimed to identify ageing associated gene signatures conserved across multiple species and tissues (61,62). In their review on molecular damage in ageing, Gladyshev et al. raise the point that only recently ageing studies that use RNA-seq have become big or granular enough to attempt to probe if ageing-associated transcriptomic changes are due to RNA damage or adaptive responses to this type of damage (41).

Protein damage is a result of both enzymatic and non-enzymatic reactions, the latter being characterised by oxidations as well as pathways where aspartic acid and asparagine residues racemize, isomerize and deamidate into deleterious products that have been associated with ageing (63,64). Protein damage via post-translational modifications is an understudied area, but protein carbamylation has been highlighted as being associated with ageing particularly of the skin (65). An example of the importance of the protein repair or clearance in ageing is represented by the role of the protein L-isoaspartyl methyltransferase (PCMT) that converts L-isoaspartyl residues, toxic in most cases, back to L-aspartyl residues via the L-isoaspartyl methyl ester and which has been shown that when overexpressed can increase the lifespan on C. elegans and when its gene is knocked out in mice can produce a phenotype in mice characterised by seizures and shortened lifespan (66,67). A decline in cellular proteostasis has been shown to be associated with age, as human primary fibroblasts from young individuals were able to initiate the unfolded protein response-related transcriptional and translational responses, but this was not the case for fibroblasts from older individuals that were in a senescent state despite showing a heightened translational regulation and endoplasmic reticulum stress sensing (68). Autophagy is a key component of the protein degradation machinery and its rate has been associated with human longevity, with descendants of centenarians having better proteostasis through preserved macro-autophagy in peripheral $CD4^+$ T-cells than their non-centenarian descended spouses and this observation is correlated with increased activation-induced interferon-γ (IFNγ) expression in $CD4^+$ T-cells (69).

Lipid damage particularly through oxidation via reactive oxygen species (ROS) generates hydroxylated, epoxidated or highly reactive short-chain lipids, which can accumulate in deposits of protein-lipid aggregates of lipofuscin, the presence of such aggregates being associated with cellular senescence (70,71). Lipid peroxidation reactions can generate compounds known to form ethenoadducts with DNA which in turn can disrupt transcription (72). Moreover, lipofuscin has been shown to negatively interfere with both the ubiquitin-proteasome system and autophagy-lysosomal pathway, key pathways in mitigating the impact of molecular damage and its accumulation in cardiomyocytes in humans has been correlated with age and sudden death (73–75).

Thus, molecular damage represents a probable driving force behind biological ageing. Understanding how molecular damage is produced and its effects can be mitigated could represent a paradigm for biological ageing at both a cellular, tissue, organ and organismal level and possibly reconciling multiple theories of ageing.

The impact of ageing on the structure and functionality of the haematopoietic stem cell compartment and haematopoiesis at large

The fundamental properties of a stem cell are self-renewal or the ability to maintain an undifferentiated stem cell pool for the life of an organism and multipotency or the potential to produce differentiated cell lineages (76). Transplantation assays in lethally irradiated or immunosuppressed murine hosts are conducted to functionally assess Haematopoietic stem cell (HSC) self-renewal and HSC's long-term repopulation and reconstitution of haematopoiesis (> 16 weeks and at least a second round of transplantation) (77). HSC self-renewal has been shown to be dependent on how quickly an HSC exits a quiescent state (78). Moreover, HSC self-renewal has also been shown to be dependent on a metabolic state defined by low mitochondrial activity (79) and tightly regulated protein synthesis (80).

There are many immunophenotypic definitions of the HSC compartment in mice and humans, but given the type of the datasets that will be studied in this thesis, for the human HSC compartment we will discuss the impact of ageing on the compartment defined by Majeti, Park and Weissman as Lin-CD34+CD38-CD90+CD45RA- (81) and the murine compartment defined by Kiel et al. as Lin-Sca-1+c-Kit+CD150+CD48- (82).

In their seminal review, López-Otín et al. highlight stem cell exhaustion as one of the hallmarks of ageing, which refers to the gradual decline in the ability of the adult, tissue specific stem cells to maintain homeostasis of the tissue in their niche (2). HSCs have a limited capacity for self-renewal evident in situations when there is an increased

proliferative stress such as serial transplantations at short intervals (83). Evidence from mouse haematopoiesis has shown that HSCs from aged donor mice when they are serially transplanted in young recipients are functionally less frequent and have poorer engraftment rates than HSCs from young donor mice (84). Biological ageing plays a role in HSC self-renewal capacity as shown by competitive transplantation of HSCs isolated from mouse strains with longer and shorter lifespans will see the HSCs from the longer lived mouse strain outcompete the ones from the mice with shorter lifespans (85).

The HSC compartment in mice and humans as defined by the most stringent phenotypic definitions used for prospective isolation by flow cytometry for use in transplantation assays is containing both bona-fide HSCs (up to 50%) as well as multipotent progenitors, thus pointing a limitation in the studies that highlighted an ageing-associated lineage bias in HSCs (86). Even with these caveats and as reviewed by Yang and de Haan (87), there is mounting evidence that with ageing the heterogeneity of the HSC compartment increases. As reviewed by Yang and de Haan (87), there are phenotypically defined HSC populations in mice which exhibit a bias towards progeny that will generate platelets (marked by the expression of von Willebrand factor or CD41) and myeloid lineage cells (marked by the expression of CD150 at high levels, Neo1, CD61, IL27Ra or Alcam) which increase in frequency with age in contrast with the HSC populations biased towards a lymphoid output (marked by the expression of CD86, Satb1, or low levels of CD150) which diminish in frequency with age.

The lineage bias of an HSC clone is determined by its relative contribution to a given lineage versus another one, with a lineage biased HSC clone being one that would predominantly give rise to progeny that is fate restricted to a certain lineage or just a limited number of lineages, but not to a balanced lineage output (88). Quantifying lineage biases in HSCs using single cell transcriptomics and single cell lineage tracing has helped confirm previous reports of HSC lineage bias, particularly regarding the megakaryocytic bias (89) without the usage of single HSC transplantations and provided estimates on the output of transcriptomic and functionally distinct HSC subpopulations (89,90). Several lineage tracing technologies utilise single cell transcriptomics to sudy HSCs including the insertion of known sequences (the LARRY system) (89,91) or by a CRISPR array (CARLIN) (92) or by tracking mutations at the level of the mitochondrial genome (93).

The CARLIN system has allowed for the study of fate decisions in the setting of unperturbed haemopoiesis and showed that multiple haematopoietic hierarchies coexist in a single mouse, each with distinct regulatory features imprinted during development and persisting well into adulthood (92). Some of the most robust evidence in terms of the lineage biased HSC's transcriptional state and output comes from the LARRY system, in which HSCs were *ex vivo* transfected with a lentiviral vector containing a library of nucleotide barcodes that allowed the labelling of each HSC clone and their progeny. The output of each HSC clone was evaluated in the setting of a primary transplantation before serially transplanting all the clones competitively into secondary recipients (94). Leveraging the capability of the LARRY system, Rodriguez-

Fraticelli et al. pointed that in mouse haematopoiesis transcriptomic distinct megakaryocytic output biased HSCs can be found, they are situated at the apex of the haematopoietic hierarchy and are mostly in a state of quiescence (89). However, in this experimental setting no purely myeloid, lymphoid or erythroid biased HSCs have been identified, highlighting maybe a sampling limitation that is inherent to the single cell nature of these assays, with a limited number of HSC clones not being enough to detect rarer lineage-biased HSC clones (89,90).

It has been debated that the variation in frequency of lineage-biased HSC subpopulations and HSC self-renewal potential observed with age can be attributed to both, HSC intrinsic and niche specific factors (86,87,95). During the lifetime of a mouse or human, the HSC compartment, even with its low division rate (murine HSC undergoes a maximum of 5 divisions during the lifetime of a mouse (96)) and the majority of this compartment being in a quiescent state (90% in humans (78) and mice (97)) accumulates DNA damage (48). Moreover, in aged HSCs an accumulation of γ-H2AX foci, a marker of active DNA damage response processes can be observed (98). The full functional implications of the DNA damage that accumulates with ageing at the level of HSC clones are actively debated, but the age-correlated increase in the prevalence of somatic mutations at the level of epigenetic regulators such as DNMT3A, TET2 and ASXL1 at the level of the HSC compartment in humans has been observed and these mutations and their occurrence pattern are hallmarks of clonal haematopoiesis of indeterminate potential (CHIP) characterised by an increased risk for developing myeloid malignancies as well as cardiovascular morbidity (99).

The accumulation of senescent cells in any tissue with ageing is a known phenomenon also observed in the bone marrow of both, mice and humans (18). The impact of SASP on HSC lineage bias will be discussed later in the context of the ageing niche, but HSC senescence has not been shown to conclusively be an intrinsic property of the aged most primitive HSC, with less than 1% of HSCs expressing p16 (100). Interestingly, an increased expression of p16 with age in the HSC compartment has been documented (101).

HSC self-renewal has been linked with the asymmetric division phenomenon (76). Cell polarity, defined as the asymmetric distribution of cellular components, biomolecules and structures within the cell is regulated in murine HSCs via *Cdc42*, as well as *Dlg*, *Crumb3, Scrimbble* and Lamin A/C (as reviewed here (102)). HSC polarity is linked to the activity of *Cdc42* which in turn has been was associated with the choice between symmetric or asymmetric division in HSCs (103). HSCs from aged donors express higher levels of *Cdc42* than their counterparts from young donors and this is associated with a loss in polarity and diminished self-renewal has been shown in both mice and humans (104,105) highlighting the impact of regulation of cell polarity on HSC self-renewal in the context of ageing.

With ageing the HSCs exhibit a change in their energetic metabolism similar to the shift between the quiescent and activated state seen in young HSCs, which is marked by a switch from glycolysis to oxidative phosphorylation (OXPHOS) which entails an

increased oxidative stress associated with a diminished regenerative potential (reviewed by Verovskaya et al. (106) and Chandel et al. (107)). Ageing is associated with diminishing macroautophagy rates in the HSC compartment leading to the accumulation of mitochondria, an accelerated myeloid differentiation and loss in self-renewal capacity (102,108). The transition from quiescent to activated HSC is dependent on the regulation of proteostasis and fatty acid metabolism as well as the energetic metabolism and chaperone-mediated autophagy (CMA) has been shown to be crucial for the regulation of proteostasis and fatty acid metabolism in the setting of murine HSCs during this transition (102,109). CMA rates are diminished with ageing, generating a poor activation response following 5-fluorouracil injection, diminished proteostasis with an accumulation of higher levels of carbonylated peptides, oxidized proteins and protein inclusions culminating in reduced self-renewal capacity, but all these phenomena are alleviated by CMA pharmacological activation using by retinoid derivatives (109,110).

Ageing-associated changes in the epigenome of HSCs are less dramatic than in other tissues, with the hypomethylation in ageing HSCs usually being more modest compared to other tissues (2,102). It is speculated that this phenomenon is related to the quiescence of this compartment in adult life (2,102,111). At the level of stem cells, including HSCs, polycomb group proteins, as epigenetic regulators, have been shown to be crucial for the maintenance of self-renewal with ageing (112). Expression of *Ezh2* and *Bmi1*, genes coding for components of the polycomb group proteins complexes which target the *Cdkn2a* locus, have been linked with the maintenance of HSC self-

renewal during serial transplantations and ageing, via the repression of p16 and p19 (113,114). The loss of polarisation at the level of the nucleus of histone H4 at lysine 16 acetylation (H4K16ac) in murine HSCs has been linked an increase in expression of *Cdc42* and associated with ageing and low of self-renewal, but this has been able to be rescued pharmacologically (104). Overall, it has been shown that the aged-related changes registered in the epigenome lead to induction of interferon related inflammatory responses, across different tissues upon ageing including murine HSC (115,116). Evidence from murine HSCs points out that the fact that the landscape of epigenetic changes shown to be age-dependent shapes the formation of HSC clones with distinct lineage outputs (116,117). Interestingly, this phenomena mirrors at least in the case of myeloid biased HSC fate the outcome of *Tet2* mutations in in murine HSCs (118).

The ageing HSC niche represents a major extrinsic factor affecting HSC functionality, with the ageing niche being usually seen as more proinflammatory and lymphoid differentiation averse milieu than the young one (as reviewed by Yang and de Haan (87)). With ageing the rapport of HSCs to other cells in their niche changes, with HSCs in the aged BM being in close proximity to perivascular Nestin^{dim} perivascular cells and sinusoids compared to arterioles and megakaryocytes in the young BM niche (119,120). Even though mesenchymal stromal cells increase in numbers with ageing at the level of the HSC niche, they have lower clonogenic potential *in vitro* and produce less Cxck12, Scf and Angpt1, factors usually associated with the maintenance of the HSC self-renewal (120–122). It has been shown that sympathetic denervation of the

HSC niche in young mice can lead to HSCs that exhibit an aged phenotype (120). Moreover, HSCs as well as non-haematopoietic components of the niche express adrenergic receptors, ADRβ2 and ADRβ3 and treatment of mice with ADRβ3 agonists improves donor engraftment whereas ADRβ3 deletion led to aged phenotype in HSCs (120,123). Megakaryocytes known for regulating HSC quiescence via CXCL4 and TGFβ1 increase their frequency and secretory output in the HSC niche with age in tandem with macrophages accumulation in the aged HSC niche which stimulate the expansion of platelet biased vWF^+ HSC (119,121,124–127). Ageing is associated with a state of low grade chronic and systemic inflammation and parallels between inflammation-associated stress haematopoiesis and aged haematopoiesis can be drawn (87,128,129). Thus, IL1-β levels at the level of the HSC niche increase with age, being produced at the level of the niche by monocytes, macrophages and endothelial cells and inducing a myeloid differentiation skew of the HSCs and multipotent progenitors (MPPs) as well as an impaired repopulation potential (121,123,130,131). TNFα, IL-6, GM-CSF levels are increased with age in the HSC niche and promote myeloid differentiation and are produced by macrophages (TNFα, IL-6, GM-CSF), T cells (TNFα, GM-CSF), MSCs (IL-6), endothelial cells (GM-CSF) and natural killer cells (TNFα) (as reviewed by Yang and de Haan (87)). Interestingly, even though IFNα/β induce a state of activation in HSCs and proliferation, this state is not sustained in the case of a chronic stimulation in which HSCs will return to quiescence following the expression of p27 and p57, hallmarks of replicative stress (132). The repression of cell cycle and translation machinery genes associated with the quiescent state under chronic inflammation is mediated via the action of NF-κB signalling dependent PU.1

activation (130,133). Given the heterogenous nature of the immunophenotypic HSC compartment, a spectrum of responses to the inflammatory stimuli associated with the aged niche have been recorded in this compartment (87). Type I IFN, TNF and IL1-β induce expansion of a $CD41^{hi}$ $Selp^{+}$ subset of HSCs in mice and this expansion has been associated with an activation in megakaryopoiesis (131,134). TNFα chronic stimulation promotes the expansion of an IL27Ra+ HSC population with diminished self-renewal potential and a myeloid-lineage bias (135). Even though the impact of chronic stimulation using IL1-β can induce a myeloid bias and a diminished self-renewal capacity in HSCs, these characteristics are not persisting after secondary transplantation, whereas HSC from aged organisms have a persistent self-renewal deficit even after secondary transplantation, highlighting the fact that solely extrinsic factors can't explain the functionality of aged HSCs (131).

Even though there is ample evidence of the existence of lineage-biased HSCs in mice and their association with a certain age group, such HSC subsets in humans have only been speculated, with evidence from xenografts of HSCs from old donors producing more myeloid and less lymphoid lineage cells than the ones of young donors (136). Though not linked to ageing there is evidence for the existence of lineage biased human HSC subsets as shown in data from gene therapy trials and clonal tracking experiments using lentiviral barcoding platforms, but this evidence is not offering information about the transcriptome of these lineage biased HSC clones (137–139) to relate it with evidence from the LARRY system (89). Using an approach that combined single cell transcriptomics, index sorting and single cell HSC cultures to explore the

HSC/MPP compartment, Belluschi et al. observed that CLEC9A^{lo}CD34^{hi}CD49f^{+} HSCs are myelo-lymphoid committed and have little to no erythroid potential and characterised their transcriptome (140). Moving away from the paradigm of the most primitive human HSC subpopulation being the CD49f+ one (141), Anjos-Afonso et al. show that using the expression of EPCR, a CD90^{+} EPCR^{-} population in the HSC compartment has a dramatically lower repopulation capacity than the EPCR+ fraction of the HSC compartment and a lymphoid-bias in terms of its progeny (142). The impact of lineage biased HSCs on the unperturbed haemopoiesis in humans remains to be evaluated, but it should be noted that evidence in mouse points to the fact the contribution of long-term HSCs to steady state haemopoiesis mature cell numbers is modest compared to the contribution of the MPPs (95), thus making us speculate that the impact on the mature blood cell counts of the lineage biased HSCs in the context of ageing to be subtle.

Haemopoiesis at large is a process that shows variation along ontogeny and with ageing in both humans and mice, a skew towards myelopoiesis and megakaryopoiesis at the expense of lymphopoiesis can be observed, a phenomenon that impacts on blood counts which have been used to infer lifespan limit (143–145). Evidence from studies that highlight the rejuvenating effects of senolytic interventions on haematopoiesis indicate the cardinal role that proinflammatory cytokines that are part of SASP have on the differentiation biases observed in aged haemopoiesis (146). This raises the question if haemopoietic ageing is a function of the accumulation of proinflammatory cytokines at the level of the HSC niche that becomes increasingly

senescent, thus driving forward the selection of HSCs, bearing CHIP-associated mutations that could survive this milieu (as reviewed by Caiado et al. (147)) for which there is an indication of a lineage bias or transcriptomic priming as well as malignant potential (118). As Caiado et al. mention in their review, whether inflammation is a cause or consequence (or both) of myelodysplastic syndromes, myeloproliferative neoplasms, chronic myeloid leukaemia and acute myeloid leukaemia remains to be determined (147).

Thus, in the context of ageing, the study of lineage-biased HSCs, their molecular features, origins and frequency changes across age groups in humans is an area that needs further investigation and could yield insights with clinical implications for alleviating the deleterious effect of CHIP and potentially immunosenescence.

The impact of ageing on the structure and functionality of the murine and human immune system

The murine and human immune system changes with age and some of these changes, grouped under the umbrella term of immunosenescence, are associated with increased susceptibility to infectious diseases, neoplasia, cardiovascular disease and autoimmunity (148). It has been proposed that aspects of immunosenescence that hinge on adaptive immunity could be understood through the lens of evolutionary pressures, in which humans have evolved to expend vast amounts of resources to build a proficient immune system before puberty as a way of alleviate an immediate selective pressure and later in their life to rely on diminishing pool of naïve T & B cells and a repertoire of memory T cells shaped by their ecological niche as resources for further building immune system capabilities are diverted towards reproduction at the cost of diminishing the capacity to mount proficient immune responses to new pathogens, but mitigating against developing autoimmunity (36,148–150). Though at a glance the innate immunity does not exhibit the same overt decline with age, it can be seen as overactive at times, with monocyte counts trending upwards with age and an increase in cytokine production in humans and mice alike, there is evidence that with age the innate immunity is no longer functioning optimally (151,152).

The connection between the phenomenon of cellular senescence and immunosenescence can be made as with age, levels of p16 and p21 increase in macrophages, T cells and B cells and levels of the compounds that make SASP

increase (153–155). Work conducted by Yousefzadeh et al. has demonstrated that DNA damaged induced senescence via Ercc1 knockout at the level of mouse haematopoietic cells produced a phenotype in 10-12 month mice similar to wild type mice twice that age in terms of expression of p16 and p21 at the level of $CD4^{+}CD44^{+}PD1^{+}$T cells, B cells, NKT cells and CD11b+ myeloid cells as well as an increase of senescence markers in solid organs and SASP protein levels in the peripheral blood (156). These observations were associated with a significant diminished lifespan in the Ercc1 knockout mice compared with their wild type counterparts (156). The interactions between immune and senescent cells are complex and the nexus of them is the SASP, produced by senescent cells via the activation of p38 mitogen-activated protein kinase, cGAS–STING pathways and DNA damage responses under the control of NK-κB and GATA4, which can trigger the elimination of senescent cells by CD8+ T cells, NK cells via MICA/ULBP2–NKG2D interaction and macrophages (as reviewed by Mogilenko et al. (157)). SASP can induce senescence in by-stander cells by chemoattraction of neutrophils, that will exacerbate telomere disfunction in adjacent cells via ROS, and PD1+TOX+CD8+ T cells through granzyme K (GZMK) expression (as reviewed by Mogilenko et al. (157)).

Some of the components of SASP are proinflammatory cytokines such as IL-6 and TNF-α which have been shown to increase systemically with age, but independently of acute immune challenges, a phenomena known as inflammaging (158). The presence of proinflammatory cytokines at escalating levels with age generates a low-level activation of the Janus kinase (JAK)–signal transducer and activator of transcription

(STAT), MyD88, and nuclear factor (NF)-κB pathways which results in a high basal activity of these pathways which is associated with a sub-optimal immune cell response with further cytokine and pattern-recognition receptor stimulation ((159) and reviewed by Rea et al. (160)). Functionally, these processes render many immune cell types hyporesponsive to acute challenges (159). Thus, the dysfunctions associated with inflammaging have been associated with an impaired antigen presentation and naïve T cell priming, corroborated with a decrease in phagocytic function in innate immune cell types and CD8+ T cell cytotoxic function, a dysfunctional type I IFN response and a restricted naïve T and B cell repertoire contrasted by a myeloid differentiation bias in bone marrow progenitors, as reviewed elsewhere (17,161,162). These ageing-associated immunological phenomena have been associated with poor vaccination responses, as well as increased mortality following the infection with influenza and coronaviruses (17,163,164).

Understanding what are the biological factors that are modulating immunosenescence is one of the great challenges of the field and among them gender and infectious diseases play a pivotal role (165). Observations in humans have pointed out that female organisms age at a different rate compared to male ones and with distinct age-associated immunological phenotypes (38). Márquez et al. using data from bulk Assay for Transposase-Accessible Chromatin with high-throughput sequencing (ATAC-seq) of peripheral blood mononuclear cells (PBMNCs) have inferred that during adult lifespan, the epigenome is undergoing two discrete periods of rapid changes in accessibility of genes associated with specific cellular identities (monocytes, NK cells,

naïve T cells, activated CD8+ T cells, B cells and plasma cells), the first one centred for women between ages 38-41 and for men between the ages of 40-42 and the second one that for women is substantially later than for men, at ages of 66-71 and 62-64, respectively, with one possible interpretation for this observation being that men age from an epigenetic standpoint faster than women (38). Evidence from a single cell RNA-seq study has pointed out that, in humans, women have more plasma cells in the circulation and an increase in activity of the BAFF/APRIL system, a hallmark of a more effective adaptive immune response, but also of B cell mediated autoimmunity, whereas in men a higher proportion of NK cells in blood, an overall higher expression of component genes of the TNF, IFN-γ, and IL-1 pathways, and more monocytes in circulation with age are recorded compared to women (166,167). An important role in the shaping of the immune system is played by sex steroids as in mice it has been observed that oestrogen and progesterone are repressing NK activity, but this is not the case for androgens and this observation is conserved in humans as well, with women taking oral contraceptives having reduced NK counts in the peripheral blood (168,169). A functional consequence of the sexual dimorphism observed in humans at the level of the immune system is the poorer response to vaccination in men compared to women, testosterone being highlighted as having immunosuppressive properties when it comes to influenza vaccine responses (170). Linking the influence of infectious disease to the processes associated with ageing in the immune system has been done while observing the similarities between the immune systems of the geriatric population and the ones of HIV-infected patients and the high prevalence of frailty as clinical state in both cohorts (165). Tedeschi et al. discuss that chronic viral

infections through persistent antigen stimulation induce a senescent state via telomere attrition and DNA damage accumulation in the CD8+ T cell compartment with an accumulation of cells expressing CD57, but negative for CD28 and expressing high levels of p16 and p21 and components of SASP, exacerbating the proinflammatory milieu that is observed during ageing (171).

With ageing, myeloid lineage populations expand relative to lymphoid lineage ones, as thymic activity decreases and a myeloid skew in haemopoiesis is present (95,144,172). Thus, in mice and humans, flow cytometry studies have showed that there is an age dependent increase in abundance of monocytes in peripheral blood, with such an increase in frequency being recorded as well in the spleens of old mice versus their younger counterparts (151,173,174). Interestingly, the phenotype of these circulating monocytes in humans is skewed towards the non-classical phenotype in humans (175). Macrophage frequency fluctuates with age and it is also dependent of the tissue it is quantified, with alveolar macrophages diminishing in numbers and functionality, peritoneal ones following a similar pattern, but $Fn1^{+}Ccr2^{+}$ macrophages in the lung interstitium as well as CX3CR1+ ones in the liver and kidney increasing in frequency in mice (176,177). In mice, dendritic cells show decreased frequencies in spleen for the conventional dendritic cells 1 (cDC1), in the peritoneum for the conventional dendritic cells 2 (cDC2), for the plasmacytoid dendritic cells (pDCs) in the spleen and liver (176,178). In humans, available data from peripheral blood indicate that pDCs decrease in frequency with age (175). Neutrophils in mice increase in frequency with age in lungs and liver (176,179).

Another cellular compartment that is affected by ageing in both mice and humans is the innate lymphoid one which comprises the natural killer cells, the group 1, 2 and 3 innate lymphoid cells (ILCs) (180). In older humans, the NK compartment is more enriched in the CD14+CD56hi fraction and overall, a diminished cytokine production and cytotoxic capacity (181–183). Evidence from mice points out to the fact that the aged microenvironment differentially interferes with NK differentiation and proliferation depending on the tissue, with a decrease in frequency of NK cells in spleen, peritoneum, lungs and liver, but not in neurogenic niches (176,184). ILC1s through their secretion of IFNγ and function as a first line of defence against viral and bacterial pathogens at the level of barrier epitheliums have been shown to decrease in frequency with age in murine livers and when it comes to ILC2s, in the lungs and brains of mice (176,185).

During ageing, a remodelling of the adaptive immune system has been observed with both B and T cell compartment being affected at different magnitudes (157). In mice it has been observed that with ageing there is an increase in the frequency of a CD43-CD21/CD35-CD23- B cell population in the spleen and a CD11b+CD11c+ B cell one in the meninges (186,187). Plasma cells have been shown to increase in abundance with age in the renal parenchyma, adipose tissue and bone marrow (188,189). With age in mice, at the level of the spleen, two B cell populations have been shown to accumulate, one Apoe+ and another Zbtb32+ and at the level of the peritoneum a Zcwpw1+ B1 B cell population (176,190). The splenic B cell populations that are

expanding with age exhibit features of antigen experience and high levels of somatic hypermutation (191). The increase in abundance with age in mice of plasma cells in both bone marrow, spleen as well as in the periphery i.e. adipose tissue and renal parenchyma and the propensity of plasma cells to secrete pro inflammatory cytokines and enhance myelopoiesis could hint at the possibility of plasma cells to be a driver of the ageing associated proinflammatory milieu and detected in the previously mentioned tissues (188,192). There are parallels between the ageing associated B cell population size fluctuation trends in mice and humans and this is reflective of accumulation of B1-like cells in old mice and humans, with such cells having an increase in expression with age of the 4-1BBL, a TNF ligand superfamily member, and exhibiting an activated phenotype which has been linked with the induction of a cytotoxic phenotype in CD8+ T cells and an inflammatory response to commensal bacteria (193–195). Interesting, the B1 B cell population as a whole decreases in frequency with age in humans and its IgM antibody repertoire is shrinking, hinting at possible reduction in flexibility when responding to emergent pathogens (196).

Before discussing the ageing-associated phenomena observed in the T cell compartment of the immune system in a greater detail as it is required given their dramatic shifts in subpopulation frequency with age (172,197), it would be important to highlight what are the current therapeutical targets in combating one of the aspect of immune system ageing, inflammaging.

Thus, Chambers and Akbar mention inhibitory ligand blockade, senolytics, p38 MAP kinase blockade and mTOR blockade as the main therapeutical angles in combating inflammaging (198). mTOR and p38 MAP kinase blockade have been used in human clinical trials to improve vaccine responses and antigen-specific cutaneous immunity respectively, but the mTOR blockade treatment was not without substantial adverse effects (stomatitis, diarrhoea, nausea, cytopenia, hyperlipidaemia and hyperglycaemia) (199,200). Senolytic small molecules and even chimeric antigen receptor T cells have been tested in mice with promising results yielding a diminished proinflammatory state and functional rejuvenation of the milieu of solid organs such as the liver (201,202). There has been little to no translation of this therapeutic approach in humans, with only a handful of trials using senolytics in humans for applications such as mitigating for the effects of diabetic kidney disease (203). One of the great dilemmas of the gerontologists and ageing scientist remains whether therapies such as senolytics, that would strike at the very core of the phenomenon of inflammaging could be translated into human use and increase the period of life spent in good health (156,204).

The impact of ageing on the structure and functionality of the T cell compartment of the murine and human immune system

Mittelbrunn and Kroemer in their review describe the ageing process in the T cell compartment through a system of ten molecular hallmarks, grouped into four primary ones (thymic involution, mitochondrial dysfunction, genetic and epigenetic alterations, and loss of proteostasis), four secondary ones,(reduction of the TCR repertoire, naive–memory imbalance, T cell senescence, and lack of effector plasticity) under the direct influence of the phenomena described by the primary hallmarks and 2 integrative ones (immunodeficiency and inflammaging), explained by the interplay between the primary and secondary hallmarks (25).

Loss of proteostasis, mitochondrial disfunction and genetic and epigenetic alterations associated with ageing are in alignment with the current ageing theory of molecular damage and are encountered across other immunological compartments but, thymic involution is a hallmark of T cell ageing that plays a fundamental role in the functionality of the T cell compartment during the lifespan (25,157). The direct consequence of thymic involution has been linked to one of the most well documented feature of the ageing of the T cell compartment, the reduction in size and clonal complexity of the $CD8^+$ naïve T cell compartment, a phenomenon that is conserved across mice and humans (176,205,206). The age-dependent diminished functionality of the thymus is linked to a decline in thymocyte numbers and change in the thymic niche, a process under the control of the increase in sex steroids characterising the transition towards

puberty of the organism and later on during more advanced ages the reduction of growth factors such as the growth hormone, insulin-like growth factor 1 (IGF1) and keratinocyte growth hormone (KGF) (207,208). Exogenous growth hormone, leptin and ghrelin can prevent stress mediated thymic atrophy that can occur during starvation in mice and physical activity promotes in humans the maintenance of elevated levels of IL-7 that acts as thymoprotective cytokine (209,210). Though more and more is being learned about the ageing process at the level of the thymus, the precise mechanisms that govern the thymic endothelial cell dysfunction, thymocyte reduction and ultimately a reduced thymic output remain largely unknown (25).

Mitochondrial dysfunction in T cells plays a pivotal role in the disfunctions that are reported in T cells with age, as in older organisms where OXPHOS is impaired, presumably due to the accumulation of dysfunctional mitochondria as a result of an autophagy deficit (211). Interestingly, the mitochondrial dysfunction in T cells has been linked with increased in DNA damage (212). A characteristic of the aged T cell mitochondrion is represented by a dysfunction in the one-carbon metabolism that is affecting the naïve T cell activation dynamics (213). Moreover, mitochondrial dysfunction plays a role in the switch towards a more pro-inflammatory phenotype with age via the accumulation of inflammatory metabolites and the release of mitochondrial DNA in the cytoplasm with the engagement of the cGAS-STING pathway (214). In aged T cells there is an increased basal activation of the PI3K–AKT–mTOR and MAPK signalling and a link between aerobic glycolysis and an excessive proinflammatory T cell phenotype has been made by observing the effects in mice of the deletion of the

Mpc1 gene, coding for a key unit in the mitochondrial pyruvate carrier in the thymocyte as well as αβ T cells development (215,216). Moreover, the knockout of mitochondrial transcription factor A (TFAM) in T cells generates a mitochondrial disfunction coupled with perturbed proteostasis resulting an aged-like T cell phenotype characterised a type 1 helper T proinflammatory phenotype (217). TFAM as well as PGC1α expression can be restored by IL-15 with positive effect on the fitness of regulatory T cells in HIV-infected patients (218). Treatment of Mycobacterium tuberculosis infected mice with metformin, a known modulator of TFAM expression has yield positive result, with an increased speed and proportion in infection resolution in the metformin arm of the study (219).

Evidence from studies carried out using cohorts recruited from the Japanese population, point that with age, it has been shown that T cells accumulate chromosomal alteration which in turn were associated with an increase in T cell leukaemia incidence with age (220). CHIP-associated mutations, have been shown to affect T cell function with enhanced CAR-T cell activity (TET2 mutations) (221) and increased graft-vs-host disease and reduced relapse in allogeneic bone marrow transplantation (DNMT3A mutations) (222). The impact of CHIP-associated mutations on the clonal structure of the T cell compartment is not as great as in the case of other lineages and the working hypothesis regarding this observation is that there is minimal thymic activity in older adults driven by a mutant HSC bearing a CHIP mutation as well as the stringent thymic selection (223–225). ROS accumulation due to mitochondrial stress has been linked with increased DNA damage and telomere attrition, thus promoting genomic instability

in T cells, a phenomenon that intensifies with age (212). Impaired high fidelity DNA repair via loss of ATM and MRE11 functionality and dysregulated histone expression via SIRT1 expression play a role in the genomic instability that increases with age and in the context of rheumatoid arthritis in T cells (226–229). From an epigenetic standpoint, in naïve CD4+ T cells ageing-associated variation in CpG sites were enriched at the level of genes associated with TCR signalling, apoptosis, mTOR and MAPK signalling (230). Hu et al undertook a study of both the memory and naïve T cell compartments in the context of ageing in healthy humans subjects and an increased differentiation state in both compartment can be observed which authors claim is driven by the gain in accessibility to bZIP sites in BATF for both CD4 and CD8 T cells (231). To complicate matters further, at a single cell level, there is an increased transcriptional variability in H3K27me3-marked genes in naïve CD4+ T cells with ageing, but this trend is not recapitulated at the level of the population (232).

The loss in proteostasis associated with ageing has been linked to diminishing levels of proteolytic enzymes such as calpain and tripeptidyl peptidase II, the genetic deficit of the latter being associated with CD8+ premature immunosenescence as well as a diminished autophagic capacity and dysfunctional proteasome (233–235). Autophagy inhibition has a negative impact on T cell differentiation dynamics, with impaired memory T cell clone formation and maintenance as well as the activation of MYC and mTORC1 in Tregs diminishing the stability of FOXP3 and apoptosis of T regs (235). Autophagy dysfunctions have been detected in T cell with age and a hallmark of this dysfunction is represented by a diminished capacity for mitophagy in order to remove

damaged mitochondria (211). IGF1 receptor mediated activation of mTORC1 signalling is correlated with inhibition of autophagy and yielded a skew in T cell differentiation towards Th17 over T regs, thus promoting a proinflammatory state (236). Observations regarding the positive effects of mTORC1 inhibition on the rate of infections in older individuals and the fact that improved activation-induced autophagic activity is a hallmark of CD4+ T cells from subjects belonging to families with exceptional longevity lends credence to the hypothesis that autophagy regulation in T cells is a vital component in the maintenance of a high performing adaptive immunity (69,199).

The lack of plasticity and increase in prevalence of the senescent T cell phenotype with age is a consequence of the mitochondrial dysfunction, loss of proteostasis and accumulation of genetic alteration that accumulates with age (25). The ageing associated senescent T cell phenotype has been postulated to be a result of lifelong antigen stimulation and it encompasses features that are seen in other senescent cell types such as an accumulation of γH2AX foci, apoptosis resistance, increased β-galactosidase activity and SASP as well as T cell specific characteristics such as loss of CD27 and CD28 expression and upregulation of terminal differentiation markers, chief among them being KLRG1 and CD57 (237,238). Not all human T cells senesce at the same rate with CD8+ T cells doing so faster than their CD4+ counterparts and this has been linked to the state of the mitochondrion of each T cell type, with the observation that the terminally differentiated effector memory CD45RA+ T cells (TEMRA) that are CD4+ having mitochondria that are less damaged than their CD8+ counterparts (215). Senescent CD8+ T cells manifest a phenotype that is more innate-

like with a diminishing TCR signalling and the acquisition of the natural killer receptor NKG2D and adapter molecule DAP12 (239). Buffering ROS levels via the activity of glutathione S-transferase has been linked to expression of DDB1- and CUL4−associated factor-1 (DCAF1) which diminish with age in T regs, thus pointing out a possible explanation for the more acute accumulation of senescent cells in the T reg compartment compared to the effector one with age (240). The diminished plasticity in T cell differentiation with age is attested by the propensity of observing Th1 and Th17 T cell phenotypes associated with extreme differentiation, with features of exhaustion and cytotoxicity with age, a phenomenon linked with the impact of cytokines such as IL-6, IL-27 and IFNβ associated with SASP on the differentiation trajectory of T cells (241). Moreover, a single cell transcriptomic study has shown in mice and humans have shown that with age there is an expansion of an oligoclonal exhausted TOX+ PD-1+ T cell population secreting a senescent inducing factor granzyme K (176).

A direct consequence of thymic involution is represented by the naïve-memory imbalance and the diminished TCR repertoire that is observed with age (25). One of the most constant observations made with regards to the ageing of the T cell compartment is that, with age, the naïve T cell compartment contracts, more so the CD8+ naïve subpopulation compared to the CD4+ one in the peripheral blood of both mice and humans and the effector memory T cell subpopulation expands (176,242). Though in mice the thymus continues to be active and export naïve T cells, albeit at a very diminished rate in older mice, in humans, the naïve T cells pool after the age of 40 is solely maintained by naïve T cells that are not recent thymic emigrants in a

process termed homeostatic peripheral proliferation (197,243). Though the imbalance between T cells with a naïve and memory phenotype can be attributed to thymic involution with age and a lifetime of antigenic stimulation, recently it has been shown in both mice and humans that in the context of a niche abundant in IL-15 and IL-4, naïve T cells will differentiate into a phenotype that exhibits the features of a memory T cells even in the absence of an antigenic stimulus, a virtual memory T cell (244). Virtual memory T cells have been shown to have high affinity to self-antigens, have a propensity to acquire a senescent phenotype (245,246). T cell receptor (TCR) repertoire reduction has been linked to ageing, with the naïve T cell compartment being affected to a greater extent than other as a direct effect of thymic involution (247,248). Interestingly, evidence from a single cell study points out that in humans the TCR repertoire shrinks with age through 2 main processes: 1) reduction with age of the contribution of the naïve T cell compartment of recent thymic emigrants and 2) through clonal selection at the level of the memory T cell compartment (247). It has been suggested that one of the driving forces for the clonal selection present in the memory T cell compartment is the persistent antigen stimulation that is associated with chronic viral infections such as the one with cytomegalovirus (CMV)(249).

Understanding how clonal haematopoiesis factors in the phenomenon of TCR repertoire shrinkage with age is still a challenge given the sparsity of evidence, though there is data pointing out that genetic determinants can influence the TCR repertoire's size as certain polymorphisms at the human leukocyte antigen class I (HLA-I) loci are associated with a range of TCR repertoire sizes (249). The diminishing size of the TCR

repertoire in older individuals has been linked with diminished vaccine efficacy particularly for respiratory viruses and therapies such as the one with recombinant human IL-7, which have shown induce an expansion of the TCR repertoire in the naïve T cell compartment could be useful to alleviate the effect of ageing on vaccination efficacy (250,251).

A result of the processes that are associated with the ageing of the T cell compartment represents an ageing-associated immunodeficiency which has been speculated to be one of the culprits for the disproportionate COVID-19 and influenza mortality among individuals over 65 years old (17). Understanding how inflammaging plays a role in the development of this ageing associated immunodeficiency as well what is its role in post-acute infectious syndromes remain open questions with potential consequential public health implications particularly in the wake of the COVID-19 pandemic which has highlighted yet again the burden of frailty on healthcare systems and the looming spectre of a public health crisis with almost a third of patients recuperating from COVID-19 manifesting some type of symptom persistence and a distinct proinflammatory state (252,253).

The impact of ageing on the immune system in the context of the coronavirus disease 2019 (COVID-19)

COVID-19 is a disease caused by the infection with the severe respiratory syndrome coronavirus 2 (SARS-CoV2), a viral pathogen from the *Betacoronavirus* genus with a single stranded positive sense RNA genome spanning approximatively 30000 bases, closely related to the etiologic agent of SARS, SARS-CoV and the Middle East respiratory syndrome coronavirus (MERS-CoV) (254). SARS-CoV2 has a tropism for cells expressing angiotensin-converting enzyme 2 (ACE2), such as the nasal epithelium, alveolar type II pneumocytes, superficial conjunctival cells and enterocytes as well as beta pancreatic cells, attaching to the cells expressing ACE2 using the viral spike protein on its surface (255–257). Following entry into such cells, the viral replication and destruction of infected cells that ensues triggers an innate immune response with these processes happening during the 5 day viral incubation period (17,258). Then, in the majority of cases, the host will clear out the virus due to an efficient coordinated immune response between the innate and the adaptive branches of the immune system with mild symptoms that could include fever, cough, shortness of breath, fatigue, myalgias, nausea, vomiting, diarrhoea, headache, weakness, rhinorrhoea, anosmia, and ageusia (259–262). Host will experience severe symptoms (pneumonia, cytokine storm, acute respiratory distress syndrome (ARDS), sepsis and coagulopathy (259,262)) if there are lapses in the interferon responses at the level of the innate immunity amounting to a failure to control the primary SARS-CoV2 infection, compounded by a delayed anti-viral adaptive immune response, as it is the case in old

patients (262). A milestone in the evolution of a COVID-19 case is day 12 after symptom onset, at which point in the case of severe cases ARDS will develop which in most cases will resolve in either death or recovery 7 to 12 days later (259,263). Overall, after 30 days post symptom onset, 80% of all unvaccinated patients will be asymptomatic (264).

COVID-19 severity can be seen as a function of how well the immune system detects the viral infection, mounts a response against it and resolves the inflammatory response after the clearance of the viral infection (24,262). Age is one of the most important prognostic factors in the clinical evolution of COVID-19 as shown by data made available from the Centers for Disease Control and Prevention (CDC): individuals aged 18 to 29 years accounting to only 0.7% of all the COVID-19 related deaths and individuals aged 65 to 74 years accounting to 22.6% of all COVID-19 related deaths, even though the individuals aged 18 to 29 years old account for 16.4% and the ones aged 65 to 74 for only 9.6% of the total US population (265). A study of unvaccinated COVID-19 patients has shown that infection fatality rate grows exponentially with age from a minimum recorded at the age of seven (266). Apart from age, diabetes mellitus, hypertension, obesity and chronic kidney disease as well as being a male patient increases the risk to develop a severe case of COVID-19 and this could be because all the above mentioned factors have been linked with a proinflammatory state or vascular damage, which in turn are key components in the pathogenesis of severe COVID-19 (267–269).

The SARS-CoV2 intrinsic immune evasive mechanisms accentuate ageing-associated deficits in the recruitment of innate immune cells at infection site, elimination of infected cells and priming of the adaptive immune response (164,270). Among those immune evasive mechanisms, the blockade of the type I IFN inducing pathways, expression of IFN-stimulated genes (ISGs) by SARC-CoV2 proteins leading to uncontrolled viral propagation and delayed type I IFN via the dysregulation of primary and secondary retinoic acid-inducible gene (RIG) have been shown to potentiate ageing-associated immune deficits (164,270,271). With age there is a heightened base activation of the JAK/STAT and NF-κB signalling as a result of SASP which makes difficult to initiate the induction of a type I interferon and in the case of COVID-19 this ultimately leads to uncontrolled viral replication and an accumulation of damage- and pathogen-associated molecular patterns (DAMPs, PAMPs) which in turn stimulate the activity of NF-κB signalling at the level of the monocytes and neutrophils that start to accumulate at the site of the infection (17,159,160,272). Consequently, in the elderly by the time an efficient antiviral type I IFN response is mounted, the site of the infection is in a hyper-inflammatory state, characterised by high levels of cytokines that trigger the cytokine storm, like TNFα and IFNγ and are encountered in the cytokine storm and in inflammaging such as IL-6, IL-8, IL-1β, IL-18, CXCL10, IL-1α and CCL2, resulting in tissue damage and ARDS (17,272). At the interface between the innate and adaptive branch of the immune response against SARS-CoV2 lies the dendritic cell, an important player in the success of the development of a durable immunity against any pathogen, which is negatively affected by age with impaired maturation, reduced IFNα

production and a reduction in their activation following TLR stimulation that is associated with diminished antigen presenting capacity (273,274).

The adaptive branch of the immune response against SARS-CoV2 is crucial for viral clearance and for ensuring durable immunity against the pathogen, but in aged individuals generating the cellular and humoral immunity against this pathogen is hampered by a series of factors such as: 1) low TCR diversity making the development of a SARS-CoV2 epitope specific T cell clones difficult (247,275) ; 2) low expression of CD40L on T cells, thus an impairment of germinal centre response (276); 3) the propensity of the aged B cells to produce low affinity antibodies due to reduced class switching and somatic hypermutation (277) and 4) lymphopenia that has been associated by the IL-6 and TNFα-triggered apoptosis (278). The importance of an effective T cell response for the prognosis of the development of a protective immunity against SARS-Cov2 cannot be understated as SARS-CoV-2-specific CD4+ and CD8+ T cell population size correlated with reduced disease severity, while neutralizing antibodies in the same individuals did not and data from patients that undergone therapeutic B cell depletion has shown that they can mount effective protective responses against SARS-Cov2 (24,279). Flow cytometry as well as single cell transcriptomic studies have shown that T cell responses to SARS-Cov2 are long lived and are mirroring to an extent the phenotype observed during ageing in the T cell compartment from a population dynamic standpoint, with an increase in frequency of memory T cell types with increased expression of proinflammatory cytokines and a slight shrinkage of the naïve T cell compartment (280–282).

The recovery from COVID-19 has been shown to not be complete in up to a third of patient at 30 days post symptom onset (253). An incomplete recovery from an infectious disease is not necessary a phenomenon that has not been encountered before, with post-SARS syndrome, Q fever fatigue syndrome, post-dengue fatigue syndrome as well as post-Ebola syndrome serving as examples (253,283–286). Though definitely a serious public health crisis waiting in the wings, the post-acute COVID-19 syndrome (PACS) lacks a unified definition with the CDC, the World Health Organisation (WHO) and UK's National Institute for Health and Care Excellence (NICE) setting different thresholds for symptom persistence after the acute form and levels of exclusion of other causes for those symptoms (252). Thus, the CDC defines PACS as a range of new, returning or ongoing health issues that individuals can experience four or more weeks after the infection with SARS-CoV2, regardless if they were asymptomatic after the diagnosis and become symptomatic only after 4 weeks from the infection date (287). The WHO has a stricter definition of PACS as it requires that the patient to have a confirmed SARS-CoV2 infection, with symptoms persisting 3 months after the onset of the acute disease for at least 2 months, in the absence of any other alternative explanation for them (288). Positioning between the stricter WHO and the more lenient CDC definitions, NICE's one states that PACS patients would have symptoms persisting between 4 to 12 weeks after acute symptom onset (289). The list of symptoms comprised by the 3 definitions shows significant overlaps and Choutka et al in their review of post-acute infection syndrome compile a list of them in the context of existing studies surveying for them: changes in taste and smell, fatigue,

dyspnoea, neuro-cognitive deficits, memory issues, sleep issues, palpitations, tightness/pain, arthralgia, myalgia, chest, blurred vision, headache, dizziness, anxiety, loss of appetite, reduced lung function, wheezing (252). Current evidence suggests that PACS patients could be stratified in 2 groups: 1) patients recovering from severe COVID-19 which can present symptoms resembling post-ICU syndrome (290) and 2) patients that present an intolerance to exertion, cognitive and sensory deficits, myalgias and flu-like symptoms (252), which usually did not experience severe symptoms during the acute phase of the disease and are predominantly women (odds ratio for recovery when compared to men: 0.62 – 95% confidence interval : 0.43-0.92)(291).

The pathogenesis of post-acute infectious syndromes is currently an understudied field, but several hypotheses have been brought forward: the persistence of a pathogen reservoir or antigen, the development of autoimmunity following infection, dysbiosis or pathogen reactivation and tissue damage (252). The deleterious effects of a persistent pathogen reservoirs have been studied in the context of CMV and they could be summarised as constant engagement of TLR signalling via the PAMPs generated by the constant pathogen presence (292). Chronic SARS-CoV2 infections have been documented in immunocompromised patients (293), a category of patients which would be vulnerable to CMV reactivation (294). Even though both CMV and SARS-CoV2 escape immune evasion by dampening interferon responses (294), in the case of chronic SARS-CoV2 infections in immunocompromised patients, there is an association between these infections and variants presenting antibody evasion

mutations (293) which could highlight a difference in mechanisms of between CMV and SARS-CoV2 persistence and how SARS-CoV2 persistence might maintain an proinflammatory state. Persistence of SARS-CoV2 in a post-acute setting has been shown in a study of gastrointestinal tract endoscopic biopsies harvested 3 months post COVID-19 symptom onset have shown that in more than a third of them SARS-CoV2 antigen can be detected and in 21% of them viral RNA was detectable, suggesting viral persistence past the 3-month mark in the enterocytes (295). A post-acute infection syndrome could be generated by the onset of an autoimmune disease and this was the case post Epstein-Barr virus (EBV) infection in which in the antibodies against the viral protein EBVNA1 cross react with the human central nervous system protein glial antigen 1 and this interaction has been causally linked to the development of multiple sclerosis (296). In the case of COVID-19, autoantibodies against type I interferons have been detected both in the acute and convalescent setting with positive corelation between the levels of these auto-antibodies in the blood and the frequency of gastro-intestinal and respiratory PACS and in a different cohort autoantibodies against G-protein coupled receptors were found in all the 31 patients included in the study with 29 of them experiencing PACS (253,297). A large multiomics study has shown that in the case of PACS the reactivation of EBV in the acute phase of COVID-19 is positively associated with the presence of PACS, building the case for the dysbiosis and pathogen reactivation hypothesis behind the pathogenesis of this post-acute infection syndrome (253). Unmitigated damage following ARDS in the context of COVID-19 could explain the presence of respiratory sequalae during the convalescence as vascular damage and lung fibrosis occurring during acute respiratory infections can

lead to respiratory disfunctions that remain unresolved (298). In support of this hypothesis of tissue damage as driver of COVID-19 severity and possibly by proxy of respiratory PACS, Guardela et al. have shown that the quantification of an idiopathic pulmonary fibrosis 50 gene expression signature in the peripheral blood of COVID-19 patients can be used to stratify their cohort study according to their need for intensive care unit admission, mechanical ventilation, and in-hospital mortality with a receive operating curve area under the curve of 0.77, 0.75, and 0.74 (299).

Understanding the pathogenesis of acute COVID-19 and the biology of recovery post COVID-19 will help the scientific community to better understand how human physiology reacts to a viral pathogen months after initial onset of it symptoms (252). The fact that one of the main risk factors for developing severe COVID-19 is old age and the fact that T cell responses are so vital to both viral clearance and protection reinforce the importance for the field of immunosenescence of the study of this pathology in great depth (262). Studying the COVID-19 specific or dependent T cell changes that can persist past the first month from symptoms onset threshold and relating them to the development of PACS forms that have been associated with severity and disability inducing such as the respiratory ones could help both our understanding of the aftermath of viral respiratory disease and identify new therapies for mitigating such adverse effects.

The benefits and challenges of utilising single cell transcriptomics in the study of ageing

In 2013, Nature Methods named single cell sequencing the Method of the Year which signalled the beginning of the single cell multiomics age (300). Single cell RNA sequencing (scRNA-seq) is a method of quantifying the abundance of polyadenylated (polyA) messenger RNA (mRNA) species at the level of single cells by first using oligo-dT primers to capture the polyA mRNA molecules and then converting them into complementary DNA (cDNA) for later construction of sequencing libraries compatible with sequencing by synthesis workflows (301). The modality of partitioning the cell for the generation of the cDNA from each cell's mRNA repertoire has segregated the majority of platforms used in ageing research for generating scRNA-seq datasets into plate based and droplet based ones, with consequences on both the throughput (hundreds vs thousands of cells/experiment) and the representation of the transcriptome offered by each type of technique (302,303). A comparison between the prototypical plate-based scRNA-seq protocol, SMART-seq2 and the industry standard droplet-based scRNA-seq one, 10X Genomics Chromium 3' V2 has shown that the plate-based protocol was more sensitive for gene detection than the droplet based one (4000 vs 2000 genes detected per cell), with increased levels of gene expression dropout in the case of the droplet based platform, and platform specific sensitivities of detection for different gene types, with the plate-based method detecting more mitochondrial and membrane protein genes compared to droplet based one, whereas

the droplet based one detected more ribosome-related process genes and long non-coding RNAs than the plate-based methods (303).

One of the benefits of studying ageing using scRNA-seq is that it allows to identify cell populations characterised by a certain transcriptomic signature that fluctuates in frequency with age in an unbiased way, thus allowing for the discovery of novel ageing-associated phenotypes inside an already predefined cellular compartment (304). In the case of studying the haematopoietic system and how ageing affects its cellular composition, scRNA-seq based studies have pointed out that during ageing in mice there is an expansion of long-term HSCs in the bone marrow, contrasting to what was observed in short term HSC and the transcriptome of old short-term HSCs resemble young long-term HSCs, suggesting that they exist in a less differentiated state (305). Single cell transcriptomics have also helped elucidate the gene expression patterns associated with the megakaryocytic biased von Willebrand factor-positive long term murine HSCs that have been observed to increase in frequency with age, with this population exhibiting a priming of transcriptomic programs associated with megakaryocyte and myeloid progenitors (306). Moreover, single cell transcriptomics have been able to show that following an inflammatory challenge (LPS and Pam3csk4) HSCs from old mice will increase the output of myeloid lineage cells in stark contrast to what would happen to HSCs from young donors and this functional outcome is linked with the activity of *Klf5, Ikzf1, and Stat3* (135). Apart from understanding the heterogeneity of a cellular compartment, single cell transcriptomics can be used to investigate the existence of cell-to-cell interactions inside a particular niche, by probing the expression patterns of receptors and their cognate ligands in the cell types

identified in a scRNA-seq dataset using computational tools such as CellPhoneDB and CellChat (307,308). Huang et al. have shown using scRNA-seq datasets generated from PBMNCs of healthy human donors of different ages that there is an increased in the BAFF/APRIL signalling between dendritic and B cell in young versus old women, the authors speculating that this observation could be linked with the higher incidence of B cell autoimmunity in women (166). Single cell transcriptomics can also be used to infer differentiation trajectories and computational tools such as tradeSeq can be used to understand which genes are differentially expressed between different stages of the trajectory or how a perturbation can affect the gene expression programmes that are associated with a differentiation trajectory (309,310). Le et al. have used trajectory inference methods to understand the gene expression programs governing the initial stages of human thymopoiesis, a vital process in the development of the human T cell compartment (311).

Unfortunately, studying the impact of ageing in a cellular compartment using scRNA-seq comes with the inherent challenges that producing and analysing a scRNA-seq dataset come with. From a wet lab perspective, knowing the frequency of a certain cell population that one wants to profile inside a cellular compartment will dictate the protocol used and the costs of the experiment (312). Baran-Gale et al. suggest the usage of high througput scRNA-seq methods, such as droplet-based ones, when the aim of project is characterising rare populations, thus allowing the profiling of large enough cell numbers in order to find the low frequency subpopulation of interest (312). If the aim of the project is to further characterise the transcriptome and dissect the heterogeneity of population containing relatively abundant subpopulations, then plate-

based methods such as Smart-seq2 and 3 would be more appropriate than droplet based ones, sacrificing throughput for allowing an increase in the gene counts observed per cell and full transcript capture (303,312,313). Similar to conventional RNA-sequencing experiments it is crucial that the experimental conditions that we are investigating to not be confounded by technical batches such in the following scenario: all the samples coming from old individuals to be processed using one scRNA-seq protocol and the samples from young donors to be processed using another scRNA-seq protocol, thus making any conclusions about the differences between old and young transcriptomic profiles in this scenario unreliable (312).

Before delving into the challenges posed by analysing single cell RNA-seq datasets, I will outline the steps in a basic scRNA-seq data processing workflow and mention some of the most performant and popular scRNA-seq computational tools used at every step of this workflow.

The first step in the analysis of a scRNA-seq dataset is the elimination of non-viable cells and doublets (314). In scRNA-seq datasets, cells with a low read or unique molecular identifier (UMI) count depth, low counts of detected genes, and a high percentage of their library size allocated to mitochondrial genes are considered non-viable cells with a damaged cell membrane (314). Thus, non-viable cells are usually eliminated using thresholds set on read/UMI counts and on the percentage of mitochondrial gene read/UMI counts, with peripheral or bone marrow mononuclear cells with less than 10% of read/UMI counts allocated to mitochondrial genes being considered viable (315). Doublets are a technical artefact in which data labelled as

coming from one cell is generated from more than one cell and they are eliminated using methodologies ranging from thresholds on read/UMI counts set to demarcate such cells from singlets to methods that profile cells to find the ones that match the transcriptome of computationally generated doublets (314,316).

Normalisation procedures are applied to the scRNA-seq data before any further processing, thus minimising the variation concerning transcript capture, reverse transcription and sequencing depth between cells and the odds that transcriptomic differences observed between cells are solely due to sampling effects (314). Currently the most used normalisation method is count depth scaling followed by log(x+1) transformation (314).

Usually following normalisation, if the analysed scRNA-seq dataset is not generated from multiple biological or technical replicates, the dimensionality of the dataset is reduced by first performing variable gene selection, a procedure that helps identifying genes that are informative for the variability of the data, reduce noise and computational burden (314,317). Among the most used methods for variable gene selection is the one implemented in the Seurat open-source R scRNA-seq analysis toolkit (318) which uses a variance stabilised transformation method (319) to study the mean-variance relationship for each gene in the data (318). Following the selection of variable genes for the scRNA-seq dataset, dimension reduction methods are used in order to visualise the dataset and summarise the gene expression patterns observed in the dataset to its essential components or dimensions (314). Reduced dimensions can be produced via linear or non-linear combinations of gene expression vectors, but the distances in the lower dimensional space generated using non-linear methods

between cells can not be interpreted intuitively (314,320). Two of the most used dimension reduction methods used in the study of scRNA-seq data are principal component analysis (PCA) (321), which employs linear combinations of gene expression vectors to summarise the main gene expression patterns observed in the dataset and Uniform Manifold Approximation and Projection (UMAP) (322), a non-linear method used primarily for visualisation purposes and to approximate the global structure of the dataset (314,320).

After dimensionality reduction, scRNA-seq data is clustered in order to identify cell groups based on the similarity of their gene expression profiles. Similarity between cells is assessed via distance metrics determined using dimensionality-reduced representations of the data as input, for example Euclidean distances that are calculated on the principal component-reduced gene expression space (314). A popular approach to determine clusters at the level of the dataset is the one employed by the Seurat open-source R scRNA-seq analysis toolkit (318), in which cells are nodes in a k-nearest neighbour (KNN) graph, where the connections in the graph (edges) are drawn between cells with similar gene expression patterns (318). Following the construction of the KNN graph based on the Euclidean distances in the PCA space, clusters are called by applying the Louvain modularity optimisation technique which will group cells iteratively with the goal of optimizing the standard modularity function i.e. until cells from inside each cluster are more connected at the level of KNN graph than the cells from different clusters (318,323).

Clustering scRNA-seq data marks an inflection point in any analysis workflow of such a dataset, as at this point batch effects can be visualised and known and novel cell

types can be identified. Cell type cluster annotation can be done by associating the expression of known cell type marker genes to clusters in which those genes are highly expressed or by employing cluster-cell type annotation methodologies such as SingleR (324). Batch effects can be assessed by studying if cells that have been profiled by a certain technique or in a different sequencing run are overrepresented in a particular cluster or by specialised methodologies for batch effect evaluation such as CellMixS (325).

If data from different sequencing runs, labs or scRNA-seq methods are used, methods of batch correction will need to be applied as to minimise for the impact of dataset-specific technical covariates on the transcriptome (314,326). One of the most used methods for batch correction and dataset integration is the one built in the Seurat open-source R scRNA-seq analysis toolkit (318) which is capable of mitigating for significant batch effects, but is less suitable for large datasets and may be more prone to overcorrection due to its usage of canonical correlation analysis than other methods (327). Another popular batch correction method is Harmony, which is designed to handle large datasets and due to its usage of soft clustering can be tuned to avoid overcorrection, but is less potent than the Seurat method in regressing very large batch effects (326–328).

scRNA-seq data analysis workflows drastically diversify following the data clustering step either focussing on cell level analyses that would involve differential abundance analysis (DAA) and trajectory inference methods or on gene level analyses such as differential gene expression analysis (DGEA) between different cell populations, gene

set enrichment and gene regulatory network analyses or more often than not on a combination of cell and gene level analyses (314).

DAA aims to quantify the effect of a perturbation on the cellular composition captured by a single cell RNA-seq dataset and tools for such analyses have just recently started being developed (314,329). Initially, DAA has been caried out by assessing the overrepresentation of cells from a certain experimental condition at the level of each cluster identified in an scRNA-seq dataset (314). Milo represents one of the most promising DAA methods with its ability to detect changes in cellular composition between experimental conditions staring from the k-nearest neighbour graph generated from the distances between cells in the a low dimension gene expression space, thus being able to forego the limitations of the clustering methods (329). Another cell level type of analysis are trajectory inference methods which aims to track differentiation trajectories or cell state transitions capture in a scRNA-seq dataset (310). A recent benchmarking of trajectory inference methods (310) has nominated Slingshot as being one of the most flexible and robust method of this kind (330).

DGEA is an essential component of any scRNA-seq data analysis workflow as it is a type of analysis that highlights the genes used to define cell types (cluster markers) and the ones whose expression is the most affected by a perturbation (331). Interestingly, for the purpose of cluster marker gene identification, methods relying on logistic regression, Student's t-test or the Wilcoxon rank-sum test performed very well (331) whereas for other purposes, methods that used pseudobulk aggregation and the edgeR (332) methodology have been shown to perform the best in terms of false discovery rate (FDR) control (333). Gene set enrichment analysis (GSEA) facilitates

the interpretation of the results of DGEA by testing if there are overrepresentations of gene sets associated with known biological functions at the level of the genes that were shown to be either upregulated or downregulated by the DGEA (314). The algorithm behind GSEA, initially designed by Subramanian et al. (334) for usage for microarray data analysis and improved and implemented as the fgsea R package by Korotkevich et al. (335) has been extensively used in field of scRNA-seq data analysis.

Gene regulatory network analysis (GRNA) is performed based on measurements of gene co-expression as to quantify the complex interplay of regulatory interactions governing gene expression (336). Among the most popular GRNA tools designed for scRNA-seq is SCENIC, which relies on identifying co-expression gene expression modules and quantifying their expression (337).

There are challenges at every step of the scRNA-seq data analysis and they stem primarily from the inherent sparsity and high dimensional nature of scRNA-seq data (338,339). Quality control of scRNA-seq datasets is complicated by the sparsity of scRNA-seq data, with shallowly sequenced datasets being up to 99% composed of zeros which makes setting thresholds of read/UMI counts for identifying viable cells challenging (340). As part of dataset quality control, doublet identification remains problematic as doublets made from cells of the same cell type being more difficult to identify than ones produced by co-encapsulation of cells of different cell types (316) and no consensus being reached on which is the computational method that is best suited for most experimental setups (340). Choosing a certain method of normalisation can influence the results of variable gene selection, dimensional reduction, clustering,

visualisation (319) as well as DGEA (341), but no consensus has been reached yet on which normalisation method is the most appropriate for the largest set of downstream analyses (314). Current popular methodologies used to perform dimensionality reduction of scRNA-seq datasets have inherent limitations such as the fact they can not be used effectively for data summarisation and visualisation at the same time, such an example being PCA (320). Moreover, non-linear dimension reduction methods are capable to capture the non-linear nature of scRNA-seq better linear methods (320), but are limited in preserving cell to cell distance information for downstream usage in methods such as trajectory inference ones, with UMAP having a bias for fully connected cluster structures as visualisations of the data (340). Stemming from the difficulty of finding a dimension reduction strategy that accurately approximates the topology of the dataset, choosing the right method for trajectory inference is a daunting challenge and only recently benchmark and choice methodologies for this kind of methods have been devised (310).

Handling the sparsity of scRNA-seq data is in particular a challenge in the context of studying ageing using scRNA-seq publicly available datasets as most of such data is from droplet-based protocol which when is pseudo-bulk aggregated does not behave like a bulk RNA-seq sample (303). Moreover, an inherent issue of performing DGEA in the context of scRNA-seq experiments in which multiple biological replicates are available per condition is pseudoreplication bias, as cells from the same individual are not statistically independent making commonly used statistical methods used for DGEA liable to this bias (342). Moreover, Kharchenko points out that in the case of DGEA done in scRNA-seq experiments it will always be difficult to deconvolute if a gene is

differentially expressed between two cell populations because it is expressed by a different number of cells in each group or at different magnitudes in all the cells tested or a combination of both scenarios previously mentioned (338). It is important to highlight that even though GSEA may have the potential to hint at the functionality of the cell types identified in a scRNA-seq dataset, this family of methods is inherently limited by the assumption that genes from different pathways act independently (343) and inferences obtained from them are particularly influenced by gene expression dropouts (344). GRNA methods have the potential to indicate gene regulatory mechanisms at the level of the cell types identified in scRNA-seq datasets but, Chen and Mar have shown in their benchmarking study that current GRN methods perform poorly when used on either experimental or simulated single cell RNA-seq data (336).

Finally, one of the most challenging aspects of scRNA-seq data analysis is the study of durable cell-cell complexes, such as the T cell – monocyte ones described by Burel et al. which could hold potential valuable insights with regards to inflammatory states such as post-acute infection ones (345,346). Studying durable cell-cell complexes is problematic, particularly when utilising droplet-based scRNA-seq platforms, because they will be indistinguishable from an artefactual doublet (316,345,346).

Summary and aims

With age, molecular damage accumulates and deleteriously affects the functionality of all the cellular compartments of an organism. The accumulation of molecular damage is associated with cellular senescence which in turn is associated with the development of an inflammatory state in the cellular niche where senescent cells accumulate. Haematopoiesis shows great variability with age. In mice there is an age-dependent megakaryocytic and myeloid lineage bias in their haematopoiesis and the HSC compartment contributes to this bias, whereas in humans the existence of a lineage biased HSC population that fluctuates in size and output with age in unperturbed haematopoiesis has not been shown. In both mice and humans, the T cell immune response has been shown to become increasingly deficient with age which has been linked to a reduced naïve T cell pool as well as a plethora of mitochondrial and proteostasis dysregulations and accumulation of DNA damage. The recovery from an infection has been shown to be a function of the functionality of the T cell compartment, particularly when it comes to COVID-19.

The advent of single cell transcriptomics can allow us to study the process of ageing at the level of the HSC and memory T cell compartment at an unprecedented resolution and help us confirm results obtained using bulk transcriptomics, as well as lead to the generation of new hypothesis on which are the signalling pathways that are associated with age in the context of health and disease. Thus, this project aims to answer the following questions utilising single cell RNA-seq datasets:

1. Can a human bone marrow HSC subpopulation exhibiting the gene expression patterns of lineage-biased murine HSCs be identified in the single cell RNA-seq datasets from healthy human bone marrow samples and is this subpopulation exhibiting an inflation with age?
2. Does the ageing phenomenon in the memory T cell compartment and the recovery from COVID-19 share common transcriptomic features? Are these features able to stratify a cohort of convalescent COVID-19 patients based on disease severity during the acute phase, thus highlighting potential pathways to target to alleviate deleterious adaptive immune processes associated with both experiencing severe COVID-19 and ageing?

Chapter II. Materials and methods

Datasets

For the chapter pertaining the analysis of the impact of ageing on the human bone marrow HSC compartment the scRNA-seq datasets have been generated from FACS-sorted phenotypic human HSCs (defined as Lineage(CD2, CD3, CD4, CD7, CD8a, CD10, CD11b, CD14, CD19, CD20, CD56, CD235ab)$^{-}$CD34^{+}CD38^{-}CD90^{+}CD45RA^{-}) from fresh bone marrow aspirates of 3 healthy young male donors (aged 21, 22 and 24 years old) sourced from AllCells (Berkeley, CA) and from the frozen CD34^{+} magnetic-activated cell sorted (Miltenyi Biotec, 130-046-702) bone marrow mononuclear cells (BM-MNC) obtained from orthoplastic surgery specimens after informed consent as part of the Mechanisms of Age-Related Clonal Haematopoiesis (MARCH) Study (NHS REC Ref: 17/YH/0382) of 3 old male donors (aged 68, 71 and 75 years old). The 3 male donors from the MARCH study have been previously screened for CHIP-associated mutations and no somatic driver mutations with a variant allele fraction ≥ 0.01 were found. No CHIP-associated mutation status data is available for the samples acquired from AllCells. Following the FACS of the phenotypic human HSCs from the samples mentioned above the cells were washed in 1× PBS + 0.04% BSA (Ambion, AM2616) and 12000 HSCs for each young donor and 13130, 6658 and 7078 HSCs for each old donor were loaded as a separate reaction on two Chromium Single Cell A Chips (10X Genomics, 2000019), one for each donor type, young or old. Following the loading of the cells on the chips the GEM Generation & Barcoding steps,

followed by post GEM-RT clean-up, cDNA amplification and library construction was carried out using the components of the Chromium Single Cell 3' Reagent Kits v2 (10X Genomics, 1000009) following the Chromium Single Cell 3' Reagent Kits v2 User Guide protocol. The scRNA-seq libraries were sequenced in two batches one for each donor age group. For each sequencing batch, each cell was sequenced at an expected depth of 100,000-200,000 reads per cell, in a 125bp paired end reads sequencing configuration on a S4 flow cell of a NovaSeq600 system (Illumina, 20043131) at a Novogene sequencing facility (Beijing, China). The sample processing, FACS, the GEM Generation & Barcoding, the post GEM-RT clean-up, cDNA amplification and library construction was carried out by a team formed from Vyas and Nerlov lab members: Bilyana Stoilova, Mario Buono, Marlen Metzner and Merve Aksöz. Asger Jakobsen performed the mutational screening for the samples collected from old donors. The demultiplexing of the .bcl files generated from sequencing of the HSC scRNA-seq libraries as well as the processing of the. fastq files and the subsequent analysis of the raw UMI count x cell matrices pertaining this dataset was carried out by Grigore-Aristide Gafencu.

The results of the differential gene expression analysis carried out by Merve Aksöz and Claus Nerlov on the scRNA-seq data generated from human HSCs clones that have been lineage-tracked and exhibited either a platelet-biased or multilineage functional output generated by Merve Aksöz as part of DPhil thesis project have been used to validate the similarity between the experimentally-determined lineage-biased human HSC clones and the computationally-determined ones. The differential gene

expression analysis methodology relied on the usage of Seurat's (v4.1.0) (347) FindMarkers function with the following parameters and using the log-normalised read counts produced by running Seurat's (v4.1.0) (347) NormalizeData at default parameters: test.use = MAST, logfc.threshold = 0, min.pct = 0.

The datasets analysed in the chapter pertaining the impact of ageing on the T cell compartment have been selected from publicly available studies that had their data obtained by profiling most of their samples using the 10X Genomics Chromium scRNA-seq platform 5' prime biased V2 or V3 scRNA-seq platform, had their samples processed in a similar fashion (PBMNCs isolated using density gradient centrifugation), contained data either from subjects that were never exposed to COVID-19 or were recovering from COVID-19 (> 30 days post symptom onset) and had suitable sample metadata available: age and gender for the clinically healthy cohort and for the convalescent COVID-19 cohort, age, gender, comorbidity, acute COVID-19 severity (WHO Ordinal Scale for Clinical Improvement score) and symptoms data at > 30 days post symptom onset. Thus the Ren (348) and Stephenson (349) datasets were highlighted for further usage of the data pertaining the healthy donor cohorts used in these studies normalised and the Su (253) dataset for its convalescent COVID-19 cohort data.

The selected datasets were downloaded either as non-normalised UMI count x cell matrices for the Ren (348) and Stephenson (349) datasets or as normalised counts per million UMI count x cell matrices for the Su (253) dataset as they were deposited and

accessible via publicly accessible websites especially conceived for the dissemination of these datasets or repositories:

- Ren dataset: http://covid19.cancer-pku.cn/ - direct download link: https://drive.google.com/file/d/1IwWcn4W-YKgNbz4DpNweM2cKxlx1hbM0/view
- Stephenson dataset: https://www.covid19cellatlas.org/ - direct download link: https://covid19.cog.sanger.ac.uk/submissions/release1/haniffa21.processed.h5ad
- Su dataset: ArrayExpress Archive of Functional Genomics Data accession: E-MTAB-10129

The datasets accessed from publicly available sources were all generated using 10X Genomics Chromium scRNA-seq platform, both 3' and 5' prime biased V2 and V3 kits being both used (Chromium Single Cell 3' v2 Reagents (10x Genomics; PN-120237), Chromium Single Cell 3' v3 Reagents (10x Genomics; PN-1000075), Chromium Single Cell 5' Feature Barcode Library Kit (10x Genomics, 1000080), Chromium Next GEM Single Cell 5' v1.1 (10x Genomics, 1000165)), starting from both frozen or fresh PBMNCs. The alignment to a reference genome of the sequencing data and the transcript quantification that generated the initial cell UMI counts x cell matrix using was done by either the CellRanger pipeline (10X Genomics) v3.1.0 for the Su dataset and v4.0 for the Stephenson dataset or the kallisto/bustools (KB, v0.24.4) (350) for the Ren dataset and the reference genome was GRCh38 for the Ren and Su datasets and the GRCh38 concatenated with the SARS-CoV-2 genome (NCBI SARS-CoV-2 isolate Wuhan-Hu-1). These datasets were freely available at the sources mentioned above after they have undergone a certain degree of processing that ranged from the removal

of cells with poor data quality and doublets (Ren, Stephenson and Su datasets) to genotype-based sample demultiplexing for pooled samples using souporcell (v2) (351) (Stephenson dataset) and the performing of gene expression normalisation (Su dataset). The data quality control for the Ren dataset consisted in the elimination of cells with less than 1000 unique molecular identifiers (UMI) counts and 500 detected genes, as well as cells with more than 10% of their UMI counts being allocated to mitochondrial genes. For the Ren dataset potential doublets were eliminated based on a cell's UMI (> 25000) and detected genes (>5000) counts. For the Stephenson dataset, the data quality control consisted in the elimination of cells with less than 200 genes detected and with more than 10% of their UMI counts being allocated to mitochondrial genes as well as the doublets identified by 2 strategies: a) doublets identified by the doubletCells function of scran (352) based on highly variable genes (HVGs) used in conjunction with the 'cluster_walktrap' function of scran (352) on the shared nearest neighbour (SNN) graph computed on the HVGs data, deeming any cell with a median doublet score > median + 2.5× median absolute deviation (MAD) or clusters containing more than the median + 2.5× MAD genotype doublets as doublets; b) doublets identified using DoubletFinder (v2.0.3) (316) and the ground truth to model the gene expression of putative doublets using the doublets identified by souporcell (v2) (351). For the Su dataset the data quality control consisted in eliminating doublets using scrublet (353) and then proceeding in eliminating the cells with < 200 detected genes and > 10000 UMIs/cell then cells with >2500 detected genes / cell and with more than 10% of their UMI counts being allocated to mitochondrial genes. The gene expression was normalised in the Su dataset utilising the scanpy.pp.normalize_total

function of Scanpy (v1.6.0) (354) with the target_sum parameter set to 10^6. For the data regarding the convalescent COVID-19 patient cohorts, cells from donors sampled less than 30 days post symptom onset were not used in further analyses. Only data from samples profiled using the 10X Genomics's 5' scRNA-seq platform were used when it comes to data sourced from publicly available sources.

Methods

Alignment and transcript quantitation

The .bcl files resulting from sequencing the scRNA-seq libraries generated from adult human bone marrow HSCs were demultiplexed by sample using the *mkfastq* function of the CellRanger pipeline (v3.1.0, 10X Genomics) at default parameters. The reads contained in the .fastq files generated from demultiplexing the .bcl files were then aligned against the *H. sapiens* GRCh38 (Ensembl 93) reference genome (10X Cell Ranger reference GRCh38 v3.1.0) and the gene UMI count x cell matrices for each sample were generated by utilising the *count* function of the CellRanger pipeline (v3.1.0, 10X Genomics) at default parameters.

Data importing and quality control

In the case of the human HSC dataset, for each donor, gene UMI count x cell matrices, filtered for empty drops, that constituted one of the outputs of the *count* function of the CellRanger pipeline (v3.1.0, 10X Genomics) were first imported as dgTMatrix using Seurat's (v4.1.0) (347) Read10X function into an R (v4.1.2) environment and converted into Seurat objects using Seurat's (v4.1.0) (347) CreateSeuratObject function with the following parameters modified from their default values: min.cells = 3, min.features = 200, thus ensuring that not cells with less than 200 detected (nonzero UMI counts) genes, a threshold suggested by the Seurat v4.1.0 documentation, are taken further

for analysis and no gene that is not expressed in at least 3 cells is considered for further analyses. In order to eliminate cells that could be in an apoptotic or necrotic state, cells with more than 10% of their UMI counts being allocated to mitochondrial genes were discarded, as suggested by the conduct in previous single cell RNA-seq data quality studies (315). In order to mitigate for the contamination of the dataset with doublets, a known artefact in droplet-based scRNA-seq platforms (355), cells that had the number of detected genes more than twice the median per sample of detected gene counts were discarded.

In the case of the datasets sourced from publicly available sources, the datasets were downloaded from the previously mentioned sources and subset to include the samples that were deemed of interest. For the Ren dataset, the data pertaining the PBMNCs from healthy controls was extracted from the downloaded .h5ad file by first loading the object into a Python (v3.9) environment using Scanpy's (v1.7) (354) read_h5ad function and further subsetting this dataset by selecting only the cells with the cell barcodes associated samples from the healthy control cohort, marked in the original dataset in the metadata column 'Sample time' as "control". Following this procedure, the .h5ad files containing the Ren's dataset healthy control subset was converted into h5seurat files using SeuratDisk's (v0.0.0.9019) (356) Convert function and the relevant dataset subsets were loaded into an R (v4.1.2) environment and converted into Seurat objects using SeuratDisk's (v0.0.0.9019) (356) LoadH5Seurat function at default parameters and saved as a .rds files for later usage. For the Stephenson dataset the data pertaining the PBMNCs from healthy control donors was extracted from the

downloaded .h5ad file by first loading the object into a Python (v3.9) environment using Scanpy's (v1.7) (354) read_h5ad function and further subsetting this dataset by selecting only the cells with the cell barcodes associated samples from the healthy control, marked in the original dataset in the metadata column 'Status' as "Healthy". Following this procedure, the .h5ad files containing the Stephenson dataset's healthy control subset were converted into h5seurat files using SeuratDisk's (v0.0.0.9019) (356) Convert function and loaded into an R (v4.1.2) environment and converted into a Seurat object using SeuratDisk's (v0.0.0.9019) (356) LoadH5Seurat function at default parameters for later usage and saved as a .rds file for later usage. For the Su dataset, for each sample that was sampled at the T3 timepoint in the study from which the Su dataset originates (253), the pre-processed normalised UMI counts x cell matrices in a .txt format were downloaded from the ArrayExpress E-MTAB-10129 accession and imported into R (v4.1.2) using the data.table's (v1.14.2) (357) fread function and then each normalised UMI counts x cell matrix was used to generate a Seurat object using Seurat's (v4.1.0) CreateSeuratObject function at default parameters. Following the creation of a Seurat object for each sample selected from the ArrayExpress E-MTAB-10129 accession, all the Seurat objects have been merged into one Seurat object using SeuratObject's (v4.0.4) (358) merge function and saved as a .rds file for later usage.

Data quality control for the healthy cohort data extracted from the Ren and Stephenson datasets consisted in eliminating the cells with < 200 detected genes and > 10000 UMIs/cell then cells with >2500 detected genes / cell and with more than 10% of their UMI counts being allocated to mitochondrial genes, the same gene count-based criteria

used to perform the quality control for the Su dataset. If samples from either the healthy or the convalescent cohorts did not have more than 20 cells in the naïve or memory T cell clusters those samples would not be used for further analysis.

Data normalisation, highly variable gene selection and batch effect correction

For data generated from human HSCs, following quality control the UMI counts have been normalised using Seurat's (347) implementation of the scTransform normalisation procedure (359) (scTransform function) carried out at a sample level. In order to mitigate the batch generated during the library preparation procedures, each sample was considered a batch, and after normalization, 3000 integration anchors across samples were defined using the Seurat's (347) FindIntegrationAnchors function ran on the list of Seurat objects containing data from each sample following the scTransform procedure. Data from old donors was processed in isolation from data from young donors and the batch correction was aimed to mitigate for inter-sample variability inside each donor type cohort. Once the integration anchors were defined, data was batch corrected using the Seurat's (347) IntegrateData function, with the function's argument normalization.method = "SCT". The integration anchors served afterwards as the highly variable genes, for which their batch corrected and normalised counts were used for PCA. In the case of the integrative analysis of the old and young HSC datasets, the analysis procedure differed from the previously mentioned one at the stage of finding the 3000 integration anchors which were defined using the Seurat's (347) FindIntegrationAnchors function ran on the list of Seurat objects containing data from

all available sample following the scTransform procedure and the Seurat's (347) IntegrateData function, with the function's argument normalization.method = "SCT" was ran on the the list of Seurat objects containing data from all available sample using the 3000 integration anchor genes determined on all available samples' data.

For the data representing the healthy donor control PBMNCs datasets, the data was initially normalised using Seurat's (347) NormalizeData function with the normalization.method = "LogNormalize" and scale.factor = 1000000 parameters on the data of the Seurat object resulted from merging all the Seurat objects resulted from the quality control procedure performed for the data representing the Ren and Stephenson dataset's healthy cohort data. The selection of 3000 highly variable genes that were used for PCA was done by utilising Seurat's (347) FindIntegrationAnchors function on a list of the outputs of the Seurat's (347) FindVariableFeature function ran at default parameters, which had as inputs the data of each analysed sample. The batch correction was done at the level of the principal component embeddings using the Harmony methodology (328). The normalised UMI counts that have been previously computed on the merged Seurat object containing the Ren and Stephenson dataset's healthy cohort data were centred and scaled using Seurat's (347) ScaleData function at default parameters and a PCA was carried out, using Seurat's (347) RunPCA function, in which only the gene expression data, as represented by the normalised, centred and scaled UMI counts of the highly variable genes previously identified was used. Next the batch effects caused by variability between samples as well as variability between the two data sources, the Ren and Stephenson datasets

used to assemble these datasets were mitigated by correcting for the influence of these variables at the level of the principal component embeddings using Harmony's (328) RunHarmony function at default parameters except for the theta parameter that was increased from 2 to 4 to improve batch mixing at the level of local neighbourhoods, with the covariates to regress being sample identity and data source.

Data from the Su dataset was downloaded as already normalised counts and highly variable genes for the data coming from each patient were determined using the Seurat's (347) FindVariableFeatures function at default parameters (selection.method = "vst"). The normalisation procedure used by the authors of the Su dataset was identical to the one employed in the processing of the Ren and Stephenson datasets. The selection of 3000 highly variable genes that were used for PCA was done by utilising Seurat's (347) FindIntegrationAnchors function on a list of the outputs of the Seurat's (347) FindVariableFeatures function. The normalised UMI of the Su dataset were then centred and scaled using Seurat's (347) ScaleData function at default parameters and a PCA was carried out, using Seurat's (347) RunPCA function, in which only the gene expression data, as represented by the normalised, centred and scaled UMI counts of the highly variable genes previously identified was used. Next the batch effects caused by variability between samples were mitigated by correcting for the influence of these variables at the level of the principal component embeddings using Harmony's (328) RunHarmony function at default parameters except for the theta parameter which was set to 4, with the covariate to regress being the sample identity.

Dimensionality reduction, clustering and cluster – cell type identity assignation

For the human HSC dataset, a PCA was carried out by using Seurat's (347) RunPCA function and the input of the function was the batch-corrected UMI counts x cell matrices including data only for the previously identified 3000 integration anchor genes. The resulting principal component representation of the data was then used as the input for the UMAP visualisation performed using Seurat's (347) RunUMAP function, used for the visualisation of the clustered data. The principal components used for the UMAP visualisation were selected using an elbow plot describing a ranking of principle components based on the number of standard deviations of the gene expression variance can be explained by each one, and only the principal components that could explain at least more than 1 standard deviation of the gene expression variance in each HSC dataset subset were selected.

In the case of the datasets that have been sourced from publicly available sources, dimensionality reduction was carried out using a PCA for which only the normalised data pertaining the highly variable genes that were identified as mentioned previously for these datasets has been used as input for the Seurat's (347) RunPCA function with default parameters. For the UMAP visualisation of the data clustering results in the case of the publicly available datasets, the Harmony batch-corrected principal component embeddings were used as the input to Seurat's (347) RunUMAP function used at default parameters. The Harmony batch-corrected principal components used

for generating the UMAP visualisation were selected using the elbow plot-based method previously described.

For of all the data that was analysed in this study, the first step in clustering single cell data based on the similarity of cell transcriptomic identity was to compute a k-nearest-neighbourhood (k-NN) graph, with edges drawn between the cells with similar gene expression patterns using the algorithm implemented in Seurat's (347) FindNeighbors function at default parameters and utilising as input the gene expression data summarised by either the principal components computed from batch corrected UMI counts x cell matrices used for the UMAP visualisation of the HSC datasets or the Harmony batch-corrected principal components used for generating the UMAP visualisation of the publicly available datasets. Using the previously computed k-NN graph, the cells were clustered using the Louvain algorithm's implementation in Seurat's (347) FindClusters function used at default parameters and at the following resolutions r = [0.2, 0.3, 0.4, 0.5, 0.6, 0.7, 0.8, 0.9]. The resolution parameter in the FindClusters function applied in the analysis of the HSC dataset was determined using the chooseR (360) methodology. Given the size of the publicly available datasets the resolution parameter of the FindCluster function could not computed in a time sensitive manner using the chooseR (360) methodology, so this parameter's value was selected by using clustering tree visualisation computed using the clustree's (361) clustree function with the prefix parameter set to monitor the cluster identities generated by iteratively running the FindClusters function at the previously mentioned range of r resolution parameters. The clustering tree visualisation (361) describes how the cluster

identify of the cells in one dataset is changing as the resolution parameter changes, and the r resolution parameter chosen for the clustering of the publicly available datasets was the resolution that is before the one in which cell cluster identity becomes unstable (i.e. clusters are no longer marking distinct topological features on the UMAP and are not stable at the resolution change).

In order to ascertain the cell type composition of the HSC dataset for each cell a number of gene expression scores have been computed based on a number of gene lists that have a cell type identity or functional property associated to them, thus indicating based on the relative value of these scores if a cell is of a certain cell type or associated with a certain functional phenotype. The gene expression scores have been computed using the AUCell module of the SCENIC suite for scRNA-seq data analysis (337). The gene expression score was computed in 2 steps: firstly, for each cell genes are ranked according to their expression (AUCell's (337) AUCell_buildRankings function used with default parameters' values), then in order to ascertain if the gene signatures of interest are expressed the, the "Area Under the Curve" of the recovery curve is used to compute a score by evaluating if the genes in the gene signature are within the top 5% of the ranking that was previously calculated (AUCell's (337) AUCell_calcAUC function used with default parameters' values). The AUCell gene expression scores can be interpreted as the proportion of expressed genes in the gene signature of interest (337).

In the case of the HSC dataset, the gene ranking was computed for the young donor HSC dataset subset starting from the log transformed Pearson's residuals generated

from the UMI counts as generated by processing the UMI counts of all the cells from the young donors using Seurat's scTransform function (359) and separately for the old donor HSC dataset subset. In the case of the integrative analysis, the gene ranking was computed starting from the log transformed Pearson's residuals generated from the UMI counts as generated by processing the UMI counts of all the cells from all the donors using Seurat's scTransform function (359). The choice of the usage of the scTransform normalisation in favour of the default gene expression normalisation implemented in Seurat was instructed by the results of a recent benchmarking study (362). The gene signatures used for scoring single cell data in the human HSC dataset were compiled from studies carried out in humans and in mice and thus when the gene sets (89,363–367) were utilising murine gene symbols, the following murine to human gene symbol conversion procedure was employed: the murine gene symbols were converted into their human counterparts when possible, by utilising the getLDS function from the biomaRt (v2.46.3) (368) R package and utilising the H. sapiens (GRCh38.p13) and M. musculus (GRCm39) Ensembl gene symbol annotation for the gene symbol conversion. Gene lists that were used for the computation of AUCell scores and were generated using the above mentioned procedure are available at Appendix methods table 1.

Clusters were assigned into clusters groups, reported as platelet biased output HSCs, multilineage output HSCs or the intermediate state between these 2 transcriptomic states, based on the hierarchical clustering of the Euclidean distance computed for each cluster's median platelet bias, multilineage, high and low output AUCell scores

computed from the gene scores derived from Rodriguez-Fraticelli's description of the megakaryocytic-biased output murine HSCs (89), using the ward.D2 agglomeration method as implemented in stats R package (v4.1.2). The choice of hierarchical clustering method was informed by the maximal agglomerative coefficient computed by the function agnes from the cluster (369) R package (v2.1.3) having as input the scaled and centred values of the median per cluster values of the AUCell scores and evaluating the following clustering algorithms available in the function hclust function of stats R package (v4.1.2): "average", "single", "complete" and "ward". The differences in gene expression score distributions across the clusters and clusters groups determined in the datasets were evaluated using the Wilcoxon rank-sum test, as implemented in the pairwise.wilcox.test and wilcox.test function in the stats R package (v4.1.2). When comparing gene expression scores between 3 or more clusters, the significance of the differences in distributions observed was quantified by using the Wilcoxon rank-sum test in a pairwise fashion and the p-value of the test was corrected for multiple comparisons using the Benjamini & Hochberg correction as implemented in the p.adjust function of the stats R package (v4.1.2).

In the case of the publicly available data cluster identity was assigned by first determining the genes that are differentially expressed for each cluster in a one vs all approach using the function wilcoxauc of the presto (370) (v1.0.0) R package and default parameters and the parameter group_by set to the name of the column in the metadata slot of the Seurat object that indicates the most stable clustering. Then for each cluster a metric representing the product of the AUC value and either 1 or -1

depending if the gene was upregulated or downregulated in the cluster that was analysed which in turn was used to rank all the genes expressed in the cluster. This ranking was next used to perform GSEA and a collection of gene sets representing known genes associated with CD4+ and CD8+ naïve, central memory (TCM), effector memory (TEM), CD45RA+ effector memory (TEMRA), regulatory (Treg), follicular helper (Tfh), helper 1/17, helper 2 (Th1/17), γδ and mucosal associated invariant (MAIT) T cells sourced from 2 publications (371,372) utilising the fgsea function from the fgsea (335) R package (v1.20.0) run at the following parameters: minSize=5, maxSize=2500, nPermSimple = 10000, eps = 0. Appendix methods table 2 contain the gene sets used for the GSEA employed for the T cell type cluster assignation. Clusters were assigned into seven clusters groups, reported as CD4+ naïve, CD8+ naïve, CD4/CD8 TCM, CD4/CD8 TEM, CD4/CD8 TEMRA, MAIT and γδ based on the hierarchical clustering of the Euclidean distance computed for each cluster's normalised enrichment score for each gene set reported with an FDR < 0.25 using the ward.D2 agglomeration method as implemented in stats R package (v4.1.2). The choice of hierarchical clustering method was informed by the maximal agglomerative coefficient computed by the function agnes from the cluster (369) R package (v2.1.3) having as input the scaled and centred values each cluster's normalised enrichment score for each gene set reported with an FDR < 0.25 and evaluating the following clustering algorithms available in the function hclust function of stats R package (v4.1.2): "average", "single", "complete" and "ward". Following the cluster grouping, the expression of the following T cell subpopulation cell type markers (CCR7, PECAM1, CCR7, CD27, EOMES,TEMRA, EOMES, KLRG1, FOXP3, ZBTB16, TRDC)(371–373)

was assessed to establish if their expression patterns differ substantially from one cluster group to another in order to validate the cluster annotation, using the Wilcoxon rank-sum test in a pairwise fashion with the p-value of the test being corrected for multiple comparisons using the Benjamini & Hochberg correction as implemented in the p.adjust function of the stats R package (v4.1.2).

T cell data extraction from peripheral blood mononuclear cell single cell RNA-seq datasets and preparation for downstream analysis

In order to study the T cell compartment in isolation starting from data from scRNA-seq datasets generated from PBMNCs, such as the Ren, Stephenson and Su datasets, first the clusters in the PBMNCs datasets in which the highest expression of CD19 and CD14 were identified. Next, for each cell in the dataset the sums of the normalised UMI counts for the α, β,γ and δ T cell receptor (TCR) chains loci fragments were computed, resulting 4 parameters, each for a type of chain that could make-up a T cell receptor, thus summarising the expression of the TCR for each cell in the dataset. Then, we established which are the clusters that are T cell-rich by identifying the clusters that register median values per cluster of the 4 parameters summarising the expression of the TCR receptor that are higher than the ones registered in the cluster with the highest CD19 median expression, as this cluster is the one that is B cell-rich. In order to eliminate any cell that could express a hybrid myeloid-T cell transcriptomic profile as would be the case for the T cell-monocyte complexes identified by Burel et al. (345) which in the current datasets would be indistinguishable from an artefactual doublet,

the expression profile of CD14, SPI1 (PU.1), CD36 were quantified in the cluster with the highest CD14 expression present in the dataset. Next in the newly identified T cell-rich clusters all the cells that are expressing CD14 or SPI1 at levels over the median – 2 x median absolute deviation normalised expression in the cluster deemed as being monocyte rich (highest median per cluster CD14 expression) or CD36 at levels over the median – median absolute deviation normalised CD36 expression in the cluster deemed as being monocyte rich are marked as doublets and eliminated from further analyses.

The data representing the T cell cluster rich following the elimination of the doublets are then prepared for further usage using the workflow for highly variable gene selection, batch effect correction dimensionality reduction, clustering and cluster – cell type identity assignation that was previously described for data from publicly available sources.

Differential gene expression, gene set enrichment and gene signature intersection analysis

DGEA comparing HSCs from different cluster groups as well as memory T cells from samples from donors of different COVID-19 severity or respiratory PACS statuses was done by first subsetting the dataset of interest to contain only the cells that were used in the comparison using Seurat's (v4.1.0) (347) subset function with the cells parameter being a vector of cell barcodes for the cluster groups or samples used in the comparison. Then the data subset Seurat object was converted into an

SingleCellExperiment object utilising Seurat's (v4.1.0) (347) as.SingleCellExperiment function with the argument assay = "RNA". Next the SingleCellExperiment was filtered to contain only genes that have non-zero normalised counts and a SingleCellAssay object that is suitable for the DGEA workflow using the MAST methodology (374) was created starting from the previously processed SingleCellExperiment by using the MAST's (v1.20.0 or higher) (374) FromMatrix function with the arguments exprsArray set to the cell by normalised gene counts of the SingleCellExperiment object and the cData argument set to the cell metadata data frame of the SingleCellExperiment object. In order to ensure that the models used by MAST for DGEA can converge in the context of a mixed-effect model genes with low expression frequency were filtered using MAST's (v1.20.0 or higher) (374) filterLowExpressedGenes function with the parameter threshold = 0.1, thus making sure than any gene that is expressed in less than 10% of the dataset is not used in the DGEA. Following the filtering of the lowly expression frequency genes the zero-inflated regression model used by MAST for DGEA was created using MAST's (v1.20.0 or higher) (374) zlm function following design formula ~condition + cngeneson + (1|orig.ident), in which condition represent the vector of cell labels for the conditions the DGEA is carried out on, cngeneson is a vector containing the dataset-scaled number of genes detected per cell as way of informing the model on the detection profile of each gene in the dataset (374) and 1|orig.ident representing the random intercept component of the model based on the biological sample identity that aims to mitigate for the pseudoreplication bias inherent to single cell DGEA methods (342) as well as the parameters 'glmer', ebayes=FALSE, fitArgsD=list(nAGQ=0) to accommodate for this design. In order to next identify which

are the differentially expressed genes between the samples or cluster groups of interest a likelihood ratio test is used by using MAST's (v1.20.0 or higher) (374) summary function on the previously computed model with the following parameters doLRT='conditiontest', indicating the element in the design matrix in the condition column that is the group I want to find genes upregulated, and fitArgsD=list(nAGQ=0, tolPwrss=1e-3) to accommodate for the requirements of the mixed-effect nature of the model. The p-value adjusted for multiple hypothesis testing of the likelihood ratio test run for each gene is adjusted using the p.adjust function of the stats R package (v4.1.2) using as the input the p-values of the likelihood ratio test and the Benjamini & Hochberg p-adjusted methodology marked as "fdr" is used for the method parameter of the function.

In order to determine what are the differentially expressed genes between old and young donor cells at the level of each computationally defined HSC populations as determined in the integrated HSC dataset analysis, the wrapper around the pseudobulk edgeR likelihood ratio test pseudobulk (LRT) methodology developed by Squair et al., Libra R package (v1.0.0) (333) was used. To this end, the Seurat object containing data from all available donors, old and young, was used as the input for Libra's (v1.0.0) (333) run_de function with the following parameters: replicate_col = "donor" (metadata column indicating donor identity), cell_type_col = "grouped_cluster_AUCell" (metadata column indicating the HSC population), label_col = "age_group" (metadata column indicating the donor age group), min_cells = 3 (minimum nuber of cell expressing a gene to be considered for analysis), min_reps = 2 (minimum number of donors per

conditions), min_features = 0 (the minimum number of counts for a gene to considered for analysis), de_family = "pseudobulk", de_method = "edgeR", de_type = "LRT".

DGEA in order to infer age-associated gene expression trends across the whole interval of ages studied in the healthy cohort PBMNCs scRNA-seq has been done by utilising the edgeR pseudobulk LRT methodological framework suggested by Squair et al. for its favourable profile in controlling false discovery rates (333). First, data from the memory T cell compartment of the healthy cohort PBMNCs scRNA-seq dataset was aggregated as donor pseudobulk by summing the counts from all the cells of one donor on a gene-by-gene basis by utilising the aggregateAcrossCells function from the scuttle (v1.4.0) (317) R package. Next the DGEList object used by edgeR DGEA method (332,375,376) was created using the DGEList function of the edgeR (v3.36.0) R package starting from the SingleCellExperiment object generated following the pseudobulk aggregation procedure. Following the creation of the DGEList object, the DGEList object was filtered to contain gene counts that could be handled optimally by edgeR by using the filterByExpr edgeR (v3.36.0) function at default parameter except the group parameter set on the column in the metadata where the age group of each sample is stated, young < 40 years old , middle-aged between 40 and 65 years old and old > 65 years old, thus filtering genes that are not present in at least 10 read count-per-million (CPM) in at least 70% of the samples in the smallest group of samples, the old donor cohort. Scaling factors to convert raw library sizes into effective library sizes were computed using the calcNormFactors function from edgeR (v3.36.0) at default parameters and the estimation of the common, trended and gene wise

dispersions across all genes of the read counts was computed using the estimateDisp edgeR (v3.36.0) function at default parameter and taking into account the following design matrix generated using the model.matrix function of the stats (v4.1.2) R package: ~ age + dataset + sex, where age is a numerical value of the number of years each donor has recorded in the metadata of the DGEList object, dataset is a vector with the labels of the dataset either Ren or Stephenson from which the sample was extracted and sex is a vector of the gender label of the samples used in this analysis. Next the generalised linear model used by edgeR for DGEA was created using the glmFit edgeR (v3.36.0) function with the previously generated DGEList object after the processing underwent through the function estimateDisp of edgeR (v3.36.0) and the previously mentioned design matrix as inputs with the robust parameter set to TRUE. The previously generated generalised linear model was used to perform a likelihood ratio test using the glmLRT edgeR (v3.36.0) function and the parameter coef set to 2, indicating what is the column form the design matrix of the model that is used for the likelihood ratio test, thus testing which gene is changing its expression significantly along the age interval. The topTags edgeR (v3.36.0) function was used to tabulate the result of the likelihood ratio test.

GSEA was carried out using 2 types of gene sets, one from relevant publications for the topic of HSC lineage bias and self-renewal or T cell type annotation and one from curated lists such as the Hallmark v7.5.1 and Reactome Pathways v79 and the methodological framework offered by the fgsea (335) (v1.20.0) R package. The metric for gene ranking used in the GSEA when the purpose of cluster annotation was the

product of the AUC value and either 1 or -1 depending if the gene was upregulated or downregulated in the cluster that was analysed using the wilcoxauc function of the presto (370) (v1.0.0) R package was employed to detect cluster marker genes. The metric for gene ranking used for GSEA on other occasions was the product of the log fold change times minus the log10 of the statistical test's p-value for each gene analysed. The list of the gene ranking was not filtered by a threshold of p-value of AUC/log fold change and the parameters of the fgsea function were the following for the cluster cell type identity annotation: minSize=5, maxSize=2500, nPermSimple = 10000, eps = 0. In the analysis pertaining the HSC datasets, the parameters of the fgsea function were as follows: minSize=5, maxSize=1500, nPermSimple = 10000. In the case of the publicly available datasets, the parameters of the fgsea function were as follows: minSize=4, maxSize=2000, nPermSimple = 1000, in order to accommodate the size of the Reactome's collection gene sets

In order to ascertain if the size of the overlap or intersection between 2 sets of gene signatures comprising differentially expressed genes between conditions or between 2 sets of gene lists that are significantly enriched or depleted between conditions is large enough not to be considered that is just due to chance, the methodology implemented in the GeneOverlap (v1.30.0) (377) R package was used. This method employs the Fisher's exact test to assess the magnitude of the intersection size between gene signatures or gene list enriched or depleted using contingency tables containing the counts of gene or gene lists overlapping between the analysed sets of gene signatures or gene lists. Firstly the sets of gene signatures or gene lists that will be compared are

created as lists of R objects and used as arguments for GeneOverlap's (v1.30.0) (377) newGOM function. The size of the statistical domain used by the Fisher's exact test is specified in the genome.size argument of the newGOM function which for the gene signature analyses is set to the size of the list of genes that have been used for the DGEA in the datasets where the procedure was executed and for the gene list analysis is set to the size of the list of genes used for the GSEA.

Trajectory inference and trajectory-informed differential gene expression analysis

In order to better understand which are the genes associated with cell state transitions, the slingshot (330) trajectory inference method was used as implemented in the R package with the same name (2.4.0) by employing the following workflow. First the genes that had zero raw UMI counts for across all cells were eliminated and then the dataset analysed was converted into SingleCellExperiment object using Seurat's (v4.1.0) (347) as.SingleCellExperiment function with the assay parameter set to "RNA". Then using the slingshot function from the slingshot (330) (2.4.0) R package a Slingshot object was created containing the cell state transitions metric of progression along a cell state transition (pseudo-time) and of the matrices describing the principal curves and cell weights along the curves describing the cells state transitions, with the following parameters: data = the matrix of the UMAP cell embeddings previously computed for that dataset retrieved from the original Seurat object using Seurat's (v4.1.0) (347) Embeddings function, clusterLabels = the vector in the

SingleCellExperiment's metadata with the label for each cell's cluster or cluster group and start.clust = cluster that was the platelet bias HSC one.

In order to next understand which genes are differentially expressed along the previously computed cell state transition trajectories the statistical and computational apparatus of the tradeSeq (309) method was used, as implemented in the tradeSeq (v1.10.0) R package. First, a generalised additive model that allows the quantification of the differences in gene expression trends along the trajectory was computed using the fitGAM function from the tradeSeq (v1.10.0) R package using the following parameters: counts = the raw UMI counts matrix from the SingleCellExperiment object previously prepared for the cell state transition step, sds = the name of the Slingshot object previously generated, U = a design matrix computed using the sample identifier column from the metadata of the SingleCellExperiment object and the model.matrix function of the stats (v4.1.2) R package (~donor) and condition = a factor vector containing the condition label to compare cells one against the other from the metadata of the SingleCellExperiment object. Finally, the resulting S4 object generated by the fitGAM function from the tradeSeq (v1.10.0) R package was passed to the function conditionTest from the tradeSeq (v1.10.0) R package at default parameters in order to produce the list of genes that are shown to have statistically significant differences in their UMI counts distributions along the state transition's trajectory.

Machine learning-based methodology for establishing the importance of ageing-associated gene signatures to the severity stratification of the COVID-19 cohort

Single cell transcriptomic data from the memory T cell compartment of each donor was aggregated using Seurat's v4.1.0) (347) AverageExpression function ran at default parameters on the Surat object containing data from the Su dataset. Next, utilising the methodological framework offered by the caret (v6.0-92) (378) R package, 4 types of machine learning algorithms were tested to evaluate their performance in correctly classifying the severity label assigned to the previously aggregated data utilising only the genes from the ageing memory T cell gene signature. To this end, a 10 times repeated 4-fold cross validation methodology was used which was set-up utilising caret's (v6.0-92) (378) R package trainControl function with the following arguments: method="repeatedcv", number=4, repeats = 10, search="grid", classProbs = T, savePredictions = "all", summaryFunction = twoClassSummary. This configuration ensured that the 10 times repeated 4-fold cross validation methodology is used to train and evaluate the models, as well to compute the area under the curve (AUC) of the receive operating curve (ROC) as well as the specificity and sensitivity of each model in the classification task.

The models were trained using caret's (v6.0-92) (378) R package train function with the following arguments: severity_use~. (indicating the column containing the labels to classify), data=hospit_ageingDEGS_hosp_enrich_input (indicating the data frame containing the information from each gene from the gene signature investigated as a column and each row a donor to be analysed), method="lda"/" knn"/"svmRadial"/"rf"

(indicating the type of machine learning algorithm tested: lda = linear discriminant analysis, knn= k-nearest neighbour, svmRadial = support vector machine with radial kernel, rf = Random forrest) and preProcess = c("center", "scale")) (indicating the fact that before the execution of the algorithm, data is centered and scaled). The best model at the classification task is selected based on the highest median ROC AUC recorded following the iterations dictated by the repeated 4-fold cross validation methodology and utilising caret's (v6.0-92) (378) R package varImp function ran on the caret object generated by the train function with the scale argument set to TRUE, the importance for the performance of the classification algorithm is ranked descending for each gene used in generating the model.

Ageing memory T cell gene score computation

In order to compute the gene expression score for summarising the expression of either the ageing upregulated or downregulated genes in significant manner (FDR < 0.05) in the memory T cell compartment of the healthy cohort dataset, the UCell methodology (379) was employed which is conceptually similar to the one used for the calculation of the AUCell scores, but its implementation in the UCell (v1.3.1) R package is better suited for the size of the dataset. The computation of the scores was done using UCell's (v1.3.1) AddModuleScore_UCell function ran at default parameters on the Seurat object containing the data for the memory T cell compartment of the healthy donor cohort and the features argument set to the list of the ageing memory T cell signatures, the one that is upregulated and the one that is downregulated with age.

Chapter III. The impact of ageing on the heterogeneity and transcriptome of the human haematopoietic stem cell compartment using single cell transcriptome analysis

Quality control

scRNA-seq data was generated as per the Material & Methods section from FACS-sorted phenotypic human HSCs from bone marrow aspirates of 3 healthy male young (aged 21, 22 and 24 years old) and 3 old male donors (aged 68, 71 and 75 years old). Following the data quality control (QC) procedure, the vast majority of the data passed the QC standards (Figure 1C), but the cells that pass the QC standards in the young donors had higher detected gene counts compared to what was observed in the old donors (Figure 1B). The higher gene counts in the young donors' data (HSCs sorted from fresh BM-MNCs) compared to the old donors' data (HSCs sorted from thawed BM-MNCs) could be attributed to the differences in processing of the samples between the two donor types. These observations made the case for the initial analysis of the datasets in separation, first the one from young donors and then the one from old donors followed by an analysis that integrates data from both young and old donors in the same low dimension transcriptomic space.

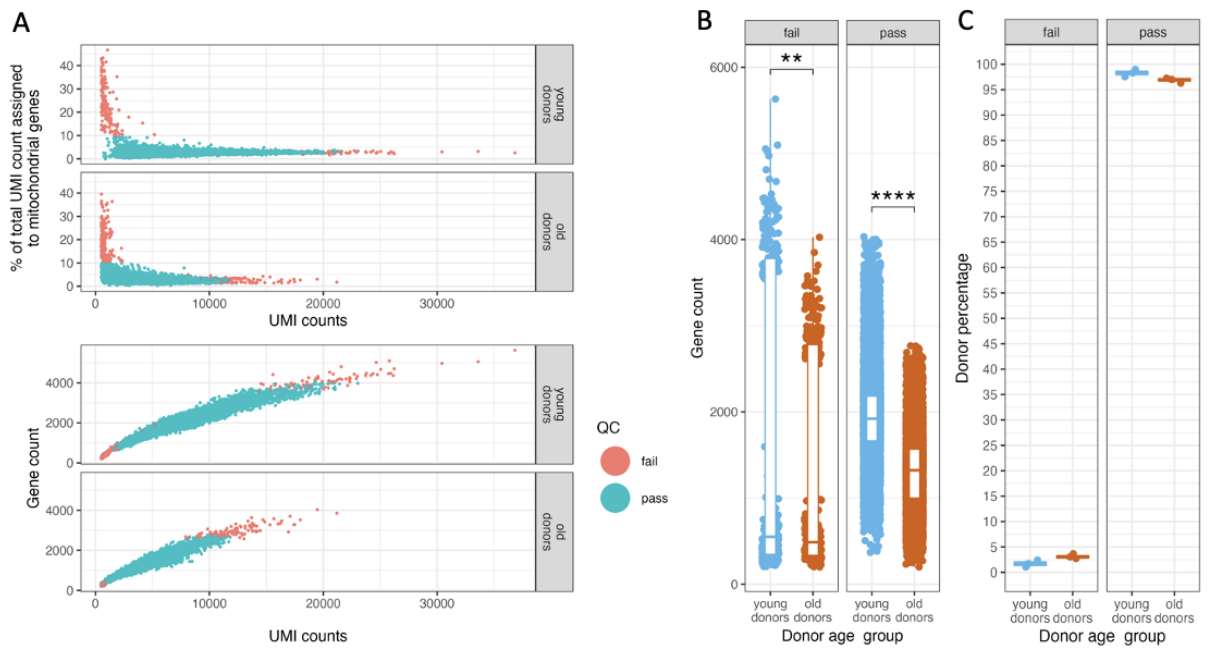

Figure 1 – Quality control procedure – human HSC scRNA-seq datasets

A) Relationship between UMI counts and gene counts / percentage of total UMI count assigned to mitochondrial genes. B) The distribution of gene counts in HSCs that failed or passed QC procedure in the young and old donor human HSC datasets. The Wilcox rank sum test was used to assess the magnitude of the differences between the distributions–p value: **** = <1e-05, ** = <0.001. C) The percentage of cells in each dataset that passed or failed the QC procedure – donor & donor age group breakdown

Young donor dataset analysis – transcriptomic data clustering and cluster characterisation

Following the batch correction procedure and the computing of a UMAP representation of the data from all young donors (Figure 2A), 8 cell clusters (Figure 2C) have been identified in the young donor dataset for the resolution 0.5 used by Seurat's (347) clustering algorithm which yielded the most stable to random subsampling clustering (Figure 2B) as indicated by the chooseR method (360).

In order to identify the clusters that express the genes sets associated with a particular lineage bias (89) or a higher self-renewal capacity (363–367), AUCell gene expression scores have been computed. The correlation patterns between the AUCell gene expression scores at the level of the whole young donor dataset were analysed and showed that the expression of gene sets associated with platelet-bias and/or low HSC output are positively correlated with gene sets associated with high self-renewal capacity HSCs (Figure 3A). In an effort to group clusters according to the patterns of AUCell scores observed for each cluster (Appendix Figure 1) a hierarchical clustering approach was used, as detailed in the Material and Methods section. Thus, 3 types of clusters (Figure 3B), from now on denominated as computationally defined HSC subpopulations were identified: one designated as platelet-biased in which we can find the cluster with the highest AUCell scores for the platelet-biased and low output HSC scores described by Rodriguez-Fraticelli et al. (89), one designated as multilineage output in which the cluster the highest AUCell scores for the multilineage and high output HSC scores described by Rodriguez-Fraticelli et al. (89) and one that encompasses all the other clusters designated as intermediate.

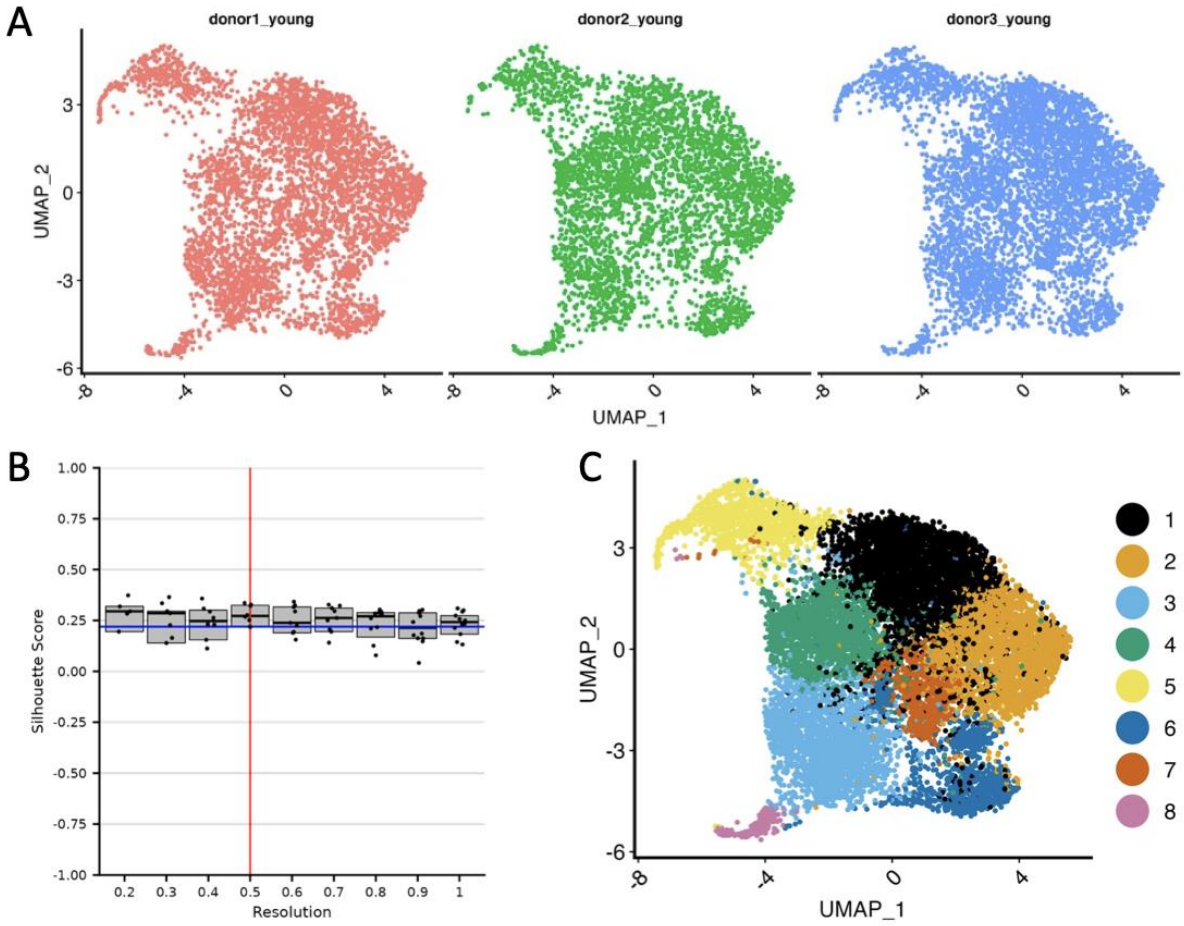

Figure 2 – Batch correction and data clustering – young donor human HSC scRNA-seq datasets

A) UMAP representation of the data from each young donor following the batch correction procedure. B) Silhouette score distribution plot for the young donor dataset. Each dot represents a cluster at a given resolution value. Medians with 95% CI are shown for each resolution value following 50 clustering iterations on randomly subsampled data. The vertical red line marks the optimal resolution, and the blue line represents the decision threshold for choosing the optimal resolution. C) Resolution 0.5 clustering overlayed on the UMAP representation of the data from all the cells available from all the young donors

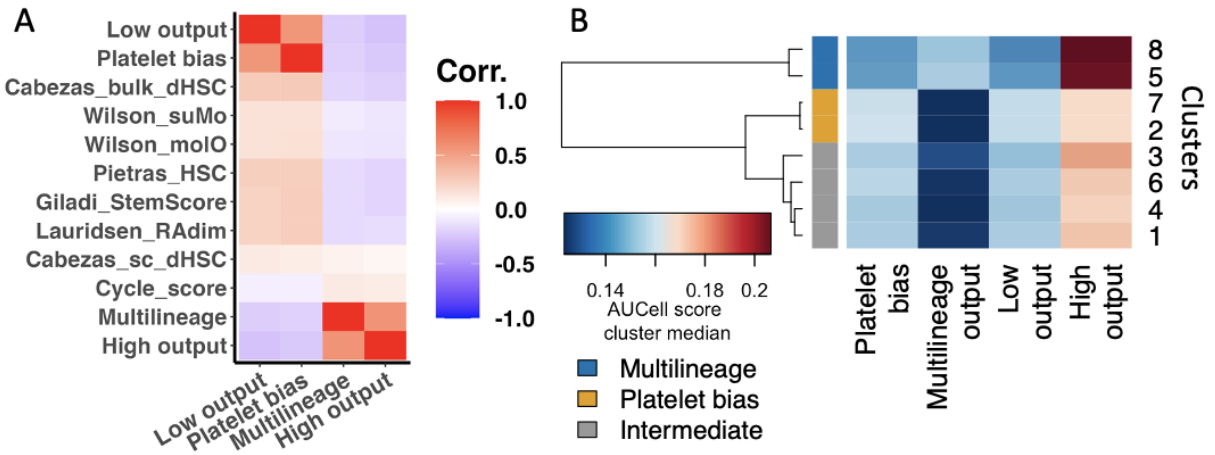

Figure 3 – AUCell score dataset-wide correlation (A) and cluster-wise aggregation (B) patterns – young donor human HSC scRNA-seq datasets. The strength and directionality of the correlation was quantified using Kendall's τ correlation coefficient. Only correlations that had a p-value < 0.05 were represented.

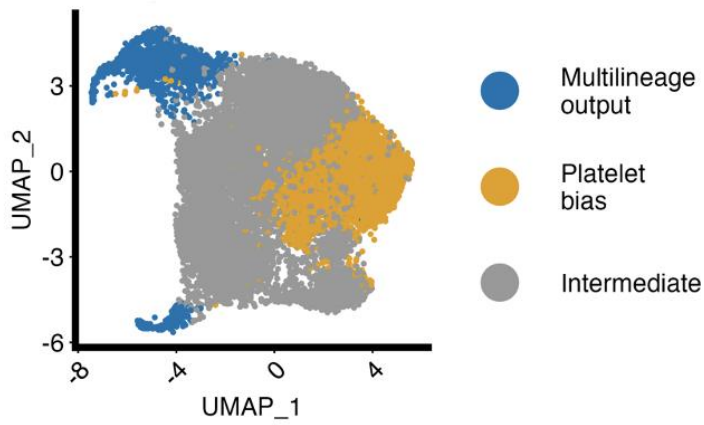

Figure 4 – UMAP representation of the computationally defined HSC subpopulations - young donor human HSC scRNA-seq dataset

Utilising this methodology, a platelet-biased HSC subpopulation has been computationally inferred as being present in the human bone marrow (Figure 4, 3D UMAP representation – Appendix figure 11A).

Next, we tried to corroborate this finding with another study in which the Nerlov lab has tracked the output of lentiviral barcoded human HSCs in xenotransplantation assays and generated the transcriptomic signatures for the HSC clones that showed a lineage bias in their lineage tracing experiments. In an effort to understand if the platelet biased computationally defined human HSCs identified in our study are similar from a

transcriptomic standpoint with the lineage biased HSCs described by the Nerlov lab study, the correlation between the expression of the gene signature of upregulated genes in the platelet biased computationally defined HSCs, determined through comparisons of these cells with the cells from the multilineage output and intermediate computationally defined subpopulations in a combinatorial manner and the expression of the upregulated genes in platelet-biased lineage traced human HSC clones compared to their multilineage output counterparts was investigated in the young donor human HSC scRNA-seq dataset. A positive correlation between the AUCell scores derived from the genes sets pertaining the cellular identity of both the computationally-identified and the functionally validated platelet biased human HSC was identified in the young donor human HSC scRNA-seq (Figure 5A). The GSEA carried out on the results of the DGEA comparing platelet biased versus multilineage human HSC identified either through computational means or in the context of the lentiviral barcoding lineage tracing experiments caried out by the Nerlov lab showed a high degree of similarity in terms of the enrichment patterns in the platelet-biased HSCs in the computational and lineage-tracing experimental setting (Figure 5B). A volcano plot representation of the expression of genes common between the ones that were differentially expressed (FDR <0.05) between the lineage tracked HSC clones that exhibited a platelet biased versus the ones with a multilineage output, the genes that were differentially expressed in the comparison between the computationally inferred platelet biased versus their multilineage counterparts in the HSCs of the young donors and the genes. used to calculate the AUCell representing the transcriptomic identity of

the computationally defined HSC populations in the young dataset and depicted in Figure 5A is found at Appendix Figure 2.

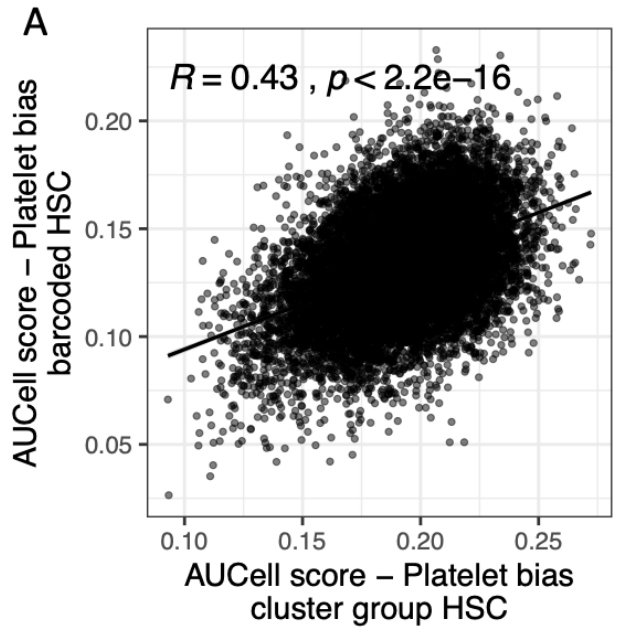

Figure 5 – Computationally defined human platelet biased HSCs identified in the young donor human HSC scRNA-seq exhibit similar gene expression patterns as platelet-biased lineage-traced human HSC clones. A) Correlation between AUCell scores derived from the genes sets pertaining the cellular identity of both the computationally-identified and the functionally validated platelet biased human HSC in the young donor human HSC scRNA-seq. B) Heatmap of normalised enrichment scores of the gene sets exhibiting an enrichment or depletion in both computationally and lineage tracing-defined platelet biased human HSC; # - FDR >0.25

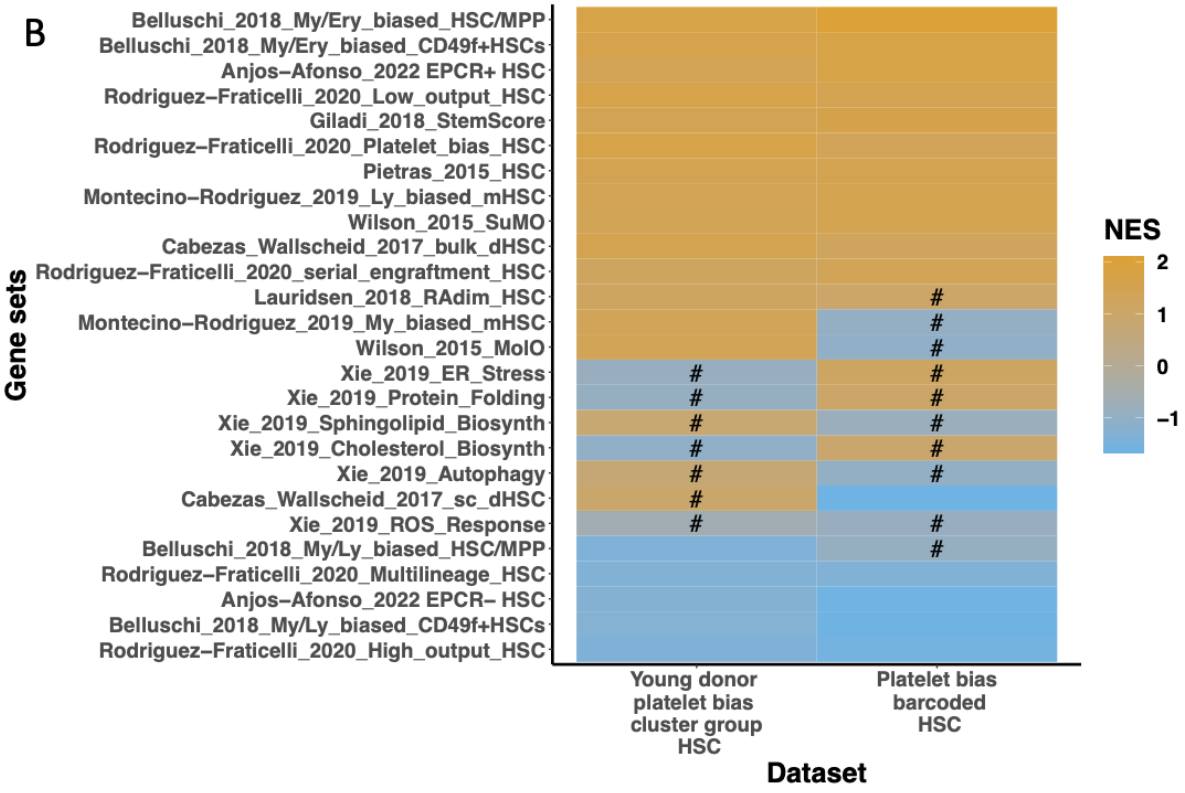

Old donor dataset analysis – transcriptomic data clustering and cluster characterisation

Following the batch correction procedure and the computing of a UMAP representation of the data from all old donors (Figure 6A), 9 cell clusters (Figure 6C) have been identified in the old donor dataset for the resolution 0.4 used by Seurat's (347) clustering algorithm which yielded the most stable to random subsampling clustering (Figure 6B) as indicated by the chooseR method (360).

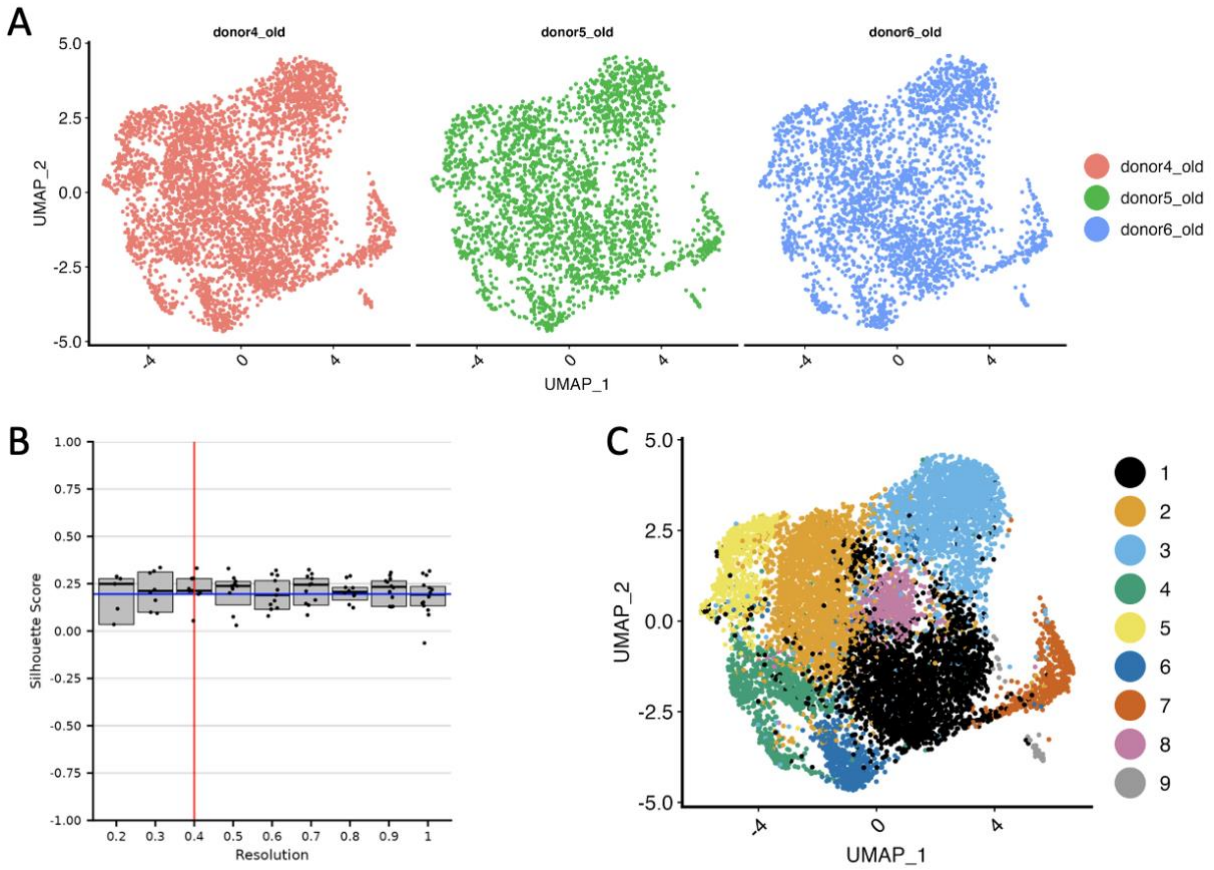

Figure 6 – Batch correction and data clustering – old donor human HSC scRNA-seq datasets. A) UMAP representation of the data from each old donor following the batch correction procedure. B) Silhouette score distribution plot for the old donor dataset. Each dot represents a cluster at a given resolution value. Medians with 95% CI are shown for each resolution value following 50 clustering iterations on randomly subsampled data. The vertical red line marks the optimal resolution, and the blue line represents the decision threshold for choosing the optimal resolution. C) Resolution 0.4 clustering overlayed on the UMAP representation of the data from all the cells available from all the old donors

In order to identify the clusters that express the genes sets associated with a particular lineage bias (89) or a higher self-renewal capacity (363–367), the same procedure as the one applied in the case of the young donor HSC scRNA-seq dataset was applied for the old donor one. The correlation patterns between the AUCell gene expression scores at the level of the whole old donor dataset showed that the expression of gene sets associated with platelet-bias and/or low HSC output are positively correlated with gene sets associated with high self-renewal capacity HSCs, mirroring the observations made in the young donor dataset (Figure 7A). Moreover, using the same procedure used for the young donor dataset, 3 types of clusters (Figure 7B), the platelet-biased one, the multilineage output and the intermediate cluster groups, or computationally defined HSC populations, were identified as well in the old donor dataset.

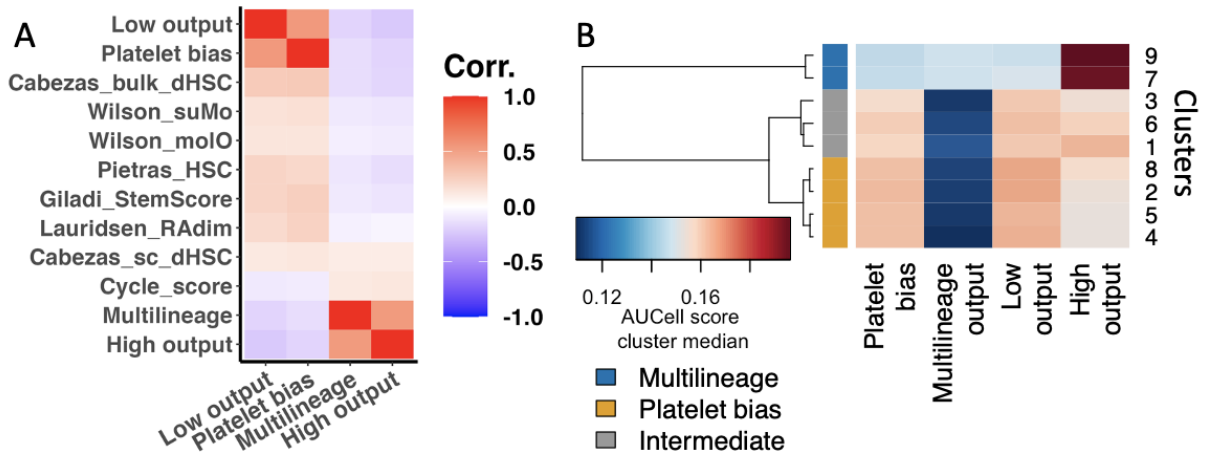

Figure 7 – AUCell score dataset-wide correlation (A) and cluster-wise aggregation (B) patterns – old donor human HSC scRNA-seq datasets. The strength and directionality of the correlation was quantified using Kendall's τ correlation coefficient. Only correlations that had a p-value < 0.05 were represented.

As it was observed in the young donor dataset, a computationally derived platelet-biased HSC subset was identified in the old donor dataset (Figure 8, 3D UMAP representation – Appendix figure 11B). In order to assess if the computationally inferred platelet-biased HSCs identified in both the young and old datasets are similar in terms

of the expression of the platelet bias gene signature, derived from the work of Rodrigue-Fraticelli et al. (89) used to define this subpopulation, the relationship between the mean of each gene in the gene signature at the level of the platelet-biased HSC subpopulation in both the young and old donor datasets was analysed. Thus, from the standpoint of the gene expression of the platelet bias gene signature, derived from the work of Rodrigue-Fraticelli et al. (89), the computationally defined platelet-biased HSCs identified in both the young and old datasets are similar (Figure 9).

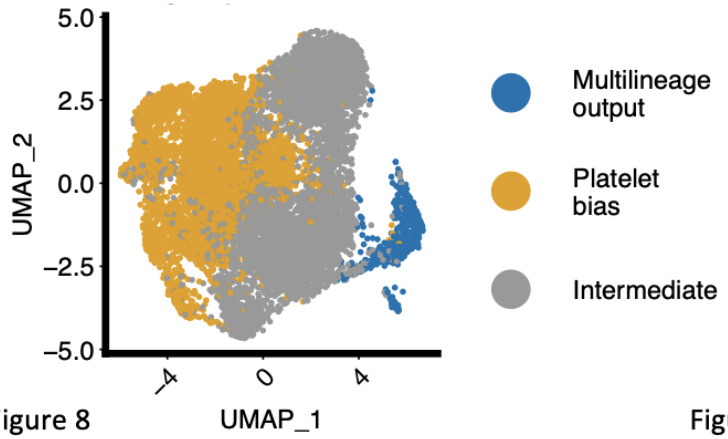

Figure 8

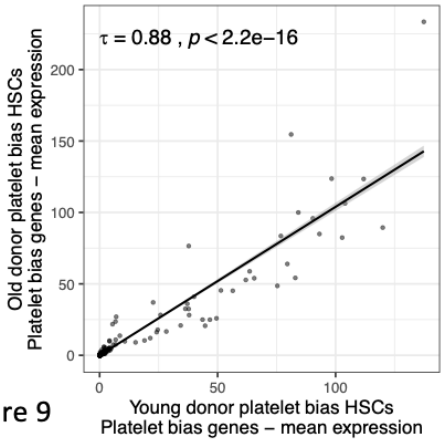

Figure 9

Figure 8 – UMAP representation of the cluster groups - old donor human HSC scRNA-seq dataset
Figure 9 – Correlation between the mean expression of platelet-bias genes at the level of the platelet-biased HSC subpopulations in the young and old datasets.

Age-associated HSC subpopulation frequency fluctuation and transcriptomic phenomena

Meta-analysis of the young and old HSC datasets

The computationally inferred HSC subpopulation previously described were compared in terms of relative abundance across age groups. Statistically significant differences were recorded between the size of the HSC subpopulations in the old versus the young donor datasets (Figure 10A) and a positive association between the old donor dataset and an increase in abundance of the platelet biased HSCs and a decrease in the multilineage output ones was observed (Figure 10B).

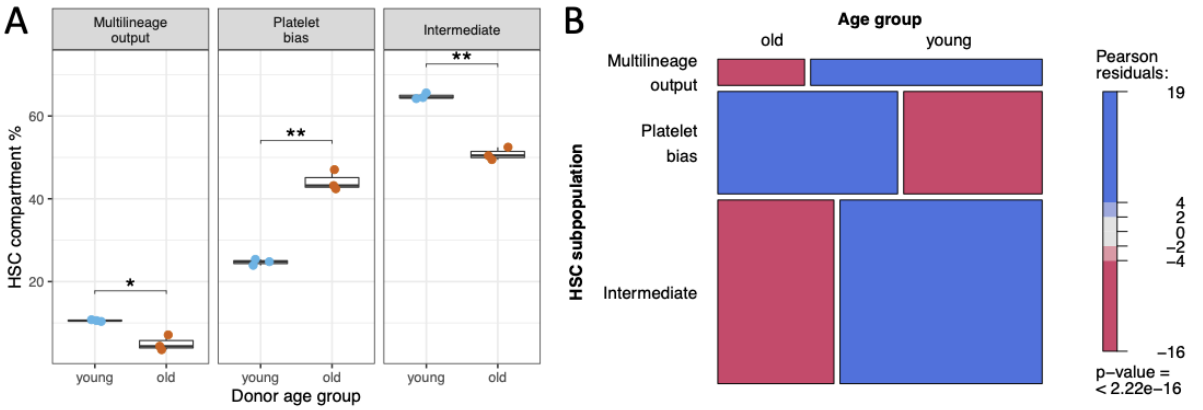

Figure 10 – Age dependent fluctuations in the size of the computationally defined human HSC subpopulations.
A) Percentage of HSC subpopulation contribution to the size of the whole HSC compartment, reported per donor; p-value symbols of the unpaired Student's t-test: * = < 0.05, ** = <0.001. B) Mosaic plot representing the proportion of each HSC subpopulation from the total cells in the old and young HSC scRNA-seq dataset; shading represents the Pearson residual of the χ^2 test used to assess (p-value listed in the figure) the dependency relationship between age group and the HSC subpopulation.

Next, the expression of the platelet bias and multilineage output gene signatures used to define the previously identified HSC subpopulations was compared between the data from the HSCs sampled from the old and young donors. With age there was an

increase in the platelet bias signature across all HSC subpopulations, but particularly so in the platelet biased subpopulation (Figure 11A) and this was recapitulated by the behaviour of the platelet biased HSC gene signature derived from the lentiviral barcoded human HSC lineage tracing experiments (Figure 11B). A decrease in the expression of the expression of the multilineage output HSC gene signature with age has been observed across all computationally defined HSC subpopulations (Figure 11C), but this gene expression pattern has not been recapitulated if the multilineage output HSCs gene signature derived from the lentiviral barcoded human HSC lineage tracing experiments was considered (Figure 11D).

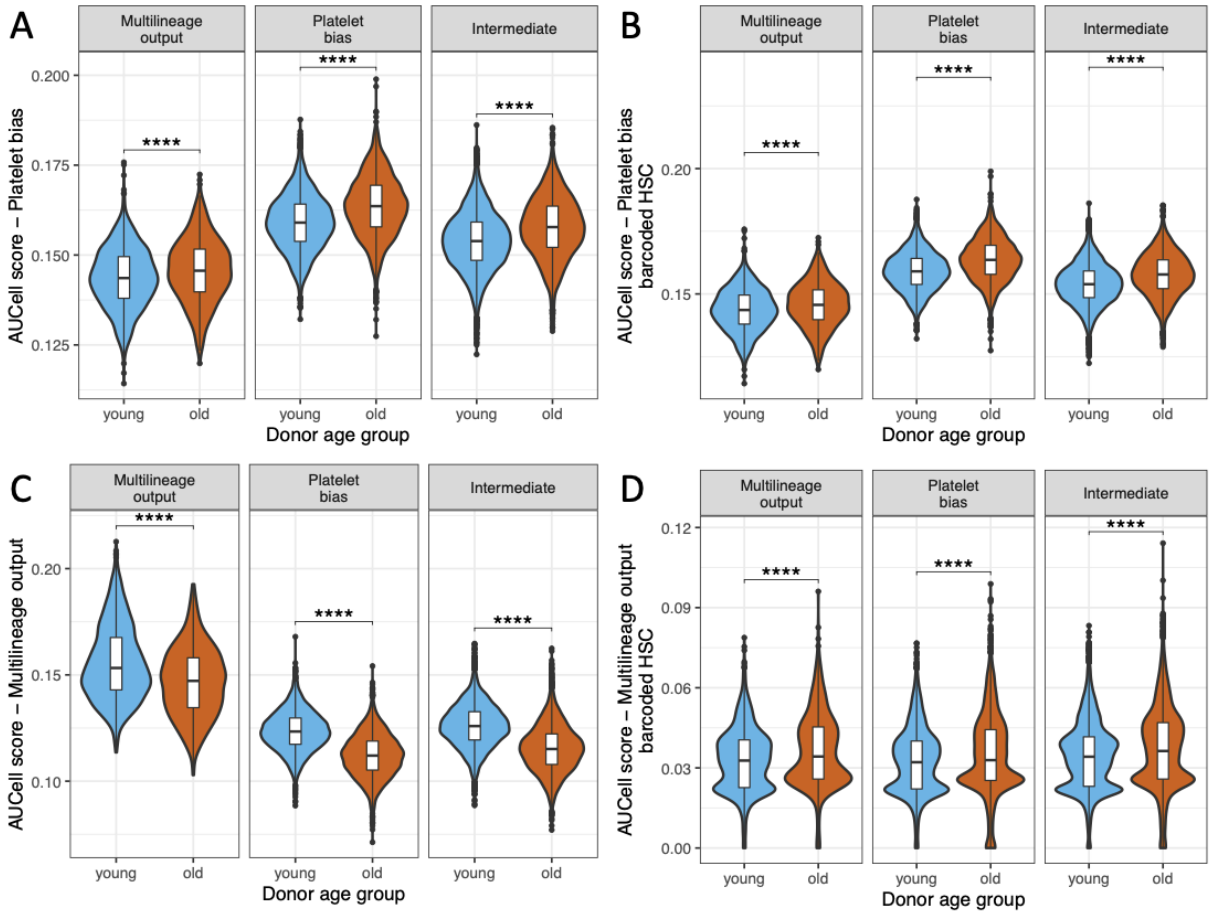

Figure 11 – Platelet bias and multilineage output HSC gene expression signature relationship with the age group of the donor at the level of the computationally derived HSC subpopulations. **** = Wilcox rank sum test, p-value < 1e-05

The lack of congruency between the expression pattern with age observed between the gene expression signatures for the multilineage output HSCs derived from the lentiviral barcoded human HSC lineage tracing experiments and the one derived from the experiments carried out by Rodriguez-Fraticelli et al. can be due to a number of factors ranging from the statistical apparatus used to determine them to the mouse – human differences in terms of HSC activation and the differences between syngeneic and xenotransplantation impact on the HSC transcriptome.

By comparing the correlation patterns observed between the AUCell score in the young and old HSC datasets, it can be observed that with age there is a diminishing in the modulus of the correlation coefficient that could reflect either the change in HSC subpopulation size previously described with age or an increase heterogeneity in expression levels of the genes that were shown to be associated with lineage fate decisions in HSCs or HSC activation in the context of murine HSCs (89) (Figure 12 & Appendix Figure 3).

In order to better understand how ageing shapes the differences between the transcriptome of the computationally identified human platelet biased and multilineage HSCs, a GSEA utilising the Hallmark collection (380) of gene sets as well as a compilation of gene sets pertaining HSC lineage bias (89,136,140,142,381) as well as the HSC self-renewal phenomena (363,364,366,367,382) and a gene expression ranking done as described in the Methods section by comparing the human platelet biased HSCs with their multilineage counterparts was performed for this comparison in the young donor dataset as well as the old one separately. By analysing the enrichment pattern of the gene sets that have shown a significant enrichment (FDR <0.25) in the

GSEA perform as mentioned above, with age the HSCs show a similar enrichment in the platelet biased HSCs in young compared to old donors (Figure 13). Out of the gene sets that showed a discordant enrichment pattern with age, none of them has an enrichment value with an FDR < 0.25.

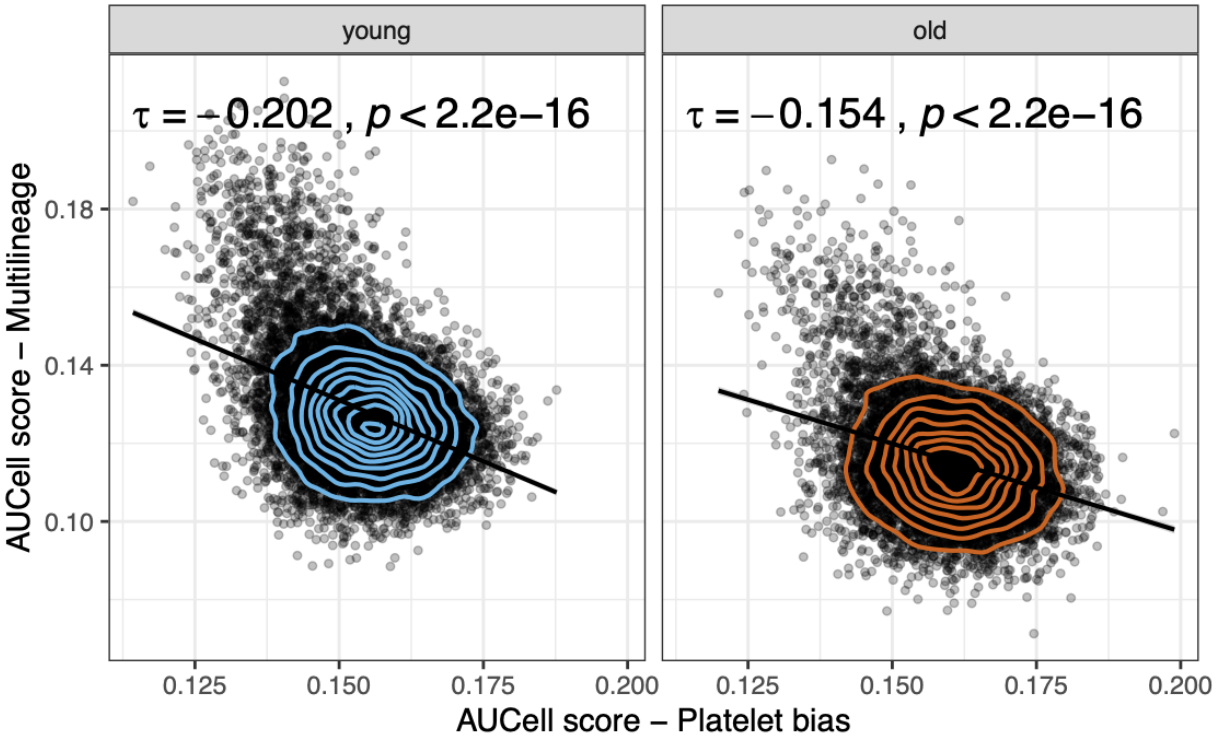

Figure 12 - Correlation between AUCell scores derived from the genes sets used to define the computationally derived HSC subpopulations in the young and old datasets. All the HSCs profiled in the old and young HSC datasets visualised. Contour plot of the 2D density estimate of all the HSCs in each dataset reside in the orthogonal system determined by the AUCell scores. The strength and directionality of the correlation was quantified using Kendall's τ correlation coefficient.

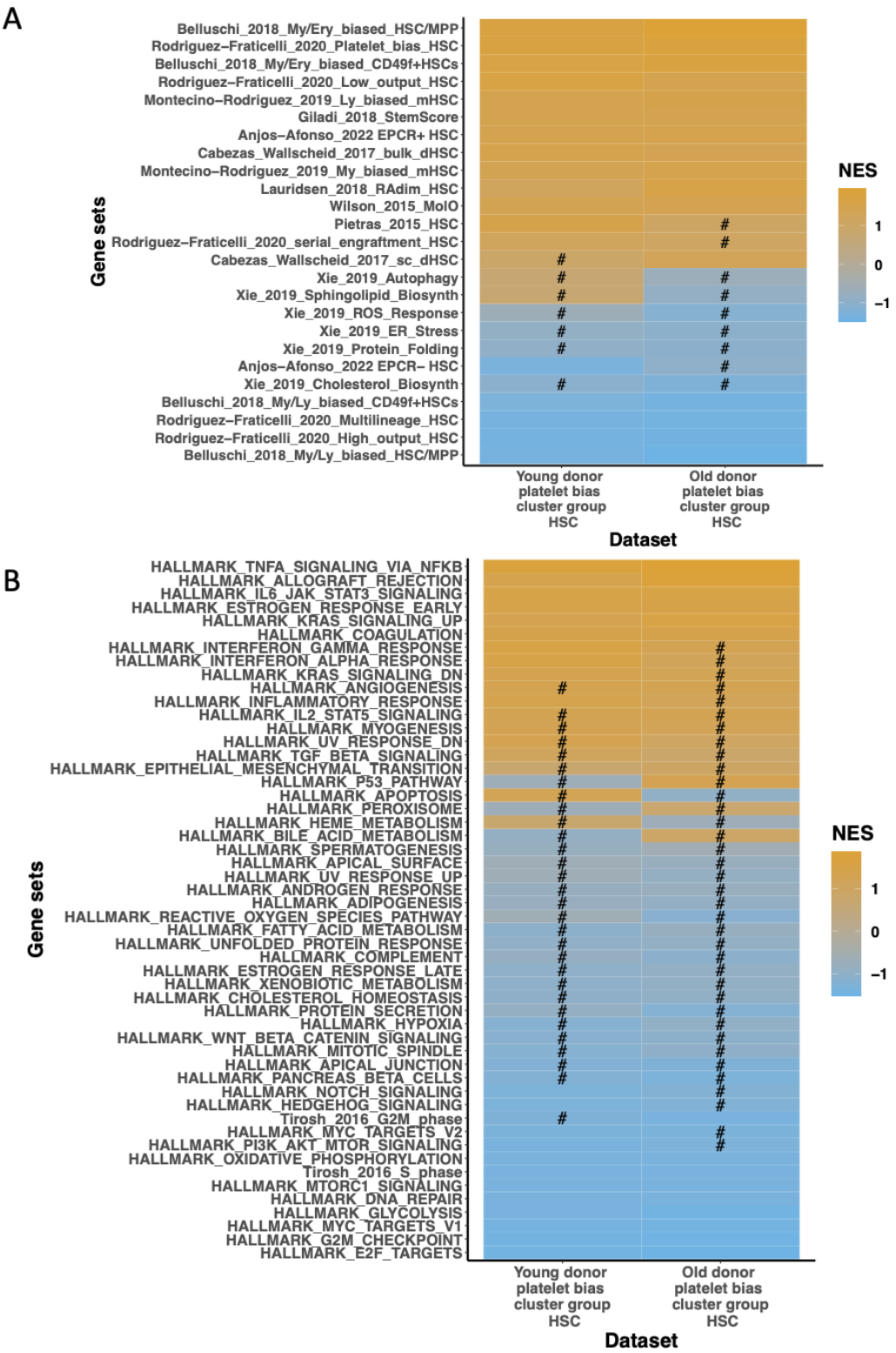

Figure 13 - Heatmap of normalised enrichment scores of the gene sets exhibiting an enrichment or depletion in both old and young dataset computationally defined platelet biased human HSC – meta-analysis of the young and old donor HSC datasets; #- FDR >0.25. A. Compilation of gene sets pertaining HSC lineage bias (89,136,140,142,381) as well as the HSC self-renewal phenomena (132,363,364,367,382); B. Hallmark collection (380) of gene sets

The gene sets that have enrichments or depletions with a FDR <0.25 in only one age group do not show age group discordant enrichment patterns, thus with ageing in the platelet biased HSCs there is only an exacerbation or dampening of an already present transcriptional program. With age there is an enrichment in the gene sets associated with vitamin A signalling in HSCs (367) and a depletion in the gene sets associated with the G2/M phases of cell cycle (383). In the young donors' platelet biased HSCs there is significant enrichment in the expression of genes associated with serial engraftment and self-renewal in HSCs (89,366), but a depletion in the ones associated with the EPCR negative HSCs (142). Moreover, in this HSC population in the young donors there is a significant enrichment in the expression of genes in Hallmark's (380) gene sets associated with inflammatory interferon gamma and alpha responses as well as KRAS pathway downregulation, but a depletion of the expression of genes in the NOTCH, Hedgehog, MYC and mTOR signalling . Lists of the leading-edge genes for the previously mentioned gene sets that have enrichments or depletions with an FDR <0.25 only in one age group have been compiled in Appendix Table 1.

Integrative analysis of the young and old HSC datasets

The purpose of analysing the young and old HSC dataset by merging them and determining computationally inferred HSC subpopulation after performing batch correction with the interpatient variability being the variable to correct for was to:

1. robustly assess which genes are differentially expressed between age groups in each HSC subpopulation
2. identify the genes that show different expression patterns between age groups along the transition state between the cells from the computationally inferred platelet biased HSCs and the ones in the multilineage ones

The integrative analysis of the young and old HSC datasets generated after batch correction a clustering configuration consisting of 10 cell clusters (Figure 14C) for the resolution 0.6 of Seurat's (347) clustering algorithm which was the most stable to random subsampling clustering (Figure 14B) following the usage of the chooseR method (360).

The correlation patterns between the AUCell gene expression scores at the level of the integrated dataset showed that the expression of gene sets associated with platelet-bias and/or low HSC output are positively correlated with gene sets associated with high self-renewal capacity HSCs, mirroring the observations made in the young and old donor datasets analysed in isolation (Figure 15A). Moreover, 3 types of clusters (Figure 15B, 3D UMAP – Appendix figure 11C), the platelet-biased one, the multilineage output and the intermediate cluster groups were identified as well in the integrated dataset.

Similar to what was observed in the case of analysing the HSC datasets, young and old, in isolation, the platelet priming was a characteristic of the HSCs from old donors which was substantiated by both the AUCell scores using the gene sets derived from the work of Rodriguez-Fraticelli et al. (89) as well as the lentiviral barcoding lineage tracing experiments carried out by the Nerlov lab (Figure 16 & Appendix Figure 3).

Assessing the relative frequency of the computationally defined HSC subpopulations in the integrated dataset highlighted some discrepancies when it comes to what was previously observed in the meta-analysis. Thus, the magnitude of the difference in the relative abundance of the HSC subpopulations, assessed as percentage of the whole HSC compartment for each donor separately, between data from old and young donors did not reach statistical significance for any of the HSC subpopulations (Figure 17A), but there was a statistically significant association between the higher frequency of platelet biased HSCs and data from all old donors as well as higher frequency of multilineage output HSCs and data from all young donors (Figure 17B). In all possible donor pairs containing one donor from each age group, it was observed a statistically significant association between the old donor data and a higher frequency of platelet biased HSCs as well as a higher frequency of multilineage output HSCs and data from young donors, as quantified using a χ^2 test (Appendix Figure 4). These observations highlighted that analysing the young and old datasets in isolation could possibly inflate the impact that age has on the size of the computationally inferred HSC population. Consequently, this study shows that with age there is a subtle enrichment in a computationally defined platelet biased HSC subpopulation.

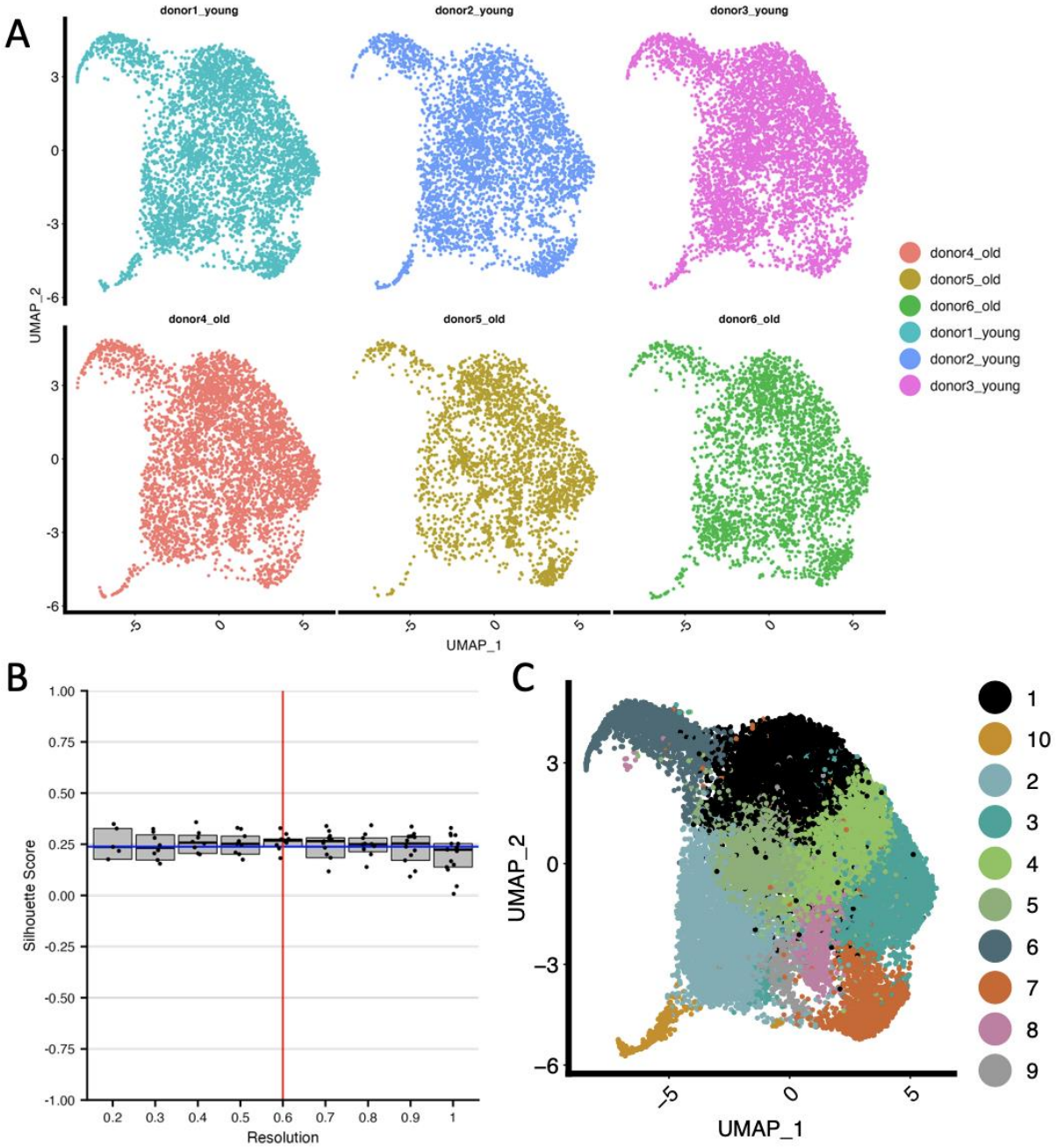

Figure 14 – Batch correction and data clustering –integrated human HSC scRNA-seq dataset
A) UMAP representation of the data from each old and young donor following the batch correction procedure. B) Silhouette score distribution plot for the integrated dataset. Each dot represents a cluster at a given resolution value. Medians with 95% CI are shown for each resolution value following 50 clustering iterations on randomly subsampled data. The vertical red line marks the optimal resolution, and the blue line represents the decision threshold for choosing the optimal resolution. C) Resolution 0.6 clustering overlayed on the UMAP representation of the data from all the cells available from all the old and young donors

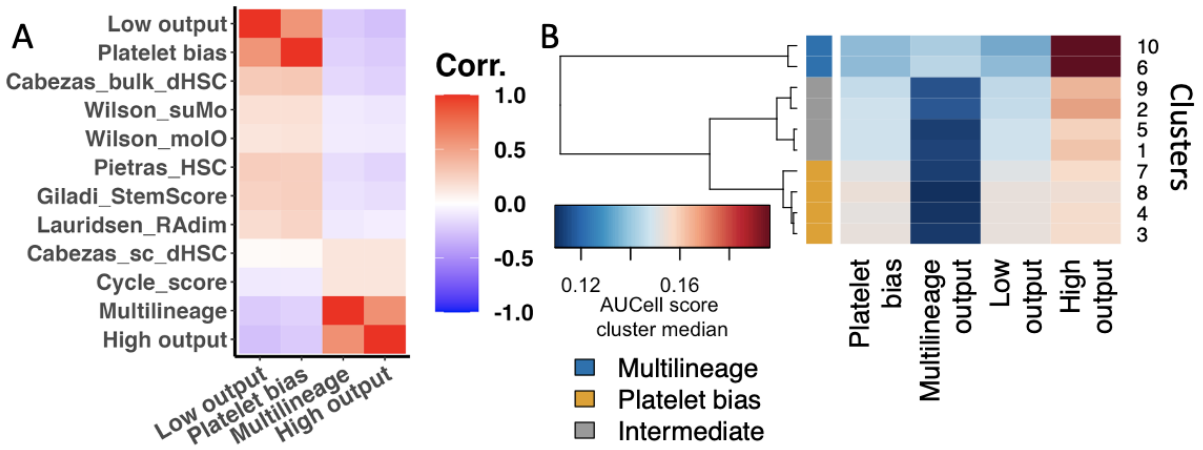

Figure 15 – AUCell score dataset-wide correlation (A) and cluster-wise aggregation (B) patterns – integrated HSC scRNA-seq dataset. The strength and directionality of the correlation was quantified using Kendall's τ correlation coefficient. Only correlations that had a p-value < 0.05 were represented.

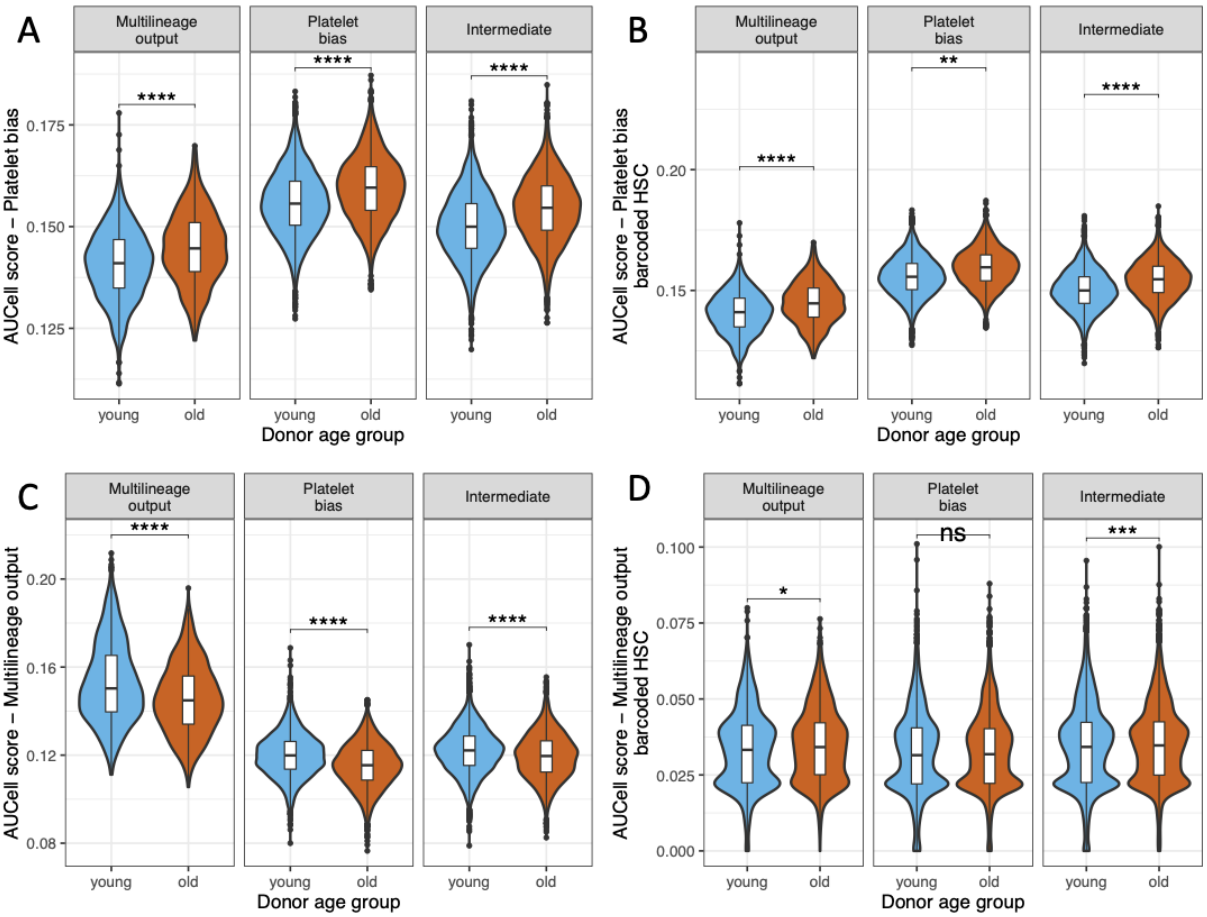

Figure 16 – Platelet bias and multilineage output HSC gene expression signature relationship with the age group of the donor at the level of the computationally derived HSC subpopulations in the integrated HSC scRNA-seq dataset.

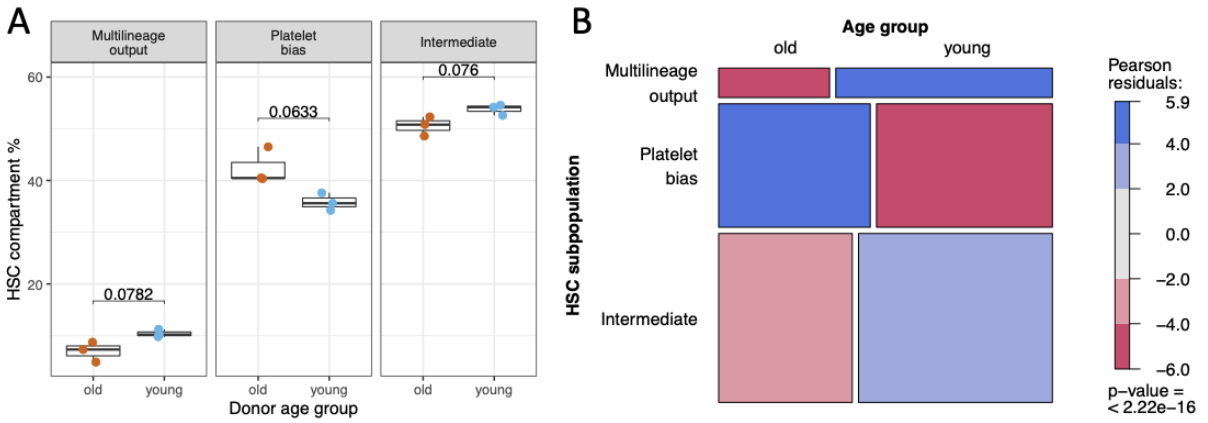

Figure 17 – Age dependent fluctuations in the size of the computationally defined human HSC subpopulations in the integrated HSC dataset.
A) Percentage of HSC subpopulation contribution to the size of the whole HSC compartment, reported per donor; p-value symbols of the unpaired Student's t-test. B) Mosaic plot representing the proportion of each HSC subpopulation from the total cells in the integrated HSC scRNA-seq dataset; shading represents the Pearson residual of the χ^2 test used to assess (p-value listed in the figure) the dependency relationship between age group and the HSC subpopulation.

Next, the impact of ageing on the transcriptome of the platelet bias and multilineage output HSC subpopulations was evaluated by comparing the single cell data from each donor type aggregated as donor pseudobulks at the level of each subpopulation, following the pseudobulk edgeR likelihood ratio test methodology shown by Squair et al. (333) as the best performing one in this type of scenario and implemented in the Libra R package (v1.0.0) (333). A GSEA utilising the Hallmark collection (380) of gene sets as well as a compilation of gene sets pertaining HSC lineage bias (89,136,140,142,381) as well as the HSC self-renewal phenomena (363,364,366,367,382) was caried out on 2 sets of gene expression rankings computed using the log2 fold changes multiplied by the -log10 of the p-value associated with each gene computed during the DGEA carried out by comparing: 1) old versus young dataset platelet biased human HSCs and old versus young dataset multilineage output human HSCs; 2) old donor platelet biased HSCs versus old donors multilineage output

HSCs and young donor platelet biased HSCs versus young donors multilineage output HSCs. By studying which gene sets are significantly enriched (FDR < 0.25) in the computationally defined platelet biased or multilineage HSCs in the context of either the young or the old donor's data, it was possible to identify gene sets that are specifically enriched in platelet biased HSCs from old donors (Figure 18 A,B) and in multilineage output HSCs from young (Figure 18C) and old donors (Figure 18D). In an effort to highlight the genes which could best describe the ageing phenomenon at the level of the computationally defined platelet biased and multilineage human HSCs we studied the intersect between the leading edge genes, driving the enrichment observed in the genes sets highlighted in Figure 18 as well as the differentially expressed (FDR < 0.05) ones determined while comparing 1) old versus young platelet biased human HSCs and old versus young multilineage output human HSCs; 2) old donor platelet biased HSCs versus old donor multilineage output HSCs and young donor platelet biased HSCs versus young donor multilineage output HSCs (Figure 19). The results of the GSEA for the gene sets with a significant (FDR <0.25) enrichment or depletion are available at Appendix Table 2 and the lists of differentially expressed genes (FDR < 0.05) for the following comparisons are available at Appendix Table 3: old versus young dataset platelet biased human HSCs, old versus young dataset multilineage output human HSCs, old donor platelet biased HSCs versus old donors multilineage output HSCs and young donor platelet biased HSCs versus young donors multilineage output HSCs.

Throughout this project it has been noticeable that the computationally defined platelet biased HSCs express genes associated with gene sets derived from studying cells which are in a quiescent state, a state associated with a higher capacity for self-renewal in HSC (89,140,367) (Figure 13A). Moreover, the multilineage output HSC subpopulation express genes associated with cell cycle progression (383) (Figure 13B) as well as MTORC1 signalling (Figure 13B), which could indicate that these HSC are in an activated state (384). Thus, a trajectory of state transition between the platelet biased HSCs and the multilineage ones in the integrated dataset was inferred using the methodological framework offered by slingshot (330) (Figure 20 A,B) and the influence of age on the genes that are associate with this trajectory was assessed using the Wald test statistic computed using the tradeSeq DGEA method (309). Among the genes that were identified as having their variability along the trajectory influenced significantly (FDR <0.05) by age (Appendix table 4), there were also cell surface marker genes that were previously identified as being specifically differentially expressed in multilineage output HSCs (B2M) from old donors (Figure 20 C).

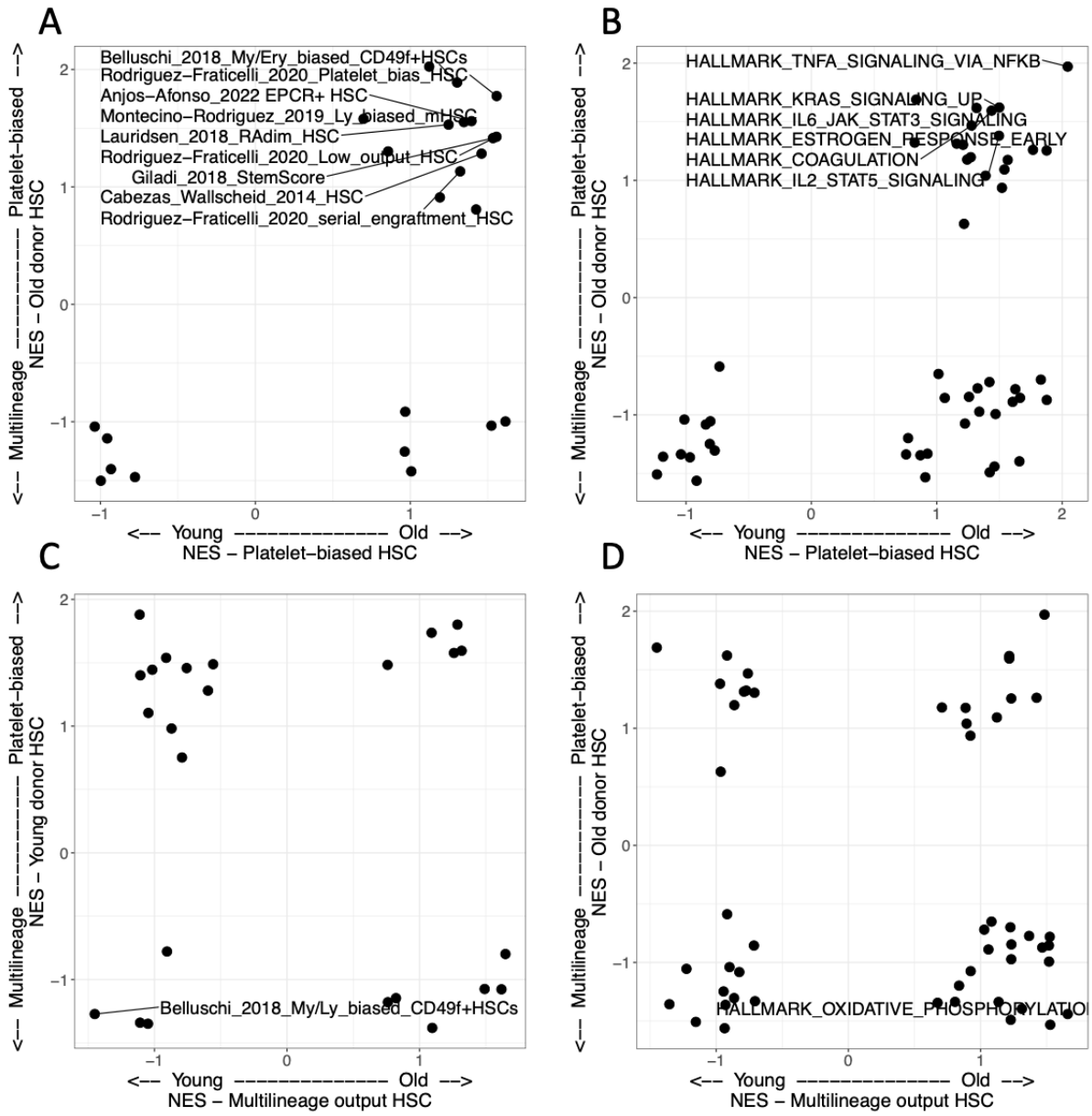

Figure 18 – Scatter plots of the normalised enrichment scores (NES) for each gene set utilised in the GSEA aiding the interpretation of which gene sets are specifically enriched in either platelet biased or multilineage output HSCs of a certain age group donor. Only gene sets with an enrichment associated with an FDR <0.25 and concordant NES sign are labelled.

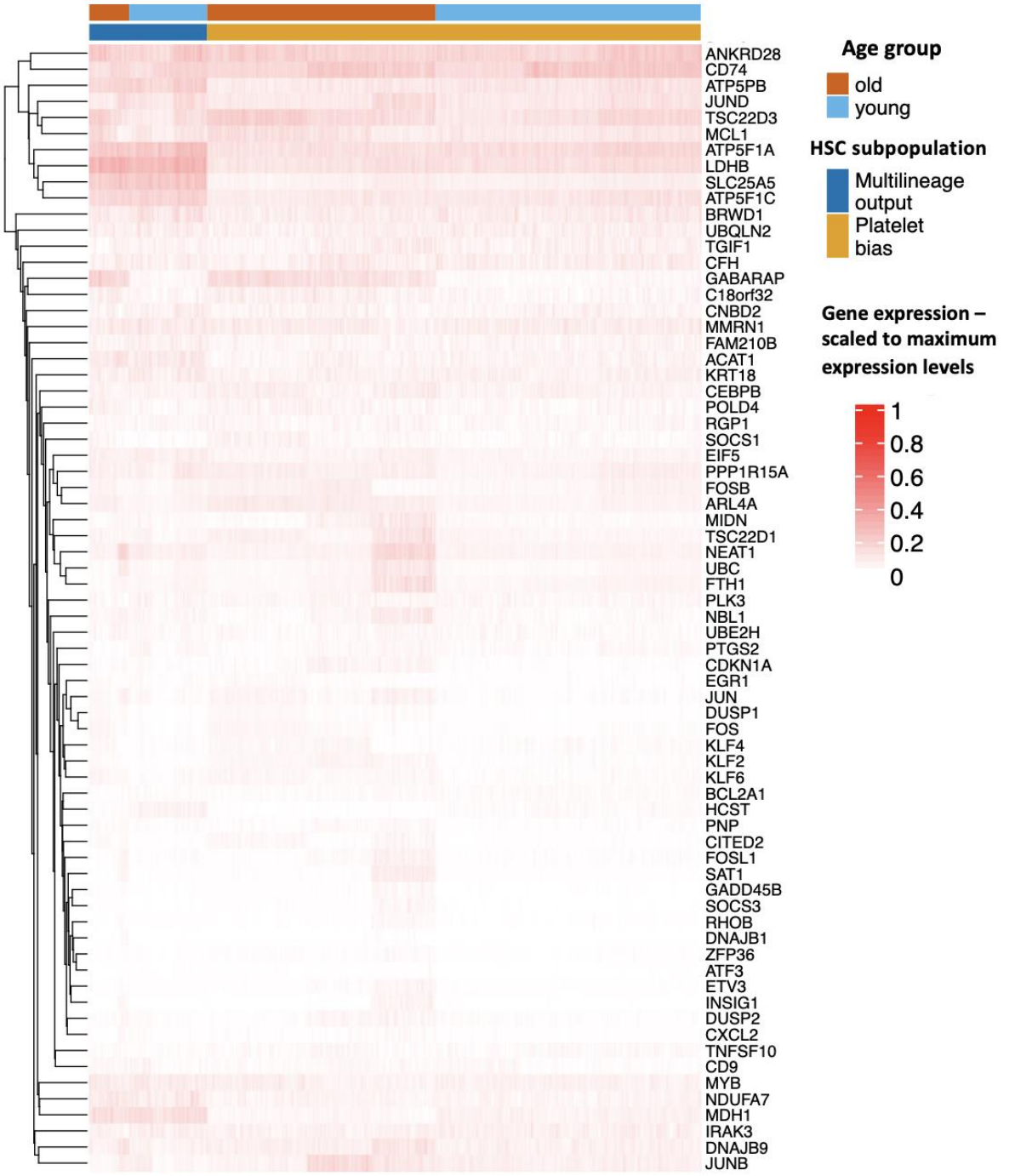

Figure 19 – Heatmap representing the expression of the leading-edge genes of the gene sets highlighted in Figure 18 which are at the same time differentially expressed (FDR <0.05) in at least one of the following set of comparisons: 1) old versus young dataset platelet biased human HSCs and old versus young dataset multilineage output human HSCs; 2) old donor platelet biased HSCs versus old donors multilineage output HSCs and young donor platelet biased HSCs versus young donors multilineage output HSCs

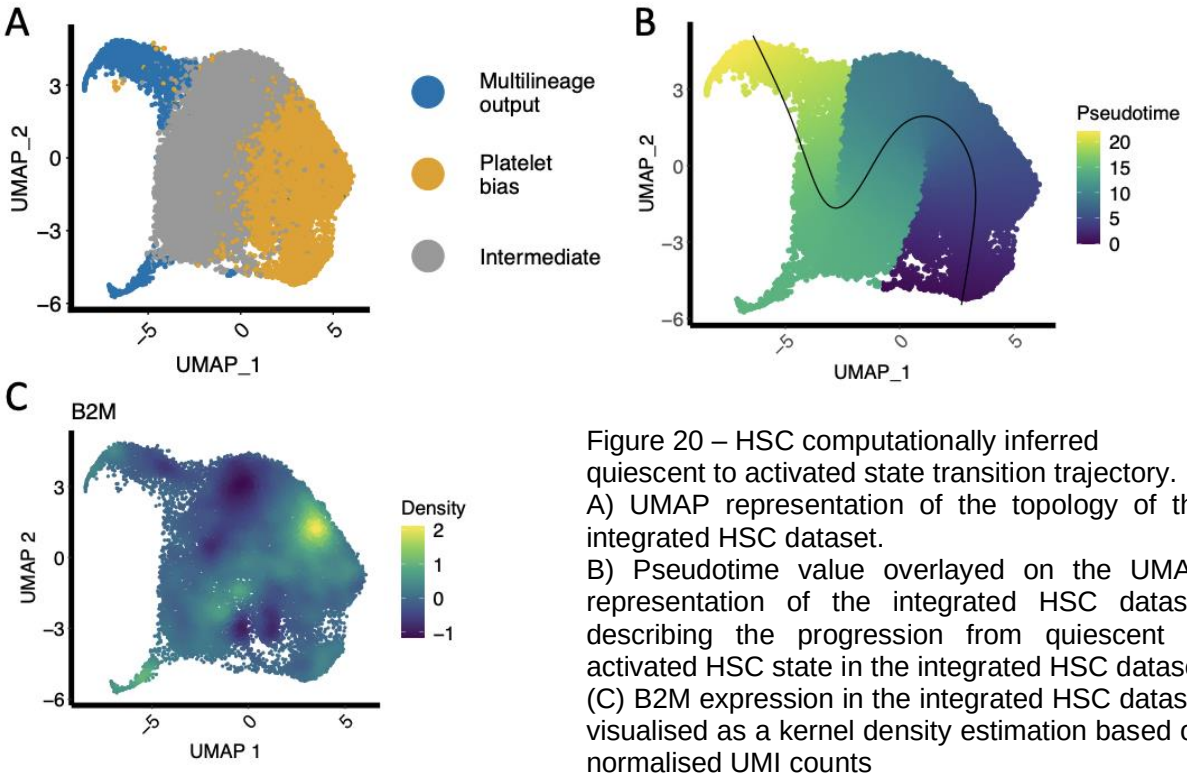

Figure 20 – HSC computationally inferred quiescent to activated state transition trajectory.
A) UMAP representation of the topology of the integrated HSC dataset.
B) Pseudotime value overlayed on the UMAP representation of the integrated HSC dataset describing the progression from quiescent to activated HSC state in the integrated HSC dataset
(C) B2M expression in the integrated HSC dataset visualised as a kernel density estimation based on normalised UMI counts

Chapter IV. The ageing-associated transcriptomic features of the memory T cell compartment in the context of post COVID-19 recovery

A description of the age-related transcriptomic changes in the memory T cell compartment of a healthy cohort

Initial quality control of the healthy cohort scRNA-seq datasets

In order to ensure that age-associated transcriptional phenomena observed in the healthy cohort scRNA-seq dataset can be related to the ones observed in the COVID-19 convalescent one, data from the healthy donor cohorts PBMNCs scRNA-seq datasets published in the Stephenson et al (349) and Ren et al. (348) studies have been filtered for any cells that would not fit the data quality control criteria used in Su et al. (253) PBMNCs scRNA-seq dataset that constituted the convalescent COVID-19 cohort, as detailed in Materials and Methods section (Figure 21). The differences in the distribution of median per sample gene counts and percentage of cells passing or failing quality control per sample in the Ren dataset compared to the Stephenson did not reach statistical significance (Figure 21 C,D) which incentivised an analysis that integrated the data from both datasets.

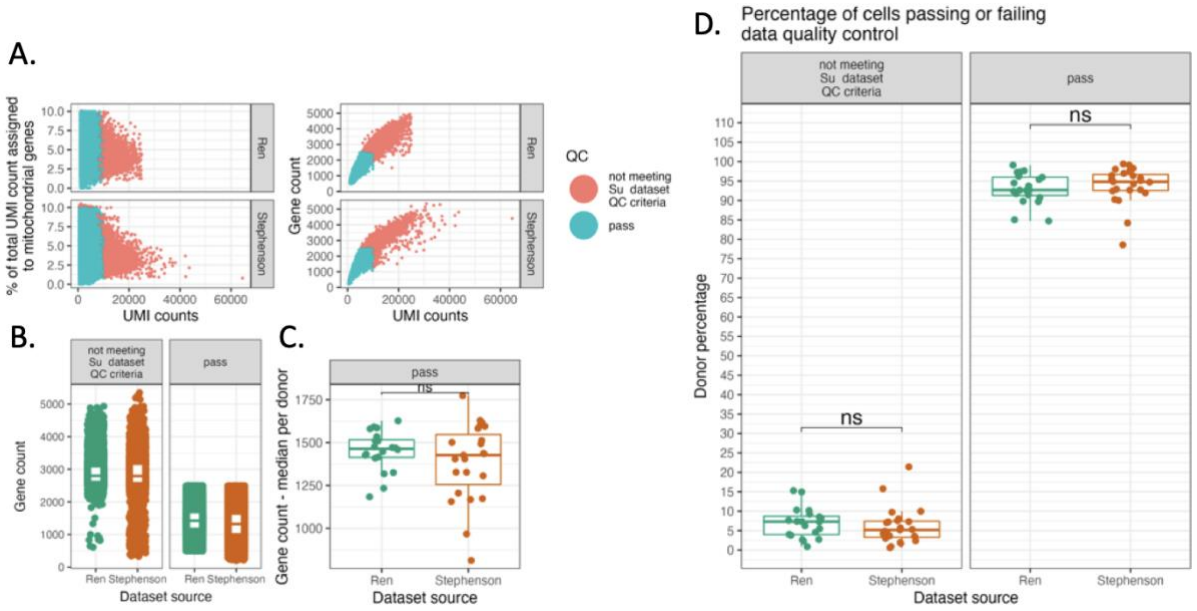

Figure 21 – Quality control procedure –healthy cohort scRNA-seq datasets

A) Relationship between UMI counts and gene counts / percentage of total UMI count assigned to mitochondrial genes. B-C) The distribution of gene of gene counts that failed or pass QC procedure in the healthy cohort scRNA-seq datasets. D) The percentage of cells in each dataset that passed or failed the QC procedure – donor & donor age group breakdown. The Wilcox rank sum test was used to assess the magnitude of the differences between the distributions; NS – p value > 0.05

Healthy donor cohort scRNA-seq datasets integrated analysis – transcriptomic data clustering and cluster characterisation

Following the batch correction procedure and the computing of a UMAP representation of the data from all the 43 donors of the healthy cohort (Figure 22A), 12 cell clusters (Figure 22B) have been identified in the integrated healthy donor dataset for the resolution 0.3 used by Seurat's (347) clustering algorithm which was highlighted as stable after using a clustering tree visualisation (361) (Appendix figure 5).

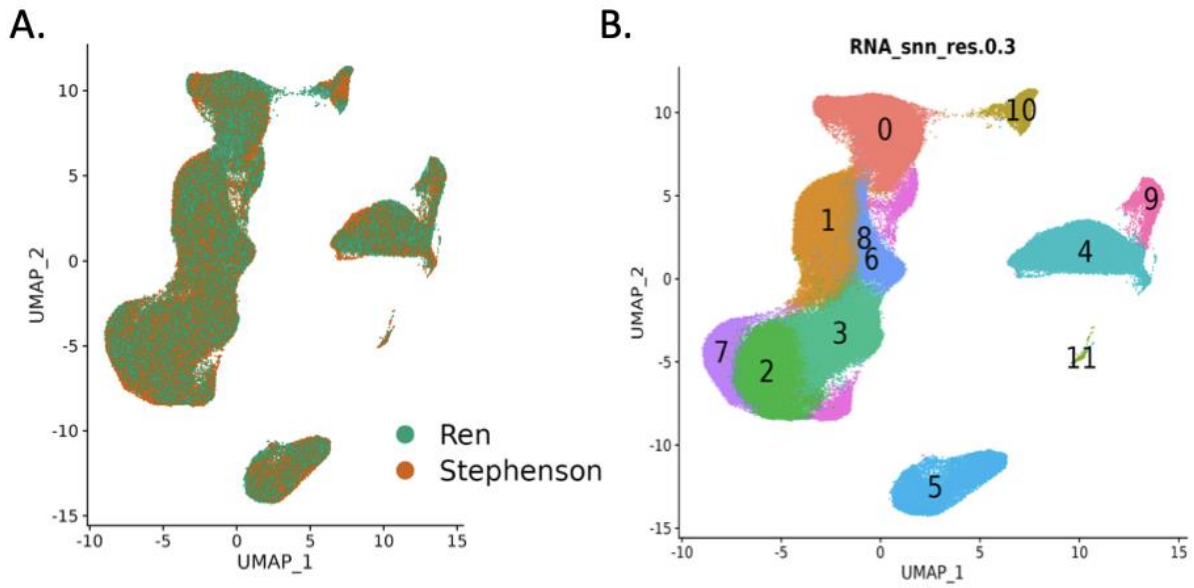

Figure 22 – Batch correction and data clustering – integrated healthy donor dataset
A) UMAP representation of the data from each dataset following the batch correction procedure.
B) Resolution 0.3 clustering overlayed on the UMAP representation of the data from all the cells available from all the 43 donors of the healthy cohort.

The T cell subset of the integrated healthy donor cohort dataset was extracted by first finding which of the clusters were rich in cells expressing the T cell receptor chains loci fragments, following the procedure described in the Materials and Methods section (Figure 23 A,B,C). Then, cells exhibiting a hybrid myeloid-T cell transcriptomic profile as would be the case for the T cell-monocyte complexes identified by Burel et al. (345)

which in the current datasets would be indistinguishable from an artefactual doublet (Figure 23 D) and clusters with an important contamination of such cells (Figure 24 A,B) were eliminated which reduced the initial size of the T cell rich subset of the integrated healthy donor cohort dataset by 6.27%. The cluster that was completely eliminated due to a significant enrichment in doublets was cluster 10 (χ^2 test, p value < 1e-16)

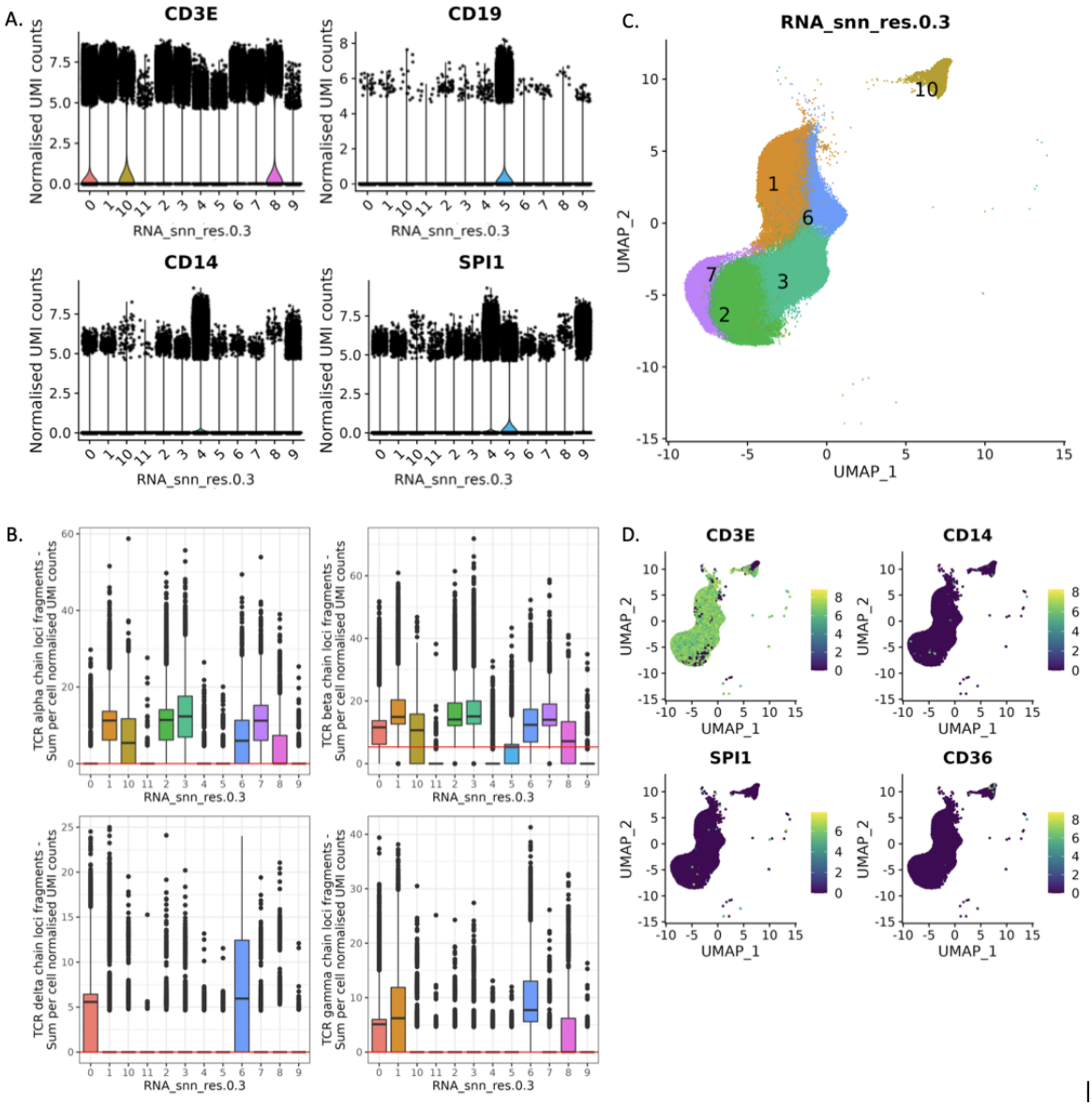

Figure 23 – T cell rich subset extraction – healthy cohort integrated dataset; A) Normalised expression of CD3E and canonical myeloid and B lymphoid markers to facilitate the B cell rich cluster identification. B) Distribution of TCR chain loci fragments across clusters. C) UMAP of T cell rich clusters of the integrated healthy donor dataset. D) Expression of canonical myeloid markers in the T cell rich clusters – normalised UMI counts

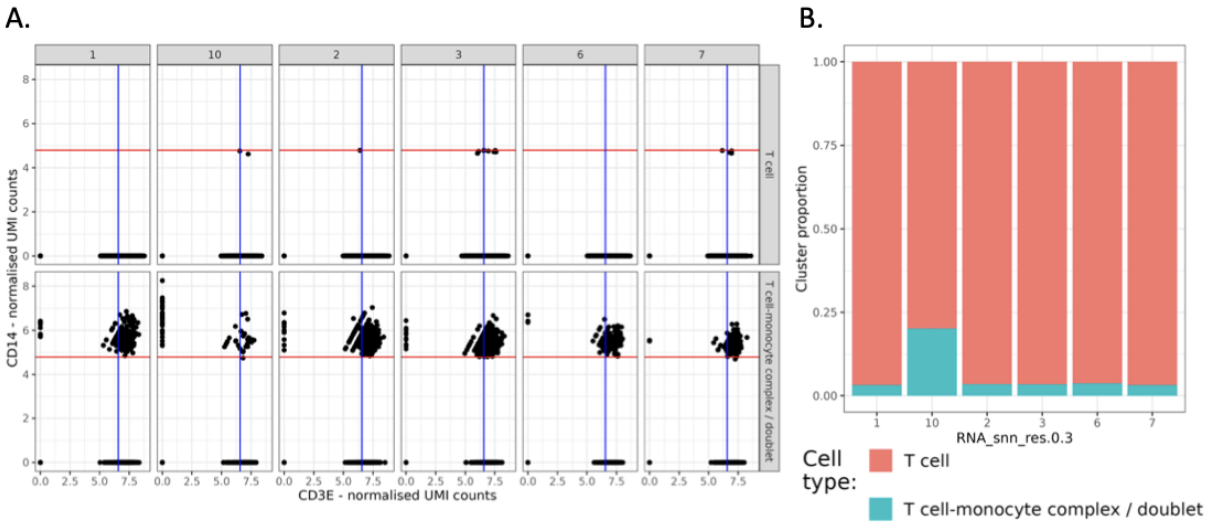

Figure 24 – Doublet identification – healthy cohort integrated dataset; A) CD14 and CD3E normalised expression in the cells labelled either as T cells or T-cell – monocyte complexes as defined by the expression levels of CD14, SPI1 (PU.1) and CD36 quantified in the cluster with the highest CD14 expression present in the dataset; red line – median-2*MAD of the CD14 expression level in the .monocyte rich cluster; blue line – median-MAD of the CD3E expression level in the T cell rich clusters B) Cluster proportion of T cells and T-cell – monocyte complexes

Following the extraction of the T cell subset of the healthy donor integrated dataset and the elimination of the doublets, the purified T cell subset was re-clustered (Figure 25A) and the marker genes for each cluster were identified. In order to ascertain the T cell type that was represented by each cluster a GSEA was conducted for the gene ranking determined by comparing the gene expression of each cluster versus all the other clusters and the marker gene sets (371,372) of the following T cell populations: CD4+ naïve, CD8+ naïve, central memory (TCM), effector memory (TEM), CD45RA+ effector memory (TEMRA), mucosal-associated invariant (MAIT), regulatory (Treg), γδ (gamma-delta) (Figure 25 B,C). The normalised enrichment scores of the gene sets that were found to have an FDR <0.25 in all clusters were used to ascertain the cluster cell type identity (Figure 25C). The T cell type annotation of each cluster was evaluated by analysing the expression of canonical T cell markers (371,373) for naïve (CCR7, PECAM1), TCM (CCR7, CD27), TEM (EOMES), TEMRA (EOMES, KLRG1), Treg

(FOXP3), MAIT (ZBTB16), γδ (TRDC) with results concordant with the GSEA-based cluster annotation (Figure 26). Appendix figure 6 details the statistical assessment of the differences recorded between the expression of the T cell subpopulation marker genes at the level of each cluster.

In an effort to ensure the reliability of the results of the DGEA aiming to find genes exhibiting gene expression patterns associated with age in the memory T cell compartment comprising TCMs, TEMs, TEMRAs, Tregs, MAITs and γδ T cells only data from samples that contained at least 20 cells in either the naïve T cell compartment or the memory T cell compartment were used in this analysis. This stringent quality control step was inspired by the one used in a previous high impact study (349) and eliminated 264 cells from the dataset, which was data from samples MH8919226 and MH8919227. An overview of the age group, sex and data source composition of the healthy cohort after the elimination of the low-quality samples is available in Figure 27.

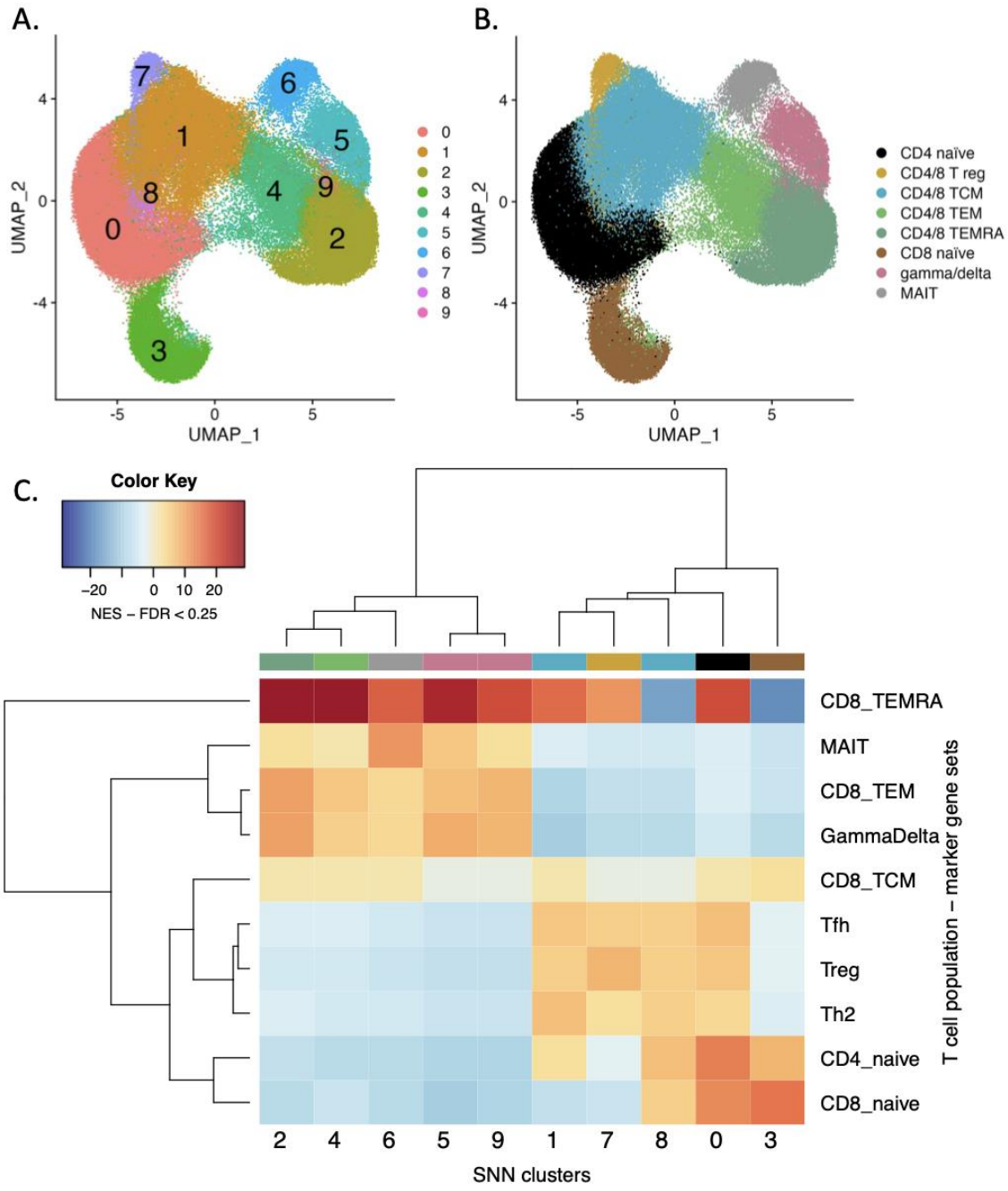

Figure 25 – T cell type assignation – healthy cohort integrated dataset. A) UMAP representation of the T cell rich clusters of the healthy cohort integrated dataset. B) UMAP representation of the T cell rich clusters of the healthy cohort integrated dataset after T cell type assignation. C) Heatmap of the normalised enrichment score (NES) of the T cell marker gene sets computed on the gene expression rankings computed for each cluster while comparing the expression of the genes detected in one cluster versus all the other T cell rich clusters of the dataset. Colours of the column labels match the colours of the UMAP at B).

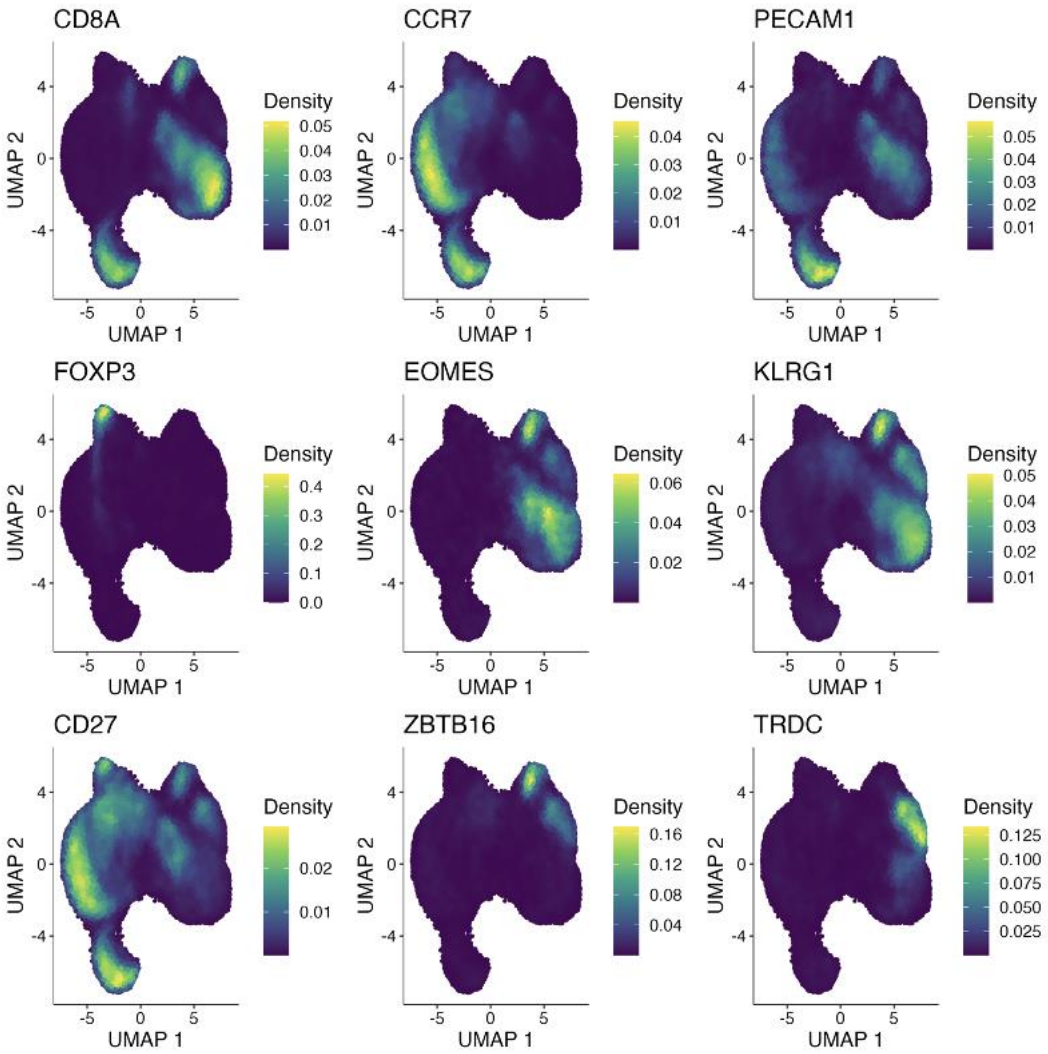

Figure 26 - Gene expression of T cell type canonic markers overlaid on the UMAP representation of the data from the T cell rich clusters of the healthy cohort integrated dataset. Gene expression visualised as a kernel density estimation based on normalised UMI counts.

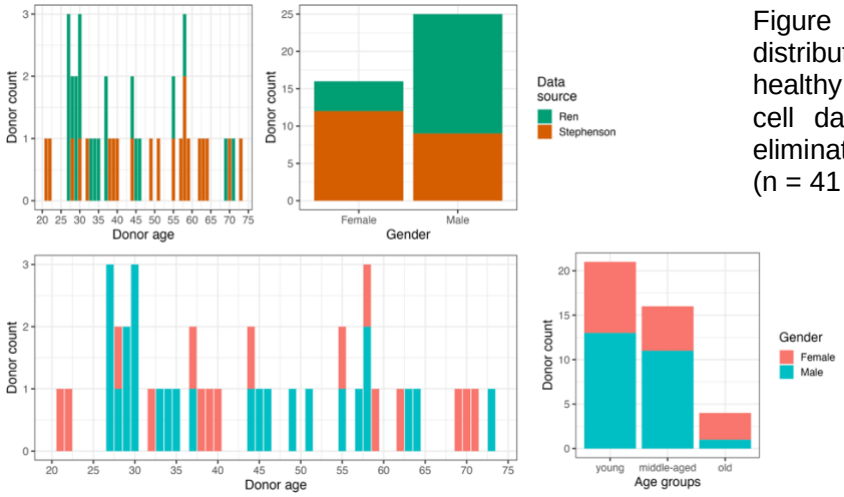

Figure 27 – Age and gender distribution of the donors of the healthy donor cohort from which T cell data is available after the elimination of low-quality samples (n = 41 donors)

Age-associated T cell population size fluctuation and gene expression patterns recorded in the healthy donor cohort

In the T cell compartment of the donors studied in the healthy donor cohort it could be observed a statistically significant negative correlation between the size of the CD8 naïve T cell compartment and the age of the donor, but the memory T cell compartment's size did not show correlations with age that reached statistical significance (Figure 28). A more granular breakdown of these trends pertaining all the T cell types identified in the healthy donor cohort integrated analysis is available in Appendix figure 7.

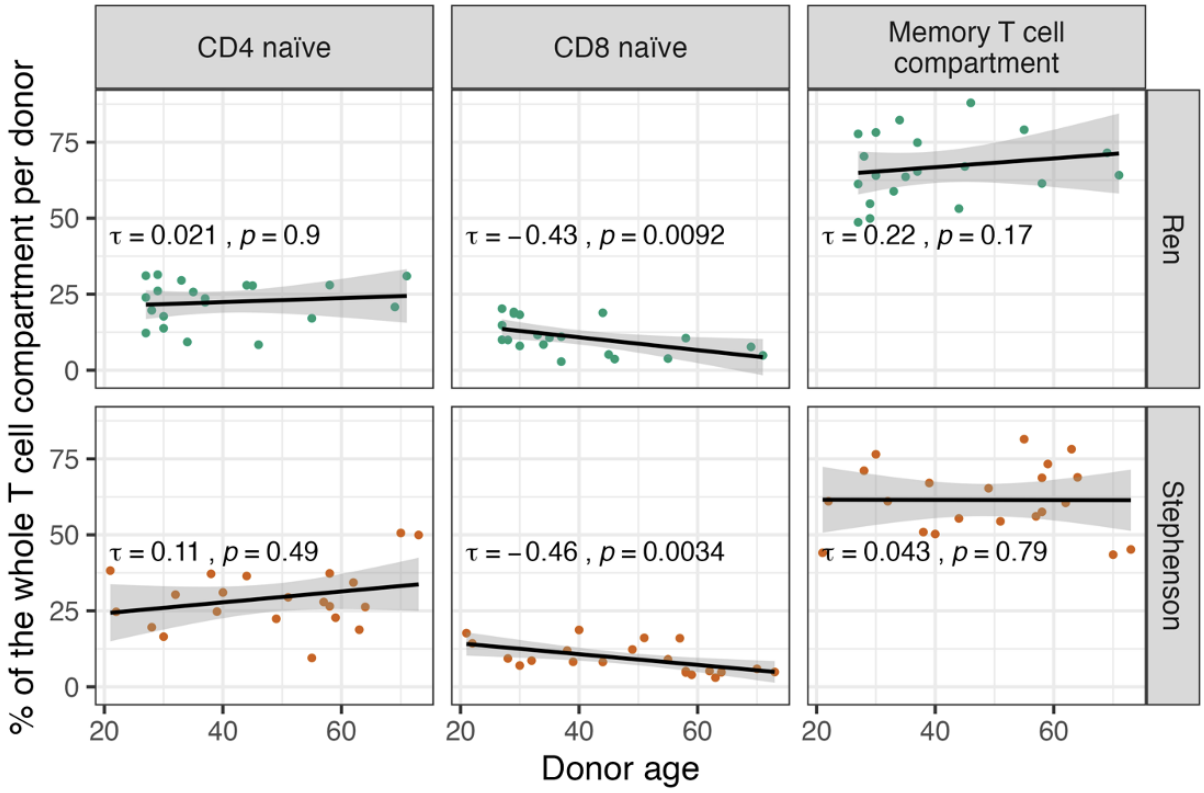

Figure 28. Relationship between the size of the naïve and memory T cell compartments and the age of the donor in the healthy donor dataset. The strength and directionality of the correlation was quantified using Kendall's τ correlation coefficient

Even if the correlation between the size of the memory T cell compartment and donor age did not reach statistical significance in this cohort, the importance of this compartment for the immune responses following reinfections as well as a record of past immunological events such as the infection with SARS-CoV2 warranted an analysis of the age-dependent gene expression patterns that could be observed in this compartment. Thus, by considering the age of the donor a continuous variable, the genes that were differentially expressed across the whole age spectrum of the healthy donor cohort were determined and resulted in a gene signature representing the ageing phenomenon as recorded in the memory T cell compartment with 20 upregulated and 18 downregulated genes with a FDR <0.05 (Figure 29).

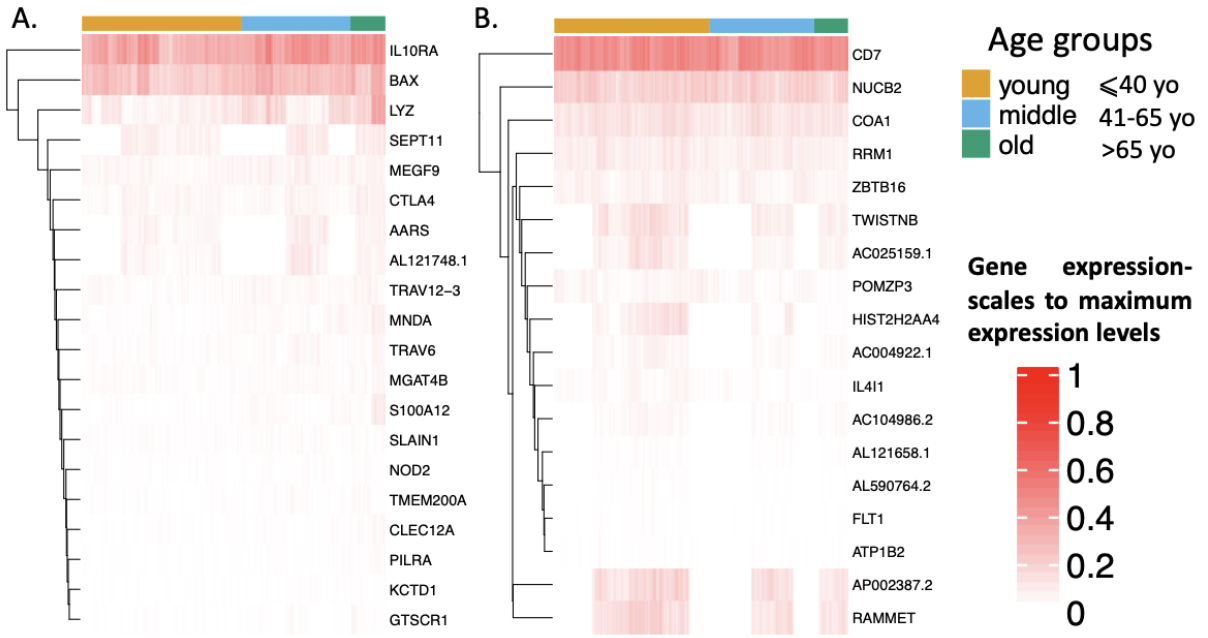

Figure 29 - Heatmap representing the gene expression scaled to the maximum expression level recorded in the in the memory T cell subset of the healthy cohort dataset of the ageing upregulated (A) and downregulated (B) genes in the memory T cell compartment.

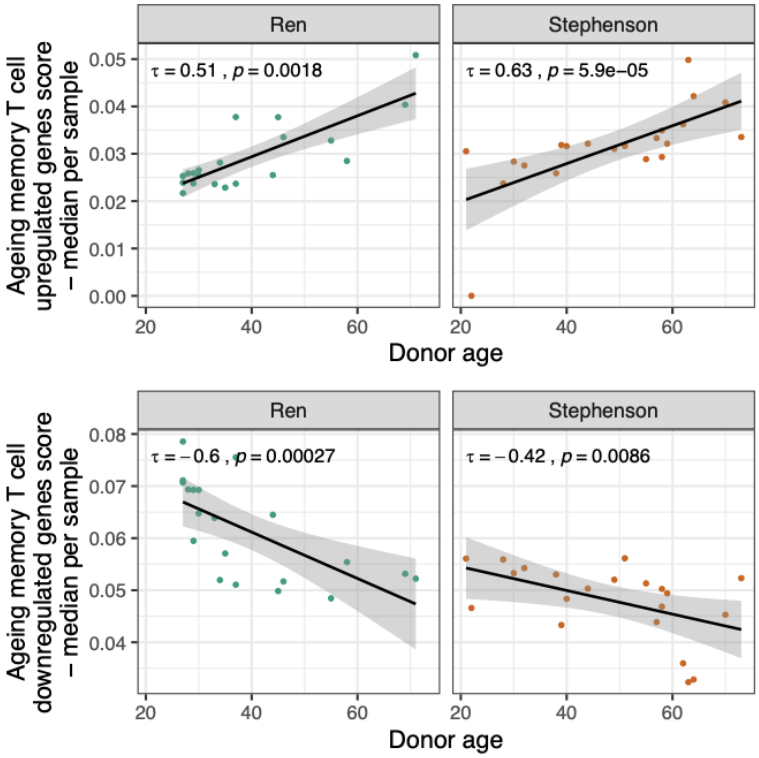

Figure 30 – Relationship between the gene expression scores computed using the ageing memory T cell signature genes at the level of the memory T cell compartment and the donor's age. The strength and directionality of the correlation was quantified using Kendall's τ correlation coefficient

To evaluate if the previously age-dependent genes identified in memory T cell compartment can be used to compute a metric to assess ageing at a transcriptomic level, the expression of the upregulated and downregulated genes with age in the memory T cell compartment was summarised in 2 scores, using the UCell methodology for computing gene expression scores (379). Then, the median per donor value of these scores as computed using the data from the memory T cell compartment for each donor was assessed in the context of the age of the donor revealing a statistically significant corelation between donor age and the gene expression scores (Figure 30).

Determining the common transcriptomic features between the ageing memory T cell compartment phenomenon and the recovery from COVID-19.

Utilising the scRNA-seq data from 100 patients that were recovering from COVID-19, were assessed at least 30 days post symptom onset and had respiratory PACS metadata, published by Su et al in 2022 (253), we set to understand what are the common gene expression patterns that are observed between the ageing of the memory T cell compartment and the recovery from COVID-19 recorded in the memory T cell compartment.

Extraction of the memory T cell data from the convalescent COVID-19 cohort dataset

Using the same methodology as the one used in the healthy cohort dataset, the PBMNC scRNA-seq datasets from each donor were integrated into a singular one and the gene expression data was batch corrected, mitigating for inter-sample variance, and clustered. The visual inspection of the distribution of samples from female and male donors, as well as donors from different age groups in the UMAP representation of the batch corrected integrated dataset did not show an overt failure of the batch correction procedure (Figure 31). T cell rich subset of the convalescent COVID-19 dataset was extracted (Figure 32), depleted of doublets (9.41% of the T cell rich subset Figure 33) and T cell type annotated (Figure 34,35) yielding a dataset comprising 95 samples (5 samples were eliminated due to low quality, totalling 779 cells).

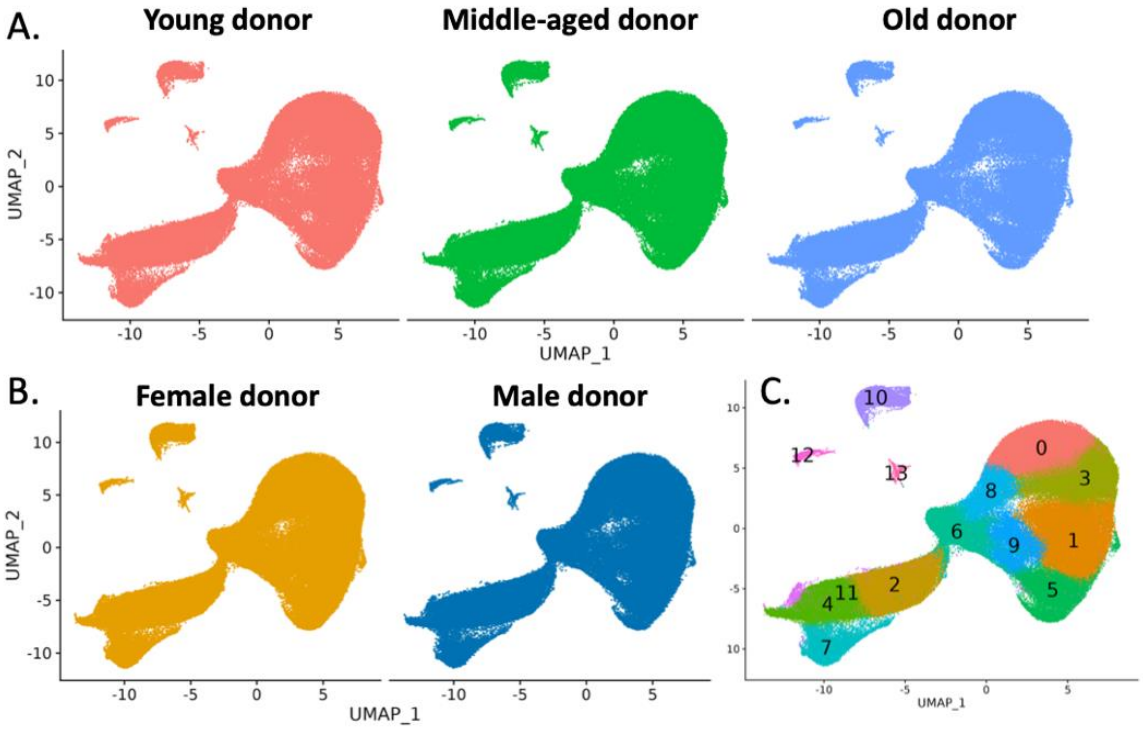

Figure 31 – Batch correction and data clustering – integrated convalescent COVID-19 donor dataset. UMAP representations of the integrated convalescent COVID-19 donor dataset following the batch correction procedure, split by age group (A) and gender (B).
C) Resolution 0.4 clustering overlayed on the UMAP representation of the data from all the cells available from all the 100 donors of the convalescent COVID-19 donor dataset. Resolution chosen based on the clustering tree visualisation available in Appendix Figure 8.

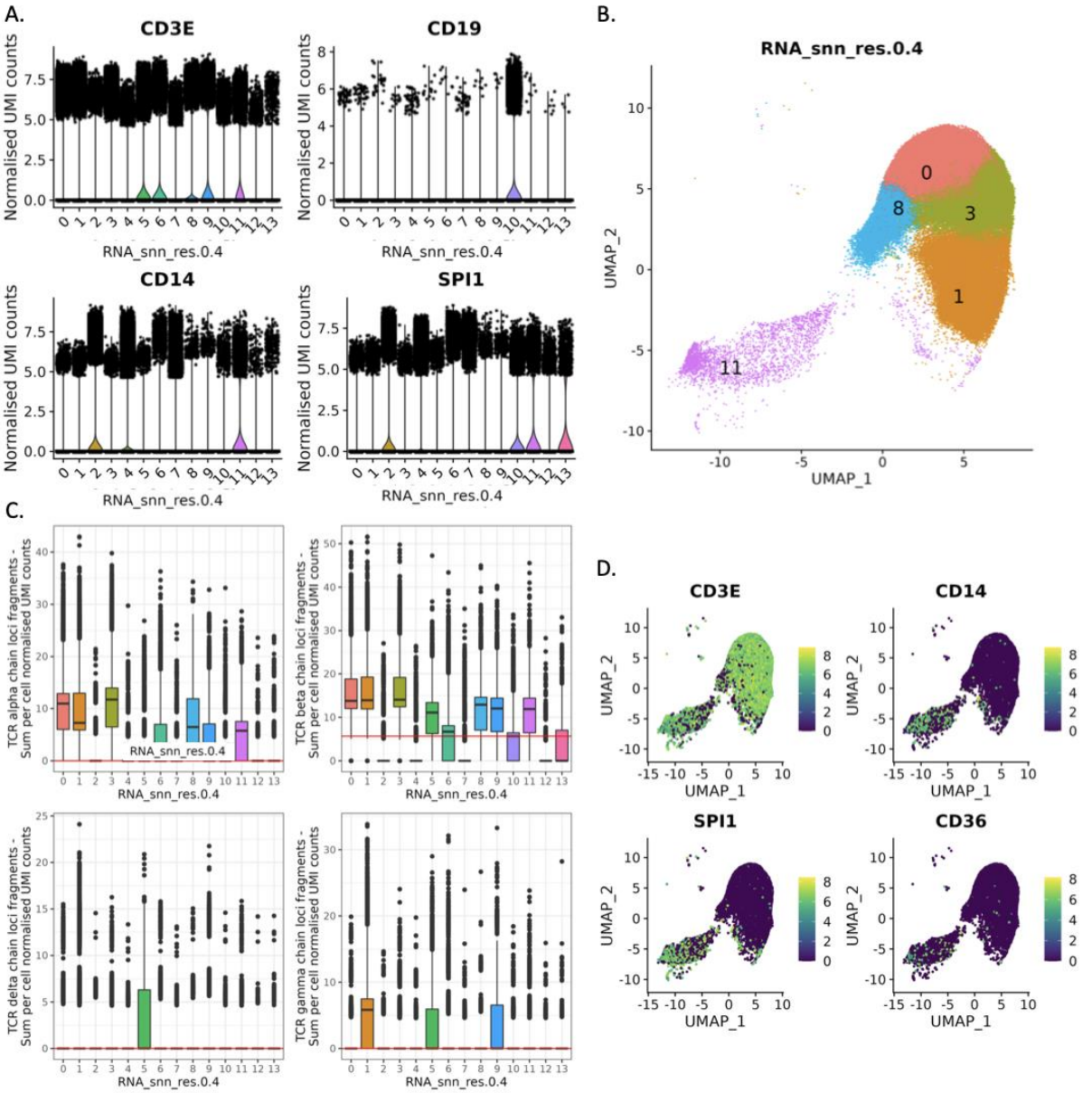

Figure 32 – T cell rich subset extraction – integrated convalescent COVID-19 donor dataset; A) Normalised expression of canonical myeloid and B lymphoid markers to facilitate the B cell rich cluster identification. B) UMAP of T cell rich clusters of the integrated convalescent COVID-19 donor dataset. C) Distribution of TCR chain loci fragments across clusters. D) Expression of canonical myeloid markers in the T cell rich clusters – normalised UMI counts

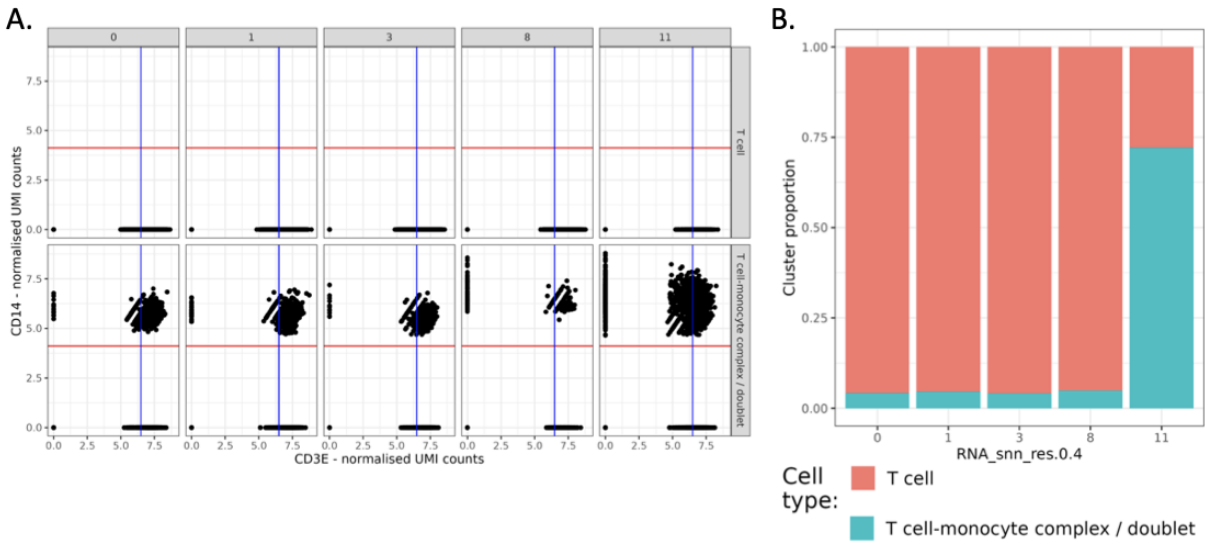

Figure 33 – Doublet identification – integrated convalescent COVID-19 donor dataset; A) CD14 and CD3E normalised expression in the cells labelled either as T cells or T-cell – monocyte complexes as defined by the expression levels of CD14, SPI1 (PU.1) and CD36 quantified in the cluster with the highest CD14 expression present in the dataset; red line – median-2*MAD of the CD14 expression level in the .monocyte rich cluster; blue line – median-MAD of the CD3E expression level in the T cell rich clusters B) Cluster proportion of T cells and T-cell – monocyte complexes.

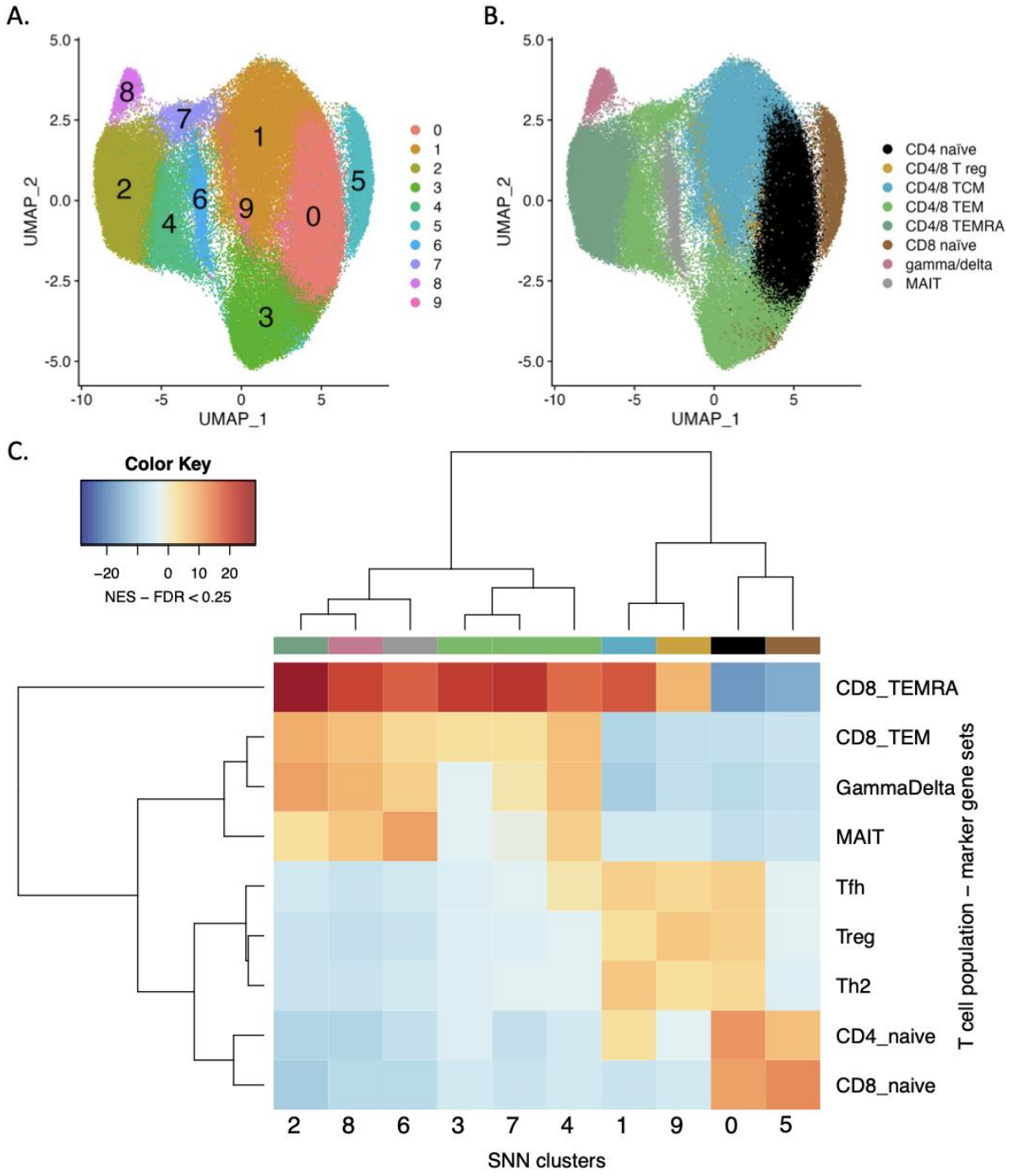

Figure 34 – T cell type assignation – integrated convalescent COVID-19 donor dataset. A) UMAP representation of the T cell rich clusters of the integrated convalescent COVID-19 donor dataset. B) UMAP representation of the T cell rich clusters of the integrated convalescent COVID-19 donor dataset after T cell type assignation. C) Heatmap of the normalised enrichment score (NES) of the T cell marker gene sets computed on the gene expression rankings computed for each cluster while comparing the expression of the genes detected in one cluster versus all the other T cell rich clusters of the dataset. Colours of the column labels match the colours of the UMAP at B).

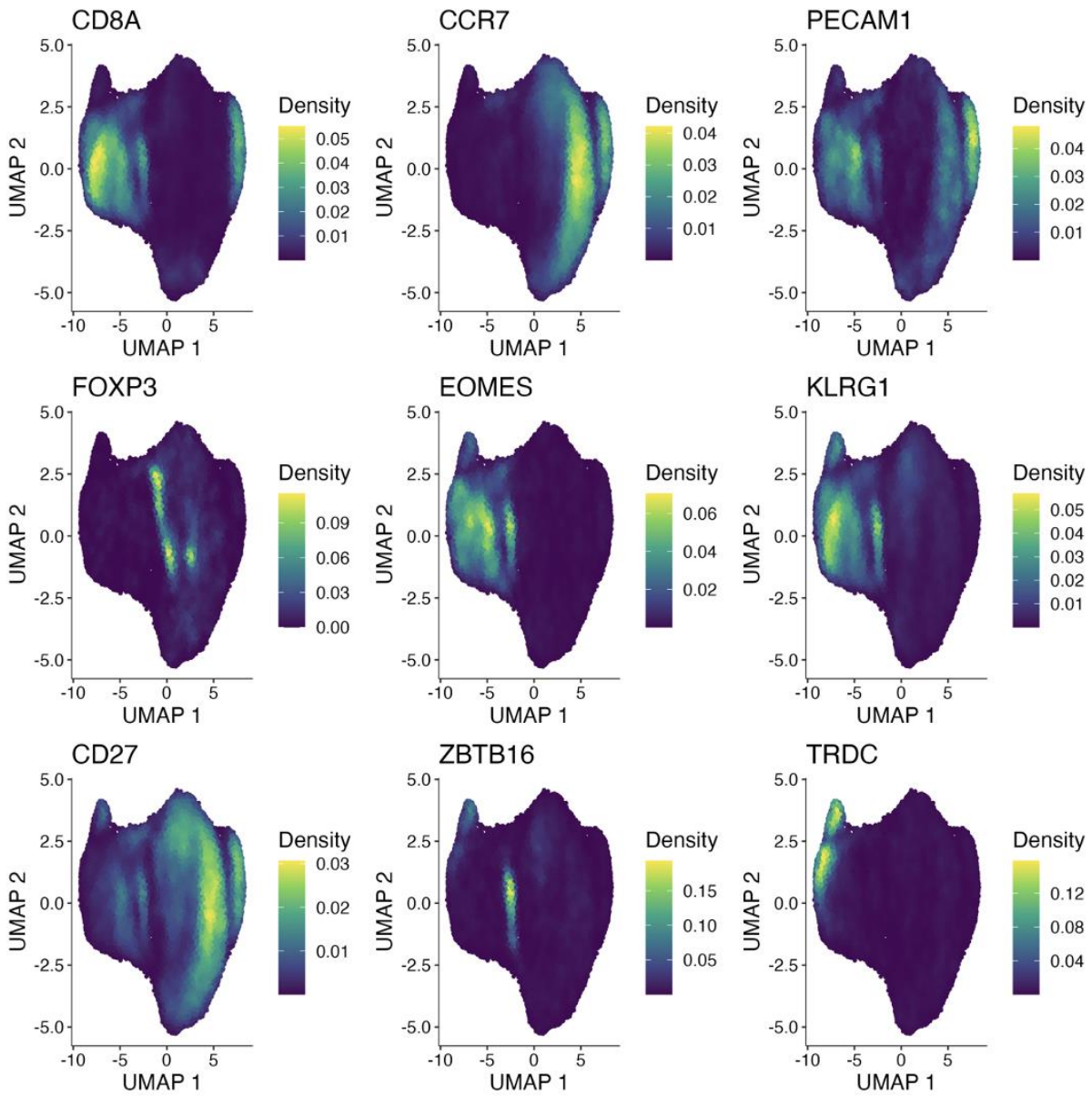

Figure 35 - Gene expression of T cell type canonic markers overlaid on the UMAP representation of the data from the T cell rich clusters of the integrated convalescent COVID-19 donor dataset. Gene expression visualised as a kernel density estimation based on normalised UMI counts. Appendix figure 9 details the statistical assessment of the differences recorded between the expression of the T cell subpopulation marker genes at the level of each cluster.

Probing the association between age group, gender and comorbidities and the acute phase COVID-19 severity or respiratory PACS in the convalescent COVID-19 cohort

Figure 36 offers a summary of the demographic parameters, severity and respiratory. PACS sample labels available in the sample metadata of the 95 samples from which high quality T cell data was available. The association between the demographic parameters, patient comorbidities, SARS-CoV2 and EBV viraemia during the acute infection stage and the frequency of severe cases of COVID-19 or respiratory PACS was assessed to inform the DGEA for comparisons of interest.

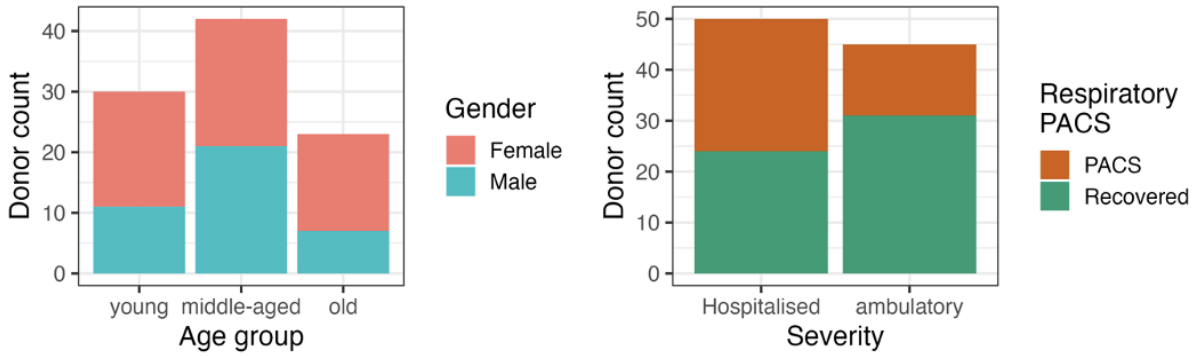

Figure 36 – Age group, gender, COVID-19 severity and respiratory PACS sample label distribution in the convalescent COVID-19 cohort. Sample metadata information from all 95 donors analysed.

Disease severity discretised as hospitalised (maximal WHO Ordinal Scale for Clinical Improvement score (WOS) ≥ 3 during follow-up) or ambulatory (maximal WOS < 3 during follow-up) was associated in a statistically significant manner with the age group of the patient, with older individuals being more frequently hospitalised than younger patients (Figure 37A). Moreover, patients with type 2 diabetes were more frequently hospitalised than normoglycemic ones, with this association reaching statistical significance (Figure 37B). All patients in this study that had congestive heart failure (Figure 37C) or were obese (body mass index (BMI) ≥ 30) (Figure 37G) necessitated hospitalisation as well as the ones in which SARS-CoV2 viraemia was detected during

the acute period (timepoint T1 (one week post symptom onset) and T2 (two weeks post symptom onset)) (Figure 37EF). Similarly, all patients in which EBV viraemia was detected at the T1 timepoint required hospitalisation (Figure 37D). The presence of respiratory PACS as defined in the publication from which the analysed dataset is originating (253) (≥ two of the following symptoms that were not present before the COVID-19 diagnosis and were present after at least month after the acute symptoms onset: cough, fatigue, shortness of breath, fever or chills, muscle/body aches, nausea) was associated the type 2 diabetes and SARS-CoV2 or EBV viraemia detected at timepoint T1 to a degree that reached statistical significance (Figure 38 A,B,C). Interestingly, EBV viraemia detected at least a month post symptom onset was associated with the presence of respiratory PACS (Figure 38D). Moreover, all the patients that had the diagnostic of congestive heart failure before the COVID-19 diagnosis or were treated with steroids during the acute phase of COVID-19 were experiencing respiratory PACS (Figure 38 E,F).

The associations of sample metadata labels that did not reach statistical significance in the assessment of their independence are represented in Appendix figure 10

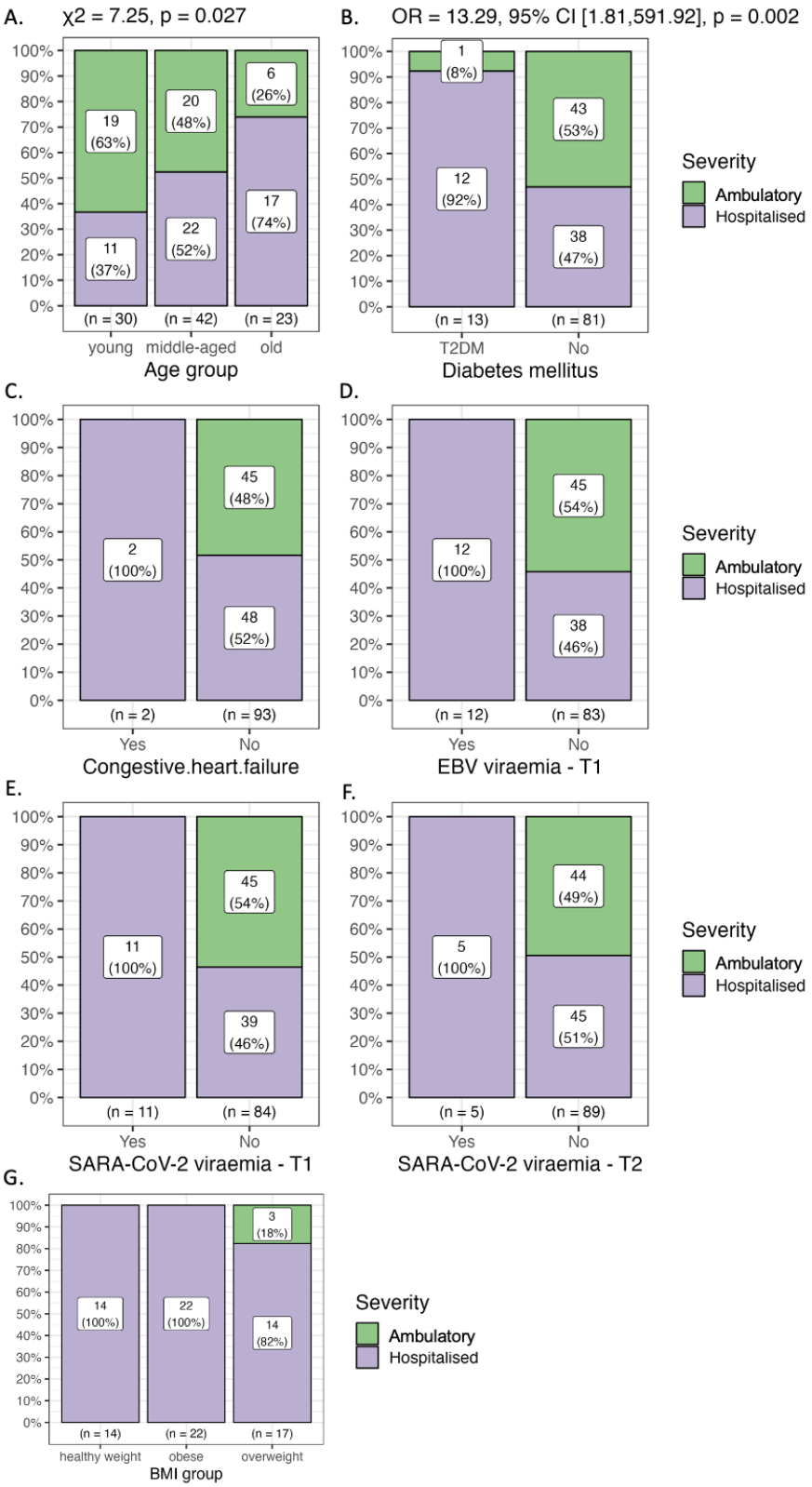

Figure 37 – The association between the acute severity class for each donor and age-group (A), type 2 diabetes (T2DM) diagnosis, the congestive heart failure diagnosis (C), BMI group (G), or EBV and SARS-CoV2 viraemia at different timepoints during the acute phase (DEF).

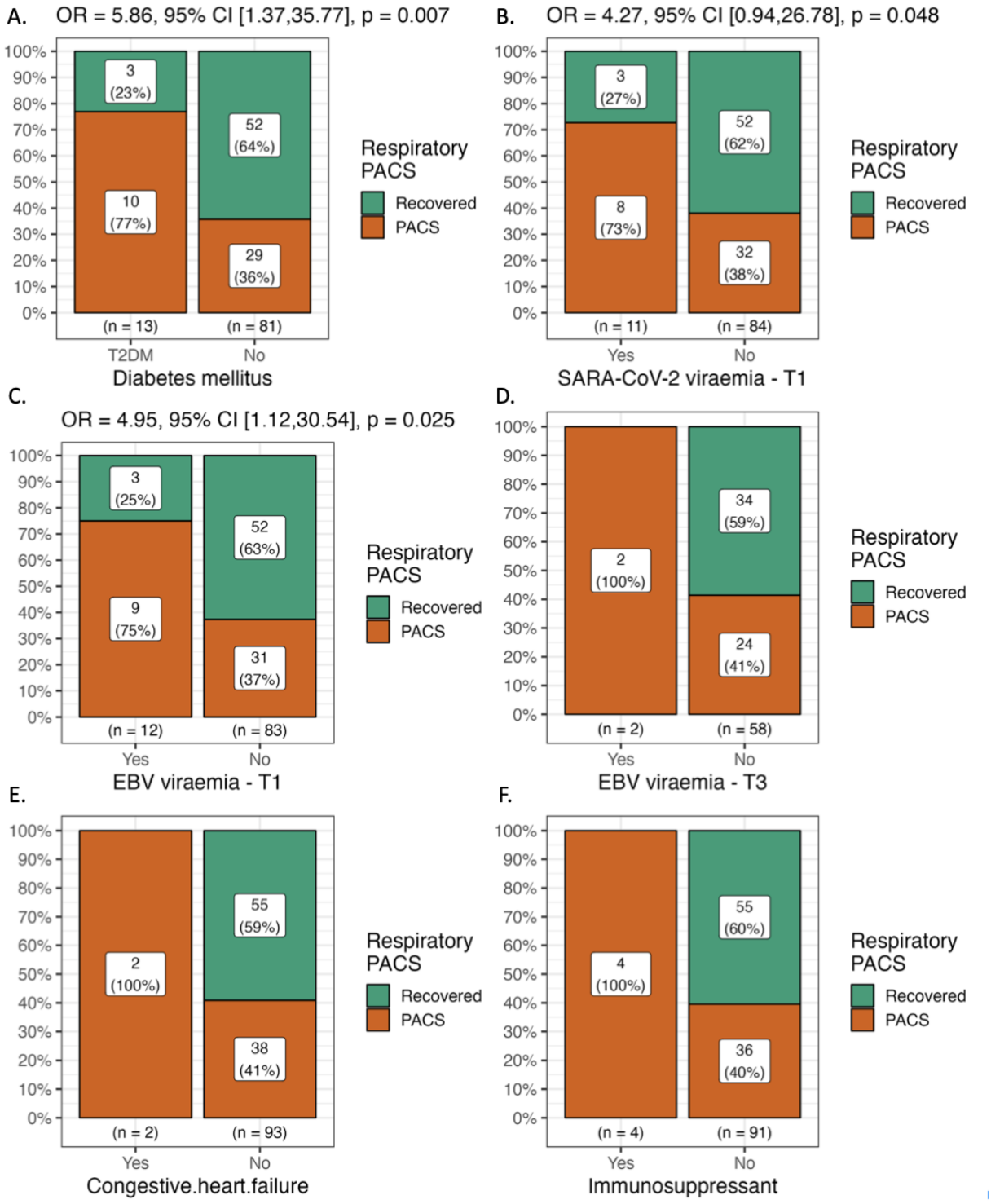

Figure 38 – The association between the respiratory PACS status of each donor and type 2 diabetes (T2DM) diagnosis (A), EBV and SARS-CoV2 viraemia at T1 timepoint during the acute phase (BC), EBV viraemia during convalescence and congestive heart failure (E) or steroid treatment during the acute phase of COVID-19 (F).

Taking into consideration the association between sample metadata labels and sample number available from each donor type, the following donor comparisons were evaluated for differentially expressed genes: samples from the convalescent COVID-19 donors versus the samples from the healthy donor cohort, hospitalised patients versus ambulatory ones, respiratory PACS patients versus completely recovered ones, type 2 diabetic patients with respiratory PACS versus type 2 diabetic patients that completely recovered from COVID19, patients with SARS-CoV2 viraemia at T1 which later on developed respiratory PACS versus their counterparts that did not developed respiratory PACS, patients with EBV viraemia at T1 which later on developed respiratory PACS versus their counterparts that did not developed respiratory PACS, old hospitalised patients versus old ambulatory ones, middle-aged hospitalised patients versus middle-aged ambulatory ones, young hospitalised patients versus young ambulatory ones, hospitalised type 2 diabetes patients versus hospitalised normoglycemic ones and respiratory PACS patients that received steroids versus the respiratory PACS ones that did not received steroids.

The overlaps between the ageing memory T cell signature detected in the healthy cohort and the genes with a FDR <0.05 considered as differentially expressed in the previously mentioned comparisons were evaluated and none of the gene signature overlaps were deemed to be large enough not to be synonymous with one that would have occurred by chance (Figure 39).

In order to understand if ageing in the memory T cell compartment of the healthy cohort donor shares at least some biological processes, as illustrated by the Hallmark and Reactome collections, with the recovery from COVID-19 of any of the donor types that were analysed, we assessed what size are the overlaps in the gene set lists that were shown to be enriched or depleted (FDR <0.25) in the convalescent donor comparisons previously mentioned and the gene sets lists observed when analysing the ageing phenomenon in the memory T cell compartment of the healthy cohort. An overlap big enough not to be attributed to chance between the gene sets that were significantly enriched with ageing in the memory T cell compartment of the healthy cohort and the ones that were enriched in all patients recovering from COVID-19 hospitalisation, and in particular the ones that were middle-aged or young was observed (Figure 40). Looking at which are the gene sets that are significantly enriched or depleted in both the ageing of the memory T cell compartment of the healthy cohort and during recovery post COVID-19, only the respiratory electron transport gene set from the Reactome collection showed a discordant enrichment pattern (Figure 41). A detailed breakdown of the leading-edge genes highlighted by the GSEA and determining the enrichment and depletions of the gene sets are available at Appendix table 5.

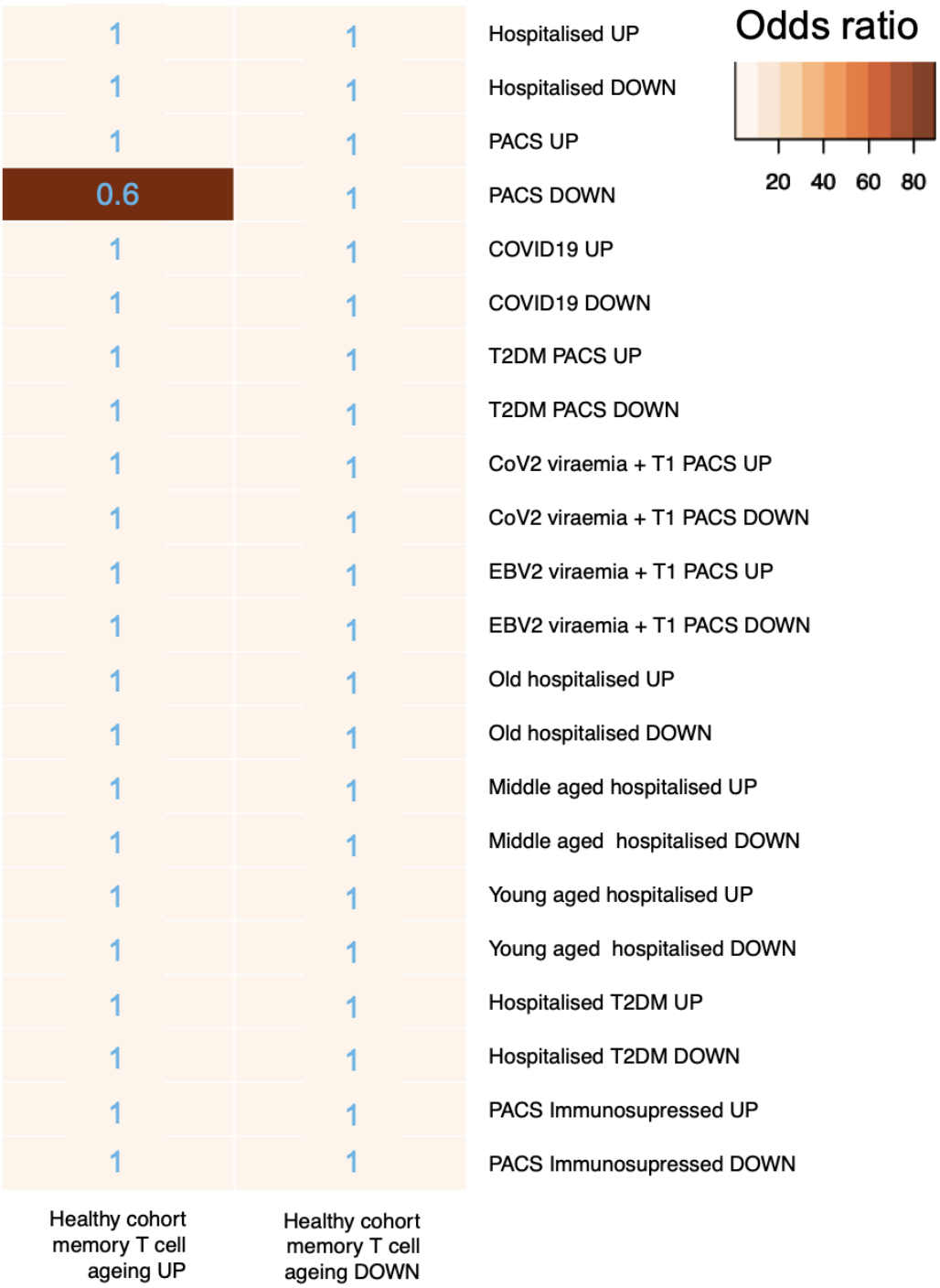

Figure 39 – Quantification of the odds ratio for the overlap between gene signatures associated with the donor types in which significant associations between acute disease severity or respiratory PACS status were found with a clinical or demographic parameter and the ageing memory T cell gene signatures. UP denotes the gene signatures that are upregulated in the labelled donor type and DOWN the gene signatures that are down regulated. Numerical values in blue are the adjusted p-values (Benjamin-Hochberg method) of the pairwise Fisher exact test used to assess the significance of the size of the overlap between the ageing memory T cell signatures and the signatures for each donor type.



Figure 40 – Quantification of the odds ratio for the overlap between significantly enriched or depleted Hallmark and Reactome gene sets associated with the donor types in which significant associations between acute disease severity or respiratory PACS status were found with a clinical or demographic parameter and the ones associated with ageing in the memory T cell compartment of the healthy cohort. UP denotes the gene sets that are enriched in the labelled donor type and DOWN the gene sets that are depleted. Numerical values in blue are the adjusted p-values (Benjamin-Hochberg method) of the pairwise Fisher exact test used to assess the significance of the size of the overlap between the ageing memory T cell gene sets and the ones for each donor type; N.S. = adjusted p-value > 0.05.

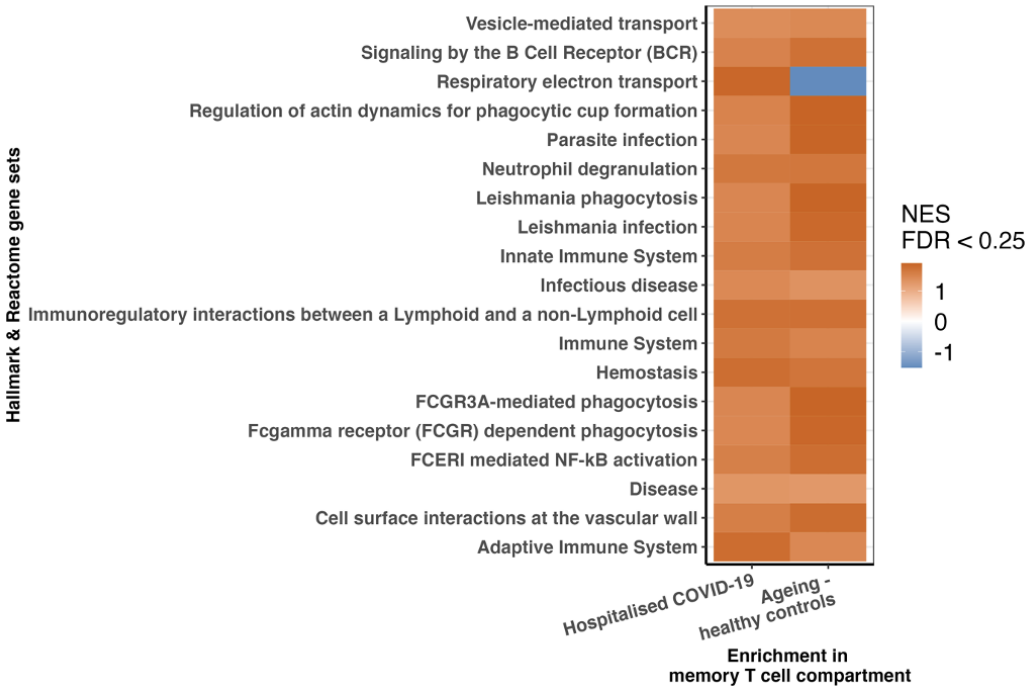

Figure 41 - Heatmap of normalised enrichment scores (NES) of the Hallmark and Reactome gene sets exhibiting an enrichment or depletion with a FDR <0.25 in both the context of the ageing memory T cell compartment of the healthy cohort and in the context of the memory T cell compartment of patients recovering from COVID-19 hospitalisation.

Genes associated with the ageing of the memory T cell compartment in healthy cohort are capable of stratifying a convalescent COVID-19 one based on the severity of the acute disease starting from scRNA-seq data collected months after symptoms onset.

Previously we have shown that the ageing of the memory T cell compartment in a healthy cohort shares biological processes with the recovery from COVID-19 hospitalisation as recorded in the memory T cell compartment of convalescent COVID-19 patients sampled at least a month after the onset of the acute symptoms.

By quantifying the capacity of the genes that were associated with memory T cell ageing to capture the differences in the transcriptome of the memory T cells from patients recovering from either hospitalised or mild COVID-19 using a machine learning approach, I tried to highlight the genes that could be prioritised for further studies at the intersect between ageing and recovery from COVID-19. Following the sample

aggregation of the single cell gene expression data from the memory T cell compartment of all the 95 convalescent donors previously analysed, 4 types of classification models, comprising both linear (LDA) and non-linear ones (random forest, KNN, support vector machine with radial kernel), aiming to predict the acute severity label of each donor were evaluated using the repeated cross-validated methodology, with the specificity, sensitivity and the ROC AUC being the parameters used to assess the best classification model.

The best type of classification model was the random forest one, with a mean across all cross-validation iterations of ROC AUC = 0.8255488 (95% confidence interval (CI): 0.75-0.91) (Figure 42A, Appendix table 7). Investigating the importance of each gene for the prediction accuracy of the random forest model revealed that BAX and IL10RA were in the top three most important genes for the performance of the prediction model (Figure 42B) and were at the same time the only two genes that overlapped between the upregulated genes (FDR <0.05) with age in the memory T cell compartment of the healthy cohort donors and in the patients that were hospitalised during the acute stage of COVID-19 compared to the ones that did not required hospitalisation in the convalescent COVID-19 cohort (Figure 42C).

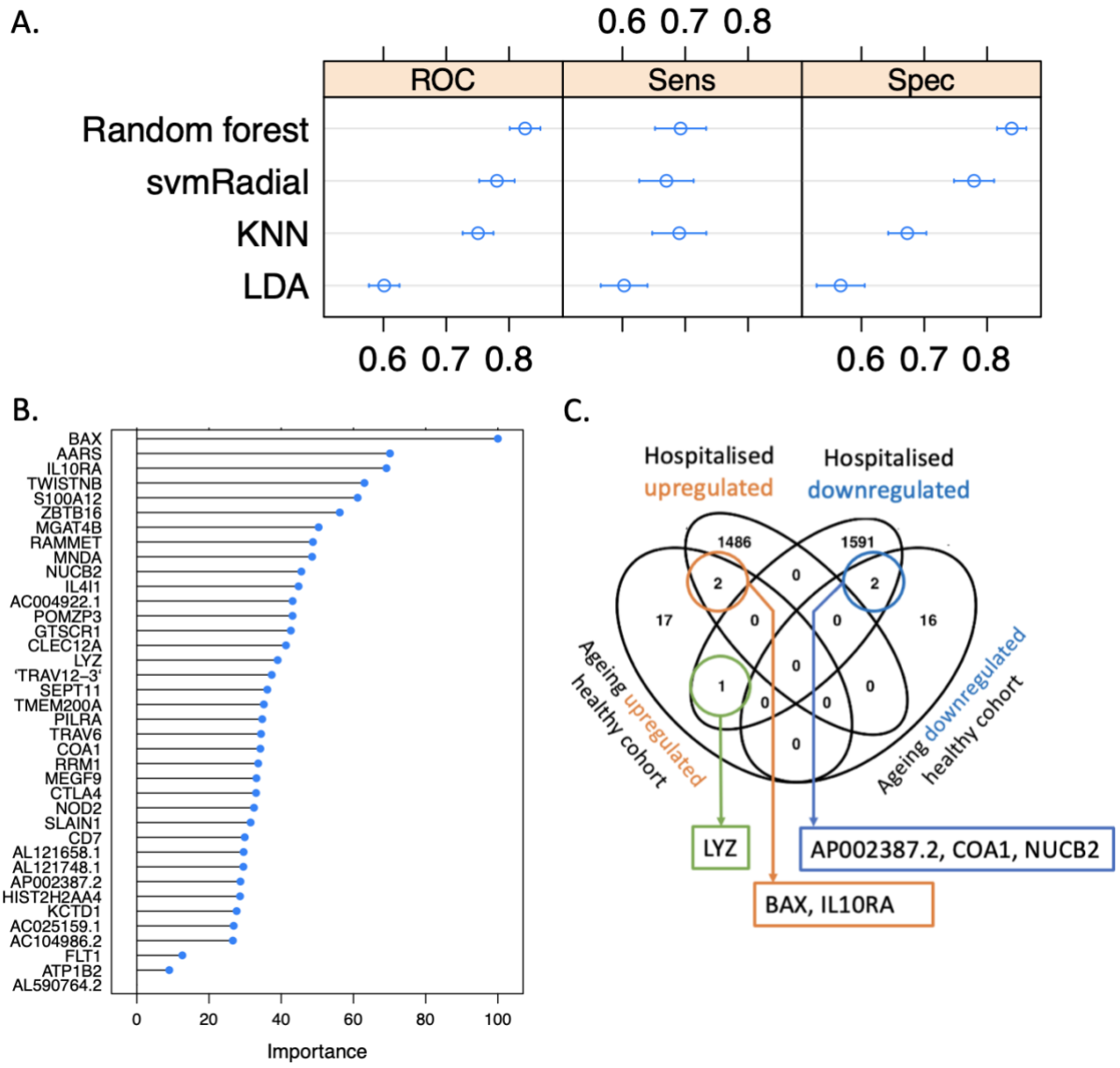

Figure 42 – Performance metrics of classification models and the relationship between the ageing memory T cell signature and the COVID-19 hospitalised case recovery one. A) AUC ROC, sensitivity and specificity of the severity classification models evaluated using the repeated 4-fold cross-validation methodology in the setting of the analysed convalescent COVID-19 cohort. Mean and 95% CI represented for each performance parameter of the models tested. B) Scaled importance metric for the genes making the random forest recovery classification model. C) Venn diagram of the lists of significantly upregulated and downregulated genes with ageing in the memory T cell compartment of the healthy cohort donors and in the patients that were hospitalised during the acute stage of COVID-19 compared to the ones that did not required hospitalisation. Appendix table 6 contains the gene lists used to produce Figure 42C

Chapter V. Discussion

HSCs exhibiting the transcriptomic features of platelet lineage bias can be identified in human HSC single cell RNA sequencing datasets

Before an analysis of the results outlined in chapter IV is made, it needs to be acknowledged that the differences observed between the frequencies of HSC subpopulations identified at the level of the young and old donors are confounded to an extent by the fact that the HSCs from old donors have been sorted from thawed BM-MNCs compared to fresh BM-MNCs from HSCs from young donors. In addition, the old and young donor HSCs were sorted on two different days and sequenced on two different sequencing runs. However, a study conducted on bone marrow aspirates from multiple myeloma patients processed using the 10X Chromium platform starting from either fresh or thawed samples has shown that gene expression patterns from fresh and frozen samples are highly correlated, but there were small differences in the relative abundance of progenitors when data from fresh samples is compared to data from thawed ones (385).

Our analysis of human HSC scRNA-seq datasets has shown that an HSC subpopulation exhibiting a gene expression programme, which in mouse haematopoiesis has been functionally linked to a bias towards megakaryopoiesis, and low output (89) can be identified in data from young (Figures 3 and 4) as well as old (Figures 7 and 8) clinically healthy males. The transcriptome of the computationally defined platelet biased HSC subpopulation was marked by the expression of gene sets associated with types of human HSCs that exhibit very high repopulation potential as

the EPCR+ HSCs (142) and are situated at the apex of the HSC compartment like the CLEC9Ahi CD34lo CD49f+ HSCs (140) (Figure 13A). Hallmark gene sets (380) associated with oxidative phosphorylation, MYC, E2F targets and mTORC1 signalling were shown to be depleted among the upregulated genes in the computationally defined platelet biased HSC subpopulation in both young and old donors compared to their multilineage counterparts (Figure 13B). This observation points to a positive association between the transcriptomic features of computationally defined platelet biased HSCs and the gene expression patterns of human and murine HSCs that have the highest self-renewal capacity (106,386). Interestingly, the depletion of the Hallmark gene set associated with glycolysis in the computationally defined platelet biased HSCs is highlighting that in this subpopulation there might be generally a lower energetic demand compared to what is needed in other HSC subpopulations. The depletion of the Hallmark gene set regarding DNA repair in the platelet biased subpopulation highlights another attribute of this population that is usually associated with quiescent HSCs (387,388).

The gene expression signature determining the transcriptomic identity the computationally defined platelet biased human HSCs has been shown to be positively correlated with the gene signature of the platelet biased human HSCs described in the lineage tracing experiments carried out by the Nerlov Lab in the analysed scRNA-seq datasets (Figure 5A & Appendix figure 3A,B). The gene set enrichment patterns obtained by studying the gene expression patterns in the computationally defined platelet biased HSCs compared to their multilineage counterparts and in the lineage

tracked platelet biased HSCs compared to their multilineage counterparts show a high degree of similarity in the gene sets that are enriched or depleted (FDR <0.25) in both comparisons (Figure 5B). The fact that in the platelet biased HSCs from lineage tracing experiments there is depletion in the gene set associated vitamin A signalling in HSCs (367) highlights the replicative needs that could be associated with the xenotransplantation step of the lineage tracing experiments.

The genes that were found to be significantly upregulated in both the computationally defined and lineage traced platelet biased HSCs when compared to their multilineage counterparts (Appendix Figure 2) were genes previously associated with higher self-renewal capacity (MLLT3, HLF, TSC22D3)(389,390), with maintenance of the HSC pool (NFE2L2, SOCS2) (391,392) and upregulated in quiescent human HSCs as part of their lysosomal machinery (LAPTM4A) (393), but downregulated in senescent human haematopoietic stem and progenitor cells (APOL3) (394). Interestingly, among the genes significantly upregulated in both the computationally defined and lineage traced platelet biased HSCs when compared to their multilineage counterparts there were as well genes part of the HLA class II family (HLA−DQA2, HLA−DRA) and relevant for HLA class II receptor assembly (CD74). HLA-DR expressing human HSCs have better engraftment capacity than their HLA-DR negative counterparts (395). Among the genes that were significantly downregulated in both the computationally defined and lineage traced platelet biased HSCs when compared to their multilineage counterparts were DNMT3A and RPS26, which in the case of its reduced expression has been linked with lineage biases, but not with a megakaryocytic one (396,397).

Human HSCs exhibiting the transcriptomic features of platelet lineage bias increase in frequency with age, but to a lesser extent than in mice

Comparing the relative and absolute frequency of the previously computationally defined human HSC subpopulation in old versus young donors highlighted an increase with age of the platelet biased HSC subpopulation size (Figures 10 and 17). This observation is in agreement with the one made by Grover et al, in which the platelet biased murine von Willebrand factor (vWf) positive HSC subpopulation was seen to increase in size with age (306). The magnitude of the size increase of the computationally defined platelet biased human HSC population with age was evaluated in the setting of two data analysis methodologies, one in which all the datasets from the young donors are analysed in isolation from the old donor ones using the same methodology for the identification of the HSC subpopulations and one in which all datasets are merged into one and using Seurat's integration batch correction (318) method with the sample specific variance being regressed and then the identification of the HSC subpopulations being carried out as before. Both analysis methodologies highlighted two types of statistically significant associations between the donor groups and the size of a computationally defined human HSCs population: an enrichment in platelet biased HSCs and a depletion of multilineage output HSCs in old donors (Figures 10B and 17B). The previously mentioned observation was reported as well in a recent preprint (398). These associations were not dependent on any particular donor pairs, as they could be observed in all possible old-young donor pairs and they always reached statistical significance (Appendix figure 4).

The differences observed between the magnitude of the difference in percentage of the computationally inferred HSC subpopulation per donor when comparing old versus young donors observed in the two data analysis methodologies would stem from two phenomena. Firstly, by using Seurat's integration batch correction method to ensure that the clustering subsequently generated using all the available data does not contain clusters that are made predominantly of data from one particular donor, some of the biological signal attributed to the age difference between donors will be regressed and this is known caveat of such a methodology (339). Though the integration methodology has the potential to diminish the impact of the ageing phenomenon on the size of the computationally defined HSC populations, it has the advantage that all the cells assigned to an HSC population have a better controlled transcriptomic identity. This aspect brings us to the second phenomena that could explain this discrepancy in effect sizes attributed to ageing in the two methodologies: analysing the two dataset types, the one from the young donors and the one from the old donors in isolation and utilising the same set of rules for defining the same computationally inferred HSC population would not mean that the transcriptomic identity of the populations in the 2 types of datasets will be well controlled. This differences in transcriptomic identity are due to different variable genes detected in the two types of datasets used for dimensionality reduction and influencing the clustering results in the end. Opting for the same list of genes to be used for dimensionality reduction and then clustering could mean using uninformative genes for one dataset type and introducing additional unwanted variance into an already "noisy" type of data (339). Thus, there is the risk of not comparing like with like in the methodology that analyses dataset types in isolation. The integrative

approach risks regressing some of the effects of the biological signal, but it controls the transcriptomic identity of the computationally inferred HSC population at the level of the variable gene selection, thus ensuring a better controlled definition of a computationally inferred populations.

Both methodological approaches agree that the fluctuation in size with age of the computationally inferred platelet biased human HSC is less dramatic than what was seen in mice, with a 1.18 to 1.79 fold change old vs young in the frequency of the platelet biased HSCs in humans, depending on the analysis methodology, compared to the 100 fold increase in the vWf+ murine platelet biased HSCs recorded in old mice compared to young ones (306). Interestingly the size of the computationally inferred platelet biased HSC population relative to the size of the whole HSC compartment is in a similar range as the one described by Rodriguez-Fraticelli et al., with a mean population size between 34.43% (min=23.9%, max=47.03%) and 39.14% (min=34.23%, max=46.52%) depending on the methodology in the case of the human HSCs and a mean 28.18% of the whole HSC compartment (min= 11.8%, max = 48.6%) the in the case of the data published by Rodriguez-Fraticelli et al. (89).

The frequency of the human lineage biased HSCs stated in our analysis should be interpreted in the context of the purity of functional human HSCs in the Lin-CD34+CD38-CD90+CD45RA- compartment which is not higher than 1/50 (81). Thus, any firm conclusions made about the frequency of functional human lineage-biased HSC populations found in the above-mentioned compartment will require prospective

isolation of such HSC starting from the expression of specific cell surface marker combinations and functional validation of their output given the functional impurity of this compartment. Moreover, it should be acknowledged that the lineage bias HSC gene signatures that were used to identify the computationally defined platelet biased human HSCs were derived from data generated from mouse HSCs defined as a cellular compartment that is far richer in functional HSC (1/2.1) (82) than the human immunophenotypic HSC compartment defined by Majeti, Park and Weissman (81) and analysed in our study. Consequently, there will be elements of the transcriptomic identity of the mouse lineage-biased HSC that would not be necessarily associated with the transcriptome of a functional human platelet-biased HSC.

To conclude, the cell population identified at the level of the immunophenotypic human HSC compartment that exhibits the gene expression patterns of a mouse platelet-biased HSC could contain functional human platelet-biased HSCs as well as more mature progenitor populations incapable of long term engraftment, but ascertaining what is the frequency of the functional human platelet-biased HSC in the cell compartment defined by Majeti, Park and Weissman (81) will require further studies and our findings provide a starting point for them.

The transcriptomic differences between the computationally inferred platelet biased and multilineage HSCs populations present in young donors are exacerbated by ageing

Both data analysis methods deployed on the human HSC scRNA-seq datasets have shown that overall, with ageing there is an increase of the expression of the gene signature associated with the platelet bias across all HSC subpopulations, but particularly so in the platelet biased subpopulation (Figures 11A, 16A) and this was recapitulated by the behaviour of the platelet biased HSC gene signature derived from the lentiviral barcoded human HSC lineage tracing experiments (Figures 11B, 16B). An opposite phenomenon was observed for the expression of the multilineage output HSC gene signature (Figures 11C,16C), but this gene expression pattern has not been recapitulated if the multilineage output HSCs gene signature derived from the lentiviral barcoded human HSC lineage tracing experiments was analysed (Figures 11D, 16D). A comparative analysis of the correlation coefficients between the AUCell scores as recorded in the young versus the old datasets shows a diminishing in the modulus of the correlation coefficient with age, regardless of the analysis methodology employed (Appendix Figure 3).This observation could reflect either the change in HSC subpopulation size previously described with age or an increase heterogeneity in expression levels of the genes that were shown to be associated with lineage fate decisions in HSCs or HSC activation in the context of murine HSCs (89). An increased in cell-to-cell gene expression heterogeneity with age has been previously documented in murine CD4+ T cells (399).

The more well controlled HSC population identity afforded by the integrative analysis methodology has pointed out that the gene sets that are specifically enriched in upregulated genes for the computationally inferred platelet-biased HSCs from old donors are the ones that are associated with a quiescent state (364) and high self renewal capacity (140,142) (Figure 18A). Interestingly, the gene set associated with murine lymphoid-biased HSCs (381) shows a positive enrichment in the old donor platelet biased HSCs (Figure 18A), but this could be due to the fact the leading edge genes determining this enrichment were genes that there were common between that gene set and the platelet bias gene set derived from the work of Rodriguez-Fraticelli et al. (89), such as MLLT3, CLU and FLI1. The Hallmark gene sets associated with the TNFα via the NF-κB and IL-6-JAK-STAT3 signalling are enriched significantly in the old donor computationally inferred platelet biased HSCs which is in agreement with the proinflammatory milieu of the ageing HSC niche (87) (Figure 18B). In the case of the computationally defined human multilineage human HSCs there was one gene set that was specifically enriched in the old donors for this HSC population and it was Hallmark's oxidative phosphorylation one which is concordant with the literature around the switch between glycolysis and oxidative phosphorylation during HSC activation (106,107) (Figure 18D). The gene set associated with the CLEC9Alo CD34hi CD49f+ HSCs which are associated with an activated phenotype (140) was the only gene set that was significantly and specifically enriched in an HSC population of the young HSC datasets, the multilineage one (Figure 18D), highlighting the possibility that the computationally derived multilineage output human HSC population to have an activated HSC phenotype (140,384).

Even though the analysis of the young and old donor HSC datasets in isolation might not have the advantage of the better controlled computationally inferred HSC population definitions found in the integrated analysis, a couple of gene sets have shown an age group specific enrichment or depletion at the level of the transcriptome of the platelet biased HSCs (Figure 13). Of note, in this analysis none of gene sets reaching statistical significance had a discordant pattern of enrichment or depletion across age groups. Among the gene sets that were significantly enriched in platelet biased HSCs of old donors was the one associated with vitamin A signalling in dormant murine HSCs (367). Interestingly, among the upregulated genes in computationally defined platelet-biased human HSCs of old donors a significant depletion in the gene set associated with the G2/M cell cycle phase (383) was recorded which could be linked with the deeper quiescent state recorded in long term HSCs from old mice compared to younger animals (400).

The gene sets associated with the computationally inferred multilineage and platelet-biased HSC populations suggest that there is an activation gradient between the cells in the computationally defined platelet biased HSC population and the ones in the multilineage one. The transition between the quiescent (platelet biased population) and activated (multilineage population) HSCs has been investigated and under the influence of ageing in our study. B2M was shown to be differentially expressed along the state transition trajectory and exhibited a gene expression pattern different in HSCs from old donors versus young ones. Thus, there is an opportunity for the study of the

inflection point in which an HSC transitions between quiescent and activated states by prospectively isolating HSCs expressing B2M (Figure 21).

Ageing of the memory T cell compartment is characterised by an inflammatory gene signature and a heterogenous effect on the size fluctuations of its subpopulations

By considering the age as a continuum in the DGEA and evaluating which genes are shown to increase or decrease with age in the memory T cell compartment of the studied cohort, our study manages to highlight a gene expression signature that is not tied to age intervals and tries to understand the continuum of accumulation of molecular damage that is ageing (41).

Among the genes that were shown be significantly upregulated with age (FDR <0.05), we can find a number of genes that have been previously associated with T cell ageing and some that have not been previously documented to be (Figure 29A). CTLA4 and BAX has been shown to be upregulated with age in the memory T cell compartment of donors in the healthy donor cohort, which is in agreement with a report from murine CD4+ TEM where CTLA4 and BAX were found to be upregulated with age (401). NOD2 upregulation with age in the memory T cell compartment is conceptually in agreement with its role as an inducer of the activation of NF-κB pathway in the memory CD4+ T cells (402), a key pathway involved in T cell ageing (248). Though a gene usually associated with the monocyte compartment (345), Lysozyme (LYZ) expression has been shown to be upregulated with age in naïve T cells in mice (403) and in our healthy donor cohort we observed its upregulation in memory T cells. Interleukin (IL) 10

receptor subunit alpha (IL10RA) expression was upregulated with age in the memory T cell compartment of the healthy donor cohort. A causal link between this expression pattern and the ageing of the memory T cell compartment has not been established yet, but high levels of serum IL-10 have been recorded in aged mice and humans and the blockade of the IL-10 receptor has improved the vaccine response in murine models, highlighting the role of IL-10 as part of the adaptive immune system dysfunction seen in old organisms (404). Moreover, IL10RA has been found to be upregulated chronic hepatitis C patients, a category of individuals associated with an accelerated ageing phenotype, when compared to healthy controls (405,406). TRAV12-3 was recorded as being upregulated with age in the healthy cohort. The mechanism and role of the upregulation of TRAV12-3 with age in the memory T cell compartment are yet to be determined, but a study of supercentenarians has shown that the largest clone present in a CD4+ cytotoxic population was expressing TRAV12-3 and the authors of the study speculate that this population has a role in immunosurveillance and is an adaptation to the late stage of aging (407). Though not directly related reports from the literature about the process of T cell ageing, the upregulation of MGAT4B in the healthy cohort could be supported as a mark of inflammaging, as the upregulation of this gene is seen in T cell from patients with systemic lupus erythematosus, a condition associated with a hyperinflammatory state (408). Moreover, the upregulation of AARS with age in the healthy cohort could be related to the role of the family of aminoacyl-tRNA synthetases, of which AARS is part of, in the regulation of telomerase activity which has been linked to the regulation of cellular senescence (409). Intriguingly, some of the genes that were shown to be

upregulated in the memory T cell compartment, like S100A12 and MNDA, which are not usually reported as being expressed in T cells have been reported to be expressed at lower levels in aged individuals during acute COVID-19 compared to their much younger counterparts (410), raising the question of their role in the prognosis of COVID-19, a condition in which age is a known prognostic factor (17).

Among the genes that were shown be significantly downregulated with age (FDR <0.05), we can find a number of genes that have been previously associated with T cell ageing and some that have not been previously documented to be (Figure 29B). CD7 and FLT1 downregulation with age has been previously reported in T cells, with CD7 downregulation being implicated in enhanced T cell cytotoxicity (401,403,411). RRM1, a regulator of telomere length in yeasts which was downregulated with age in the healthy cohort has been shown to be one of the loci relevant for the association between telomere length and human lifespan in a Dutch population cohort, thus hinting at its relevance in a phenomenon that influences human lifespan, T cell ageing (25,412). COA1, a component of the MITRAC complex which regulates cytochrome c oxidase assembly (413) was found to be downregulated with age in our study. A link between the expression of COA1 in T cells and longevity has not been shown yet, but a study of genetic variability in supercentenarians versus the general population has shown that there are specific polymorphisms for COA1 positively associated with longevity (413).

Overall, the ageing memory T cell gene signature is an inflammatory one and is in agreement with the paradigm of inflammaging as a focal point in the phenomenon of ageing in the memory T cell compartment (25).

The trends pertaining all the T cell types identified in the healthy donor cohort integrated analysis available in Appendix figure 7 are highlighting known population size fluctuations with age, with the CD8+ naïve T cell compartment shrinking with age, the central memory expanding at least in the data from the Ren dataset and the TEMRA compartment not fluctuating in size with age (176). Our study highlights as well a known observation in the field, that the only robustly reproduced size fluctuation with age across the majority of studies is the shrinkage with age of the CD8+ naïve T cell compartment (148).

Thus, our study of the ageing phenomenon in the memory T cell compartment has generated a gene expression signature that highlights known and novel aspects of the ageing phenomenon in the T cells compartment. Moreover, this gene signature has the potential to indicate the impact of a perturbation on the rate of which ageing in this compartment progresses, given the robust correlative behaviour of the gene expression scores computed using this signature in relation with the age of the donors (Figure 30).

At the level of the memory T cell compartment, recovering from a COVID-19 - related hospitalisation and ageing share common biological processes

Utilising the data published by Su et al. (253) offered us the opportunity to test a number of hypotheses chief among them being if recovering from a form of COVID-19 that required hospitalisation shares certain biological processes with the ageing phenomenon at the level of the memory T cell compartment. Identifying these biological processes could highlight potential therapeutical targets for alleviating deleterious adaptive immune processes associated with both experiencing severe COVID-19 and ageing.

Despite eliminating 5 samples during the quality control step from the original cohort, we observed similar patterns of associations between acute COVID-19 severity and respiratory post-acute COVID-19 syndrome (PACS), as well as age groups and comorbidities and gender (Figures 37 and 38) as reported in the original publication from which the data was extracted (253). In their publication, Su et al. define respiratory PACS as two or more of the following symptoms persisting more 30 days after COVID-19 clinical onset: cough, fatigue, dyspnoea, fever/chills, muscle/body aches, nausea (253). We opted to study the samples that had respiratory PACS as in this study this category of patients required the highest number of symptoms to be met in order to be labelled as exhibiting PACS, thus more stringently assigning this label. Though directly there was no statistically significant association between respiratory PACS and acute COVID-19 severity (Appendix Figure 10), there was a statistically significant association between type 2 diabetes and both COVID-19 severity and respiratory PACS, hinting at the vulnerability of these patients to poor outcomes in the context of

COVID-19 (Figures 37B, 38A). Interestingly, in this study, there was no statistically significant association relationship between obesity and respiratory PACS (Appendix figure 10B) which is not in agreement with the literature (414), but all obese patients required hospitalisation (Figure 37G), a fact that aligns with the reports of obesity being a risk factor for severe COVID-19 (269). Moreover, the fact that EBV viraemia during the acute disease stage was associated with both acute disease severity and respiratory PACS (Figures 37D, 38C) could hint at the involvement EBV reactivation in the pathogenesis of severe COVID-19 and lending evidence to the dysbiosis theory of post-acute infectious disease syndrome pathogenesis (252).

Surprisingly, at least 30 days post-acute symptom onset, the transcriptomic differences between patients that experienced respiratory PACS and the ones that successfully recovered from COVID19 or between the ones that were hospitalised and the ones that were not did not overlap with the ageing memory T cell signature to a statistically relevant extent (Figure. 39). One interpretation of this finding might be that at least a month after acute symptom onset the inflammatory signature that could be shared with immunological ageing in the memory T cell compartment has been attenuated in the respiratory PACS or hospitalised patients to levels similar to the ones recorded in completely recovered COVID-19 or ambulatory COVID-19 patients, a phenomenon that has been described by Su et al (253).

When we looked at pathways and biological processes as represented by the gene sets from the Hallmark and Reactome collections, there was a significantly large

overlap between the gene sets that were enriched in patients that were recovering from COVID-19 hospitalisation and the ones that were enriched with age in a cohort that never experienced COVID-19 (Figure 39). Interestingly, IL10RA was the only differentially expressed gene with age at the level of the memory T cell compartment that was common with the leading-edge genes determining the enrichment of the gene sets commonly enriched or depleted to a statistically significant degree in patients recovering from COVID-19 hospitalisation and were enriched with age in a cohort that never experienced COVID-19 (Figure 40).

The observation regarding the size of the overlaps of gene signatures and gene sets associated with COVID-19 hospitalisation recovery and ageing in the context of a healthy cohort suggested a degree of commonality between these two phenomena as recorded at the level of the memory T cell compartment. We focused next on understanding which of the genes found in the ageing memory T cell gene signature could be important for differentiating between convalescent COVID-19 patients recovering from hospitalisation versus the ones that did not such support. It is known that older COVID-19 patients require hospitalisation more often (17) and recover less well than younger ones (264) and it has been shown that recovering from COVID-19 induces a process of accelerated ageing (415), so our analysis would try to just highlighting potential pathways to target to alleviate deleterious adaptive immune processes associated with both experiencing severe COVID-19 and ageing. To this end we first assessed a number of machine learning algorithms that were suitable for classifying the convalescent COVID-19 cohort's samples into their respective acute

severity classes utilising only the information of the ageing memory T cell gene signature recorded in their memory T cell compartments and chose the best performing model at this task after its evaluation in a repeated cross-validation set-up. The random forest model had the best performance parameters (Figure 42A) and given good classification performance reflected by its ROC AUC score (0.8255488, 95% confidence interval (CI): 0.75-0.91) when trained only on the ageing memory cell, it highlights the importance of the ageing process genes in the context of the recovery from COVID-19 hospitalisation. Out of these ageing genes that were shown to have a significant contribution to the performance of the random forest model (Figure 42B), BAX and IL10RA were of particular interest given the fact that they have been shown to be the only 2 genes that were significantly (FDR <0.05) upregulated in both hospitalised COVID-19 patients and upregulated with age in the healthy cohort (Figure 42C).

IL10RA encodes the α chain of the IL-10 receptor, which was first described as an anti-inflammatory cytokine, but in the context of the high plasma levels of bacterial DNA and lipopolysaccharides, originating from the bacteriemia with a gut origin encountered in severe COVID-19 (416) acts as a proinflammatory factor associated with the cytokine storm encountered in severe COVID-19 patients (417). The paradoxical pro-inflammatory action of IL-10 has been recorded as well in type 2 diabetes patients, a demographic that is particularly vulnerable to COVID-19 and presents a proinflammatory state compared to their normoglycemic counterparts (259,418). High levels of serum IL-10 have been recorded in aged mice and humans and the blockade

of the IL-10 receptor has improved the vaccine response in murine models, highlighting the role of IL-10 as part of the adaptive immune system dysfunction seen in old organisms (404). Our study highlights a possible scenario in which during the recovery from severe COVID-19, elevated levels of IL10RA persist in the memory T cell compartment, thus maintaining a characteristic of ageing in this compartment and possibly a disfunction of the adaptive immune system.

The expression of BAX, a pro-apoptotic protein has been linked with the lymphopenia and the exacerbated T cell apoptosis recorded in the acute phase of severe COVID-19 (419). The persistence of a T cell population manifesting a VDAC1-mediated mitochondrial dysfunction that is associated with BAX-mediated apoptosis past 90 days after acute symptom onset in convalescent COVID-19 (420) could suggests that during COVID-19 recovery there is an ongoing mitochondrial dysfunction present. Mitochondrial dysfunction is one of the hallmarks of T cell ageing and an increase in BAX-mediated apoptosis with age in memory T cells has been previously documented (25,421,422).

Our study has the potential to suggest IL-10 signalling and BAX-mediated apoptosis at the level of the memory T cell compartment as targets of future research for therapeutical intervention to alleviate adaptive immune disfunctions linked to inflammaging and potentially PACS. Islam et al. speculate on the opportunity of using SHIP agonists to alleviate the proinflammatory IL-10 signalling associated with severe COVID-19 cases (417) and Almanan et al. have shown that IL-10 receptor blockade improves vaccine responses (404). Drugs modulating the activity of BAX, such as navitoclax have been shown to have a senolytic activity (26) and our current study

highlights this class of drugs as potential target of future research for a therapeutical approach in combating both inflammaging and post COVID-19 immunological sequalae.

Future studies

The scope of the conclusions of our study of the impact of ageing on the transcriptome of the human HSC and memory T cell compartments are limited by several factors.

Firstly, being a purely computational study any of the conclusions or conjectures made about the impact of ageing on the biology of the above-mentioned cellular compartments will need extensive experimental validation.

Secondly, the nature of the analysed datasets is less than optimal. Given the fact that the differences in sample preparation could affect the relative frequencies of the HSC subpopulations that were identified in the analysed datasets, it would be critical to validate that the fluctuations observed with age in the analysed datasets are observed as well when both young and old donor HSCs are sorted from either fresh or thawed bone marrow and preferably processed using the same microfluidics chip and sequenced in the same sequencing run. Moreover, the human HSC compartment an ideal dataset would have been made from paired scRNA-seq datasets generated from sequential HSC samples gathered from a small cohort of both men and women under the age of 40 and over the age of 65, ages at which ageing rates accelerate at least in the immune system. A clonal architecture inference technique such as the one relying on the study of accumulation of mitochondrial mutations starting from the single RNA-seq data (93) could be used to reconstruct the clonal architecture at both timepoints. Furthermore, such a technique would allow us to associate a clonal expansion with a certain transcriptomic profile, thus allowing a more robust assignation of the

transcriptomic profiles found in the HSC clones that expand with age. In the case of the study regarding the ageing of the memory T cell compartment, a sample distribution with a gender ratio reflective of the population it was sampled from across the whole available age range would allow for understanding the impact of gender in the ageing of this compartment. Moreover, in order to rigorously assess the impact of COVID-19 recovery on the ageing associated phenotype, ideally samples before the infection, during the acute phase of the infection and convalescence would be needed from the same individuals, thus allowing to deconvolute which are the ageing and which are the COVID-19 dependent transcriptomic features with a high degree of confidence. Such samples could be collected during the next COVID-19 epidemic waves.

Thirdly, the conclusions of these studies will need to be validated by the analysis of technically similar datasets from different sources. This is particularly obvious in the case of the study regarding the impact of ageing on the memory T cell compartment in which the ageing memory T cell signature's properties need to be validated using a cohort extracted from a different genetic background. Moreover, the observations made about the capacity of the ageing memory T cell signature to segregate a COVID-19 convalescent patients starting from the transcriptomic data of the memory T cell compartment will need to be validated using an independent patient cohort.

Lastly, in the field of computational biology there are active debates on how to perform DGEA in the context of scRNA-seq data from multiple biological replicates (333,342,423) as well as how to mitigate for the unwanted variance caused by technical

factors without compromising the integrity of the biological signal that is investigated by the experiment (326,339). Given the influence of the batch correction and differential gene expression procedures to the conclusion of our study, in future studies that will be aimed to confirm the findings of this one, the analysis methodology will need to be updated to reflect the current state of the art in terms of the computational tools available for those analyses.

Conclusions

Human biological ageing comprises the molecular and physiological changes that negatively affect homeostasis with age and are strongly associated with susceptibility to disease and ultimately death (1–7). Understanding the biological processes underpinning ageing has the potential to revolutionise how we understand the pathophysiology of many diseases and in the process alleviate societal pressures.

In this thesis, we have aimed to use single cell transcriptomics to study two cellular compartments and how ageing impacts on their transcriptome and potentially the functionality in the context of health and disease.

Firstly, we have studied the HSC compartment to understand if a phenomenon encountered in mice with ageing, the existence of HSCs with an output biased towards platelet generation that expand with age, also occurs in humans. Secondly, we have studied how ageing shapes the transcriptome of the memory T cell compartment followed by a study to understand if recovering from a severe case of COVID-19 shares similar biological processes with ageing in the context of the memory T cell compartment of a healthy donor cohort.

Our study of the HSC compartment has shown that computationally defined HSC subpopulations exhibiting the gene expression patterns associated with platelet bias in

murine HSCs can be identified in healthy adult human males. By comparing data from healthy old and young males, it was shown that the previously identified HSC populations is enriched in old individuals. Moreover, this population exhibited the transcriptomic features associated with previously documented HSC populations with high self-renewal capacity and quiescence. Interestingly, with ageing there were no major shifts in which pathways were upregulated or downregulated, but more of an accentuation of the transcriptomic programmes already present at younger ages.

An inflammatory gene expression signature was shown to be characteristic of the phenomenon of ageing as observed at the level of the transcriptome of the memory T cell compartment of a healthy human cohort that was analysed. This observation was done by considering age as a continuum and described known signalling pathways associated with the ageing phenomenon in the T cell compartment such IL-10 signalling as well hinted at the evolvement of family of gene that have not been previously linked to T cell ageing such the aminoacyl-tRNA synthetases. Our study of the gene expression pattern associated with aging in the healthy cohort as well as the ones observed while comparing different types of COVID-19 patients during their recovery has revealed that at the level of the memory T cell compartment ageing and recovering from a severe case of COVID-19 share common biological pathways. By leveraging a machine learning-based methodology, it was shown that the most important aspects that are shared between ageing as a perturbation and recovering from COVID-19 are IL-10 signalling and BAX-mediated apoptosis, at least at the level of the memory T cell compartment.

The potential functional implications of the ageing associated observations made in the human HSC and memory T cell compartments remain open questions that could potentially allow us to understand what are the signals that determine fate specifications in HSCs and the long-term deleterious effects of experiencing a respiratory viral infection on the functionality of the adaptive immune system.

Appendices

Appendix figures

Appendix figure 1

A. Distribution of AUCell scores used to determine the computationally defined HSC populations in each cluster in the young donor HSC dataset. The AUCell distributions were compared between clusters in a pairwise fashion and the magnitude of the differences observed in these comparisons was quantified using the Wilcoxon rank sum test. Comparisons in with the magnitude of the difference between the clusters compared did not reach statistical significance (Benjamini Hochberg adjusted p-value <0.05) were not highlighted.

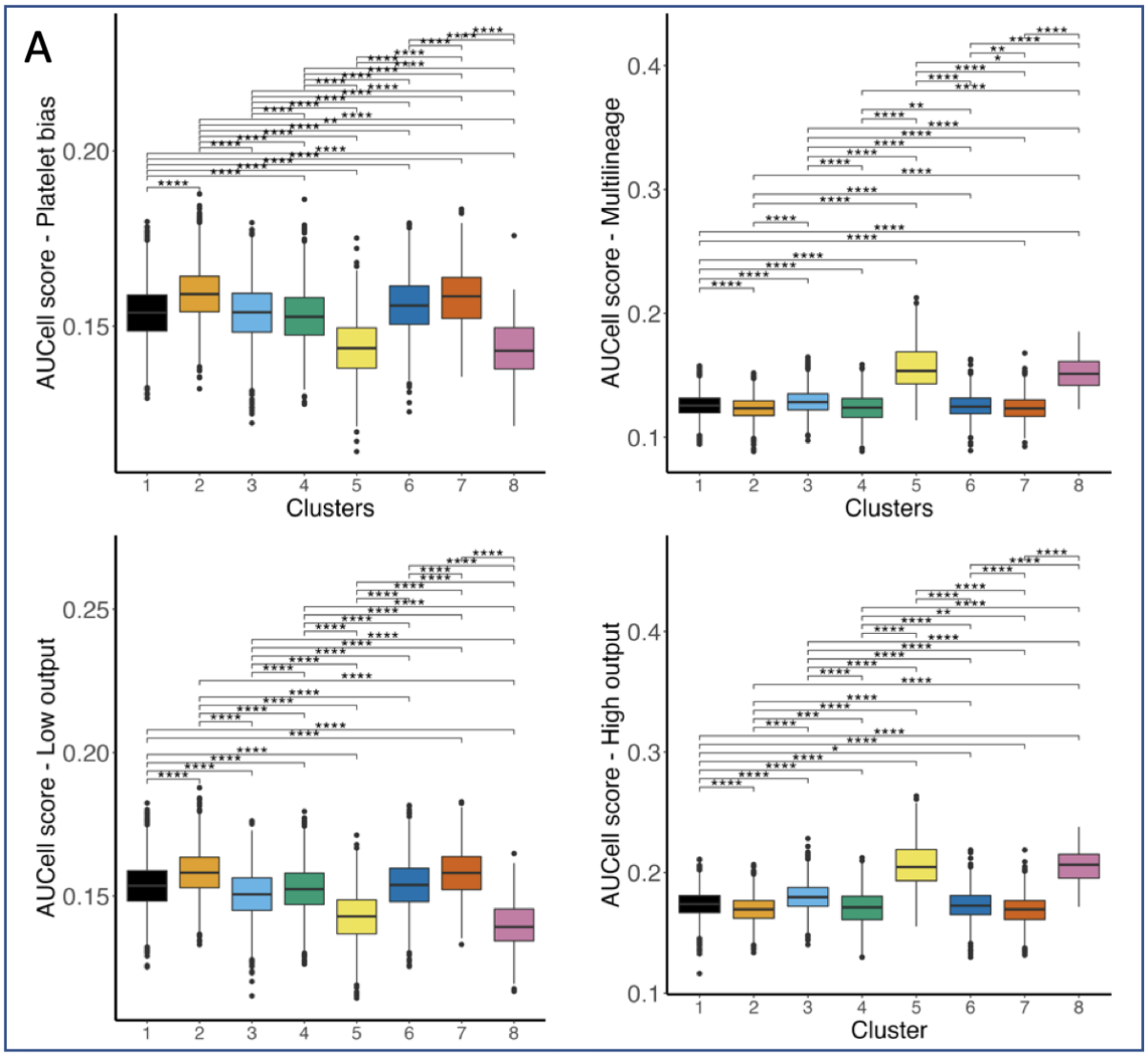

B. Distribution of AUCell scores used to determine the computationally defined HSC populations in each cluster in the old donor HSC dataset. The AUCell distributions were compared between clusters in a pairwise fashion and the magnitude of the differences observed in these comparisons was quantified using the Wilcoxon rank sum test. Comparisons in with the magnitude of the difference between the clusters compared did not reach statistical significance (Benjamini Hochberg adjusted p-value <0.05) were not highlighted.

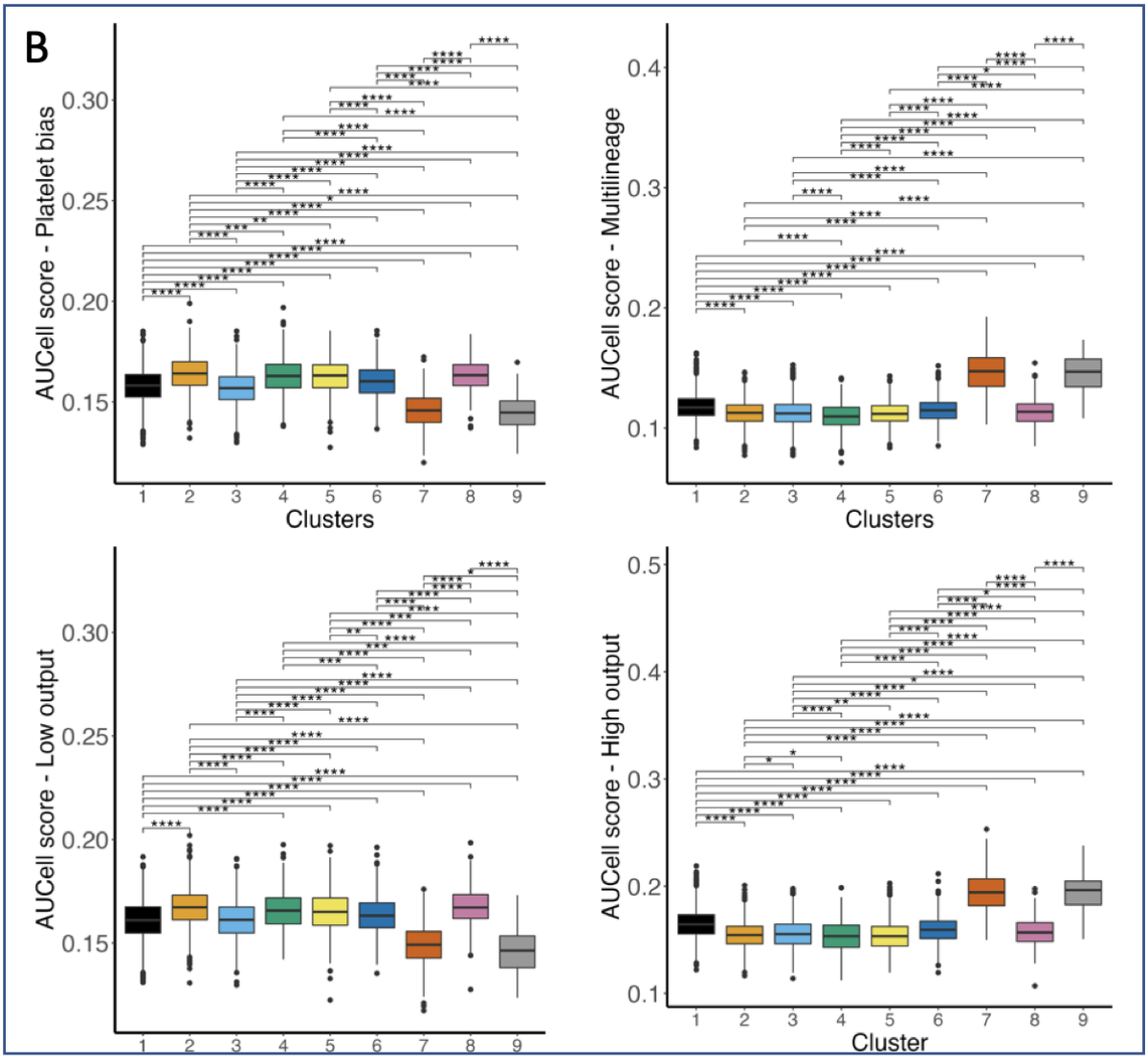

C. Distribution of AUCell scores used to determine the computationally defined HSC populations in each cluster in the integrated HSC dataset. The AUCell distributions were compared between clusters in a pairwise fashion and the magnitude of the differences observed in these comparisons was quantified using the Wilcoxon rank sum test. Comparisons in with the magnitude of the difference between the clusters compared did not reach statistical significance (Benjamini Hochberg adjusted p-value <0.05) were not highlighted.

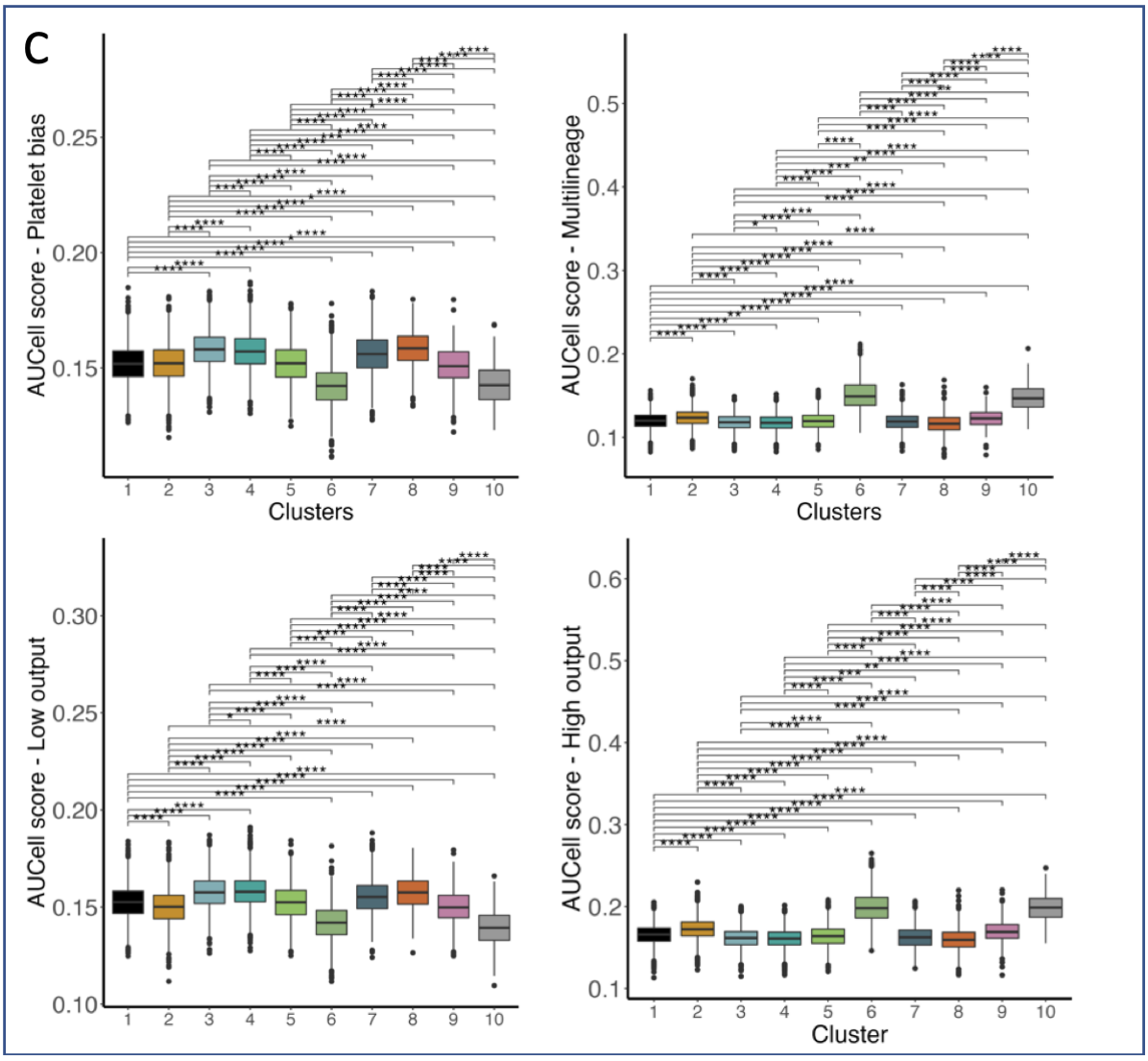

Appendix figure 2

Genes differentially expressed in computationally defined platelet biased (right) versus the computationally defined multilineage output (left) HSCs from the young donor dataset. Labelled genes represent the genes common between the ones that were differentially expressed (FDR <0.05) between the lineage tracked platelet biased HSC clones versus the multilineage output ones, the genes that were differentially expressed between the computationally defined platelet biased HSCs versus their multilineage counterparts in the the young donors and the genes used to calculate the AUCell scores representative of the computationally defined platelet biased and multilineage HSC populations in the young dataset (Figure 5A and Appendix figure 3)

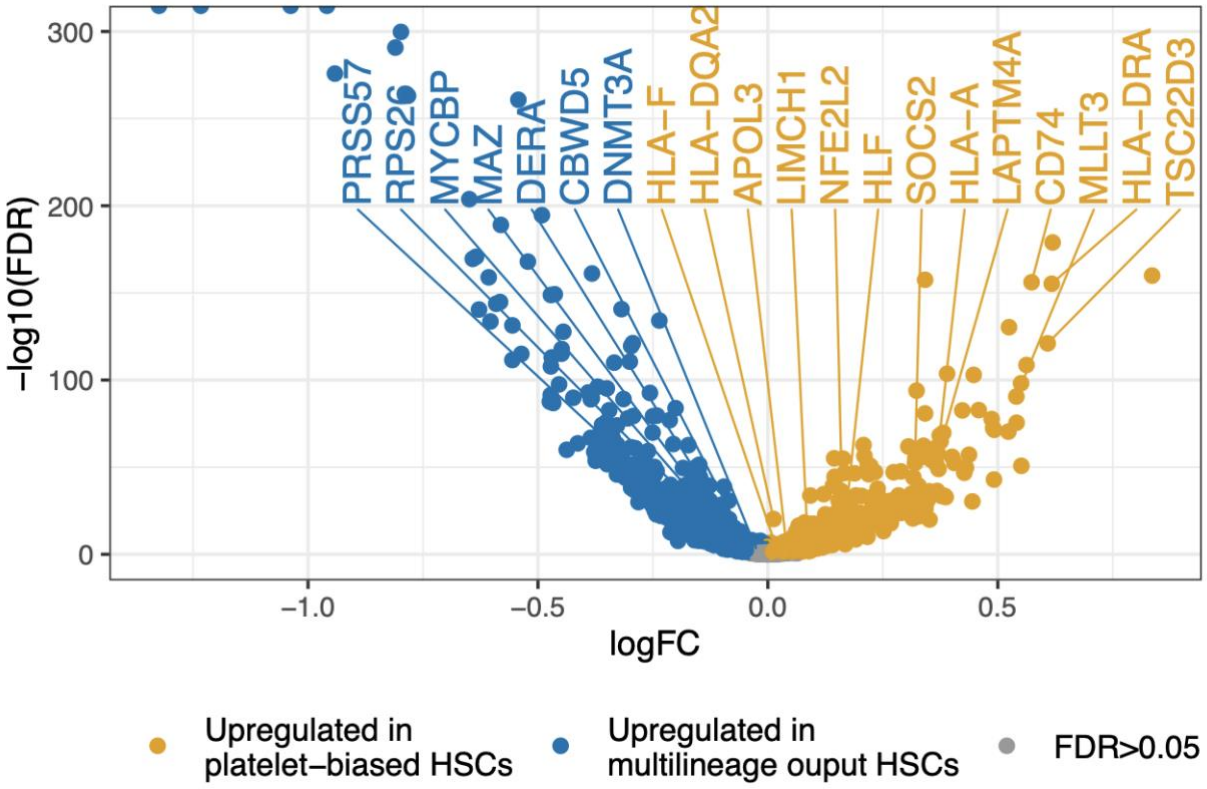

Appendix figure 3

A. Correlation between AUCell scores computed for young and old HSC datasets separately. All the HSCs profiled in the old and young HSC datasets are represented. The strength and directionality of the correlation was quantified using Kendall's τ correlation coefficient.

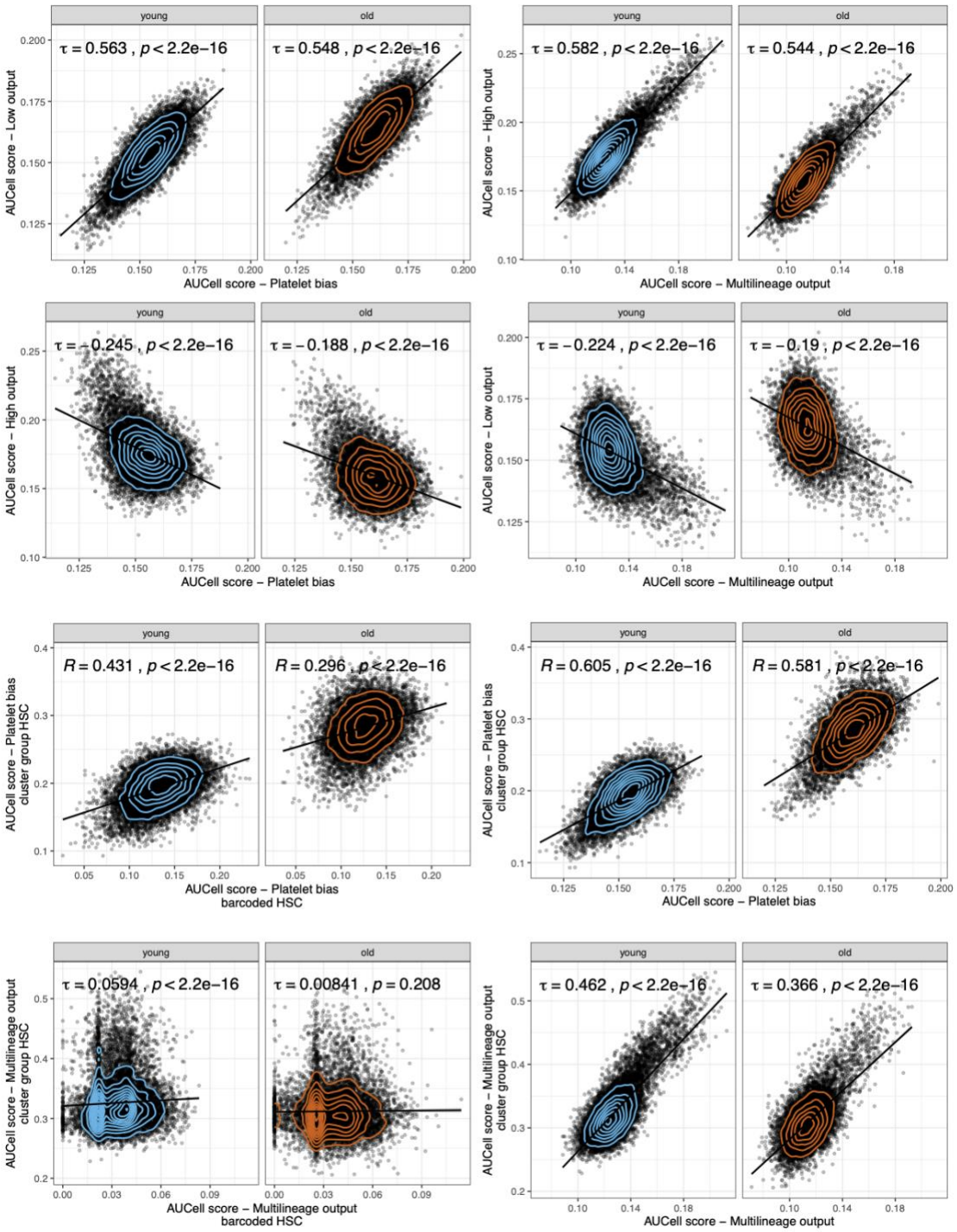

B. Correlation between AUCell scores computed for the integrated HSC dataset. All the HSCs profiled in the old and young HSC datasets are represented. The strength and directionality of the correlation was quantified using Kendall's τ correlation coefficient.

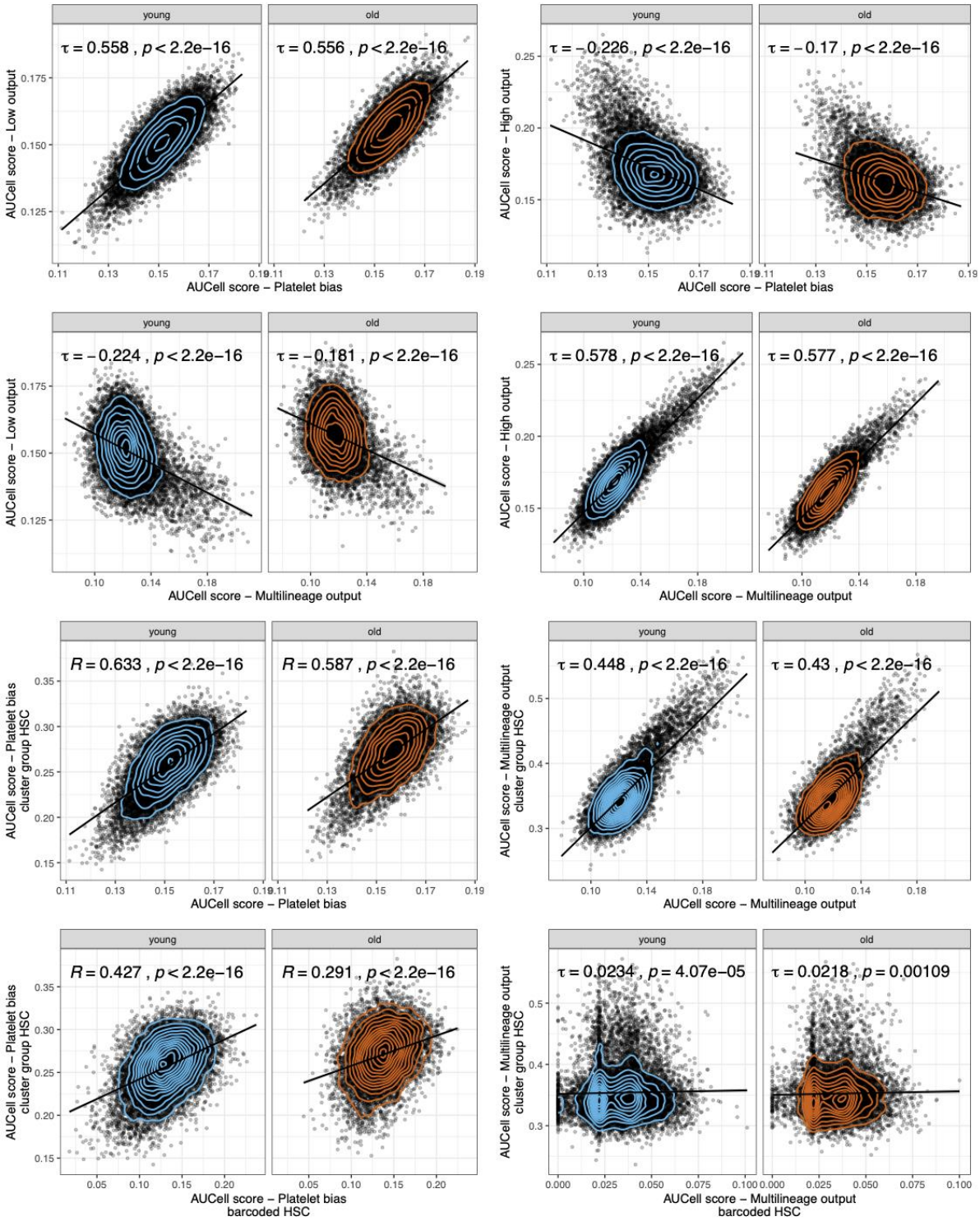

Appendix figure 4

Mosaic plot representing the frequency of each HSC subpopulation from the total cells in all the possible donor pair configurations including one young and one old donor. The HSC population assignation was done in the context of the integrated HSC dataset analysis; shading represents the Pearson residual of the χ^2 test used to assess (p-value listed in the figure) the dependency relationship between donor age group and the HSC subpopulation.

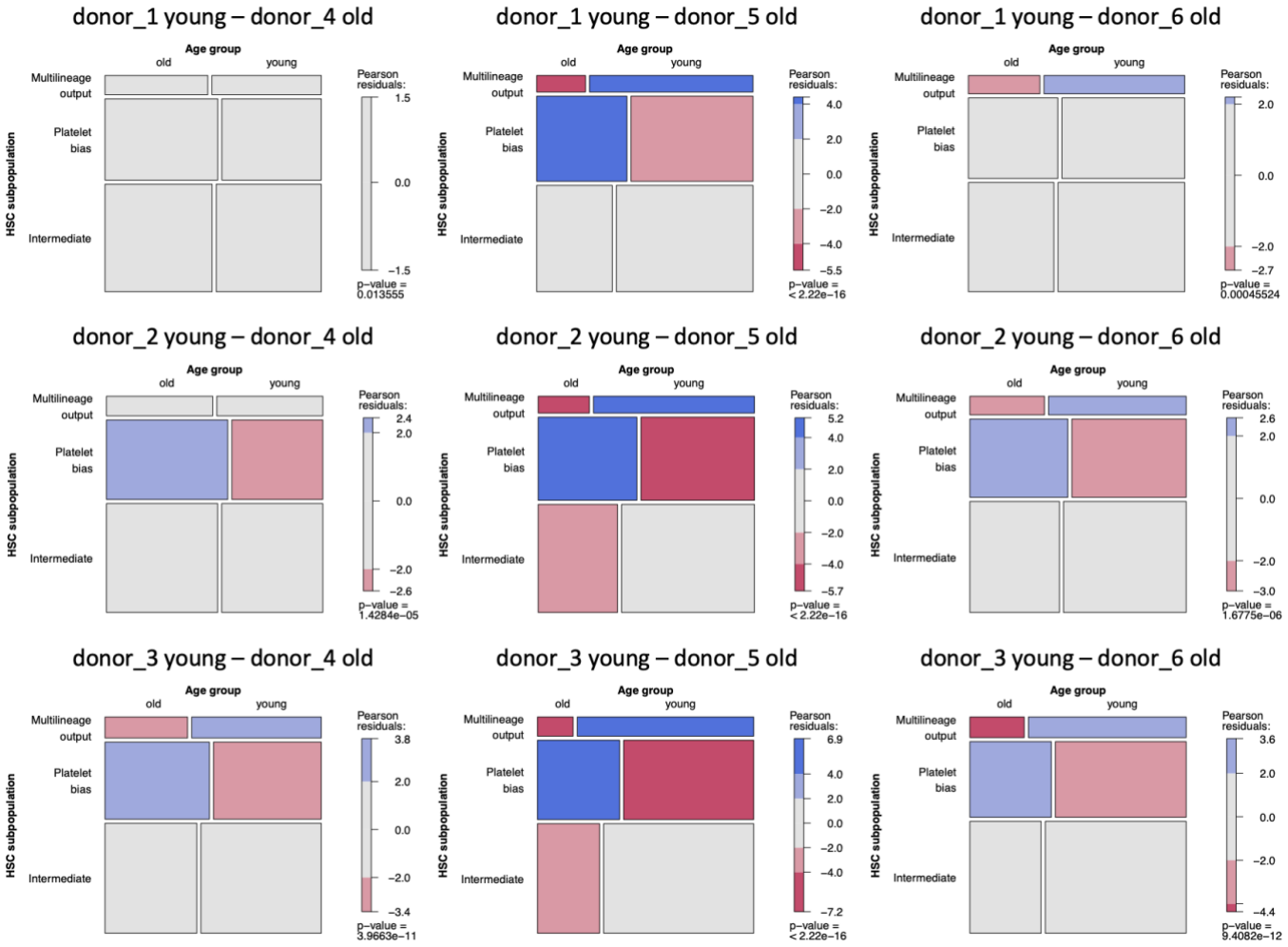

Appendix figure 5

Clustering tree visualisation (361) describing how the cluster identify of the cells in the healthy donor cohort dataset is changing as the resolution parameter changes; the size of the cluster is represented by the size of the circle and the shading of the arrow connecting the clusters the proportion of how many cells from cluster changes cluster identity with the change in the resolution parameter of the clustering algorithm.

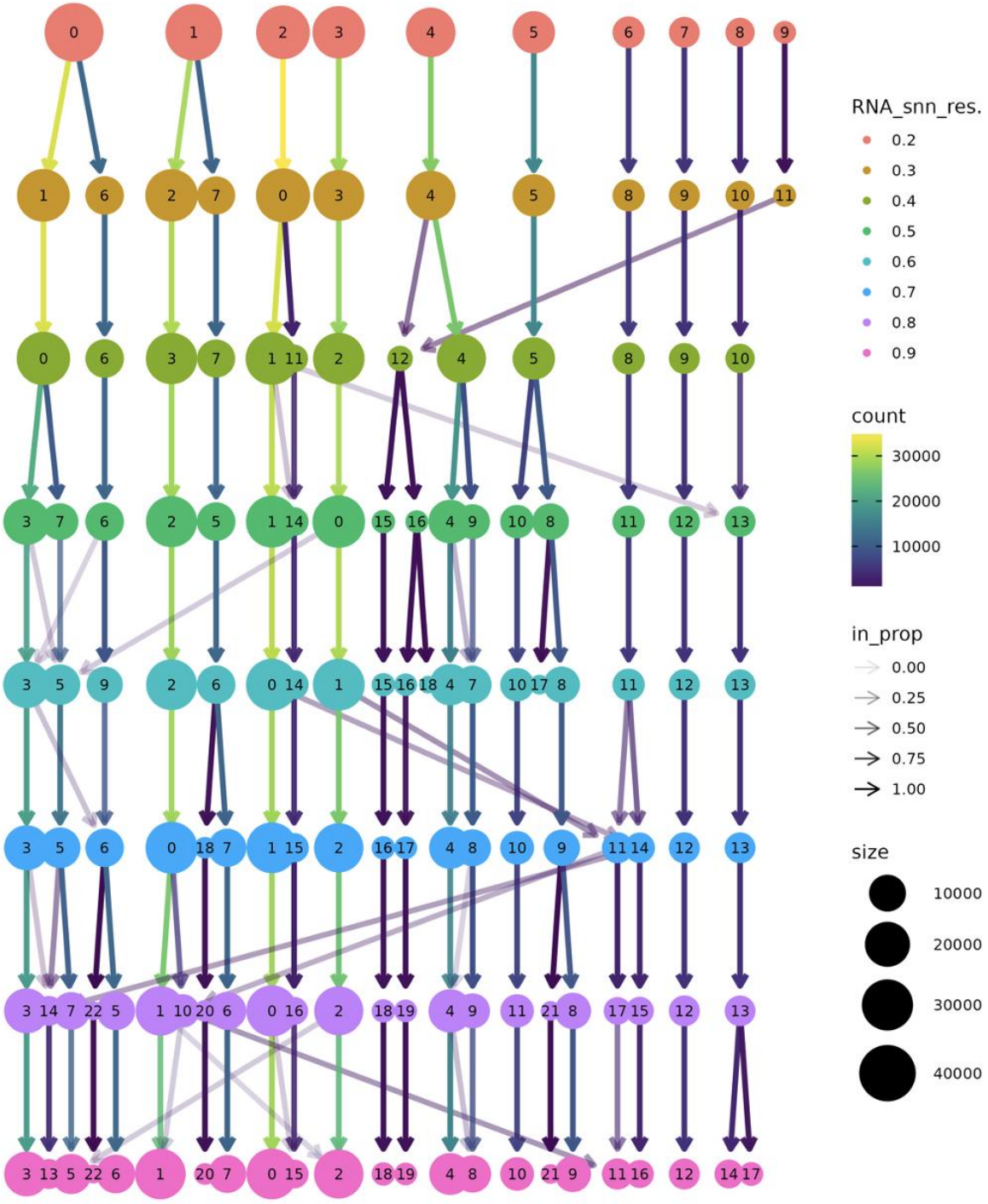

Appendix figure 6

The distribution of the normalised UMI counts across T cell types in the healthy cohort donor dataset for the canonical markers for the following T cell types: naïve (CCR7, PECAM1), TCM (CCR7, CD27), TEM (EOMES), TEMRA (EOMES, KLRG1), Treg (FOXP3), MAIT (ZBTB16), γδ (TRDC). The magnitude of the differences observed while comparing the normalised UMI distributions for each gene between cell types was quantified using the Wilcoxon rank sum test in a pairwise manner. Comparisons in with the magnitude of the difference between T cell types compared did not reach statistical significance (Benjamini Hochberg adjusted p-value <0.05) were not highlighted.

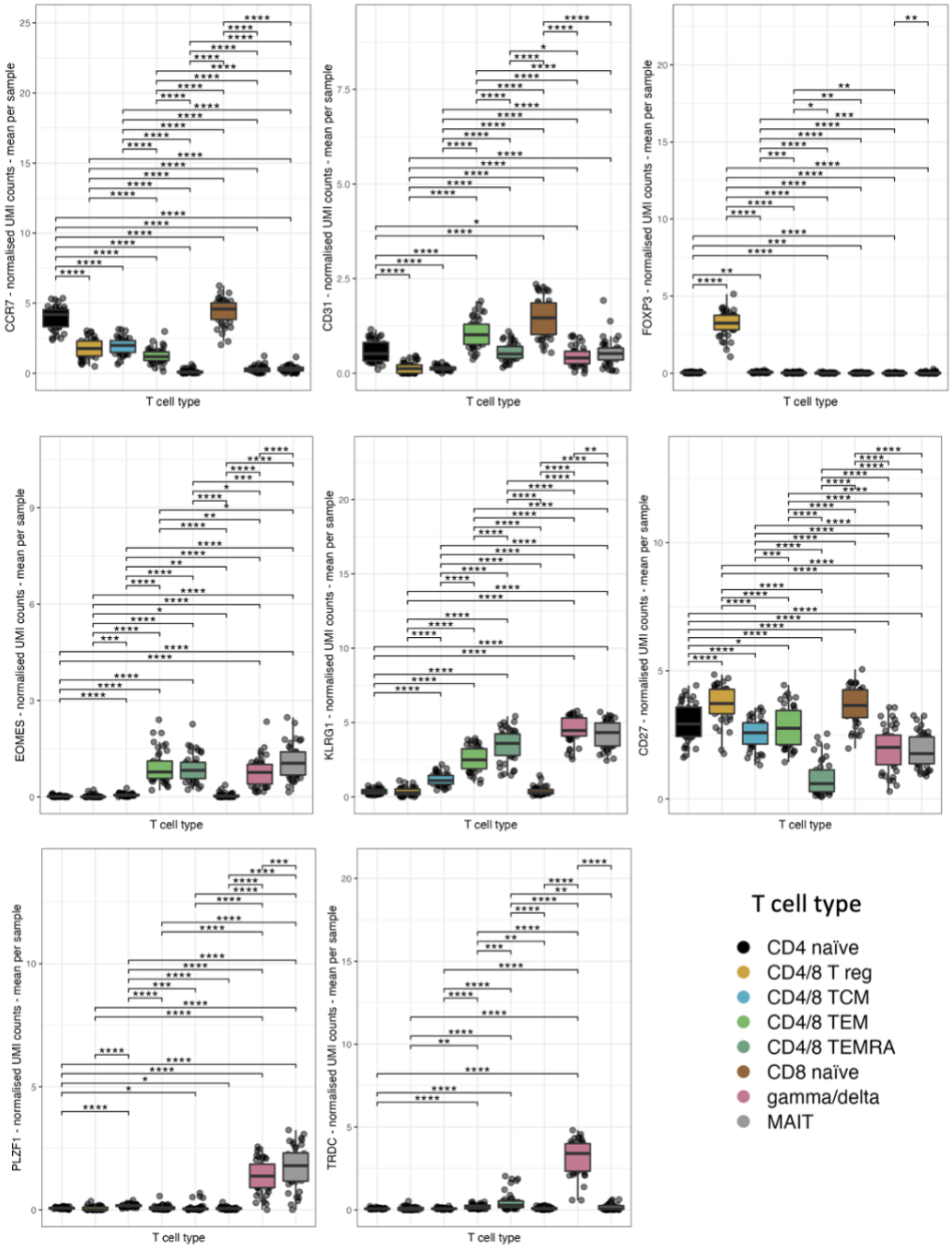

Appendix figure 7

Relationship between the size of the T cell populations and the age of the donor in the healthy donor dataset. The strength and directionality of the correlation was quantified using Kendall's τ correlation coefficient. Data from the Ren dataset and the Stephenson one is represented side by side to emphasise which trends are robustly reproduced across datasets.

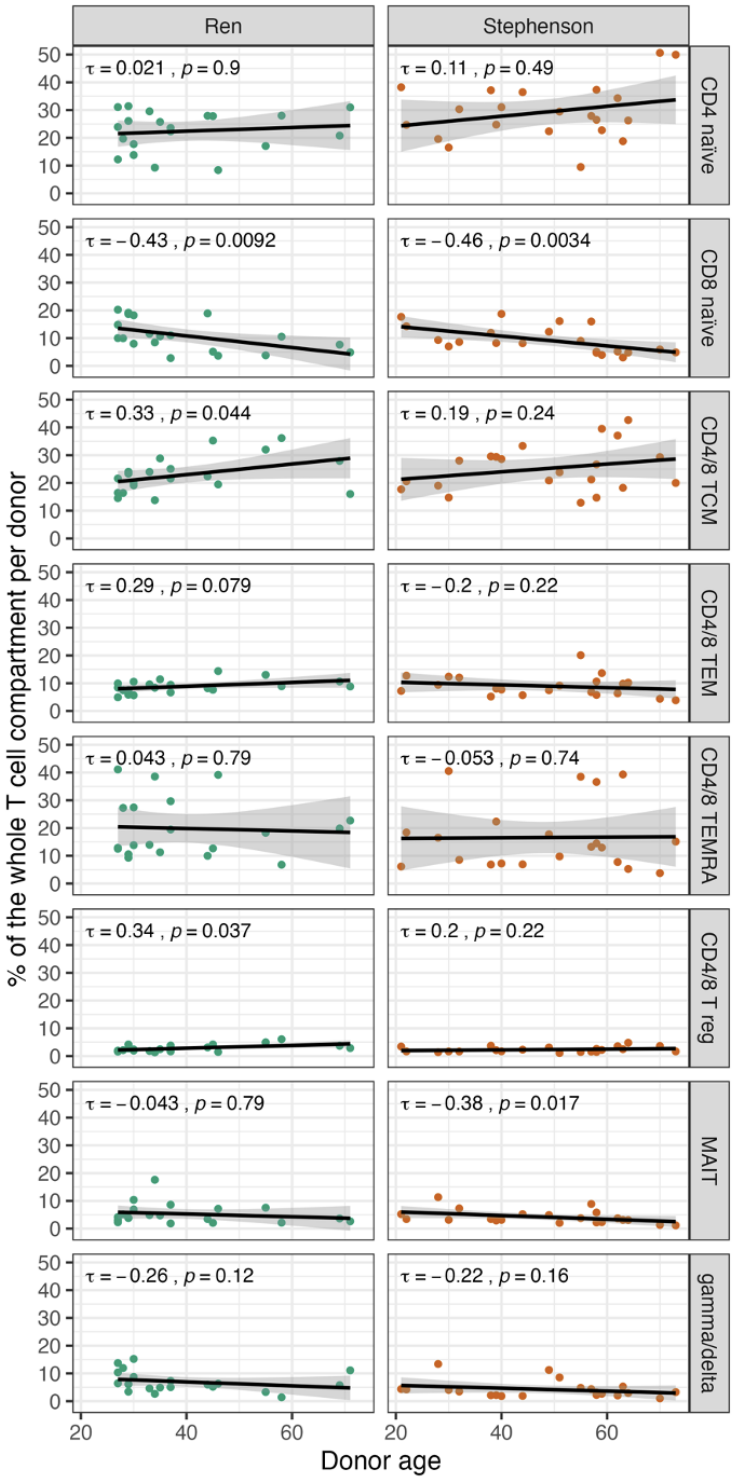

Appendix figure 8

Clustering tree visualisation (361) describing how the cluster identify of the cells in the COVID-19 convalescent cohort dataset is changing as the resolution parameter changes; the size of the cluster is represented by the size of the circle and the shading of the arrow connecting the clusters the proportion of how many cells from cluster changes cluster identity with the change in the resolution parameter of the clustering algorithm.

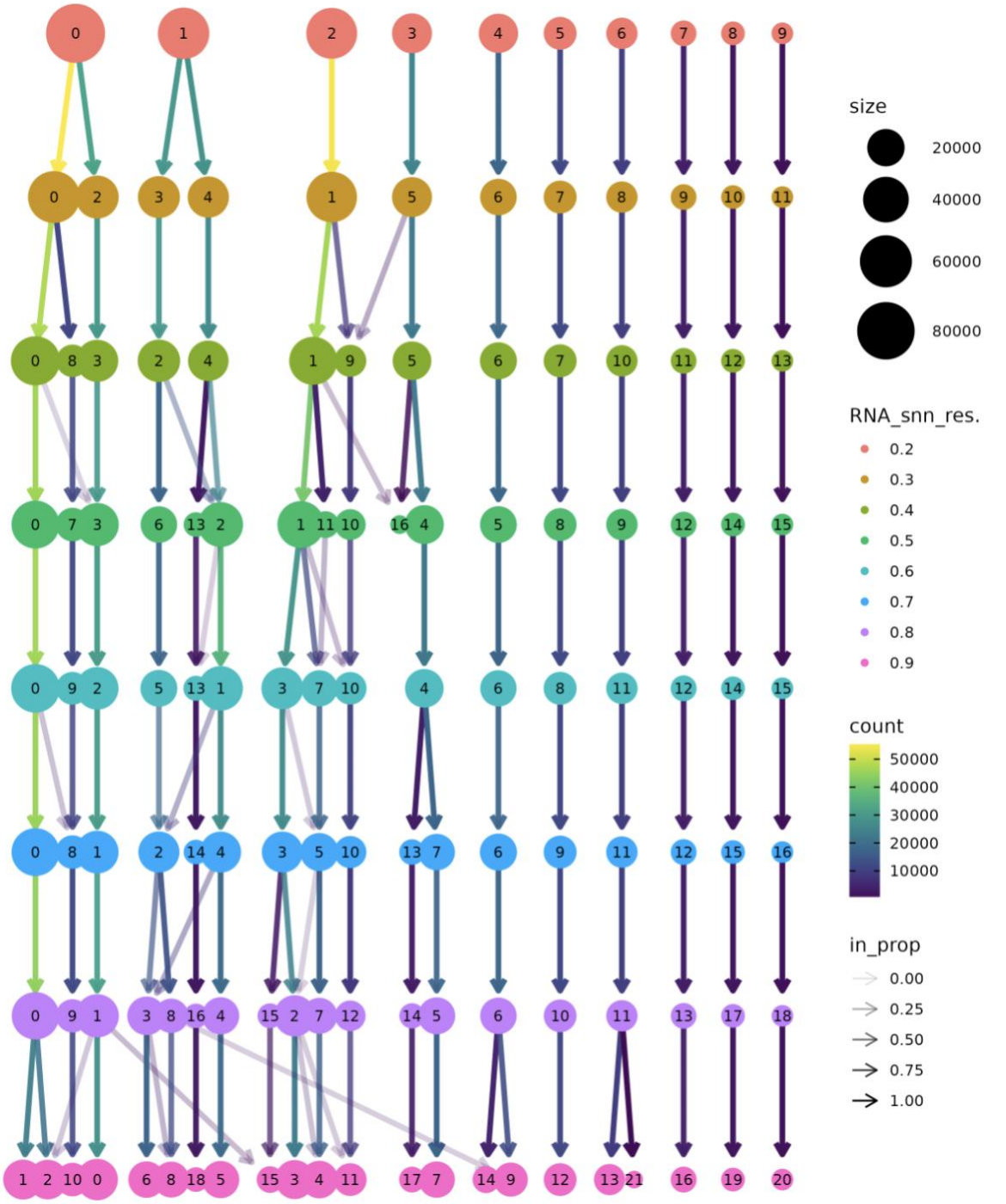

Appendix figure 9

The distribution of the normalised UMI counts across T cell types in the he COVID-19 convalescent cohort dataset for the canonical markers for the following T cell types: naïve (CCR7, PECAM1), TCM (CCR7, CD27), TEM (EOMES), TEMRA (EOMES, KLRG1), Treg (FOXP3), MAIT (ZBTB16), γδ (TRDC). The magnitude of the differences observed while comparing the normalised UMI distributions for each gene between cell types was quantified using the Wilcoxon rank sum test in a pairwise manner. Comparisons in with the magnitude of the difference between T cell types compared did not reach statistical significance (Benjamini Hochberg adjusted p-value <0.05) were not highlighted.

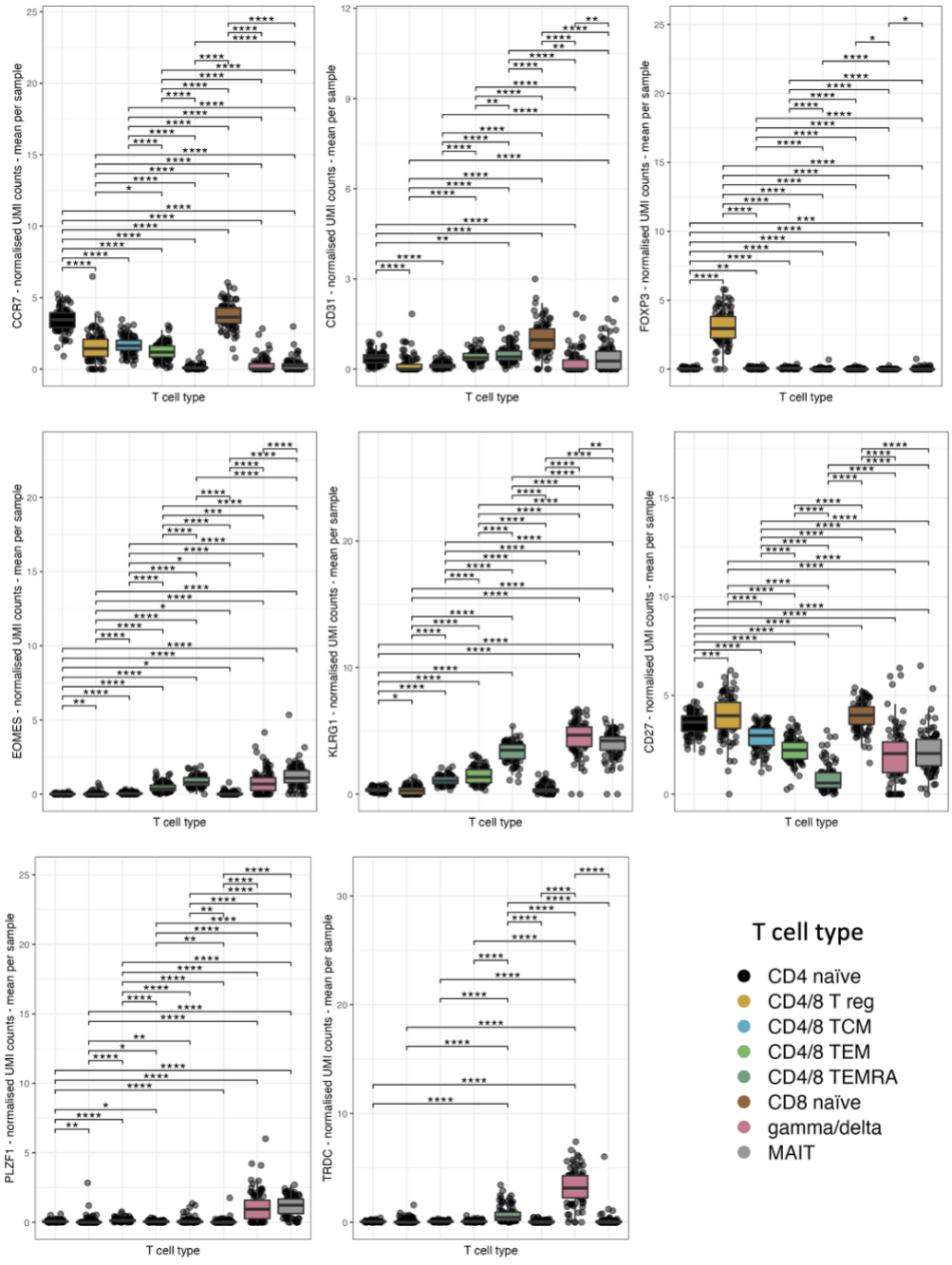

Appendix figure 10

A. Association between the frequency of acute severity class for each donor and demographic, comorbidity or viraemia status labels. Only the associations that with a p-value for the Fisher's exact test or the χ^2 test are represented.

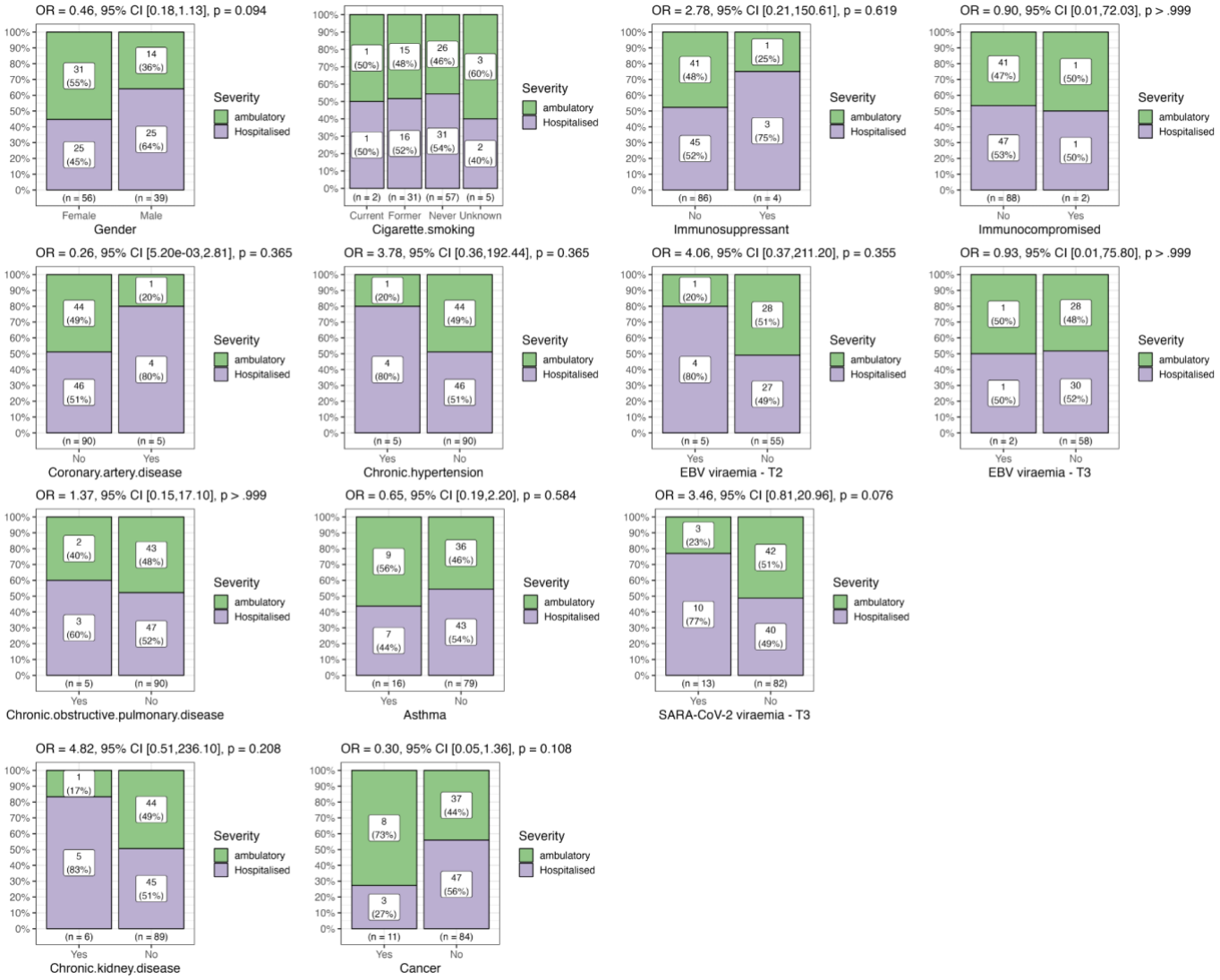

B. Association between the frequency of respiratory PACS class for each donor and acute severity, demographic, comorbidity or viraemia status labels. Only the associations that with a p-value for the Fisher's exact test or the χ^2 test are represented.

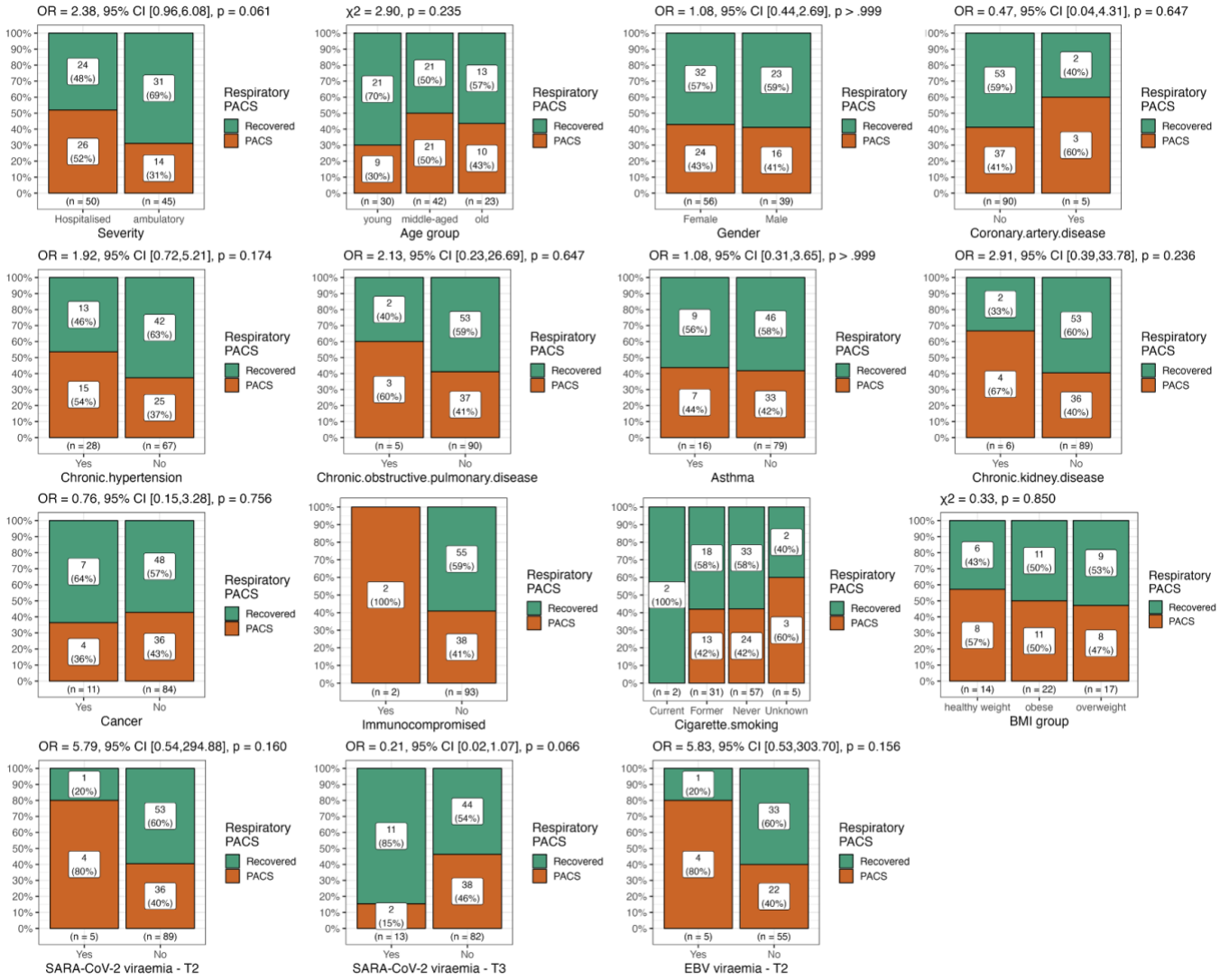

Appendix figure 11

3D UMAP representations of the HSC scRNA-seq datasets and the computationally defined HSC populations in the case of young donors (A), old donors (B) and in the context of the integrated analysis (C).

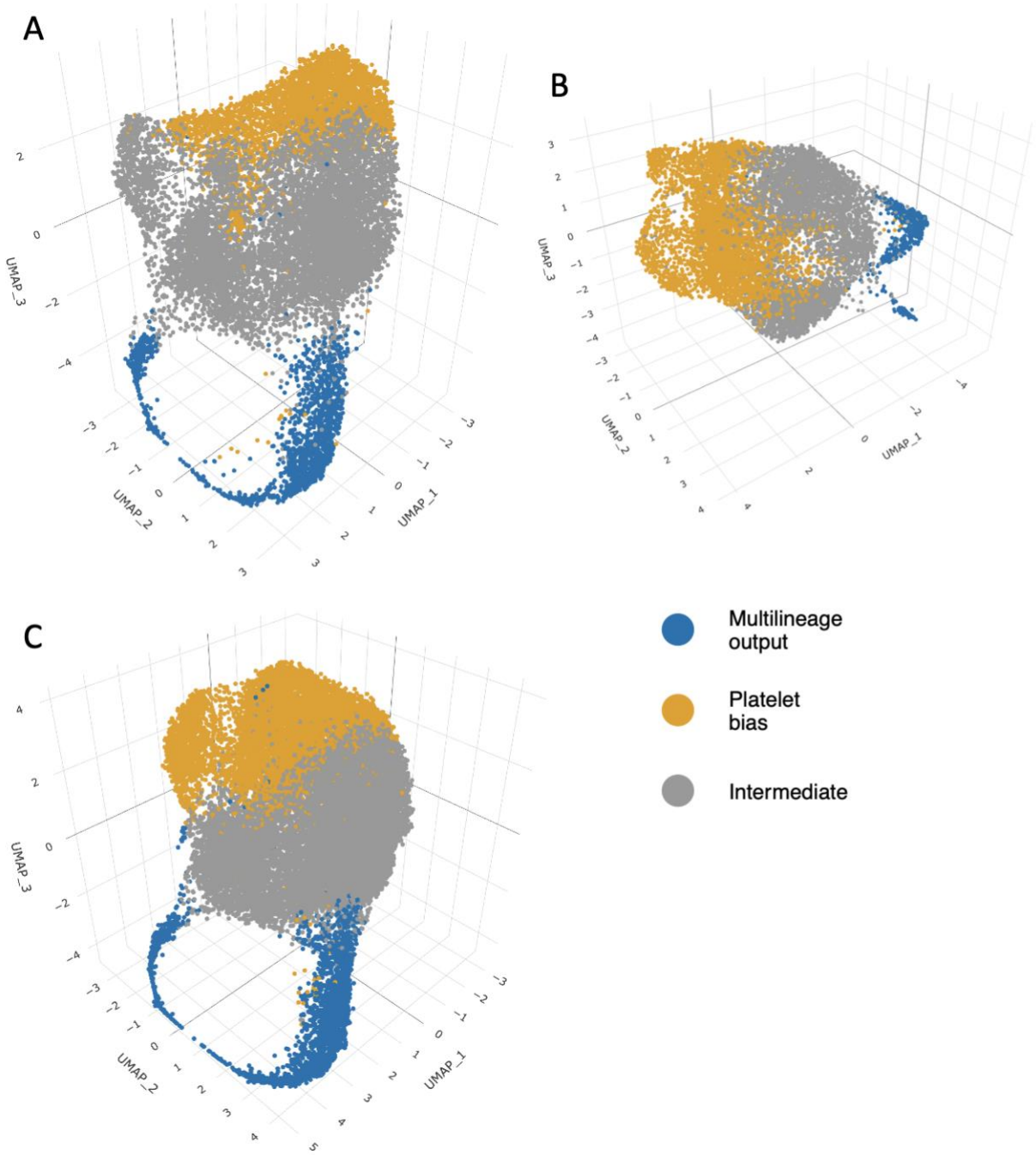

Appendix tables

Appendix table 1

Lists of the leading-edge genes for the previously gene sets that have enrichments or depletions with an FDR <0.25 only in one age group – meta-analysis of the young and old donor HSC datasets.

Gene sets significantly enriched only in platelet-biased HSC from young donors						
Pietras_2015_HSC	Rodriguez-Fraticelli_2020 serial_engraftment_HSC	Anjos-Afonso_2022 EPCR- HSC	HALLMARK_INTERFERON_ GAMMA_RESPONSE	HALLMARK_INTERFERON ALPHA_RESPONSE	HALLMARK_KRAS_ SIGNALING_DN	HALLMARK_INFLAMMATORY RESPONSE
HLA-E	SRGN	SNRPD1	CD74	CD74	NR4A2	BST2
MLLT3	MLLT3	SNRPE	HLA-DRB1	BST2	SELENOP	PTGER4
SOCS2	JUNB	CDK6	BST2	HLA-C	TENT5C	IL18
N4BP2L2	NR4A2	ATP5MF	HLA-A	TXNIP		EMP3
TXNIP	CLU	LDHB	HLA-B	ELF1		NAMPT
ALDH1A1	ITM2B	IGLL1	HLA-DMA	GBP4		SCARF1
PTGS1	PTGER4	RPS21	HLA-DQA1			CD82
MYCT1	NACA	ABRACL	TXNIP			SELL
MAGED2	SOCS2	EEF1B2	ARL4A			TNFSF10
EEF2	N4BP2L2	MZT2B	CFH			
MAFF	S100A6	SMIM24	VAMP5			
CTSF	PNRC1	IGFBP7	STAT3			
HLF	ALDH1A1	RFC2	GBP4			
ARL4A	TSC22D1	CD69				
GATA3	LST1	RPS3A				
TMEM59	HLF	RPS7				
EID1	SAT1	MATK				
BEX4	GATA3	HSBP1				
BEX2	BEX4	VRK1				
TFPI	BEX2	CKS2				
EMCN	TFPI	ARMH1				
ARMCX1	POU2F2	MDH1				
DST		RPS17				
RPL7						
GSTM3						
PRKACB						
ZSCAN18						
PHLDB2						
TBXAS1						
ROBO4						
SPART						
GBP2						
PBX1						
GABARAPL1						
SLC3A2						

Appendix table 1 -cont.

Gene sets significantly depleted only in platelet-biased HSC from young donors				Gene sets significantly enriched only in platelet-biased HSC from old donors	Gene sets significantly depleted only in platelet-biased HSC from old donors
HALLMARK_NOTCH_SIGNALING	HALLMARK_HEDGEHOG_SIGNALING	HALLMARK_MYC_TARGETS_V2	HALLMARK_PI3K_AKT_MTOR_SIGNALING	Cabezas_Wallscheid_2017_sc_dHSC	Tirosh_2016_G2M_phase
RBX1	CDK6	MCM4	PFN1	HLA-E	HMGB2
		MCM5	CFL1	SRGN	CKS1B
		UNG	CALR	CD37	
		CDK4	CDK4	FTH1	
		HSPD1		RPL35A	
		CBX3		RPL12	
		DCTPP1		EEF2	
		PA2G4		RPL31	
		HSPE1		RPS27	
		SRM		RPL30	
		TMEM97		RPS9	
				RPL13	
				EIF1	
				RPL18	
				RPL24	
				FAU	
				EEF1A1	
				RPL32	
				RPS2	
				RPS29	
				RPL38	
				RPL23A	
				RPS8	
				RPS25	
				RPL28	
				RPL29	
				RPL37	
				RPL19	
				RPL8	
				FTL	
				TPT1	
				PABPC1	
				RPL27A	
				RPL15	
				RPL10A	
				DDX5	
				PTPRC	
				RPL23	
				HSP90AB1	
				TXNIP	
				RPS20	
				TSC22D3	
				RPS11	
				ITM2B	
				RPS23	
				RPS28	
				SON	

Appendix table 2

A. GSEA – old donor vs young donor platelet-biased HSCs defined in the integrative analysis - gene sets pertaining HSC lineage bias (89,136,140,142,381) as well as the HSC self-renewal phenomena (132,363,364,367,382). Positive NES values indicate enrichment in the old donor platelet biased HSCs; only gene sets with an associated FDR < 0.25 are listed

Gene set	pval	FDR	log2 err	ES	NES	size	leadingEdge
Xie_2019_ER_Stress	4.27E-04	2.88E-03	4.98E-01	6.04E-01	1.61E+00	292	HSPA6, HSPA5, JUN, TXNDC5, HSPA2, HERPUD1, ATF3, IFIT1, VEGFA, SLC7A5, EIF4A3, DNAJB9, DNAJB1, PPP1R15A, LMNA, CEBPB, DNAJB5, ERLIN1, THBS1, STUB1, UBQLN2, CXCL8, HSPD1, HSP90B1, EIF4A2, PDIA3, DDIT3, EIF2B5, EIF2S1, PSMC2, TMX4, CLU, UBQLN1, XBP1, SDF2L1, DNAJA1, TXNDC11, EIF4E, EXOSC8, DDIT4, PIK3R2, DNAJB11, FAF2, DDX10, SPCS1, PDIA6, DCP1A, KDELR3, ACADVL, TRIM13, SEC63
Rodriguez-Fraticelli_2020_Platelet_bias_HSC	1.77E-06	2.38E-05	6.44E-01	5.44E-01	1.56E+00	696	GABARAP, KLF2, MYOF, C18orf32, PGR, DUSP1, JUN, CITED2, PPIC, KLF6, PDZK1IP1, ZFP36, FOS, AK1, SELP, ADGRL4, INSIG1, PIANP, AMIGO3, PCDHB10, NOS1AP, JUNB, TSC22D1, CADPS2, B2M, TM4SF1, PPP1R15A, GIMAP5, MSMO1, CD9, TMEM176A, RGP1, COL4A2, RUNX1T1, CEBPB, RPL7, CDKN1C, ABCG2, ASAP3, TNFSF10, MICA, IER2, NKX2-3, JUND, MMRN1, RGS1, CRACR2B, CLEC14A, CISH, CD74, KIFC3, KRT18, MAP2K1, PANX2, EVC, TMEM158, NEURL3, LDHB, ECSCR, TGM2, ZFP36L2, RPL34, PTPRM, WT1, ID2, PTGS1, FAM210B, ST7L, ALDH1A1, HOXB6, DLG2, APP, SRXN1, FAM43A, ADTRP, BHLHE40
Rodriguez-Fraticelli_2020_Low_output_HSC	4.79E-09	1.29E-07	7.61E-01	5.29E-01	1.56E+00	1109	GABARAP, SNX15, KLF2, MYOF, TJP2, PGR, PNP, IFNB1, HSPA5, DUSP1, CAMK2A, CITED2, PPIC, KLF6, PDZK1IP1, RHOB, IFIT2, FOS, IFIT3, AK1, TSPAN9, SELP, ADGRL4, CA2, INSIG1, MSRB2, CCL20, AMIGO3, PCDHB10, NOS1AP, DNAJB9, TSC22D1, CADPS2, ACOT2, B2M, TM4SF1, PPP1R15A, TSC22D3, DKKL1, TCEAL6, GIMAP5, CTF1, TMEM176A, RGP1, COL4A2, CEBPB, APBA2, MCL1, KLF4, RPL7, CDKN1C, AFAP1L1, FOSB, ABCG2, ASAP3, RASL11A, TNFSF10, MICA, FAF1, NKX2-3, JUND, BBC3, MMRN1, GAS6, BHLHE41, IL21R, RGS1, CD81, CRACR2B, ISG20, ADRB2, CISH, UBQLN2, CD74, UPP1, KRT18, MAP2K1, PANX2, EVC, TMEM158, NEURL3, LDHB, DNALI1, IRAK3,

							ECSCR, FAM107A, MOBP, TGM2, STARD4, PLPP2, ZFP36L2, WT1, HES1, FTL, DMXL2, FAM210B, ALDH1A1, TXNDC15, HOXB6, DLG2, APP, DCAF12L2, FAM43A, VWA5A, BHLHE40, ANG, ATPAF1, RCHY1, MTUS1, FAS, GFI1, CLU, MARVELD1, GRAMD1C, PCF11, PRICKLE1, COPS8, LRPAP1, S100A6, XBP1, PFDN5, SLC6A6, NR4A2, PIM1, APOL4, NOC3L, BEX1, EIF1, SH3BP5, EIF4E, FKBP7, RHOF, BEX4, KCNK5, ITGA6, EHD4
Giladi_2018_StemScore	2.95E-02	7.96E-02	1.41E-01	7.22E-01	1.53E+00	48	PDZK1IP1, CA2, ACOT2, DKKL1, TMEM176A, RGS1, CD81, CISH, CD74, KRT18, CD274, LDHB
Xie_2019_Protein_Folding	6.38E-03	3.44E-02	3.35E-01	6.12E-01	1.52E+00	155	HSPA6, HSPA5, TXNDC5, HSPA2, DNAJB1, UBC, SPHK1, HSPD1, HSP90B1, PDIA3, CCT8, TMX4, CLU, TXNDC11, PFDN2, FKBP7, TRAP1, RGS9, EMC4, FKBP5, GNB2, PDIA6, CHORDC1, VAPA, GNAI3, EMC2
Cabezas_Wallscheid_2017_bulk_dHSC	1.16E-04	1.04E-03	5.38E-01	5.15E-01	1.46E+00	610	HBA2, FABP4, KLF2, MYOF, HBA1, PNP, GPR183, PDZK1IP1, HSPA2, ZFP36, SAT1, DUSP2, NRP1, INSIG1, TSC22D1, ACOT2, B2M, EPHX1, TSC22D3, DKKL1, GIMAP5, TMEM176A, XDH, RUNX1T1, RPL7, IFNGR1, GPR171, MICA, NOVA1, NUDT12, CISH, TRIB1, LDHB, BRWD1, CNBD2, MB21D2, ECSCR, TGM2, ZCCHC12, ID2, FTL, XRN1, CD247, ANXA1, SESN1, SRXN1, HBP1, VPS45, PPP1R16B, PRKAA2, GFI1, BLZF1, S100A6, XBP1, SNRPN, CDC26, RBM47, CTSS, BTG1, IDH1, SH3BP5, CD2, LPIN1, ARID5A, TP53INP1, LGALS3, ATP6V1B2, GLUL
Xie_2019_Autophagy	1.79E-02	6.04E-02	1.99E-01	5.71E-01	1.42E+00	158	GABARAP, UBC, CHMP4B, TRIM17, SNF8
Anjos-Afonso_2022 EPCR+ HSC	1.16E-02	4.48E-02	2.70E-01	5.22E-01	1.40E+00	295	MYOF, TNFRSF12A, CPE, ETV3, MIR29B2CHG, STX1A, MIDN, ABI3, FGL2, VEGFA, RTN1, PLK3, MIR22HG, COL9A3, SLC2A3, NOTCH4, MAFB, AQP1, COL4A2, EMP2, PELI1, ALOX5, PLAUR, ANXA2, GAS6, IL21R, THBS1, ZNF331, TUBA4A, CLEC14A, RELT, UPP1, ALOX15B, DDN, PHLDB1, PLB1, TGM2, STARD4, TBC1D9, HES1, AHRR, PTGS1, CD36, DLGAP2, ID1, CLEC3B, ABI3BP, EPPK1, CPVL, IER3, PLVAP, THBD, CCDC149, CRYBG3, NR4A2, NDEL1, ZC3H12A, LONRF3, LRRC32, ARMCX4, EHD4, TOB1, CXCL16, ADM, IL13RA1, DENND3, ZNF423, SIRPB2, CLMN, TCOF1, PLEC, S100A11, TUBB4B, SPEG, ARFGEF3, VWF, NRIP3, LYZ, PDGFA, SORBS2
Pang_2011_elderlyHSC	1.09E-01	2.23E-01	6.91E-02	8.03E-01	1.37E+00	12	FOS, SELP, ANXA3, PTGS1, HOXA9

Montecino-Rodriguez_2019_Ly_biased_mHSC	9.12E-02	2.05E-01	8.01E-02	6.18E-01	1.35E+00	58	MYOF, MMRN1, CISH, DLG2, CLU, MAP9, ITGA6
Rodriguez-Fraticelli_2020_serial_engraftment_HSC	1.13E-02	4.48E-02	2.97E-01	4.79E-01	1.32E+00	439	CDKN1A, MYOF, GNG10, PGR, PNP, HSPA5, SH3GL3, SAT1, SELP, ADGRL4, DUSP2, ACKR1, JUNB, TSC22D1, TM4SF1, GIMAP5, UBE2H, DUSP4, TACSTD2, COL4A2, CEBPB, CDKN1C, TNFSF10, BHLHE41, TGIF1, MAP2K1, PANX2, TMEM158, TGM2, ZFP36L2, PTPRM, ID2, ALDH1A1, HOXB6, LYPLAL1, SESN1, DLG2, APP, FAM43A, GFI1, CLU, THBD, MARVELD1, SPCS2, S100A6, NR4A2, PIM1, NDEL1, BEX1, PFDN2
Belluschi_2018_My/Ery_biased_CD49f+HSCs	1.16E-01	2.23E-01	7.14E-02	5.83E-01	1.30E+00	68	MTRNR2L1, DUSP1, JUN, GRASP, HSPA1B, DNAJB1, UBC, TSC22D3, NEAT1, EIF5, FTH1, PELI1, FOSB, JUND, ANKRD28, CD74, ZFP36L2, FTL
Lauridsen_2018_RAdim_HSC	4.88E-02	1.20E-01	1.30E-01	4.68E-01	1.25E+00	288	MYOF, PDZK1IP1, SMAD7, POLD4, DUSP2, PTGES, TSC22D1, ACOT2, DKKL1, GIMAP5, TMEM176A, COL4A2, ABCG2, GAS6, CD74, UPP1, NEURL3, LDHB, ECSCR, FTL, TXNDC15, HOXB6, SESN1, HBP1, DDIT3, POLI, HOXA9, PPCDC, PIM1, CTSS, LPIN1, ARID5A
Pietras_2015_HSC	2.78E-02	7.96E-02	2.23E-01	4.13E-01	1.19E+00	748	MYOF, ARL4A, TJP2, ADAMTS1, SOX6, PPIC, ETV3, ASPA, SELP, CA2, LDB2, MAOA, ST14, COPZ2, CADPS2, EPHX1, TCEAL6, PHLDA2, STOX1, GIMAP5, GALNT5, DUSP4, TMEM176A, RPL7, AFAP1L1, TNFSF4, ABCG2, C11orf1, MMRN1, TCEA2, TNFRSF18, CD81, ISG20, CISH, FGFBP3, UPP1, KRT18, SPA17, CCDC28A, PPT1, LDHB, PRPS1, IRAK3, PAIP2, PON3, TGM2, STARD4, TMEM59, ACAT1, PTGS1, NOMO1, ALDH1A1, LYPLAL1, FAM110B, SUCLG2, GHR, SESN1, ACSS3, ARPP19, DLG2, SRXN1, CAV2, VWA5A, VPS45, TNFSF9, GRAMD1C, SERINC1, CTSW, BEX1, FKBP7, LPIN1, RHOF, BEX4, KCNK5, ITGA6, SPRED2, GLUL, CRYZ, PPP2R2B, CTNNA1

B. GSEA – old donor vs young donor platelet-biased HSCs defined in the integrative analysis – Hallmark (380) and cell cycle progression (383) gene sets

Gene set	pval	padj	log2err	ES	NES	size	leadingEdge
HALLMARK_ADIPOGENESIS	5.06E-04	3.92E-03	4.77E-01	6.61E-01	1.66E+00	179	FABP4, BCKDHA, ARL4A, ANGPTL4, COL15A1, DNAJB9, CMPK1, UBC, ACADL, IFNGR1, CAVIN2, PFKFB3, PHLDB1, SPARCL1, CD36, RNF11, UBQLN1, ATP5PO, IDH1, PPM1B, DLD, TOB1, DHRS7
HALLMARK_ANDROGEN_RESPONSE	8.54E-02	1.85E-01	8.51E-02	5.74E-01	1.33E+00	91	AKAP12, ADAMTS1, SAT1, INSIG1, DNAJB9, TSC22D1, B2M, SGK1, MYL12A, IDI1, RRP12
HALLMARK_APOPTOSIS	1.29E-05	1.68E-04	5.93E-01	7.42E-01	1.83E+00	149	CDKN1A, GADD45B, TNFRSF12A, IFNB1, JUN, RHOB, SMAD7, SAT1, ATF3, IL6, CCNA1, IL1B, LMNA, LEF1, MCL1, IFNGR1, PMAIP1, TNFSF10, CD69, ISG20, CASP1, KRT18, PPT1, PLAT, ANXA1, BIK, APP, DDIT3, FAS, BIRC3, IER3, CLU, BCAP31, DNAJA1, CD2, ETF1, PEA15, EMP1, LGALS3
HALLMARK_CHOLESTEROL_HOMEOSTASIS	1.20E-02	4.28E-02	2.26E-01	7.26E-01	1.61E+00	66	TNFRSF12A, MAL2, ATF3, CD9, PLAUR, STARD4, IDI1, CHKA, CLU, LDLR, TP53INP1, LGALS3, MVD, CXCL16, S100A11, ECH1
HALLMARK_COAGULATION	1.12E-01	2.15E-01	7.41E-02	5.52E-01	1.28E+00	94	TFPI2, MSRB2, CFB, DUSP6, CD9, C1S, PROS1, MMP14, THBS1, APOA1, SERPINE1, CFH, PLAT, CRIP2, PROC, ANXA1, ANG, F8, CLU, THBD, KLF7, CPQ, GNB2, CTSK, MMP7, LTA4H, ISCU, VWF, CAPN2, USP11, CFD, TIMP1, APOC1, GSN, PRSS23, DCT
HALLMARK_COMPLEMENT	1.16E-01	2.15E-01	7.65E-02	4.92E-01	1.22E+00	161	HSPA5, TFPI2, CTSL, IL6, CA2, CFB, NOTCH4, DUSP6, COL4A2, CEBPB, C1S, PLAUR, MMP14, SERPINE1, CASP1, CFH, PLAT, CD36, ANG, F8, CLU, PIM1, CTSS, KCNIP2, LGALS3, CPQ, KYNU, GNB2, CXCL1, DOCK4, LTA4H, PRSS3
HALLMARK_EPITHELIAL_MESENCHYMAL_TRANSITION	1.32E-01	2.21E-01	7.04E-02	4.93E-01	1.21E+00	144	GADD45B, TNFRSF12A, JUN, NNMT, RHOB, SAT1, TFPI2, IL6, VEGFA, SFRP4, CADM1, COL4A2, PLAUR, CXCL6, MMP14, THBS1, SERPINE1, ITGA5, CXCL8, GAS1, ITGB5, FBLN1, TGM2, ID2, SGCB, ABI3BP, CALD1, FAS, PFN2
HALLMARK_ESTROGEN_RESPONSE_EARLY	1.86E-02	5.65E-02	1.95E-01	5.75E-01	1.44E+00	169	MYOF, PGR, FOS, OVOL2, RAB31, SYBU, PTGES, NBL1, SLC7A5, CHPT1, TFF3, SLC7A2, KLF4, PMAIP1, TIPARP, SIAH2, CISH, KRT18, DHRS3, MYB, TGM2, HES1, FRK, RRP12, BHLHE40, KCNK15, XBP1, SLC19A2, SH3BP5, KCNK5, TOB1, FKBP5, KAZN, MUC1

HALLMARK_ESTROGEN_RESPONSE_LATE	1.37E-03	8.88E-03	4.55E-01	6.53E-01	1.63E+00	162	MYOF, PERP, PGR, CPE, ZFP36, FOS, TFPI2, CA2, OVOL2, DUSP2, RAB31, PTGES, NBL1, SLC7A5, ST14, CHPT1, TFF3, SGK1, CCNA1, GAL, CD9, EMP2, KLF4, ISG20, LSR, SIAH2, CISH, MYB, KIF20A, ID2, FRK, RNASEH2A
HALLMARK_FATTY_ACID_METABOLISM	5.65E-02	1.47E-01	1.09E-01	5.49E-01	1.34E+00	139	CA2, PTPRG, MAOA, ACOT2, EPHX1, YWHAH, ACADL, CYP1A1, TDO2, ACSM3, INMT, IDI1, CD36, ALDH1A1, SUCLG2, PTS, VNN1, SERINC1, IDH1, HSD17B11, DLD, GLUL, CRYZ, HMGCL, ECH1, ACADVL, BPHL, ADSL, GABARAPL1, HSD17B7
HALLMARK_G2M_CHECKPOINT	1.20E-01	2.16E-01	4.70E-02	-5.36E-01	-1.23E+00	193	ORC6, CDC20, EXO1, CDC45, NEK2, PLK4, CTCF, MYBL2, MKI67, UPF1, HMMR, XPO1, CENPF, CCNF, KIF2C, CDK1, JPT1, KIF4A, E2F2, NOTCH2, SLC12A2, NUSAP1, PBK, MEIS2, CHMP1A, NDC80, FBXO5, MCM5, E2F1, KMT5A, ATF5, MEIS1, GINS2, NASP, SLC38A1, POLQ, BIRC5, CHEK1, TMPO
HALLMARK_GLYCOLYSIS	1.96E-02	5.65E-02	1.91E-01	5.67E-01	1.42E+00	173	HSPA5, CITED2, ANGPTL4, TKTL1, GPC4, ARTN, VEGFA, TFF3, GPR87, DSC2, DPYSL4, ABCB6, ISG20, PRPS1, KIF20A, P4HA2, BIK, ARPP19, ANG, LHPP, SPAG4, IER3, FAM162A, UGP2, IDH1, DLD, TXN, DDIT4, SRD5A3, IL13RA1
HALLMARK_HEDGEHOG_SIGNALING	7.89E-02	1.82E-01	8.33E-02	7.27E-01	1.42E+00	27	UNC5C, NRP1, VEGFA, RTN1, NKX6-1, NRP2
HALLMARK_HEME_METABOLISM	1.76E-02	5.65E-02	2.02E-01	5.65E-01	1.42E+00	178	HBB, PDZK1IP1, CA2, SMOX, YPEL5, HBZ, ACKR1, RHCE, DMTN, ABCG2, ABCB6, CCDC28A, ANK1, P4HA2, HAGH, CLIC2, SLC10A3, PICALM
HALLMARK_HYPOXIA	1.01E-06	2.63E-05	6.44E-01	7.51E-01	1.88E+00	169	CDKN1A, AKAP12, HSPA5, DUSP1, JUN, CITED2, CAVIN3, KLF6, ANGPTL4, ZFP36, TKTL1, ATF3, FOS, GPC4, IL6, VEGFA, PPP1R15A, SLC2A3, STBD1, PLAUR, CDKN1C, DPYSL4, SRPX, ANXA2, HAS1, TIPARP, ISG20, SERPINE1, PFKFB3, SIAH2, LXN, IDS, TGM2, P4HA2, NEDD4L, DDIT3, BHLHE40, IER3, SLC6A6, PIM1, FAM162A, UGP2
HALLMARK_IL2_STAT5_SIGNALING	5.95E-03	3.44E-02	3.55E-01	5.94E-01	1.50E+00	182	GADD45B, ARL4A, PNP, KLF6, RHOB, NCS1, SELP, CA2, SOCS1, NRP1, FGL2, CXCL10, SLC2A3, TNFRSF9, CD86, CDKN1C, IFNGR1, TNFSF10, TNFRSF18, CD81, PHLDA1, CISH, DHRS3
HALLMARK_IL6_JAK_STAT3_SIGNALING	1.11E-01	2.15E-01	7.26E-02	5.89E-01	1.32E+00	71	SOCS3, TNFRSF12A, JUN, IL6, SOCS1, CXCL10, IL1B, CD9, IFNGR1, IL1R1

HALLMARK_INFLAMMATORY_RESPONSE	8.06E-02	1.82E-01	9.21E-02	5.12E-01	1.27E+00	158	CDKN1A, GPR183, KLF6, HAS2, IL6, CCL20, CCR7, SGMS2, CXCL10, IL1B, TNFRSF9, SLC7A2, PLAUR, TNFSF10, CXCL6, MMP14, CD70, IL1R1, RGS1, VIP, SPHK1, CD69, SERPINE1, NFKB1, ITGA5, CXCL8, SRI, ICOSLG, KCNA3, OSM, SCN1B, SELENOS, TNFSF9, RGS16, BEST1, LDLR, GPR132, PTGIR, MXD1, LAMP3, ADM
HALLMARK_INTERFERON_ALPHA_RESPONSE	1.23E-02	4.28E-02	2.29E-01	6.75E-01	1.57E+00	96	IFI27, IFIT2, IFIT3, CXCL10, B2M, C1S, ISG20, CASP1, OASL, CD74
HALLMARK_INTERFERON_GAMMA_RESPONSE	5.27E-06	9.13E-05	6.11E-01	7.42E-01	1.88E+00	185	CDKN1A, ARL4A, IFI27, SOCS3, PNP, IFIT2, IFIT3, SELP, IFIT1, IL6, SOCS1, FGL2, CFB, CXCL10, B2M, PSMA2, CD86, PELI1, C1S, PTGS2, TNFSF10, CD69, ISG20, NFKB1, CASP1, HLA-DMA, OASL, CD74, UPP1, CD274, CFH
HALLMARK_KRAS_SIGNALING_UP	1.19E-02	4.28E-02	2.42E-01	6.07E-01	1.50E+00	150	AKAP12, GADD45G, CPE, ANGPTL4, ADGRL4, CA2, NRP1, CCL20, CFB, CXCL10, PPP1R15A, IL1B, DUSP6, MAFB, TMEM176A, KLF4, PLAUR, YRDC, PTGS2, BTC, USP12, TRIB1, TMEM158, CFH, SPARCL1, PLAT, ID2, GPNMB, VWA5A, CDADC1, SCN1B, BIRC3, PLVAP, RGS16, PDCD1LG2, MYCN, CTSS
HALLMARK_MTORC1_SIGNALING	5.27E-04	3.92E-03	4.77E-01	6.53E-01	1.66E+00	196	CDKN1A, PNP, HSPA5, INSIG1, FGL2, SLC7A5, PPP1R15A, SLC2A3, CD9, IGFBP5, TUBA4A, HSPD1, HSP90B1, STARD4, IDI1, DDIT3, BHLHE40, ARPC5L, PSMC2, XBP1, SDF2L1, SLC6A6, IFRD1, LDLR, IDH1, ETF1, DDIT4
HALLMARK_MYOGENESIS	1.10E-01	2.15E-01	7.71E-02	5.10E-01	1.24E+00	137	CDKN1A, GADD45B, AK1, COL15A1, CTF1, RYR1, TEAD4, COL4A2, SPHK1, TCAP, KIFC3, ITGB5, EIF4A2, CD36, MYOM2, APP, BHLHE40, CKB, CLU
HALLMARK_OXIDATIVE_PHOSPHORYLATION	7.51E-03	3.90E-02	3.18E-01	5.74E-01	1.46E+00	199	BCKDHA, NDUFA7, TIMM10, LDHB, CYCS, SLC25A5, ACAT1, ATP5PB, ATP5F1C, MRPL35, ATP5F1A, ATP5PO, IDH1, DLD, HADHA, ATP5MG, NDUFA6, TIMM17A, PDK4, UQCRFS1, ISCU, ECH1, COX7A2L, ACADVL, ATP6V0E1, ACADSB, ATP5PF, SLC25A4, UQCRC1, PMPCA, ATP6V1F, ABCB7, BAX, ATP5MC1, CYB5R3, COX7A2, SDHC, DECR1, ECHS1, NDUFA4, NDUFA9, LDHA, HSPA9, NDUFB8, CYB5A, ALDH6A1, VDAC3, SDHD
HALLMARK_P53_PATHWAY	2.98E-05	3.10E-04	5.76E-01	7.01E-01	1.77E+00	183	CDKN1A, PERP, JUN, SAT1, ATF3, FOS, AK1, SERTAD3, SOCS1, ST14, TSC22D1, PLK3, TM4SF1, EPHX1, PPP1R15A, KLF4, RRAD, SPHK1, CD81, CASP1, UPP1, ALOX15B, LDHB, PHLDA3, DNTTIP2, ZBTB16, RALGDS, SESN1, NINJ1, APP, DDIT3, VWA5A, RCHY1, FAS, TNFSF9, IER3, RGS16, HEXIM1, FAM162A, SLC19A2, BTG1, TOB1, DDIT4, MXD1

HALLMARK_PEROXISOME	1.27E-01	2.19E-01	6.96E-02	5.44E-01	1.26E+00	93	ABCB4, CRABP1, YWHAH, ABCD2, CADM1, DHRS3, IDI1, ALDH1A1, CNBP, MSH2, IDH1, HSD17B11, PABPC1, HMGCL
HALLMARK_TGF_BETA_SIGNALING	7.61E-02	1.82E-01	8.74E-02	6.52E-01	1.39E+00	52	SMAD7, RAB31, JUNB, PPP1R15A, SKIL, CDKN1C, THBS1, TGIF1, SERPINE1, ID2, ID1
HALLMARK_TNFA_SIGNALING_VIA_NFKB	4.95E-10	2.57E-08	8.01E-01	8.06E-01	2.04E+00	190	KLF2, CDKN1A, GADD45B, SOCS3, DUSP1, JUN, GPR183, KLF6, RHOB, EGR1, ZFP36, SAT1, ATF3, IFIT2, FOS, SIK1, IL6, CXCL2, FOSL1, DUSP2, EGR2, VEGFA, CCL20, JUNB, TSC22D1, CXCL10, PPP1R15A, SLC2A3, SGK1, PHLDA2, IL1B, TNFRSF9, DUSP4, CEBPB, MCL1, KLF4, SPSB1, PLAUR, YRDC, PTGS2, FOSB, IER2, CXCL6, TIPARP, SPHK1, TGIF1, PHLDA1, CD69, SERPINE1, NFKB1, PFKFB3, BIRC2, TRIB1, BCL2A1, ID2, HES1, ICOSLG, NINJ1, BHLHE40, TNFSF9, BIRC3, IER3
HALLMARK_UNFOLDED_PROTEIN_RESPONSE	2.39E-02	6.54E-02	1.65E-01	6.23E-01	1.47E+00	108	HSPA5, HERPUD1, ATF3, IFIT1, VEGFA, SLC7A5, EIF4A3, DNAJB9, CEBPB, HSP90B1, EIF4A2, EIF2S1, XBP1, EIF4E, DDIT4, DDX10, SPCS1, PDIA6, DCP1A, KDELR3
HALLMARK_UV_RESPONSE_DN	9.51E-03	4.28E-02	2.65E-01	6.43E-01	1.54E+00	120	DUSP1, CITED2, SMAD7, HAS2, NRP1, INSIG1, PTGFR, IGFBP5, ANXA2, SERPINE1, NFKB1, IRS1, PTPRM, SRI, ID1, BHLHE40, LDLR, RBPMS, SFMBT1, PLPP3, TFPI
HALLMARK_UV_RESPONSE_UP	1.11E-02	4.28E-02	2.49E-01	6.21E-01	1.52E+00	141	RHOB, HSPA2, ATF3, FOS, IL6, CA2, CXCL2, MAOA, CDO1, JUNB, DNAJB1, EPHX1, GAL, EIF5, CDKN1C, RRAD, FOSB, CYP1A1, MMP14, TUBA4A, FGF18, PPT1

C. GSEA – old donor vs young donor multilineage output HSCs defined in the integrative analysis - gene sets pertaining HSC lineage bias (89,136,140,142,381) as well as the HSC self-renewal phenomena (132,363,364,367,382). Positive NES values indicate enrichment in the old multilineage output HSCs; only gene sets with an associated FDR < 0.25 are listed

Gene set	pval	padj	log2err	ES	NES	size	leadingEdge
Xie_2019_Autophagy	8.10E-03	7.01E-02	3.55E-01	6.42E-01	1.65E+00	158	GABARAP, SNF8, UBC, TP53INP1, ATG3, EI24
Xie_2019_Protein_Folding	1.14E-02	7.01E-02	2.97E-01	6.32E-01	1.62E+00	155	HSPA6, HSPA5, TXNDC5, DNAJB1, CCT8, HSPD1, UBC, HSP90B1, PDIA6, FKBP7, RAD23B, PDIA3, EMC4, PFDN2, CCT4, CCT5, SIL1, FKBP3, RUVBL2, CCT6B, CHCHD4, TMX4, HSPE1, FKBP5
Xie_2019_ER_Stress	5.74E-03	7.01E-02	4.07E-01	5.49E-01	1.49E+00	293	HSPA6, HSPA5, TXNDC5, HERPUD1, PIK3R2, DNAJB9, DNAJB1, IFIT1, JUN, TRIM13, HSPD1, KDELR3, DDIT3, XBP1, HSP90B1, GET4, SDF2L1, PDIA6, STUB1, ATF3, PDIA3, PPP1R15A, SPCS1, UBQLN2, CEBPB, EIF2S1, EIF2B5, THBS1, DERL2, SDAD1, EIF4A2, SHC1
Rodriguez-Fraticelli_2020_Platelet_bias_HSC	1.30E-02	7.01E-02	3.81E-01	4.41E-01	1.29E+00	676	GABARAP, C18orf32, KLF2, DUSP1, CITED2, FOS, AMIGO3, KLF6, CADPS2, PDZK1IP1, MSMO1, ZFP36, RPL7, B2M, LDHB, JUN, INSIG1, SELP, AK1, RPL34, ABCG2, ECSCR, MYOF, FMNL2, COL16A1, CSGALNACT1, RGS1, SPR, CCDC181, MMRN1, TSC22D1, BMP4, SRXN1, NMUR1, DHRS11, TNFSF10, FKBP7, FPGT, CD9, RUNX1T1, ZFP36L2, PTGS1, CD74, PPP1R15A, JUNB, NR4A2, CEBPB, PODXL, GLUL, ALDH1A1, AIG1, EVC2, JUND
Rodriguez-Fraticelli_2020_Low_output_HSC	6.58E-03	7.01E-02	4.07E-01	4.11E-01	1.26E+00	1080	GABARAP, SNX15, HSPA5, IFIT2, ACOT2, KLF2, RND3, DUSP1, CITED2, FOS, AMIGO3, KLF6, PNP, CADPS2, PDZK1IP1, MSRB2, DNAJB9, TJP2, TSC22D3, FBXO16, RPL7, B2M, LDHB, INSIG1, SELP, AK1, NOC3L, KLF4, FOSB, ABCG2, TRMT11, ECSCR, MYOF, XBP1, CA2, FMNL2, COL16A1, CSGALNACT1, RGS1, MMRN1, TSC22D1, MCL1, BMP4, IFIT3, TCEAL6, SELENBP1, MOBP, RHOB, TCF7L1, DHRS11, HMGCL, TNFSF10, FKBP7, FPGT, GAS6, CD81, ZFP36L2, CD74, PPP1R15A, ATPAF1, UBQLN2, LRPAP1, NR4A2, CEBPB, PODXL, GLUL, DMXL2, ALDH1A1, PRDX4, AIG1, EVC2, JUND, PPA1
Belluschi_2018_My/Ly_biased_CD49f+HSCs	3.62E-02	1.63E-01	9.09E-02	-7.96E-01	-1.45E+00	20	JCHAIN, HCST, B9D2

D. GSEA – old donor vs young donor multilineage output HSCs defined in the integrative analysis – Hallmark (380) and cell cycle progression (383) gene sets. Positive NES values indicate enrichment in the old multilineage output HSCs; only gene sets with an associated FDR < 0.25 are listed

Gene set	pval	padj	log2err	ES	NES	size	leadingEdge
HALLMARK_OXIDATIVE_PHOSPHORYLATION	2.31E-03	1.20E-01	4.32E-01	6.26E-01	1.66E+00	199	BCKDHA, NDUFA7, LDHB, ACAT1, MDH1, ATP5PB, SLC25A5, ATP5F1C, ATP5F1A, SDHD, TIMM10, DLD, IDH1, NDUFA9, ATP5PF, ATP5PO, ATP5MC1, ATP5MG, CYCS, PDHB, UQCRFS1, VDAC3, NDUFS2, SDHC, NDUFB5, ECH1, TIMM17A, ATP6V1C1, ECHS1, UQCRC2, HADHA, NDUFA5, COX7A2L, ISCU, NDUFA6, COX7A2, NDUFB8, ETFA, CYB5A, UQCRC1, HCCS, NDUFA4, ATP6V1F, ACADSB, LDHA, MTX2, VDAC2, PRDX3, PMPCA, SDHA, UQCR11, NDUFB3, FH, GLUD1, IDH3A

E. GSEA – old donor platelet-biased vs old donor multilineage output HSCs defined in the integrative analysis - gene sets pertaining HSC lineage bias (89,136,140,142,381) as well as the HSC self-renewal phenomena (132,363,364,367,382). Positive NES values indicate enrichment in the old donor platelet biased HSCs; only gene sets with an associated FDR < 0.25 are listed.

Gene set	pval	padj	log2err	ES	NES	size	leadingEdge
Anjos-Afonso_2022 EPCR+ HSC	1.56E-02	3.75E-02	2.29E-01	8.06E-01	1.56E+00	30	TCOF1, CST3, NR4A2, PTGS1, ID1, NAMPT, MIDN, HLA-DMB, ZNF331, PER1, CCNL1, EMCN, ETV3, SLC2A3, PLK3, TACC1, LYZ, HLF, LIMCH1, AMPD2, ARRDC2, MECOM, TUBB4B
Belluschi_2018_My/Ery_biased_CD49f+HSCs	3.84E-06	2.30E-05	6.11E-01	8.83E-01	1.89E+00	54	FTH1, HLA-E, SRGN, UBC, CD74, EIF1, MLLT3, RPS27, MALAT1, HLA-DRB1, FOSB, FXYD5, FTL, JUN, DUSP1, DDX5, TSC22D3, NFKBIA, TXNIP, NAMPT, PTPRC, SBDS, NEAT1
Belluschi_2018_My/Ery_biased_HSC/MPP	8.46E-10	2.03E-08	8.01E-01	9.15E-01	2.02E+00	65	HLA-DRA, HLA-E, SRGN, CD74, HLA-DPB1, CD37, EIF1, MLLT3, HLA-DQB1, HLA-DRB1, SAT1, ZFP36, HIST2H2BE, MAFF, ID2, HLA-DMA, NR4A2, CXCL8, PTGS1, HIST1H2BG, MYCT1, CCNH, NAMPT, ALDH1A1
Belluschi_2018_My/Ly_biased_CD49f+HSCs	3.86E-02	7.00E-02	8.69E-02	-9.29E-01	-1.40E+00	11	MT-CO2, CALM2, TFDP1, MT-CO1, CDK6
Belluschi_2018_My/Ly_biased_HSC/MPP	4.31E-03	1.41E-02	2.61E-01	-9.63E-01	-1.50E+00	18	H2AFZ, HMGN2
Cabezas_Wallscheid_2017_bulk_dHSC	4.08E-02	7.00E-02	2.80E-01	5.07E-01	1.28E+00	177	HLA-E, MLLT3, EEF2, SAT1, TSC22D1, ZFP36, KLF2, S100A6, FTL, ID2, TSC22D3, EEF1A1, CIRBP, LST1, PSAP, TXNIP, CTSS, CTSF, SNRPN, PTPRC, FIS1, SQSTM1, ABHD14B, MYADM
Cabezas_Wallscheid_2017_sc_dHSC	3.63E-02	7.00E-02	2.97E-01	5.15E-01	1.30E+00	177	FTH1, HLA-E, SRGN, CD37, EIF1, RPL31, RPL35A, RPL30, RPS27, RPL12, RPL13, EEF2, RPS9, RPL18, FAU, RPL24, RPL38, FTL, DDX5, RPS29, TSC22D3, EEF1A1, RPL27A, TPT1, RPS25, RPL32, RPL37, RPL29, RPL8, RPL23A, RPL28, RPS8, RPL19, TXNIP, PTPRC, RPS20
Giladi_2018_StemScore	8.05E-02	1.29E-01	9.54E-02	7.81E-01	1.42E+00	19	HLA-E, SRGN, CD74, MLLT3, PNRC1, MYCT1, TXNIP
Lauridsen_2018_RAdim_HSC	4.69E-03	1.41E-02	4.07E-01	6.55E-01	1.53E+00	94	HLA-E, CD74, CD37, MLLT3, RPS27, TSC22D1, FAU, PNRC1, FTL, LAPTM5, EEF1A1, RPL27A, RPL28, LST1, RPL19, CTSS, CTSF, FIS1, VAMP2, RNF125, IL18, RPS23, PIK3IP1, LYL1, TSPYL2, CD82, ARID5A, TCF25, PBXIP1, RABAC1, LIMD2

Montecino-Rodriguez_2019_Ly_biased_mHSC	1.83E-02	3.99E-02	1.97E-01	8.92E-01	1.55E+00	14	MLLT3, CLU, FLI1
Montecino-Rodriguez_2019_My_biased_mHSC	9.95E-03	2.65E-02	3.11E-01	7.70E-01	1.58E+00	43	HLA-E, CD37, VIM, ACAP1
Rodriguez-Fraticelli_2020_High_output_HSC	2.92E-07	3.51E-06	6.75E-01	-7.94E-01	-1.47E+00	455	STMN1, TUBA1B, RANBP1, TUBB, SLC25A5, DUT, HMGB2, PFN1, YBX1, SNRPB, DEK, LSM4, FABP5, CKS1B, UQCRQ, HSPE1, MIF, SNRPD1, MCM3, HNRNPA2B1, MCM7, C1QBP, TXN, CENPH, CHCHD2, PRDX2, GAPDH, NME1, PSMA2, HNRNPA1, HNRNPM, CDK4, COX6C, NASP, PGAM1, PHGDH, ATP5MC3, USP1, DCTPP1, NDUFB2, SLBP, TMED2, PSMB3, PARK7, MAD2L1, HNRNPF, HNRNPA3, COX5A, ABRACL, NDUFA4, NAP1L1, NUCKS1, ACTB, CDK6, DNAJC9, NCL, RRM1, PA2G4, RNASEH2B, SIVA1, COX6A1, PRKDC, RPN2, SRSF2, BANF1, PPP1CA, RBBP4, SF3B6, PAICS, HDAC2, SNRPF, HNRNPAB, CKS2, SMS, ATP5ME, CBX3, SMC3, TMED9, EIF5A, NHP2, TCP1, SMC4, SNRPD3, LSM7, ANP32B, COX8A, TMEM14C, UQCR11, SRSF3, NDUFB6, CYC1, NDUFB8, ATP1B3, RPA1, SERBP1, GTF3C6, CD69, MARCKSL1, FUS, PSMB6, RBMX, SAE1, PHF5A, MTHFD1, SRM, UBE2I, VAMP8, HMGB3, VRK1, EXOSC8, EEF1E1, DYNLL1, COX7A2, NDUFS8, RPA2, HNRNPDL, MRPL51, ISYNA1, SOD1, ACTR3, TAF9, RNPS1, HNRNPD, ATP5F1C, RBM3, ETFB, COX5B, RPS19, HACD3, HMGN5, OAZ1
Rodriguez-Fraticelli_2020_Low_output_HSC	3.41E-04	1.37E-03	4.98E-01	5.26E-01	1.43E+00	339	HLA-E, CD74, EIF1, MLLT3, RPL30, RPL13, EEF2, RPS9, FOSB, TSC22D1, CLU, PPP1R15A, KLF2, RPL24, S100A6, S100A4, MAFF, RPL38, FTL, DUSP1, FOS, MCL1, TSC22D3, NR4A2, PFDN5, RPL37, PTGER4, SRSF5, LST1, PSAP, MYCT1, TXNIP, EIF4B, ALDH1A1, RPS20, STAT3, NR4A1, KDELR1, ITM2B, CEBPB, MYADM, EIF1B, KLF4, BEX2, PHF1, CITED2, RPL36A, GATA2, ELMO1, PIK3IP1, TFPI, CARD19, WBP2, BEX4, CD82, DNAJB9, MT-CO3, APP, TCF25, PNRC2

Rodriguez-Fraticelli_2020_Multilineage_HSC	2.29E-04	1.10E-03	5.19E-01	-7.69E-01	-1.42E+00	351	STMN1, TUBA1B, RANBP1, TUBB, SLC25A5, DUT, HMGB2, YBX1, DEK, FABP5, CKS1B, HSPE1, SNRPD1, MCM3, HNRNPA2B1, MCM7, C1QBP, CENPH, HSP90AA1, CHCHD2, GAPDH, CACYBP, NME1, SPCS2, HNRNPM, CDK4, COX6C, NASP, PGAM1, PHGDH, HSPA8, RBX1, ATP5MC3, USP1, DCTPP1, SLBP, OSTC, TMED2, MAD2L1, HNRNPF, COX5A, NDUFA4, NAP1L1, NUCKS1, CDK6, DNAJC9, NDUFC2, RRM1, RHEB, PA2G4, SRSF10, RNASEH2B, SIVA1, SUMO3, SRSF2, BANF1, ARL6IP6, RBBP4, SF3B6, PAICS, HDAC2, SNRPF, HNRNPAB, SLIRP, CKS2, SMS, ATP5ME, CBX3, SMC3, PSMA7, EIF5A, TCP1, PSMB2, SMC4, SNRPD3, TMEM258, ANP32B, NUTF2, TMEM14C, UQCR11, CYC1, ATP1B3, RPA1, SERBP1, GTF3C6, CD69, PSMB6, PHF5A, MTHFD1, SRM, UBE2I, EIF2S2, PARP1, HMGB3, VRK1, EEF1E1, DYNLL1
Rodriguez-Fraticelli_2020_Platelet_bias_HSC	5.20E-07	4.16E-06	6.59E-01	6.68E-01	1.77E+00	259	HLA-E, CD74, RPL31, RPL35A, MLLT3, RPL30, JUNB, RPL13, EEF2, RPS9, TSC22D1, CLU, ZFP36, PPP1R15A, RACK1, KLF2, RPL24, S100A6, S100A4, MAFF, JUN, DUSP1, FOS, ID2, RPS29, NR4A2, RPL32, RPL37, PTGER4, RPL8, RPL28, LST1, PTGS1, PSAP, RPS8, MYCT1, SYF2, NFKBIA, TXNIP, CTSF, ALDH1A1, RPS20, STAT3, ITM2B, CEBPB
Rodriguez-Fraticelli_2020_serial_engraftment_HSC	1.63E-01	2.34E-01	1.14E-01	4.61E-01	1.13E+00	132	SRGN, MLLT3, RPL12, JUNB, SAT1, TSC22D1, CLU, NACA, S100A6, PNRC1, ID2, NR4A2, PTGER4, LST1, EIF4B, ALDH1A1, ITM2B, CEBPB, MAX, BEX2, CDKN1A, RPL36A
Xie_2019_Cholesterol_Biosynth	1.66E-01	2.34E-01	3.77E-02	-7.55E-01	-1.25E+00	40	RAN, PARK7, FDPS, KPNB1, CNBP, ISYNA1, EBP

F. GSEA – old donor platelet-biased vs old donor multilineage output HSCs defined in the integrative analysis - Hallmark (380) and cell cycle progression (383) gene sets. Positive NES values indicate enrichment in the old donor platelet-biased HSCs; only gene sets with an associated FDR < 0.25 are listed.

Gene set	pval	padj	log2err	ES	NES	size	leadingEdge
HALLMARK_ALLOGRAFT_REJECTION	6.63E-04	8.45E-03	4.77E-01	7.85E-01	1.69E+00	57	HLA-DRA, HLA-E, SRGN, CD74, HLA-A, RPS9, HLA-DMA, HLA-DQA1, RPL9, EIF3D, CTSS, PTPRC
HALLMARK_APICAL_JUNCTION	7.53E-02	2.48E-01	5.80E-02	-8.18E-01	-1.36E+00	43	PFN1, ARPC2, ACTB, YWHAH, MDK
HALLMARK_COAGULATION	4.98E-02	2.12E-01	1.26E-01	7.64E-01	1.47E+00	27	CLU, MAFF, ISCU, ANXA1, GSN, USP11, CPQ, CFH, KLF7, CD9
HALLMARK_DNA_REPAIR	8.57E-02	2.48E-01	5.21E-02	-7.67E-01	-1.33E+00	75	DUT, RPA3, NME1, PRIM1, RBX1, TMED2, HPRT1, GTF2A2, DAD1, NME4, RPA2, TAF9, MPC2, POLR2K, POLR2E, SSRP1, NUDT21, GPX4, DGUOK, SF3A3, BCAP31, POLR2I, POLR2J, ARL6IP1, COX17, POLR2F
HALLMARK_E2F_TARGETS	1.80E-04	3.06E-03	5.19E-01	-9.03E-01	-1.56E+00	73	STMN1, RANBP1, TUBB, DUT, HMGB2, RAN, SNRPB, DEK, HMGA1, CKS1B, MCM3, MCM7, RPA3, NME1, CDK4, RBBP7, NASP, PRDX4, USP1, DCTPP1, SLBP, MAD2L1, PSIP1, NAP1L1, NAA38, PA2G4, PRKDC, SRSF2, POLD2, PAICS, CKS2, SMC3, XRCC6
HALLMARK_ESTROGEN_RESPONSE_EARLY	1.27E-02	6.49E-02	2.57E-01	8.16E-01	1.60E+00	30	AREG, CD44, FOS, TIPARP, KLF4
HALLMARK_G2M_CHECKPOINT	3.06E-03	3.13E-02	2.91E-01	-8.80E-01	-1.51E+00	62	STMN1, HMGN2, HMGA1, CKS1B, SNRPD1, MCM3, CDK4, NASP, HSPA8, MAD2L1, TFDP1, NCL, SRSF10, SRSF2, CKS2, BUB3, SMC4
HALLMARK_GLYCOLYSIS	7.14E-03	4.55E-02	1.93E-01	-8.87E-01	-1.49E+00	47	STMN1, TPI1, PPIA, PKM, ENO1, MIF, TXN, MDH1, NASP, PGAM1
HALLMARK_IL2_STAT5_SIGNALING	6.41E-02	2.48E-01	1.25E-01	6.48E-01	1.38E+00	53	CD44, ARL4A, MAFF, GADD45B, SWAP70, GBP4, KLF6, RNH1, SLC2A3, SOCS2

HALLMARK_IL6_JAK_STAT3_SIGNALING	7.06E-03	4.55E-02	3.26E-01	8.84E-01	1.62E+00	20	CD44, JUN, STAT3, SOCS3
HALLMARK_KRAS_SIGNALING_UP	1.05E-02	5.97E-02	2.97E-01	7.85E-01	1.62E+00	42	CD37, PPP1R15A, LAPTM5, ID2, CTSS, KLF4, BIRC3, TFPI, GUCY1A1, PTGS2, USP12
HALLMARK_MTORC1_SIGNALING	2.81E-02	1.30E-01	9.13E-02	-7.91E-01	-1.40E+00	98	ATP5MC1, TPI1, HSPE1, PSMA4, HSPD1, PPIA, ENO1, GAPDH, CACYBP, PRDX1, PHGDH, PPA1, HPRT1, LDHA, RPA1, EIF2S2, EEF1E1, PSMG1, GMPS, HSP90B1, ACTR3, HSPA5, DDX39A, PGK1, EBP
HALLMARK_MYC_TARGETS_V1	4.45E-05	1.14E-03	5.57E-01	-8.45E-01	-1.53E+00	168	RANBP1, DUT, ERH, RAN, DEK, HSPE1, PSMA4, YWHAQ, HSPD1, PPIA, SNRPD1, HNRNPA2B1, MCM7, C1QBP, NME1, PSMA2, HNRNPA1, CDK4, ILF2, PRDX3, PRDX4, USP1, HNRNPR, PSMB3, MAD2L1, HNRNPA3, COX5A, TFDP1, YWHAE, NAP1L1, SET, VDAC1, RRM1, PA2G4, HPRT1, SRSF2, POLD2, PTGES3, HDAC2, CBX3, SSBP1, PSMA7, LDHA, XRCC6, BUB3, NHP2, TCP1, PSMB2, GLO1, SNRPD3, LSM7, PHB, VBP1, CCT5, SRSF3, CYC1, SNRPG, KPNB1, SERBP1, CNBP, POLE3, SRM, EIF1AX, ACP1, EIF2S2
HALLMARK_MYC_TARGETS_V2	9.08E-02	2.48E-01	5.47E-02	-8.50E-01	-1.34E+00	20	HSPE1, HSPD1, CDK4, DCTPP1, PA2G4, CBX3, PHB, SRM
HALLMARK_OXIDATIVE_PHOSPHORYLATION	4.28E-03	3.64E-02	2.32E-01	-7.99E-01	-1.44E+00	149	SLC25A5, ATP5MC1, UQCRQ, LDHB, ATP5MF, IDH2, COX7B, UQCR10, COX6C, MDH1, PRDX3, ATP5MC3, NDUFB2, COX5A, ATP5PF, NDUFA4, VDAC1, NDUFC2, COX6A1, NDUFB1, ATP5ME, LDHA, COX8A, UQCR11, NDUFB6, CYC1, NDUFB8, NDUFB3, COX7A2, UQCRH, NDUFS8, ETFA, NDUFAB1, NDUFA6, ATP5F1C, ETFB, COX5B, NDUFA5, ECH1, UQCRC1, NDUFA9, ATP5F1E, COX6B1, MRPL11, SDHD, GPX4, NDUFA3, NDUFS6, ATP5PB, ATP5F1A, ACADM, NDUFA1, ATP5MG, ATP5F1B, TIMM13, HSD17B10, MDH2, VDAC3, NDUFA2
HALLMARK_PI3K_AKT_MTOR_SIGNALING	8.74E-02	2.48E-01	5.42E-02	-8.23E-01	-1.34E+00	35	PFN1, CFL1, CDK4, PPP1CA, YWHAB, AP2M1, HSP90B1, ACTR3, UBE2N

HALLMARK_TNFA_SIGNALING_VIA_NFKB	9.19E-08	4.69E-06	7.05E-01	8.70E-01	1.97E+00	78	EIF1, AREG, CD44, JUNB, SAT1, FOSB, TSC22D1, ZFP36, PPP1R15A, KLF2, MAFF, PNRC1, JUN, DUSP1, FOS, ID2, MCL1, NR4A2, PTGER4, NFKBIA, GADD45B, NAMPT, GADD45A, TIPARP, NR4A1, CXCL2, SOCS3, SQSTM1, CEBPB, KLF4, ATF3, BIRC3, CDKN1A, IL18, BTG1, PER1, CCNL1, PTGS2, BCL2A1, IER2, KLF6, TGIF1, SLC2A3
Tirosh_2016_G2M_phase	7.71E-02	2.48E-01	6.13E-02	-9.01E-01	-1.36E+00	10	HMGB2, CKS1B, CKS2, SMC4
Tirosh_2016_S_phase	9.24E-02	2.48E-01	5.66E-02	-9.11E-01	-1.34E+00	7	PRIM1, NASP, USP1, SLBP, RRM1, MSH2, RPA2

G. GSEA – young donor platelet-biased vs young donor multilineage output HSCs defined in the integrative analysis - gene sets pertaining HSC lineage bias (89,136,140,142,381) as well as the HSC self-renewal phenomena (132,363,364,367,382). Positive NES values indicate enrichment in the young donor platelet biased HSCs; only gene sets with an associated FDR < 0.25 are listed.

Gene set	pval	padj	log2err	ES	NES	size	leadingEdge
Anjos-Afonso_2022 EPCR+ HSC	5.72E-02	1.02E-01	1.34E-01	7.82E-01	1.44E+00	44	NR4A2, PTGS1, CST3, HLA-DMB, HLF, PER1, TCOF1, MECOM, EMCN, ZNF331, CPED1, LIMCH1, LINC01122, TIE1, NAMPT, ARRDC2, LYZ
Belluschi_2018_My/Ery_biased_CD49f+HSCs	1.20E-04	4.99E-04	5.38E-01	9.17E-01	1.74E+00	55	HLA-E, CD74, SRGN, TSC22D3, EIF1, MLLT3, HLA-DRB1, FXYD5, LAPTM4A, UBC, FTL, HSP90AB1, DDX5, TXNIP, DUSP1, HLA-DRB5, FOSB, SBDS, PTPRC, ANKRD28
Belluschi_2018_My/Ery_biased_HSC/MPP	3.17E-09	7.91E-08	7.75E-01	9.48E-01	1.88E+00	79	HLA-E, CD74, SRGN, HLA-DRA, CD37, EIF1, MLLT3, HLA-DPB1, HLA-DQB1, HLA-DRB1, HIST2H2BE, LAPTM4A, NR4A2, HLA-DMA, ALDH1A1, HLA-DRB5, SOCS2, MYCT1, HIST1H2BG, PTGS1, ZFP36, MAFF, HLA-DMB, THEMIS2, ELMO1, SAT1, SORL1, CXCL8, CCNH, BEX5, NR1H2
Belluschi_2018_My/Ly_biased_CD49f+HSCs	1.58E-01	2.47E-01	4.02E-02	-8.85E-01	-1.27E+00	16	TFDP1, CDK6, MT-CO1, MT-CO2, RPL6, NDUFAB1, PRSS2, CALM2, RPLP1
Belluschi_2018_My/Ly_biased_HSC/MPP	1.73E-02	4.31E-02	1.26E-01	-9.49E-01	-1.38E+00	25	H2AFZ, HMGN2, IGLL1, CDK6
Cabezas_Wallscheid_2017_bulk_dHSC	4.86E-04	1.73E-03	4.98E-01	6.62E-01	1.54E+00	243	HLA-E, TSC22D3, MLLT3, FTL, EEF2, CIRBP, TXNIP, TSC22D1, PSAP, SOCS2, S100A6, CTSF, ANXA1, ZFP36, CTSS, CD52, CD53, ZBTB20, PTPRC, SNRPN, LST1, ABHD14B, SAT1, CCNDBP1, FIS1, IL16, SORL1, HLF, ANKRD12, BTG1, USE1, SARAF, CD82, GATA3, RPL7, MECOM, UBE2F, XBP1, TSPAN31, SQSTM1, RENBP, UBA7
Giladi_2018_StemScore	1.24E-02	3.44E-02	3.81E-01	9.27E-01	1.59E+00	25	HLA-E, CD74, SRGN, MLLT3, PNRC1, TXNIP, MYCT1
Lauridsen_2018_RAdim_HSC	2.28E-02	5.18E-02	2.97E-01	6.62E-01	1.40E+00	124	HLA-E, CD74, CD37, MLLT3, FTL, PNRC1, PBXIP1, TSC22D1, FAU, IL18, VAMP2, LAPTM5, CTSF, CTSS, ZBTB20, LST1, PIK3IP1, FIS1, TSPYL2, IL16, RNF125, ACAP1, LIMD2, HLF, USE1, CD82, MVP, GBP4, POU2F2, MECOM, LYL1
Montecino-Rodriguez_2019_Ly_biased_mHSC	4.74E-02	9.88E-02	1.33E-01	8.65E-01	1.49E+00	25	MLLT3, CLU, SNAP23, FLI1

Montecino-Rodriguez_2019_My_biased_mHSC	1.47E-01	2.46E-01	8.79E-02	6.73E-01	1.28E+00	57	HLA-E, CD37, VIM, ACAP1
Pietras_2015_HSC	1.01E-03	3.15E-03	4.55E-01	6.20E-01	1.46E+00	285	HLA-E, MLLT3, ALDH1A1, EEF2, TXNIP, N4BP2L2, SOCS2, MAGED2, MYCT1, PTGS1, CTSF, MAFF, HLF, ARMCX1, PRKACB, BEX2, GATA3, RPL7, BEX4, TFPI, EMCN, PHLDB2, ROBO4, DST, NAP1L3, P2RX1, ARL4A, GABARAPL1, SLC3A2, SPART, GBP2, EID1, TMEM59, RAB27B, TBXAS1, MEIS1, PBX1, WDR45, GNAI1, PCMTD2, TIE1
Rodriguez-Fraticelli_2020_High_output_HSC	1.59E-06	1.32E-05	6.44E-01	-8.42E-01	-1.35E+00	589	TUBA1B, STMN1, TUBB, RANBP1, DEK, DUT, SNRPB, MCM7, LSM4, SLC25A5, MIF, GAPDH, EIF5A, FABP5, NASP, YBX1, NUCKS1, PCNA, MCM3, CENPH, PFN1, SRSF2, SNRPD1, CKS1B, CDK4, DNMT1, MCM5, PHGDH, USP1, HMGB2, CALR, UNG, HNRNPA2B1, HNRNPH1, UQCRQ, SIVA1, HNRNPA1, CHCHD2, NME1, NCL, PA2G4, DCTPP1, SNRPF, DNAJC9, HSPE1, HNRNPF, HNRNPAB, C1QBP, CBX3, ACTB, SMS, COX5A, NDUFS6, PGAM1, PRKDC, ATP5MC3, CDK6, FUS, SLBP, PPM1G, SMC2, SRSF3, COX8A, TXN, NDUFB2, PAICS, NAP1L1, RBBP4, SSRP1, TMED2, BANF1, RRM1, HNRNPM, CARHSP1, COX6C, SMC3, MAD2L1, SNRNP25, COX6A1, DTYMK, SERBP1, RNPS1, NDUFS8, RNASEH2B, NHP2, HMGB3, ANP32B, ANP32E, RALY, CENPW, HNRNPA3, ISYNA1, PARK7, UBA2, HDAC2, CALM3, ABRACL, LSM7, PRDX2, HMGN5, ATP5ME, EZH2, CYC1, CKS2, NDUFA4, MRPL51, TMEM14C, SMC4, MIS18BP1, NDUFB6, POLR2I, TCP1, RFC2, HACD3, SRM, NDUFS5, HNRNPL, EEF1B2, HNRNPD, SNRPD3, MRPS26, MTHFD1, UBE2I, RPA2, MSH6, PSMB3, VRK1, PIN1, COTL1, PSMB6, PPP1CA, TOMM40, RBMX, DAZAP1, SAE1, ETFB, BAZ1B, PRPS2, ATP5F1E, IPO5, HNRNPA0, COX5B, CCT2, SF3B6, SRSF7, CORO1A, MLEC, ACTL6A, TOMM22, SFXN1, NONO, SFPQ, RPA1, EXOSC8, RPN1, TMED9, PPP1CC, NUDT21, NDUFB7, ATP1B3, UQCRC1, PDAP1, HNRNPU, NOP56, PSMA2, RPSA, SUZ12, SNRNP40, RBM3, CAPZA1, KIF22, ATP5PD, NMRAL1, MRPL18, EEF1E1, ATP5F1B
Rodriguez-Fraticelli_2020_Low_output_HSC	9.41E-06	5.88E-05	5.93E-01	6.39E-01	1.58E+00	472	HLA-E, CD74, TSC22D3, EIF1, MLLT3, LAPTM4A, NR4A2, CLU, PFDN5, SRSF5, FTL, ITM2B, ALDH1A1, PTGER4, EEF2, TXNIP, DUSP1, TSC22D1, PSAP, MCL1, SOCS2, MAGED2, RPL30, MYCT1, RPL38, S100A6, GATA2, FOSB, MAFF, S100A4, FOS, ZBTB20, ELMO1, LST1, PIK3IP1, RPL24, LAMP2, PHF1, MT-ND2, LIMD2, HLF, CARD19, STAT3, HMGA2, ANXA7, BEX2, CD82, NR4A1, GATA3, GBP4, TPST2, RPL7, NDFIP1, BEX4, SAMSN1, POU2F2, MECOM, WBP2, FLI1, DNAJB9, KDELR1, TTC14, TFPI, EMCN, XBP1, ROBO4, DDX17, DST, CALCOCO1, UBA7, CEBPB, P2RX1, EIF1B, MYADM, GABARAPL1, KLF2, GBP2, EID1

Rodriguez-Fraticelli_2020_Multilineage_HSC	6.08E-05	3.04E-04	5.57E-01	-8.36E-01	-1.34E+00	450	TUBA1B, STMN1, TUBB, RANBP1, TYMS, DEK, DUT, MCM7, SLC25A5, GAPDH, EIF5A, FABP5, NASP, YBX1, NUCKS1, PCNA, MCM3, CENPH, HELLS, SRSF2, SNRPD1, CKS1B, CDK4, DNMT1, MCM5, PHGDH, USP1, HMGB2, CALR, UNG, HNRNPA2B1, HNRNPH1, SIVA1, CHCHD2, NME1, HSPA8, HSP90AA1, PA2G4, DCTPP1, SNRPF, PSMA7, DNAJC9, HSPE1, HNRNPF, HNRNPAB, C1QBP, CBX3, SMS, COX5A, NDUFS6, PGAM1, CACYBP, ATP5MC3, CDK6, SLBP, PPM1G, SMC2, PAICS, NAP1L1, RBBP4, SSRP1, TMED2, BANF1, SRSF10, RBX1, RRM1, HNRNPM, TPM4, ARL6IP6, COX6C, SMC3, MAD2L1, DTYMK, SERBP1, NUTF2, RAD21, RNASEH2B, HMGB3, ANP32B, ANP32E, SLIRP, SUMO3, CENPW, SPCS2, HDAC2, TP53, TMEM97, PARP1, NDUFC2, MTHFD2, HMGN5, ATP5ME, EZH2, CYC1, CKS2, NDUFA4, TMEM14C, SMC4, MIS18BP1, TCP1, RFC2, POLR2J, RHEB, OSTC, SRM, NDUFS5, PSMB2, HNRNPL, EEF1B2, HNRNPD, SNRPD3, MTHFD1, UBE2I, RPA2, VRK1, PIN1, COTL1, PSMB6
Rodriguez-Fraticelli_2020_Platelet_bias_HSC	3.63E-08	4.54E-07	7.20E-01	7.51E-01	1.80E+00	329	HLA-E, CD74, MLLT3, JUNB, RPL35A, LAPTM4A, NR4A2, RPL31, CLU, ITM2B, ALDH1A1, PTGER4, EEF2, RACK1, TXNIP, DUSP1, TSC22D1, PSAP, SOCS2, MAGED2, RPL30, MYCT1, S100A6, GATA2, PTGS1, CTSF, ZFP36, MAFF, S100A4, FOS, ZBTB20, SYF2, LST1, CCNDBP1, RPL24, LAMP2, IL16, LIMD2, HLF, CARD19, STAT3, HMGA2, PRKACB, SARAF, BEX2, GATA3, GBP4, TPST2, RPL7, NFKBIA, BEX4, SAMSN1, MECOM, WBP2, VAMP5, TTC14, TFPI, SDCBP, ROBO4, SERINC3, UBA7, CEBPB, P2RX1, GABARAPL1, KLF2, GBP2, RPS29, EID1, TMBIM4, RPL39, SSBP3, TBXAS1, SCARF1, CHPF2, MEIS1, CITED2, PBX1, CREBRF
Wilson_2015_MolO	5.33E-02	1.02E-01	1.09E-01	9.40E-01	1.48E+00	9	MLLT3, CTSF, LIMD2, CD82

H. GSEA – young donor platelet-biased vs young donor multilineage output HSCs defined in the integrative analysis - Hallmark (380) and cell cycle progression (383) gene sets. Positive NES values indicate enrichment in the young donor platelet-biased HSCs; only gene sets with an associated FDR < 0.25 are listed.

Gene set	pval	padj	log2err	ES	NES	size	leadingEdge
HALLMARK_ALLOGRAFT_REJECTION	6.57E-02	2.01E-01	1.40E-01	7.01E-01	1.37E+00	72	HLA-E, CD74, SRGN, HLA-DRA, HLA-A, HLA-DMA, HLA-DQA1, EIF3D, IL18, CTSS, HLA-DMB, PTPRC, NPM1, CCND3, IL16
HALLMARK_DNA_REPAIR	1.76E-02	1.01E-01	1.17E-01	-8.74E-01	-1.34E+00	94	TYMS, DUT, PCNA, RPA3, NME1, NME4, PRIM1, GPX4, HPRT1, SSRP1, TMED2, RBX1, TP53, POLR2I, RFC2, POLR2J, RPA2
HALLMARK_E2F_TARGETS	6.45E-05	1.68E-03	5.38E-01	-9.33E-01	-1.44E+00	102	STMN1, TUBB, RANBP1, DEK, DUT, HMGA1, SNRPB, MCM7, NASP, PCNA, MCM3, HELLS, SRSF2, CKS1B, CDK4, DNMT1, MCM5, RAN, USP1, RPA3, HMGB2, UNG, NAA38, NME1, PA2G4, DCTPP1, PSIP1, RBBP7, CBX5, PRKDC, SLBP, POLD2, PAICS, NAP1L1, SSRP1, PTTG1, TMPO, PRDX4, SMC3, MAD2L1, RAD21, SMC1A, HMGB3, ILF3, ANP32E, TP53, RFC1, MTHFD2, EZH2, CKS2, SMC4, RFC2, XRCC6, ATAD2
HALLMARK_ESTROGEN_RESPONSE_EARLY	3.82E-02	1.32E-01	1.63E-01	7.91E-01	1.46E+00	47	CD44, AREG, FOS, TIPARP, XBP1, ELF1, KRT8
HALLMARK_G2M_CHECKPOINT	4.35E-04	7.54E-03	4.98E-01	-9.16E-01	-1.41E+00	98	STMN1, HMGN2, HMGA1, NASP, MCM3, SRSF2, SNRPD1, CKS1B, CDK4, MCM5, HSPA8, NCL, TFDP1, SMC2, SRSF10, PTTG1, TMPO, MAD2L1, DTYMK, MT2A, RAD21, KPNB1, SMC1A, HMGB3, ILF3
HALLMARK_GLYCOLYSIS	1.25E-02	8.89E-02	1.41E-01	-9.02E-01	-1.36E+00	66	STMN1, MIF, NASP, PPIA, PKM, TPI1, ENO1, PGAM1, TXN
HALLMARK_IL6_JAK_STAT3_SIGNALING	3.78E-02	1.32E-01	1.50E-01	8.77E-01	1.49E+00	26	CD44, STAT3, CXCL3
HALLMARK_INFLAMMATORY_RESPONSE	3.24E-02	1.32E-01	1.82E-01	7.80E-01	1.46E+00	52	BST2, PTGER4, IL18, CXCL8, EMP3, CD82, NFKBIA, SCARF1, NAMPT, SELL, ICAM4, TNFSF10

HALLMARK_INTERFERON_ALPHA_RESPONSE	2.80E-02	1.32E-01	1.95E-01	7.92E-01	1.48E+00	50	CD74, BST2, HLA-C, TXNIP, GBP4
HALLMARK_INTERFERON_GAMMA_RESPONSE	1.37E-02	8.89E-02	3.26E-01	7.47E-01	1.50E+00	86	CD74, HLA-DRB1, BST2, HLA-A, HLA-B, HLA-DMA, HLA-DQA1, TXNIP, STAT3, BTG1, MVP, GBP4, NFKBIA, CFH, VAMP5
HALLMARK_KRAS_SIGNALING_UP	2.00E-02	1.04E-01	2.38E-01	7.85E-01	1.49E+00	58	CD37, LAPTM5, CTSS, ADAM8, BIRC3, GUCY1A1, CFH, TFPI, JUP, MAP7
HALLMARK_MTORC1_SIGNALING	4.33E-03	4.51E-02	2.32E-01	-8.73E-01	-1.36E+00	131	GAPDH, PPIA, TPI1, PHGDH, ATP5MC1, CALR, UNG, HSPD1, ENO1, HSPE1, CACYBP, HPRT1, PSMA4, PPA1, TMEM97, MTHFD2, EBP, LDHA, TOMM40, PSMD14, HSP90B1, PSMG1, PRDX1, TCEA1, DDX39A, GMPS, CORO1A, RPA1, RPN1, EIF2S2, PDAP1, PGK1
HALLMARK_MYC_TARGETS_V1	6.23E-04	8.10E-03	4.77E-01	-8.83E-01	-1.39E+00	177	RANBP1, TYMS, DEK, DUT, MCM7, PCNA, SET, PPIA, SRSF2, SNRPD1, CDK4, MCM5, RAN, ERH, USP1, HNRNPA2B1, HNRNPA1, NME1, YWHAQ, YWHAE, PA2G4, HSPD1, PSMA7, HSPE1, C1QBP, CBX3, HNRNPR, COX5A, SNRPG, TFDP1, HPRT1, PPM1G, POLD2, SRSF3, NAP1L1, RRM1, PSMA4, VDAC1, PRDX4, MAD2L1, SERBP1, KPNB1, RNPS1, NHP2, GLO1, HNRNPA3, UBA2, HDAC2, POLE3, LSM7, PRDX3, CYC1, CDK2, TCP1, RPL6, ILF2, XRCC6, VBP1, TUFM, SRM, PSMB2, EEF1B2, HNRNPD, SNRPD3, PTGES3, PSMB3, LDHA, PSMD14, CCT5, PRPS2, CCT2, ACP1, SRSF7, NDUFAB1, PHB, EIF1AX, IMPDH2, EIF2S2, SRSF1, HNRNPU, PGK1, NOP56, PSMA2
HALLMARK_MYC_TARGETS_V2	7.53E-02	2.17E-01	5.77E-02	-8.88E-01	-1.31E+00	36	CDK4, MCM5, UNG, PA2G4, HSPD1, DCTPP1, HSPE1, CBX3, TMEM97, SRM
HALLMARK_OXIDATIVE_PHOSPHORYLATION	1.19E-02	8.89E-02	1.36E-01	-8.41E-01	-1.33E+00	170	SLC25A5, IDH2, ATP5MC1, UQCRQ, ATP5MF, COX7B, GPX4, COX5A, NDUFS6, ATP5MC3, LDHB, COX8A, NDUFB2, VDAC1, COX6C, COX6A1, MRPL11, UQCR10, NDUFS8, NDUFC2, PRDX3, ATP5ME, NDUFB1, CYC1, NDUFA4, NDUFB6, SLC25A6, NDUFA3, LDHA, ETFB, UQCRH, ATP5F1E, NDUFA2, COX5B, NDUFA6, NDUFAB1, TOMM22, ATP5PF, NDUFB7, UQCRC1, MDH1, POLR2F, TIMM8B, ATP5PD, ATP5F1B, UQCR11, NDUFA1, SLC25A3, NDUFB3
HALLMARK_PI3K_AKT_MTOR_SIGNALING	3.59E-02	1.32E-01	8.34E-02	-8.90E-01	-1.33E+00	56	CFL1, PFN1, CDK4, CALR, CDK2, PIN1, PPP1CA, HSP90B1

HALLMARK_TNFA_SIGNALING_VIA_NFKB	9.30E-07	4.84E-05	6.59E-01	8.94E-01	1.82E+00	92	EIF1, JUNB, CD44, NR4A2, AREG, PTGER4, PNRC1, DUSP1, TSC22D1, MCL1, IL18, GADD45A, FOSB, ZFP36, MAFF, FOS, SAT1, NFE2L2, TIPARP, PER1, BTG1, BIRC3, NR4A1, NFKBIA
Tirosh_2016_S_phase	4.70E-02	1.53E-01	7.74E-02	-9.49E-01	-1.36E+00	14	TYMS, NASP, PCNA, HELLS, MCM5, USP1, UNG, PRIM1, SLBP, RRM1

Appendix table 3

A. Lists of differentially expressed genes (FDR < 0.05) when comparing old donor vs young donor platelet-biased HSCs defined in the integrative analysis. Base of the log is 2.

A1 – upregulated in old donors

Gene	logFC	FDR	Gene	logFC	FDR	Gene	logFC	FDR
FABP4	9.16E+00	2.79E-05	NXF3	4.12E+00	1.70E-02	SOX6	2.87E+00	3.79E-04
HSPA6	7.90E+00	2.05E-02	ADAMTS1	4.06E+00	4.41E-04	CTSL	2.83E+00	1.82E-02
IL11	7.54E+00	3.15E-02	HERPUD1	4.02E+00	2.84E-02	INSIG1	2.81E+00	2.93E-02
HBA2	7.32E+00	4.00E-11	PPIC	3.98E+00	9.94E-03	EIF4EBP3	2.79E+00	8.77E-16
IFNB1	7.18E+00	4.11E-02	TNFRSF12A	3.90E+00	6.95E-04	RHOB	2.75E+00	1.97E-03
AKAP12	7.08E+00	2.76E-03	AC139795.3	3.71E+00	3.39E-02	AC020916.1	2.74E+00	3.83E-19
LINC01731	6.87E+00	2.67E-08	WNT11	3.71E+00	1.47E-02	TRHDE	2.72E+00	8.86E-03
MYOF	6.33E+00	4.03E-04	ADGRV1	3.70E+00	1.79E-02	Z98752.4	2.72E+00	1.86E-02
IFI27	6.23E+00	9.26E-03	IFIT3	3.67E+00	3.61E-02	PLSCR3	2.69E+00	4.78E-03
ZNF804B	6.22E+00	3.16E-05	RASD1	3.57E+00	3.09E-04	TOGARAM2	2.67E+00	9.45E-04
PGR	6.07E+00	1.23E-02	AC114490.2	3.53E+00	6.64E-06	AC116407.2	2.64E+00	4.78E-13
HAMP	5.92E+00	2.47E-02	SNX15	3.51E+00	1.09E-14	MAOA	2.61E+00	3.88E-02
PRSS16	5.68E+00	4.57E-03	AL138995.1	3.42E+00	1.65E-05	SPAG6	2.60E+00	3.50E-03
ANKRD20A1	5.61E+00	1.31E-03	ASPA	3.37E+00	9.95E-03	AC000093.1	2.60E+00	9.54E-05
IGLC2	5.42E+00	9.48E-03	IFIT1	3.35E+00	3.43E-02	TJP2	2.59E+00	7.89E-07
PABPC1L2A	5.22E+00	1.39E-02	AL162457.1	3.35E+00	8.65E-06	HSPA2	2.58E+00	1.49E-03
FIGN	5.21E+00	9.18E-14	AC126283.1	3.33E+00	1.66E-03	CDKN1A	2.57E+00	2.69E-11
UNC5C	5.18E+00	2.93E-02	PERP	3.32E+00	9.55E-06	CEP83-DT	2.55E+00	7.29E-11
AC123777.1	5.01E+00	3.28E-02	GATD3B	3.30E+00	6.04E-10	PACERR	2.53E+00	9.33E-03
HSPA5	4.99E+00	6.63E-03	RNASEK-C17o	3.23E+00	3.19E-08	AP000894.4	2.51E+00	1.38E-02
MDGA1	4.92E+00	7.82E-03	GABARAP	3.22E+00	2.86E-28	AL139286.2	2.50E+00	3.02E-02
CPE	4.91E+00	1.08E-02	MIA-RAB4B	3.18E+00	9.33E-06	AC009831.1	2.49E+00	3.81E-04
SLC44A5	4.86E+00	1.54E-02	AC048382.5	3.13E+00	1.55E-02	SAT1	2.49E+00	3.21E-03
AC083973.1	4.77E+00	3.81E-02	HBB	3.13E+00	6.58E-07	AC093462.1	2.48E+00	4.98E-07
ABCB4	4.69E+00	1.70E-02	RNASE4	3.11E+00	5.19E-11	LRRC70	2.48E+00	7.69E-11
CAVIN3	4.68E+00	3.25E-02	EEF1G	3.09E+00	8.95E-25	AC007881.3	2.47E+00	1.07E-02
LINC01233	4.68E+00	3.25E-02	HIST1H2AC	3.06E+00	3.14E-02	SMAD7	2.47E+00	7.45E-04
AC092718.8	4.66E+00	2.65E-02	TDRP	3.05E+00	2.05E-03	RAB31	2.45E+00	1.58E-02
AP001046.1	4.63E+00	2.96E-02	SOCS3	3.04E+00	3.48E-05	SLCO4A1	2.44E+00	3.16E-02
MAL2	4.58E+00	6.64E-03	DDX47	3.01E+00	6.36E-25	BCKDHA	2.43E+00	1.78E-08
DLX2	4.47E+00	3.28E-02	CPLX1	3.01E+00	1.11E-04	AL359541.1	2.42E+00	1.97E-03
AC097504.2	4.45E+00	3.23E-02	GADD45G	3.01E+00	2.26E-05	AC074044.1	2.40E+00	2.79E-02
AP000446.1	4.45E+00	3.23E-02	SMOX	2.98E+00	3.62E-02	HIPK1-AS1	2.40E+00	1.34E-05
HBA1	4.44E+00	6.64E-06	CA2	2.98E+00	2.81E-02	TUSC3	2.39E+00	1.53E-02
KIF26A	4.40E+00	4.38E-02	SEMA3E	2.97E+00	3.91E-05	AC093512.1	2.38E+00	1.17E-02
KRT86	4.40E+00	4.38E-02	AC096733.2	2.95E+00	1.49E-02	AC010422.3	2.35E+00	2.47E-02
IDI2-AS1	4.32E+00	8.62E-03	ABHD16A	2.94E+00	8.14E-15	ETV3	2.34E+00	4.43E-04
NHEJ1	4.26E+00	6.16E-15	GADD45B	2.92E+00	6.21E-08	AC004771.4	2.34E+00	6.90E-04
IGKC	4.18E+00	7.45E-04	AC019129.2	2.90E+00	6.09E-03	KLF2	2.33E+00	1.11E-17
MTRNR2L1	4.16E+00	2.69E-03	AC069148.1	2.87E+00	9.24E-04	TXNDC5	2.33E+00	2.26E-05

Gene	logFC	FDR	Gene	logFC	FDR	Gene	logFC	FDR
CYGB	2.31E+00	2.21E-02	QPCT	2.02E+00	8.94E-08	AC073195.1	1.75E+00	1.54E-02
SIK1	2.31E+00	3.95E-03	RAVER1	1.99E+00	6.22E-05	AC083829.2	1.74E+00	5.24E-03
EIF5AL1	2.30E+00	3.65E-04	MIR22HG	1.98E+00	2.94E-02	PAGR1	1.74E+00	4.14E-04
C19orf81	2.29E+00	1.91E-12	CCDC183	1.98E+00	2.53E-02	STOX1	1.74E+00	3.02E-02
SNURF	2.29E+00	6.63E-03	PNP	1.98E+00	2.01E-08	NBPF15	1.73E+00	6.68E-05
EGR2	2.26E+00	1.04E-02	PYDC1	1.97E+00	3.02E-02	DEPP1	1.73E+00	1.25E-03
FOSL1	2.24E+00	6.53E-03	AC087239.1	1.97E+00	8.30E-04	ATF3	1.72E+00	9.88E-05
SH3GL3	2.24E+00	3.61E-04	HSPA1B	1.96E+00	2.02E-03	ATP2B1-AS1	1.72E+00	1.05E-08
NOS1AP	2.23E+00	2.98E-02	NBL1	1.96E+00	8.62E-03	C18orf32	1.72E+00	2.51E-12
RUNDC3B	2.23E+00	9.19E-05	GPR183	1.95E+00	5.45E-06	MIR29B2CHG	1.71E+00	4.80E-05
PCOLCE-AS1	2.22E+00	2.70E-02	TMPO-AS1	1.94E+00	2.73E-06	FOS	1.69E+00	9.19E-05
CITED2	2.16E+00	1.81E-05	AL355388.2	1.93E+00	1.29E-02	LIN7A	1.69E+00	2.41E-02
CHRM3-AS2	2.16E+00	1.71E-02	PRR16	1.92E+00	5.06E-03	DOK5	1.69E+00	9.40E-05
RTN1	2.16E+00	2.34E-02	DUSP2	1.92E+00	2.18E-03	AL132639.2	1.69E+00	7.03E-05
AC010173.1	2.15E+00	8.23E-03	CCDC15	1.92E+00	2.19E-03	AC012615.1	1.69E+00	8.35E-09
ASPHD1	2.15E+00	4.12E-02	ACY1	1.90E+00	3.03E-06	FGL2	1.69E+00	1.63E-03
AC011773.4	2.15E+00	4.26E-02	MRPL38	1.90E+00	2.69E-08	TRAPPC5	1.68E+00	7.86E-06
OSBPL6	2.15E+00	3.02E-02	PDZK1IP1	1.90E+00	3.97E-05	COL9A3	1.68E+00	1.34E-02
AL118516.1	2.15E+00	6.20E-03	AC020659.1	1.89E+00	2.81E-02	AL117379.1	1.68E+00	3.51E-03
IQCJ-SCHIP1	2.14E+00	1.49E-04	EGLN2	1.87E+00	6.09E-03	AC069544.1	1.67E+00	4.62E-03
TM4SF1	2.14E+00	4.14E-02	JUN	1.86E+00	4.69E-07	SELP	1.66E+00	1.52E-04
ODF3L1	2.13E+00	2.24E-02	AP001437.1	1.86E+00	4.05E-02	MRC1	1.66E+00	2.98E-02
AC072061.1	2.12E+00	4.34E-04	ARL5A	1.83E+00	4.29E-15	PNMT	1.65E+00	9.26E-03
FAM218A	2.11E+00	1.21E-02	HAUS4	1.83E+00	6.81E-17	SKIL	1.63E+00	2.16E-02
AC012368.1	2.10E+00	1.58E-02	AL731569.1	1.83E+00	3.34E-03	AC010531.6	1.63E+00	8.15E-03
GNG10	2.10E+00	8.22E-12	WBP1	1.83E+00	5.59E-04	DDN-AS1	1.62E+00	4.57E-03
AC092053.2	2.10E+00	1.41E-02	SERTAD3	1.83E+00	1.45E-03	DUSP6	1.62E+00	3.02E-02
AC015912.3	2.09E+00	9.51E-03	EGR1	1.82E+00	2.75E-05	HIF3A	1.62E+00	4.83E-02
MFSD14A	2.08E+00	8.94E-08	AK1	1.80E+00	3.08E-04	AC017083.1	1.60E+00	4.69E-02
AC093635.1	2.08E+00	8.30E-04	GLRB	1.80E+00	1.20E-02	SOCS1	1.60E+00	5.38E-04
AL445228.2	2.07E+00	8.81E-04	DUSP1	1.80E+00	7.99E-08	AC020765.2	1.59E+00	6.37E-05
SGK1	2.07E+00	4.28E-02	KMT2E-AS1	1.80E+00	1.63E-11	UBC	1.58E+00	6.72E-03
MIDN	2.06E+00	2.62E-03	AC034236.2	1.80E+00	2.94E-03	TSC22D1	1.58E+00	4.81E-03
FAM71D	2.05E+00	4.98E-02	STOX2	1.79E+00	4.69E-02	ARF6	1.58E+00	1.33E-03
AC091271.1	2.05E+00	1.02E-08	ANKDD1B	1.78E+00	1.58E-02	AL627171.1	1.57E+00	3.23E-05
LINC01970	2.05E+00	1.11E-05	AL360270.1	1.77E+00	1.36E-02	AL353708.3	1.57E+00	2.94E-02
HAS2	2.03E+00	2.19E-03	CCDC80	1.77E+00	2.23E-02	NEAT1	1.57E+00	1.24E-02
MPZ	2.03E+00	3.21E-02	PHLDA2	1.77E+00	3.08E-02	ZFP36	1.57E+00	5.75E-06
Z83847.1	2.02E+00	2.75E-02	AC007032.1	1.76E+00	6.34E-06	TCEA3	1.56E+00	1.50E-02
MRPL53	2.02E+00	6.57E-18	ARL4A	1.75E+00	9.13E-12	NGRN	1.56E+00	2.15E-06

Gene	logFC	FDR	Gene	logFC	FDR	Gene	logFC	FDR
ZSWIM4	1.55E+00	9.12E-04	DSC2	1.37E+00	4.96E-02	CEBPB	1.14E+00	1.09E-02
RARRES1	1.55E+00	2.98E-03	AL121832.2	1.35E+00	9.91E-03	MSRB2	1.13E+00	1.59E-05
AL391121.1	1.54E+00	7.19E-05	KLF4	1.35E+00	3.41E-02	LMNA	1.13E+00	4.57E-03
CAHM	1.53E+00	7.58E-07	IER5L	1.34E+00	4.85E-03	MICA	1.13E+00	3.66E-02
KLF6	1.53E+00	6.72E-07	C8orf82	1.33E+00	4.63E-02	PPP1R15A	1.13E+00	7.96E-04
AC024257.3	1.53E+00	7.98E-03	JUNB	1.33E+00	1.14E-03	AC008764.8	1.13E+00	3.94E-03
CXCL2	1.53E+00	2.29E-04	YWHAH	1.33E+00	6.74E-03	MID1IP1	1.13E+00	2.45E-02
AL359513.1	1.53E+00	2.97E-04	EPB41L5	1.32E+00	3.59E-02	CHPT1	1.12E+00	1.22E-04
NOTCH4	1.52E+00	9.47E-03	DNAJB9	1.32E+00	9.51E-04	AL050341.2	1.12E+00	6.88E-04
C11orf80	1.51E+00	1.97E-03	ACOT2	1.32E+00	2.13E-03	RMI2	1.12E+00	1.18E-02
EPS8	1.51E+00	2.66E-04	DNAJB1	1.32E+00	1.24E-03	SHLD1	1.10E+00	8.23E-03
THSD7A	1.50E+00	2.85E-02	AC073389.1	1.32E+00	4.82E-03	TAF9	1.09E+00	2.65E-02
TMEM107	1.50E+00	8.14E-04	CLDND2	1.30E+00	1.04E-02	AL121944.1	1.09E+00	3.33E-02
CTF1	1.50E+00	1.86E-02	SERTAD1	1.29E+00	9.35E-05	CSRNP1	1.08E+00	1.19E-03
AC026979.2	1.50E+00	2.10E-03	RGCC	1.29E+00	4.45E-04	ILF3-DT	1.08E+00	3.04E-05
GOLGA6L9	1.50E+00	2.18E-03	CD9	1.29E+00	1.01E-02	PCDH9	1.08E+00	7.36E-03
AC093677.2	1.48E+00	1.07E-03	LINC01023	1.29E+00	7.41E-07	SGSM3	1.07E+00	2.02E-03
MZF1-AS1	1.47E+00	3.98E-04	AC025159.1	1.28E+00	8.77E-04	TRAPPC2B	1.07E+00	7.43E-03
AC023157.3	1.47E+00	4.20E-05	EIF4A3	1.28E+00	4.74E-04	Z93930.2	1.07E+00	3.08E-02
EMP2	1.46E+00	2.90E-02	KCNK12	1.25E+00	3.75E-02	NKX2-3	1.06E+00	3.02E-02
RAB24	1.46E+00	3.95E-06	RASSF6	1.24E+00	1.52E-02	MLF1	1.06E+00	1.72E-02
GRASP	1.46E+00	1.04E-04	H1F0	1.24E+00	1.22E-03	EIF5	1.06E+00	1.69E-03
AC099778.1	1.46E+00	1.12E-03	AC007541.1	1.24E+00	3.84E-02	TIMM10	1.05E+00	8.77E-03
CDK2AP1	1.46E+00	1.37E-06	AC006333.2	1.23E+00	7.71E-07	PTGS2	1.05E+00	1.74E-02
ZNF674-AS1	1.44E+00	3.64E-04	AC016727.1	1.22E+00	1.54E-02	B2M	1.04E+00	2.60E-04
HAR1B	1.44E+00	3.46E-02	THAP2	1.22E+00	2.99E-03	PLK3	1.04E+00	1.28E-04
H3F3B	1.43E+00	1.69E-02	IL1B	1.21E+00	3.80E-03	ANXA3	1.03E+00	1.19E-02
AL691403.2	1.42E+00	6.09E-03	PPP1R10	1.21E+00	4.99E-03	AC078846.1	1.03E+00	9.89E-03
LINC01116	1.42E+00	1.24E-03	EPHX1	1.20E+00	1.29E-03	MCL1	1.02E+00	6.79E-03
AC124016.1	1.41E+00	2.53E-02	TUBA1A	1.19E+00	3.59E-03	TLNRD1	1.01E+00	1.58E-02
LRP2BP	1.40E+00	4.46E-03	AL355353.1	1.19E+00	1.76E-02	TTC19	1.01E+00	6.17E-05
FTH1	1.40E+00	2.79E-02	FOSB	1.18E+00	3.30E-02	APOA1	1.00E+00	4.52E-02
AC004982.2	1.40E+00	1.54E-02	CMPK1	1.18E+00	5.83E-04	RGP1	1.00E+00	2.17E-03
AC099522.2	1.40E+00	3.88E-02	AL137802.2	1.18E+00	1.01E-02	MMP24OS	9.95E-01	1.58E-03
POLD4	1.39E+00	7.06E-07	TSC22D3	1.18E+00	1.14E-03	LINC01560	9.94E-01	3.70E-02
SRSF7	1.38E+00	9.00E-08	UBE2H	1.17E+00	3.94E-03	PSMA2	9.78E-01	6.79E-04
ANKRD65	1.38E+00	5.95E-03	YPEL5	1.16E+00	7.26E-05	JUND	9.77E-01	2.13E-02
SELENOK	1.38E+00	3.62E-02	ERVK3-1	1.14E+00	2.88E-05	CD81	9.74E-01	3.75E-02
AC022364.1	1.38E+00	2.67E-03	CDKN1C	1.14E+00	2.24E-02	AC097534.2	9.68E-01	1.24E-03
FAM133A	1.38E+00	4.38E-05	JPH4	1.14E+00	3.16E-02	ERLIN1	9.63E-01	2.47E-02

Gene	logFC	FDR	Gene	logFC	FDR	Gene	logFC	FDR
TGIF1	9.62E-01	3.88E-02	COQ7	8.23E-01	2.37E-03	PAIP2	7.07E-01	3.51E-02
SKP1	9.49E-01	8.57E-04	AL035563.1	8.17E-01	2.07E-02	IDS	7.00E-01	2.89E-02
CCNH	9.39E-01	2.18E-02	LXN	8.16E-01	3.95E-02	PLGRKT	6.94E-01	1.79E-02
C2orf74	9.35E-01	2.59E-02	CEACAM4	8.15E-01	1.65E-02	RPL34	6.84E-01	4.07E-02
CYYR1	9.33E-01	5.89E-03	RCC1L	8.09E-01	4.59E-02	TAX1BP1	6.81E-01	4.60E-02
ASH1L-AS1	9.31E-01	5.49E-03	STX8	8.09E-01	4.52E-02	POLE4	6.80E-01	2.07E-02
CAMTA1	9.27E-01	9.08E-03	DPH3	8.06E-01	1.21E-02	PRKAR1A	6.77E-01	2.24E-02
SELENOM	9.26E-01	2.58E-02	CD74	8.05E-01	3.02E-02	BEX5	6.75E-01	4.97E-02
AC090204.1	9.24E-01	7.76E-04	CMTM8	8.00E-01	3.18E-02	MYL12A	6.75E-01	3.03E-02
ASTE1	9.21E-01	1.38E-02	MYB	7.99E-01	3.46E-02	OCIAD2	6.74E-01	3.05E-02
CXorf40B	9.14E-01	4.08E-02	CLEC2B	7.96E-01	2.52E-02	IRAK3	6.74E-01	2.51E-02
SLC9A3R2	9.10E-01	8.49E-03	MMRN1	7.93E-01	8.23E-03	COMMD10	6.71E-01	3.18E-02
RPL7	9.09E-01	3.87E-03	HLA-DMA	7.87E-01	2.45E-02	IMMP2L	6.71E-01	2.58E-02
SRP14-AS1	9.08E-01	6.06E-03	C11orf1	7.80E-01	5.22E-03	EIF4A2	6.69E-01	4.60E-02
BBS2	9.05E-01	3.05E-02	TCEA2	7.79E-01	8.86E-03	BRWD1	6.63E-01	2.16E-02
RPL17	9.03E-01	9.23E-03	MGST2	7.79E-01	1.62E-02	ZFAND1	6.62E-01	4.46E-02
AL022328.4	9.02E-01	2.21E-02	ACSM3	7.74E-01	4.17E-02	FAM120AOS	6.56E-01	3.49E-02
TNFSF10	8.99E-01	1.18E-02	RBBP6	7.58E-01	1.40E-02	ACAT1	6.56E-01	4.12E-02
JMJD1C	8.96E-01	4.85E-02	RSL1D1	7.57E-01	1.29E-02	TMEM59	6.55E-01	3.41E-02
FZR1	8.92E-01	3.51E-02	C12orf66	7.53E-01	1.74E-02	SRI	6.52E-01	3.59E-02
FAF1	8.82E-01	1.19E-02	AC008267.5	7.49E-01	3.18E-02	TXNDC15	6.46E-01	4.94E-02
NDUFA7	8.82E-01	4.64E-04	CRYZL1	7.39E-01	8.67E-03	MAP3K13	6.43E-01	3.18E-02
YRDC	8.79E-01	4.84E-03	AC027644.3	7.39E-01	3.15E-02	AK6	6.28E-01	3.15E-02
LSR	8.73E-01	3.20E-02	AL162377.1	7.38E-01	3.27E-02	MRPL32	6.27E-01	3.15E-02
STUB1	8.57E-01	2.75E-02	CNBD2	7.37E-01	3.89E-02	RALB	6.24E-01	3.90E-02
FGFBP3	8.53E-01	3.82E-02	BCL2A1	7.36E-01	4.19E-02	FAM210B	6.23E-01	3.84E-02
TMLHE	8.51E-01	2.12E-02	VPS29	7.35E-01	1.08E-02	FBXL5	6.16E-01	4.77E-02
ISG20	8.47E-01	2.45E-02	CFH	7.34E-01	3.20E-02	ACYP1	5.94E-01	3.60E-02
TUBA4A	8.44E-01	1.97E-02	C11orf74	7.32E-01	1.58E-02	SMIM20	5.94E-01	4.25E-02
AC012306.2	8.42E-01	1.81E-02	LDHB	7.27E-01	3.10E-02			
GIPC2	8.40E-01	4.72E-02	CISD1	7.25E-01	2.03E-02			
CASP1	8.40E-01	3.15E-02	PPT1	7.25E-01	2.93E-02			
ANKRD28	8.39E-01	1.10E-02	CHURC1	7.24E-01	1.55E-02			
MDP1	8.38E-01	4.34E-02	HSPD1	7.23E-01	2.12E-02			
ANXA2R	8.35E-01	1.66E-02	CCDC28A	7.18E-01	2.58E-02			
SNHG10	8.34E-01	7.82E-03	GGPS1	7.18E-01	9.14E-03			
NEU1	8.33E-01	1.72E-02	KRT18	7.16E-01	1.93E-02			
TLE4	8.33E-01	2.54E-02	INTS13	7.15E-01	3.43E-02			
PNMA1	8.31E-01	1.47E-02	UBQLN2	7.08E-01	1.60E-02			
PGRMC2	8.29E-01	1.50E-02	DIAPH2	7.07E-01	3.92E-02			

A2 – downregulated in old donors

Gene	logFC	FDR	Gene	logFC	FDR	Gene	logFC	FDR
CPT1A	-6.17E-01	4.52E-02	UBXN6	-7.84E-01	2.96E-02	ZNF7	-8.64E-01	2.12E-02
ARHGAP30	-6.40E-01	3.58E-02	CNP	-7.85E-01	2.87E-02	DDX49	-8.67E-01	4.04E-03
TEX30	-6.54E-01	3.15E-02	ZDHHC7	-7.87E-01	2.54E-02	WDR35	-8.68E-01	4.23E-02
CREBRF	-6.55E-01	2.43E-02	ATF4	-7.87E-01	4.98E-02	CDK6	-8.71E-01	1.53E-02
EGFL7	-6.62E-01	3.99E-02	SYTL1	-7.88E-01	9.43E-03	COQ8B	-8.76E-01	1.10E-02
TTC37	-6.66E-01	2.58E-02	NOL10	-7.88E-01	2.91E-02	UBR5-AS1	-8.76E-01	1.21E-02
SUMF2	-6.80E-01	2.05E-02	JUP	-7.95E-01	2.12E-02	AP5S1	-8.79E-01	3.05E-02
TRAF7	-6.85E-01	3.28E-02	SASH3	-7.96E-01	2.84E-02	SRP19	-8.81E-01	1.24E-03
RAMMET	-6.87E-01	2.58E-02	NSA2	-8.00E-01	1.72E-02	NCBP2-AS2	-8.81E-01	9.74E-03
ETS2	-6.89E-01	4.58E-02	PI4KA	-8.01E-01	4.02E-02	AP002748.3	-8.84E-01	3.87E-03
CAVIN1	-7.02E-01	2.77E-02	GCC1	-8.01E-01	2.37E-02	BOD1L1	-8.85E-01	3.16E-02
CSF3R	-7.04E-01	2.58E-02	GPATCH11	-8.02E-01	1.58E-02	POLR2D	-8.87E-01	1.18E-02
TOR1AIP2	-7.10E-01	4.93E-02	AC020910.4	-8.06E-01	1.18E-02	WDR36	-8.90E-01	9.43E-03
SEPHS2	-7.11E-01	3.62E-02	NLE1	-8.06E-01	3.46E-02	PIK3R1	-8.97E-01	1.73E-02
GNPDA2	-7.12E-01	4.69E-02	CDK11A	-8.19E-01	1.55E-02	HEATR5B	-8.99E-01	4.52E-02
MRPL4	-7.16E-01	2.10E-02	EPSTI1	-8.19E-01	2.96E-02	ATP6V1H	-9.00E-01	1.19E-03
TMED7	-7.19E-01	1.74E-02	TRIM11	-8.20E-01	3.56E-02	FZD3	-9.05E-01	2.94E-02
STMN3	-7.24E-01	1.65E-02	ARHGAP25	-8.21E-01	1.82E-02	RMND5A	-9.09E-01	5.28E-03
MRPS12	-7.25E-01	2.05E-02	LETM1	-8.27E-01	1.58E-02	SMG1	-9.10E-01	1.60E-02
PCNA	-7.27E-01	3.15E-02	TNFRSF21	-8.29E-01	3.15E-02	CTCF	-9.19E-01	5.37E-03
TPT1	-7.31E-01	3.12E-02	SLC3A2	-8.33E-01	4.67E-03	ESYT2	-9.19E-01	1.82E-02
SFXN1	-7.32E-01	3.58E-02	DNAJC30	-8.34E-01	2.10E-02	MUS81	-9.25E-01	8.77E-03
ZC3H18	-7.35E-01	4.57E-02	PPME1	-8.40E-01	1.73E-02	RAB33B	-9.30E-01	2.10E-02
AHR	-7.36E-01	3.33E-02	RPL37	-8.42E-01	1.18E-02	C8orf59	-9.32E-01	8.53E-03
TKT	-7.36E-01	1.97E-02	ZNF669	-8.43E-01	4.43E-02	OSBPL7	-9.33E-01	4.36E-02
RPL38	-7.37E-01	3.15E-02	SLC48A1	-8.44E-01	1.86E-02	DGCR8	-9.36E-01	4.25E-02
RNF6	-7.40E-01	2.60E-02	XPO1	-8.44E-01	3.30E-02	DCLRE1C	-9.37E-01	6.72E-03
MED8	-7.41E-01	3.23E-02	TK2	-8.47E-01	2.02E-02	NSUN5	-9.37E-01	9.25E-04
XRRA1	-7.42E-01	4.34E-02	PPP1R8	-8.49E-01	1.33E-02	FAM241B	-9.39E-01	3.33E-02
PICK1	-7.43E-01	2.75E-02	C6orf47	-8.51E-01	3.24E-02	IL12A-AS1	-9.42E-01	4.06E-02
KCTD18	-7.43E-01	3.63E-02	TMEM115	-8.53E-01	1.69E-02	SLC19A1	-9.44E-01	3.46E-02
RPL28	-7.46E-01	1.97E-02	TNFRSF14	-8.54E-01	1.29E-03	TACO1	-9.45E-01	1.79E-02
ZNF431	-7.60E-01	2.65E-02	TP53	-8.55E-01	3.82E-03	AC092683.1	-9.49E-01	3.23E-02
SF3A2	-7.60E-01	1.61E-02	COG2	-8.57E-01	3.02E-02	HDHD3	-9.51E-01	2.25E-02
RASA4	-7.63E-01	4.12E-02	NFYA	-8.58E-01	4.40E-02	PLCG2	-9.52E-01	9.47E-03
DDHD2	-7.63E-01	4.17E-02	VHL	-8.59E-01	1.47E-02	COMMD5	-9.57E-01	2.33E-02
ZNF44	-7.64E-01	1.80E-02	MTPAP	-8.60E-01	1.69E-02	ZNF521	-9.58E-01	8.77E-04
AAK1	-7.68E-01	3.16E-02	YTHDF1	-8.63E-01	3.95E-02	SPNS2	-9.59E-01	2.07E-02
ARPC4	-7.78E-01	1.20E-02	LRRC58	-8.63E-01	3.36E-03	ING1	-9.60E-01	1.24E-02

Gene	logFC	FDR	Gene	logFC	FDR	Gene	logFC	FDR
POP7	-9.69E-01	2.23E-02	GSR	-1.12E+00	1.38E-02	PLAU	-1.35E+00	2.98E-02
FAM76A	-9.79E-01	3.56E-02	AFF3	-1.14E+00	2.96E-02	TONSL	-1.36E+00	4.35E-02
HCST	-9.80E-01	3.51E-02	P2RX1	-1.15E+00	1.53E-05	STARD5	-1.37E+00	3.28E-02
MPDU1	-9.82E-01	2.96E-03	ZNF16	-1.16E+00	3.48E-02	MOCS3	-1.37E+00	1.54E-02
CCDC18	-9.86E-01	3.56E-02	SPRY2	-1.16E+00	1.59E-02	ZNF738	-1.37E+00	3.68E-03
HMGB2	-9.86E-01	2.25E-03	IL16	-1.17E+00	2.46E-02	LINC01521	-1.38E+00	3.43E-02
SP1	-9.87E-01	4.41E-02	ST3GAL6	-1.18E+00	3.69E-02	SHLD3	-1.38E+00	1.28E-04
ETV5	-9.90E-01	2.62E-03	GHRL	-1.18E+00	2.96E-02	ZNF433	-1.39E+00	9.43E-03
GRAMD4	-9.91E-01	2.45E-02	CCDC71L	-1.18E+00	1.37E-03	ZNF668	-1.40E+00	3.24E-05
SCAI	-9.94E-01	5.05E-03	ZNF564	-1.18E+00	2.27E-02	ZNF844	-1.42E+00	5.77E-05
POMGNT1	-9.94E-01	1.68E-02	PREPL	-1.18E+00	2.97E-04	DPY19L3	-1.42E+00	3.28E-02
GPATCH3	-1.01E+00	1.78E-02	TWNK	-1.22E+00	4.41E-02	FRAT2	-1.42E+00	3.96E-02
CNEP1R1	-1.01E+00	2.93E-02	LANCL2	-1.22E+00	7.89E-03	NOG	-1.43E+00	2.09E-05
ICMT	-1.01E+00	3.08E-02	INTS5	-1.22E+00	1.55E-02	DOPEY2	-1.43E+00	3.28E-02
RNF144B	-1.01E+00	2.47E-02	ARVCF	-1.23E+00	1.85E-02	HDAC9	-1.45E+00	1.97E-03
PAPOLG	-1.01E+00	2.66E-02	GBGT1	-1.23E+00	1.84E-02	NHSL2	-1.46E+00	3.37E-02
SAC3D1	-1.02E+00	8.82E-03	ARRDC3	-1.23E+00	1.55E-02	TRBC2	-1.47E+00	4.58E-02
TAF5L	-1.02E+00	4.47E-02	CCDC137	-1.24E+00	2.18E-04	HPS6	-1.48E+00	1.69E-03
RETREG3	-1.02E+00	7.09E-03	MTA2	-1.24E+00	2.18E-03	EID2	-1.48E+00	1.37E-04
HIST1H2BN	-1.02E+00	2.15E-02	NPAS1	-1.25E+00	4.40E-02	AC005921.2	-1.48E+00	8.77E-03
C6orf62	-1.02E+00	9.12E-04	MIATNB	-1.26E+00	2.37E-03	IGHM	-1.49E+00	1.99E-04
TOR2A	-1.02E+00	4.46E-03	SDHAF1	-1.27E+00	9.19E-05	LIMD1	-1.50E+00	1.30E-02
NET1	-1.03E+00	4.34E-03	NEURL1	-1.27E+00	1.20E-03	ARL4D	-1.51E+00	3.13E-02
COLGALT1	-1.04E+00	3.86E-02	ANKRD49	-1.28E+00	2.45E-07	SPSB2	-1.52E+00	1.44E-02
SOX4	-1.04E+00	7.42E-04	KBTBD6	-1.28E+00	4.86E-02	AVPI1	-1.53E+00	1.15E-02
MYLIP	-1.05E+00	4.47E-03	DSEL	-1.28E+00	1.15E-02	HYLS1	-1.53E+00	2.27E-02
ZBTB24	-1.05E+00	6.80E-03	PPIF	-1.28E+00	1.31E-02	HLX	-1.54E+00	4.49E-04
AC092140.1	-1.05E+00	1.34E-02	RASSF2	-1.28E+00	4.94E-02	IGHD	-1.58E+00	3.40E-09
FEM1A	-1.05E+00	2.17E-03	SPATA5L1	-1.29E+00	9.88E-03	AC133550.2	-1.59E+00	3.98E-03
XPO4	-1.06E+00	1.84E-02	ENTR1	-1.31E+00	6.09E-03	TMIGD2	-1.59E+00	4.04E-03
TWF1	-1.07E+00	2.13E-04	C1QTNF4	-1.31E+00	7.42E-06	GSPT2	-1.60E+00	5.34E-07
VIRMA	-1.07E+00	3.94E-03	TGFBR2	-1.31E+00	7.45E-04	SAMSN1	-1.60E+00	4.09E-09
SNX11	-1.07E+00	3.27E-02	MT-ATP8	-1.31E+00	1.62E-02	PLK4	-1.61E+00	3.20E-02
SMG6	-1.08E+00	2.36E-03	MED23	-1.31E+00	2.44E-04	AREL1	-1.61E+00	4.51E-02
AC067852.2	-1.08E+00	1.24E-02	BASP1	-1.33E+00	6.98E-03	NEFH	-1.62E+00	4.82E-02
BRF2	-1.08E+00	1.19E-02	DDX28	-1.33E+00	2.25E-05	WASHC1	-1.63E+00	1.90E-09
TAF13	-1.09E+00	2.03E-02	NAGLU	-1.33E+00	3.16E-02	NAIF1	-1.64E+00	2.92E-03
ZNF441	-1.09E+00	4.88E-02	PMS2	-1.34E+00	1.24E-03	SLC15A4	-1.65E+00	1.49E-02
MKL1	-1.10E+00	2.97E-03	COL5A1	-1.34E+00	1.67E-03	CARD11	-1.65E+00	3.50E-02

Gene	logFC	FDR	Gene	logFC	FDR	Gene	logFC	FDR
IL10RA	-1.66E+00	4.60E-02	CD48	-2.21E+00	4.59E-03	GTF2H4	-3.67E+00	1.16E-02
AL390728.6	-1.68E+00	5.54E-09	HIST1H2AK	-2.29E+00	5.92E-03	ZC3H11B	-3.73E+00	1.33E-04
RIOX1	-1.68E+00	5.61E-04	SLC2A1-AS1	-2.33E+00	1.12E-02	AC138904.3	-3.79E+00	9.40E-03
MZB1	-1.69E+00	2.75E-02	RAB3IL1	-2.34E+00	8.90E-05	DCBLD1	-3.90E+00	9.19E-05
ZKSCAN2	-1.70E+00	3.47E-03	ACTL10	-2.35E+00	1.61E-02	HIST1H4F	-3.92E+00	3.01E-10
CNOT6	-1.70E+00	3.20E-02	AC135050.1	-2.38E+00	3.46E-02	RGS17	-4.11E+00	6.90E-04
TOR1B	-1.71E+00	1.69E-03	CA8	-2.44E+00	9.26E-03	COLEC12	-4.18E+00	9.35E-05
ZNF77	-1.73E+00	2.55E-02	AL935212.1	-2.47E+00	3.28E-02	TMPPE	-4.24E+00	1.52E-04
ZNF674	-1.73E+00	3.70E-02	STAG3	-2.47E+00	1.93E-03	DND1	-4.31E+00	2.87E-02
AC009093.2	-1.74E+00	2.02E-03	SLC16A14	-2.53E+00	3.51E-02	ITGA1	-4.40E+00	3.65E-04
HMGN4	-1.75E+00	3.69E-03	AC008040.5	-2.55E+00	2.05E-02	GPR137C	-4.73E+00	4.64E-02
URB2	-1.76E+00	2.62E-03	MAGI3	-2.57E+00	2.05E-02	AC009812.3	-4.74E+00	4.89E-02
XKR8	-1.76E+00	3.67E-03	ZNF57	-2.57E+00	1.99E-04	RASIP1	-4.77E+00	3.82E-02
AC090559.1	-1.76E+00	2.25E-02	AC008079.2	-2.57E+00	5.05E-03	AC011444.1	-4.82E+00	3.95E-02
FZD1	-1.78E+00	9.82E-03	NKG7	-2.62E+00	3.20E-03	CCDC3	-4.83E+00	3.59E-02
MILR1	-1.79E+00	4.25E-02	AC104248.1	-2.62E+00	4.15E-02	SLFNL1-AS1	-4.83E+00	3.93E-02
CRYBG1	-1.80E+00	3.75E-02	CDC20	-2.66E+00	4.95E-03	KLB	-4.84E+00	4.03E-02
AC074117.1	-1.80E+00	4.35E-05	SPDYE3	-2.66E+00	9.72E-04	CYP2D6	-4.84E+00	3.59E-02
PAM16	-1.80E+00	1.23E-03	SLC16A13	-2.71E+00	1.20E-02	AC020917.3	-4.85E+00	4.64E-02
AL360012.1	-1.82E+00	2.09E-02	MYLK	-2.72E+00	4.93E-02	LINC01798	-4.85E+00	4.64E-02
IGLL1	-1.84E+00	1.65E-04	GTF2IRD1	-2.74E+00	2.18E-02	KIZ-AS1	-4.85E+00	2.88E-09
AC008555.5	-1.85E+00	2.53E-02	AL512770.1	-2.78E+00	5.90E-03	S100A9	-4.88E+00	1.02E-02
RWDD3	-1.86E+00	8.77E-03	HIST1H4B	-2.85E+00	1.11E-06	PEBP4	-4.91E+00	3.41E-02
AC090825.1	-1.88E+00	4.28E-03	AL445686.2	-2.90E+00	8.19E-05	BX640514.2	-4.92E+00	3.07E-02
POLR2J3	-1.89E+00	4.91E-04	AC074386.1	-2.90E+00	4.62E-02	IKZF3	-4.92E+00	4.61E-02
CHRDL1	-1.93E+00	3.00E-02	AC084036.1	-2.91E+00	7.82E-03	DARS-AS1	-4.93E+00	2.96E-02
ZNF845	-1.98E+00	9.83E-04	LINC00937	-2.92E+00	1.27E-06	AL592295.4	-4.94E+00	4.43E-02
MARS2	-1.99E+00	3.65E-04	KIAA0087	-2.92E+00	2.02E-02	AC007228.2	-4.94E+00	2.96E-02
AC010737.1	-2.00E+00	2.07E-02	GNG11	-2.99E+00	3.33E-04	UPB1	-4.94E+00	2.96E-02
SPOCK2	-2.04E+00	4.42E-03	AC124283.1	-3.00E+00	3.65E-04	FAXC	-4.95E+00	3.25E-02
ORC6	-2.05E+00	2.90E-05	ADGRG5	-3.06E+00	8.53E-03	UMODL1	-4.96E+00	4.31E-02
DYTN	-2.08E+00	4.66E-03	AC007383.2	-3.06E+00	3.86E-03	AC092069.1	-4.96E+00	1.97E-03
ZSCAN32	-2.08E+00	2.70E-04	PDE6A	-3.06E+00	1.15E-02	AL449266.1	-4.98E+00	3.88E-02
AC018638.7	-2.09E+00	4.23E-02	FBLIM1	-3.07E+00	2.20E-03	CPB2-AS1	-4.98E+00	3.88E-02
THSD1	-2.15E+00	1.12E-02	DOCK6	-3.23E+00	2.97E-04	AL590652.1	-5.02E+00	2.21E-02
ZNF442	-2.17E+00	4.73E-04	SLC51A	-3.32E+00	5.81E-03	MIR193BHG	-5.03E+00	3.15E-02
NFATC4	-2.18E+00	3.21E-02	GATD3A	-3.33E+00	3.55E-03	OR3A3	-5.03E+00	2.50E-02
AC138696.2	-2.18E+00	1.51E-02	VASH2	-3.49E+00	3.96E-02	AP000552.1	-5.04E+00	3.90E-02
SIDT1-AS1	-2.20E+00	2.67E-04	CFAP58-DT	-3.50E+00	3.96E-02	AC010245.2	-5.05E+00	2.89E-02

Gene	logFC	FDR	Gene	logFC	FDR	Gene	logFC	FDR
TRPV3	-5.07E+00	3.70E-02	SYNPO2L	-5.53E+00	7.95E-03	AC008914.1	-6.51E+00	3.70E-03
TRIM60	-5.09E+00	2.05E-02	AL590867.1	-5.57E+00	9.47E-03	ANKRD20A8P	-6.62E+00	4.04E-03
LRRC74B	-5.09E+00	3.41E-02	PCAT7	-5.58E+00	3.04E-03	AC091891.2	-6.85E+00	9.35E-05
Z95114.2	-5.11E+00	1.86E-02	AL132657.1	-5.60E+00	2.97E-03	AC015987.1	-6.86E+00	1.42E-04
AP000487.1	-5.15E+00	2.77E-02	ITCH-AS1	-5.61E+00	1.35E-02	NACA2	-6.91E+00	7.42E-06
AL627309.1	-5.16E+00	3.36E-02	AC107982.3	-5.65E+00	2.84E-02	RPS6KB2-AS1	-7.16E+00	1.94E-04
SLC30A2	-5.18E+00	1.85E-02	HEATR4	-5.66E+00	3.89E-02	AC008763.2	-7.21E+00	1.15E-06
AC092634.3	-5.18E+00	1.37E-02	Z98885.2	-5.68E+00	3.44E-03	TEKT4	-7.24E+00	2.18E-03
AC004922.1	-5.19E+00	1.58E-02	AL445248.1	-5.69E+00	2.87E-07	FAM239B	-7.32E+00	6.31E-03
AC093525.7	-5.19E+00	1.29E-02	AP000962.1	-5.69E+00	1.36E-02	GSTT2B	-7.34E+00	8.30E-04
AC002116.2	-5.19E+00	1.39E-02	GABRD	-5.75E+00	4.66E-03	HLA-DRB5	-7.42E+00	9.88E-05
C9orf41-AS1	-5.20E+00	1.41E-02	TMEM9B-AS1	-5.76E+00	1.63E-03	RBFOX1	-7.76E+00	1.56E-02
MAP3K10	-5.21E+00	1.63E-02	GAS7	-5.79E+00	9.33E-03	PRDM6	-8.11E+00	2.18E-02
AL358075.2	-5.21E+00	2.45E-02	KCNJ5	-5.83E+00	6.33E-03	AC008083.2	-8.14E+00	5.29E-10
CR936218.1	-5.22E+00	1.86E-02	DDTL	-5.83E+00	1.21E-02	OR2A25	-8.25E+00	2.35E-13
LINC01770	-5.23E+00	1.43E-05	COL8A1	-5.83E+00	1.86E-03	LRRC7	-8.31E+00	1.10E-11
AGAP2-AS1	-5.25E+00	1.92E-02	AC117503.1	-5.85E+00	7.15E-03	CRYBB2	-8.36E+00	6.53E-03
APOBEC3A	-5.26E+00	4.39E-02	AL512625.3	-5.87E+00	4.44E-04	AC243829.5	-8.59E+00	3.99E-02
ZNF556	-5.26E+00	2.73E-02	AP003392.1	-5.87E+00	3.11E-03	AC073896.3	-9.07E+00	7.09E-22
FSCN3	-5.29E+00	1.60E-02	GLIPR1L1	-5.90E+00	4.89E-03	MTRNR2L8	-9.63E+00	2.86E-28
NGFR	-5.30E+00	2.31E-02	AC084871.2	-5.96E+00	5.66E-03	MTRNR2L12	-1.05E+01	6.03E-38
AL117190.1	-5.31E+00	1.29E-02	AL354977.2	-5.96E+00	4.77E-04			
AC068389.4	-5.34E+00	1.17E-02	CU634019.6	-5.99E+00	2.14E-02			
AC008731.1	-5.38E+00	1.79E-02	AL160191.1	-6.01E+00	4.49E-04			
SLC37A2	-5.39E+00	2.57E-06	OR4D9	-6.04E+00	4.57E-03			
AC092849.1	-5.40E+00	2.40E-02	OR10G3	-6.05E+00	4.36E-04			
KCNN1	-5.44E+00	2.95E-02	STEAP4	-6.07E+00	1.45E-03			
SLC14A2	-5.45E+00	1.11E-02	OR51M1	-6.12E+00	1.52E-02			
TSGA13	-5.45E+00	2.86E-02	STAC2	-6.19E+00	6.92E-03			
AL137003.1	-5.47E+00	1.04E-02	AC138207.2	-6.23E+00	1.90E-04			
AL355312.2	-5.48E+00	1.55E-02	MPO	-6.27E+00	1.95E-04			
SLC3A1	-5.48E+00	1.55E-02	LINC01209	-6.27E+00	2.05E-03			
AC131212.1	-5.48E+00	4.57E-03	SLC28A2	-6.40E+00	4.07E-03			
AC013468.1	-5.48E+00	5.70E-03	AL359397.2	-6.40E+00	7.45E-04			
Z95114.1	-5.48E+00	1.39E-02	CADM2	-6.42E+00	5.58E-03			
PART1	-5.49E+00	2.10E-02	HIGD1B	-6.45E+00	6.90E-04			
AL157938.2	-5.49E+00	7.06E-03	AC092718.5	-6.47E+00	4.44E-04			
AC079305.1	-5.51E+00	2.08E-09	PCDH9-AS1	-6.48E+00	5.37E-04			
FAM83F	-5.52E+00	3.69E-03	AC007014.1	-6.50E+00	2.96E-05			

B. Lists of differentially expressed genes (FDR < 0.05) when comparing old donor vs young donor multilineage output HSCs defined in the integrative analysis. Base of the log is 2

B1 – upregulated in old donors

Gene	logFC	FDR	Gene	logFC	FDR	Gene	logFC	FDR
HSPA6	7.51E+00	4.43E-03	PIK3R2	2.26E+00	1.42E-02	GADD45B	1.48E+00	2.18E-04
FABP4	5.90E+00	1.05E-02	MRPL38	2.20E+00	1.65E-05	DNAJB9	1.47E+00	6.61E-04
SEMA3E	5.82E+00	1.56E-04	CYR61	2.20E+00	2.82E-02	Z93930.2	1.45E+00	1.79E-02
ZCCHC12	5.71E+00	1.38E-02	SOCS3	2.19E+00	1.33E-09	AC010531.6	1.44E+00	2.69E-02
ANGPTL4	5.58E+00	4.41E-02	CEP83-DT	2.17E+00	4.28E-03	AC091271.1	1.42E+00	3.59E-03
LINC02158	5.43E+00	3.25E-03	SH3GL3	2.10E+00	1.02E-03	AC087239.1	1.39E+00	4.94E-03
NECAB1	5.40E+00	6.48E-03	EIF5AL1	2.10E+00	6.54E-04	IL1B	1.36E+00	5.20E-04
MTRNR2L1	5.27E+00	2.71E-03	MFSD14A	2.10E+00	4.11E-08	ETV3	1.36E+00	6.46E-05
HBA2	5.14E+00	9.46E-03	PAGR1	2.08E+00	4.63E-04	AC012615.1	1.33E+00	1.50E-04
HSPA5	5.03E+00	1.10E-03	LINC01970	2.04E+00	2.79E-04	CCDC15	1.32E+00	2.21E-02
FIGN	5.03E+00	1.41E-17	PDZK1IP1	2.04E+00	8.32E-03	PNP	1.32E+00	6.46E-05
LINC01731	5.02E+00	2.38E-02	C19orf81	2.02E+00	1.82E-09	SNHG10	1.31E+00	7.77E-04
CHODL	4.84E+00	2.40E-02	TJP2	1.99E+00	9.44E-03	KLF6	1.29E+00	3.71E-05
RND3	4.70E+00	4.76E-02	AC069544.1	1.99E+00	2.64E-02	KDM4B	1.29E+00	2.51E-02
AC245884.8	4.60E+00	4.80E-02	GNG10	1.99E+00	5.87E-05	ARL4A	1.28E+00	2.12E-05
COPZ2	4.45E+00	4.76E-02	BOLA2-SMG1I	1.98E+00	4.60E-03	MIR155HG	1.27E+00	3.82E-02
GATD3B	4.45E+00	6.05E-06	RAB24	1.95E+00	2.42E-04	CHPT1	1.27E+00	7.84E-05
IFIT2	4.27E+00	1.57E-02	NBPF15	1.92E+00	4.28E-03	CDK2AP1	1.27E+00	2.01E-05
HERPUD1	4.19E+00	1.03E-02	AC007541.1	1.86E+00	3.67E-02	ZFP36	1.26E+00	5.54E-04
SNX15	3.80E+00	1.99E-06	ARL5A	1.85E+00	2.34E-12	DUSP2	1.24E+00	2.21E-02
AL162457.1	3.43E+00	5.85E-03	ACY1	1.84E+00	1.02E-02	TSC22D3	1.24E+00	1.96E-04
RUNDC3B	3.41E+00	5.94E-06	LINC01116	1.82E+00	4.01E-05	CCNQ	1.20E+00	2.69E-02
PERP	3.39E+00	1.13E-08	CITED2	1.82E+00	4.00E-05	MSRB2	1.20E+00	5.11E-05
AC010173.1	3.38E+00	2.68E-02	POLD4	1.79E+00	4.01E-07	CNST	1.20E+00	3.84E-02
EEF1G	3.31E+00	4.04E-29	DUSP6	1.78E+00	1.07E-02	RMI2	1.19E+00	7.49E-03
ACSS3	3.27E+00	2.09E-02	MRPL53	1.75E+00	2.60E-07	JUN	1.18E+00	1.44E-02
SNAI3-AS1	3.24E+00	2.23E-02	ACOT2	1.74E+00	7.48E-07	AL050341.2	1.17E+00	4.16E-03
MACROD2	3.21E+00	4.25E-02	SOCS1	1.70E+00	7.25E-03	KMT2E-AS1	1.14E+00	9.00E-03
RNASE4	3.16E+00	1.16E-05	C18orf32	1.70E+00	6.31E-08	CDKN1A	1.13E+00	6.02E-03
GABARAP	3.12E+00	5.41E-41	SAT1	1.69E+00	2.21E-02	ATP2B1-AS1	1.09E+00	1.06E-02
MIA-RAB4B	2.96E+00	2.60E-02	DNAJC12	1.68E+00	6.52E-04	AC025159.1	1.09E+00	2.81E-03
AC114490.2	2.92E+00	6.80E-03	AC124016.1	1.64E+00	5.91E-03	PCDH9	1.07E+00	1.83E-02
EIF4EBP3	2.88E+00	3.09E-13	FOS	1.64E+00	1.49E-05	UBE2H	1.07E+00	1.61E-02
RNASEK-C17o	2.76E+00	2.86E-02	IQCJ-SCHIP1	1.63E+00	3.35E-02	HAUS7	1.07E+00	2.21E-02
VWA1	2.75E+00	4.09E-03	WHRN	1.61E+00	4.97E-02	TUBA1A	1.07E+00	1.89E-03
HSPA1B	2.75E+00	2.71E-03	DUSP1	1.61E+00	4.31E-06	C2orf74	1.04E+00	2.21E-02
AC020916.1	2.70E+00	4.49E-13	DNAJB1	1.60E+00	6.80E-03	ILF3-DT	1.04E+00	5.11E-05
AC116407.2	2.63E+00	1.93E-05	AC092803.2	1.59E+00	4.75E-02	RNASEH2A	1.04E+00	1.19E-02
BCKDHA	2.63E+00	9.38E-07	AL139089.1	1.58E+00	2.24E-02	PSMA2	1.03E+00	4.56E-06
NHEJ1	2.60E+00	4.86E-02	TRAPPC5	1.57E+00	8.96E-03	NDUFA7	1.02E+00	5.20E-04
ABHD16A	2.54E+00	3.16E-07	KLF2	1.57E+00	1.23E-07	NME7	1.01E+00	1.03E-03
EGLN2	2.54E+00	2.91E-05	AC093635.1	1.56E+00	3.30E-02	TAF9	1.01E+00	4.94E-03
RAVER1	2.47E+00	5.23E-07	HAUS4	1.56E+00	1.33E-10	SGSM3	1.01E+00	4.81E-02
HIPK1-AS1	2.42E+00	1.05E-05	NGRN	1.55E+00	9.00E-03	TBC1D7	1.00E+00	1.43E-02
DDX47	2.41E+00	1.17E-07	C8orf44	1.51E+00	1.35E-03	AL359504.2	9.97E-01	4.69E-02
TXNDC5	2.41E+00	2.16E-05	ZNF883	1.51E+00	2.64E-02	NBL1	9.92E-01	2.82E-02
TUSC3	2.40E+00	3.63E-04	AC023157.3	1.51E+00	1.07E-02	TTC19	9.87E-01	6.46E-05
SIK1	2.36E+00	3.90E-03	AL132639.2	1.50E+00	4.65E-02	OMA1	9.74E-01	3.36E-02
CCDC80	2.30E+00	2.16E-05	MZF1-AS1	1.49E+00	8.49E-04	FOSB	9.55E-01	4.04E-02

Gene	logFC	FDR	Gene	logFC	FDR
C11orf74	9.54E-01	4.43E-04	DARS	6.82E-01	1.48E-02
ZMYM5	9.52E-01	2.08E-02	LSM5	6.76E-01	1.55E-02
CCT8	9.49E-01	4.22E-03	AK6	6.75E-01	2.59E-02
SPARC	9.41E-01	4.28E-03	ALG5	6.73E-01	3.96E-02
RPL7	9.37E-01	6.80E-04	TMEM59	6.71E-01	3.07E-02
ACAT1	9.24E-01	2.51E-03	ATP5PB	6.70E-01	2.11E-02
YWHAH	9.22E-01	7.84E-03	CSTF3	6.64E-01	3.69E-02
SDE2	9.10E-01	1.38E-02	SLC25A5	6.53E-01	2.79E-02
RPL17	9.05E-01	8.85E-03	DGUOK	6.50E-01	3.98E-02
TRIM13	9.05E-01	3.29E-02	ILF2	6.32E-01	3.19E-02
CYSTM1	9.03E-01	1.41E-02	PDIA6	6.27E-01	3.30E-02
PLGRKT	8.95E-01	4.40E-03	ATP5MPL	6.19E-01	2.82E-02
B2M	8.93E-01	1.02E-03	ATP5F1C	6.12E-01	3.98E-02
MGST2	8.93E-01	1.35E-03	ATP5F1A	6.02E-01	4.69E-02
EPDR1	8.85E-01	3.77E-02			
FARSB	8.83E-01	4.18E-03			
NOC3L	8.82E-01	1.07E-02			
C3orf14	8.82E-01	2.89E-02			
H2AFY2	8.66E-01	2.46E-02			
LDHB	8.62E-01	7.62E-04			
RSL1D1	8.45E-01	4.28E-03			
RARS	8.41E-01	2.21E-02			
SKP1	8.35E-01	2.90E-03			
SNF8	8.35E-01	2.24E-02			
ANKRD28	8.14E-01	1.48E-02			
MRPL32	8.13E-01	1.02E-02			
SRSF7	7.96E-01	6.53E-03			
UCHL3	7.94E-01	1.22E-02			
CLEC2B	7.75E-01	2.84E-02			
MSH2	7.71E-01	9.54E-03			
RPL34	7.70E-01	8.32E-03			
CRYZL1	7.64E-01	4.13E-02			
STX8	7.61E-01	4.66E-02			
PPA2	7.57E-01	4.60E-03			
AC008124.1	7.56E-01	1.79E-02			
CHURC1	7.53E-01	3.26E-03			
SRI	7.49E-01	7.94E-03			
HSPD1	7.28E-01	1.17E-02			
HSD17B12	7.20E-01	2.17E-02			
PSMB3	7.19E-01	1.22E-02			
N4BP2L1	7.15E-01	4.71E-02			
PRDX2	7.12E-01	2.85E-02			
MMRN1	7.11E-01	3.86E-02			
PPT1	6.99E-01	1.01E-02			
CDC26	6.99E-01	2.21E-02			
TMEM230	6.97E-01	2.08E-02			
HIKESHI	6.94E-01	1.53E-02			
MDH1	6.85E-01	1.37E-02			
HIGD1A	6.83E-01	3.98E-02			

B2 – downregulated in old donors

Gene	logFC	FDR	Gene	logFC	FDR
EIF2S3	-6.13E-01	4.19E-02	SIK3	-1.07E+00	3.07E-02
NOP53	-6.15E-01	4.00E-02	SAV1	-1.08E+00	4.80E-02
POLR2J3.1	-6.57E-01	4.27E-02	TXNIP	-1.09E+00	1.07E-02
TKT	-6.59E-01	2.86E-02	THEMIS2	-1.09E+00	1.01E-02
PTGER4	-6.65E-01	3.45E-02	PLEKHA2	-1.09E+00	2.69E-02
STMN3	-6.74E-01	4.88E-02	EP300	-1.09E+00	1.02E-02
RPS11	-6.79E-01	3.51E-02	MYLIP	-1.11E+00	2.07E-02
RPL30	-6.81E-01	4.20E-02	AAK1	-1.11E+00	2.52E-02
SOX4	-7.00E-01	3.79E-02	UBXN6	-1.13E+00	1.95E-02
ZNF292	-7.28E-01	4.87E-02	FEM1A	-1.15E+00	3.59E-03
EGFL7	-7.32E-01	1.04E-02	SLC48A1	-1.15E+00	2.41E-02
RPLP2	-7.42E-01	1.51E-02	LYZ	-1.15E+00	2.45E-02
TNFRSF14	-7.69E-01	3.29E-02	VHL	-1.15E+00	6.10E-03
MT-ND4L	-7.74E-01	3.98E-02	MKI67	-1.16E+00	2.88E-02
INPP5D	-7.75E-01	2.23E-02	ARMC5	-1.16E+00	4.62E-02
RPSA	-7.76E-01	1.02E-02	ZFYVE27	-1.16E+00	4.06E-02
RPS12	-7.80E-01	1.15E-02	METTL16	-1.17E+00	4.03E-02
WDR45B	-7.83E-01	3.49E-02	FOSL2	-1.17E+00	3.90E-03
RPL7A	-7.90E-01	1.15E-02	CTCF	-1.17E+00	1.92E-03
MRPL43	-7.94E-01	3.30E-02	LUZP1	-1.17E+00	2.44E-03
TACC3	-8.00E-01	3.35E-02	C1QTNF4	-1.20E+00	2.67E-05
RPL37A	-8.03E-01	1.49E-02	PDE4B	-1.21E+00	3.06E-03
DUSP10	-8.08E-01	4.83E-02	ATF4	-1.22E+00	1.05E-05
ELF2	-8.11E-01	3.86E-02	ZBTB10	-1.23E+00	1.34E-02
CAVIN1	-8.16E-01	7.94E-03	COMMD5	-1.23E+00	3.42E-02
RPL28	-8.59E-01	2.61E-03	ZBTB24	-1.23E+00	1.83E-02
TPT1	-8.60E-01	2.51E-03	EID3	-1.23E+00	2.75E-02
MAFF	-8.64E-01	8.32E-03	GPATCH11	-1.24E+00	1.03E-02
XPO1	-8.71E-01	2.85E-02	ERO1B	-1.25E+00	1.02E-02
POP7	-8.73E-01	2.40E-02	GCC1	-1.26E+00	4.79E-02
PIK3R1	-8.74E-01	1.01E-02	RNF113A	-1.27E+00	2.77E-03
MGAT1	-8.80E-01	2.08E-02	C6orf62	-1.27E+00	8.63E-07
RPL38	-8.84E-01	2.36E-03	MED23	-1.29E+00	7.25E-03
BOD1L1	-8.92E-01	3.96E-02	ATG13	-1.30E+00	3.15E-02
MAPKAPK5-A	-9.03E-01	2.08E-02	P2RX1	-1.32E+00	7.68E-03
IGHD	-9.13E-01	3.34E-02	LTB	-1.33E+00	4.21E-03
SPTY2D1	-9.25E-01	4.41E-02	MUS81	-1.35E+00	6.07E-03
NOL10	-9.68E-01	4.05E-02	ZNF266	-1.35E+00	2.86E-02
CHD8	-9.73E-01	4.58E-02	SMPD2	-1.36E+00	4.41E-02
BROX	-9.77E-01	7.49E-03	VILL	-1.36E+00	4.58E-02
NRDE2	-9.85E-01	4.95E-02	MTA2	-1.38E+00	4.69E-02
HCST	-9.88E-01	8.08E-03	FANCF	-1.39E+00	1.07E-02
RPL37	-9.93E-01	1.50E-04	LGALS1	-1.39E+00	1.86E-04
ARPC4	-9.95E-01	1.89E-03	ZNF521	-1.40E+00	1.56E-04
THAP1	-1.01E+00	4.69E-02	DDX28	-1.41E+00	5.99E-04
AC020910.4	-1.01E+00	4.17E-02	PREPL	-1.43E+00	3.46E-02
NR4A1	-1.01E+00	7.90E-03	AC092140.1	-1.43E+00	4.79E-02
C8orf59	-1.02E+00	6.45E-04	ANKRD49	-1.44E+00	6.46E-05
MAP3K8	-1.03E+00	7.46E-03	TNFAIP8L1	-1.45E+00	5.58E-03
RPP38	-1.07E+00	2.88E-02	SAMSN1	-1.45E+00	4.23E-06

Gene	logFC	FDR	Gene	logFC	FDR
AC005921.2	-1.46E+00	4.41E-02	MPO	-3.43E+00	1.47E-07
ALKBH4	-1.47E+00	7.90E-03	DYTN	-3.45E+00	2.08E-02
IL3RA	-1.48E+00	4.52E-02	COLEC12	-3.53E+00	4.91E-03
MEPCE	-1.49E+00	5.91E-03	RTN4RL2	-3.58E+00	9.41E-03
ZFY	-1.54E+00	8.96E-03	HIST1H4F	-3.65E+00	4.43E-05
AL031777.3	-1.58E+00	2.03E-03	GATD3A	-3.67E+00	1.64E-03
IQCH-AS1	-1.61E+00	1.95E-02	MEG8	-3.70E+00	8.32E-03
DGCR8	-1.62E+00	1.10E-02	AL445686.2	-3.78E+00	6.70E-03
HEATR5B	-1.64E+00	1.61E-02	NLRP2	-3.78E+00	6.48E-03
POLR2J3	-1.65E+00	2.90E-02	DCBLD1	-4.07E+00	1.43E-02
NEFH	-1.68E+00	4.45E-02	HIST1H4B	-4.53E+00	8.10E-04
LANCL2	-1.69E+00	1.06E-02	IRF8	-4.94E+00	1.89E-03
PILRB	-1.71E+00	1.18E-03	AC007611.1	-5.38E+00	4.69E-02
PMS2	-1.74E+00	8.38E-03	ZFP3	-5.41E+00	4.95E-02
ARRDC3	-1.77E+00	9.17E-07	PRICKLE3	-5.41E+00	4.69E-02
WASHC1	-1.80E+00	3.97E-09	IL10RA	-5.49E+00	4.71E-02
SLC25A28	-1.82E+00	2.09E-02	AC015987.1	-5.51E+00	4.86E-02
CD48	-1.85E+00	1.53E-02	MS4A3	-5.52E+00	3.12E-02
PPP2R3B	-1.86E+00	4.52E-02	AC092069.1	-5.57E+00	9.11E-06
TADA1	-1.86E+00	9.66E-03	AC079305.1	-5.98E+00	4.28E-03
ZNF668	-1.88E+00	1.22E-03	KIZ-AS1	-6.03E+00	4.94E-03
RIOX1	-1.91E+00	7.59E-05	RNASE2	-6.03E+00	3.51E-02
TGFBR2	-1.92E+00	1.07E-02	AC008763.2	-6.07E+00	4.28E-03
NR4A3	-1.93E+00	1.03E-03	TEKT4	-6.11E+00	4.79E-02
AC074117.1	-2.02E+00	5.54E-04	OR2A25	-6.20E+00	4.74E-03
SPSB2	-2.04E+00	7.03E-03	AL445248.1	-6.25E+00	8.85E-03
RPS6KL1	-2.04E+00	2.68E-02	AL512625.3	-6.34E+00	6.08E-03
AC067852.2	-2.05E+00	1.33E-02	SLC37A2	-6.38E+00	4.45E-03
HIST1H1B	-2.05E+00	5.85E-03	AC008083.2	-6.66E+00	1.75E-03
MAN2B1	-2.06E+00	3.01E-02	LRRC7	-6.99E+00	6.89E-05
HS1BP3	-2.08E+00	3.24E-02	HLA-DRB5	-7.42E+00	1.23E-05
GNE	-2.08E+00	2.40E-02	AC073896.3	-7.69E+00	3.65E-08
AL390728.6	-2.15E+00	1.36E-05	CRYBB2	-7.91E+00	1.01E-02
HPS6	-2.15E+00	1.27E-02	MTRNR2L8	-8.06E+00	8.67E-11
TAF13	-2.17E+00	7.70E-03	AZU1	-8.44E+00	8.05E-10
ZKSCAN2	-2.17E+00	1.79E-02	ELANE	-8.91E+00	1.02E-08
LPAR6	-2.22E+00	1.01E-02	MTRNR2L12	-8.99E+00	1.43E-15
CDC42EP4	-2.22E+00	4.87E-02	PRTN3	-9.41E+00	4.66E-08
AC090825.1	-2.26E+00	2.29E-02			
AC008555.5	-2.43E+00	3.69E-02			
HLX	-2.45E+00	4.82E-04			
GNG11	-2.48E+00	2.81E-03			
RBAK	-2.51E+00	1.61E-02			
FRAT2	-2.57E+00	2.08E-02			
PPIP5K1	-2.64E+00	4.13E-02			
AC133550.2	-2.79E+00	6.07E-04			
HIST1H2AH	-3.04E+00	6.46E-05			
STAG3	-3.18E+00	6.46E-03			
XKR8	-3.29E+00	2.81E-03			
HIST1H2AL	-3.37E+00	4.79E-02			

C. Lists of differentially expressed genes (FDR < 0.05) when comparing old donor platelet -biased HSCs versus old donor multilineage output HSCs defined in the integrative analysis. Base of the log is Euler's number

C1- upregulated in old donor platelet -biased HSCs

Gene	logFC	FDR	Gene	logFC	FDR	Gene	logFC	FDR
A1BG	6.23E-02	1.14E-10	AKIRIN2	2.39E-02	1.32E-08	ARMCX3	3.01E-02	2.15E-10
AAED1	1.69E-01	7.11E-15	AKR1C3	7.69E-02	1.63E-03	ARMCX6	2.54E-02	7.14E-09
AATF	1.51E-02	4.03E-13	AL118516.1	1.74E-01	1.16E-11	ARPC4	3.30E-02	1.47E-10
ABCB1	3.57E-02	2.05E-06	AL121944.1	1.54E-01	2.64E-12	ARRDC2	8.38E-02	1.22E-09
ABCB7	3.40E-02	1.44E-11	AL359504.2	1.76E-02	3.72E-07	ARRDC3	8.02E-02	2.38E-08
ABHD14B	2.03E-01	8.74E-17	AL592183.1	3.88E-02	4.02E-08	ASAH1	9.80E-02	2.90E-09
ABI1	1.94E-02	2.57E-11	ALCAM	2.92E-02	6.50E-06	ASH1L	7.28E-02	2.40E-10
ABLIM1	4.32E-02	1.60E-10	ALDH1A1	3.09E-01	7.90E-17	ATF1	8.38E-03	8.27E-06
ABRAXAS1	8.14E-02	2.11E-13	ALDH2	4.82E-02	1.89E-10	ATF3	2.14E-01	2.05E-14
AC008124.1	1.65E-03	4.04E-07	ALG13	1.67E-01	7.14E-15	ATF4	1.03E-01	1.06E-19
AC011139.1	6.07E-01	3.15E-97	ALKBH5	4.05E-02	2.37E-16	ATF6B	3.45E-02	6.43E-11
AC012615.1	1.20E-02	6.42E-07	ALKBH7	1.99E-01	3.38E-24	ATF7IP2	1.22E-01	1.92E-06
AC020916.1	5.01E-01	8.35E-29	AMD1	4.77E-02	8.23E-07	ATG16L2	7.54E-02	4.59E-13
AC025159.1	1.70E-04	1.64E-07	AMPD2	6.15E-02	3.72E-14	ATP1B1	6.83E-02	1.06E-12
AC026369.3	3.65E-02	3.21E-11	ANGPT1	3.45E-02	7.90E-06	ATP2B1-AS1	1.97E-01	8.36E-18
AC026979.2	7.35E-02	1.10E-09	ANKRD11	1.41E-02	1.01E-07	ATP2C1	2.13E-02	1.05E-09
AC087239.1	5.35E-02	3.83E-06	ANKRD12	1.18E-01	2.09E-09	ATP5F1D	1.50E-01	1.22E-10
AC090204.1	1.05E-01	7.23E-13	ANKRD28	2.29E-01	2.64E-09	ATP6AP1	4.03E-02	5.73E-13
AC091271.1	2.62E-02	1.54E-08	ANXA1	2.18E-01	6.72E-06	ATP6V0A1	6.61E-02	7.00E-09
AC092171.3	8.00E-02	4.80E-14	ANXA11	2.31E-02	4.14E-07	ATXN3	3.32E-02	2.26E-09
AC100810.1	3.24E-02	9.40E-12	ANXA6	9.28E-02	5.09E-12	ATXN7L3B	1.76E-02	1.01E-08
AC114760.2	2.21E-01	7.88E-16	ANXA7	1.11E-01	1.22E-13	AVP	4.00E-01	2.64E-21
AC245297.3	9.60E-02	3.44E-11	AP002387.2	1.92E-02	2.40E-10	BABAM2	3.97E-03	6.10E-12
ACAA1	2.90E-02	6.65E-07	AP1G2	5.32E-02	4.77E-11	BAG5	2.28E-02	4.07E-11
ACAP1	1.30E-01	4.67E-12	AP2B1	3.79E-02	1.12E-10	BAG6	7.06E-02	3.00E-16
ACO2	1.31E-03	5.97E-09	APEH	2.30E-02	1.21E-05	BAZ2A	4.01E-02	4.65E-08
ACSM3	3.49E-01	2.53E-45	APH1A	6.76E-02	9.50E-19	BAZ2B	5.30E-02	3.82E-11
ACSS1	8.72E-05	4.80E-11	APLP2	9.01E-02	3.83E-10	BBX	1.12E-03	3.67E-10
ACTG1	9.45E-02	1.71E-02	APMAP	1.98E-02	8.14E-07	BCAS2	1.72E-01	1.95E-17
ACTR1A	2.52E-02	3.63E-07	APOBEC3C	1.46E-02	1.07E-07	BCAT1	1.52E-02	2.62E-05
ACTR1B	4.25E-02	5.09E-14	APP	1.68E-01	7.06E-12	BCL11A	3.34E-02	1.60E-09
ACYP2	2.63E-02	1.55E-04	APRT	1.26E-01	5.42E-10	BCL2A1	1.01E-01	1.22E-17
ADAM28	1.99E-01	3.28E-27	AREG	8.55E-01	5.81E-53	BCL2L13	7.58E-03	3.27E-10
ADAR	3.00E-02	1.81E-07	ARF1	9.86E-02	5.34E-09	BCL7B	7.52E-02	3.82E-12
ADD1	2.01E-02	4.12E-12	ARF3	2.77E-02	4.60E-10	BEX1	3.16E-02	1.20E-03
ADGRG6	4.89E-02	2.13E-08	ARF4	1.45E-02	3.21E-12	BEX2	2.21E-01	2.50E-14
ADPRM	6.74E-02	1.11E-18	ARF6	1.18E-01	3.66E-13	BEX4	1.68E-01	9.41E-13
AES	6.07E-02	6.47E-14	ARFGAP2	1.59E-02	1.75E-11	BEX5	1.75E-01	1.66E-16
AFF4	7.28E-02	2.08E-12	ARFGAP3	3.97E-02	4.65E-09	BFAR	4.09E-02	3.66E-08
AFTPH	4.44E-02	9.19E-10	ARHGAP15	1.06E-01	2.16E-08	BHLHE40	8.69E-02	5.07E-08
AGPS	1.24E-02	5.43E-17	ARHGAP45	3.75E-02	4.46E-07	BIN1	2.18E-02	5.51E-10
AHNAK	6.54E-02	9.86E-08	ARHGAP9	2.35E-03	2.26E-06	BIN2	3.97E-02	1.01E-09
AIDA	1.62E-02	5.83E-12	ARHGEF1	6.15E-02	4.23E-14	BIRC2	1.21E-01	7.06E-10
AIF1	8.00E-02	6.09E-04	ARHGEF2	5.94E-02	1.24E-08	BIRC3	1.70E-01	1.55E-17
AIMP1	4.11E-02	2.55E-09	ARID4A	2.94E-02	4.42E-07	BISPR	6.14E-02	1.02E-11
AIP	2.90E-02	5.59E-12	ARID5A	1.41E-01	9.07E-15	BLOC1S6	4.23E-03	5.07E-14
AJ009632.2	1.67E-01	8.85E-14	ARIH2	4.72E-04	2.74E-08	BLVRA	3.89E-02	5.81E-13
AKAP13	1.24E-01	7.76E-13	ARL14EP	4.20E-02	7.27E-08	BLVRB	1.96E-02	3.22E-13
AKAP17A	5.03E-02	9.64E-06	ARL4A	5.32E-01	6.63E-37	BMI1	3.87E-02	4.30E-12
AKIRIN1	6.95E-02	2.79E-08	ARMCX1	1.15E-01	2.10E-10	BNIP2	1.12E-01	2.43E-13

Gene	logFC	FDR	Gene	logFC	FDR	Gene	logFC	FDR
BNIP3	2.36E-02	5.28E-12	CBX6	5.10E-02	1.85E-05	CEP68	4.77E-02	2.60E-08
BNIP3L	9.55E-02	9.30E-11	CCDC115	9.03E-04	8.06E-15	CEP70	5.07E-03	8.13E-11
BORCS7	7.28E-03	8.94E-06	CCDC12	1.36E-02	5.10E-17	CFAP20	3.99E-02	1.29E-04
BPTF	3.92E-02	8.28E-13	CCDC42	1.17E-01	1.95E-15	CFAP36	4.27E-02	4.33E-10
BRAF	4.49E-02	9.41E-10	CCDC57	1.82E-02	4.32E-08	CFAP97	5.56E-03	5.31E-14
BRD4	1.56E-02	2.31E-06	CCDC59	4.03E-02	1.18E-11	CFH	9.57E-02	3.74E-09
BRMS1	4.24E-02	1.84E-09	CCDC85B	4.66E-02	1.89E-11	CFLAR	2.80E-02	1.29E-05
BRWD1	8.16E-02	1.74E-12	CCDC91	1.65E-02	1.02E-05	CGGBP1	7.94E-03	1.96E-13
BSDC1	2.72E-02	1.47E-06	CCND2	3.52E-02	1.80E-11	CHCHD5	6.00E-03	1.07E-05
BSPRY	3.19E-02	1.07E-09	CCND3	4.54E-02	8.23E-11	CHCHD7	3.55E-02	6.37E-09
BST2	5.03E-01	3.28E-40	CCNDBP1	1.08E-01	8.68E-10	CHD1	1.54E-02	1.39E-08
BTG1	2.50E-01	6.84E-10	CCNG1	4.03E-02	8.91E-12	CHD2	1.53E-02	1.19E-10
BTG2	9.82E-02	3.16E-05	CCNH	2.68E-01	5.89E-20	CHD9	8.26E-02	9.87E-10
BTN3A2	4.43E-02	5.47E-07	CCNI	3.33E-01	8.14E-14	CHIC2	1.07E-04	4.42E-08
BUD23	2.82E-02	1.27E-20	CCNL1	2.00E-01	2.29E-10	CHMP1B	2.90E-01	8.74E-18
C11orf1	4.73E-02	3.41E-14	CCPG1	3.53E-02	5.91E-06	CHMP2A	2.08E-02	8.79E-10
C12orf10	6.67E-02	3.25E-07	CCSER2	5.37E-02	1.28E-07	CHMP3	5.82E-02	1.06E-10
C12orf76	5.36E-03	6.73E-07	CD109	1.85E-02	1.13E-06	CHMP4B	4.26E-03	1.45E-10
C15orf40	2.49E-02	2.05E-08	CD151	7.79E-02	7.56E-18	CHP1	6.82E-02	3.46E-10
C16orf54	8.21E-02	6.06E-09	CD164	1.23E-01	2.56E-03	CHST11	3.67E-02	7.61E-09
C18orf32	4.36E-02	2.42E-16	CD300A	4.80E-02	1.94E-07	CHTOP	9.30E-03	2.49E-11
C19orf24	8.25E-03	6.27E-07	CD302	3.51E-02	3.10E-09	CHURC1	7.00E-02	1.30E-05
C19orf53	2.00E-02	4.72E-18	CD34	4.86E-02	4.52E-07	CIR1	1.03E-01	4.40E-11
C19orf66	3.44E-03	7.76E-14	CD37	7.68E-01	5.88E-79	CIRBP	3.30E-01	2.75E-32
C1orf162	6.07E-02	1.35E-11	CD44	6.19E-01	1.64E-63	CITED2	2.91E-01	3.08E-10
C1orf21	5.83E-02	3.24E-10	CD46	7.90E-02	1.92E-12	CLDND1	5.31E-02	4.88E-10
C2orf69	3.04E-02	1.62E-10	CD52	1.19E-01	3.07E-03	CLEC2B	1.12E-01	3.30E-09
C6orf48	7.51E-01	1.42E-64	CD53	6.70E-02	4.89E-08	CLEC9A	1.34E-01	2.03E-14
C6orf62	3.74E-02	8.96E-10	CD55	5.24E-02	7.38E-11	CLIC1	1.73E-01	1.01E-06
C7orf50	1.45E-02	1.50E-07	CD63	5.55E-02	2.05E-16	CLIC2	7.39E-02	5.29E-13
C8orf59	6.73E-02	4.39E-10	CD74	6.11E-01	3.43E-157	CLINT1	6.83E-02	3.64E-16
C9orf43	7.28E-02	4.53E-08	CD79B	2.38E-02	1.14E-04	CLK1	1.20E-01	2.12E-08
C9orf72	1.51E-02	1.82E-11	CD82	1.17E-01	1.45E-17	CLN5	1.13E-02	3.99E-12
CACUL1	3.48E-02	7.34E-08	CD9	5.60E-02	1.70E-12	CLTA	3.29E-02	1.28E-10
CALCOCO2	5.37E-02	8.16E-10	CDADC1	7.64E-02	7.58E-15	CLTB	4.38E-02	6.37E-19
CALHM6	6.13E-02	8.23E-14	CDC40	1.22E-02	4.27E-06	CLU	5.27E-01	8.83E-41
CALN1	8.42E-02	2.13E-12	CDC42	7.44E-02	1.52E-06	CMBL	5.10E-02	1.48E-14
CAMLG	9.62E-02	2.49E-07	CDC42SE1	4.97E-03	5.65E-07	CMPK1	2.30E-01	1.02E-11
CAPN1	3.97E-02	4.63E-07	CDC42SE2	3.67E-02	7.32E-06	CMTM6	1.93E-02	1.17E-15
CAPN2	3.02E-02	9.27E-11	CDC73	2.07E-02	3.19E-11	CNBD2	4.10E-02	1.58E-08
CAPN7	3.87E-02	2.82E-11	CDIP1	2.80E-02	6.39E-07	CNIH1	3.53E-02	4.42E-09
CARD19	1.55E-01	1.06E-14	CDIPT	2.12E-02	1.39E-07	CNOT1	3.23E-02	3.28E-10
CARD8	1.06E-01	4.99E-13	CDK5RAP3	1.98E-02	1.19E-07	CNOT2	3.61E-02	3.60E-09
CASP1	4.09E-02	1.11E-12	CDKN1A	1.74E-01	2.63E-16	CNOT4	2.78E-02	4.62E-12
CASP4	1.10E-01	9.90E-08	CDV3	5.52E-02	5.31E-15	CNPPD1	1.40E-02	7.34E-10
CAST	8.51E-02	3.64E-14	CEBPB	2.14E-01	6.62E-17	CNST	3.29E-02	8.80E-12
CAVIN1	6.90E-02	5.59E-11	CEBPZ	2.17E-02	1.12E-08	COMMD6	3.24E-01	3.16E-28
CAVIN2	4.08E-01	1.06E-24	CEBPZOS	7.33E-02	5.94E-16	COPA	7.33E-03	5.57E-10
CBWD5	2.15E-02	6.58E-13	CELF2	4.74E-02	2.58E-09	COPB1	3.08E-02	2.81E-12
CBX2	2.57E-02	1.49E-07	CENPC	4.68E-02	4.20E-10	COPS2	2.32E-02	2.77E-08

Gene	logFC	FDR	Gene	logFC	FDR	Gene	logFC	FDR
COPZ1	1.84E-02	1.04E-11	CYSLTR1	1.54E-01	2.36E-19	DUSP11	6.96E-03	2.68E-09
COQ10B	6.78E-02	4.04E-14	CYTH2	1.53E-02	1.22E-15	DUSP2	1.36E-01	4.72E-05
COQ8A	3.80E-03	2.21E-09	CYTIP	3.20E-02	3.12E-05	DYNC1H1	1.17E-02	3.66E-12
CORO1B	2.26E-02	1.82E-05	CYTL1	8.74E-02	3.06E-08	DYNC1I2	8.84E-02	6.08E-14
CORO1C	3.16E-02	1.43E-09	CYTOR	1.34E-01	1.82E-08	DYNLRB1	6.88E-02	2.53E-09
COX19	5.39E-02	1.47E-10	DAP	4.95E-02	6.97E-15	DYNLT3	7.59E-02	2.09E-13
COX20	5.50E-02	2.36E-14	DAP3	6.00E-03	1.52E-12	EAPP	5.14E-02	4.56E-09
COX4I1	6.73E-02	2.94E-02	DAZAP2	1.67E-01	1.86E-09	EBAG9	2.12E-04	3.85E-09
COX7A2L	2.31E-02	4.54E-07	DCAF11	6.69E-03	8.39E-06	EBLN3P	4.68E-02	4.77E-08
COX7C	4.16E-02	1.72E-04	DCAF8	6.17E-02	1.81E-10	EBPL	4.86E-02	8.89E-04
CPNE1	1.64E-02	5.28E-06	DCP1A	4.33E-02	1.09E-08	ECSIT	5.07E-02	4.34E-08
CPNE3	9.70E-02	2.13E-12	DCTN2	2.91E-02	1.37E-15	EDEM2	6.28E-03	6.31E-09
CPPED1	5.53E-04	6.31E-08	DCTN6	1.19E-02	3.09E-08	EDF1	1.46E-01	6.80E-11
CPQ	7.17E-02	1.41E-12	DDA1	1.34E-02	2.28E-13	EEF1A1	2.09E-01	8.77E-53
CRBN	1.15E-01	7.73E-11	DDAH2	2.39E-01	2.19E-21	EEF1AKMT2	6.09E-03	9.73E-15
CREG1	9.78E-02	6.66E-11	DDRGK1	2.65E-02	1.19E-08	EEF1D	9.35E-02	1.08E-03
CRHBP	6.63E-01	1.28E-52	DDX17	1.25E-01	8.26E-10	EEF2	3.68E-01	1.14E-76
CRTAP	8.65E-03	9.65E-12	DDX18	2.65E-02	3.90E-10	EGFL7	1.73E-01	2.39E-09
CRYGD	1.08E-01	5.03E-15	DDX24	1.66E-01	5.94E-11	EGR1	1.32E-01	4.16E-10
CRYL1	7.20E-02	1.52E-11	DDX27	3.85E-02	4.74E-06	EHMT1	3.57E-03	5.49E-07
CRYZL1	7.41E-02	1.33E-10	DDX3X	2.44E-01	1.78E-16	EHMT2	2.29E-02	2.72E-09
CSDE1	1.72E-01	4.94E-06	DDX3Y	1.14E-01	4.86E-08	EID1	1.06E-01	2.06E-04
CSNK1A1	9.56E-03	7.01E-09	DDX5	3.93E-01	4.23E-34	EIF1	4.57E-01	7.20E-132
CSNK1D	7.55E-02	1.27E-07	DDX54	1.68E-02	1.22E-15	EIF1B	2.36E-01	1.17E-13
CSRNP1	3.06E-01	3.00E-35	DEF6	6.56E-03	9.80E-04	EIF2A	2.57E-01	5.80E-17
CSRP1	5.65E-02	3.31E-10	DEPTOR	2.79E-02	4.35E-09	EIF2AK4	3.43E-03	1.58E-04
CST3	4.25E-01	1.86E-26	DERL1	2.22E-02	1.74E-10	EIF2B1	8.17E-04	4.24E-12
CTBP2	6.98E-04	7.03E-14	DGKZ	4.81E-02	7.66E-09	EIF2D	6.37E-02	4.72E-10
CTDSP1	1.81E-02	1.05E-12	DHPS	4.33E-02	3.67E-13	EIF2S3	1.76E-01	5.26E-10
CTDSP2	2.41E-02	1.07E-08	DHRS7	7.82E-02	1.39E-12	EIF3D	3.76E-01	7.64E-20
CTNNA1	2.33E-02	2.18E-08	DIAPH2	9.83E-03	1.26E-05	EIF3E	3.25E-01	1.56E-58
CTNNB1	4.18E-02	3.44E-07	DLK1	1.65E-01	5.54E-24	EIF3F	1.69E-01	1.70E-04
CTSB	2.12E-02	4.35E-08	DNAJB1	3.57E-02	3.01E-07	EIF3G	2.38E-01	5.96E-15
CTSC	2.38E-02	4.51E-10	DNAJB14	6.08E-02	2.15E-10	EIF3H	2.74E-01	3.82E-12
CTSD	1.61E-01	1.32E-19	DNAJB6	1.39E-01	2.85E-04	EIF3I	3.06E-02	4.91E-10
CTSF	1.87E-01	6.91E-28	DNAJB9	1.28E-01	7.04E-16	EIF3K	7.69E-02	1.13E-07
CTSO	2.16E-02	1.78E-06	DNAJC10	1.41E-02	6.06E-12	EIF3M	1.11E-01	1.37E-07
CTSS	2.71E-01	1.66E-20	DNAJC3	3.25E-03	3.31E-13	EIF4A1	1.24E-01	1.40E-12
CTSW	1.51E-01	3.28E-11	DNAJC4	1.92E-01	1.69E-22	EIF4A2	5.81E-01	7.71E-79
CUL5	3.70E-02	2.64E-09	DNAJC7	1.37E-02	9.80E-11	EIF4B	3.21E-01	5.90E-18
CUX1	4.44E-03	1.22E-09	DOCK8	5.18E-02	1.22E-05	EIF4G2	5.94E-03	2.17E-14
CWC25	4.24E-02	1.29E-06	DPF2	1.15E-02	2.45E-08	EIF4H	1.28E-01	1.32E-14
CWF19L2	2.41E-02	2.63E-07	DPH3	2.74E-02	8.97E-05	EIF5	3.03E-02	1.44E-07
CXCL2	2.87E-01	6.60E-14	DPH5	3.42E-02	3.24E-07	ELF1	6.79E-02	3.43E-05
CXCL3	1.29E-01	2.79E-05	DPM1	1.69E-02	5.83E-11	ELF2	1.36E-02	3.28E-06
CXCL8	4.17E-01	4.76E-20	DPPA4	6.48E-03	3.06E-05	ELK3	5.79E-02	2.38E-07
CXCR4	2.19E-01	1.57E-05	DRAM2	3.42E-02	4.27E-10	ELK4	3.93E-02	2.66E-08
CYB5R1	2.57E-02	3.11E-08	DST	7.17E-02	4.38E-13	ELMO1	1.73E-01	4.63E-14
CYHR1	3.26E-02	3.67E-09	DTNBP1	5.31E-03	4.34E-09	ELOF1	7.82E-03	5.18E-07
CYLD	4.13E-02	1.67E-06	DUSP1	4.15E-01	5.08E-33	ELOVL5	2.28E-02	5.16E-12

Gene	logFC	FDR	Gene	logFC	FDR	Gene	logFC	FDR
ELP2	6.23E-02	7.55E-13	FAM53C	4.86E-02	1.98E-09	GGA1	4.42E-02	3.61E-04
EMB	2.30E-03	7.44E-10	FAM96B	3.58E-02	9.22E-14	GGNBP2	7.16E-03	2.21E-09
EMC3	3.44E-02	1.34E-10	FAU	3.02E-01	3.22E-66	GID8	2.20E-02	4.20E-13
EMC6	1.78E-03	5.27E-11	FBXL15	3.52E-02	1.45E-15	GIMAP2	1.03E-01	1.61E-17
EMCN	1.04E-01	1.30E-16	FBXL5	9.47E-02	6.73E-18	GINM1	3.86E-02	3.28E-13
EMD	2.14E-02	1.68E-06	FBXO7	2.39E-02	1.42E-12	GIT2	4.66E-03	1.49E-09
EMP1	1.19E-01	5.67E-10	FBXW5	1.16E-02	4.16E-08	GLIPR1	1.93E-01	3.33E-14
EMP3	2.66E-01	5.11E-16	FCER1A	1.28E-01	2.31E-13	GLTP	6.55E-02	1.24E-12
EPB41L4A-AS	3.91E-01	2.57E-39	FCGRT	1.03E-01	3.50E-10	GMPR2	8.17E-02	4.70E-12
EPC1	7.31E-02	3.52E-12	FERMT3	1.76E-02	6.16E-12	GNA15	9.79E-02	6.58E-06
EPM2AIP1	1.16E-02	8.05E-06	FES	5.67E-02	1.84E-11	GNAI2	1.17E-02	1.01E-16
EPS15	2.18E-02	1.45E-09	FEZ2	3.35E-02	4.54E-09	GNAI3	2.03E-02	3.39E-03
ERAP2	2.98E-03	2.24E-06	FGD5-AS1	6.05E-03	1.16E-15	GNB2	1.88E-02	4.12E-05
ERCC1	1.33E-02	5.88E-09	FHIT	3.67E-02	3.18E-06	GNG7	2.67E-02	2.29E-10
EREG	1.06E-01	2.02E-04	FHL1	2.06E-02	9.69E-06	GOLGB1	3.89E-02	3.29E-08
ERG	4.52E-02	2.22E-06	FIS1	2.30E-01	2.58E-17	GPAT3	7.42E-02	6.99E-10
ERGIC1	3.88E-02	1.91E-11	FKBP8	5.85E-02	2.19E-17	GPATCH8	1.45E-02	8.48E-09
ERGIC3	8.47E-02	6.64E-03	FLI1	8.87E-02	1.50E-13	GPBP1L1	5.45E-02	7.09E-10
ERICH1	1.66E-01	1.13E-15	FLII	1.96E-02	6.01E-07	GPI	4.64E-03	2.92E-12
ERLIN1	2.58E-02	1.84E-10	FLOT1	6.21E-02	2.94E-10	GPSM2	2.66E-04	4.28E-07
ERP29	1.20E-01	3.11E-08	FMNL1	5.57E-02	1.53E-09	GPSM3	1.57E-01	9.11E-16
ERP44	2.81E-02	1.37E-14	FNBP1	1.18E-01	6.38E-07	GRAMD1A	3.37E-02	7.83E-08
ERV3-1	2.10E-03	3.89E-12	FNBP4	1.57E-02	1.42E-09	GRB2	8.01E-03	5.96E-11
ESD	1.34E-01	1.60E-07	FNIP1	2.52E-02	4.15E-15	GRHPR	2.31E-02	9.66E-09
ETFRF1	7.27E-02	1.03E-11	FOPNL	2.69E-03	8.32E-12	GRINA	5.81E-02	2.33E-11
ETNK1	1.18E-02	1.00E-16	FOS	3.80E-01	8.03E-36	GRK2	2.33E-02	7.66E-07
ETS2	5.00E-02	5.16E-07	FOSB	5.74E-01	3.12E-43	GRN	1.64E-02	3.64E-08
ETV3	1.51E-01	6.19E-11	FOSL1	9.95E-02	3.01E-12	GRSF1	5.72E-03	1.39E-07
ETV6	4.08E-02	8.38E-10	FOXN3	8.41E-02	1.14E-09	GSDMD	1.64E-02	2.35E-03
EVI2A	6.12E-02	1.12E-09	FOXO3	8.82E-02	6.68E-12	GSN	8.69E-02	3.82E-12
EVI2B	2.65E-01	1.51E-21	FOXP1	6.72E-02	2.46E-07	GSTK1	2.31E-01	1.21E-18
EVL	1.80E-02	8.38E-12	FRA10AC1	1.56E-02	3.95E-09	GSTM3	8.33E-02	1.36E-11
EXOC7	6.68E-02	2.71E-09	FRMD4B	2.84E-02	1.53E-07	GSTM5	8.38E-02	7.48E-11
EXOSC7	1.88E-03	2.68E-08	FTH1	7.19E-01	5.36E-185	GSTO2	3.14E-02	1.60E-07
EZR	4.87E-02	6.93E-03	FTL	2.76E-01	1.90E-54	GTF2B	3.84E-02	4.64E-07
F2R	6.99E-03	5.71E-07	FTX	9.30E-02	1.78E-16	GTF2F1	1.68E-01	1.83E-20
FAAP20	2.27E-02	6.24E-18	FXR1	6.23E-02	1.33E-12	GTF2F2	6.30E-03	7.87E-11
FAHD2A	5.04E-03	1.64E-06	FXYD5	4.53E-01	6.32E-43	GUCY1A1	1.71E-01	2.27E-12
FAM118A	2.06E-02	2.18E-07	G3BP2	4.50E-02	1.80E-10	GUCY1B1	8.27E-02	2.52E-10
FAM124B	5.25E-02	3.77E-09	G6PD	3.05E-02	5.20E-08	H1F0	6.06E-01	2.26E-52
FAM162A	2.07E-02	1.13E-11	GABARAP	1.62E-01	3.84E-09	H1FX	2.63E-01	4.86E-11
FAM177A1	8.44E-02	7.60E-06	GABARAPL2	2.42E-01	7.76E-17	H2AFJ	4.27E-02	1.22E-10
FAM19A2	7.94E-02	2.07E-10	GABPB1-AS1	1.16E-01	1.61E-07	H3F3B	1.89E-01	3.29E-10
FAM200B	7.26E-03	2.14E-11	GADD45A	2.93E-01	2.39E-16	HACD4	1.02E-02	2.90E-11
FAM204A	1.19E-02	1.61E-10	GADD45B	2.46E-01	4.76E-22	HADHA	2.26E-01	1.26E-16
FAM210B	2.84E-02	7.41E-07	GAPT	4.06E-02	6.34E-17	HADHB	2.35E-02	3.88E-12
FAM215B	3.21E-02	2.65E-09	GATA2	1.68E-01	2.71E-15	HARS	4.08E-02	1.73E-10
FAM219B	3.12E-02	1.42E-06	GBP4	1.42E-01	2.41E-12	HAX1	5.62E-02	5.35E-07
FAM228B	5.55E-03	2.62E-09	GCC2	3.78E-02	2.32E-18	HBP1	4.90E-02	1.32E-10
FAM3C	3.24E-02	1.31E-09	GCSAML	1.59E-02	4.09E-06	HDAC5	3.74E-02	3.93E-09

Gene	logFC	FDR	Gene	logFC	FDR	Gene	logFC	FDR
HEBP1	8.09E-02	8.90E-10	ICAM2	5.04E-02	5.77E-12	JUP	2.11E-02	4.64E-05
HEBP2	2.47E-02	1.93E-13	ICAM3	2.98E-01	4.10E-12	KAT2A	1.66E-02	2.99E-05
HECTD1	3.22E-02	4.22E-05	ID1	3.34E-01	2.71E-20	KAT6B	6.10E-05	1.80E-06
HERC2	3.29E-02	1.28E-10	ID2	4.84E-01	6.38E-28	KCNAB2	2.92E-02	1.11E-08
HEXA	4.59E-02	1.21E-08	IDH3G	8.43E-03	8.02E-12	KCNQ1OT1	7.07E-02	4.19E-06
HGSNAT	5.37E-02	2.63E-10	IDS	5.95E-01	2.78E-44	KDELR1	2.05E-01	2.47E-19
HIF1A	8.83E-02	1.68E-11	IER2	2.26E-01	4.04E-08	KDM5B	3.32E-02	6.90E-10
HIGD2A	2.16E-02	9.87E-10	IFI16	7.41E-02	9.42E-14	KDM6B	9.24E-02	3.68E-12
HIPK1	3.72E-03	3.44E-11	IFI27L2	8.65E-02	7.28E-17	KDSR	7.24E-03	1.49E-07
HIST1H1C	7.33E-01	1.91E-107	IFIT2	5.01E-02	8.06E-04	KHDC4	2.17E-02	4.24E-09
HIST1H1D	6.17E-02	6.34E-10	IFITM3	3.20E-02	2.60E-05	KHDRBS1	6.29E-02	1.13E-12
HIST1H2AC	4.18E-01	5.37E-41	IFNGR1	4.23E-02	2.78E-06	KLF10	1.26E-01	2.15E-05
HIST1H2AE	1.56E-01	6.90E-40	IFRD1	1.22E-01	7.58E-12	KLF13	5.04E-02	1.41E-10
HIST1H2BC	2.10E-01	4.75E-28	IFT20	1.85E-02	5.90E-04	KLF2	4.33E-01	1.62E-42
HIST1H2BG	1.63E-01	2.87E-38	IFT57	6.31E-03	3.62E-16	KLF3	1.31E-01	3.81E-10
HIST2H2AC	1.15E-01	7.47E-14	IGBP1	2.03E-01	1.12E-15	KLF4	2.12E-01	4.19E-15
HIST2H2BE	3.35E-01	8.79E-55	IGF2BP2	4.75E-02	4.71E-10	KLF6	2.58E-01	3.36E-07
HIST3H2A	1.18E-01	6.31E-18	IK	4.05E-02	6.31E-07	KLF7	5.96E-02	2.20E-12
HLA-A	6.30E-01	1.65E-47	IL18	1.39E-01	7.56E-20	KLF9	6.38E-02	4.01E-10
HLA-B	6.46E-01	9.82E-56	IL27RA	2.23E-02	4.78E-09	KLHDC2	7.62E-03	4.17E-12
HLA-C	4.10E-01	7.13E-23	ILF3-DT	8.85E-02	1.48E-10	KLHL24	3.83E-03	3.19E-05
HLA-DMA	4.47E-01	2.34E-27	IMMP2L	2.38E-02	1.03E-10	KLHL6	4.94E-02	3.69E-08
HLA-DMB	1.45E-01	2.71E-22	IMPACT	3.22E-03	7.05E-10	KMT2A	1.83E-02	3.38E-07
HLA-DOA	9.76E-02	8.05E-16	ING4	4.91E-03	4.37E-10	KMT2E	6.66E-02	2.49E-06
HLA-DPA1	8.04E-01	5.15E-95	INO80E	1.75E-02	1.15E-10	KPNA4	4.85E-02	7.49E-13
HLA-DPB1	7.04E-01	2.22E-86	INPP5D	1.40E-01	2.06E-15	KRAS	2.55E-02	2.52E-07
HLA-DQA1	3.21E-01	8.83E-29	INSIG1	1.46E-01	5.32E-04	KRCC1	2.92E-02	1.06E-11
HLA-DQA2	9.15E-02	1.25E-10	INSIG2	2.56E-02	2.35E-09	KRT18	8.46E-02	2.13E-09
HLA-DQB1	6.14E-01	3.27E-58	INTS6	2.00E-02	1.71E-08	KRT8	7.96E-02	4.28E-08
HLA-DRA	6.96E-01	7.95E-167	INTS8	1.64E-02	1.92E-07	KYAT3	3.63E-02	3.53E-10
HLA-DRB1	6.16E-01	6.66E-48	IPO11	2.55E-02	3.43E-09	LAIR1	1.62E-01	9.02E-21
HLA-E	8.86E-01	2.08E-129	IQGAP2	4.19E-02	5.40E-15	LAMP2	4.10E-02	4.48E-07
HLF	8.90E-02	3.80E-11	IRAK3	1.00E-01	2.75E-10	LAMTOR1	3.09E-01	4.35E-21
HMGA2	6.71E-02	2.95E-09	IRF1	3.53E-02	3.14E-02	LAMTOR4	1.09E-01	3.17E-12
HNRNPH2	7.12E-02	4.85E-09	IRF2BP2	4.14E-02	2.30E-07	LAPTM4A	1.84E-01	1.96E-06
HOPX	1.96E-01	8.61E-06	IRF3	3.74E-02	2.01E-12	LAPTM5	5.03E-01	2.08E-27
HOXA10	3.38E-03	1.86E-09	ISCA1	4.07E-02	2.73E-08	LCOR	1.90E-02	1.15E-10
HOXA5	2.87E-02	3.16E-02	ISCU	1.40E-01	1.67E-13	LDLR	2.86E-03	4.69E-08
HOXB-AS3	4.44E-02	7.99E-07	IST1	1.03E-02	1.13E-13	LENG8	3.68E-02	5.23E-09
HPCAL1	4.15E-02	1.70E-07	ITM2B	2.92E-01	1.14E-12	LEPROT	2.56E-01	1.40E-17
HPS4	2.00E-02	1.22E-06	ITSN2	1.00E-01	8.31E-12	LEPROTL1	3.30E-02	3.48E-02
HSBP1L1	4.72E-02	8.44E-11	JAGN1	6.26E-02	9.65E-09	LETMD1	1.72E-01	3.13E-17
HSD17B11	6.88E-01	2.81E-60	JAK1	4.79E-02	2.21E-10	LGALS9	4.52E-02	1.29E-07
HSF1	7.43E-02	2.78E-20	JAML	2.93E-01	3.18E-32	LIMCH1	8.77E-02	1.59E-10
HSH2D	5.10E-03	2.15E-04	JARID2	2.33E-03	2.93E-10	LIMD2	1.63E-01	1.07E-11
HSP90AB1	1.79E-01	7.95E-19	JMJD1C	8.12E-02	2.40E-06	LIMS1	2.82E-01	4.34E-15
HTR1F	6.67E-02	1.36E-09	JPX	3.99E-02	1.78E-12	LINC00667	2.23E-02	4.86E-15
HTRA2	6.06E-03	6.73E-09	JUN	5.52E-01	6.39E-26	LINC01116	1.68E-02	1.02E-09
HYI	9.57E-03	1.71E-08	JUNB	7.13E-01	1.01E-48	LINC01122	2.47E-02	7.43E-11
ICA1	7.93E-02	2.91E-12	JUND	1.94E-01	3.05E-08	LINC02573	1.25E-01	2.16E-16

Gene	logFC	FDR	Gene	logFC	FDR	Gene	logFC	FDR
LIPA	4.25E-02	3.67E-13	MCL1	4.53E-01	9.00E-27	MSN	1.05E-01	1.64E-12
LITAF	3.35E-02	2.81E-06	MCRIP1	4.69E-03	5.29E-11	MSRB3	1.43E-01	3.13E-14
LLPH	1.31E-02	1.58E-12	MCRIP2	1.50E-02	6.62E-05	MT-CO3	1.41E-01	1.70E-14
LMNA	6.82E-01	1.80E-61	MCTS1	7.20E-03	8.48E-09	MT-ND1	5.98E-02	4.87E-04
LMO2	8.59E-02	2.15E-07	MDM4	5.90E-03	1.77E-12	MT-ND2	1.21E-01	1.32E-07
LMO4	3.30E-02	4.29E-07	MECOM	7.25E-02	2.04E-10	MT-ND3	5.73E-02	4.53E-02
LONP2	1.07E-01	2.99E-15	MECP2	3.26E-02	4.52E-09	MTA1	1.00E-02	9.66E-11
LPCAT2	6.00E-02	5.42E-09	MED12L	1.23E-02	7.19E-04	MTFR1L	4.20E-02	3.47E-07
LPIN1	1.04E-01	8.17E-13	MED17	3.10E-02	2.70E-07	MTIF3	2.36E-02	1.94E-08
LRBA	2.18E-02	9.88E-09	MED28	1.51E-02	4.54E-07	MTPN	2.98E-02	1.66E-04
LRCH4	6.49E-02	1.91E-09	MED6	3.14E-02	1.76E-12	MTURN	2.36E-02	2.44E-05
LRRC41	2.05E-02	1.92E-06	MEG3	5.89E-01	7.03E-68	MUC20-OT1	3.95E-02	1.98E-11
LRRFIP1	7.73E-02	6.26E-03	MEIS1	8.40E-02	1.66E-13	MUM1	9.86E-04	1.91E-08
LRRFIP2	8.14E-02	8.26E-13	METTL23	2.32E-02	1.19E-10	MYADM	2.39E-01	2.27E-14
LSM2	2.57E-02	3.87E-06	MFNG	2.16E-02	2.89E-08	MYB	6.18E-02	7.50E-06
LST1	3.81E-01	1.71E-19	MFSD10	4.46E-02	1.51E-06	MYCBP2	3.86E-02	2.57E-07
LTBP4	1.36E-02	1.97E-11	MGLL	5.81E-02	8.74E-09	MYCT1	2.46E-01	1.70E-25
LTC4S	2.17E-02	1.29E-11	MGMT	1.72E-02	6.58E-07	MYH9	3.55E-02	6.57E-05
LXN	1.01E-01	1.43E-13	MID1IP1	2.82E-02	6.02E-04	MYL12B	8.02E-02	8.79E-13
LY6E	4.53E-02	2.61E-11	MIDN	2.49E-01	8.48E-19	MYO1G	3.49E-02	1.16E-06
LYL1	1.73E-01	1.50E-13	MIER1	1.58E-02	1.06E-08	N4BP2L1	5.11E-02	5.61E-07
LYN	5.00E-02	3.54E-09	MIF4GD	1.02E-03	1.55E-05	N4BP2L2	1.56E-01	7.93E-10
LYRM1	7.13E-02	4.63E-08	MIR155HG	2.94E-02	1.10E-05	NAAA	1.87E-02	3.38E-09
LYRM9	5.97E-02	1.94E-11	MIR4435-2H	3.94E-02	9.73E-11	NAALADL1	7.03E-02	1.98E-09
LYZ	7.95E-02	7.05E-13	MITD1	6.47E-03	8.30E-07	NACA	3.13E-01	3.31E-63
MACF1	2.24E-02	2.05E-10	MKRN1	9.00E-03	3.69E-08	NAMPT	2.36E-01	1.89E-22
MAF1	6.54E-02	7.15E-15	MLF1	1.06E-01	1.59E-07	NAPA	3.91E-03	6.71E-10
MAFF	4.51E-01	2.93E-36	MLF2	9.58E-02	4.44E-13	NAPRT	7.60E-02	1.05E-13
MAFG	7.43E-02	9.95E-10	MLLT10	2.65E-02	3.05E-14	NAT9	4.73E-02	5.44E-08
MAGED2	1.25E-01	9.15E-11	MLLT3	6.47E-01	6.85E-75	NBEAL1	3.61E-02	2.78E-07
MAGEF1	2.55E-02	2.42E-07	MLXIP	3.34E-03	6.44E-06	NBL1	8.87E-02	9.29E-07
MALAT1	3.09E-01	5.49E-104	MMP24OS	4.95E-02	1.84E-11	NCK1	2.24E-02	5.33E-10
MAP1LC3B	5.33E-02	1.80E-11	MMRN1	7.61E-02	1.36E-11	NCKAP1L	3.80E-03	1.24E-06
MAP3K13	1.91E-02	5.71E-13	MOAP1	5.63E-02	5.11E-10	NCOA4	2.83E-02	4.03E-09
MAP3K8	7.78E-02	1.65E-04	MPG	3.79E-02	4.00E-05	NCOA7	8.00E-03	1.53E-05
MAP7	3.64E-02	3.02E-07	MPHOSPH8	1.65E-01	8.11E-16	NDFIP1	8.75E-02	3.57E-13
MAP7D1	1.76E-02	7.63E-09	MPI	1.62E-02	1.90E-05	NDUFAF3	1.68E-02	3.08E-12
MAP7D3	9.18E-03	1.55E-04	MPP1	3.68E-03	7.41E-14	NDUFB4	8.64E-03	8.18E-09
MAP9	3.88E-02	3.46E-06	MRFAP1	1.45E-02	1.59E-06	NDUFC1	4.14E-02	2.15E-14
MAPK1IP1L	9.17E-02	1.22E-07	MRPL10	7.32E-02	3.25E-09	NDUFS7	1.34E-02	2.92E-12
MAPK6	1.18E-02	5.81E-07	MRPL43	9.38E-02	3.48E-13	NEAT1	3.07E-01	2.41E-14
Mar-06	1.17E-01	1.53E-13	MRPL45	3.71E-02	8.72E-07	NECAP1	3.13E-02	5.92E-07
Mar-07	6.13E-02	5.61E-14	MRPL52	1.25E-02	4.75E-06	NECAP2	1.06E-02	4.85E-11
MAT2A	8.08E-03	1.13E-06	MRPL53	7.41E-02	3.77E-17	NECTIN2	4.15E-02	5.91E-12
MAT2B	6.15E-04	1.15E-09	MRPL54	2.11E-02	3.03E-12	NEMF	1.07E-02	1.16E-09
MAX	1.62E-01	1.02E-19	MRPS18B	7.53E-03	8.06E-12	NFE2L2	1.53E-01	3.27E-10
MBD5	6.90E-03	1.41E-07	MRPS21	8.13E-02	4.66E-09	NFIA	8.77E-02	4.71E-08
MBNL1	1.19E-01	1.92E-07	MRPS27	6.85E-02	7.93E-10	NFKBIA	4.16E-01	3.46E-15
MBOAT7	1.00E-01	3.47E-10	MRPS33	5.54E-03	1.87E-07	NFKBIZ	4.98E-02	4.17E-03
MBP	6.81E-02	1.99E-11	MSI2	5.65E-03	1.41E-05	NFU1	4.39E-02	1.08E-13

Gene	logFC	FDR	Gene	logFC	FDR	Gene	logFC	FDR
NGDN	2.41E-03	2.98E-09	OXLD1	1.64E-02	1.59E-07	PLAUR	1.08E-01	5.99E-06
NHLRC3	1.29E-02	1.55E-08	P4HTM	2.52E-02	3.57E-11	PLD3	1.40E-01	1.37E-18
NIFK	1.48E-02	2.07E-10	PABPC1	1.58E-01	2.06E-19	PLD4	9.54E-03	8.48E-11
NIPSNAP1	1.35E-03	2.00E-10	PAFAH1B2	5.64E-02	8.05E-12	PLEKHA5	3.56E-02	1.97E-11
NKTR	1.64E-01	2.49E-12	PAK2	1.87E-02	7.70E-14	PLEKHB2	2.62E-02	4.93E-09
NME3	7.58E-02	1.36E-08	PAN3	4.53E-02	1.14E-08	PLEKHF2	2.35E-02	1.64E-09
NMT1	1.16E-03	2.64E-10	PARVB	2.61E-02	6.80E-11	PLK3	9.33E-02	7.49E-15
NOA1	9.00E-02	1.67E-15	PBX1	5.94E-02	1.02E-07	PLP2	1.05E-02	1.60E-06
NOB1	1.04E-01	4.45E-09	PBXIP1	1.26E-01	3.87E-15	PLPP5	5.73E-02	1.07E-09
NOC2L	8.69E-03	1.32E-10	PCBD1	4.60E-02	2.38E-06	PLSCR1	1.64E-02	2.32E-12
NOP53	5.87E-01	1.82E-55	PCDH9	2.40E-01	9.86E-17	PLXDC2	6.59E-02	1.47E-10
NORAD	7.71E-02	4.09E-11	PCF11	2.19E-02	4.49E-07	PMPCB	1.04E-01	4.32E-10
NPC2	7.78E-02	1.43E-15	PCMTD1	6.16E-02	3.27E-10	PNISR	2.02E-01	1.25E-06
NPDC1	1.24E-01	9.27E-14	PDCD2	1.67E-02	2.13E-15	PNMA1	6.64E-02	2.50E-09
NPR3	6.58E-02	5.59E-09	PDCD4	3.28E-02	5.91E-12	PNP	4.13E-02	6.43E-06
NR1H2	1.75E-01	1.25E-18	PDCD6IP	1.10E-02	3.67E-06	PNPLA8	6.81E-02	1.45E-08
NR3C1	4.86E-02	1.20E-10	PDCL	1.55E-02	1.36E-11	PNRC1	4.93E-01	5.82E-33
NR4A1	2.38E-01	2.68E-17	PDE4B	1.09E-01	1.33E-10	PNRC2	1.43E-01	1.39E-13
NR4A2	4.12E-01	1.69E-26	PDLIM2	2.24E-02	2.06E-05	POLD4	5.48E-02	1.60E-12
NRBP1	1.10E-02	4.43E-08	PDZD8	1.95E-02	9.73E-09	POLK	1.21E-02	7.80E-12
NRIP1	3.92E-02	1.15E-07	PECAM1	1.18E-04	9.28E-08	POLR1D	2.87E-02	4.22E-09
NSA2	3.07E-02	1.18E-10	PER1	1.64E-01	6.08E-14	PPCS	2.80E-02	1.72E-09
NSFL1C	3.51E-02	1.36E-15	PEX16	4.55E-02	6.59E-06	PPDPF	7.45E-02	1.17E-04
NSMAF	1.84E-02	8.99E-09	PFDN1	3.12E-02	1.91E-15	PPIL3	2.70E-02	6.43E-07
NSMCE1	4.59E-02	3.22E-09	PFDN5	2.41E-01	2.95E-38	PPIL4	2.22E-02	7.76E-14
NSRP1	6.67E-02	2.56E-10	PGLS	6.75E-03	5.57E-09	PPIP5K2	5.35E-04	1.16E-05
NT5C	5.74E-03	6.23E-06	PHACTR1	1.41E-01	5.49E-10	PPM1B	3.05E-03	1.52E-11
NT5C3B	2.68E-02	1.57E-06	PHACTR2	2.37E-02	2.19E-06	PPM1K	3.33E-02	2.63E-08
NTHL1	2.64E-02	9.28E-08	PHACTR4	4.59E-02	1.04E-07	PPP1CB	2.75E-01	2.94E-12
NUB1	7.23E-02	7.12E-10	PHB2	1.89E-02	7.10E-11	PPP1R10	4.46E-02	3.83E-12
NUCB1	1.04E-01	2.54E-11	PHF1	1.18E-01	7.02E-24	PPP1R11	2.33E-02	4.73E-10
NUDT2	2.13E-02	1.29E-07	PHF11	7.91E-02	1.89E-12	PPP1R12A	2.02E-02	1.64E-09
NUDT3	3.15E-03	3.15E-07	PHF14	7.67E-03	2.33E-10	PPP1R15A	5.68E-01	3.98E-36
NUDT4	4.32E-02	2.67E-09	PHF20	3.54E-02	2.82E-05	PPP1R2	9.49E-02	2.67E-13
NUMB	3.99E-02	3.97E-10	PHF20L1	6.68E-04	4.68E-09	PPP2R5C	3.77E-02	3.11E-06
OARD1	5.46E-02	3.60E-12	PHF3	5.24E-02	4.45E-14	PPP2R5E	1.51E-02	1.72E-06
OAZ2	3.98E-02	2.33E-09	PHTF1	7.99E-02	3.33E-10	PPP4R2	1.38E-02	5.10E-12
OFD1	1.23E-01	1.48E-10	PHYH	1.11E-02	3.42E-10	PPP6C	2.07E-02	1.41E-06
OGA	4.54E-02	7.04E-10	PHYKPL	9.43E-02	3.48E-16	PQBP1	1.13E-01	1.26E-09
OGT	2.19E-02	1.15E-05	PIAS1	3.76E-02	1.74E-08	PQLC3	1.55E-02	2.14E-09
OPTN	7.21E-02	1.34E-12	PIGP	1.47E-03	4.19E-08	PRCC	2.66E-03	3.65E-08
ORAI2	2.83E-03	2.59E-07	PIK3IP1	1.26E-01	8.95E-19	PRCP	1.15E-02	4.85E-08
ORAI3	4.70E-02	4.78E-08	PIK3R1	3.72E-03	7.99E-12	PRDM2	2.65E-02	2.84E-06
ORC4	6.20E-03	2.42E-10	PIM1	1.67E-02	3.76E-04	PRKACB	1.03E-01	7.13E-11
OS9	1.43E-01	3.62E-18	PIM2	2.18E-02	3.75E-06	PRKAR1A	1.68E-01	2.50E-15
OSBPL8	8.14E-03	1.77E-12	PIM3	1.30E-01	4.76E-08	PRKCB	4.24E-02	3.49E-08
OST4	1.68E-01	5.64E-07	PIP4K2A	2.47E-02	3.87E-11	PRKCH	4.98E-02	3.08E-13
OTUB1	4.79E-02	7.54E-12	PJA2	8.37E-02	3.89E-11	PRKCSH	5.29E-02	2.30E-09
OTUD6B-AS1	1.21E-02	1.74E-07	PKN1	7.99E-02	7.90E-11	PRKD3	1.36E-02	1.24E-11
OXA1L	1.52E-01	1.56E-11	PKN2	1.39E-02	4.47E-16	PRKG2	1.54E-02	1.58E-08

Gene	logFC	FDR	Gene	logFC	FDR	Gene	logFC	FDR
PRMT2	7.02E-02	4.87E-09	RANBP2	3.17E-03	1.55E-05	RNF114	8.91E-02	1.07E-10
PRNP	5.49E-02	1.13E-08	RARRES3	1.69E-01	4.00E-16	RNF115	1.88E-02	3.48E-11
PRPF38A	3.31E-02	3.59E-15	RASAL3	8.25E-02	2.44E-09	RNF125	1.80E-01	5.37E-16
PRPF38B	1.08E-02	5.11E-10	RASSF1	4.64E-02	2.66E-09	RNF126	1.84E-03	2.39E-15
PRPF6	6.31E-02	2.41E-14	RB1CC1	9.84E-02	1.78E-10	RNF13	4.83E-02	4.99E-08
PRPF8	5.57E-03	2.39E-10	RBBP6	1.63E-02	4.14E-12	RNF139	3.84E-02	2.75E-12
PRRC2C	8.85E-02	1.00E-12	RBCK1	8.22E-02	1.16E-15	RNF145	6.04E-02	1.16E-07
PSAP	3.25E-01	3.52E-21	RBM22	4.58E-02	2.64E-07	RNF168	4.68E-02	2.44E-07
PSENEN	2.91E-02	1.44E-14	RBM23	1.06E-01	1.25E-12	RNF187	9.05E-03	7.91E-09
PSMA3-AS1	1.02E-01	3.68E-09	RBM25	1.83E-02	6.88E-09	RNF19A	1.55E-02	6.19E-09
PSMB10	1.27E-02	2.63E-13	RBM39	1.19E-01	8.10E-05	RNF220	4.36E-02	5.30E-07
PSMB8-AS1	1.06E-02	1.40E-05	RBM4	1.73E-02	4.26E-11	RNF24	2.47E-02	1.21E-08
PSMC2	1.90E-03	1.26E-09	RBM5	4.53E-02	4.71E-07	RNF7	9.69E-02	2.85E-13
PSMD12	1.95E-02	1.46E-09	RBM6	9.49E-03	8.16E-09	RNH1	1.16E-01	4.98E-14
PSMD3	1.01E-03	2.86E-19	RBM7	8.03E-02	6.94E-16	RNMT	5.67E-02	1.05E-15
PSMG2	1.95E-02	5.05E-11	RBM8A	6.30E-03	1.74E-15	ROBO3	5.99E-02	3.38E-13
PTAR1	1.52E-02	1.06E-11	RBMS1	2.08E-02	1.09E-12	ROCK1	1.27E-02	4.77E-09
PTEN	9.48E-02	3.13E-11	RBPJ	5.37E-02	7.58E-13	RPL10	2.57E-01	1.14E-115
PTGER4	3.30E-01	9.64E-26	RBPMS	9.29E-02	7.29E-11	RPL10A	1.41E-01	5.65E-23
PTGS1	2.48E-01	1.68E-28	RCHY1	3.85E-02	7.52E-14	RPL11	2.54E-01	5.65E-83
PTGS2	1.41E-01	2.06E-13	RCSD1	8.61E-02	6.55E-09	RPL12	3.16E-01	3.74E-120
PTP4A1	9.83E-02	8.42E-08	REL	2.33E-02	3.04E-05	RPL13	2.69E-01	1.21E-108
PTPN2	3.98E-02	1.75E-09	RENBP	6.85E-02	4.07E-10	RPL13A	2.35E-01	1.56E-81
PTPN6	4.63E-02	1.11E-07	REPIN1	5.05E-02	4.17E-12	RPL14	1.21E-01	3.19E-11
PTPRA	1.06E-02	5.74E-07	RERE	4.94E-02	2.06E-10	RPL15	1.21E-01	5.41E-27
PTPRC	2.80E-01	8.30E-18	REST	8.02E-03	7.40E-10	RPL17	1.11E-01	1.06E-09
PUM1	1.25E-02	5.13E-15	RETREG2	1.79E-02	2.92E-03	RPL18	3.02E-01	2.08E-69
PWP1	1.23E-02	1.52E-08	REV1	1.01E-02	1.25E-06	RPL18A	3.23E-02	1.31E-02
PYCARD	2.61E-02	1.66E-11	REX1BD	6.81E-02	1.65E-12	RPL19	1.84E-01	9.24E-34
PYGL	2.59E-04	2.73E-05	RFTN1	4.70E-02	2.37E-06	RPL22	4.19E-02	2.08E-02
QARS	7.31E-02	2.66E-11	RGL2	7.49E-02	1.23E-12	RPL23	2.00E-01	2.88E-17
QTRT1	1.06E-02	5.39E-13	RGL4	4.52E-03	1.12E-03	RPL23A	1.92E-01	1.21E-41
R3HDM4	7.41E-02	1.99E-12	RGP1	5.77E-02	5.12E-09	RPL24	3.15E-01	9.23E-58
RAB11B	1.19E-02	2.18E-13	RGS10	8.52E-02	9.91E-13	RPL26	7.96E-02	1.23E-10
RAB13	1.09E-01	8.40E-10	RGS19	4.44E-02	6.73E-09	RPL27A	2.21E-01	3.12E-46
RAB14	1.69E-02	3.66E-18	RHOB	8.03E-02	1.50E-08	RPL28	2.12E-01	1.01E-36
RAB18	4.85E-02	7.26E-15	RHOC	8.95E-02	1.96E-10	RPL29	2.07E-01	4.59E-40
RAB1A	7.05E-02	1.83E-10	RHOF	3.80E-02	1.28E-10	RPL30	3.86E-01	1.50E-109
RAB2A	8.92E-03	2.45E-16	RHOG	1.70E-02	2.45E-06	RPL31	3.54E-01	5.88E-139
RAB34	1.54E-01	4.60E-21	RHOH	8.42E-02	1.47E-05	RPL32	1.70E-01	1.05E-54
RAB37	1.97E-01	2.78E-25	RHOT2	6.04E-03	5.77E-10	RPL35A	3.44E-01	1.55E-142
RAB3GAP1	3.20E-02	8.00E-15	RIC3	2.55E-02	1.60E-07	RPL36	2.47E-01	1.58E-66
RAB5A	3.20E-02	1.30E-06	RICTOR	5.70E-02	1.43E-10	RPL36A	1.46E-01	2.23E-18
RAB6A	1.45E-02	7.15E-10	RILPL2	3.49E-01	7.10E-24	RPL36AL	4.66E-01	4.31E-39
RABAC1	1.60E-01	4.87E-12	RIMKLB	3.18E-02	1.03E-12	RPL37	2.33E-01	9.17E-38
RABGAP1	3.31E-02	2.71E-13	RING1	3.91E-02	1.87E-06	RPL37A	1.24E-01	1.47E-12
RAC2	4.83E-02	4.30E-06	RIPK2	8.30E-02	1.95E-09	RPL38	3.11E-01	9.23E-51
RACK1	2.74E-01	7.20E-68	RIPOR2	9.42E-02	1.20E-07	RPL41	8.70E-02	8.82E-18
RALB	3.12E-02	6.89E-09	RNASET2	2.10E-01	6.62E-16	RPL5	2.44E-01	1.15E-49
RALBP1	5.10E-04	2.10E-10	RNF11	1.37E-01	3.64E-11	RPL7A	1.89E-01	5.81E-25

Gene	logFC	FDR	Gene	logFC	FDR	Gene	logFC	FDR
RPL8	2.01E-01	2.82E-40	SCN9A	7.78E-02	9.75E-09	SLC50A1	2.06E-02	2.20E-14
RPL9	2.14E-01	1.09E-41	SCRN2	5.19E-02	5.96E-16	SLU7	8.55E-02	1.25E-07
RPLP2	2.82E-01	9.61E-62	SDCBP	5.79E-02	6.63E-09	SMARCA2	3.57E-02	7.55E-06
RPS10	1.09E-01	7.80E-08	SDCCAG8	5.65E-02	1.76E-06	SMARCC2	5.25E-02	7.28E-09
RPS11	1.73E-01	1.33E-11	SDE2	3.16E-02	8.77E-08	SMCHD1	2.69E-02	2.32E-10
RPS12	2.82E-01	7.14E-84	SDF2	2.57E-03	1.26E-10	SMDT1	3.50E-01	2.41E-17
RPS13	4.45E-02	2.73E-03	SDF4	1.64E-02	3.85E-10	SMIM10L1	5.64E-02	2.78E-12
RPS15	8.91E-02	3.51E-14	SDHAF2	2.84E-02	7.85E-09	SMIM20	6.06E-02	2.14E-13
RPS15A	6.54E-02	1.76E-06	SEC14L1	5.48E-02	2.22E-06	SMIM26	3.38E-01	7.58E-26
RPS2	1.13E-01	3.10E-22	SEC23A	2.84E-02	1.31E-09	SMIM27	4.25E-02	5.68E-07
RPS20	1.88E-01	6.89E-26	SEC31A	7.68E-02	9.36E-17	SMIM3	3.55E-02	5.29E-05
RPS23	1.23E-01	4.49E-20	SEC62	1.10E-01	2.36E-08	SMIM7	7.25E-03	1.14E-12
RPS24	8.47E-02	3.76E-09	SECISBP2	2.23E-02	1.99E-05	SNAP23	3.69E-02	1.13E-08
RPS25	2.20E-01	1.22E-42	SELENOK	2.00E-01	5.65E-07	SNHG7	6.09E-01	4.25E-57
RPS27	2.83E-01	2.30E-142	SELENOM	3.06E-01	8.49E-48	SNHG8	6.39E-01	5.18E-52
RPS27A	1.49E-01	5.46E-31	SELENOP	2.58E-01	1.03E-20	SNRK	8.89E-02	3.34E-09
RPS28	8.99E-02	1.55E-11	SELENOS	4.34E-02	1.19E-09	SNRNP200	7.44E-03	9.34E-09
RPS29	2.17E-01	2.45E-56	SELENOT	1.71E-02	8.25E-10	SNRPN	2.50E-01	8.43E-21
RPS4Y1	3.43E-01	4.43E-12	SENP6	4.32E-02	1.08E-05	SNW1	4.29E-03	1.35E-14
RPS6KB2	1.55E-02	1.76E-08	SEPHS2	1.51E-02	6.81E-10	SNX14	1.48E-02	4.72E-09
RPS8	1.73E-01	3.37E-38	SEPT9	1.79E-02	1.20E-09	SNX17	3.03E-02	5.53E-14
RPS9	2.83E-01	2.14E-92	SERINC1	6.05E-02	4.56E-11	SOCS1	8.87E-02	7.93E-10
RPSA	7.20E-02	5.38E-05	SERINC3	1.08E-01	3.98E-14	SOCS2	2.05E-01	4.68E-08
RRBP1	5.80E-02	4.19E-14	SERP1	2.19E-01	4.15E-08	SOCS3	2.30E-01	9.24E-16
RSBN1	1.09E-01	7.29E-11	SERPINB6	1.59E-01	2.68E-08	SOD2	4.89E-02	3.50E-03
RSBN1L	2.70E-02	4.36E-07	SERPING1	2.45E-02	2.40E-06	SON	2.56E-01	8.55E-17
RSL24D1	1.06E-01	3.39E-04	SERTAD2	8.44E-03	2.76E-06	SORL1	6.33E-02	1.23E-04
RSRC2	4.37E-02	7.22E-11	SESN1	3.02E-02	7.79E-09	SP100	5.78E-02	2.49E-07
RSRP1	2.06E-01	8.08E-16	SETD2	6.67E-03	4.85E-10	SP110	6.71E-02	2.38E-11
RTCB	8.63E-03	4.23E-11	SF1	2.11E-01	2.28E-10	SPAG7	2.49E-02	9.95E-07
RTF2	6.19E-02	6.27E-11	SGK3	1.30E-04	8.64E-16	SPAG9	2.95E-02	2.21E-09
RTN4	1.13E-01	6.42E-08	SH3BGRL3	2.15E-01	2.10E-07	SPART	1.93E-02	4.36E-14
RUNX1	3.71E-02	8.92E-07	SH3GLB1	2.51E-02	1.22E-10	SPG7	1.61E-02	1.46E-10
RWDD1	8.69E-02	1.39E-10	SH3KBP1	2.78E-03	1.04E-11	SPINT2	7.94E-02	3.84E-07
RYBP	4.69E-02	1.01E-07	SHARPIN	7.22E-03	2.11E-09	SPN	1.88E-02	9.53E-09
S100A11	7.16E-02	3.61E-08	SHISA5	4.91E-02	1.51E-10	SPRY1	7.51E-02	2.27E-05
S100A4	5.49E-01	1.02E-32	SHKBP1	3.72E-02	1.29E-10	SPSB3	3.76E-02	5.51E-11
S100A6	4.96E-01	2.93E-36	SIAH2	1.87E-02	1.23E-05	SPTBN1	2.46E-02	3.14E-11
SAFB2	6.18E-02	7.62E-11	SIGIRR	2.29E-02	3.59E-08	SQOR	6.09E-02	5.80E-13
SAMD9	6.42E-03	6.66E-11	SIL1	8.35E-02	2.23E-09	SQSTM1	2.04E-01	1.08E-17
SAR1A	1.55E-02	2.71E-13	SKAP1	8.41E-02	4.16E-17	SREK1IP1	5.83E-03	8.84E-13
SARAF	1.37E-01	1.28E-03	SKAP2	3.00E-03	3.62E-12	SRGN	9.35E-01	2.56E-106
SARNP	3.29E-02	6.42E-07	SKIL	1.96E-01	5.13E-15	SRP68	2.44E-02	4.30E-12
SART1	9.44E-03	8.12E-08	SLC17A9	7.55E-03	3.95E-07	SRRM2	3.30E-02	2.08E-12
SAT1	6.33E-01	2.04E-41	SLC25A36	2.33E-02	2.68E-11	SRSF5	3.50E-01	4.01E-22
SAT2	1.59E-01	2.78E-19	SLC2A3	1.51E-01	1.01E-10	SRSF6	1.94E-01	7.55E-14
SBDS	2.68E-01	7.18E-17	SLC35C2	8.54E-03	2.50E-09	SRSF7	2.12E-02	1.62E-06
SCAMP2	3.76E-02	5.51E-08	SLC38A2	2.87E-03	1.36E-06	SRSF8	2.47E-02	9.73E-08
SCAND1	3.13E-02	2.57E-05	SLC40A1	5.76E-02	7.44E-08	SS18	1.53E-02	5.98E-09
SCARB2	1.98E-02	1.71E-07	SLC44A1	9.07E-04	4.71E-10	SSBP3	6.31E-02	4.62E-08

Gene	logFC	FDR	Gene	logFC	FDR	Gene	logFC	FDR
SSBP4	3.53E-02	1.04E-10	TBL1XR1	1.16E-02	1.01E-07	TNFAIP3	1.19E-01	9.96E-05
SSR2	9.35E-02	1.19E-07	TBXAS1	7.92E-02	1.40E-12	TNFRSF14	8.12E-02	1.25E-14
ST13	1.64E-01	1.42E-04	TCEA2	4.30E-02	2.08E-12	TNFRSF1A	1.87E-02	1.85E-03
STARD10	4.24E-02	3.32E-07	TCEAL1	3.66E-02	7.25E-14	TNFSF10	8.82E-02	3.58E-11
STARD3	7.04E-02	1.09E-12	TCEAL2	1.48E-01	1.68E-25	TNIP1	4.49E-02	3.20E-06
STARD3NL	4.71E-02	1.06E-12	TCEAL3	4.56E-02	1.06E-07	TNRC6B	1.34E-01	6.04E-15
STAT3	2.17E-01	7.18E-20	TCEAL4	1.20E-01	3.23E-15	TOB1	8.74E-02	1.16E-07
STAT5A	6.98E-02	1.64E-09	TCEAL8	8.86E-02	3.22E-10	TOB2	5.88E-02	3.82E-10
STAU1	1.19E-02	6.12E-11	TCF25	1.62E-01	4.50E-12	TOMM20	3.95E-02	1.81E-10
STK17B	2.28E-01	7.43E-19	TCF4	3.47E-02	3.09E-10	TOMM7	4.18E-01	9.04E-23
STK4	1.03E-01	1.73E-09	TCF7	8.48E-02	2.27E-14	TOP1MT	5.31E-02	1.47E-10
STMN3	1.89E-02	1.86E-07	TCOF1	3.42E-01	1.82E-36	TOR1AIP1	3.59E-02	5.31E-09
STN1	5.53E-02	7.46E-08	TCTA	5.19E-02	1.51E-10	TP53TG1	2.56E-02	1.14E-13
STOM	3.20E-02	3.38E-10	TCTEX1D1	4.83E-02	7.24E-13	TPGS1	6.90E-02	1.47E-06
STX16	6.23E-02	1.68E-08	TERF2IP	1.37E-02	2.08E-14	TPP1	5.02E-02	1.32E-07
STX3	2.28E-02	1.66E-10	TESPA1	5.10E-02	1.03E-07	TPST2	1.28E-01	9.54E-11
STX4	7.55E-02	8.58E-11	TFPI	1.80E-01	6.58E-13	TPT1	2.45E-01	1.55E-40
STX7	2.74E-04	2.05E-09	TFPT	7.09E-03	4.67E-10	TRABD	2.96E-02	1.05E-05
STXBP2	1.02E-02	5.47E-05	TGFB1	2.66E-02	4.49E-11	TRAF3IP3	9.19E-03	3.39E-08
STXBP3	1.02E-02	2.83E-08	TGIF1	1.05E-01	2.96E-15	TRAF5	2.12E-02	2.66E-05
SUCLG2	6.83E-02	2.34E-19	THEM4	1.90E-02	1.22E-16	TRAPPC2B	6.29E-02	9.64E-10
SUN2	8.81E-02	2.49E-14	THUMPD1	7.53E-02	2.09E-09	TRIM13	7.36E-04	6.28E-10
SUPT3H	4.95E-02	1.73E-09	TIAL1	2.27E-02	1.08E-07	TRIM22	5.46E-02	2.08E-13
SUPT4H1	3.04E-02	1.00E-15	TIMM9	5.45E-02	6.39E-06	TRIM24	1.95E-02	3.89E-06
SURF1	4.14E-02	3.12E-12	TIPARP	2.39E-01	1.10E-17	TRIM4	8.71E-02	2.27E-12
SVBP	1.64E-02	3.52E-12	TKT	1.28E-01	2.15E-06	TRIM56	3.23E-02	5.24E-07
SWAP70	1.47E-01	2.51E-15	TLE4	1.79E-01	3.03E-13	TRIM58	5.75E-02	9.82E-09
SYAP1	1.31E-01	5.22E-07	TLK1	4.16E-02	4.00E-10	TRIM8	4.94E-02	2.18E-08
SYF2	3.30E-01	3.87E-19	TLN1	5.41E-02	4.64E-08	TRIP6	1.71E-02	1.37E-10
SYK	4.64E-03	4.49E-07	TM2D1	5.91E-03	2.24E-13	TRIR	3.68E-02	3.87E-07
SYMPK	6.70E-02	3.10E-08	TM2D3	7.82E-02	1.63E-12	TRMT1	2.13E-02	1.23E-07
SYNGR1	2.74E-02	2.65E-16	TMC8	7.36E-02	3.79E-10	TSC22D1	6.17E-01	1.25E-37
SYNGR2	1.19E-03	2.36E-14	TMED3	1.55E-01	6.95E-11	TSC22D3	3.61E-01	1.51E-32
SYNJ2BP	2.05E-02	2.35E-08	TMEM101	2.36E-03	3.00E-05	TSC22D4	3.18E-03	1.88E-07
SYPL1	7.54E-02	8.29E-04	TMEM106B	2.91E-03	4.07E-08	TSG101	2.34E-02	1.55E-09
SYTL1	5.06E-02	1.55E-06	TMEM141	1.65E-02	2.76E-07	TSPAN32	1.06E-01	5.41E-14
SYTL4	3.46E-02	1.32E-03	TMEM167B	8.16E-02	3.63E-15	TSPO	3.42E-01	1.81E-21
TACC1	1.21E-01	1.63E-11	TMEM170A	1.83E-02	1.43E-08	TSPYL1	1.53E-01	5.17E-12
TACC3	5.61E-02	9.21E-10	TMEM173	2.28E-01	3.61E-26	TSPYL2	1.43E-01	7.72E-15
TAF11	9.09E-03	4.97E-12	TMEM205	1.62E-02	5.65E-13	TSR2	1.28E-02	1.13E-10
TAF1D	1.65E-01	4.98E-09	TMEM219	1.02E-01	6.18E-14	TSSC4	6.66E-02	4.35E-11
TAGAP	4.63E-02	2.37E-08	TMEM243	4.32E-02	2.39E-13	TTC14	4.76E-02	1.13E-08
TANK	2.07E-02	2.65E-06	TMEM248	4.42E-03	8.66E-18	TTC17	3.53E-02	6.96E-11
TAPBP	1.15E-01	1.20E-09	TMEM256	1.31E-01	1.91E-13	TUBA1A	3.50E-01	1.45E-14
TAPBPL	3.09E-02	8.39E-06	TMEM42	2.02E-02	3.23E-09	TUBA1C	1.01E-02	1.76E-12
TARBP1	2.16E-02	6.49E-07	TMEM43	4.97E-02	6.10E-09	TUBB4B	6.15E-02	4.52E-12
TATDN1	1.04E-01	3.86E-12	TMEM69	4.12E-02	7.87E-08	TUBGCP2	4.06E-02	3.91E-12
TAX1BP1	7.17E-02	2.20E-09	TMEM91	1.21E-01	1.57E-13	TWSG1	8.59E-03	2.31E-06
TBC1D10C	5.05E-02	8.06E-08	TMEM9B	4.50E-02	5.83E-08	TXN2	1.39E-02	5.45E-11
TBCC	7.96E-03	2.38E-22	TMF1	2.37E-02	8.76E-13	TXNIP	2.61E-01	2.15E-23

Gene	logFC	FDR	Gene	logFC	FDR	Gene	logFC	FDR
UAP1	5.52E-03	7.64E-07	VSIR	1.31E-01	7.22E-18	ZNF106	1.09E-03	9.42E-10
UBA52	6.46E-02	6.15E-03	WAC	1.32E-02	1.82E-11	ZNF131	6.22E-02	3.01E-11
UBA7	6.42E-02	9.09E-08	WAC-AS1	3.75E-02	2.90E-10	ZNF148	1.54E-02	7.43E-12
UBAC2	2.07E-02	3.78E-12	WAPL	3.32E-02	3.05E-12	ZNF207	3.41E-03	2.32E-12
UBC	7.68E-01	8.82E-129	WAS	4.64E-02	8.32E-11	ZNF24	3.97E-02	9.27E-06
UBE2B	4.71E-02	9.15E-08	WASF2	7.71E-02	1.05E-09	ZNF277	5.99E-02	1.05E-10
UBE2E1	3.05E-02	3.19E-09	WASHC4	2.46E-02	6.60E-05	ZNF281	6.14E-02	1.05E-07
UBE2F	5.32E-02	7.86E-14	WBP2	1.13E-01	3.60E-19	ZNF292	9.64E-03	1.40E-06
UBE2H	3.03E-02	8.82E-09	WDR13	6.16E-02	2.95E-10	ZNF32	2.10E-02	2.93E-06
UBE2R2	2.55E-02	6.78E-08	WDR33	8.25E-03	3.09E-05	ZNF331	2.09E-01	5.06E-15
UBQLN1	3.40E-03	3.23E-11	WDR45	6.46E-02	3.31E-13	ZNF33B	2.62E-02	1.14E-07
UBQLN2	5.41E-02	1.61E-10	WDR45B	8.28E-02	1.95E-09	ZNF394	7.17E-02	2.62E-15
UBXN1	4.42E-01	3.14E-43	WDR46	2.16E-03	4.88E-10	ZNF512	1.28E-02	2.35E-05
UCHL1	2.72E-02	1.43E-06	WDR6	4.03E-02	2.21E-09	ZNF580	3.30E-02	1.03E-06
UCP2	2.24E-02	8.28E-03	WDR74	1.18E-02	2.32E-06	ZNF581	5.58E-02	4.99E-08
UFC1	6.76E-02	3.50E-07	WDR83OS	7.08E-02	1.57E-14	ZNF593	2.79E-02	3.50E-04
UFL1	5.47E-03	8.38E-07	WIPF1	4.27E-02	1.36E-10	ZNF638	3.56E-02	2.71E-11
UFM1	2.11E-03	4.38E-13	WSB1	2.24E-01	1.37E-15	ZNF644	2.09E-02	3.67E-13
ULK3	3.04E-02	1.29E-08	XAB2	1.77E-02	5.01E-06	ZNF667	9.94E-03	3.31E-08
UNC13D	6.48E-02	8.11E-09	XPA	5.22E-02	1.05E-08	ZNF766	5.55E-03	3.97E-10
UNC45A	3.52E-02	3.47E-11	XPC	3.64E-02	2.15E-14	ZNF83	7.09E-02	4.17E-11
UPF2	2.62E-02	3.20E-10	YBEY	5.45E-02	1.83E-08	ZNHIT3	1.48E-03	1.42E-08
UQCRB	1.90E-02	4.71E-02	YBX3	1.45E-01	3.03E-07	ZNRD1	1.41E-02	8.07E-12
UQCRC2	6.07E-02	2.15E-07	YIPF2	5.19E-02	1.64E-08	ZRANB2	1.34E-02	2.28E-12
URI1	1.51E-02	1.36E-09	YIPF3	3.59E-02	4.03E-07	ZSCAN18	8.34E-02	2.03E-14
URM1	1.08E-02	8.49E-10	YIPF4	6.10E-03	1.19E-10	ZSWIM7	5.44E-02	8.14E-10
USE1	7.17E-02	3.94E-11	YME1L1	2.83E-02	8.35E-06	ZYX	8.55E-02	1.45E-09
USO1	1.01E-02	1.60E-09	YPEL5	5.86E-01	1.78E-38			
USP11	8.02E-02	7.16E-12	YTHDC1	5.64E-02	3.27E-08			
USP12	1.32E-01	1.43E-13	YWHAZ	1.22E-01	2.13E-08			
USP15	1.17E-01	1.38E-08	ZBTB16	4.91E-02	2.55E-10			
USP16	4.24E-03	6.08E-12	ZBTB20	9.08E-02	1.23E-13			
USP22	3.37E-02	2.14E-12	ZC3H7A	4.16E-02	3.09E-09			
USP34	4.23E-02	4.72E-07	ZC3HAV1	1.25E-02	2.06E-06			
USP47	1.58E-02	2.45E-09	ZCCHC7	6.32E-02	3.96E-09			
USP8	2.29E-02	7.44E-06	ZDHHC24	1.18E-02	1.19E-09			
UTRN	5.19E-02	6.37E-09	ZFAND1	2.59E-01	7.22E-18			
UXT	3.87E-02	3.64E-04	ZFAND2B	2.57E-02	3.25E-07			
VAMP2	2.90E-01	1.23E-12	ZFAND5	1.29E-01	1.36E-07			
VAMP5	1.58E-01	1.11E-08	ZFAND6	3.62E-02	6.59E-07			
VAPA	5.53E-02	2.54E-05	ZFAS1	6.11E-01	6.61E-65			
VASP	9.04E-02	1.47E-12	ZFC3H1	3.42E-02	5.91E-07			
VCP	1.22E-01	4.20E-11	ZFP36	5.95E-01	3.53E-35			
VIM	5.71E-01	1.27E-50	ZFP36L2	1.06E-01	5.00E-02			
VMP1	2.35E-02	4.09E-09	ZFR	7.14E-03	2.39E-13			
VPS13C	4.30E-02	2.10E-05	ZFYVE21	8.99E-02	9.43E-17			
VPS28	7.66E-02	1.15E-11	ZKSCAN1	2.95E-02	2.29E-07			
VPS37B	1.38E-01	7.28E-14	ZMAT2	1.30E-02	1.80E-11			
VPS4A	6.97E-03	3.46E-15	ZMYM2	3.92E-02	1.75E-11			
VPS51	1.22E-01	7.67E-14	ZMYND8	4.55E-02	2.09E-06			

C2- downregulated in old donor platelet -biased HSCs

Gene	logFC	FDR	Gene	logFC	FDR	Gene	logFC	FDR
PABPC4	-4.96E-05	1.44E-11	IQGAP1	-2.70E-03	2.26E-05	CCDC66	-5.72E-03	2.21E-08
MIEN1	-1.44E-04	4.62E-14	ZNHIT1	-2.73E-03	1.15E-09	HPS1	-5.75E-03	5.39E-10
ARHGAP5	-2.15E-04	2.09E-06	ARHGEF6	-2.85E-03	3.72E-06	GNL1	-5.81E-03	4.66E-08
ATP6V0E1	-3.31E-04	9.19E-12	ARID4B	-2.92E-03	4.43E-07	PCMTD2	-5.87E-03	1.38E-05
SHOC2	-3.57E-04	2.00E-05	ZC3H15	-2.92E-03	1.57E-04	IARS	-5.89E-03	9.12E-15
ZBED5	-4.61E-04	2.66E-05	APBB1IP	-2.94E-03	1.32E-05	GPATCH2L	-5.93E-03	4.04E-10
SMU1	-4.64E-04	5.69E-11	FAH	-3.04E-03	3.59E-08	APOPT1	-6.01E-03	4.56E-10
TOX4	-5.12E-04	2.81E-09	CARD16	-3.05E-03	6.09E-11	XRN1	-6.02E-03	1.29E-09
DYM	-6.04E-04	3.06E-08	COX11	-3.07E-03	1.23E-11	AFG3L2	-6.24E-03	2.85E-09
UBL7	-6.38E-04	2.33E-15	AMZ2	-3.07E-03	1.23E-14	DHRS4L2	-6.26E-03	3.95E-08
MRPS5	-6.57E-04	1.29E-06	VAMP7	-3.09E-03	1.28E-08	TMUB1	-6.26E-03	2.19E-19
CHPT1	-7.49E-04	6.61E-13	ZC3H13	-3.22E-03	3.08E-15	FYTTD1	-6.26E-03	1.05E-07
ATP6V0A2	-7.51E-04	1.00E-09	DNAJA2	-3.24E-03	2.03E-11	ETHE1	-6.29E-03	5.09E-07
CCDC25	-7.81E-04	1.07E-05	VRK3	-3.25E-03	4.36E-05	ARL2BP	-6.29E-03	4.71E-17
FSCN1	-8.44E-04	1.50E-08	MARCH5	-3.42E-03	4.04E-07	DDX6	-6.30E-03	1.56E-06
BRD2	-8.53E-04	2.63E-06	UBALD2	-3.50E-03	4.22E-08	MPV17	-6.32E-03	1.33E-10
ZNF330	-9.25E-04	4.80E-12	AC090152.1	-3.52E-03	2.09E-07	TMEM220	-6.38E-03	1.65E-13
KANSL1	-9.94E-04	5.40E-07	PAPSS1	-3.64E-03	1.50E-11	IAH1	-6.47E-03	2.22E-07
INTS11	-1.01E-03	6.25E-08	RHOT1	-3.77E-03	4.64E-13	LCMT1	-6.47E-03	1.36E-16
M6PR	-1.10E-03	1.22E-15	TSTD1	-3.77E-03	6.80E-15	DNAJC21	-6.52E-03	1.74E-10
NDUFS5	-1.12E-03	2.63E-10	MICU2	-3.80E-03	7.84E-10	PTPN7	-6.67E-03	8.91E-08
TIMM44	-1.21E-03	6.16E-06	ARL6IP4	-3.81E-03	1.52E-10	BCAS4	-6.71E-03	4.05E-08
LTA4H	-1.29E-03	2.07E-08	UBE2G2	-3.81E-03	3.60E-11	CCDC88A	-6.71E-03	1.78E-07
STRADB	-1.30E-03	8.39E-11	USP5	-3.92E-03	1.63E-11	TMEM192	-6.73E-03	9.71E-12
ZCRB1	-1.31E-03	7.97E-14	CHMP2B	-3.93E-03	2.12E-13	OSBPL9	-6.76E-03	2.03E-12
TUT4	-1.33E-03	7.26E-08	SNHG25	-4.15E-03	1.04E-08	PDXDC1	-6.81E-03	9.36E-06
ATP6V1E1	-1.45E-03	2.56E-08	FUNDC2	-4.20E-03	9.08E-08	QPRT	-7.01E-03	1.50E-06
NDUFA10	-1.50E-03	2.64E-13	ADH5	-4.33E-03	7.86E-08	ATP6V1F	-7.02E-03	1.17E-15
FKBP2	-1.53E-03	4.99E-08	ARMC8	-4.37E-03	8.14E-09	PHIP	-7.02E-03	3.73E-16
ZEB2	-1.54E-03	8.95E-12	MAPK14	-4.40E-03	9.73E-12	SNX6	-7.05E-03	1.16E-12
MRPL40	-1.69E-03	2.44E-13	C19orf70	-4.51E-03	1.62E-11	ERLEC1	-7.06E-03	2.20E-09
PRPSAP2	-1.75E-03	7.10E-09	CMTM3	-4.54E-03	1.74E-11	SUGT1	-7.08E-03	9.83E-16
AAMDC	-1.80E-03	1.94E-10	ARHGDIA	-4.60E-03	1.09E-09	IDI1	-7.15E-03	1.48E-06
MRPS9	-1.83E-03	4.27E-11	RTRAF	-4.67E-03	1.12E-09	FIP1L1	-7.15E-03	3.34E-12
PLPBP	-1.97E-03	2.00E-11	CREB1	-4.69E-03	4.25E-14	TMEM50B	-7.25E-03	1.31E-09
AP1M1	-2.00E-03	1.05E-07	AGPAT2	-4.70E-03	6.76E-10	TIMP1	-7.31E-03	6.32E-06
CCNB1IP1	-2.07E-03	1.32E-12	PEPD	-4.79E-03	4.31E-14	SLC25A26	-7.42E-03	7.65E-09
TROVE2	-2.18E-03	5.54E-12	XPOT	-4.83E-03	2.28E-10	PDS5B	-7.43E-03	3.12E-08
LBR	-2.21E-03	1.02E-17	CFDP1	-4.91E-03	3.45E-10	CHTF8	-7.67E-03	7.93E-12
MXD1	-2.26E-03	5.94E-05	PEF1	-5.04E-03	1.02E-06	ITGA4	-7.72E-03	3.39E-09
CTNNBL1	-2.35E-03	2.88E-07	EIF4EBP3	-5.09E-03	6.69E-08	RNF10	-7.78E-03	2.11E-10
VTI1B	-2.43E-03	1.79E-09	SSBP2	-5.14E-03	3.15E-12	DBNL	-7.78E-03	6.12E-15
NT5C3A	-2.44E-03	3.29E-10	HCLS1	-5.16E-03	1.89E-10	AZIN1	-7.79E-03	2.23E-08
ADAM17	-2.47E-03	6.26E-05	RNF181	-5.20E-03	8.12E-11	DNPEP	-7.91E-03	1.72E-05
PITPNB	-2.51E-03	4.84E-08	DMAC2	-5.22E-03	5.65E-07	GGPS1	-7.92E-03	9.78E-10
IGSF10	-2.58E-03	3.59E-09	SMYD3	-5.31E-03	1.62E-11	PARVG	-7.92E-03	6.27E-10
GDE1	-2.59E-03	2.53E-11	PTOV1	-5.50E-03	1.57E-08	SPEN	-7.93E-03	1.66E-14
ILVBL	-2.62E-03	2.88E-05	KAT7	-5.53E-03	1.17E-09	CAMK2G	-7.93E-03	4.14E-12
OSBPL1A	-2.63E-03	6.98E-07	SF3B2	-5.72E-03	5.73E-17	GFM1	-8.08E-03	1.25E-10

MOB4	-8.12E-03	3.67E-13	WDR1	-1.09E-02	5.71E-17	WDFY2	-1.42E-02	3.15E-10
DMAC1	-8.19E-03	3.16E-10	MRPL34	-1.09E-02	1.93E-13	NUFIP2	-1.44E-02	3.47E-13
RNF167	-8.21E-03	3.94E-08	SNHG19	-1.09E-02	4.54E-09	C1orf43	-1.44E-02	8.42E-19
COL4A3BP	-8.22E-03	9.99E-08	SNHG9	-1.10E-02	4.01E-14	C5orf24	-1.46E-02	4.09E-11
FBXW9	-8.23E-03	3.54E-06	TMEM38B	-1.10E-02	4.57E-22	GOLPH3	-1.47E-02	3.56E-12
RASGRP2	-8.26E-03	2.53E-11	SMIM4	-1.11E-02	2.42E-12	UQCC3	-1.47E-02	3.19E-14
ZNF302	-8.29E-03	4.02E-08	MAPKAPK3	-1.12E-02	1.11E-08	SPTLC2	-1.48E-02	4.40E-08
SRPRA	-8.30E-03	1.82E-17	JKAMP	-1.12E-02	1.73E-08	ARL16	-1.48E-02	3.40E-13
DEGS1	-8.38E-03	5.10E-18	IFI6	-1.13E-02	4.70E-10	GPATCH4	-1.50E-02	1.97E-04
ALDH9A1	-8.40E-03	7.66E-06	COMMD10	-1.14E-02	1.99E-12	ARHGAP4	-1.50E-02	1.23E-14
PAXIP1-AS1	-8.44E-03	6.52E-11	DTD1	-1.15E-02	3.92E-12	RAB5C	-1.51E-02	1.06E-13
AUP1	-8.52E-03	4.47E-09	SAP30BP	-1.15E-02	3.85E-09	TMEM87A	-1.52E-02	7.83E-13
ARID1A	-8.77E-03	5.57E-09	PPP2R2A	-1.16E-02	4.64E-09	NXT1	-1.52E-02	4.96E-09
NBN	-8.77E-03	2.03E-09	MEF2C	-1.18E-02	1.52E-12	CUL4A	-1.52E-02	4.17E-07
RPL7L1	-8.90E-03	4.16E-08	ATAD1	-1.18E-02	3.62E-11	ATG12	-1.53E-02	3.47E-07
TM9SF3	-8.95E-03	4.27E-07	TMED4	-1.19E-02	2.01E-07	FAM133B	-1.54E-02	1.03E-08
ODF2	-9.00E-03	7.29E-18	DHX36	-1.19E-02	2.51E-10	NENF	-1.55E-02	3.61E-26
PCM1	-9.02E-03	4.12E-08	NOL7	-1.20E-02	4.56E-09	NABP2	-1.55E-02	7.20E-10
RAC1	-9.06E-03	3.05E-11	ODF2L	-1.20E-02	6.55E-12	COMT	-1.55E-02	3.80E-09
TPD52L2	-9.06E-03	9.91E-16	CXXC5	-1.21E-02	3.26E-06	CNN2	-1.56E-02	3.25E-09
TMEM59	-9.21E-03	7.10E-10	PPP3CA	-1.23E-02	2.53E-10	SCFD1	-1.56E-02	3.33E-06
PFDN6	-9.33E-03	2.56E-10	PRKAG1	-1.23E-02	2.94E-12	CREBRF	-1.57E-02	5.99E-06
NELFCD	-9.50E-03	5.43E-13	ZCCHC10	-1.23E-02	9.96E-13	RDH11	-1.57E-02	4.23E-09
ANAPC16	-9.57E-03	2.41E-08	ARPC1A	-1.25E-02	2.54E-15	CHST12	-1.57E-02	4.74E-08
SPOP	-9.59E-03	1.18E-15	DNAJC1	-1.27E-02	1.74E-07	MAPRE2	-1.58E-02	9.17E-08
BTK	-9.61E-03	1.79E-10	NAA15	-1.29E-02	1.84E-11	IL2RG	-1.59E-02	3.20E-05
C1orf56	-9.68E-03	3.28E-10	VPS36	-1.29E-02	2.16E-09	TMEM134	-1.59E-02	1.04E-13
CCDC28A	-9.75E-03	4.73E-10	RALA	-1.30E-02	2.15E-11	TYW3	-1.60E-02	8.18E-10
HINT3	-9.78E-03	3.03E-08	SLC25A33	-1.31E-02	1.63E-05	TEX264	-1.60E-02	3.27E-09
ESYT1	-9.78E-03	6.01E-07	CHMP4A	-1.31E-02	9.80E-09	TWF2	-1.60E-02	3.92E-12
EFCAB14	-9.88E-03	8.98E-10	TRIM44	-1.32E-02	2.77E-11	METAP2	-1.61E-02	3.63E-14
TSEN34	-9.90E-03	4.37E-10	PCIF1	-1.32E-02	2.47E-08	DNAAF2	-1.62E-02	1.91E-08
POLR2C	-9.92E-03	4.37E-14	ZNF706	-1.32E-02	4.99E-17	EIF3B	-1.62E-02	1.08E-05
HDLBP	-9.92E-03	3.13E-10	DTWD1	-1.33E-02	9.04E-12	THUMPD3-A	-1.63E-02	2.20E-10
C2orf74	-9.96E-03	2.28E-10	SZRD1	-1.34E-02	1.77E-19	PCID2	-1.63E-02	4.13E-08
TBC1D15	-1.01E-02	4.88E-05	IDH3B	-1.34E-02	3.49E-13	ATP5S	-1.63E-02	6.05E-10
NMD3	-1.01E-02	3.30E-09	FAM213A	-1.34E-02	6.64E-14	UTP6	-1.63E-02	1.01E-05
SLC3A2	-1.02E-02	1.31E-11	AKAP9	-1.35E-02	7.35E-05	NOSIP	-1.64E-02	5.30E-11
WIPI2	-1.02E-02	1.01E-06	FBXO21	-1.35E-02	1.45E-09	NIT2	-1.64E-02	4.90E-15
SUPT20H	-1.03E-02	1.37E-10	HHEX	-1.36E-02	4.03E-08	MRPL28	-1.64E-02	1.15E-13
BCKDK	-1.04E-02	7.74E-13	USP14	-1.36E-02	4.22E-13	TRAPPC3	-1.65E-02	1.08E-18
REXO4	-1.06E-02	1.69E-09	SUMF2	-1.36E-02	8.74E-13	FMC1	-1.65E-02	1.65E-10
CFAP298	-1.06E-02	1.39E-07	PTP4A2	-1.37E-02	1.87E-16	PPP2CA	-1.67E-02	3.72E-13
OSTF1	-1.07E-02	2.77E-08	SRPK2	-1.38E-02	3.64E-08	SATB1	-1.69E-02	8.52E-08
RAB7A	-1.07E-02	1.90E-19	TTC19	-1.39E-02	1.31E-10	CBFB	-1.70E-02	1.17E-15
MRPS36	-1.07E-02	3.80E-13	DNAJC15	-1.39E-02	4.29E-18	PTTG1IP	-1.70E-02	5.18E-12
EMC7	-1.08E-02	8.54E-18	ISY1	-1.39E-02	2.90E-10	PFDN4	-1.71E-02	8.75E-05
RPS19BP1	-1.08E-02	1.22E-14	TGOLN2	-1.41E-02	2.10E-14	PSMB4	-1.71E-02	8.59E-12
YAF2	-1.09E-02	8.54E-08	RIOK3	-1.41E-02	3.12E-12	TES	-1.72E-02	5.28E-07

Gene	logFC	FDR	Gene	logFC	FDR	Gene	logFC	FDR
METTL5	-1.72E-02	4.94E-15	TMEM179B	-2.01E-02	4.07E-11	ADSS	-2.41E-02	2.78E-10
ZNF511	-1.72E-02	1.18E-07	PSPC1	-2.01E-02	1.10E-09	MAGED1	-2.41E-02	3.31E-09
IMP3	-1.72E-02	2.33E-11	SNX5	-2.02E-02	2.37E-09	TMEM218	-2.42E-02	3.53E-15
HTATIP2	-1.73E-02	1.29E-14	IMP4	-2.04E-02	3.58E-14	TMEM9	-2.43E-02	8.43E-16
FAM120AOS	-1.73E-02	1.69E-13	MRPS31	-2.04E-02	6.62E-09	C4orf3	-2.44E-02	1.74E-17
SAMM50	-1.74E-02	2.27E-13	ITPA	-2.05E-02	2.91E-14	IKZF1	-2.45E-02	5.21E-13
ZCCHC17	-1.75E-02	2.21E-08	MAPRE1	-2.05E-02	7.59E-14	FLYWCH2	-2.45E-02	1.28E-12
WNK1	-1.76E-02	1.25E-08	SRFBP1	-2.06E-02	1.10E-07	IMPDH2	-2.46E-02	5.43E-10
PRR13	-1.77E-02	5.76E-09	NCOR1	-2.07E-02	1.06E-10	DCTD	-2.46E-02	7.23E-13
CHMP5	-1.77E-02	5.13E-16	HMG20B	-2.08E-02	8.42E-13	LRRC75A	-2.46E-02	8.26E-13
IP6K2	-1.78E-02	6.06E-21	MRPL21	-2.09E-02	8.41E-15	TRA2B	-2.47E-02	6.40E-14
TTC32	-1.79E-02	6.46E-08	OXR1	-2.10E-02	1.99E-08	BIVM	-2.49E-02	3.35E-05
ARID1B	-1.79E-02	1.51E-10	C1orf52	-2.13E-02	4.35E-13	NDUFB5	-2.49E-02	7.34E-10
VGLL4	-1.81E-02	7.32E-14	MED10	-2.15E-02	3.98E-17	TPD52	-2.49E-02	1.30E-23
PPIE	-1.81E-02	1.11E-12	STUB1	-2.15E-02	1.41E-15	GLRX	-2.50E-02	1.52E-09
GSPT1	-1.82E-02	5.19E-09	LYRM2	-2.15E-02	1.38E-15	FAM111A	-2.50E-02	1.26E-20
TMEM30A	-1.83E-02	7.22E-18	ANXA4	-2.16E-02	7.89E-14	MTDH	-2.50E-02	2.68E-11
YWHAG	-1.83E-02	2.56E-08	ACADVL	-2.17E-02	5.99E-18	SSSCA1	-2.51E-02	1.45E-08
CYB5R3	-1.83E-02	3.91E-11	GABPB1	-2.19E-02	8.87E-13	BABAM1	-2.51E-02	1.22E-15
NUTM2B-AS	-1.83E-02	1.12E-10	UNK	-2.19E-02	1.07E-15	TSNAX	-2.52E-02	8.63E-04
CDK2AP2	-1.85E-02	1.95E-12	PLAGL1	-2.20E-02	3.77E-13	SLC39A1	-2.54E-02	1.76E-13
ASNSD1	-1.85E-02	1.09E-13	DR1	-2.21E-02	1.78E-09	HDAC3	-2.55E-02	1.64E-08
COPS4	-1.86E-02	4.21E-11	DCTN3	-2.22E-02	5.82E-21	TFDP2	-2.55E-02	1.11E-10
TP53I13	-1.87E-02	1.38E-13	HNRNPUL1	-2.24E-02	3.16E-16	ENOSF1	-2.56E-02	2.66E-09
KDM5A	-1.87E-02	4.48E-11	SMIM15	-2.24E-02	1.31E-11	DVL2	-2.56E-02	1.34E-15
KIF2A	-1.88E-02	4.37E-12	HSD17B12	-2.24E-02	3.09E-16	PARL	-2.58E-02	8.02E-13
GNAI1	-1.88E-02	4.86E-07	EEF1G	-2.25E-02	6.18E-14	KIF5B	-2.58E-02	4.41E-16
GUK1	-1.89E-02	2.45E-20	EIF4A3	-2.25E-02	2.12E-03	HOXA9	-2.59E-02	3.11E-08
TMEM98	-1.89E-02	8.05E-16	TERF1	-2.26E-02	2.56E-10	UBE2K	-2.59E-02	7.52E-12
FAM122B	-1.89E-02	5.06E-11	C1orf123	-2.28E-02	8.20E-09	NT5DC1	-2.60E-02	3.51E-13
POLR2J3.1	-1.89E-02	2.60E-13	EPRS	-2.28E-02	2.55E-05	GNL2	-2.61E-02	1.79E-11
SLTM	-1.90E-02	4.62E-13	TIMM10	-2.28E-02	5.27E-11	COA4	-2.63E-02	1.11E-11
UHMK1	-1.90E-02	4.94E-09	CHID1	-2.28E-02	1.41E-09	ZNF667-AS1	-2.64E-02	7.91E-20
PRELID3B	-1.92E-02	8.31E-13	HNRNPL	-2.30E-02	3.20E-10	RPF2	-2.64E-02	1.86E-12
NPEPPS	-1.92E-02	1.74E-13	CCDC82	-2.31E-02	5.43E-09	SEC63	-2.65E-02	1.07E-13
PLEK	-1.92E-02	2.63E-06	DIAPH1	-2.31E-02	2.58E-07	GYG1	-2.65E-02	1.93E-14
SLC30A9	-1.93E-02	8.77E-12	MCFD2	-2.31E-02	1.29E-15	TPP2	-2.65E-02	1.75E-07
CAPZA2	-1.94E-02	1.03E-11	LYRM4	-2.31E-02	7.91E-18	DNAJC2	-2.66E-02	3.62E-09
MSRA	-1.94E-02	9.55E-10	SPIN1	-2.32E-02	7.14E-11	CPXM1	-2.67E-02	8.44E-11
PPP1R7	-1.94E-02	1.18E-13	GCA	-2.33E-02	1.57E-10	ZMYM5	-2.68E-02	4.53E-08
ZNF146	-1.95E-02	3.23E-11	KRR1	-2.34E-02	1.45E-17	CYCS	-2.69E-02	6.73E-06
MMADHC	-1.95E-02	3.39E-11	EMC10	-2.36E-02	1.25E-14	FDX1	-2.70E-02	1.75E-10
ASPH	-1.96E-02	8.18E-08	RBM42	-2.36E-02	4.47E-12	ARL1	-2.71E-02	8.72E-13
TRAP1	-1.96E-02	7.58E-11	IFITM2	-2.37E-02	1.62E-09	RFXANK	-2.71E-02	2.66E-10
DIMT1	-1.98E-02	3.85E-09	MRPS30	-2.37E-02	3.87E-07	APIP	-2.73E-02	2.88E-14
PPP1R18	-1.99E-02	3.95E-12	TCERG1	-2.38E-02	8.72E-09	RPAIN	-2.73E-02	5.94E-16
RXYLT1	-1.99E-02	1.19E-10	CKB	-2.38E-02	6.14E-13	ACTN4	-2.73E-02	6.04E-14
TAOK3	-1.99E-02	2.13E-09	CSF3R	-2.39E-02	2.72E-07	PSMF1	-2.73E-02	1.54E-08
BCKDHB	-1.99E-02	1.50E-12	DRAP1	-2.41E-02	1.40E-10	DHX29	-2.74E-02	2.03E-14

Gene	logFC	FDR	Gene	logFC	FDR	Gene	logFC	FDR
DDX50	-2.74E-02	1.27E-08	RAB11A	-3.06E-02	1.94E-17	GARS	-3.45E-02	1.76E-10
ACIN1	-2.74E-02	3.17E-12	BUD31	-3.06E-02	9.29E-16	UTP18	-3.47E-02	1.83E-13
SNCA	-2.76E-02	4.04E-17	MYL6B	-3.06E-02	2.88E-14	NRDC	-3.50E-02	2.67E-12
MAPKAPK5	-2.76E-02	6.43E-09	TRAPPC6A	-3.09E-02	2.79E-13	OSGEP	-3.51E-02	1.79E-10
TMEM126B	-2.77E-02	8.14E-07	CAPRIN1	-3.10E-02	6.84E-14	MCCC1	-3.51E-02	1.48E-11
XBP1	-2.78E-02	3.37E-07	GOLIM4	-3.11E-02	7.30E-07	COMMD1	-3.51E-02	1.95E-14
PIGT	-2.78E-02	4.53E-12	STX8	-3.12E-02	1.33E-11	MEA1	-3.51E-02	1.05E-13
TIA1	-2.80E-02	2.23E-07	SELENOW	-3.12E-02	2.19E-17	DNAJC19	-3.51E-02	1.15E-16
PGD	-2.81E-02	1.01E-11	RABGGTB	-3.14E-02	2.89E-11	UGP2	-3.53E-02	3.40E-19
SNU13	-2.81E-02	5.85E-13	AIG1	-3.14E-02	1.01E-13	TRAPPC4	-3.55E-02	3.48E-13
FLT3	-2.81E-02	1.07E-09	SNHG15	-3.14E-02	4.77E-06	CEP57	-3.56E-02	5.32E-13
F8A1	-2.81E-02	2.52E-09	USP33	-3.15E-02	1.09E-13	MFF	-3.57E-02	3.73E-13
TPM1	-2.81E-02	1.54E-09	TM9SF2	-3.15E-02	1.63E-13	FAM192A	-3.58E-02	1.13E-13
HEXB	-2.81E-02	1.72E-18	CMTM7	-3.17E-02	4.39E-16	ANKLE2	-3.58E-02	9.00E-09
NBDY	-2.83E-02	5.05E-15	INTS10	-3.17E-02	3.60E-12	UPF3B	-3.58E-02	4.64E-12
ALDOA	-2.83E-02	3.64E-10	BAD	-3.18E-02	7.16E-23	OSER1	-3.59E-02	6.35E-15
MED21	-2.84E-02	1.90E-22	NFIC	-3.18E-02	1.08E-17	HIBCH	-3.60E-02	1.08E-15
SDR39U1	-2.85E-02	2.53E-14	C16orf87	-3.18E-02	8.07E-14	C1QTNF4	-3.61E-02	8.44E-05
TAF15	-2.85E-02	7.96E-10	LYSMD2	-3.20E-02	2.70E-12	NSMCE4A	-3.61E-02	5.00E-19
API5	-2.86E-02	1.93E-14	MT-CYB	-3.20E-02	5.44E-03	SMIM30	-3.62E-02	2.22E-16
ETF1	-2.86E-02	1.89E-11	COMMD2	-3.20E-02	5.93E-15	DFFA	-3.63E-02	2.42E-10
DCAF16	-2.87E-02	7.05E-13	SDHC	-3.21E-02	1.43E-18	YDJC	-3.63E-02	3.82E-11
FAM216A	-2.88E-02	1.01E-14	POLR3GL	-3.22E-02	1.69E-12	MOB1A	-3.64E-02	2.93E-18
LRRC58	-2.88E-02	2.75E-08	BDP1	-3.23E-02	2.02E-08	CHD4	-3.64E-02	6.33E-15
CAPNS1	-2.88E-02	1.27E-06	SAFB	-3.24E-02	1.11E-14	RPS21	-3.64E-02	9.54E-03
KARS	-2.88E-02	4.28E-22	GNB4	-3.25E-02	5.04E-16	ORMDL1	-3.64E-02	5.78E-14
CCAR1	-2.89E-02	3.48E-18	BCAP29	-3.26E-02	1.64E-17	ZDHHC4	-3.64E-02	4.69E-19
DPYSL2	-2.89E-02	9.44E-13	STAG2	-3.26E-02	2.67E-05	CALM1	-3.65E-02	4.83E-12
UXS1	-2.90E-02	1.19E-10	STX10	-3.28E-02	6.94E-13	HDHD2	-3.65E-02	1.10E-15
B3GNT2	-2.90E-02	5.93E-06	LAS1L	-3.28E-02	2.16E-15	PPHLN1	-3.66E-02	1.71E-12
CHCHD10	-2.91E-02	3.85E-19	SEC22B	-3.32E-02	9.69E-13	ATP5MC2	-3.67E-02	2.62E-02
COMMD9	-2.91E-02	9.05E-12	TMBIM4	-3.33E-02	5.31E-14	CCDC90B	-3.67E-02	1.80E-14
KPNA3	-2.92E-02	1.69E-13	KRT10	-3.34E-02	1.13E-13	SF3B4	-3.67E-02	3.32E-15
DYNC1LI1	-2.94E-02	5.10E-10	OAT	-3.35E-02	5.68E-11	RAB10	-3.68E-02	3.50E-15
RSF1	-2.94E-02	1.46E-14	PSMG4	-3.35E-02	1.56E-08	RAB4A	-3.68E-02	4.56E-17
IARS2	-2.96E-02	8.92E-09	GCFC2	-3.35E-02	1.46E-17	LSM14A	-3.68E-02	5.92E-14
CAND1	-2.97E-02	6.01E-08	CHRAC1	-3.35E-02	6.81E-12	SBNO1	-3.69E-02	7.46E-15
UBA5	-2.97E-02	1.26E-07	KRTCAP2	-3.35E-02	1.80E-18	KXD1	-3.69E-02	1.75E-17
ZPR1	-2.99E-02	3.34E-13	USP10	-3.38E-02	3.39E-13	LSM8	-3.70E-02	4.55E-20
SMARCE1	-2.99E-02	1.21E-07	BRD3	-3.38E-02	5.16E-08	NDUFAF2	-3.70E-02	2.16E-09
CD59	-2.99E-02	4.88E-16	BTF3L4	-3.39E-02	1.32E-12	NIPBL	-3.71E-02	2.29E-13
RBM26	-3.02E-02	5.87E-10	MESD	-3.40E-02	3.13E-11	DPP7	-3.73E-02	4.23E-17
CWC15	-3.02E-02	3.39E-10	NOL8	-3.42E-02	3.16E-08	PRPF4B	-3.74E-02	1.66E-11
TMEM18	-3.03E-02	5.00E-09	SMIM8	-3.43E-02	1.02E-11	SLC25A11	-3.75E-02	6.37E-16
NAP1L4	-3.03E-02	4.23E-13	DHX30	-3.43E-02	7.79E-08	NOP56	-3.75E-02	1.57E-16
ZNF326	-3.03E-02	1.83E-12	TAF12	-3.44E-02	2.55E-11	NUP54	-3.75E-02	4.31E-20
WASHC3	-3.03E-02	1.25E-09	MRPL33	-3.45E-02	1.65E-21	ZNF711	-3.76E-02	1.53E-11
MRPL24	-3.03E-02	9.01E-16	ZBTB44	-3.45E-02	2.54E-07	ATIC	-3.76E-02	2.97E-15
ECI2	-3.05E-02	3.33E-16	NANS	-3.45E-02	2.18E-16	CLPP	-3.76E-02	3.25E-10

Gene	logFC	FDR	Gene	logFC	FDR	Gene	logFC	FDR
SDAD1	-3.77E-02	1.06E-12	LARP7	-4.15E-02	2.66E-12	DECR1	-4.66E-02	1.68E-10
ANKRD36	-3.77E-02	1.26E-08	SPAG16	-4.15E-02	2.82E-13	DGCR6L	-4.66E-02	5.22E-23
DCXR	-3.79E-02	7.34E-22	SPI1	-4.15E-02	3.33E-10	ARPC5L	-4.69E-02	3.70E-03
PPP4R3B	-3.80E-02	1.52E-08	PNN	-4.18E-02	2.43E-09	PRDX6	-4.69E-02	6.97E-17
SHMT2	-3.80E-02	1.33E-08	TTC1	-4.20E-02	1.99E-14	AL157938.3	-4.70E-02	2.21E-10
NAA10	-3.83E-02	1.48E-16	CNPY3	-4.21E-02	2.32E-12	MFSD1	-4.70E-02	2.14E-14
MRPL19	-3.83E-02	2.16E-08	FKBP5	-4.21E-02	3.57E-07	ANKRD36C	-4.70E-02	7.21E-16
SFT2D1	-3.84E-02	9.81E-18	PMVK	-4.22E-02	1.75E-12	SEPT11	-4.71E-02	4.70E-13
MRPS15	-3.84E-02	4.35E-13	NME7	-4.22E-02	4.57E-20	SNHG21	-4.72E-02	3.04E-13
ING3	-3.84E-02	3.52E-10	MBD4	-4.23E-02	2.59E-06	IFRD2	-4.73E-02	3.22E-12
FUBP1	-3.84E-02	4.20E-09	FADS1	-4.24E-02	8.20E-11	TRAPPC2L	-4.73E-02	7.25E-16
ATRX	-3.85E-02	1.23E-11	TRMT10C	-4.26E-02	6.47E-13	SEC11A	-4.76E-02	1.46E-09
SNAPIN	-3.85E-02	3.69E-13	SF3B1	-4.26E-02	3.08E-05	ANAPC13	-4.76E-02	3.36E-13
MTCH1	-3.85E-02	1.39E-15	STT3B	-4.27E-02	4.23E-12	RSRC1	-4.76E-02	3.12E-08
EIF1AY	-3.86E-02	1.33E-12	ATP6V1G1	-4.28E-02	1.76E-05	TNPO1	-4.79E-02	4.12E-12
BCLAF1	-3.86E-02	5.36E-11	NCBP2-AS2	-4.31E-02	3.99E-12	NDUFA7	-4.79E-02	1.67E-13
HDGF	-3.87E-02	1.37E-23	ZSCAN16-AS	-4.34E-02	2.53E-13	CCNC	-4.80E-02	1.98E-15
CNDP2	-3.88E-02	7.77E-12	HINT1	-4.34E-02	3.56E-03	SEC13	-4.80E-02	1.96E-13
RAP1B	-3.90E-02	3.05E-22	RRP7A	-4.35E-02	2.63E-16	PUF60	-4.80E-02	3.59E-23
THOC2	-3.91E-02	3.17E-12	NIPSNAP2	-4.35E-02	1.65E-17	TIMMDC1	-4.81E-02	2.80E-11
NCF4	-3.92E-02	3.96E-12	BCL7A	-4.37E-02	2.03E-08	OCIAD1	-4.81E-02	2.08E-13
SCNM1	-3.92E-02	6.04E-10	KIAA1143	-4.41E-02	1.28E-12	PSMC6	-4.82E-02	7.70E-17
REXO2	-3.93E-02	2.57E-13	FKBP4	-4.41E-02	2.54E-15	MTX2	-4.82E-02	2.72E-09
DENR	-3.93E-02	2.71E-17	RAP1A	-4.43E-02	2.75E-13	CELF1	-4.83E-02	6.91E-17
ACBD6	-3.93E-02	8.99E-14	CNTRL	-4.43E-02	4.46E-13	TIMM10B	-4.83E-02	3.91E-07
PSMD13	-3.93E-02	8.10E-16	PMPCA	-4.43E-02	2.71E-20	LSM1	-4.83E-02	2.30E-16
MRPS25	-3.94E-02	3.83E-14	MANF	-4.44E-02	7.09E-05	GTPBP4	-4.84E-02	5.57E-07
LMAN1	-3.95E-02	1.01E-15	FXN	-4.45E-02	3.59E-18	EXOSC5	-4.85E-02	9.16E-12
LSP1	-3.95E-02	1.20E-14	PRPSAP1	-4.47E-02	1.07E-10	PMF1	-4.87E-02	1.75E-15
PTMS	-3.96E-02	2.44E-30	SH3BGRL	-4.49E-02	1.82E-07	DDX21	-4.88E-02	2.06E-07
C11orf74	-3.97E-02	8.37E-14	TMEM123	-4.49E-02	1.13E-16	SND1	-4.90E-02	4.58E-10
ABHD14A	-3.97E-02	6.32E-11	PSMD6	-4.49E-02	6.78E-20	PNKD	-4.91E-02	1.86E-20
CDC5L	-3.99E-02	1.31E-08	PRPF31	-4.51E-02	1.03E-11	DNTTIP2	-4.92E-02	6.46E-13
C9orf78	-4.00E-02	5.00E-18	FAM117A	-4.52E-02	6.54E-11	STARD7	-4.92E-02	6.12E-17
MPC1	-4.00E-02	4.95E-16	TMEM208	-4.52E-02	1.40E-13	MRPS7	-4.92E-02	1.66E-13
ATP2B1	-4.02E-02	2.62E-13	MRPL32	-4.52E-02	1.72E-16	GMFG	-4.93E-02	7.58E-05
TXNRD1	-4.02E-02	6.31E-09	FGFR1OP2	-4.53E-02	8.84E-11	BTG3	-4.94E-02	2.16E-09
RPF1	-4.03E-02	5.28E-08	C4orf48	-4.55E-02	1.61E-13	TMEM183A	-4.97E-02	1.44E-12
POP5	-4.04E-02	5.51E-19	LUC7L3	-4.56E-02	1.62E-08	KPNA2	-4.98E-02	9.16E-10
UBXN4	-4.05E-02	5.59E-12	VMA21	-4.57E-02	2.53E-20	CISD1	-4.99E-02	1.08E-12
STIP1	-4.06E-02	4.14E-13	NDUFS4	-4.57E-02	1.25E-09	TRA2A	-4.99E-02	4.25E-14
SSNA1	-4.07E-02	4.11E-16	C9orf16	-4.60E-02	1.41E-17	RER1	-5.00E-02	7.68E-15
ADPGK	-4.11E-02	1.83E-12	TIPRL	-4.60E-02	1.91E-23	GNB1	-5.00E-02	1.49E-13
EIF2B5	-4.11E-02	7.15E-15	TMEM242	-4.61E-02	9.98E-12	QDPR	-5.00E-02	2.26E-12
FNTA	-4.12E-02	9.02E-09	TRAPPC1	-4.62E-02	1.24E-13	TARDBP	-5.02E-02	4.74E-13
ASH2L	-4.13E-02	1.44E-19	PSMB9	-4.63E-02	1.10E-21	ZBTB8OS	-5.02E-02	7.28E-16
CERS2	-4.13E-02	1.96E-13	DNAJA1	-4.63E-02	2.22E-17	PFDN2	-5.03E-02	4.96E-13
SFXN4	-4.13E-02	2.40E-08	TALDO1	-4.63E-02	2.20E-10	GSTO1	-5.04E-02	1.22E-22
NELFE	-4.14E-02	4.91E-19	PPP2R1A	-4.64E-02	2.78E-12	PLRG1	-5.04E-02	7.12E-15

Gene	logFC	FDR	Gene	logFC	FDR	Gene	logFC	FDR
ABCE1	-5.05E-02	2.18E-15	POLR2H	-5.46E-02	2.27E-15	CCDC124	-5.88E-02	3.31E-20
HEMGN	-5.05E-02	1.17E-09	DCAF7	-5.47E-02	9.22E-12	SEPT11	-5.90E-02	4.99E-13
MRPL9	-5.05E-02	6.47E-15	ASF1A	-5.47E-02	3.95E-16	BST1	-5.90E-02	7.31E-14
BID	-5.06E-02	1.18E-17	MYDGF	-5.48E-02	9.22E-24	CAPZA1	-5.90E-02	1.19E-15
MRPL50	-5.07E-02	2.73E-16	CNTLN	-5.51E-02	3.72E-07	NUBP2	-5.92E-02	1.43E-06
HIBADH	-5.08E-02	6.68E-13	PTDSS1	-5.51E-02	1.58E-13	CWC27	-5.92E-02	2.51E-15
UTP11	-5.11E-02	1.28E-13	WBP11	-5.52E-02	1.41E-14	NDUFS2	-5.94E-02	3.58E-13
KDELR2	-5.11E-02	1.07E-14	CRLS1	-5.52E-02	3.09E-20	MZT1	-5.94E-02	4.32E-21
SLC25A6	-5.13E-02	2.87E-09	SRP19	-5.52E-02	1.39E-14	SEC11C	-5.95E-02	3.74E-17
HDDC2	-5.13E-02	1.67E-15	EXTL2	-5.52E-02	1.29E-18	ELP5	-5.95E-02	8.07E-15
DUSP23	-5.14E-02	2.31E-13	UBE2J1	-5.53E-02	7.80E-14	ICE2	-5.97E-02	1.39E-11
C22orf39	-5.15E-02	1.20E-13	PSMC1	-5.54E-02	1.50E-17	RPS17	-5.99E-02	6.55E-04
AAMP	-5.15E-02	4.50E-12	INTS13	-5.54E-02	4.12E-14	ESF1	-5.99E-02	3.08E-12
MRPL55	-5.15E-02	2.13E-19	POLR2G	-5.54E-02	1.00E-16	NSD3	-6.00E-02	2.14E-13
SDHB	-5.16E-02	2.15E-23	ADD3	-5.55E-02	1.17E-09	UBE3A	-6.01E-02	9.91E-14
PTGER2	-5.16E-02	9.73E-05	SF3A2	-5.55E-02	9.22E-13	MRPS18C	-6.02E-02	7.79E-20
PSMD9	-5.16E-02	1.32E-15	CYB5B	-5.55E-02	1.72E-16	RGS1	-6.06E-02	6.39E-04
YIF1A	-5.17E-02	3.37E-14	MSRB2	-5.55E-02	1.84E-13	CMAS	-6.06E-02	2.44E-18
BLOC1S2	-5.19E-02	1.76E-10	LAT2	-5.60E-02	8.25E-10	CRIPT	-6.07E-02	5.44E-16
SPG21	-5.19E-02	1.01E-12	PDLIM1	-5.62E-02	5.31E-15	COMMD3	-6.07E-02	5.60E-11
SRRT	-5.20E-02	1.74E-11	MEAF6	-5.62E-02	5.21E-16	REC8	-6.08E-02	2.61E-11
CSTB	-5.21E-02	1.15E-15	SSR3	-5.62E-02	6.47E-12	KLHDC3	-6.10E-02	6.07E-17
EAF2	-5.22E-02	5.93E-15	ITM2C	-5.63E-02	4.95E-17	DCAF13	-6.11E-02	1.33E-19
ZNF428	-5.23E-02	8.88E-12	MAP3K20	-5.64E-02	5.63E-18	ABI2	-6.11E-02	1.36E-11
SLC30A5	-5.23E-02	1.24E-11	ME2	-5.65E-02	7.47E-13	NUP107	-6.13E-02	2.71E-14
SERPINB1	-5.23E-02	4.58E-02	AP002360.1	-5.67E-02	1.70E-13	RBM14	-6.15E-02	5.14E-13
ARF5	-5.23E-02	7.48E-16	XRN2	-5.70E-02	1.43E-15	TMEM167A	-6.15E-02	1.50E-17
NSD1	-5.23E-02	1.01E-12	METTL21A	-5.70E-02	1.20E-13	PPP2R3C	-6.17E-02	6.39E-15
PBRM1	-5.25E-02	6.63E-12	MGST3	-5.70E-02	5.05E-22	VPS26A	-6.18E-02	2.19E-22
BRK1	-5.25E-02	1.03E-08	GORASP2	-5.71E-02	3.94E-18	ARMH1	-6.20E-02	7.84E-13
ARGLU1	-5.25E-02	7.93E-11	ARRB2	-5.71E-02	1.04E-11	MRPL20	-6.23E-02	3.66E-18
FKBP11	-5.29E-02	2.62E-16	TWISTNB	-5.71E-02	1.50E-13	SMARCA5	-6.23E-02	2.52E-12
FAM32A	-5.29E-02	2.21E-14	HM13	-5.73E-02	5.47E-14	CSNK2A1	-6.27E-02	1.43E-16
PRPS1	-5.29E-02	1.05E-19	PRPF19	-5.74E-02	6.78E-14	TARS	-6.27E-02	4.23E-16
PITHD1	-5.34E-02	2.64E-15	NDUFB7	-5.75E-02	6.37E-19	PDIA4	-6.29E-02	1.10E-15
ATRAID	-5.34E-02	1.75E-14	DDT	-5.75E-02	8.10E-15	MORF4L2	-6.32E-02	4.21E-14
CAPZB	-5.35E-02	1.95E-12	SNF8	-5.76E-02	2.64E-25	RAB8A	-6.32E-02	3.42E-31
GALNT1	-5.36E-02	1.46E-11	TMA16	-5.77E-02	3.77E-13	LRPAP1	-6.35E-02	1.32E-23
MTHFD2L	-5.36E-02	8.67E-15	UBE2L6	-5.77E-02	6.60E-14	PUS7L	-6.36E-02	1.62E-17
FAM234A	-5.37E-02	7.13E-12	ADSL	-5.78E-02	2.74E-17	ACTR10	-6.37E-02	2.26E-21
CANX	-5.38E-02	1.22E-14	TMBIM6	-5.79E-02	1.45E-13	RPL27	-6.37E-02	1.20E-03
HSPH1	-5.40E-02	6.21E-11	BCCIP	-5.79E-02	1.25E-16	RNF138	-6.38E-02	4.91E-10
PSMD11	-5.42E-02	1.66E-22	ISOC2	-5.81E-02	9.75E-08	PLIN3	-6.38E-02	2.02E-13
CTNNBIP1	-5.42E-02	2.00E-14	METTL9	-5.81E-02	1.58E-19	GNPAT	-6.38E-02	1.18E-15
DNAJB11	-5.43E-02	4.88E-15	TFG	-5.81E-02	6.62E-16	MRPL22	-6.41E-02	1.63E-16
RDX	-5.43E-02	7.04E-15	NDUFA8	-5.82E-02	5.99E-10	GNAQ	-6.42E-02	7.65E-15
SNX2	-5.44E-02	2.02E-16	ANKRD10	-5.83E-02	2.40E-20	DDB1	-6.42E-02	5.43E-13
COPS5	-5.45E-02	3.48E-16	YY1	-5.85E-02	8.21E-14	HBS1L	-6.42E-02	3.78E-21
TMEM126A	-5.46E-02	1.52E-13	PTRHD1	-5.86E-02	3.04E-11	RPL3	-6.43E-02	6.73E-08

Gene	logFC	FDR	Gene	logFC	FDR	Gene	logFC	FDR
WDR18	-6.44E-02	6.69E-12	RALY	-7.20E-02	6.05E-26	RNF130	-7.96E-02	8.36E-15
PDHB	-6.48E-02	2.98E-16	SEPT6	-7.21E-02	7.31E-06	PCBP1	-7.96E-02	4.29E-19
TXNL4A	-6.49E-02	1.03E-12	MRPS14	-7.22E-02	1.00E-11	TMX2	-7.97E-02	1.04E-12
MYL12A	-6.49E-02	1.20E-07	HNRNPA0	-7.22E-02	1.04E-12	PDHA1	-7.99E-02	4.62E-15
TRIM28	-6.51E-02	6.12E-14	COX14	-7.25E-02	7.05E-25	KATNBL1	-8.06E-02	2.51E-23
TBCA	-6.51E-02	2.79E-13	LYRM7	-7.25E-02	9.75E-20	MED30	-8.12E-02	6.84E-25
NARF	-6.52E-02	5.40E-13	SS18L2	-7.27E-02	6.20E-14	PCNP	-8.13E-02	1.20E-11
UBE2A	-6.53E-02	3.43E-15	NDUFV1	-7.28E-02	4.66E-20	DHX9	-8.14E-02	4.95E-12
MRPL41	-6.55E-02	1.61E-19	SNRNP70	-7.30E-02	1.20E-15	CUEDC2	-8.16E-02	1.13E-20
SUCLG1	-6.58E-02	1.27E-14	TXNDC17	-7.31E-02	6.08E-14	NIPSNAP3A	-8.18E-02	6.09E-17
CPSF6	-6.58E-02	5.83E-17	C1D	-7.33E-02	1.63E-19	MTF2	-8.20E-02	2.50E-10
RSU1	-6.59E-02	4.55E-11	FDFT1	-7.33E-02	1.08E-18	OLA1	-8.22E-02	1.77E-18
TXNL1	-6.60E-02	2.55E-13	EIF6	-7.34E-02	4.06E-15	CETN2	-8.24E-02	1.13E-14
ERGIC2	-6.64E-02	2.49E-28	NDUFS3	-7.35E-02	1.70E-22	SPCS3	-8.27E-02	1.76E-25
MRPS35	-6.64E-02	7.04E-18	EIF3J	-7.35E-02	7.40E-14	CKAP2	-8.36E-02	6.80E-21
LINC02001	-6.69E-02	7.48E-14	CDC37	-7.37E-02	5.35E-12	PSMA1	-8.36E-02	2.71E-16
ITFG1	-6.69E-02	7.67E-18	MRPL23	-7.37E-02	1.61E-20	IMMP1L	-8.37E-02	1.74E-14
ANAPC15	-6.72E-02	2.95E-14	DPM2	-7.38E-02	1.42E-19	CSNK2B	-8.38E-02	1.49E-16
PABPN1	-6.73E-02	4.27E-14	UFD1	-7.39E-02	5.19E-18	BZW1	-8.39E-02	1.73E-15
SSR1	-6.74E-02	7.34E-18	DCK	-7.42E-02	1.83E-25	DPM3	-8.41E-02	1.03E-23
RAB32	-6.77E-02	8.30E-20	PAIP1	-7.45E-02	9.25E-13	ACAA2	-8.41E-02	1.58E-21
UPF3A	-6.78E-02	3.34E-12	HNRNPC	-7.48E-02	1.40E-10	ADA	-8.44E-02	5.98E-13
NDUFB10	-6.82E-02	4.60E-09	GCHFR	-7.52E-02	5.68E-18	NCBP2	-8.46E-02	1.78E-16
SPTLC1	-6.83E-02	6.26E-19	EIF4E2	-7.53E-02	1.10E-17	PIN4	-8.47E-02	6.28E-18
MRPL16	-6.84E-02	1.97E-09	CCDC47	-7.53E-02	1.52E-17	RPL21	-8.47E-02	3.43E-12
SSU72	-6.85E-02	3.45E-18	UBE2D2	-7.54E-02	1.78E-18	SRSF4	-8.50E-02	4.74E-13
LRPPRC	-6.85E-02	2.53E-14	PYCR2	-7.55E-02	1.31E-13	SAP18	-8.50E-02	2.02E-13
PSMD8	-6.86E-02	1.20E-28	RPN1	-7.57E-02	7.23E-16	PRPS2	-8.51E-02	2.21E-20
WDR43	-6.88E-02	3.08E-16	ACTR2	-7.57E-02	2.03E-15	CIB1	-8.52E-02	1.59E-16
PSMC4	-6.88E-02	2.08E-11	DRG1	-7.62E-02	6.63E-17	ING2	-8.52E-02	1.41E-13
TFAM	-6.89E-02	3.07E-14	SCOC	-7.62E-02	3.29E-22	GAMT	-8.54E-02	2.49E-19
GPBP1	-6.90E-02	3.21E-11	LAP3	-7.62E-02	9.64E-22	EIF2AK1	-8.57E-02	2.49E-17
ALG3	-6.91E-02	1.32E-13	GAR1	-7.66E-02	1.20E-13	RTF1	-8.57E-02	1.85E-16
CYB5A	-6.92E-02	1.62E-18	TMEM107	-7.69E-02	3.72E-12	BAALC	-8.58E-02	1.93E-16
NTPCR	-6.92E-02	1.33E-10	BRIX1	-7.70E-02	6.68E-13	LMAN2	-8.58E-02	2.46E-29
SMARCA4	-6.92E-02	9.57E-18	TIMM17A	-7.70E-02	8.23E-17	AKR7A2	-8.59E-02	1.67E-22
C20orf27	-6.95E-02	1.17E-12	SNRPD2	-7.72E-02	1.23E-06	DAZAP1	-8.60E-02	1.27E-20
MSMO1	-6.96E-02	2.52E-12	NARS	-7.72E-02	1.19E-13	COPS8	-8.62E-02	3.96E-19
DNM1L	-6.97E-02	6.57E-16	THOC6	-7.75E-02	4.75E-16	ADIPOR1	-8.62E-02	5.61E-16
APPL1	-6.99E-02	1.15E-18	MRPL1	-7.76E-02	2.19E-11	MRPL3	-8.66E-02	8.69E-26
SNX10	-7.00E-02	7.17E-16	DDX52	-7.77E-02	1.81E-12	PIH1D1	-8.68E-02	1.19E-21
MATK	-7.06E-02	6.91E-13	TBCB	-7.79E-02	4.82E-22	TAF7	-8.71E-02	5.74E-10
DERL2	-7.06E-02	2.36E-23	MRPL57	-7.80E-02	2.35E-18	ATOX1	-8.71E-02	1.29E-22
PDCL3	-7.06E-02	6.58E-13	DDX46	-7.80E-02	7.80E-22	DHX15	-8.73E-02	3.39E-17
PFKL	-7.09E-02	2.54E-19	SDHA	-7.85E-02	2.64E-17	PSMB7	-8.76E-02	1.53E-23
PROM1	-7.11E-02	5.56E-14	EIF4E	-7.86E-02	2.28E-19	SMC5	-8.77E-02	1.20E-16
CDKN2AIPNL	-7.13E-02	2.97E-11	GLUD1	-7.87E-02	1.45E-24	COPS9	-8.77E-02	7.92E-17
POLDIP2	-7.15E-02	3.20E-13	TOP2B	-7.94E-02	1.21E-16	SNX3	-8.78E-02	1.40E-11
UBB	-7.17E-02	8.41E-05	OXCT1	-7.95E-02	3.82E-19	SRRM1	-8.80E-02	2.14E-16

Gene	logFC	FDR	Gene	logFC	FDR	Gene	logFC	FDR
CNOT7	-8.82E-02	3.65E-14	SLC39A8	-9.72E-02	3.10E-22	PIN1	-1.07E-01	2.12E-30
RPL6	-8.84E-02	3.39E-07	NMRAL1	-9.75E-02	1.14E-25	DDOST	-1.07E-01	7.84E-15
DDX1	-8.84E-02	1.52E-22	ARPC3	-9.78E-02	3.00E-17	AK3	-1.07E-01	4.88E-21
GNAS	-8.85E-02	1.60E-14	AP1S1	-9.79E-02	1.12E-22	TXNDC12	-1.08E-01	8.01E-25
ADK	-8.91E-02	4.14E-32	YTHDF2	-9.81E-02	8.39E-17	DNAJC8	-1.08E-01	2.43E-23
SCP2	-8.94E-02	1.15E-21	HSPA9	-9.82E-02	4.86E-28	PCBP2	-1.08E-01	1.81E-07
UBE2L3	-8.96E-02	1.58E-23	NOLC1	-9.83E-02	5.43E-16	RFC1	-1.08E-01	4.65E-23
GPAA1	-9.00E-02	1.12E-25	ODC1	-9.84E-02	1.77E-20	CHD1L	-1.08E-01	2.64E-20
HDAC1	-9.03E-02	1.20E-22	SRPK1	-9.85E-02	1.05E-19	BAX	-1.08E-01	1.44E-14
ATP6AP2	-9.04E-02	4.58E-21	PLEKHJ1	-9.85E-02	9.76E-25	DERA	-1.08E-01	8.27E-24
CBWD1	-9.04E-02	8.17E-20	PSMD4	-9.86E-02	6.84E-25	SELENOH	-1.08E-01	1.49E-16
MRPS6	-9.05E-02	1.72E-18	PDCD10	-9.87E-02	3.30E-16	EIF2AK2	-1.08E-01	2.37E-23
ECHS1	-9.06E-02	7.31E-24	PLGRKT	-9.89E-02	7.63E-20	SELL	-1.09E-01	2.34E-05
TMEM165	-9.10E-02	7.46E-23	BAZ1A	-9.90E-02	1.64E-14	ADRM1	-1.09E-01	1.63E-23
MT-ND4L	-9.13E-02	4.09E-19	ATP6V0B	-9.92E-02	3.37E-25	TIMM8B	-1.10E-01	1.66E-20
MRPL48	-9.13E-02	5.52E-18	TOMM40	-9.93E-02	6.00E-28	LRRC59	-1.11E-01	5.92E-19
MRPL15	-9.17E-02	7.46E-23	B2M	-9.99E-02	8.80E-11	C8orf33	-1.11E-01	3.86E-24
LAPTM4B	-9.18E-02	4.13E-12	RPIA	-1.01E-01	1.54E-16	HACD1	-1.11E-01	1.28E-18
LAMP1	-9.20E-02	4.01E-20	GLRX3	-1.02E-01	2.42E-23	DCUN1D5	-1.11E-01	1.05E-18
SERPINE2	-9.23E-02	6.51E-16	GPN1	-1.02E-01	5.68E-25	CAPG	-1.11E-01	8.14E-16
WRB	-9.24E-02	3.04E-20	CALU	-1.02E-01	1.54E-19	POLE4	-1.11E-01	7.96E-21
FRG1	-9.25E-02	3.54E-12	ENOPH1	-1.02E-01	6.93E-23	IMMT	-1.12E-01	2.09E-25
TOMM22	-9.25E-02	3.01E-16	CDK2AP1	-1.02E-01	4.91E-21	SFPQ	-1.12E-01	3.87E-14
TOPORS	-9.25E-02	1.80E-15	ITGB1	-1.03E-01	1.04E-16	PSMD7	-1.12E-01	1.26E-18
RARS	-9.28E-02	3.79E-15	NMI	-1.03E-01	6.61E-13	GNL3	-1.12E-01	3.06E-20
GADD45GIP1	-9.35E-02	7.32E-21	MRPL4	-1.03E-01	2.79E-19	FBL	-1.12E-01	6.81E-16
UROS	-9.35E-02	4.55E-18	PRDX5	-1.03E-01	2.22E-27	GDI2	-1.12E-01	5.08E-12
CD99	-9.37E-02	7.97E-20	DLD	-1.04E-01	1.22E-15	PRELID1	-1.12E-01	2.53E-16
CMC2	-9.38E-02	1.05E-14	ARL6IP5	-1.04E-01	2.42E-07	ERG28	-1.12E-01	2.86E-22
SF3B5	-9.43E-02	2.70E-18	LARS	-1.04E-01	3.69E-29	UBE2E3	-1.13E-01	1.18E-24
GOLGA7	-9.43E-02	7.19E-26	ARL6IP1	-1.04E-01	2.69E-32	UBE2D3	-1.13E-01	3.91E-11
MRPS10	-9.44E-02	1.92E-16	NUDT5	-1.04E-01	2.36E-17	ATXN10	-1.13E-01	4.81E-20
COX16	-9.45E-02	9.16E-22	TMCO1	-1.04E-01	1.13E-19	WTAP	-1.13E-01	3.26E-15
PSMA6	-9.46E-02	4.71E-21	TSPAN13	-1.05E-01	9.22E-18	NDUFV2	-1.13E-01	1.87E-22
TRIAP1	-9.48E-02	9.28E-18	MORF4L1	-1.05E-01	4.25E-08	ILF3	-1.13E-01	7.13E-26
MRPL47	-9.51E-02	7.40E-19	HPF1	-1.05E-01	5.93E-33	PLAC8	-1.14E-01	8.96E-12
USP48	-9.52E-02	4.52E-19	NGLY1	-1.05E-01	2.20E-17	AP1S2	-1.14E-01	1.16E-21
GTF2H5	-9.54E-02	4.11E-19	ARMC10	-1.05E-01	3.17E-19	CCT3	-1.14E-01	5.16E-17
IPO7	-9.55E-02	3.70E-11	PSMB8	-1.05E-01	1.39E-19	RPS16	-1.14E-01	8.01E-09
SRSF1	-9.55E-02	6.55E-24	TRAM1	-1.05E-01	2.74E-23	SLC39A3	-1.14E-01	9.93E-20
MRPS16	-9.55E-02	5.86E-19	RNF5	-1.05E-01	4.17E-25	HP1BP3	-1.14E-01	5.96E-20
TMED10	-9.57E-02	2.83E-12	PDAP1	-1.05E-01	5.78E-21	EIF2S1	-1.14E-01	5.96E-30
ACAT1	-9.58E-02	1.13E-20	VPS35	-1.06E-01	1.53E-23	PSMD1	-1.15E-01	4.08E-26
DYNLT1	-9.60E-02	1.36E-13	WDR61	-1.06E-01	1.90E-21	ITGAE	-1.15E-01	2.04E-28
RAD23A	-9.63E-02	1.49E-18	CUTC	-1.06E-01	1.05E-22	G3BP1	-1.15E-01	3.91E-18
AHSA1	-9.64E-02	2.68E-20	HADH	-1.06E-01	7.14E-22	CAP1	-1.15E-01	6.60E-24
TMEM50A	-9.66E-02	2.62E-33	BTF3	-1.06E-01	2.30E-09	CMSS1	-1.15E-01	2.15E-23
MRPL14	-9.68E-02	2.66E-24	NPM3	-1.07E-01	1.88E-19	IPO5	-1.15E-01	2.32E-21
SNHG10	-9.71E-02	2.14E-16	SSB	-1.07E-01	8.47E-16	RUVBL2	-1.15E-01	4.02E-27

Gene	logFC	FDR	Gene	logFC	FDR	Gene	logFC	FDR
RIF1	-1.16E-01	2.72E-28	HNRNPA1P4	-1.28E-01	7.22E-20	CBX1	-1.38E-01	2.95E-35
FARSB	-1.16E-01	2.18E-25	SMIM19	-1.28E-01	6.82E-24	NDUFS6	-1.39E-01	2.72E-32
PRKRA	-1.16E-01	6.42E-19	HSD17B10	-1.28E-01	6.32E-29	SSR4	-1.39E-01	1.44E-20
ISOC1	-1.16E-01	1.70E-27	CHCHD3	-1.28E-01	1.64E-28	MAD2L2	-1.39E-01	2.73E-32
RCN1	-1.17E-01	3.55E-20	SREK1	-1.28E-01	1.16E-22	HIKESHI	-1.39E-01	3.41E-23
ROMO1	-1.17E-01	7.21E-20	PET100	-1.28E-01	1.82E-29	PGRMC1	-1.40E-01	3.76E-31
MT2A	-1.18E-01	6.76E-11	HAUS4	-1.28E-01	1.17E-20	BAG1	-1.40E-01	4.70E-26
PRPF40A	-1.19E-01	1.14E-18	PTBP1	-1.29E-01	2.30E-29	MGST2	-1.40E-01	2.29E-19
SRD5A3	-1.19E-01	2.78E-23	MTHFD2	-1.29E-01	4.61E-27	MTCH2	-1.41E-01	7.93E-33
EMC4	-1.19E-01	5.17E-25	LAMTOR2	-1.29E-01	1.30E-18	CSTF3	-1.41E-01	1.81E-18
RCN2	-1.19E-01	4.16E-30	MRPL37	-1.29E-01	1.07E-24	FAM49B	-1.41E-01	4.25E-25
DARS	-1.19E-01	4.01E-14	PRSS57	-1.29E-01	4.90E-19	ARHGDIB	-1.41E-01	2.91E-14
MRPS34	-1.19E-01	3.98E-28	EEF1B2	-1.29E-01	9.98E-11	SNRNP40	-1.41E-01	8.46E-31
THOC7	-1.19E-01	2.18E-26	ITM2A	-1.29E-01	1.37E-23	NREP	-1.42E-01	1.12E-21
NDUFAF8	-1.19E-01	5.32E-32	SMARCB1	-1.30E-01	2.49E-28	THYN1	-1.42E-01	1.07E-35
PSMA3	-1.19E-01	2.02E-26	HENMT1	-1.30E-01	4.18E-24	CISD2	-1.42E-01	7.81E-18
CENPV	-1.20E-01	1.68E-25	CCDC14	-1.30E-01	1.32E-23	MRPS26	-1.42E-01	2.35E-28
PPIB	-1.20E-01	1.48E-16	HIGD1A	-1.30E-01	3.10E-25	CDC123	-1.42E-01	6.39E-26
AC245014.3	-1.20E-01	1.15E-12	TTC3	-1.30E-01	2.43E-19	RNASEH2C	-1.43E-01	1.81E-40
UCHL3	-1.20E-01	4.46E-20	UQCRFS1	-1.30E-01	1.09E-19	MRPL13	-1.43E-01	1.37E-36
SMARCC1	-1.21E-01	4.14E-24	METTL26	-1.31E-01	7.39E-30	CCT6A	-1.43E-01	8.18E-27
AHCY	-1.21E-01	3.04E-23	TMEM14A	-1.31E-01	1.21E-34	NUDCD2	-1.44E-01	5.26E-22
ATP5PD	-1.22E-01	6.33E-21	PAXX	-1.31E-01	2.51E-32	DBI	-1.44E-01	5.16E-12
ANP32A	-1.22E-01	1.15E-23	PAFAH1B3	-1.31E-01	5.88E-24	RPS19	-1.44E-01	2.86E-38
ASNA1	-1.22E-01	7.25E-28	CDC26	-1.31E-01	3.92E-25	SNRPA1	-1.44E-01	3.83E-36
CD47	-1.22E-01	6.13E-26	SKP1	-1.31E-01	3.50E-11	SDF2L1	-1.44E-01	8.90E-13
ITGB1BP1	-1.22E-01	9.04E-29	PSMB5	-1.32E-01	2.05E-20	CLEC11A	-1.45E-01	7.91E-18
APEX1	-1.22E-01	2.56E-11	EBNA1BP2	-1.32E-01	1.41E-27	TMEM160	-1.45E-01	1.39E-41
FAM136A	-1.23E-01	5.15E-24	CNN3	-1.32E-01	8.39E-23	CLNS1A	-1.45E-01	2.34E-14
MPHOSPH6	-1.23E-01	2.88E-22	MIS18BP1	-1.33E-01	1.10E-22	NAE1	-1.46E-01	2.80E-27
MRPL12	-1.23E-01	3.25E-23	SF3A3	-1.33E-01	2.22E-32	PDCD5	-1.46E-01	8.20E-31
NONO	-1.24E-01	2.72E-28	EIF5B	-1.33E-01	7.98E-29	TSPAN3	-1.46E-01	6.52E-29
NDUFB9	-1.24E-01	3.19E-16	MDH2	-1.33E-01	1.09E-27	GLOD4	-1.46E-01	7.03E-28
TMEM147	-1.24E-01	1.58E-27	SOX4	-1.34E-01	2.28E-07	TAGLN2	-1.46E-01	3.79E-15
THRAP3	-1.24E-01	2.26E-28	RPS27L	-1.34E-01	1.83E-27	SSRP1	-1.47E-01	2.38E-34
SRP72	-1.24E-01	9.07E-19	ANXA5	-1.34E-01	1.37E-22	MED4	-1.47E-01	5.18E-28
WDR54	-1.24E-01	3.43E-18	ARPP19	-1.35E-01	3.38E-20	NDUFA9	-1.47E-01	1.32E-34
ANP32E	-1.25E-01	6.78E-20	MPLKIP	-1.35E-01	1.20E-32	TECR	-1.47E-01	4.50E-25
PSME1	-1.25E-01	1.75E-13	PSMD2	-1.35E-01	1.87E-32	TCEA1	-1.47E-01	3.00E-25
PPP1CC	-1.25E-01	1.55E-29	SUB1	-1.35E-01	9.21E-24	TPM4	-1.47E-01	2.75E-17
GUSB	-1.25E-01	1.03E-24	POLR2J	-1.36E-01	4.19E-25	ENSA	-1.48E-01	6.79E-20
UBA2	-1.26E-01	3.07E-31	GTF2I	-1.36E-01	1.72E-18	TSN	-1.48E-01	1.28E-27
COA3	-1.26E-01	5.68E-25	COMMD7	-1.36E-01	3.65E-23	RAD23B	-1.49E-01	2.13E-30
C12orf57	-1.26E-01	1.13E-20	VDAC2	-1.36E-01	1.48E-19	RAB5IF	-1.49E-01	2.49E-20
ARL5A	-1.26E-01	2.65E-19	SNRPB2	-1.36E-01	1.59E-11	RPL34	-1.49E-01	8.59E-29
TNFSF13B	-1.27E-01	6.41E-23	LSM6	-1.37E-01	8.87E-24	ATP5F1B	-1.50E-01	3.81E-27
BZW2	-1.27E-01	3.22E-19	SPCS1	-1.37E-01	5.39E-18	HERPUD1	-1.50E-01	1.53E-05
POLR2F	-1.27E-01	3.53E-24	COX17	-1.37E-01	2.73E-23	EI24	-1.50E-01	1.92E-33
RTN3	-1.27E-01	2.81E-15	PPIG	-1.38E-01	8.10E-23	GYPC	-1.50E-01	5.93E-08

Gene	logFC	FDR	Gene	logFC	FDR	Gene	logFC	FDR
ERI3	-1.51E-01	1.34E-22	ARPC1B	-1.66E-01	1.47E-15	NAA50	-1.81E-01	2.88E-26
AURKAIP1	-1.51E-01	4.35E-26	FIBP	-1.66E-01	2.50E-26	DDX39A	-1.81E-01	5.30E-34
VDAC3	-1.51E-01	2.64E-24	EBP	-1.67E-01	2.01E-34	STMP1	-1.82E-01	1.70E-21
HTATSF1	-1.52E-01	4.64E-31	NDUFAB1	-1.67E-01	2.20E-37	SYNCRIP	-1.82E-01	1.99E-28
SNRPA	-1.52E-01	6.75E-30	SRSF11	-1.67E-01	8.61E-23	MRPL18	-1.82E-01	3.93E-25
COPS3	-1.52E-01	4.18E-35	AKR1B1	-1.67E-01	1.14E-36	MAGOH	-1.82E-01	1.33E-38
ACADM	-1.53E-01	1.07E-27	FAM96A	-1.67E-01	5.01E-29	AKR1A1	-1.82E-01	6.24E-22
HINT2	-1.54E-01	6.12E-23	SEPT2	-1.68E-01	1.35E-32	ALG5	-1.82E-01	4.31E-35
PSMA5	-1.54E-01	5.02E-25	TM7SF3	-1.69E-01	7.86E-23	C11orf58	-1.83E-01	7.61E-15
POLR2I	-1.54E-01	2.12E-22	ETFB	-1.69E-01	8.40E-35	EWSR1	-1.83E-01	9.16E-26
SVIP	-1.54E-01	1.27E-27	BLOC1S1	-1.69E-01	2.58E-46	SDHAF3	-1.84E-01	1.85E-38
PCMT1	-1.55E-01	1.15E-24	CBX5	-1.69E-01	4.66E-31	SAE1	-1.84E-01	7.49E-46
IGHM	-1.55E-01	9.62E-14	TOMM5	-1.69E-01	1.67E-26	ELOC	-1.84E-01	2.30E-23
PDCD6	-1.56E-01	1.05E-22	DPY30	-1.69E-01	1.15E-35	SMIM24	-1.85E-01	9.61E-21
HACD3	-1.56E-01	6.60E-35	TIMM13	-1.69E-01	6.08E-23	LYPLA1	-1.86E-01	2.58E-26
DSTN	-1.57E-01	1.38E-16	PPM1G	-1.70E-01	1.17E-30	PSMG1	-1.87E-01	7.19E-39
PPP4C	-1.58E-01	4.33E-32	CALM3	-1.70E-01	3.77E-20	ATP5IF1	-1.87E-01	4.95E-28
NDUFA2	-1.58E-01	4.72E-23	HNRNPH3	-1.70E-01	1.50E-25	MZT2B	-1.87E-01	1.80E-26
YEATS4	-1.58E-01	8.76E-41	PSMD14	-1.71E-01	6.32E-29	SELENOF	-1.87E-01	1.47E-26
SINHCAF	-1.58E-01	1.26E-24	KTN1	-1.71E-01	4.00E-18	RAD21	-1.87E-01	1.16E-33
TUFM	-1.59E-01	1.04E-30	AP3S1	-1.72E-01	1.08E-25	GHITM	-1.88E-01	3.69E-28
TRMT112	-1.59E-01	6.13E-18	OCIAD2	-1.72E-01	4.91E-26	HNRNPU	-1.89E-01	4.40E-18
HAT1	-1.59E-01	5.92E-34	NAXE	-1.73E-01	1.15E-39	DGUOK	-1.91E-01	1.18E-24
POLR2E	-1.59E-01	2.43E-32	PMAIP1	-1.73E-01	2.16E-05	ANAPC5	-1.91E-01	2.58E-27
EIF3A	-1.59E-01	9.82E-22	LCP1	-1.73E-01	1.81E-27	PTPMT1	-1.91E-01	7.55E-38
NUDT21	-1.59E-01	2.77E-30	CCT2	-1.73E-01	6.57E-25	NDUFA5	-1.93E-01	1.83E-29
ENY2	-1.59E-01	1.77E-27	CNPY2	-1.73E-01	1.05E-22	CAT	-1.93E-01	7.87E-20
MRPL42	-1.59E-01	5.79E-31	ATP1A1	-1.75E-01	1.15E-30	NDUFA6	-1.93E-01	6.76E-31
NOP10	-1.59E-01	1.24E-23	VBP1	-1.75E-01	3.58E-55	PAIP2	-1.93E-01	7.29E-30
U2SURP	-1.60E-01	1.64E-23	HMGN5	-1.75E-01	3.79E-31	VPS29	-1.93E-01	4.04E-41
GLUL	-1.60E-01	3.75E-13	PSMB1	-1.75E-01	7.13E-20	EEF1E1	-1.94E-01	3.41E-39
CCT4	-1.60E-01	5.57E-28	SRP14	-1.75E-01	1.48E-17	HIST1H4C	-1.95E-01	8.54E-59
SLC25A3	-1.60E-01	4.94E-15	SCAF11	-1.75E-01	1.69E-21	MPC2	-1.95E-01	7.56E-32
LUC7L2	-1.60E-01	1.39E-25	MSH2	-1.75E-01	2.94E-40	VKORC1	-1.95E-01	2.38E-38
DKC1	-1.60E-01	2.12E-28	SLC25A39	-1.76E-01	4.12E-40	IER3IP1	-1.95E-01	5.03E-40
PSMC5	-1.60E-01	2.24E-26	GPX4	-1.76E-01	6.22E-27	POLR2K	-1.95E-01	1.88E-27
AK6	-1.61E-01	4.04E-30	RPA2	-1.76E-01	7.06E-39	HNRNPD	-1.96E-01	6.96E-32
MLEC	-1.62E-01	1.94E-22	ISYNA1	-1.76E-01	1.51E-37	GNG5	-1.97E-01	6.10E-32
CUTA	-1.62E-01	3.79E-23	MRPL11	-1.76E-01	1.68E-27	ACYP1	-1.97E-01	2.73E-36
SDHD	-1.62E-01	3.09E-29	CORO1A	-1.77E-01	3.58E-22	RBM17	-1.97E-01	2.31E-30
P4HB	-1.63E-01	1.44E-28	ADI1	-1.77E-01	1.34E-26	ETFA	-1.97E-01	2.10E-34
IGFBP7	-1.63E-01	2.73E-23	ATP5PO	-1.78E-01	1.48E-11	VRK1	-1.97E-01	6.25E-39
NDUFA11	-1.64E-01	3.17E-28	TCEAL9	-1.78E-01	1.93E-26	ELAVL1	-1.98E-01	6.68E-41
ZNF22	-1.64E-01	1.03E-22	RNPS1	-1.78E-01	3.30E-36	NUDT1	-1.98E-01	1.51E-36
UQCRC1	-1.64E-01	1.57E-31	JTB	-1.80E-01	4.34E-28	MZT2A	-1.99E-01	1.08E-25
BCAP31	-1.65E-01	1.99E-22	MRPL51	-1.80E-01	2.26E-37	TPR	-1.99E-01	1.65E-24
SEC61B	-1.65E-01	2.19E-30	NDUFA3	-1.80E-01	8.43E-26	PHF5A	-1.99E-01	2.35E-42
UROD	-1.65E-01	3.06E-26	MCUB	-1.80E-01	1.16E-32	ATG3	-1.99E-01	2.26E-32
NDUFA1	-1.65E-01	4.07E-25	PAPOLA	-1.81E-01	1.04E-25	HMGB3	-2.00E-01	5.15E-39

Gene	logFC	FDR	Gene	logFC	FDR	Gene	logFC	FDR
CCT7	-2.00E-01	4.74E-25	ATP5F1C	-2.24E-01	1.39E-26	SMC4	-2.56E-01	7.51E-41
GMPS	-2.00E-01	1.54E-34	UBE2I	-2.24E-01	1.85E-36	PARP1	-2.57E-01	6.47E-31
SNRPC	-2.01E-01	3.37E-38	ITGB3BP	-2.25E-01	5.48E-44	SUPT16H	-2.58E-01	1.48E-48
ATP5F1A	-2.01E-01	1.80E-21	HNRNPH1	-2.26E-01	4.84E-21	HNRNPDL	-2.58E-01	2.63E-26
ATP5MG	-2.02E-01	1.62E-20	ATP1B3	-2.27E-01	3.81E-40	TCP1	-2.59E-01	1.50E-41
UBE2N	-2.02E-01	2.69E-28	SRM	-2.27E-01	4.58E-36	DNPH1	-2.59E-01	4.31E-50
TPGS2	-2.03E-01	2.48E-38	SOD1	-2.27E-01	4.14E-29	AC103591.3	-2.60E-01	5.80E-20
PPT1	-2.03E-01	2.78E-37	NDUFB3	-2.28E-01	2.32E-37	YWHAB	-2.60E-01	4.93E-43
NDUFS8	-2.03E-01	9.08E-34	UBL5	-2.28E-01	8.82E-38	ARL6IP6	-2.61E-01	2.80E-54
ATP5PB	-2.04E-01	4.56E-22	RPL7	-2.29E-01	5.92E-68	UQCRH	-2.61E-01	5.86E-28
MEST	-2.05E-01	1.85E-33	ACP1	-2.29E-01	6.41E-35	SNRPD3	-2.61E-01	1.14E-38
NEDD8	-2.05E-01	2.16E-32	TPRKB	-2.30E-01	1.89E-32	POLD2	-2.62E-01	1.03E-58
NUDC	-2.05E-01	7.91E-38	FDPS	-2.30E-01	1.05E-48	DAD1	-2.64E-01	1.81E-40
GLO1	-2.05E-01	4.45E-50	FUS	-2.31E-01	2.18E-37	EIF5A	-2.64E-01	6.86E-42
PRMT1	-2.07E-01	1.21E-37	RPS3A	-2.31E-01	6.57E-87	CAMTA1	-2.64E-01	6.40E-41
SRI	-2.08E-01	1.54E-24	MYL6	-2.33E-01	1.12E-25	OAZ1	-2.64E-01	8.68E-21
GCSH	-2.08E-01	1.42E-50	NUTF2	-2.33E-01	2.67E-42	TMED9	-2.64E-01	3.14E-43
RPA1	-2.09E-01	3.55E-43	TMEM14C	-2.34E-01	7.43E-42	SIVA1	-2.64E-01	9.61E-61
EIF4EBP1	-2.10E-01	5.86E-35	NDUFA12	-2.34E-01	3.23E-42	RRM1	-2.65E-01	8.19E-68
MTHFD1	-2.10E-01	4.11E-40	NME4	-2.34E-01	9.62E-39	SLIRP	-2.66E-01	3.76E-46
SCCPDH	-2.12E-01	4.46E-45	RBMX	-2.35E-01	3.98E-36	HDAC2	-2.67E-01	3.65E-47
POLE3	-2.12E-01	5.58E-40	MARCKSL1	-2.36E-01	4.13E-37	RBM3	-2.68E-01	3.30E-22
ACTR3	-2.13E-01	5.08E-31	COX7A2	-2.36E-01	1.10E-31	CNBP	-2.68E-01	5.01E-32
PPA2	-2.13E-01	1.06E-24	GTF3C6	-2.37E-01	1.87E-37	NDUFB8	-2.69E-01	4.50E-34
SPTSSA	-2.13E-01	4.24E-45	TPM3	-2.37E-01	6.81E-27	SMS	-2.70E-01	1.50E-44
ATP5F1E	-2.14E-01	1.23E-23	PSMB2	-2.37E-01	3.55E-45	MT-ATP6	-2.73E-01	4.41E-43
UQCC2	-2.14E-01	7.14E-43	TAF9	-2.37E-01	1.70E-27	HSP90B1	-2.73E-01	3.27E-25
MINOS1	-2.15E-01	5.19E-36	EIF2S2	-2.39E-01	1.85E-33	MT-ND4	-2.77E-01	2.62E-54
PSMB6	-2.15E-01	1.27E-39	XRCC6	-2.39E-01	1.98E-48	RBBP4	-2.77E-01	1.09E-50
CENPX	-2.15E-01	7.40E-52	CCT8	-2.40E-01	1.32E-29	EIF1AX	-2.78E-01	4.67E-29
NDUFB6	-2.15E-01	6.11E-44	ANAPC11	-2.41E-01	8.80E-42	LSM7	-2.79E-01	6.01E-36
AK2	-2.15E-01	1.26E-37	ARL2	-2.41E-01	7.97E-43	H2AFV	-2.80E-01	3.76E-46
BUB3	-2.16E-01	1.72E-51	SMC3	-2.42E-01	1.47E-48	PPP1CA	-2.80E-01	2.83E-50
EXOSC8	-2.16E-01	3.02E-35	CCT5	-2.43E-01	1.23E-39	ANP32B	-2.83E-01	5.32E-35
LAMTOR5	-2.16E-01	7.45E-33	DYNLL1	-2.43E-01	4.08E-31	PHPT1	-2.84E-01	3.79E-48
NAA20	-2.17E-01	1.75E-38	HAUS1	-2.44E-01	3.27E-41	SSBP1	-2.84E-01	6.35E-42
BSG	-2.17E-01	4.33E-26	TMEM109	-2.44E-01	5.97E-43	SERBP1	-2.85E-01	1.31E-31
SNRPG	-2.18E-01	1.43E-42	COX6B1	-2.44E-01	3.69E-20	PEBP1	-2.85E-01	4.22E-35
CALR	-2.18E-01	4.76E-20	CYC1	-2.47E-01	7.34E-38	FKBP3	-2.86E-01	3.01E-47
ECH1	-2.19E-01	3.50E-24	ELOB	-2.49E-01	2.43E-36	PSMA7	-2.87E-01	1.04E-40
HSPB1	-2.19E-01	1.00E-22	SEC61G	-2.49E-01	1.73E-33	TMEM14B	-2.88E-01	4.31E-40
CDCA7L	-2.19E-01	1.92E-42	COPS6	-2.50E-01	1.32E-40	SRSF3	-2.88E-01	3.91E-33
STOML2	-2.20E-01	3.58E-36	HNRNPAB	-2.51E-01	5.40E-49	SNRPF	-2.88E-01	8.24E-43
STRAP	-2.20E-01	1.86E-38	TMX1	-2.51E-01	7.92E-40	COPE	-2.88E-01	4.65E-50
KPNB1	-2.20E-01	6.72E-42	AC084033.3	-2.51E-01	8.22E-22	CBX3	-2.88E-01	1.82E-41
COX5B	-2.22E-01	2.96E-26	UBE2V2	-2.51E-01	4.01E-50	PRKDC	-2.89E-01	5.21E-55
PHB	-2.22E-01	8.48E-45	UQCR11	-2.53E-01	4.06E-38	DNAJC9	-2.95E-01	1.91E-66
PGK1	-2.23E-01	8.58E-27	PAICS	-2.54E-01	1.42E-50	HPRT1	-2.95E-01	9.15E-57
AP2M1	-2.24E-01	4.59E-34	COX8A	-2.55E-01	1.88E-38	RHOA	-2.95E-01	1.22E-27

Gene	logFC	FDR	Gene	logFC	FDR	Gene	logFC	FDR	Gene	logFC	FDR
RHEB	-2.96E-01	1.24E-59	HSPB11	-3.55E-01	5.33E-74	OSTC	-4.30E-01	7.82E-57	TPI1	-6.18E-01	4.80E-134
BANF1	-2.98E-01	8.99E-48	H3F3A	-3.58E-01	3.05E-43	HNRNPA3	-4.32E-01	8.77E-53	YBX1	-6.21E-01	7.89E-183
RPL22L1	-2.99E-01	4.25E-53	H2AFY	-3.58E-01	2.44E-42	CALM2	-4.36E-01	2.39E-52	FABP5	-6.24E-01	3.62E-129
VDAC1	-3.01E-01	2.44E-61	C19orf48	-3.60E-01	7.93E-70	NME1	-4.38E-01	3.03E-87	NUCB2	-6.27E-01	4.25E-115
LAGE3	-3.01E-01	2.76E-59	TMED2	-3.62E-01	4.34E-67	GAPDH	-4.42E-01	1.40E-94	UQCRQ	-6.29E-01	1.13E-125
ATP5ME	-3.01E-01	6.55E-40	PHGDH	-3.63E-01	1.36E-76	CENPH	-4.49E-01	5.20E-107	HSPE1	-6.33E-01	5.14E-121
COX6A1	-3.01E-01	2.80E-53	SET	-3.64E-01	5.56E-51	SPINK2	-4.49E-01	2.05E-83	PPIA	-6.38E-01	9.69E-110
NHP2	-3.03E-01	6.26E-36	NDUFB2	-3.65E-01	3.28E-69	GGCT	-4.51E-01	6.95E-83	ATP5MC1	-6.39E-01	1.63E-135
POLR2L	-3.03E-01	9.47E-52	NDUFB11	-3.65E-01	1.15E-57	CYBA	-4.59E-01	2.41E-71	LSM4	-6.40E-01	1.21E-135
VAMP8	-3.03E-01	1.49E-26	HSPA5	-3.67E-01	1.27E-17	HSPA8	-4.63E-01	7.28E-60	PSMA4	-6.44E-01	6.47E-117
NDUFC2	-3.03E-01	1.04E-60	RBBP7	-3.67E-01	3.30E-80	RPA3	-4.63E-01	4.49E-107	SNRPB	-6.60E-01	3.01E-153
SRSF10	-3.04E-01	4.46E-56	LDHA	-3.69E-01	1.47E-31	IDH2	-4.64E-01	1.88E-102	HSPD1	-6.60E-01	2.83E-108
PTGES3	-3.04E-01	2.97E-45	HNRNPF	-3.70E-01	5.11E-63	CACYBP	-4.69E-01	1.20E-87	MT-CO2	-6.70E-01	2.51E-260
SF3B6	-3.06E-01	4.97E-45	NASP	-3.71E-01	2.65E-76	UQCR10	-4.73E-01	2.04E-82	YWHAQ	-6.73E-01	9.22E-108
BEX3	-3.06E-01	3.12E-36	FKBP1A	-3.71E-01	1.19E-39	MCM7	-4.75E-01	1.32E-104	DEK	-6.85E-01	3.00E-137
SUMO3	-3.07E-01	9.47E-52	CD69	-3.73E-01	9.67E-24	SPCS2	-4.76E-01	1.24E-79	LSM5	-6.86E-01	2.30E-142
TFDP1	-3.09E-01	5.98E-71	PSMB3	-3.74E-01	1.08E-64	HNRNPM	-4.78E-01	4.14E-74	HMGB1	-6.98E-01	1.44E-201
TMEM258	-3.13E-01	4.03E-32	SUMO2	-3.74E-01	9.61E-61	PRDX1	-4.79E-01	3.10E-74	HMGA1	-7.01E-01	1.52E-115
PSMC3	-3.13E-01	1.41E-57	CKLF	-3.75E-01	1.98E-76	SUMO1	-4.82E-01	8.87E-74	RAN	-7.19E-01	6.52E-154
SEPT7	-3.16E-01	4.64E-51	PYURF	-3.77E-01	8.48E-48	COX6C	-4.88E-01	1.05E-62	ERH	-7.42E-01	2.39E-153
SRSF2	-3.16E-01	4.84E-49	CDK6	-3.77E-01	2.44E-52	GTF3A	-4.88E-01	7.66E-75	PFN1	-7.60E-01	3.49E-197
GTF2A2	-3.18E-01	5.19E-50	YWHAE	-3.78E-01	1.02E-57	COX7B	-4.91E-01	6.07E-89	HMGB2	-8.34E-01	9.75E-215
NDUFB1	-3.20E-01	1.29E-41	ATP5MD	-3.78E-01	2.50E-46	HMGN3	-5.03E-01	1.74E-83	DUT	-8.82E-01	1.75E-235
PA2G4	-3.21E-01	1.00E-54	NCL	-3.81E-01	1.77E-48	ATP5MPL	-5.03E-01	4.83E-89	SLC25A5	-1.02E+00	1.93E-237
MAD2L1	-3.21E-01	2.44E-73	XRCC5	-3.82E-01	2.39E-68	POMP	-5.06E-01	4.39E-76	TUBB	-1.15E+00	0.00E+00
RPN2	-3.21E-01	1.33E-48	PSIP1	-3.83E-01	1.62E-56	MCM3	-5.07E-01	1.79E-119	RANBP1	-1.20E+00	0.00E+00
YWHAH	-3.24E-01	3.23E-49	COX5A	-3.85E-01	1.87E-57	PTMA	-5.08E-01	3.39E-220	TUBA1B	-1.30E+00	0.00E+00
MDK	-3.24E-01	1.51E-34	HNRNPR	-3.88E-01	9.05E-66	ATP5MF	-5.16E-01	1.79E-92	HMGN2	-1.40E+00	0.00E+00
SRSF9	-3.24E-01	4.76E-49	ATP5MC3	-3.92E-01	2.16E-68	PRDX2	-5.16E-01	1.17E-85	H2AFZ	-1.40E+00	0.00E+00
MT-CO1	-3.24E-01	4.16E-61	TMEM106C	-3.95E-01	2.77E-94	LSM3	-5.17E-01	3.43E-109	STMN1	-1.84E+00	0.00E+00
RNASEH2B	-3.25E-01	1.23E-49	MDH1	-3.96E-01	9.13E-72	PSMA2	-5.23E-01	2.66E-70			
SEM1	-3.25E-01	2.36E-46	ATP5PF	-3.97E-01	1.93E-55	PSME2	-5.24E-01	1.76E-99			
NOP58	-3.27E-01	9.61E-61	HSBP1	-3.98E-01	7.10E-67	CHCHD2	-5.27E-01	2.05E-86			
MGST1	-3.29E-01	6.43E-50	PRDX3	-3.99E-01	2.33E-68	PDIA6	-5.33E-01	1.48E-95			
NUCKS1	-3.42E-01	5.72E-58	RBX1	-4.02E-01	2.01E-67	TXN	-5.46E-01	2.42E-90			
NDUFA4	-3.42E-01	5.20E-62	ARPC5	-4.03E-01	1.20E-61	HNRNPA2B1	-5.51E-01	1.08E-97			
PDIA3	-3.43E-01	5.32E-39	ILF2	-4.04E-01	1.75E-71	C1QBP	-5.52E-01	9.23E-90			
DCTPP1	-3.44E-01	1.14E-75	NAP1L1	-4.04E-01	4.84E-52	SNRPE	-5.57E-01	9.22E-92			
SERF2	-3.44E-01	1.63E-55	HNRNPA1	-4.07E-01	8.94E-89	ENO1	-5.60E-01	2.93E-114			
AP2S1	-3.45E-01	3.67E-59	PRIM1	-4.12E-01	1.88E-90	HMGN1	-5.61E-01	6.52E-93			
NDUFA13	-3.46E-01	1.29E-59	PARK7	-4.14E-01	8.48E-58	GSTP1	-5.61E-01	3.37E-122			
USP1	-3.46E-01	7.25E-76	CKS2	-4.14E-01	1.56E-29	HSP90AA1	-5.64E-01	8.83E-84			
PPA1	-3.46E-01	4.46E-56	MT-ND5	-4.15E-01	4.35E-76	LDHB	-5.67E-01	1.64E-138			
NAA38	-3.50E-01	9.15E-55	TMSB4X	-4.17E-01	5.71E-83	CKS1B	-5.90E-01	1.71E-136			
PGAM1	-3.52E-01	9.50E-80	HNRNPK	-4.21E-01	3.53E-68	MIF	-5.97E-01	4.61E-106			
SLBP	-3.52E-01	1.97E-71	ARPC2	-4.21E-01	2.06E-54	SNRPD1	-5.99E-01	1.92E-102			
ABRACL	-3.53E-01	5.84E-61	CDK4	-4.22E-01	1.42E-81	PKM	-6.09E-01	2.35E-111			
PRDX4	-3.54E-01	1.91E-76	TMEM230	-4.23E-01	7.46E-65	CFL1	-6.13E-01	5.58E-120			
ACTB	-3.55E-01	1.04E-55	TMA7	-4.26E-01	7.71E-64	SRP9	-6.13E-01	9.14E-118			

D. Lists of differentially expressed genes (FDR < 0.05) when comparing young donor platelet -biased HSCs versus young donor multilineage output HSCs defined in the integrative analysis. Base of the log is Euler's number

D1- upregulated in young donor platelet-biased HSCs

Gene	logFC	FDR	Gene	logFC	FDR	Gene	logFC	FDR
A1BG	4.53E-02	1.69E-05	ADAL	1.84E-03	2.53E-02	AMPD2	4.62E-02	1.92E-05
AAED1	8.13E-02	9.07E-07	ADAM28	1.94E-01	4.05E-34	AMZ2	3.72E-02	5.07E-07
AAK1	1.37E-02	7.22E-04	ADAM8	1.13E-01	4.60E-28	ANAPC10	2.97E-03	1.69E-04
AAMDC	2.74E-02	3.11E-08	ADAR	2.73E-02	1.47E-07	ANAPC16	1.00E-01	1.39E-06
AASDHPPT	9.08E-03	1.29E-02	ADAT2	1.35E-02	2.72E-05	ANGEL2	8.35E-03	3.42E-04
ABCB1	5.08E-02	5.60E-06	ADD1	2.08E-02	1.47E-05	ANGPT1	6.21E-02	2.28E-09
ABCB7	2.95E-02	2.32E-09	ADD3	5.81E-03	6.52E-06	ANKRA2	1.05E-02	1.50E-04
ABCD4	7.13E-03	1.17E-04	ADGRE5	2.73E-02	5.65E-05	ANKRD12	1.57E-01	2.94E-16
ABCG1	2.49E-02	3.61E-06	ADGRG1	2.55E-02	7.37E-04	ANKRD13D	1.92E-02	2.02E-03
ABHD10	2.26E-02	5.85E-05	ADGRG6	7.76E-02	1.79E-09	ANKRD28	2.34E-01	1.99E-20
ABHD13	1.26E-02	1.02E-02	ADH5	6.50E-02	1.55E-06	ANKRD49	3.76E-02	6.80E-06
ABHD14B	2.06E-01	5.75E-21	ADPRHL2	1.81E-02	1.03E-07	ANKRD54	9.03E-03	1.17E-02
ABHD17A	1.39E-02	4.69E-04	ADPRM	7.61E-02	7.00E-19	ANTXR2	2.31E-02	2.26E-07
ABI1	2.92E-02	8.34E-04	AES	1.26E-03	3.07E-06	ANXA1	2.82E-01	5.34E-24
ABLIM1	3.96E-02	6.18E-05	AFF3	3.28E-02	5.40E-07	ANXA4	4.32E-02	5.61E-11
ABRAXAS1	1.12E-01	1.20E-14	AFF4	4.12E-02	1.67E-06	ANXA6	9.93E-02	1.95E-09
ABT1	3.71E-03	6.82E-03	AFTPH	3.23E-02	4.50E-09	ANXA7	1.53E-01	1.22E-14
ABTB1	4.85E-02	2.32E-10	AGAP2	1.55E-02	9.51E-04	AP000547.3	2.29E-03	2.61E-02
AC004130.1	2.83E-02	2.95E-03	AHNAK	7.63E-02	4.94E-13	AP002387.2	5.23E-02	3.72E-09
AC004540.2	2.99E-02	1.88E-05	AHR	3.09E-02	1.34E-08	AP002748.3	1.30E-02	1.79E-03
AC004687.1	1.18E-02	7.62E-07	AIF1	5.38E-02	3.82E-03	AP1G2	2.99E-02	1.34E-05
AC004865.2	5.63E-02	4.54E-09	AIMP1	6.63E-02	1.41E-07	AP2A2	4.69E-02	2.43E-07
AC008124.1	4.31E-02	9.64E-07	AIP	1.76E-02	1.43E-02	AP3M2	5.02E-02	5.67E-07
AC011139.1	2.01E-01	7.38E-51	AJ009632.2	2.14E-01	2.12E-34	APBB1IP	1.92E-02	8.42E-03
AC020910.4	6.50E-03	3.42E-05	AKAP13	5.09E-02	1.22E-06	APEH	1.33E-02	1.96E-02
AC020916.1	8.29E-02	6.65E-06	AKAP17A	2.76E-02	1.85E-07	APLP2	9.99E-02	1.22E-06
AC025159.1	1.84E-03	1.57E-04	AKAP7	7.40E-03	3.51E-02	APMAP	3.08E-02	1.41E-04
AC026369.3	1.14E-01	3.57E-14	AKAP8	1.95E-02	9.50E-06	APOBEC3G	4.70E-02	1.07E-07
AC090204.1	5.16E-02	2.35E-07	AKAP8L	3.83E-02	9.78E-06	APOL3	3.76E-02	1.42E-06
AC092171.3	9.84E-03	1.53E-06	AKAP9	6.38E-02	1.16E-04	APP	8.57E-02	4.81E-08
AC093673.1	3.91E-02	7.22E-07	AKIRIN1	5.61E-03	5.38E-06	APPBP2	1.40E-02	2.65E-05
AC097376.2	1.09E-02	8.04E-10	AKIRIN2	8.42E-02	1.11E-12	APRT	1.04E-01	4.85E-06
AC100810.1	2.67E-02	4.13E-05	AKNA	2.06E-02	4.02E-06	AREG	4.28E-01	5.11E-47
AC103591.3	1.89E-01	9.29E-11	AKR1C3	1.53E-01	4.65E-17	ARF1	3.08E-02	7.90E-03
AC114760.2	9.70E-02	4.16E-06	AKT1S1	1.30E-02	6.00E-04	ARF4	3.11E-02	3.50E-08
AC245297.3	1.05E-01	7.70E-13	AL031777.3	1.07E-01	8.63E-25	ARFGAP2	3.12E-02	1.15E-04
ACAA1	3.07E-02	2.74E-04	AL118516.1	4.09E-02	1.71E-06	ARFGAP3	1.01E-02	1.31E-08
ACADS	4.85E-03	1.40E-08	AL121944.1	6.30E-02	7.55E-08	ARFRP1	4.52E-03	1.53E-02
ACAP1	1.67E-01	8.22E-18	AL391069.3	6.59E-03	8.86E-06	ARHGAP15	1.57E-01	1.04E-22
ACOT11	2.18E-02	1.26E-05	AL590226.1	1.33E-02	1.70E-02	ARHGAP22	2.54E-02	7.43E-06
ACOT13	9.99E-04	2.15E-02	AL592183.1	1.25E-02	6.62E-03	ARHGAP25	3.26E-02	7.60E-05
ACSL1	2.58E-02	9.47E-06	AL662844.4	6.07E-02	2.17E-12	ARHGAP30	3.68E-02	2.75E-05
ACSM3	2.29E-01	1.12E-47	ALDH1A1	3.14E-01	1.30E-42	ARHGAP45	3.70E-02	1.40E-05
ACSS1	2.24E-02	1.05E-05	ALDH2	2.97E-02	1.77E-04	ARHGAP5	4.64E-02	3.97E-06
ACTG1	1.02E-01	1.00E-09	ALDH9A1	2.99E-03	6.54E-06	ARHGAP9	2.28E-02	1.54E-03
ACTR10	6.29E-03	3.55E-05	ALG13	9.77E-02	8.19E-13	ARHGDIB	7.01E-02	9.52E-06
ACTR1A	2.85E-02	2.41E-03	ALKBH3	6.87E-03	2.01E-03	ARHGEF1	3.76E-02	1.67E-03
ACTR1B	1.68E-02	8.45E-07	ALKBH5	1.30E-02	4.52E-08	ARHGEF2	6.11E-02	4.27E-09
ACTR6	6.64E-03	3.04E-04	ALKBH7	1.84E-01	2.48E-20	ARHGEF40	1.56E-02	1.60E-07
ACYP2	7.82E-03	1.03E-04	AMD1	1.13E-02	1.68E-02	ARID2	2.94E-03	2.23E-03

Gene	logFC	FDR	Gene	logFC	FDR	Gene	logFC	FDR
ARID5A	3.49E-02	4.86E-04	AVP	2.96E-01	1.15E-34	BTG1	1.78E-01	2.84E-13
ARID5B	5.66E-02	3.87E-11	AZI2	3.07E-03	5.17E-04	BTG2	8.70E-02	4.48E-06
ARL1	2.78E-03	7.30E-05	B2M	3.46E-02	2.98E-03	BTK	2.29E-02	2.80E-02
ARL14EP	7.04E-02	5.84E-11	B3GNT2	2.79E-02	1.22E-03	BTN3A2	5.24E-02	8.04E-07
ARL2BP	4.10E-02	1.03E-04	B3GNT5	4.08E-02	1.20E-06	BUD23	1.60E-02	3.21E-10
ARL4A	1.33E-01	3.90E-09	B4GALT3	2.38E-03	1.16E-07	C11orf1	3.33E-02	1.09E-05
ARL6IP5	7.82E-02	8.83E-07	BAALC	8.08E-03	4.62E-07	C11orf21	6.24E-02	2.01E-12
ARMCX1	1.26E-01	1.20E-18	BABAM2	5.24E-02	5.86E-07	C11orf54	9.78E-03	1.18E-06
ARMCX3	8.25E-02	7.91E-09	BAG2	2.49E-03	5.51E-09	C11orf71	2.36E-02	1.56E-05
ARMCX6	2.09E-03	8.25E-04	BAG5	2.23E-02	8.29E-04	C11orf74	4.77E-02	5.44E-07
ARRB1	3.62E-02	3.93E-07	BAK1	8.98E-05	2.04E-05	C12orf10	7.44E-02	4.18E-08
ARRDC2	6.62E-02	1.87E-10	BANP	1.68E-02	3.28E-06	C12orf76	3.32E-02	9.80E-08
ARRDC3	1.39E-01	1.84E-11	BAZ2A	6.47E-02	9.89E-07	C15orf39	1.80E-02	7.68E-04
ARRDC4	3.32E-02	1.01E-03	BAZ2B	5.90E-02	5.33E-08	C16orf45	3.52E-02	3.08E-05
ARSD	3.35E-02	2.85E-05	BBIP1	4.08E-03	2.15E-06	C16orf72	1.51E-02	1.70E-03
ASAH1	1.96E-01	8.82E-21	BBX	4.67E-02	1.86E-05	C16orf87	1.51E-02	7.39E-03
ASB8	4.36E-02	2.81E-07	BCAS2	9.33E-02	6.45E-08	C18orf21	7.02E-03	3.62E-03
ASB9	2.34E-03	5.46E-04	BCAT1	2.12E-02	6.79E-06	C19orf38	4.68E-02	1.00E-08
ASCC2	4.44E-03	2.60E-06	BCKDHB	8.94E-03	1.48E-02	C19orf66	4.58E-02	6.01E-07
ASF1A	1.60E-02	4.74E-05	BCL2A1	5.92E-02	2.67E-12	C1orf122	5.87E-03	4.77E-04
ASNSD1	1.62E-02	3.87E-03	BCL2L1	2.66E-02	5.87E-04	C1orf123	9.50E-04	2.09E-03
ASPSCR1	2.08E-02	1.06E-03	BCL2L13	6.61E-03	1.76E-06	C1orf162	8.88E-02	5.16E-10
ATAD1	6.12E-03	3.18E-02	BDH2	1.43E-02	7.74E-06	C1orf21	2.88E-02	1.90E-04
ATF2	2.28E-03	1.22E-02	BECN1	1.36E-03	1.26E-04	C1orf216	2.56E-02	4.45E-04
ATF3	2.93E-02	3.08E-03	BEX2	1.66E-01	2.43E-12	C20orf96	1.09E-02	7.84E-05
ATF4	2.05E-02	3.66E-05	BEX4	1.49E-01	2.61E-12	C2orf49	5.48E-03	4.79E-02
ATF6	1.74E-02	2.16E-08	BEX5	1.36E-01	3.07E-18	C2orf69	4.15E-02	6.65E-06
ATF6B	6.39E-02	7.92E-05	BFAR	2.44E-02	4.30E-05	C2orf74	1.62E-02	2.85E-04
ATF7IP2	2.35E-01	4.28E-23	BIN1	2.21E-02	1.04E-02	C2orf76	2.19E-02	8.02E-04
ATG101	4.92E-02	1.96E-09	BIN2	1.06E-01	1.20E-09	C4orf3	4.12E-02	3.45E-03
ATG16L2	4.35E-02	4.84E-05	BIRC2	6.68E-02	1.84E-10	C5orf15	2.64E-03	5.60E-06
ATG4B	9.15E-03	1.67E-05	BIRC3	1.12E-01	4.29E-18	C6orf48	3.76E-01	3.38E-86
ATG4C	2.04E-02	3.78E-05	BISPR	4.64E-02	1.18E-08	C7orf50	7.18E-03	4.69E-04
ATM	1.57E-02	8.03E-03	BIVM	1.95E-03	1.17E-04	C8orf59	1.90E-01	1.85E-15
ATP2B1-AS1	2.20E-02	1.94E-05	BLCAP	1.69E-02	4.33E-04	C9orf43	8.73E-02	1.96E-12
ATP2B4	2.09E-02	3.59E-04	BLOC1S4	6.99E-02	1.67E-13	C9orf72	2.94E-02	3.90E-05
ATP2C1	3.83E-02	1.47E-03	BLVRA	2.40E-02	7.36E-06	CA5B	4.63E-02	2.16E-05
ATP6AP1	4.63E-02	8.60E-07	BMI1	1.79E-02	1.20E-04	CABIN1	4.83E-02	5.25E-08
ATP6V0A1	7.03E-02	5.11E-15	BNIP2	1.02E-01	6.90E-10	CACNA1C-AS	1.97E-02	2.14E-02
ATP6V1A	4.34E-02	2.37E-07	BNIP3	4.68E-02	6.93E-06	CACUL1	2.06E-02	4.79E-04
ATP6V1E1	1.58E-02	5.12E-06	BNIP3L	1.02E-01	1.64E-06	CALCOCO1	6.62E-02	3.07E-19
ATP6V1F	1.41E-02	1.07E-06	BORCS7	3.06E-02	5.76E-03	CALCOCO2	5.94E-02	4.53E-12
ATP8B4	3.71E-02	6.92E-05	BPTF	8.61E-03	4.62E-03	CALHM6	4.49E-02	1.11E-06
ATRAID	3.11E-02	7.18E-07	BRI3	1.29E-02	2.63E-03	CALN1	2.92E-02	1.28E-04
ATRX	3.99E-02	4.02E-05	BRMS1	2.74E-02	1.43E-07	CAMK1D	1.62E-02	4.67E-02
ATXN1	3.05E-02	9.89E-07	BRWD1	3.14E-02	1.10E-07	CAMK2G	2.42E-02	5.63E-07
ATXN2	5.79E-03	5.70E-05	BSDC1	1.12E-02	7.79E-04	CAMLG	1.74E-01	2.82E-13
ATXN3	1.36E-02	2.90E-04	BSPRY	2.75E-02	2.06E-03	CANX	2.05E-02	1.38E-09
ATXN7L3B	3.77E-03	3.26E-03	BST2	3.93E-01	6.02E-89	CAP1	2.29E-02	1.39E-06
AUP1	2.26E-02	5.08E-08	BTF3	3.84E-02	2.84E-04	CAPN1	4.68E-02	1.27E-06

Gene	logFC	FDR	Gene	logFC	FDR	Gene	logFC	FDR
CAPN2	4.37E-02	1.17E-07	CCT3	1.76E-02	9.47E-10	CFAP36	3.76E-02	6.28E-07
CAPN7	6.17E-02	2.48E-13	CCT8	3.12E-02	1.70E-04	CFH	9.90E-02	8.60E-17
CAPZA2	8.68E-02	1.77E-06	CD109	3.00E-02	1.09E-04	CFLAR	5.90E-02	1.20E-08
CAPZB	3.52E-03	6.20E-05	CD151	9.23E-02	8.89E-12	CFP	9.87E-03	1.66E-04
CARD16	2.87E-02	6.49E-03	CD164	1.94E-01	7.91E-27	CGGBP1	4.36E-02	1.24E-07
CARD19	1.53E-01	5.37E-18	CD244	4.61E-02	2.24E-09	CGRRF1	6.45E-02	2.32E-12
CARD8	1.03E-01	1.87E-14	CD300A	4.10E-02	1.90E-04	CHCHD5	3.58E-02	6.83E-04
CASC4	2.35E-02	1.68E-05	CD300LF	2.26E-02	1.58E-03	CHCHD7	5.10E-03	3.43E-06
CASP1	2.04E-02	9.79E-08	CD302	4.45E-02	4.08E-06	CHD2	3.09E-02	8.59E-06
CASP10	5.15E-03	3.10E-02	CD34	5.15E-02	3.77E-05	CHD6	9.38E-03	1.09E-02
CASP4	1.24E-01	4.77E-09	CD37	5.58E-01	1.39E-179	CHD9	8.73E-02	3.39E-07
CAST	8.74E-02	2.76E-08	CD44	4.58E-01	2.91E-85	CHIC2	3.24E-02	3.02E-11
CAT	2.78E-02	1.79E-03	CD46	9.45E-02	1.73E-09	CHMP1B	2.72E-01	9.12E-31
CAVIN1	4.89E-02	3.27E-05	CD48	7.01E-03	5.25E-03	CHMP2A	1.84E-02	1.35E-02
CAVIN2	1.88E-01	2.23E-15	CD52	2.33E-01	1.50E-24	CHMP2B	2.66E-02	5.14E-05
CBFA2T3	2.93E-02	4.78E-04	CD53	2.21E-01	1.59E-25	CHMP3	5.73E-02	2.65E-04
CBLL1	1.53E-02	8.89E-04	CD55	5.33E-02	2.20E-06	CHMP4A	1.43E-02	1.02E-06
CBR4	3.83E-02	8.05E-08	CD58	1.68E-02	3.59E-04	CHMP5	4.39E-02	1.19E-09
CCDC107	1.90E-02	2.19E-05	CD63	1.67E-02	3.05E-08	CHMP6	1.60E-02	2.70E-04
CCDC115	4.34E-02	2.79E-08	CD74	5.69E-01	1.90E-213	CHP1	6.11E-03	9.17E-03
CCDC12	5.75E-03	1.38E-04	CD79B	4.43E-02	7.56E-05	CHPF2	7.87E-02	1.07E-12
CCDC152	1.86E-02	8.41E-05	CD82	1.35E-01	1.60E-14	CHPT1	1.66E-02	7.28E-04
CCDC159	5.75E-02	1.09E-12	CD83	8.04E-02	3.27E-09	CHRM3	1.36E-02	8.52E-06
CCDC171	1.58E-02	3.89E-05	CD9	2.14E-02	6.41E-04	CHST11	1.46E-02	2.85E-04
CCDC174	2.11E-02	5.03E-03	CDADC1	3.67E-02	3.51E-08	CHST12	5.65E-02	2.64E-06
CCDC186	4.53E-02	1.81E-06	CDC16	1.58E-02	1.63E-08	CHST13	9.66E-02	1.01E-19
CCDC22	1.10E-02	4.60E-05	CDC26	4.75E-03	2.71E-04	CHTOP	2.66E-02	1.33E-04
CCDC28A	2.03E-03	3.83E-05	CDC27	5.04E-03	2.38E-05	CHURC1	1.65E-01	9.96E-15
CCDC32	2.52E-02	2.51E-04	CDC40	2.28E-02	3.52E-08	CIITA	5.86E-02	2.32E-11
CCDC57	1.18E-02	1.76E-05	CDC42BPA	2.58E-02	7.87E-04	CIR1	1.21E-01	5.57E-15
CCDC59	1.11E-01	1.96E-10	CDC42SE2	3.57E-02	2.08E-04	CIRBP	2.16E-01	9.26E-54
CCDC6	1.16E-03	3.98E-04	CDC73	2.25E-02	1.33E-04	CITED2	1.17E-01	1.95E-08
CCDC69	5.39E-02	2.15E-11	CDH7	1.05E-01	2.91E-23	CIZ1	6.05E-03	8.60E-03
CCDC88C	1.52E-02	1.25E-03	CDIP1	1.49E-02	7.42E-06	CLCN7	1.72E-02	3.56E-05
CCDC90B	3.92E-02	4.30E-08	CDIPT	2.17E-02	5.13E-09	CLDN15	5.76E-02	7.96E-12
CCDC91	2.27E-03	9.60E-05	CDK10	3.93E-03	2.78E-03	CLDND1	1.93E-02	8.55E-06
CCDC97	2.85E-02	2.21E-07	CDK11A	1.13E-02	1.13E-06	CLEC2B	1.45E-01	6.73E-12
CCL28	1.99E-02	3.29E-07	CDK17	1.92E-02	1.12E-04	CLEC2D	2.65E-02	1.76E-05
CCM2	1.76E-02	3.95E-05	CDS2	1.62E-02	1.02E-02	CLEC9A	9.01E-02	1.01E-15
CCND2	1.56E-02	7.08E-04	CEBPB	1.05E-01	7.54E-12	CLIC1	9.01E-02	7.89E-06
CCND3	1.59E-01	1.56E-22	CEBPZOS	4.45E-02	1.49E-08	CLIC2	8.01E-02	5.59E-20
CCNDBP1	1.72E-01	7.20E-22	CELF2	2.68E-02	3.54E-02	CLINT1	3.70E-02	1.69E-05
CCNG1	8.97E-02	6.57E-05	CENPC	2.78E-02	3.11E-05	CLIP1	7.04E-03	3.35E-02
CCNH	1.48E-01	4.80E-17	CEP68	4.71E-02	2.51E-06	CLK1	3.00E-02	1.00E-04
CCNI	7.87E-02	2.09E-07	CEP70	2.62E-02	2.38E-07	CLK3	1.63E-02	4.41E-03
CCNL2	3.89E-02	2.84E-08	CEP95	5.34E-03	6.63E-06	CLK4	3.70E-02	4.00E-07
CCNT1	1.54E-03	4.96E-03	CEPT1	4.02E-04	2.64E-03	CLN5	3.16E-02	4.86E-05
CCPG1	6.16E-02	4.98E-09	CERS5	3.89E-03	7.64E-03	CLN8	2.23E-02	7.36E-04
CCS	6.55E-02	2.20E-11	CES2	6.07E-03	2.67E-02	CLSTN1	6.38E-03	2.48E-07
CCSER2	6.01E-02	1.50E-10	CFAP20	4.45E-02	6.12E-03	CLU	3.52E-01	4.54E-48

Gene	logFC	FDR	Gene	logFC	FDR	Gene	logFC	FDR
CMBL	6.40E-02	1.32E-08	CRYZL1	9.25E-02	3.44E-16	DCAF11	2.79E-02	1.28E-05
CMPK1	4.07E-02	2.42E-08	CSF3R	8.55E-02	8.13E-07	DCAF6	7.74E-03	3.05E-04
CMTM6	6.49E-03	1.03E-12	CSGALNACT2	2.96E-02	7.90E-04	DCAF8	4.15E-02	1.57E-06
CNBD2	3.27E-03	2.80E-02	CSNK1D	4.16E-02	5.29E-07	DCP1A	3.30E-02	7.44E-06
CNIH1	2.05E-02	3.95E-07	CSNK1E	1.99E-02	4.35E-02	DCP2	4.15E-03	2.37E-04
CNOT3	2.37E-02	1.30E-03	CSNK1G3	2.80E-03	3.20E-06	DCTN2	3.39E-02	3.06E-07
CNOT4	1.85E-02	4.52E-07	CSRNP1	1.48E-01	5.68E-21	DCTN3	1.96E-02	3.30E-07
CNST	8.58E-02	3.13E-14	CST3	2.46E-01	7.98E-24	DCTN4	1.08E-02	5.33E-04
COA5	7.96E-03	1.82E-06	CSTF2T	3.13E-02	1.01E-04	DCTN6	2.54E-03	5.28E-04
COASY	8.99E-03	1.30E-03	CTBS	3.70E-02	1.22E-07	DDAH2	1.08E-01	7.76E-06
COG3	4.48E-02	4.95E-09	CTDSP1	9.41E-03	2.28E-06	DDHD1	5.07E-03	2.04E-02
COL4A3BP	2.49E-02	1.67E-08	CTDSP2	5.61E-02	4.22E-10	DDHD2	7.40E-03	5.37E-06
COMMD10	1.99E-02	4.54E-05	CTDSPL	1.38E-02	3.49E-04	DDIT3	7.48E-02	1.53E-08
COMMD2	3.38E-02	4.50E-04	CTNNA1	3.46E-02	7.33E-08	DDRGK1	1.72E-02	3.30E-08
COMMD6	2.71E-01	5.85E-62	CTNNBL1	2.24E-03	3.57E-07	DDX10	3.18E-03	5.65E-05
COMMD8	4.65E-03	1.52E-02	CTR9	1.93E-02	5.36E-04	DDX17	1.34E-01	6.32E-10
COMT	2.54E-02	8.28E-08	CTSD	1.77E-01	2.66E-16	DDX24	5.79E-02	3.61E-07
COPA	2.76E-02	3.71E-09	CTSF	1.79E-01	3.51E-38	DDX28	2.15E-03	5.47E-06
COPB1	1.69E-02	1.39E-06	CTSO	4.61E-02	1.63E-08	DDX3X	1.48E-01	3.02E-12
COPB2	1.90E-03	2.46E-07	CTSS	2.12E-01	5.40E-28	DDX3Y	8.84E-02	1.41E-11
COPG2	5.15E-04	8.01E-08	CTSW	4.23E-02	9.65E-04	DDX5	2.37E-01	2.99E-48
COPS2	4.72E-02	3.56E-06	CUL4A	6.54E-03	5.89E-09	DEDD2	2.70E-02	1.10E-07
COPS7A	1.96E-02	5.32E-06	CUTC	3.94E-02	7.79E-07	DEF6	3.33E-02	2.35E-07
COPZ1	1.87E-02	6.63E-05	CWC22	7.46E-03	3.18E-02	DEGS1	2.04E-02	2.98E-08
COQ10B	9.39E-02	2.76E-08	CWF19L2	6.73E-02	4.68E-11	DELE1	3.24E-02	7.57E-05
COQ5	1.73E-02	5.32E-04	CXCL2	1.03E-01	2.89E-10	DENND1B	6.30E-03	4.54E-04
COQ8A	1.89E-02	1.30E-02	CXCL3	1.61E-01	4.61E-10	DENND5A	7.74E-04	2.78E-04
CORO1B	3.86E-02	2.13E-04	CXCL8	2.00E-01	9.68E-14	DEPTOR	3.18E-02	2.25E-05
COX11	3.57E-02	3.39E-10	CXCR4	8.85E-02	6.23E-03	DERL1	1.74E-02	7.96E-06
COX19	1.56E-02	8.31E-06	CYB561	2.45E-02	4.62E-05	DERL2	2.27E-03	4.26E-09
COX7A2L	5.53E-02	3.04E-02	CYB5D2	1.98E-02	3.41E-06	DGKZ	4.35E-02	1.80E-05
COX7C	5.55E-02	4.77E-04	CYB5R1	3.51E-02	1.56E-03	DGLUCY	8.26E-03	1.24E-04
CPED1	6.85E-02	1.60E-17	CYBRD1	4.14E-02	9.02E-08	DHPS	1.07E-04	4.13E-04
CPNE3	6.54E-02	1.11E-11	CYFIP1	3.03E-02	7.56E-06	DHRS4L2	2.68E-02	1.40E-03
CPPED1	9.99E-03	4.30E-04	CYHR1	3.23E-02	2.73E-05	DHRS7	8.20E-02	1.16E-07
CPQ	5.12E-02	4.48E-08	CYLD	4.97E-02	2.07E-07	DHRSX	2.00E-02	1.39E-04
CRBN	1.58E-01	2.96E-17	CYSLTR1	1.36E-01	2.32E-22	DICER1	5.15E-03	2.47E-08
CREB1	4.13E-02	2.55E-07	CYTH1	1.96E-02	5.41E-05	DIDO1	1.04E-02	3.42E-05
CREB3	1.61E-02	5.05E-04	CYTH2	2.75E-02	1.64E-07	DIMT1	3.68E-02	4.72E-06
CREB3L4	2.20E-02	5.93E-03	CYTIP	2.53E-02	9.19E-03	DIP2A	3.70E-02	7.97E-08
CREBBP	5.56E-03	1.37E-04	CYTL1	1.49E-01	1.37E-08	DLK1	7.06E-02	1.22E-09
CREBRF	7.70E-02	3.06E-12	CYTOR	4.13E-02	1.87E-05	DMAP1	2.78E-02	5.02E-05
CREG1	8.65E-02	3.41E-06	CYYR1	1.62E-02	1.51E-02	DMXL1	1.70E-02	1.06E-03
CRELD1	5.84E-02	9.28E-15	DAB2	3.82E-02	1.54E-06	DNAAF2	1.71E-02	2.93E-06
CREM	1.38E-02	2.00E-03	DALRD3	6.12E-02	8.08E-11	DNAJB1	2.50E-02	2.81E-03
CRHBP	5.39E-01	3.00E-99	DAP3	1.14E-02	7.28E-04	DNAJB12	1.43E-02	1.22E-05
CRLF3	1.26E-02	1.78E-05	DAPK1	1.33E-02	8.25E-03	DNAJB14	4.55E-02	6.13E-05
CRTC3	3.95E-03	6.68E-05	DAPK3	1.71E-02	1.70E-08	DNAJB6	1.16E-01	7.35E-06
CRYGD	7.83E-02	1.90E-08	DARS	2.39E-02	1.36E-04	DNAJB9	1.05E-01	6.39E-15
CRYL1	6.09E-02	7.03E-08	DAZAP2	1.76E-01	3.37E-15	DNAJC10	4.09E-03	2.20E-05

Gene	logFC	FDR	Gene	logFC	FDR	Gene	logFC	FDR
DNAJC30	4.28E-02	3.66E-09	EGFL7	6.12E-02	3.05E-02	EREG	8.02E-02	5.60E-05
DNAJC4	2.56E-01	2.32E-43	EHD2	1.72E-02	1.40E-02	ERG	4.20E-02	1.68E-04
DNASE1L1	3.62E-02	8.69E-07	EHMT1	8.35E-03	1.22E-05	ERGIC1	1.60E-02	2.20E-05
DNASE2	3.13E-02	9.25E-04	EHMT2	1.30E-02	7.02E-04	ERICH1	1.26E-01	3.51E-13
DNTTIP1	5.80E-03	1.25E-06	EID1	1.27E-01	4.37E-09	ERLEC1	1.45E-02	5.53E-04
DNTTIP2	2.44E-02	4.26E-05	EIF1	3.43E-01	6.98E-218	ERO1B	4.67E-02	8.69E-10
DOCK8	4.49E-02	7.43E-08	EIF1B	1.19E-01	2.63E-10	ERP44	3.48E-02	6.83E-10
DPF2	2.24E-02	2.73E-05	EIF2A	2.16E-01	4.08E-24	ESCO1	9.77E-03	2.80E-06
DPH3	2.41E-03	1.64E-06	EIF2B1	1.99E-02	3.98E-05	ESD	1.22E-01	6.19E-07
DPH5	5.87E-02	2.22E-07	EIF2B4	8.75E-03	4.12E-06	ESYT1	6.47E-03	2.25E-07
DPM1	1.85E-03	1.53E-11	EIF2D	5.15E-02	3.24E-05	ETFDH	1.90E-02	6.03E-04
DPPA4	2.25E-02	1.36E-08	EIF3D	2.98E-01	1.56E-45	ETFRF1	1.56E-01	4.88E-25
DRAM1	2.72E-02	1.44E-02	EIF3E	3.38E-01	1.66E-156	ETHE1	3.75E-02	2.52E-04
DRAM2	4.79E-02	8.82E-08	EIF3F	8.11E-02	1.92E-04	ETS2	1.00E-01	1.95E-09
DST	9.31E-02	6.47E-14	EIF3G	1.78E-01	8.78E-14	ETV3	3.80E-02	1.70E-06
DSTYK	2.21E-02	1.69E-02	EIF3H	1.29E-01	1.92E-11	EVA1B	5.93E-02	1.57E-10
DTD1	7.96E-03	2.43E-06	EIF3J-DT	5.31E-02	7.09E-08	EVI2A	7.17E-02	8.38E-14
DTWD1	1.64E-02	3.20E-07	EIF3K	3.42E-02	2.19E-02	EVI2B	3.54E-01	3.30E-67
DTX3	1.71E-02	3.56E-04	EIF3M	1.29E-01	3.28E-07	EVL	8.89E-02	3.40E-08
DUSP1	3.24E-01	4.81E-34	EIF4A1	5.82E-02	4.68E-04	EXOC1	3.83E-02	1.69E-06
DUSP11	5.41E-02	4.18E-08	EIF4A2	4.35E-01	4.01E-122	EXOC4	1.56E-02	4.48E-06
DUSP2	6.02E-02	2.35E-05	EIF4G3	2.41E-02	1.09E-05	EXOC7	8.93E-02	7.11E-10
DUSP22	6.78E-02	2.34E-11	EIF4H	3.52E-03	1.08E-07	EXOSC7	4.31E-03	1.44E-02
DUSP3	2.68E-02	2.47E-05	ELF1	1.44E-01	8.98E-09	F11R	3.37E-02	3.09E-06
DUSP6	4.43E-02	2.43E-03	ELK3	5.14E-02	1.34E-07	F2R	2.71E-02	1.47E-05
DXO	5.53E-03	2.37E-04	ELK4	1.25E-02	2.17E-04	FAHD2A	3.55E-03	4.53E-09
DYM	1.85E-02	2.77E-03	ELMO1	2.07E-01	3.37E-24	FAIM	3.43E-03	6.19E-05
DYNC1I2	8.50E-02	4.09E-10	ELOA	1.10E-02	6.31E-07	FAM104A	1.45E-03	6.60E-06
DYNC1LI1	6.95E-03	3.10E-09	ELP2	8.75E-02	1.71E-09	FAM118A	3.19E-02	6.82E-11
DYNC1LI2	2.77E-02	3.65E-05	EMB	1.81E-02	3.60E-03	FAM124B	2.59E-02	1.79E-03
DYNLL2	1.33E-02	1.45E-03	EMC3	2.78E-02	6.48E-07	FAM126B	1.14E-02	8.96E-05
DYNLRB1	3.87E-02	6.75E-07	EMC7	1.63E-02	7.29E-07	FAM162A	2.30E-02	2.80E-07
DYNLT1	1.76E-02	9.27E-06	EMCN	8.83E-02	6.33E-17	FAM172A	5.19E-03	5.12E-03
DYNLT3	5.28E-02	1.10E-07	EMG1	4.94E-03	2.74E-07	FAM177A1	5.94E-02	1.27E-07
DYRK4	1.29E-02	3.39E-03	EMID1	9.74E-03	3.49E-06	FAM19A2	6.25E-02	3.53E-11
DZIP3	3.15E-02	6.26E-07	EML3	2.83E-02	1.07E-04	FAM200B	4.33E-02	2.15E-05
EAF2	6.65E-02	1.95E-05	EMP1	8.46E-02	9.44E-10	FAM215B	1.96E-02	2.83E-02
EAPP	8.99E-02	1.16E-06	EMP3	1.65E-01	1.22E-13	FAM219B	5.46E-02	9.67E-09
EBAG9	5.36E-03	1.04E-03	ENDOV	9.54E-03	2.00E-03	FAM228B	3.97E-02	2.69E-07
EBLN3P	6.87E-02	7.81E-10	ENG	3.66E-02	8.23E-05	FAM234A	2.86E-03	2.61E-06
EBPL	5.75E-02	3.50E-02	ENPP4	3.20E-02	1.73E-06	FAM30A	1.75E-01	7.75E-14
ECSIT	2.52E-02	3.22E-03	ENTPD6	3.53E-02	4.52E-08	FAM3C	3.11E-02	1.14E-06
EDEM2	2.09E-02	1.01E-03	EPB41L4A-A	3.44E-01	5.13E-55	FAM53C	4.16E-02	2.91E-03
EDF1	1.22E-02	6.87E-03	EPC1	1.10E-01	6.67E-07	FAM96B	1.33E-02	1.72E-07
EEF1AKMT2	1.08E-02	5.34E-05	EPHA1-AS1	7.29E-02	3.86E-12	FAR2	7.76E-03	1.75E-04
EEF1D	4.06E-02	4.41E-03	EPM2AIP1	9.41E-03	1.24E-03	FAU	1.53E-01	1.70E-62
EEF1G	1.66E-02	4.04E-04	EPRS	1.53E-04	1.38E-09	FBXL12	1.90E-02	1.26E-06
EEF2	1.78E-01	1.36E-71	EPS15	3.99E-02	2.24E-07	FBXL15	5.22E-02	2.10E-08
EFCAB14	3.41E-03	1.63E-02	EPSTI1	3.82E-03	4.18E-02	FBXL20	9.03E-04	4.08E-07
EFHC1	3.19E-02	3.85E-05	ERCC1	1.45E-02	1.30E-02	FBXL3	2.67E-02	9.79E-07

Gene	logFC	FDR	Gene	logFC	FDR	Gene	logFC	FDR
FBXL5	6.38E-02	1.06E-07	FTX	9.66E-02	8.27E-12	GNPTAB	2.26E-02	3.94E-02
FBXO25	2.62E-02	1.15E-05	FXR1	5.10E-02	6.14E-05	GOLGA2	3.46E-02	8.77E-07
FBXO3	5.56E-02	8.60E-10	FXYD5	3.49E-01	3.15E-100	GOLGA8B	1.59E-02	3.07E-02
FBXO33	1.16E-02	6.63E-03	FXYD6	3.47E-03	1.52E-15	GOLGB1	1.87E-02	8.27E-03
FBXO34	1.36E-03	7.86E-06	G3BP2	1.39E-02	7.12E-05	GON4L	8.80E-03	3.23E-03
FBXO7	3.74E-02	1.05E-06	G6PD	3.83E-02	5.35E-04	GOPC	1.21E-02	7.55E-05
FBXW11	2.02E-02	6.93E-04	GABARAP	2.92E-02	5.78E-08	GOSR1	2.33E-02	5.02E-05
FBXW9	2.42E-02	6.92E-05	GABARAPL1	6.85E-02	5.28E-17	GOSR2	4.88E-03	5.95E-03
FCER1A	5.19E-02	2.90E-11	GABARAPL2	2.06E-01	4.42E-22	GPAT3	5.52E-02	1.99E-06
FCGRT	7.46E-02	3.93E-07	GABPB1-AS1	1.86E-01	1.16E-17	GPATCH8	7.43E-03	9.03E-06
FCHO1	2.86E-02	4.84E-06	GADD45A	2.82E-01	5.18E-31	GPBP1L1	3.39E-02	1.62E-06
FEM1B	7.67E-03	1.59E-02	GALK2	2.69E-03	3.02E-05	GPCPD1	9.35E-03	2.29E-08
FERMT3	1.08E-01	1.72E-12	GALNT2	2.04E-02	4.58E-04	GPR108	5.93E-02	9.68E-13
FES	5.72E-02	1.63E-07	GALT	3.29E-02	3.76E-05	GPR146	6.18E-02	2.27E-12
FEZ2	6.91E-02	4.70E-08	GAPT	9.10E-02	1.10E-15	GPSM3	1.71E-01	8.05E-16
FGD3	4.96E-02	2.74E-11	GATA2	2.07E-01	3.69E-35	GRAMD1A	2.48E-02	4.67E-03
FGFR1OP2	1.36E-01	1.14E-10	GATA3	9.21E-02	1.26E-20	GRINA	6.69E-02	9.99E-09
FHIT	2.55E-02	2.86E-07	GATAD1	2.59E-02	2.85E-06	GRK2	6.35E-03	1.09E-04
FHL1	6.33E-02	6.60E-04	GATD3A	5.74E-03	4.62E-02	GRN	2.28E-02	1.10E-02
FHL3	6.40E-02	7.81E-10	GBP2	8.06E-02	3.40E-14	GRSF1	1.42E-02	1.50E-03
FIS1	1.98E-01	2.73E-17	GBP4	1.32E-01	1.78E-14	GSDMD	2.37E-03	1.44E-07
FKBP9	2.22E-02	3.07E-06	GCA	2.31E-02	5.22E-04	GSE1	9.40E-03	1.31E-02
FLI1	1.18E-01	2.25E-13	GCC2	7.48E-02	5.70E-06	GSKIP	5.48E-03	8.99E-06
FLII	3.34E-02	1.38E-06	GCLM	2.18E-02	3.23E-03	GSN	5.58E-02	2.25E-04
FLNB	1.56E-02	1.05E-03	GCSAML	3.52E-02	1.95E-06	GSTK1	1.73E-01	1.99E-13
FLOT1	4.56E-02	2.74E-08	GFI1B	4.37E-02	4.80E-09	GSTM3	6.56E-02	2.30E-09
FLOT2	1.92E-02	2.76E-05	GFM1	1.04E-02	3.35E-04	GSTM4	2.48E-02	5.65E-04
FLT3	1.22E-02	4.62E-07	GFOD1	4.21E-02	1.04E-08	GSTM5	2.98E-02	6.13E-08
FMC1	3.57E-02	2.51E-05	GGA1	4.57E-02	4.45E-06	GSTO2	2.50E-02	1.27E-04
FMNL1	2.94E-02	8.17E-10	GGNBP2	3.08E-02	3.79E-07	GTF2B	4.24E-02	5.42E-05
FNBP1	1.15E-01	3.56E-08	GGPS1	1.49E-02	8.52E-05	GTF2F1	6.70E-02	8.49E-06
FNBP4	3.22E-02	2.41E-05	GHDC	3.35E-02	3.02E-07	GTF2F2	1.58E-02	7.22E-07
FNDC3A	7.40E-03	5.65E-03	GID8	1.81E-02	1.85E-07	GTF2H5	3.54E-02	5.54E-05
FNIP1	8.08E-02	1.11E-07	GIMAP2	1.29E-01	4.47E-29	GTF2IRD2	2.63E-02	4.87E-07
FNTA	4.42E-03	9.85E-05	GINM1	1.51E-02	2.58E-04	GTF3C3	1.97E-02	8.07E-03
FO393401.1	1.95E-02	1.83E-04	GIT2	1.40E-02	2.56E-11	GTPBP1	8.82E-03	1.71E-02
FOPNL	1.62E-02	4.03E-07	GLB1	1.48E-02	9.18E-05	GTPBP6	1.01E-02	1.13E-03
FOS	2.82E-01	2.90E-20	GLG1	1.77E-02	8.44E-03	GUCY1A1	1.36E-01	9.40E-13
FOSB	2.69E-01	1.26E-24	GLIPR1	2.38E-01	4.88E-39	GUCY1B1	2.82E-02	1.77E-05
FOSL2	6.06E-02	3.49E-07	GLMP	4.55E-02	9.08E-08	GYG1	1.26E-02	5.65E-07
FOXK1	1.26E-03	2.86E-02	GLRX	5.16E-02	3.14E-04	H1F0	3.61E-01	1.78E-59
FOXN3	1.07E-01	2.86E-10	GLS	2.74E-02	1.10E-04	H1FX	1.31E-01	1.77E-07
FOXO3	1.15E-02	7.63E-04	GLT8D1	5.38E-04	1.18E-08	H2AFJ	3.80E-02	2.21E-08
FOXP1	5.38E-03	5.30E-03	GMFB	4.04E-03	6.50E-07	H3F3B	2.60E-01	7.84E-62
FPGS	4.56E-03	2.41E-05	GMFG	1.13E-01	3.66E-08	HACD4	3.30E-02	2.18E-05
FRA10AC1	3.67E-02	1.95E-05	GMPR2	7.21E-02	2.29E-07	HACL1	4.69E-03	1.45E-04
FRMD4B	4.17E-02	1.65E-06	GNAI1	9.40E-02	7.11E-10	HADHA	1.16E-01	2.29E-06
FRMD8	3.87E-03	3.35E-06	GNG11	4.52E-02	3.21E-05	HADHB	5.69E-02	3.21E-06
FRYL	1.44E-02	4.40E-07	GNG7	3.60E-02	1.23E-07	HARS	2.16E-02	1.48E-04
FTL	2.11E-01	9.20E-78	GNPDA2	1.59E-02	7.28E-05	HAX1	4.45E-02	1.57E-07

Gene	logFC	FDR	Gene	logFC	FDR	Gene	logFC	FDR
HBP1	6.22E-02	3.08E-11	HLA-DRB1	4.75E-01	1.16E-87	IFITM1	1.05E-02	6.85E-03
HCFC1R1	1.22E-02	1.84E-08	HLA-DRB5	3.64E-01	1.12E-27	IFITM2	3.61E-02	1.42E-05
HCG18	2.79E-02	2.62E-06	HLA-E	6.26E-01	4.64E-238	IFITM3	7.92E-02	1.09E-05
HCLS1	3.62E-02	8.63E-04	HLA-F	2.07E-02	3.44E-04	IFNGR1	2.21E-02	8.86E-07
HDAC5	5.46E-02	1.61E-11	HLF	1.37E-01	1.72E-20	IFRD1	1.28E-02	4.30E-06
HDAC7	3.37E-02	2.26E-06	HMBOX1	2.43E-02	2.47E-04	IFT20	4.28E-02	3.95E-06
HDDC3	1.36E-02	3.54E-04	HMGA2	1.21E-01	6.68E-19	IFT27	5.74E-04	1.69E-06
HDHD3	2.76E-02	1.29E-09	HMGCS1	1.27E-02	7.86E-05	IFT74	3.08E-03	6.10E-03
HEBP1	8.84E-02	4.00E-11	HNRNPH2	1.17E-01	3.36E-12	IGBP1	2.40E-01	4.30E-35
HEBP2	1.26E-02	1.36E-03	HOOK3	2.52E-04	3.08E-05	IGF2BP2	5.56E-02	8.05E-06
HECTD1	1.03E-02	3.09E-06	HOPX	3.32E-01	3.73E-44	IGHD	5.34E-02	3.49E-05
HELZ	7.06E-03	3.62E-06	HOXA10	2.75E-02	4.13E-05	IGSF10	3.02E-02	7.26E-05
HEMGN	6.12E-02	1.07E-04	HOXA10-AS	3.32E-02	1.69E-05	IGSF8	1.22E-02	7.34E-05
HEMK1	2.61E-02	3.17E-05	HOXA7	1.54E-03	6.91E-06	IK	5.12E-02	8.79E-08
HERC1	1.21E-02	1.46E-03	HOXA9	2.75E-02	1.13E-07	IKBIP	2.85E-04	3.11E-05
HERC2	1.58E-03	1.13E-02	HOXB-AS3	3.84E-02	1.75E-06	IKZF1	7.91E-03	1.07E-02
HERC4	1.68E-02	1.25E-08	HOXB2	2.17E-03	1.66E-03	IL12A-AS1	1.48E-01	4.04E-43
HERPUD2	2.74E-02	8.00E-04	HOXB4	3.19E-02	1.54E-05	IL16	1.20E-01	3.92E-26
HEXA	8.52E-02	2.29E-08	HPCAL1	4.56E-02	1.81E-07	IL17RC	2.66E-02	7.37E-06
HEXB	1.59E-02	1.14E-09	HPS1	1.17E-02	6.02E-07	IL18	2.19E-01	2.02E-40
HEXDC	4.73E-02	3.82E-10	HSBP1L1	7.80E-02	1.52E-15	IL1B	2.21E-02	7.34E-05
HHEX	4.74E-02	4.47E-04	HSCB	3.24E-02	1.49E-06	IL27RA	3.25E-02	1.16E-06
HIBCH	3.21E-02	1.19E-09	HSD17B11	4.53E-01	5.38E-86	IL6ST	1.51E-02	1.50E-04
HIF1A	1.51E-02	1.83E-02	HSD17B12	3.60E-02	7.53E-07	ILF3-DT	5.99E-02	7.74E-11
HINT1	7.81E-02	3.37E-12	HSD17B14	6.41E-02	2.12E-14	IMMP2L	5.59E-03	7.12E-05
HINT3	2.74E-02	4.36E-08	HSF1	3.65E-02	1.81E-05	IMP3	1.63E-02	7.04E-06
HIST1H1C	4.72E-01	1.64E-94	HSP90AB1	2.05E-01	8.09E-57	IMPA1	3.08E-02	6.72E-06
HIST1H1D	2.51E-02	2.04E-12	HSPA13	1.92E-02	2.47E-07	IMPACT	1.35E-03	4.05E-06
HIST1H1E	2.94E-02	1.20E-09	HSPA1A	6.21E-02	2.84E-08	ING4	4.66E-02	5.44E-06
HIST1H2AC	1.66E-01	2.25E-58	HSPA5	6.82E-02	2.40E-07	INPP4B	3.71E-02	2.09E-05
HIST1H2AE	1.05E-01	2.02E-32	HTATIP2	1.35E-02	2.73E-04	INPP5D	1.57E-01	4.04E-16
HIST1H2BC	9.85E-02	5.50E-27	HTR1F	6.44E-02	8.49E-08	INSIG1	8.34E-03	1.74E-02
HIST1H2BG	1.76E-01	1.23E-43	HUS1	2.98E-02	1.07E-05	INSIG2	3.54E-02	1.67E-05
HIST1H2BN	9.39E-02	2.27E-22	ICA1	1.08E-01	2.97E-15	INTS11	3.08E-02	6.48E-06
HIST1H4E	5.69E-02	4.94E-12	ICAM2	9.84E-02	2.45E-13	INTS12	2.97E-02	2.01E-07
HIST2H2BE	3.71E-01	2.74E-110	ICAM3	1.10E-01	2.06E-07	INTS6	2.24E-03	1.21E-05
HIST3H2A	9.95E-02	1.59E-20	ICAM4	6.16E-02	3.70E-11	INTS6-AS1	3.66E-02	1.06E-05
HK1	8.57E-03	3.95E-03	ID1	6.28E-02	1.54E-02	INTS8	1.02E-02	2.68E-03
HLA-A	3.77E-01	1.81E-91	ID2	1.04E-01	1.49E-03	IP6K2	7.22E-02	6.91E-06
HLA-B	3.56E-01	2.22E-70	IDH3B	1.73E-02	1.33E-05	IPO11	2.63E-02	4.68E-06
HLA-C	3.41E-01	1.98E-68	IDH3G	2.53E-02	6.07E-06	IQGAP1	9.79E-04	2.16E-07
HLA-DMA	3.66E-01	2.12E-53	IDI1	6.28E-03	1.63E-07	IRAK3	5.10E-02	2.26E-05
HLA-DMB	1.55E-01	2.11E-34	IDNK	3.12E-02	1.01E-03	IREB2	9.76E-03	5.73E-05
HLA-DOA	8.08E-02	1.29E-20	IDS	2.80E-01	9.61E-30	IRF2	2.10E-02	4.57E-05
HLA-DPA1	5.35E-01	6.58E-125	IER2	5.33E-02	7.45E-04	IRF2BP2	5.41E-02	1.15E-04
HLA-DPB1	5.25E-01	2.09E-123	IFI16	1.27E-01	7.67E-10	IRF3	6.61E-02	2.07E-08
HLA-DQA1	2.79E-01	8.02E-52	IFI27L2	3.91E-02	1.67E-03	IRF5	1.54E-02	7.93E-03
HLA-DQA2	5.98E-03	1.75E-19	IFI35	3.93E-02	1.77E-06	IRS2	1.64E-02	1.85E-03
HLA-DQB1	5.09E-01	3.60E-86	IFI44	6.66E-03	1.29E-04	ISCA1	4.56E-02	5.93E-04
HLA-DRA	5.79E-01	2.14E-200	IFI44L	3.90E-02	1.46E-06	ISCA2	5.76E-04	4.68E-08

Gene	logFC	FDR	Gene	logFC	FDR	Gene	logFC	FDR
ISCU	1.35E-01	5.62E-12	KLHL6	6.36E-02	7.95E-12	LMBRD1	4.96E-02	9.17E-11
IST1	7.65E-03	5.85E-04	KLHL9	3.19E-02	1.14E-06	LMNA	3.31E-01	1.60E-41
ISY1	6.48E-03	1.17E-04	KMT2A	2.40E-02	5.78E-04	LMO2	7.44E-02	1.82E-06
ITGA4	3.01E-02	5.30E-03	KMT2C	2.21E-03	7.66E-04	LMO4	4.16E-02	4.30E-07
ITM2B	2.96E-01	5.07E-52	KMT2E	3.86E-02	1.22E-05	LONP2	4.48E-02	1.48E-03
ITM2C	1.52E-02	6.11E-05	KMT5B	4.93E-02	3.21E-11	LPCAT2	4.58E-02	4.94E-06
ITSN2	5.16E-02	4.96E-06	KPNA5	2.78E-02	1.24E-05	LPIN1	5.69E-02	3.73E-08
IVD	2.48E-02	7.26E-05	KRCC1	2.94E-02	1.82E-06	LPP	2.50E-02	6.87E-07
JAGN1	4.47E-02	1.58E-08	KRIT1	1.79E-02	1.74E-06	LRBA	3.61E-02	1.79E-04
JAK1	3.69E-02	2.69E-04	KRT18	3.35E-02	1.72E-03	LRCH4	1.03E-01	1.37E-20
JAML	2.39E-01	2.22E-54	KRT8	8.28E-02	3.32E-13	LRMDA	4.21E-03	4.00E-05
JKAMP	4.58E-02	3.82E-07	KTI12	2.56E-02	2.84E-04	LRMP	3.96E-02	3.04E-08
JMJD1C	1.01E-02	1.34E-05	KYAT3	4.41E-02	8.34E-09	LRP10	9.35E-02	5.51E-18
JMJD6	3.17E-02	1.21E-06	LAG3	2.80E-02	3.92E-03	LRRC23	1.11E-02	8.41E-05
JUNB	5.32E-01	3.13E-74	LAIR1	2.08E-01	1.48E-34	LRRC41	4.29E-02	2.97E-06
JUND	1.07E-01	2.60E-06	LAMP1	1.08E-03	1.98E-06	LRRC47	1.74E-03	8.01E-04
JUP	1.00E-01	1.50E-14	LAMP2	1.70E-01	1.58E-21	LRRFIP1	9.56E-02	2.18E-04
KANSL1-AS1	4.29E-03	2.71E-03	LAMTOR1	1.17E-01	2.38E-06	LRRFIP2	5.24E-02	1.33E-08
KARS	1.28E-02	6.01E-07	LAMTOR3	3.24E-02	8.26E-08	LSM10	3.53E-02	6.33E-06
KAT5	2.31E-02	8.11E-04	LAMTOR4	8.40E-02	9.30E-05	LSP1	1.05E-03	4.13E-04
KAT6A	8.27E-03	1.50E-03	LANCL1	1.10E-02	5.37E-04	LST1	2.26E-01	1.04E-19
KAT8	4.15E-02	7.63E-05	LAPTM4A	4.02E-01	4.75E-82	LTA4H	1.06E-01	2.56E-12
KCNN4	1.81E-02	3.77E-03	LAPTM4B	5.89E-02	2.22E-05	LTBP3	2.18E-02	6.23E-06
KCTD18	1.39E-02	4.73E-07	LAPTM5	2.38E-01	7.07E-33	LTBP4	1.35E-02	2.52E-05
KCTD20	1.93E-03	1.03E-04	LARP7	1.27E-02	1.44E-03	LTBR	1.38E-02	1.78E-04
KDELR1	1.36E-01	1.52E-11	LATS2	1.58E-02	2.56E-03	LTC4S	2.87E-02	9.77E-06
KDM2A	1.40E-02	2.64E-04	LCP2	3.93E-02	3.00E-06	LTV1	4.74E-03	1.44E-04
KDM5B	3.36E-02	8.13E-05	LDOC1	3.90E-02	1.96E-10	LUC7L	1.26E-02	1.20E-05
KDM5D	3.42E-02	1.25E-05	LENG1	4.48E-02	4.77E-07	LUC7L3	1.27E-01	3.52E-08
KDM6B	8.35E-03	5.75E-03	LENG8	6.06E-02	6.54E-09	LXN	7.72E-02	1.24E-11
KHDC4	1.66E-02	9.52E-03	LEPROT	2.02E-01	2.12E-21	LYL1	1.33E-01	1.19E-12
KIAA1109	2.73E-02	1.54E-04	LEPROTL1	7.84E-02	3.32E-08	LYN	3.89E-02	7.88E-04
KIAA1191	3.73E-02	1.17E-08	LETMD1	1.36E-01	1.23E-16	LYRM1	5.77E-02	1.77E-05
KIAA1551	2.16E-02	7.00E-07	LGALS8	3.07E-02	1.00E-03	LYRM7	8.74E-03	7.09E-08
KIAA2026	4.76E-02	4.70E-08	LGALS9	9.56E-02	4.02E-10	LYRM9	5.91E-02	2.62E-09
KIDINS220	1.92E-02	8.45E-06	LIAS	3.43E-02	8.38E-09	LYSMD2	3.76E-02	1.39E-07
KIF5B	8.10E-03	3.51E-07	LIMA1	3.45E-02	3.76E-05	LYZ	3.71E-02	3.54E-18
KIN	2.89E-02	1.92E-05	LIMCH1	7.72E-02	4.67E-15	LZTFL1	1.49E-02	8.55E-04
KLC1	4.57E-02	1.04E-06	LIMD2	1.89E-01	1.85E-15	M6PR	4.67E-03	1.41E-09
KLF10	7.84E-02	1.54E-05	LIMS1	2.51E-01	3.03E-26	MACC1	1.32E-02	2.70E-03
KLF13	1.56E-02	1.38E-03	LINC00623	5.52E-02	1.18E-09	MACF1	7.57E-03	6.26E-04
KLF2	9.31E-02	1.66E-12	LINC00667	4.82E-02	2.20E-05	MAD1L1	1.86E-02	3.24E-06
KLF3	1.14E-01	3.86E-09	LINC01089	2.17E-02	4.04E-04	MAEA	3.16E-03	1.52E-07
KLF4	8.46E-02	3.34E-08	LINC01122	8.52E-02	1.45E-13	MAF1	7.32E-03	3.90E-03
KLF5	1.19E-01	1.17E-20	LINC01184	2.03E-02	4.98E-06	MAFF	2.65E-01	1.34E-23
KLF7	2.22E-02	3.11E-05	LINC02256	7.62E-04	8.37E-03	MAFG	4.53E-02	3.28E-09
KLF9	2.32E-02	1.53E-05	LINC02573	1.83E-01	2.19E-31	MAGED2	2.41E-01	5.02E-38
KLHDC2	6.52E-02	3.23E-07	LIPA	1.11E-01	1.18E-11	MAGEF1	2.73E-02	3.25E-05
KLHDC8B	2.62E-02	7.35E-08	LITAF	2.81E-02	1.10E-03	MAN1A2	1.66E-02	1.39E-04
KLHL24	5.53E-02	2.53E-08	LIX1L	2.48E-02	5.02E-07	MAN1B1	1.83E-02	1.19E-03

Gene	logFC	FDR	Gene	logFC	FDR	Gene	logFC	FDR
MAN2A2	8.24E-02	7.91E-15	MEG3	4.09E-01	7.36E-94	MPHOSPH8	1.50E-01	1.31E-16
MAN2C1	1.27E-02	4.11E-03	MEIS1	8.89E-02	5.97E-11	MPI	4.34E-02	1.41E-06
MANSC1	7.15E-03	1.80E-11	METAP1D	2.81E-02	4.95E-05	MPP1	2.07E-02	2.54E-04
MAP1A	1.61E-02	2.58E-03	METTL15	2.62E-02	5.87E-04	MPV17	7.34E-03	7.63E-07
MAP1LC3B	5.72E-02	2.00E-08	METTL23	2.24E-02	1.07E-05	MRFAP1	3.55E-02	6.68E-05
MAP2K2	1.59E-02	4.58E-03	METTL3	2.14E-02	1.05E-02	MRM3	1.26E-02	2.81E-06
MAP2K3	2.06E-03	1.53E-06	METTL7A	3.30E-02	9.94E-09	MRPL10	5.02E-02	1.50E-08
MAP2K7	2.86E-03	3.54E-05	MFF	7.79E-04	2.42E-08	MRPL16	1.35E-01	3.90E-09
MAP3K11	3.74E-03	2.04E-06	MFSD1	5.52E-02	3.51E-06	MRPL32	1.16E-02	1.39E-03
MAP3K8	9.72E-02	3.41E-05	MFSD10	3.51E-02	5.69E-06	MRPL40	4.35E-03	1.01E-06
MAP4K2	6.21E-02	8.53E-08	MFSD11	1.66E-02	2.57E-05	MRPL43	9.36E-03	3.57E-02
MAP7	1.07E-01	6.73E-12	MGLL	9.00E-02	3.98E-09	MRPL44	1.05E-02	2.79E-05
MAP7D1	1.31E-02	1.11E-03	MGMT	4.10E-02	4.32E-07	MRPL45	6.37E-02	1.57E-08
MAP9	1.57E-02	1.46E-04	MGRN1	1.56E-03	2.82E-06	MRPS21	1.01E-01	3.25E-06
MAPK1IP1L	7.10E-02	3.64E-06	MIA2	1.39E-02	3.21E-06	MRPS27	7.80E-03	5.58E-07
MAPK6	2.07E-02	4.98E-06	MIA3	2.02E-02	9.48E-06	MRPS28	8.55E-03	6.12E-03
MAPKAPK5-A	1.71E-02	2.11E-06	MIB2	7.45E-03	1.13E-05	MRPS30	3.06E-02	9.13E-03
MAPRE1	1.91E-02	3.34E-05	MICAL1	1.15E-02	3.88E-03	MRPS33	4.76E-02	2.82E-06
MARCH5	7.70E-03	2.16E-03	MID1IP1	1.45E-02	9.74E-03	MRPS36	3.66E-02	1.05E-06
MARCH6	4.00E-02	4.14E-06	MIDN	3.89E-02	9.46E-08	MRPS5	9.91E-03	1.13E-02
MARCH7	1.11E-01	1.47E-13	MIEN1	2.14E-02	7.16E-04	MSL2	1.09E-02	4.73E-03
MARF1	2.87E-02	8.07E-04	MIF4GD	5.50E-03	4.11E-09	MSN	5.32E-02	3.13E-04
MAST4	2.21E-02	4.91E-04	MIIP	6.11E-03	9.97E-06	MSRB3	1.05E-01	9.66E-08
MAT2A	1.74E-02	7.02E-04	MIR155HG	7.49E-02	1.58E-12	MT-ATP8	1.55E-02	7.08E-03
MAT2B	1.35E-02	7.47E-09	MIR4458HG	1.49E-03	2.82E-02	MT-ND1	8.38E-02	2.27E-08
MAX	5.86E-02	2.85E-05	MIR99AHG	6.63E-02	1.49E-14	MT-ND2	1.40E-01	4.70E-25
MBD1	1.19E-02	9.37E-06	MITD1	1.43E-02	3.25E-07	MT-ND3	9.15E-02	3.97E-10
MBD5	3.98E-02	7.82E-06	MKLN1	2.93E-03	3.16E-02	MTERF4	1.71E-02	2.17E-05
MBNL1	7.40E-02	6.44E-04	MKRN1	6.33E-02	3.85E-11	MTFR1L	5.42E-02	1.39E-06
MBOAT7	3.50E-02	5.02E-03	MKRN2	1.35E-03	2.37E-04	MTIF3	7.30E-02	3.63E-08
MBP	6.38E-02	2.10E-06	MLC1	1.99E-03	7.92E-06	MTMR14	1.90E-02	3.46E-05
MBTPS1	2.39E-02	1.40E-06	MLF1	7.39E-02	8.20E-12	MTRF1L	1.04E-03	6.62E-04
MCCC1	2.92E-02	2.79E-05	MLF2	2.35E-02	1.29E-10	MTRNR2L12	9.56E-03	1.69E-06
MCL1	3.11E-01	2.44E-30	MLH3	2.41E-02	2.00E-05	MTURN	2.09E-02	5.88E-04
MCTP1	1.12E-03	5.43E-05	MLLT3	5.38E-01	8.61E-121	MTX1	1.98E-04	1.92E-06
MCTP2	1.06E-02	1.05E-03	MLLT6	4.01E-02	4.24E-06	MTX2	2.00E-02	2.77E-05
MEAF6	1.72E-02	5.01E-07	MLX	8.52E-03	2.58E-02	MUS81	1.58E-03	1.87E-03
MECOM	9.41E-02	3.22E-18	MLXIP	1.01E-02	2.18E-04	MVD	1.06E-02	2.28E-03
MECP2	1.44E-02	2.29E-04	MMADHC	5.87E-02	1.38E-04	MVP	8.05E-02	6.28E-24
MED10	8.28E-03	2.17E-05	MMGT1	1.90E-02	2.82E-03	MX1	4.39E-02	6.72E-06
MED12L	1.94E-02	5.66E-05	MMP24OS	2.65E-02	1.45E-04	MXD4	2.07E-02	1.74E-05
MED15	1.57E-02	9.81E-06	MMP28	4.62E-02	2.28E-08	MYADM	1.40E-01	7.78E-09
MED16	1.28E-02	2.26E-02	MMRN1	5.47E-02	1.84E-06	MYB	1.29E-02	1.89E-02
MED19	2.06E-02	1.03E-05	MOAP1	1.14E-01	9.57E-17	MYCBP2	4.88E-02	9.95E-07
MED21	2.78E-02	1.23E-04	MOB2	3.10E-02	8.00E-09	MYCT1	2.25E-01	4.70E-38
MED28	5.72E-02	3.40E-03	MOB4	3.37E-02	1.06E-05	MYL12A	9.60E-02	3.61E-07
MED29	1.99E-02	1.44E-03	MOCS2	8.10E-03	1.02E-03	MYL12B	9.67E-02	8.45E-06
MED6	2.88E-02	1.09E-03	MOSPD3	2.33E-02	3.79E-06	MYLIP	3.69E-02	8.87E-05
MED7	3.71E-02	2.53E-08	MPG	8.79E-02	3.89E-06	MYO1F	2.85E-02	3.80E-07
MEF2C	7.19E-02	2.08E-07	MPHOSPH10	1.45E-02	1.08E-02	MYO1G	4.07E-02	5.07E-05

Gene	logFC	FDR	Gene	logFC	FDR	Gene	logFC	FDR
MZF1	3.34E-02	8.86E-05	NFKB2	3.41E-02	3.65E-05	NT5C2	2.01E-03	2.73E-02
N4BP2L1	8.52E-02	9.59E-09	NFKBIA	1.72E-01	6.38E-11	NT5C3A	4.06E-02	6.92E-04
N4BP2L2	2.79E-01	5.40E-34	NFKBID	1.88E-02	7.83E-04	NTHL1	3.68E-02	2.79E-09
NAA30	2.12E-02	1.31E-08	NFKBIL1	4.35E-02	7.29E-08	NUB1	5.18E-02	3.08E-06
NAA60	3.24E-03	3.85E-05	NFKBIZ	2.49E-02	5.25E-04	NUBP1	1.56E-02	3.14E-04
NAA80	2.42E-02	1.77E-06	NFU1	3.54E-02	5.12E-05	NUCB1	4.42E-02	1.27E-04
NAALADL1	9.57E-02	3.41E-14	NGDN	1.14E-03	1.82E-03	NUDCD3	2.59E-02	2.16E-04
NACA	2.29E-01	1.20E-110	NIFK	2.82E-02	3.38E-06	NUDT14	4.98E-02	4.97E-11
NADSYN1	2.73E-02	2.94E-05	NIFK-AS1	3.55E-02	7.95E-06	NUDT16	4.88E-02	1.69E-09
NAF1	2.06E-02	3.70E-07	NINJ2	1.25E-02	1.55E-04	NUDT16L1	9.61E-03	1.18E-09
NAMPT	9.77E-02	1.41E-08	NIPSNAP1	4.62E-03	7.26E-05	NUDT19	8.97E-03	7.64E-03
NANS	1.68E-02	7.88E-05	NKAIN2	4.01E-02	7.57E-05	NUDT2	3.47E-02	3.08E-06
NAP1L3	8.67E-02	3.43E-14	NKTR	4.46E-02	3.33E-02	NUDT3	2.29E-02	2.46E-03
NAP1L5	2.90E-02	5.78E-06	NLRP1	3.77E-02	6.00E-13	NUDT4	3.84E-02	1.48E-04
NAPG	1.10E-03	3.44E-03	NMD3	5.07E-02	3.84E-07	NUMA1	1.50E-02	3.85E-03
NAPRT	3.13E-02	3.86E-04	NME3	1.04E-01	3.82E-14	NUMB	3.25E-02	9.77E-06
NARFL	2.02E-02	1.37E-05	NME7	2.00E-02	1.38E-03	NXF1	1.84E-02	1.64E-02
NAT9	2.76E-02	1.80E-06	NMRK1	4.42E-02	1.36E-09	OARD1	8.27E-02	6.27E-08
NBDY	4.08E-02	9.92E-05	NOA1	6.62E-02	6.26E-09	OAT	3.27E-02	1.26E-06
NBEAL1	4.55E-02	5.30E-07	NOB1	9.72E-02	7.93E-08	ODF2L	1.99E-02	2.35E-05
NBL1	4.46E-03	1.67E-02	NOG	1.98E-02	2.45E-04	ODR4	1.24E-03	4.45E-02
NBR1	4.27E-02	5.78E-06	NOL7	2.35E-02	3.43E-06	OFD1	5.82E-02	8.36E-05
NCK1	9.31E-03	3.91E-03	NOP53	2.14E-01	1.08E-52	OGA	3.87E-02	1.14E-05
NCKAP1L	5.94E-02	2.37E-06	NORAD	9.98E-03	6.36E-04	OGFR	3.04E-02	2.59E-06
NCOA4	6.85E-02	5.12E-08	NPC2	3.99E-02	2.52E-08	OGT	2.59E-02	1.41E-04
NCOA7	2.67E-02	5.78E-04	NPDC1	3.01E-02	1.94E-05	OPTN	7.57E-02	6.67E-12
NCOR1	3.16E-02	2.74E-06	NPEPPS	1.38E-02	1.30E-02	ORAI1	2.43E-02	2.08E-03
NCSTN	1.56E-02	4.73E-03	NPM1	1.20E-01	3.63E-30	ORAI2	3.21E-02	6.71E-06
NDFIP1	1.33E-01	6.78E-14	NPM2	5.29E-02	1.60E-09	ORAI3	4.27E-02	5.46E-05
NDN	1.70E-02	1.34E-05	NPR3	1.09E-01	8.47E-07	ORC4	4.56E-03	9.65E-06
NDRG2	5.02E-02	4.72E-09	NPRL3	1.25E-02	5.47E-06	ORMDL1	1.93E-02	5.54E-07
NDUFA10	5.20E-02	4.43E-04	NR1D2	1.68E-02	1.10E-02	OS9	1.11E-01	1.88E-11
NDUFAF3	2.23E-02	4.99E-04	NR1H2	1.37E-01	4.53E-18	OSER1	1.81E-02	8.11E-06
NDUFB5	9.65E-02	3.04E-06	NR3C1	6.61E-02	1.03E-08	OST4	7.04E-02	2.65E-03
NDUFC1	3.63E-02	1.60E-04	NR4A1	1.26E-01	1.90E-15	OSTF1	4.02E-02	1.58E-09
NDUFS2	2.16E-02	1.64E-03	NR4A2	4.02E-01	3.42E-69	OTUB1	6.83E-02	3.41E-12
NDUFS4	6.11E-02	5.30E-07	NRBF2	1.33E-02	3.92E-02	OTUD6B-AS1	4.70E-02	1.32E-05
NEAT1	9.57E-02	6.78E-05	NRBP1	2.36E-02	3.92E-05	OXA1L	1.36E-01	4.58E-14
NECAP1	3.05E-02	1.09E-05	NRDE2	3.91E-03	1.06E-05	OXLD1	2.72E-02	3.57E-04
NECAP2	1.75E-02	1.09E-03	NRIP1	6.54E-02	2.99E-03	OXR1	2.00E-02	3.38E-04
NECTIN2	2.57E-02	4.51E-04	NRROS	1.08E-02	4.90E-03	OXT	2.11E-02	3.84E-07
NEIL2	1.90E-02	3.59E-04	NSA2	7.10E-02	5.79E-05	P2RX1	8.30E-02	1.44E-14
NEMF	1.93E-02	8.09E-03	NSFL1C	4.32E-02	1.01E-06	P2RX4	1.72E-02	6.54E-06
NEU1	7.72E-02	1.21E-20	NSMAF	6.02E-03	7.01E-06	P2RY8	3.68E-02	1.77E-07
NFAT5	2.21E-02	4.07E-08	NSMCE1	3.95E-02	2.23E-07	P4HA1	4.87E-03	2.55E-03
NFATC1	2.36E-02	6.05E-06	NSMCE2	8.32E-03	4.96E-03	P4HTM	3.08E-02	3.98E-04
NFATC2	2.24E-02	4.08E-05	NSMCE3	3.35E-02	9.95E-06	PABPC1	1.87E-01	1.36E-66
NFE2	3.28E-02	6.36E-06	NSRP1	6.29E-03	2.98E-04	PACS1	2.51E-02	7.38E-08
NFE2L2	1.67E-01	1.25E-19	NSUN2	6.07E-03	7.13E-05	PADI4	5.38E-02	2.31E-07
NFIA	6.02E-02	2.89E-06	NSUN5	2.25E-02	9.31E-06	PAPSS1	2.97E-02	2.71E-06

Gene	logFC	FDR	Gene	logFC	FDR	Gene	logFC	FDR
PARL	4.49E-03	4.33E-04	PHYH	1.34E-02	3.40E-02	PON2	1.27E-02	2.53E-08
PARP10	4.25E-02	9.28E-08	PHYKPL	1.06E-01	2.68E-20	POU2F2	9.00E-02	3.59E-19
PARP16	1.47E-02	4.27E-06	PI4KB	1.83E-02	2.60E-05	PPCS	5.80E-02	6.10E-09
PARVG	1.38E-02	2.65E-03	PIAS1	4.03E-02	2.65E-05	PPFIBP1	4.54E-02	1.09E-09
PAXIP1-AS1	1.38E-02	5.25E-03	PIBF1	1.30E-02	3.70E-04	PPIL3	1.96E-02	6.82E-04
PBX1	8.16E-02	9.01E-12	PIGBOS1	1.12E-02	5.95E-03	PPIL4	1.86E-02	9.99E-04
PBXIP1	2.40E-01	2.74E-43	PIGP	4.28E-02	3.64E-05	PPM1B	2.27E-02	6.49E-04
PCBD1	2.93E-02	2.62E-06	PIK3CG	4.37E-02	1.72E-07	PPM1F	1.25E-02	3.16E-03
PCDH9	1.51E-01	6.99E-15	PIK3IP1	1.41E-01	1.45E-27	PPM1K	3.73E-02	5.97E-07
PCF11	1.82E-02	2.31E-08	PILRB	4.36E-03	6.47E-06	PPP1R10	1.86E-03	2.36E-04
PCGF5	1.59E-02	8.10E-03	PIM3	7.56E-02	2.81E-06	PPP1R11	5.54E-02	8.01E-07
PCID2	1.40E-02	3.75E-08	PIP4P1	7.76E-03	1.13E-06	PPP1R12A	1.04E-02	1.44E-03
PCIF1	3.37E-02	8.58E-06	PIP4P2	3.39E-02	1.56E-06	PPP1R15A	1.36E-01	5.69E-07
PCMTD1	4.30E-02	3.58E-06	PIP5K1B	3.28E-02	1.63E-08	PPP1R15B	1.15E-02	1.80E-02
PCMTD2	7.10E-02	2.73E-12	PITPNA-AS1	2.46E-02	8.95E-05	PPP1R18	2.36E-03	2.52E-06
PCNP	1.13E-02	8.04E-07	PJA2	6.59E-02	8.64E-06	PPP1R2	5.21E-02	1.42E-05
PCSK7	1.34E-02	1.92E-02	PKN1	5.23E-02	4.27E-05	PPP2R2A	1.91E-02	1.54E-05
PDCD4	1.74E-02	1.56E-04	PLCG2	1.96E-02	2.58E-04	PPP3CC	2.45E-02	2.65E-07
PDCD6IP	9.84E-03	1.87E-06	PLD3	9.39E-02	2.56E-11	PPP6C	9.46E-04	7.74E-06
PDCL	1.73E-02	4.64E-07	PLD4	3.54E-02	2.50E-05	PPP6R2	2.56E-02	6.62E-06
PDE12	2.97E-03	9.47E-04	PLEKHA2	2.71E-02	4.62E-05	PPP6R3	9.86E-03	2.09E-05
PDE4B	1.46E-02	1.77E-04	PLEKHA3	3.06E-03	9.56E-04	PPWD1	1.14E-02	3.02E-03
PDE4D	2.04E-02	1.23E-06	PLEKHA5	1.56E-02	5.60E-03	PQBP1	1.03E-01	2.63E-10
PDE4DIP	1.15E-02	1.64E-03	PLEKHF2	3.02E-02	8.80E-06	PQLC3	4.51E-02	5.07E-08
PDE6G	6.49E-02	1.32E-15	PLEKHO1	2.88E-02	2.36E-08	PRAF2	3.39E-02	5.55E-10
PDLIM2	3.47E-02	5.77E-06	PLIN3	2.03E-02	1.06E-05	PRAM1	1.18E-02	1.86E-03
PDLIM5	1.07E-02	1.45E-04	PLK3	1.94E-02	3.82E-05	PRCP	9.36E-03	1.42E-05
PDXDC1	1.68E-03	3.76E-04	PLPP5	6.34E-02	1.04E-07	PRELID2	2.70E-04	8.03E-04
PECAM1	4.63E-02	7.78E-06	PLRG1	3.08E-03	3.82E-05	PREPL	4.69E-02	7.55E-08
PEF1	3.10E-02	9.04E-06	PLSCR1	3.36E-02	1.13E-05	PREX2	5.12E-02	1.57E-08
PEPD	1.37E-02	2.50E-05	PLXDC2	5.18E-02	3.31E-07	PRH1	1.72E-02	2.61E-02
PER1	1.45E-01	2.32E-17	PML	3.91E-02	2.61E-06	PRKAA1	2.03E-02	8.56E-04
PEX16	4.93E-02	2.69E-06	PMPCB	1.19E-01	2.12E-12	PRKACB	1.39E-01	6.25E-15
PEX19	1.64E-02	3.19E-02	PNISR	3.05E-01	8.37E-47	PRKAG1	1.15E-02	2.44E-06
PEX2	1.21E-02	1.90E-05	PNMA1	1.78E-03	2.57E-05	PRKAG2	6.80E-03	7.02E-04
PEX3	4.70E-03	1.49E-03	PNPLA2	5.15E-02	2.29E-08	PRKAR1A	1.12E-01	8.51E-11
PFDN4	1.03E-01	2.64E-07	PNPLA6	2.09E-02	7.97E-06	PRKCB	2.98E-02	1.93E-04
PFDN5	2.28E-01	9.15E-73	PNPLA8	4.57E-02	1.63E-05	PRKCH	6.97E-02	1.26E-08
PFKM	2.97E-02	2.08E-05	PNRC1	3.12E-01	4.39E-38	PRKG2	3.97E-02	5.21E-05
PGGT1B	1.40E-02	1.78E-05	PNRC2	5.81E-02	8.75E-09	PRKX	3.82E-03	3.49E-02
PGM2L1	4.03E-03	3.69E-03	POLD4	4.13E-02	1.06E-09	PRMT2	7.57E-02	1.89E-07
PGPEP1	3.79E-02	3.62E-06	POLL	3.85E-02	1.77E-07	PRNP	5.68E-02	1.11E-06
PHACTR1	7.34E-02	8.85E-08	POLR1D	8.42E-02	1.39E-04	PROM1	3.55E-02	2.91E-08
PHACTR2	4.21E-02	1.03E-04	POLR2C	2.61E-02	3.83E-10	PRPF18	5.14E-03	1.79E-04
PHC3	2.01E-02	9.23E-07	POLR2M	2.21E-02	1.60E-06	PRPF38A	1.45E-02	5.24E-05
PHF1	1.28E-01	4.35E-28	POLR3D	1.39E-03	2.60E-03	PRPF6	1.39E-02	2.13E-03
PHF11	6.57E-02	1.08E-09	POLR3E	6.91E-03	1.90E-04	PRPSAP2	1.35E-02	3.17E-05
PHF20	1.27E-01	8.29E-13	POLR3GL	2.17E-02	7.94E-08	PRR13	7.40E-02	2.44E-04
PHLDB2	6.95E-02	1.25E-19	POMC	1.46E-02	3.09E-06	PRR14	5.04E-03	6.29E-03
PHTF1	3.76E-02	1.15E-04	POMGNT1	2.24E-02	1.31E-03	PRR5	5.92E-02	2.81E-10

Gene	logFC	FDR	Gene	logFC	FDR	Gene	logFC	FDR
PRR7	2.22E-02	2.04E-03	RAC2	7.16E-02	3.55E-03	RGS14	4.65E-02	9.46E-08
PSAP	2.77E-01	7.98E-35	RACK1	1.57E-01	4.75E-81	RGS19	4.83E-02	1.03E-05
PSMB1	1.31E-02	4.17E-10	RAD54L2	3.07E-02	1.31E-04	RGS2	4.48E-02	3.74E-03
PSMB8-AS1	2.70E-02	2.77E-11	RALB	1.99E-02	7.24E-08	RHOBTB3	2.00E-02	3.44E-03
PSMF1	4.45E-02	1.90E-05	RAP2B	1.20E-03	3.50E-04	RHOC	9.00E-02	6.84E-11
PSMG2	3.85E-02	1.08E-05	RAP2C	7.59E-03	1.32E-05	RHOF	1.58E-02	1.48E-04
PSTPIP2	3.06E-02	1.54E-05	RAPGEF2	2.90E-02	7.95E-05	RHOG	4.65E-02	1.16E-04
PTAR1	4.44E-02	5.49E-06	RARA	3.35E-02	1.98E-07	RHOH	1.24E-01	1.88E-12
PTBP3	2.70E-02	3.38E-04	RARRES3	1.87E-01	1.19E-22	RHPN1	1.68E-02	6.13E-04
PTEN	2.61E-02	2.94E-08	RASA2	2.08E-02	2.66E-04	RIC3	4.77E-02	8.08E-07
PTER	2.13E-02	4.99E-08	RASAL3	1.09E-01	4.87E-16	RICTOR	7.11E-03	1.92E-04
PTGER2	1.75E-02	1.02E-06	RASSF1	6.86E-03	4.95E-05	RILP	3.13E-02	5.02E-06
PTGER4	3.30E-01	5.12E-40	RASSF5	3.50E-02	4.04E-06	RILPL2	2.90E-01	5.00E-35
PTGS1	1.78E-01	7.37E-40	RB1CC1	2.02E-02	1.79E-03	RIMKLB	6.49E-02	7.07E-10
PTGS2	3.16E-02	1.63E-05	RBCK1	5.25E-02	6.91E-11	RIN3	2.93E-02	8.82E-06
PTK2B	3.33E-02	4.66E-05	RBL2	2.12E-02	6.85E-05	RIOK2	7.01E-03	1.32E-05
PTP4A1	3.57E-02	4.71E-05	RBM22	3.92E-02	6.64E-06	RIPK2	5.01E-02	3.23E-06
PTPN2	6.33E-03	2.49E-06	RBM23	4.98E-02	1.72E-07	RIPOR2	1.12E-01	3.57E-14
PTPN22	2.33E-02	1.62E-05	RBM33	1.02E-02	2.44E-06	RLIM	1.12E-02	2.85E-05
PTPN6	1.02E-01	4.12E-12	RBM4	8.07E-03	1.98E-04	RMDN3	7.81E-03	4.28E-05
PTPRA	2.86E-03	4.04E-04	RBM48	9.67E-03	1.55E-04	RMND1	4.68E-02	1.07E-09
PTPRC	2.27E-01	1.93E-21	RBM5	3.18E-02	1.84E-04	RNASET2	2.12E-01	2.21E-22
PTS	6.86E-04	8.86E-04	RBM7	4.44E-02	1.57E-03	RNF11	6.37E-02	7.18E-07
PURA	2.26E-02	2.88E-04	RBMS1	2.32E-02	1.30E-04	RNF113A	1.15E-02	1.35E-02
PURB	2.14E-02	2.66E-04	RBMX2	3.73E-02	4.92E-05	RNF114	4.91E-02	6.29E-05
PYCARD	4.62E-02	9.99E-04	RBMXL1	8.03E-03	4.96E-06	RNF115	2.28E-02	3.76E-03
QPRT	2.44E-04	2.69E-03	RBPJ	4.71E-04	5.25E-11	RNF125	1.69E-01	1.18E-18
QSOX1	2.60E-02	1.11E-04	RBPMS	6.74E-02	1.78E-09	RNF139	2.27E-02	7.94E-05
QTRT1	3.12E-02	1.41E-05	RC3H1	4.06E-03	4.65E-03	RNF145	4.48E-02	4.53E-04
R3HCC1	6.63E-03	1.38E-05	RC3H2	1.59E-02	3.09E-05	RNF166	1.89E-03	1.07E-02
R3HDM4	5.27E-02	1.19E-09	RCHY1	1.55E-02	2.81E-05	RNF167	7.30E-03	8.26E-07
RAB11B	3.29E-03	7.84E-05	RCSD1	1.55E-01	2.66E-12	RNF19A	3.62E-02	3.57E-06
RAB13	3.95E-02	6.94E-05	RDH11	1.59E-02	4.82E-06	RNF20	4.07E-03	3.10E-02
RAB18	5.39E-02	5.63E-06	RDH14	7.55E-03	1.05E-05	RNF213	2.25E-02	1.76E-05
RAB1A	6.60E-02	2.94E-09	REL	3.49E-02	1.77E-04	RNF216	1.22E-03	4.03E-02
RAB21	1.59E-02	3.99E-06	RELA	4.55E-02	2.22E-07	RNF220	7.60E-02	7.86E-06
RAB27B	7.06E-02	1.07E-14	RENBP	7.98E-02	5.87E-16	RNF24	4.06E-02	6.70E-05
RAB30-AS1	1.03E-02	3.22E-06	REPIN1	3.65E-02	8.01E-08	RNF41	7.25E-03	6.61E-04
RAB33A	4.17E-02	1.74E-08	RERE	4.10E-02	1.22E-03	RNF44	4.22E-02	1.75E-05
RAB33B	2.63E-02	8.82E-08	REST	2.32E-02	7.45E-06	RNF6	3.02E-02	4.55E-05
RAB34	3.96E-02	6.45E-05	RETREG3	5.22E-02	6.25E-13	RNF7	1.19E-01	3.92E-09
RAB37	2.55E-01	3.42E-47	REXO2	6.68E-03	6.96E-04	RNFT1	2.26E-02	2.98E-08
RAB3D	4.79E-02	1.16E-06	REXO4	1.26E-02	1.52E-02	RNH1	1.01E-01	2.32E-13
RAB3GAP1	2.34E-02	5.05E-06	REXO5	1.47E-02	4.33E-09	RNMT	3.07E-02	3.40E-05
RAB7A	2.39E-02	6.55E-08	RFTN1	5.12E-02	2.55E-07	RNPC3	1.67E-02	6.66E-05
RAB9A	2.25E-02	4.04E-05	RFX5	4.10E-02	6.54E-06	ROBO3	2.75E-02	1.05E-06
RABAC1	1.11E-01	3.72E-09	RGL2	7.55E-02	5.57E-16	ROBO4	7.73E-02	4.04E-17
RABEP2	4.91E-03	5.43E-03	RGL4	3.21E-02	5.70E-07	RPAP2	1.92E-02	9.35E-03
RABGAP1	4.97E-02	6.98E-05	RGP1	2.31E-02	6.68E-07	RPF1	4.81E-02	3.25E-05
RABGAP1L	2.49E-02	1.39E-04	RGS10	1.07E-01	8.95E-08	RPF2	1.64E-02	1.22E-06

Gene	logFC	FDR	Gene	logFC	FDR	Gene	logFC	FDR
RPL10A	3.79E-02	7.46E-07	RTRAF	2.66E-02	7.19E-06	SECISBP2	2.12E-02	2.38E-04
RPL12	1.73E-01	9.30E-118	RUNX2	1.24E-02	5.57E-03	SELENOK	4.92E-02	6.27E-03
RPL17	4.46E-02	2.84E-03	RUNX3	3.96E-03	4.45E-03	SELENOM	1.95E-01	4.41E-57
RPL18	1.02E-01	3.43E-37	RXRB	2.50E-02	1.46E-05	SELENOP	1.50E-01	2.24E-18
RPL19	2.87E-02	2.38E-04	RYBP	2.00E-02	4.49E-04	SELENOS	8.26E-03	4.31E-09
RPL23	4.34E-02	4.24E-05	S100A10	2.36E-02	3.23E-04	SELENOT	2.51E-02	9.07E-08
RPL23A	5.09E-02	1.45E-12	S100A11	1.39E-02	3.56E-03	SELL	1.27E-01	1.01E-06
RPL24	1.12E-01	1.46E-32	S100A4	2.56E-01	2.41E-24	SENP6	2.75E-02	3.29E-05
RPL28	1.48E-02	2.18E-02	S100A6	2.67E-01	9.70E-29	SENP7	2.66E-02	4.06E-06
RPL29	2.99E-02	3.13E-04	S1PR4	3.86E-02	7.82E-08	SEPT6	1.63E-02	6.22E-03
RPL30	1.35E-01	3.99E-67	SAFB2	1.68E-02	1.09E-05	SEPT9	1.69E-02	5.30E-05
RPL31	1.59E-01	7.51E-131	SAMD4B	4.01E-03	1.69E-03	SERGEF	5.10E-03	1.79E-06
RPL35A	2.00E-01	3.62E-178	SAMD9	2.06E-02	3.58E-05	SERINC1	5.81E-02	5.27E-08
RPL36	8.57E-02	2.87E-36	SAMD9L	4.76E-02	8.76E-09	SERINC3	1.09E-01	8.92E-12
RPL36A	7.02E-02	4.67E-11	SAMSN1	1.31E-01	1.43E-13	SERP1	8.83E-02	9.33E-05
RPL36AL	2.97E-01	7.50E-60	SAP30BP	9.25E-04	4.02E-05	SERPINB1	1.54E-01	2.46E-13
RPL38	1.44E-01	1.66E-54	SARAF	1.64E-01	8.75E-13	SERPINB6	8.20E-02	1.01E-04
RPL39	6.88E-02	2.27E-15	SARNP	1.31E-02	1.28E-03	SERPING1	2.07E-02	2.01E-03
RPL5	4.86E-02	6.22E-10	SART1	6.89E-03	6.88E-04	SESN3	3.16E-02	3.54E-04
RPL7	6.85E-02	6.99E-27	SAT1	2.01E-01	1.84E-21	SETD3	2.37E-02	9.45E-07
RPL7L1	6.00E-03	2.01E-03	SAT2	1.78E-01	4.90E-28	SETX	4.31E-03	1.08E-03
RPL8	4.58E-02	3.34E-08	SATB1	2.74E-02	1.17E-04	SF1	7.35E-02	1.96E-03
RPL9	7.87E-02	2.36E-23	SAV1	1.90E-03	2.36E-05	SF3B1	5.49E-02	2.38E-05
RPS11	6.49E-02	5.22E-10	SBDS	2.22E-01	3.83E-29	SFR1	1.78E-03	8.95E-05
RPS13	3.67E-02	4.09E-06	SBF2	1.40E-02	2.14E-02	SFXN3	3.75E-02	2.78E-06
RPS15A	5.98E-02	4.82E-21	SC5D	2.98E-02	4.53E-05	SFXN4	4.40E-03	6.87E-05
RPS25	6.61E-02	1.05E-16	SCAF4	1.28E-02	4.26E-04	SGF29	9.22E-03	9.87E-03
RPS27A	1.04E-01	2.33E-66	SCAMP1	3.66E-03	3.84E-03	SGK3	1.04E-02	2.30E-06
RPS29	5.44E-02	2.11E-20	SCAMP1-AS1	2.97E-02	4.67E-04	SH2B1	1.49E-02	4.45E-05
RPS4Y1	1.67E-01	1.09E-22	SCAMP2	6.63E-02	3.13E-09	SH3BGRL	1.04E-01	1.16E-05
RPS6KA1	2.47E-02	1.77E-07	SCAND1	7.45E-02	4.06E-05	SH3BGRL3	7.95E-02	5.25E-04
RPS6KA3	1.33E-02	6.55E-04	SCAP	7.91E-03	1.76E-02	SH3D21	4.55E-02	8.51E-07
RPS6KB2	1.47E-04	1.12E-04	SCARB2	1.73E-02	6.56E-04	SH3GLB1	1.50E-02	1.48E-02
RPUSD4	3.45E-02	3.22E-07	SCARF1	7.07E-02	2.91E-14	SH3KBP1	6.87E-04	6.39E-09
RRAGA	7.71E-02	3.95E-11	SCFD1	1.53E-02	3.01E-03	SH3YL1	1.56E-02	1.89E-02
RRAGB	5.00E-03	1.81E-03	SCN9A	7.69E-02	2.32E-14	SHISA5	2.91E-02	6.98E-06
RRBP1	1.81E-02	4.26E-05	SCP2	5.23E-02	1.00E-10	SHKBP1	4.25E-02	1.05E-09
RRS1	9.18E-03	2.60E-08	SCRN2	8.29E-02	7.11E-10	SHOC2	2.89E-02	6.09E-03
RSAD1	9.16E-03	1.02E-02	SDAD1	5.85E-03	3.43E-06	SIAH2	1.03E-02	3.12E-06
RSBN1	2.05E-01	3.07E-33	SDCBP	1.27E-01	9.51E-11	SIGIRR	1.27E-02	8.83E-03
RSBN1L	2.64E-02	8.60E-04	SDCCAG8	7.00E-02	2.97E-07	SIK3	2.67E-02	7.54E-06
RSF1	1.05E-02	1.48E-05	SDE2	5.26E-02	1.04E-06	SIL1	1.21E-01	9.91E-16
RSL1D1	1.83E-01	1.98E-15	SDHA	2.57E-02	3.32E-04	SIPA1	6.79E-03	2.81E-04
RSL24D1	2.01E-01	8.81E-22	SDHAF2	1.56E-02	5.35E-09	SIRT2	2.41E-02	2.99E-05
RSRP1	1.53E-01	3.95E-16	SDR39U1	2.01E-02	1.04E-05	SKAP1	7.82E-02	2.12E-11
RTCA	2.05E-02	1.27E-07	SEC14L1	4.56E-02	2.80E-04	SKAP2	8.08E-02	1.54E-08
RTCB	1.32E-03	1.19E-05	SEC23A	4.51E-03	8.43E-07	SKIL	4.36E-02	1.81E-04
RTF2	1.57E-02	1.71E-05	SEC23IP	7.41E-03	5.11E-05	SLA	2.54E-02	3.02E-03
RTL8C	1.79E-02	8.75E-03	SEC31A	3.84E-02	8.23E-04	SLC16A7	4.48E-02	3.17E-06
RTN2	5.75E-02	4.45E-16	SEC62	1.22E-01	6.28E-07	SLC25A24	5.59E-05	3.09E-11

Gene	logFC	FDR	Gene	logFC	FDR	Gene	logFC	FDR
SLC25A26	2.42E-02	6.80E-03	SNX14	5.24E-02	1.08E-08	ST6GALNAC4	1.85E-02	3.14E-05
SLC25A33	6.88E-03	1.47E-05	SNX17	9.36E-03	1.10E-07	STAMBP	7.27E-04	7.02E-04
SLC25A36	3.40E-02	8.37E-04	SNX2	3.19E-02	2.37E-03	STARD10	3.06E-02	1.46E-06
SLC25A38	3.71E-02	5.37E-04	SNX6	2.38E-02	1.17E-04	STARD3	5.25E-02	3.36E-08
SLC2A3	5.82E-02	1.59E-09	SNX9	2.91E-02	1.49E-03	STARD3NL	5.17E-02	1.00E-06
SLC30A9	4.39E-03	4.56E-06	SOCS2	2.82E-01	2.85E-33	STAT3	1.55E-01	1.48E-16
SLC35C2	3.12E-02	1.40E-04	SOCS4	2.71E-03	1.65E-05	STAT5A	6.15E-02	1.03E-03
SLC35E3	1.19E-02	9.02E-03	SOCS6	2.37E-02	1.58E-03	STAT5B	1.46E-02	1.47E-02
SLC37A1	1.38E-04	9.40E-07	SON	1.01E-01	3.13E-05	STAT6	5.62E-02	8.66E-10
SLC38A10	3.64E-03	8.00E-04	SORL1	1.61E-01	2.01E-19	STAU2	7.60E-03	1.10E-05
SLC39A1	9.67E-03	1.43E-11	SP100	6.41E-02	9.64E-10	STIM1	1.93E-02	1.54E-03
SLC39A6	8.11E-03	9.73E-03	SP110	8.31E-02	2.73E-10	STIM2	2.62E-03	3.96E-02
SLC39A7	7.32E-04	9.06E-07	SPAG7	4.14E-02	2.98E-08	STK10	3.21E-02	1.13E-10
SLC3A2	1.08E-01	7.65E-11	SPAG9	2.29E-02	4.94E-05	STK16	5.67E-03	5.63E-03
SLC40A1	5.45E-02	8.37E-06	SPART	9.65E-02	5.82E-12	STK17A	4.65E-02	1.55E-06
SLC41A3	4.61E-03	9.07E-08	SPATA20	4.48E-02	3.11E-07	STK17B	1.84E-01	8.48E-15
SLC44A1	4.87E-03	3.49E-05	SPATC1L	3.12E-02	3.96E-05	STK25	1.68E-03	1.15E-05
SLC50A1	2.87E-02	2.00E-04	SPCS1	4.45E-02	5.18E-10	STK26	1.36E-02	8.52E-05
SLCO3A1	1.61E-02	7.74E-06	SPECC1	3.04E-03	7.44E-03	STK4	1.02E-01	3.68E-10
SLU7	4.81E-02	2.89E-08	SPG11	1.66E-02	9.72E-05	STMN3	2.53E-03	1.04E-03
SMAD3	2.20E-02	6.26E-07	SPG21	9.93E-03	3.83E-05	STN1	4.71E-02	5.40E-08
SMAP2	1.19E-02	8.09E-03	SPG7	2.65E-02	1.65E-03	STOM	6.00E-02	1.32E-05
SMARCA2	3.69E-02	2.14E-07	SPI1	1.19E-02	1.63E-05	STRADA	2.08E-02	1.29E-03
SMARCC2	4.61E-02	1.09E-05	SPIN2B	4.78E-02	1.37E-06	STX16	5.22E-02	1.96E-07
SMDT1	3.08E-01	2.26E-40	SPINT1	2.71E-02	2.68E-07	STX17	5.42E-03	6.23E-06
SMIM10L1	1.38E-02	2.99E-04	SPINT2	9.97E-02	5.27E-05	STX3	5.57E-02	1.81E-07
SMIM14	4.30E-02	8.75E-09	SPOP	5.40E-02	3.90E-09	STX4	6.48E-02	2.34E-09
SMIM20	4.02E-02	1.61E-05	SPPL2B	8.22E-03	1.82E-05	STX5	6.72E-03	1.03E-03
SMIM26	3.53E-01	7.47E-57	SPRTN	3.26E-02	4.99E-06	STX7	2.03E-02	1.09E-05
SMIM27	3.81E-02	1.72E-04	SPSB3	5.52E-02	4.80E-06	STX8	1.68E-02	4.17E-06
SMIM29	4.64E-02	2.60E-12	SPTLC2	3.90E-02	2.83E-04	STXBP2	4.67E-02	1.32E-04
SMIM3	5.29E-02	3.56E-06	SPTY2D1	8.20E-03	2.32E-04	STXBP3	5.57E-03	5.92E-06
SMIM30	3.68E-03	4.45E-06	SQOR	4.19E-02	6.87E-07	SUCLG2	5.21E-02	1.72E-11
SMIM37	4.00E-03	1.16E-05	SQSTM1	1.24E-01	5.13E-11	SUCO	9.53E-04	1.50E-04
SMIM7	2.46E-02	7.82E-08	SRBD1	2.58E-02	9.65E-05	SUGT1	2.74E-02	4.57E-05
SMIM8	1.22E-02	6.73E-04	SREK1IP1	2.41E-02	3.67E-02	SULT1A1	6.24E-03	3.68E-03
SNAP23	1.61E-01	2.98E-24	SRFBP1	1.50E-03	2.98E-04	SUN1	2.49E-02	7.14E-06
SNAPC1	2.47E-02	9.23E-07	SRGN	7.10E-01	2.58E-166	SUN2	6.33E-02	2.73E-13
SNAPIN	5.53E-03	2.58E-04	SRI	2.75E-02	5.36E-08	SUPT20H	1.56E-03	1.78E-05
SNCA	9.33E-03	7.02E-07	SRP68	1.24E-02	7.92E-07	SUPT3H	3.86E-02	9.35E-08
SNHG12	1.37E-01	5.96E-32	SRPRA	4.01E-04	4.72E-08	SUPT4H1	7.93E-02	2.73E-07
SNHG25	4.34E-02	5.43E-03	SRSF5	2.82E-01	1.29E-58	SUPT5H	1.06E-02	2.64E-03
SNHG7	4.51E-01	1.09E-87	SRSF8	7.92E-02	2.66E-05	SUPT6H	1.68E-02	2.70E-04
SNHG8	2.57E-01	3.51E-43	SS18	8.34E-03	7.45E-06	SUPT7L	1.03E-02	8.67E-06
SNRK	4.61E-02	1.28E-05	SSBP2	1.44E-01	2.90E-12	SUPV3L1	9.25E-04	2.58E-04
SNRNP35	2.13E-02	2.39E-05	SSBP3	9.04E-02	1.14E-11	SURF1	5.39E-02	1.17E-07
SNRPN	1.88E-01	3.94E-24	SSBP4	6.50E-02	1.10E-07	SUSD3	4.49E-02	1.05E-08
SNTB1	3.04E-02	5.30E-07	SSR2	9.03E-02	4.98E-05	SV2A	6.49E-03	4.76E-04
SNW1	1.32E-02	6.34E-09	ST13	1.88E-01	2.25E-21	SVBP	2.43E-03	4.03E-05
SNX12	1.90E-03	3.91E-09	ST3GAL1	2.68E-02	7.24E-07	SVIL	2.92E-03	7.98E-03

Gene	logFC	FDR	Gene	logFC	FDR	Gene	logFC	FDR
SVOPL	7.24E-03	5.37E-04	TCTEX1D1	4.75E-02	1.56E-06	TMEM128	3.62E-03	2.41E-09
SWAP70	9.48E-02	3.21E-12	TCTN3	1.36E-04	1.35E-04	TMEM134	1.42E-02	5.39E-05
SWI5	3.29E-03	4.21E-07	TEN1	5.93E-03	8.31E-06	TMEM163	2.92E-02	5.84E-08
SYAP1	9.96E-02	8.61E-07	TENT2	3.38E-02	4.61E-05	TMEM167B	4.66E-02	1.85E-08
SYF2	2.33E-01	2.54E-22	TENT5A	6.33E-02	3.08E-11	TMEM170A	1.01E-02	1.16E-03
SYMPK	6.92E-02	5.89E-07	TENT5C	5.75E-02	1.48E-12	TMEM173	1.99E-01	2.46E-21
SYNJ2BP	7.45E-03	6.07E-05	TERF1	6.76E-03	3.70E-06	TMEM179B	2.65E-02	6.39E-05
SYNRG	1.87E-02	1.55E-05	TESMIN	9.10E-03	3.60E-05	TMEM192	5.86E-03	3.53E-02
SYPL1	1.65E-01	1.39E-13	TESPA1	7.32E-02	1.59E-08	TMEM205	7.27E-02	1.27E-06
SYS1	3.57E-02	2.30E-09	TET2	2.41E-02	1.16E-07	TMEM219	6.07E-02	3.56E-03
SYTL1	9.01E-02	2.88E-09	TEX264	5.84E-03	6.00E-04	TMEM222	3.23E-03	8.45E-06
SYTL4	4.89E-02	2.34E-07	TFEC	2.26E-02	7.63E-06	TMEM243	5.54E-02	1.78E-07
TAB2	1.99E-02	2.70E-04	TFPI	1.22E-01	2.00E-12	TMEM248	4.44E-03	1.89E-05
TACC1	5.73E-02	9.11E-05	TFPT	2.60E-02	1.10E-02	TMEM256	3.89E-02	2.53E-04
TAF11	2.37E-03	1.27E-03	TGFBRAP1	2.89E-03	1.83E-07	TMEM263	2.38E-02	4.70E-08
TAF1D	1.27E-01	6.37E-08	TGIF1	6.30E-02	1.78E-13	TMEM267	8.47E-03	4.65E-03
TAF7	7.93E-02	7.33E-04	TGOLN2	3.21E-03	1.49E-04	TMEM30A	1.35E-02	3.24E-06
TAF8	1.84E-03	8.08E-06	THAP1	2.48E-02	1.47E-04	TMEM38B	5.44E-02	3.32E-08
TAGAP	6.17E-02	2.90E-09	THAP4	9.73E-03	5.64E-04	TMEM42	4.24E-02	3.23E-05
TAL1	2.19E-02	9.40E-04	THEM4	8.29E-03	9.44E-06	TMEM43	6.54E-02	1.42E-12
TALDO1	2.14E-02	7.92E-04	THEMIS2	1.51E-01	1.30E-34	TMEM50B	1.54E-02	8.88E-08
TANK	5.06E-02	1.16E-06	THG1L	1.43E-02	8.17E-04	TMEM59	1.33E-01	4.18E-08
TAOK3	5.59E-02	9.31E-03	THUMPD1	1.59E-02	1.06E-05	TMEM68	7.05E-03	5.66E-06
TAPBP	2.83E-02	2.69E-05	TIE1	6.31E-02	1.63E-13	TMEM69	5.09E-02	5.11E-09
TAPBPL	5.52E-02	1.00E-09	TIMM9	9.75E-02	2.06E-09	TMEM80	2.62E-02	5.33E-07
TARBP1	5.12E-02	4.59E-04	TIMMDC1	6.46E-04	6.36E-03	TMEM9	5.48E-03	1.15E-04
TARSL2	5.40E-02	1.19E-09	TIMP1	1.75E-02	5.57E-03	TMEM91	1.38E-01	3.75E-23
TATDN1	1.28E-01	6.00E-13	TINF2	4.62E-02	6.72E-07	TMEM9B	5.93E-02	8.42E-10
TAX1BP1	8.11E-02	4.03E-08	TIPARP	1.38E-01	1.63E-19	TMF1	1.09E-02	3.45E-06
TAX1BP3	2.03E-04	6.60E-07	TIPRL	1.99E-02	1.90E-07	TMUB2	2.98E-02	2.44E-04
TAZ	1.25E-04	2.67E-04	TKT	8.11E-02	2.09E-03	TMX4	2.70E-02	8.01E-03
TBC1D10C	7.07E-02	7.42E-09	TLE4	9.50E-02	8.43E-10	TNFAIP3	9.68E-02	2.80E-05
TBC1D15	8.53E-04	1.02E-06	TLN1	3.24E-04	1.20E-02	TNFAIP8	1.93E-02	3.54E-03
TBC1D22A	1.23E-02	5.39E-04	TM2D2	2.31E-02	6.11E-04	TNFAIP8L1	2.30E-02	2.16E-03
TBC1D9B	1.71E-04	4.44E-05	TM2D3	9.01E-02	9.05E-13	TNFRSF14	1.72E-01	1.23E-27
TBCC	5.84E-02	1.97E-09	TM7SF2	3.98E-02	8.98E-09	TNFRSF1A	6.85E-02	7.31E-11
TBK1	2.76E-02	8.26E-10	TM9SF2	2.06E-02	3.47E-04	TNFSF10	5.85E-02	3.24E-11
TBRG1	9.05E-03	1.19E-05	TMBIM1	2.01E-02	4.64E-05	TNIP1	1.86E-02	1.38E-04
TBXAS1	9.36E-02	3.95E-11	TMBIM4	1.24E-01	3.88E-09	TNRC18	6.11E-03	5.92E-03
TCAIM	3.16E-02	5.44E-07	TMC6	3.38E-02	4.68E-05	TNRC6A	3.23E-02	1.14E-04
TCEAL1	5.03E-02	3.42E-06	TMC8	7.29E-02	3.73E-08	TNRC6B	3.86E-02	4.40E-05
TCEAL2	7.61E-02	3.72E-12	TMCO3	4.29E-03	3.95E-04	TOB1	2.31E-02	2.86E-03
TCEAL3	6.14E-03	2.00E-09	TMED1	1.18E-02	2.88E-03	TOB2	4.46E-02	2.39E-05
TCEAL4	1.03E-01	4.00E-08	TMED10	1.22E-02	2.02E-02	TOE1	3.07E-02	7.67E-08
TCEAL8	3.44E-02	6.97E-05	TMED3	8.03E-02	2.02E-04	TOLLIP	2.23E-02	2.16E-04
TCF25	1.12E-01	8.34E-07	TMED5	1.83E-02	1.03E-07	TOMM7	1.84E-01	1.34E-23
TCF7	2.95E-02	8.23E-05	TMED7	6.08E-02	1.53E-07	TOP1MT	4.94E-02	2.46E-07
TCF7L2	1.61E-02	1.95E-06	TMEM101	5.28E-03	8.81E-04	TOR1AIP1	3.68E-02	4.56E-08
TCOF1	1.47E-01	1.81E-14	TMEM106B	4.00E-02	7.65E-07	TOX	3.39E-02	1.15E-05
TCTA	2.96E-02	6.31E-04	TMEM126A	7.05E-03	9.68E-04	TOX4	5.98E-04	1.56E-02

Gene	logFC	FDR	Gene	logFC	FDR	Gene	logFC	FDR
SVOPL	7.24E-03	5.37E-04	TCTEX1D1	4.75E-02	1.56E-06	TMEM128	3.62E-03	2.41E-09
SWAP70	9.48E-02	3.21E-12	TCTN3	1.36E-04	1.35E-04	TMEM134	1.42E-02	5.39E-05
SWI5	3.29E-03	4.21E-07	TEN1	5.93E-03	8.31E-06	TMEM163	2.92E-02	5.84E-08
SYAP1	9.96E-02	8.61E-07	TENT2	3.38E-02	4.61E-05	TMEM167B	4.66E-02	1.85E-08
SYF2	2.33E-01	2.54E-22	TENT5A	6.33E-02	3.08E-11	TMEM170A	1.01E-02	1.16E-03
SYMPK	6.92E-02	5.89E-07	TENT5C	5.75E-02	1.48E-12	TMEM173	1.99E-01	2.46E-21
SYNJ2BP	7.45E-03	6.07E-05	TERF1	6.76E-03	3.70E-06	TMEM179B	2.65E-02	6.39E-05
SYNRG	1.87E-02	1.55E-05	TESMIN	9.10E-03	3.60E-05	TMEM192	5.86E-03	3.53E-02
SYPL1	1.65E-01	1.39E-13	TESPA1	7.32E-02	1.59E-08	TMEM205	7.27E-02	1.27E-06
SYS1	3.57E-02	2.30E-09	TET2	2.41E-02	1.16E-07	TMEM219	6.07E-02	3.56E-03
SYTL1	9.01E-02	2.88E-09	TEX264	5.84E-03	6.00E-04	TMEM222	3.23E-03	8.45E-06
SYTL4	4.89E-02	2.34E-07	TFEC	2.26E-02	7.63E-06	TMEM243	5.54E-02	1.78E-07
TAB2	1.99E-02	2.70E-04	TFPI	1.22E-01	2.00E-12	TMEM248	4.44E-03	1.89E-05
TACC1	5.73E-02	9.11E-05	TFPT	2.60E-02	1.10E-02	TMEM256	3.89E-02	2.53E-04
TAF11	2.37E-03	1.27E-03	TGFBRAP1	2.89E-03	1.83E-07	TMEM263	2.38E-02	4.70E-08
TAF1D	1.27E-01	6.37E-08	TGIF1	6.30E-02	1.78E-13	TMEM267	8.47E-03	4.65E-03
TAF7	7.93E-02	7.33E-04	TGOLN2	3.21E-03	1.49E-04	TMEM30A	1.35E-02	3.24E-06
TAF8	1.84E-03	8.08E-06	THAP1	2.48E-02	1.47E-04	TMEM38B	5.44E-02	3.32E-08
TAGAP	6.17E-02	2.90E-09	THAP4	9.73E-03	5.64E-04	TMEM42	4.24E-02	3.23E-05
TAL1	2.19E-02	9.40E-04	THEM4	8.29E-03	9.44E-06	TMEM43	6.54E-02	1.42E-12
TALDO1	2.14E-02	7.92E-04	THEMIS2	1.51E-01	1.30E-34	TMEM50B	1.54E-02	8.88E-08
TANK	5.06E-02	1.16E-06	THG1L	1.43E-02	8.17E-04	TMEM59	1.33E-01	4.18E-08
TAOK3	5.59E-02	9.31E-03	THUMPD1	1.59E-02	1.06E-05	TMEM68	7.05E-03	5.66E-06
TAPBP	2.83E-02	2.69E-05	TIE1	6.31E-02	1.63E-13	TMEM69	5.09E-02	5.11E-09
TAPBPL	5.52E-02	1.00E-09	TIMM9	9.75E-02	2.06E-09	TMEM80	2.62E-02	5.33E-07
TARBP1	5.12E-02	4.59E-04	TIMMDC1	6.46E-04	6.36E-03	TMEM9	5.48E-03	1.15E-04
TARSL2	5.40E-02	1.19E-09	TIMP1	1.75E-02	5.57E-03	TMEM91	1.38E-01	3.75E-23
TATDN1	1.28E-01	6.00E-13	TINF2	4.62E-02	6.72E-07	TMEM9B	5.93E-02	8.42E-10
TAX1BP1	8.11E-02	4.03E-08	TIPARP	1.38E-01	1.63E-19	TMF1	1.09E-02	3.45E-06
TAX1BP3	2.03E-04	6.60E-07	TIPRL	1.99E-02	1.90E-07	TMUB2	2.98E-02	2.44E-04
TAZ	1.25E-04	2.67E-04	TKT	8.11E-02	2.09E-03	TMX4	2.70E-02	8.01E-03
TBC1D10C	7.07E-02	7.42E-09	TLE4	9.50E-02	8.43E-10	TNFAIP3	9.68E-02	2.80E-05
TBC1D15	8.53E-04	1.02E-06	TLN1	3.24E-04	1.20E-02	TNFAIP8	1.93E-02	3.54E-03
TBC1D22A	1.23E-02	5.39E-04	TM2D2	2.31E-02	6.11E-04	TNFAIP8L1	2.30E-02	2.16E-03
TBC1D9B	1.71E-04	4.44E-05	TM2D3	9.01E-02	9.05E-13	TNFRSF14	1.72E-01	1.23E-27
TBCC	5.84E-02	1.97E-09	TM7SF2	3.98E-02	8.98E-09	TNFRSF1A	6.85E-02	7.31E-11
TBK1	2.76E-02	8.26E-10	TM9SF2	2.06E-02	3.47E-04	TNFSF10	5.85E-02	3.24E-11
TBRG1	9.05E-03	1.19E-05	TMBIM1	2.01E-02	4.64E-05	TNIP1	1.86E-02	1.38E-04
TBXAS1	9.36E-02	3.95E-11	TMBIM4	1.24E-01	3.88E-09	TNRC18	6.11E-03	5.92E-03
TCAIM	3.16E-02	5.44E-07	TMC6	3.38E-02	4.68E-05	TNRC6A	3.23E-02	1.14E-04
TCEAL1	5.03E-02	3.42E-06	TMC8	7.29E-02	3.73E-08	TNRC6B	3.86E-02	4.40E-05
TCEAL2	7.61E-02	3.72E-12	TMCO3	4.29E-03	3.95E-04	TOB1	2.31E-02	2.86E-03
TCEAL3	6.14E-03	2.00E-09	TMED1	1.18E-02	2.88E-03	TOB2	4.46E-02	2.39E-05
TCEAL4	1.03E-01	4.00E-08	TMED10	1.22E-02	2.02E-02	TOE1	3.07E-02	7.67E-08
TCEAL8	3.44E-02	6.97E-05	TMED3	8.03E-02	2.02E-04	TOLLIP	2.23E-02	2.16E-04
TCF25	1.12E-01	8.34E-07	TMED5	1.83E-02	1.03E-07	TOMM7	1.84E-01	1.34E-23
TCF7	2.95E-02	8.23E-05	TMED7	6.08E-02	1.53E-07	TOP1MT	4.94E-02	2.46E-07
TCF7L2	1.61E-02	1.95E-06	TMEM101	5.28E-03	8.81E-04	TOR1AIP1	3.68E-02	4.56E-08
TCOF1	1.47E-01	1.81E-14	TMEM106B	4.00E-02	7.65E-07	TOX	3.39E-02	1.15E-05
TCTA	2.96E-02	6.31E-04	TMEM126A	7.05E-03	9.68E-04	TOX4	5.98E-04	1.56E-02

Gene	logFC	FDR	Gene	logFC	FDR	Gene	logFC	FDR
WDR45B	5.94E-02	3.77E-09	ZEB1	1.42E-02	2.67E-04	ZNF521	1.28E-03	4.56E-05
WDR6	4.90E-02	3.57E-08	ZEB2	6.01E-02	1.76E-05	ZNF559	2.69E-02	1.94E-06
WDR82	5.78E-03	3.39E-02	ZFAND1	2.19E-01	1.23E-27	ZNF581	9.64E-02	1.28E-16
WDR83OS	5.25E-02	1.38E-05	ZFAND2A	4.16E-02	4.34E-09	ZNF586	1.30E-02	2.55E-02
WDSUB1	2.33E-02	6.80E-05	ZFAND3	2.60E-02	1.54E-05	ZNF609	1.35E-02	3.66E-03
WIPF1	4.90E-02	2.70E-07	ZFAND5	5.20E-02	1.49E-03	ZNF622	1.95E-03	1.54E-04
WRNIP1	9.63E-04	4.94E-05	ZFAND6	6.29E-02	5.07E-08	ZNF638	5.02E-03	3.99E-03
WSB1	2.75E-01	7.49E-37	ZFAS1	4.19E-01	1.58E-174	ZNF654	8.97E-03	2.81E-05
XAB2	3.61E-02	9.44E-06	ZFC3H1	3.33E-02	9.53E-06	ZNF655	3.98E-02	3.99E-09
XAF1	7.00E-02	5.10E-11	ZFHX3	1.34E-02	9.66E-07	ZNF660	3.76E-03	3.80E-02
XBP1	1.61E-01	2.26E-09	ZFP36	2.72E-01	4.73E-24	ZNF669	2.33E-02	2.30E-05
XPA	5.16E-02	5.13E-05	ZFPL1	5.65E-03	1.30E-02	ZNF677	2.94E-02	1.37E-06
XPC	4.61E-02	7.36E-06	ZFR	2.93E-03	2.33E-04	ZNF680	1.56E-02	1.05E-04
XPNPEP3	1.29E-02	4.87E-03	ZFYVE21	4.95E-02	7.11E-10	ZNF706	6.94E-02	6.82E-10
XPO7	2.66E-02	2.14E-07	ZKSCAN1	8.21E-02	3.28E-07	ZNF721	1.87E-02	2.98E-05
XRRA1	3.19E-02	2.97E-04	ZMAT1	2.86E-03	6.49E-03	ZNF75A	1.82E-03	4.18E-02
XXYLT1-AS2	4.18E-02	2.79E-11	ZMAT5	2.45E-02	1.67E-06	ZNF766	2.45E-02	1.53E-06
YBEY	7.24E-02	1.65E-13	ZMIZ1	1.26E-02	7.07E-04	ZNF791	1.37E-02	3.71E-05
YES1	4.42E-02	8.58E-09	ZMYM2	4.01E-02	5.89E-05	ZNF800	8.34E-04	7.64E-03
YIPF2	5.40E-02	5.29E-06	ZMYM5	2.15E-02	1.22E-03	ZNF83	4.64E-02	3.85E-06
YIPF3	3.76E-02	1.40E-09	ZMYND8	3.29E-02	5.57E-03	ZNF830	1.92E-02	4.06E-06
YIPF4	3.67E-02	2.37E-07	ZNF106	1.23E-02	8.90E-05	ZNF880	2.10E-02	1.40E-04
YIPF6	9.21E-03	2.41E-07	ZNF136	1.05E-02	1.33E-02	ZNHIT3	2.63E-02	2.09E-05
YJU2	3.07E-02	1.34E-06	ZNF148	3.27E-02	8.62E-06	ZNHIT6	9.55E-03	1.20E-03
YME1L1	1.15E-02	1.26E-06	ZNF219	4.81E-03	3.24E-03	ZNRD1	4.66E-03	6.36E-03
YPEL3	6.87E-02	3.40E-13	ZNF226	4.06E-02	1.31E-08	ZP3	4.46E-02	9.11E-09
YPEL5	2.99E-01	4.75E-31	ZNF24	4.76E-02	7.20E-07	ZRANB2	3.76E-02	2.13E-02
YTHDC1	6.06E-02	9.65E-08	ZNF254	1.94E-02	5.42E-04	ZRSR2	5.52E-03	1.89E-06
YWHAG	6.41E-03	2.02E-04	ZNF263	3.81E-03	2.08E-02	ZSCAN18	7.90E-02	1.03E-09
YWHAZ	3.15E-02	8.65E-04	ZNF274	5.64E-02	3.25E-09	ZSWIM7	3.88E-02	7.73E-05
YY1AP1	1.01E-02	3.42E-04	ZNF277	4.68E-02	6.85E-08	ZYX	9.20E-02	3.16E-10
ZBED5	1.98E-02	1.03E-03	ZNF280D	1.87E-02	3.95E-04			
ZBED5-AS1	1.73E-02	2.80E-05	ZNF281	6.46E-02	3.62E-06			
ZBTB1	1.54E-02	1.21E-03	ZNF302	7.12E-02	5.68E-11			
ZBTB10	2.15E-03	2.80E-04	ZNF32	4.43E-02	1.04E-06			
ZBTB16	3.22E-02	5.23E-11	ZNF330	2.81E-02	3.12E-04			
ZBTB20	1.91E-01	2.70E-28	ZNF331	1.01E-01	2.04E-12			
ZBTB21	2.59E-02	1.05E-09	ZNF33A	1.46E-02	1.83E-02			
ZBTB24	1.48E-02	7.69E-04	ZNF33B	3.46E-02	7.30E-05			
ZBTB38	1.49E-02	2.55E-06	ZNF350	2.00E-02	1.04E-03			
ZBTB43	2.48E-03	7.99E-05	ZNF385D	4.80E-02	9.05E-09			
ZBTB44	8.73E-03	2.45E-04	ZNF394	1.06E-01	9.06E-16			
ZBTB7A	1.24E-02	3.19E-04	ZNF395	7.28E-04	4.61E-03			
ZBTB8A	5.21E-03	2.60E-02	ZNF397	3.81E-02	3.48E-06			
ZC3H12A	5.19E-02	6.22E-08	ZNF426	1.61E-02	4.20E-07			
ZC3H7A	5.90E-03	5.14E-07	ZNF431	5.01E-04	8.11E-04			
ZCCHC10	2.23E-02	1.77E-05	ZNF439	5.86E-03	1.18E-03			
ZCCHC7	6.78E-02	7.52E-08	ZNF44	9.06E-03	2.39E-04			
ZDHHC21	1.93E-02	2.35E-04	ZNF480	1.05E-02	3.22E-04			
ZDHHC24	1.09E-02	8.52E-03	ZNF518A	1.09E-02	5.35E-04			

D2- downregulated in young donor platelet -biased HSCs

Gene	logFC	FDR	Gene	logFC	FDR	Gene	logFC	FDR
AAMP	-6.22E-02	3.14E-15	ADSL	-2.74E-02	1.32E-06	ANKRD26	-1.55E-02	1.12E-03
AATF	-2.26E-02	2.81E-05	ADSS	-4.73E-03	1.12E-04	ANKRD36	-5.23E-02	1.47E-09
ABCE1	-5.20E-02	1.19E-08	AEBP2	-2.42E-03	1.17E-05	ANKRD36B	-2.50E-03	3.04E-02
ABCF1	-6.49E-02	4.68E-09	AFF1	-6.37E-03	3.69E-03	ANKRD36C	-6.30E-02	7.26E-10
ABHD12	-2.79E-02	8.93E-08	AFG3L2	-5.44E-02	6.21E-11	ANKRD39	-1.66E-02	1.56E-06
ABHD14A	-4.76E-02	3.14E-09	AFMID	-8.41E-02	1.04E-16	ANKRD40	-5.99E-02	5.06E-11
ABHD17B	-1.03E-02	3.47E-03	AGA	-7.99E-03	1.04E-02	ANP32A	-9.56E-02	1.43E-19
ABHD5	-1.18E-02	4.06E-02	AGO1	-3.12E-03	6.81E-03	ANP32B	-2.60E-01	5.53E-51
ABI2	-6.99E-03	1.18E-03	AGO2	-3.45E-02	2.65E-05	ANP32E	-2.26E-01	5.06E-57
ABRACL	-2.22E-01	1.42E-44	AGO3	-6.26E-03	1.98E-04	ANXA11	-1.05E-02	3.91E-06
AC005921.2	-5.87E-02	6.87E-14	AGPAT2	-3.04E-02	5.15E-13	ANXA5	-1.33E-01	3.43E-23
AC007952.4	-2.20E-02	1.06E-03	AGPAT5	-2.50E-03	9.84E-05	AP002360.1	-7.42E-02	2.57E-19
AC010642.2	-2.95E-02	6.64E-07	AGPS	-2.69E-03	4.17E-06	AP1B1	-9.78E-03	1.03E-02
AC012360.3	-1.38E-02	9.48E-03	AGTRAP	-3.42E-02	1.87E-07	AP1M1	-2.15E-02	2.06E-06
AC026979.2	-1.29E-02	4.63E-04	AHCY	-1.98E-01	1.42E-43	AP1S1	-3.92E-02	6.76E-14
AC084033.3	-1.45E-01	6.41E-16	AHCYL1	-4.48E-02	1.05E-09	AP1S2	-8.16E-03	2.83E-06
AC118549.1	-4.92E-03	3.52E-04	AHI1	-3.17E-02	3.37E-05	AP2A1	-2.61E-02	4.32E-06
AC245014.3	-4.77E-02	5.16E-07	AHSA1	-9.82E-02	5.13E-20	AP2B1	-2.82E-03	6.19E-07
ACAA2	-8.73E-02	2.68E-20	AIDA	-8.97E-04	3.07E-05	AP2M1	-1.01E-01	1.69E-17
ACADM	-4.15E-02	2.60E-11	AIG1	-4.64E-03	1.37E-04	AP2S1	-2.88E-01	3.67E-87
ACADVL	-4.49E-02	4.83E-12	AK2	-1.27E-01	2.82E-21	AP3B1	-3.72E-02	3.93E-12
ACAP2	-4.47E-03	2.31E-04	AK3	-6.70E-02	4.39E-15	AP3D1	-3.35E-02	1.04E-11
ACAT1	-2.33E-02	6.27E-06	AK6	-6.82E-02	1.12E-14	AP3S1	-1.01E-01	6.28E-20
ACAT2	-6.93E-02	9.12E-17	AKIP1	-8.55E-03	1.72E-05	AP5M1	-3.33E-03	1.39E-03
ACBD6	-3.75E-02	1.04E-11	AKR1A1	-1.15E-01	7.75E-14	APEX1	-6.53E-02	1.16E-02
ACD	-5.28E-02	2.80E-17	AKR1B1	-1.23E-01	3.82E-26	APH1A	-2.55E-03	2.80E-03
ACIN1	-2.57E-02	8.56E-09	AKR7A2	-1.61E-01	4.33E-40	API5	-2.65E-02	2.94E-07
ACLY	-4.42E-02	3.08E-11	AKT2	-1.37E-02	2.71E-02	APIP	-4.87E-02	4.91E-08
ACO2	-1.82E-02	1.26E-06	AL157938.3	-6.82E-02	1.78E-13	APOBEC3C	-9.29E-02	2.50E-18
ACP1	-1.71E-01	9.18E-29	AL390728.6	-1.07E-02	6.26E-07	APOPT1	-1.64E-02	1.27E-06
ACSF3	-2.04E-03	2.37E-05	ALCAM	-4.46E-03	1.24E-02	APPL1	-5.58E-02	8.45E-11
ACSL3	-1.14E-02	1.75E-03	ALDH16A1	-4.10E-02	1.65E-08	ARAF	-1.95E-02	8.36E-06
ACTB	-2.86E-01	6.99E-92	ALDH18A1	-6.33E-02	2.68E-14	ARF3	-2.41E-02	8.43E-06
ACTL6A	-1.25E-01	8.26E-39	ALDH6A1	-1.83E-02	1.87E-05	ARF5	-3.92E-02	3.43E-09
ACTN1	-3.29E-02	1.90E-05	ALDOA	-7.11E-02	9.89E-16	ARF6	-1.36E-01	1.11E-31
ACTN4	-5.56E-02	4.06E-09	ALG3	-4.00E-02	2.06E-05	ARFIP2	-4.13E-03	1.62E-04
ACTR2	-4.41E-02	2.29E-08	ALG5	-6.43E-02	9.33E-18	ARGLU1	-2.01E-03	6.79E-11
ACTR3	-5.16E-02	3.54E-12	ALG8	-3.07E-02	1.84E-08	ARHGAP4	-2.77E-02	1.46E-05
ACYP1	-1.30E-01	1.98E-37	ALKBH2	-4.04E-03	1.98E-05	ARHGDIA	-8.65E-02	7.16E-17
ADA	-4.31E-02	4.12E-08	AMFR	-1.02E-01	1.50E-28	ARID1A	-1.38E-02	6.59E-05
ADAM10	-1.10E-02	1.22E-04	ANAPC11	-2.46E-01	2.88E-68	ARID1B	-8.26E-03	6.42E-04
ADAM15	-4.29E-02	5.11E-07	ANAPC13	-2.49E-03	2.49E-05	ARID4A	-9.24E-03	4.73E-04
ADAM17	-9.82E-02	2.41E-16	ANAPC15	-1.05E-01	4.64E-22	ARID4B	-7.09E-03	2.28E-04
ADI1	-8.24E-02	2.17E-13	ANAPC5	-1.31E-01	4.87E-20	ARIH1	-2.03E-02	4.32E-07
ADIPOR1	-7.67E-02	9.72E-25	ANAPC7	-1.44E-02	5.74E-04	ARIH2	-3.26E-02	8.84E-05
ADIPOR2	-5.00E-03	2.61E-08	ANKLE2	-3.53E-02	2.24E-06	ARL16	-3.02E-02	5.30E-06
ADK	-6.74E-02	4.31E-15	ANKRD10	-5.08E-02	2.56E-06	ARL2	-2.23E-01	2.16E-63
ADNP	-5.01E-02	2.76E-11	ANKRD11	-6.64E-02	1.45E-11	ARL3	-2.04E-02	3.23E-04
ADPGK	-1.45E-02	1.56E-08	ANKRD13A	-5.76E-03	2.53E-07	ARL5A	-1.75E-02	1.64E-06
ADRM1	-5.38E-02	1.26E-10	ANKRD17	-1.01E-02	1.45E-05	ARL6IP1	-5.32E-04	5.90E-17

Gene	logFC	FDR	Gene	logFC	FDR	Gene	logFC	FDR
ARL6IP4	-1.41E-01	3.07E-18	ATP5MG	-5.80E-02	2.07E-04	BLOC1S6	-1.46E-03	1.14E-05
ARL6IP6	-2.19E-01	6.40E-71	ATP5MPL	-2.66E-01	1.97E-45	BLVRB	-1.58E-02	1.03E-05
ARL8B	-3.45E-02	1.07E-07	ATP5PB	-5.47E-02	1.09E-05	BMS1	-3.05E-02	1.09E-08
ARMC1	-2.20E-02	1.52E-06	ATP5PD	-1.51E-01	5.52E-23	BOD1L1	-1.60E-02	1.26E-04
ARMC10	-5.83E-02	1.14E-12	ATP5PF	-1.69E-01	2.45E-27	BOLA3	-1.11E-01	1.04E-20
ARMC8	-9.39E-03	1.80E-06	ATP5PO	-3.89E-02	1.95E-06	BOP1	-4.33E-02	9.83E-08
ARMH1	-1.12E-01	3.99E-16	ATP5S	-1.62E-02	2.01E-06	BRAF	-2.02E-02	1.13E-08
ARPC1A	-9.17E-02	1.07E-18	ATP6AP2	-5.53E-03	1.10E-09	BRD2	-3.78E-02	1.30E-10
ARPC1B	-3.24E-02	2.79E-09	ATP6V0A2	-7.23E-03	7.47E-08	BRD3	-5.53E-02	4.94E-10
ARPC2	-2.93E-01	1.12E-64	ATP6V0B	-4.40E-02	1.00E-13	BRD4	-4.96E-02	3.27E-07
ARPC3	-1.34E-02	4.80E-04	ATP6V0D1	-6.62E-04	1.20E-07	BRD7	-5.95E-02	2.07E-12
ARPC4	-1.39E-01	2.31E-36	ATP6V0E1	-4.69E-02	7.37E-08	BRD9	-1.25E-02	1.92E-03
ARPC5	-1.81E-01	3.76E-27	ATP6V0E2	-4.56E-02	4.83E-15	BRIX1	-3.92E-03	1.19E-05
ARPC5L	-6.85E-02	7.76E-12	ATP6V1D	-2.38E-02	8.30E-04	BRK1	-5.04E-02	1.71E-07
ARPP19	-7.12E-02	1.35E-14	ATP6V1H	-1.10E-02	1.54E-08	BROX	-6.49E-03	1.22E-10
ARRB2	-7.45E-03	4.80E-09	ATPAF2	-4.60E-04	2.56E-05	BSG	-2.07E-01	4.52E-38
ARV1	-1.74E-02	3.18E-13	ATXN10	-4.77E-02	8.21E-11	BST1	-2.85E-02	1.93E-07
ASCC3	-1.92E-02	4.32E-06	ATXN2L	-4.76E-02	3.94E-10	BTBD1	-1.43E-02	1.12E-03
ASH1L	-5.99E-03	6.68E-03	AURKAIP1	-1.11E-01	2.23E-24	BTF3L4	-8.99E-03	2.13E-04
ASH2L	-1.08E-03	7.08E-04	AZIN1	-6.88E-02	1.03E-10	BTG3	-4.87E-02	1.86E-06
ASMTL	-1.91E-03	4.27E-06	B3GAT3	-3.44E-02	2.82E-08	BUB3	-7.96E-02	2.00E-15
ASNA1	-5.95E-02	2.61E-14	BABAM1	-2.61E-02	1.79E-08	BUD31	-5.55E-02	1.41E-11
ASPH	-2.50E-02	3.43E-06	BAD	-4.75E-02	3.25E-07	BX284668.5	-4.97E-02	1.84E-11
ASXL1	-2.14E-02	7.77E-09	BAG1	-1.23E-01	1.61E-21	BZW1	-1.02E-01	1.77E-14
ATAD2	-1.45E-01	2.15E-49	BAG6	-6.96E-03	7.85E-05	BZW2	-4.36E-02	3.82E-03
ATF1	-7.29E-03	7.95E-10	BANF1	-2.68E-01	6.79E-65	C11orf58	-9.37E-02	3.83E-17
ATF7	-1.79E-03	9.24E-03	BAX	-1.24E-01	1.89E-17	C12orf43	-2.56E-03	5.68E-04
ATF7IP	-1.34E-03	3.07E-02	BAZ1A	-5.97E-02	4.13E-08	C12orf57	-2.37E-01	1.59E-40
ATG10	-2.36E-02	1.24E-06	BAZ1B	-1.47E-01	5.13E-38	C12orf75	-1.50E-01	3.02E-43
ATG12	-1.27E-02	2.71E-04	BCAP29	-3.44E-02	1.63E-07	C15orf40	-9.50E-03	2.89E-07
ATG3	-1.04E-01	2.73E-21	BCAP31	-5.56E-02	4.22E-15	C15orf61	-6.01E-03	4.31E-02
ATG5	-1.46E-02	2.52E-07	BCAS4	-1.07E-03	1.20E-05	C16orf54	-6.01E-03	8.44E-04
ATIC	-3.26E-02	1.17E-06	BCAT2	-4.73E-02	1.78E-09	C16orf91	-4.32E-02	1.78E-08
ATL3	-5.54E-02	4.53E-15	BCCIP	-2.77E-02	1.07E-05	C19orf24	-2.58E-02	5.81E-09
ATOX1	-1.05E-01	1.14E-22	BCKDK	-1.68E-02	1.99E-07	C19orf25	-1.45E-02	3.89E-04
ATP1A1	-1.75E-01	2.09E-30	BCL10	-1.35E-02	3.33E-07	C19orf48	-3.68E-01	2.30E-102
ATP1B1	-9.86E-03	6.65E-03	BCL11A	-9.48E-02	2.73E-08	C19orf53	-3.15E-02	1.94E-07
ATP1B3	-1.69E-01	1.35E-24	BCL7A	-1.91E-02	4.63E-05	C19orf70	-2.63E-02	1.35E-07
ATP2A3	-3.73E-02	2.05E-09	BCL7B	-1.89E-02	4.92E-07	C1D	-1.95E-04	1.37E-04
ATP2B1	-1.55E-02	5.36E-05	BCL7C	-5.78E-02	2.35E-15	C1GALT1	-2.49E-02	3.08E-04
ATP5F1A	-4.70E-02	2.73E-05	BCLAF1	-1.27E-01	1.36E-11	C1QBP	-3.44E-01	4.62E-79
ATP5F1B	-1.37E-01	2.03E-24	BDP1	-8.37E-02	1.64E-09	C1QTNF4	-1.36E-01	8.06E-14
ATP5F1C	-8.57E-02	2.92E-08	BEX1	-3.22E-02	9.47E-04	C1orf131	-2.23E-02	4.04E-06
ATP5F1E	-1.81E-01	2.77E-30	BEX3	-1.75E-01	3.69E-27	C1orf174	-5.79E-02	2.23E-13
ATP5IF1	-1.58E-01	3.36E-20	BICD1	-1.17E-02	6.48E-06	C1orf35	-2.98E-02	6.18E-07
ATP5MC1	-4.07E-01	3.29E-143	BID	-6.18E-02	1.43E-11	C1orf43	-1.03E-02	2.54E-05
ATP5MC3	-3.10E-01	7.65E-75	BIRC6	-2.98E-02	2.72E-04	C1orf52	-1.93E-02	1.67E-05
ATP5MD	-2.34E-01	1.35E-42	BLMH	-5.72E-02	2.00E-11	C1orf56	-1.11E-01	5.29E-19
ATP5ME	-2.15E-01	2.76E-42	BLOC1S1	-1.91E-01	3.47E-52	C20orf27	-1.35E-01	1.41E-31
ATP5MF	-3.90E-01	1.15E-114	BLOC1S2	-6.02E-02	6.38E-12	C21orf2	-2.37E-03	1.37E-04

Gene	logFC	FDR	Gene	logFC	FDR	Gene	logFC	FDR
C22orf39	-7.00E-02	8.52E-14	CCDC66	-2.72E-02	6.24E-06	CEP350	-2.17E-02	3.34E-06
C2orf68	-1.68E-02	1.62E-05	CCDC82	-2.32E-02	9.52E-11	CEP57	-7.61E-02	2.73E-14
C3orf14	-6.85E-02	6.05E-15	CCDC85B	-1.17E-02	3.29E-07	CEP63	-4.08E-02	5.27E-08
C3orf38	-1.58E-02	1.18E-05	CCDC88A	-5.54E-02	9.17E-11	CEP83	-3.21E-02	9.04E-06
C4orf48	-4.18E-02	9.00E-12	CCNB1IP1	-5.10E-02	1.13E-07	CERS2	-1.88E-02	1.88E-08
C5orf24	-3.07E-02	1.04E-03	CCNC	-4.46E-02	3.08E-06	CERS6	-1.04E-02	2.69E-07
C5orf30	-4.12E-02	4.49E-08	CCNK	-9.62E-03	8.27E-04	CETN2	-3.71E-02	1.29E-04
C6orf62	-8.25E-02	6.28E-08	CCNL1	-6.29E-03	1.59E-02	CETN3	-6.32E-03	7.55E-05
C8orf33	-5.92E-02	5.18E-12	CCNY	-1.57E-02	1.55E-06	CFAP97	-2.39E-02	1.04E-04
C9orf16	-9.01E-02	8.02E-16	CCP110	-3.01E-02	3.41E-10	CFDP1	-8.58E-02	6.57E-10
C9orf78	-2.55E-02	1.20E-09	CCT2	-1.56E-01	1.54E-31	CFL1	-5.05E-01	2.46E-236
CACYBP	-2.71E-01	1.35E-89	CCT5	-1.53E-01	1.31E-38	CHCHD1	-6.62E-02	1.57E-10
CALM1	-1.32E-01	1.58E-17	CCT6A	-1.03E-01	1.96E-21	CHCHD10	-5.16E-02	2.61E-13
CALM2	-1.39E-01	1.15E-23	CCT7	-8.17E-02	1.76E-13	CHCHD2	-3.63E-01	3.12E-126
CALM3	-1.96E-01	1.69E-51	CCZ1	-3.30E-02	1.78E-12	CHCHD3	-1.48E-01	2.21E-29
CALR	-4.63E-01	7.18E-123	CD2AP	-2.95E-02	1.01E-06	CHD1	-2.49E-02	6.95E-07
CALU	-4.59E-02	1.54E-08	CD2BP2	-9.26E-03	1.55E-06	CHD1L	-5.39E-02	3.61E-15
CAMTA1	-1.74E-01	4.25E-37	CD47	-1.01E-01	1.60E-16	CHD3	-7.15E-03	5.47E-03
CAND1	-2.26E-02	5.91E-09	CD59	-3.81E-02	3.93E-08	CHD4	-7.90E-02	2.43E-10
CAPG	-1.37E-01	3.49E-28	CD69	-9.18E-02	4.77E-04	CHD8	-2.33E-02	3.33E-06
CAPNS1	-2.55E-02	7.88E-05	CD81	-2.44E-02	6.21E-08	CHID1	-9.23E-02	7.34E-26
CAPRIN1	-4.46E-02	2.15E-08	CD99	-1.36E-01	9.89E-16	CHMP1A	-2.33E-02	1.46E-07
CAPZA1	-1.33E-01	1.80E-26	CDC123	-6.11E-02	1.62E-10	CHMP4B	-3.60E-02	1.51E-09
CARHSP1	-2.28E-01	9.99E-72	CDC37	-5.63E-02	3.07E-08	CHRAC1	-1.38E-01	1.26E-27
CARNMT1	-1.65E-03	7.25E-04	CDC42	-2.08E-01	1.18E-22	CHTF8	-2.59E-02	4.44E-10
CASC3	-8.90E-03	5.14E-04	CDC42SE1	-6.13E-02	1.02E-08	CIAO1	-1.18E-03	1.64E-05
CASP2	-1.36E-01	1.13E-30	CDC5L	-5.79E-02	1.82E-12	CIAPIN1	-3.71E-02	7.67E-10
CASP6	-1.26E-03	7.66E-03	CDCA4	-9.74E-02	5.87E-36	CIB1	-3.75E-02	1.81E-10
CASP8	-5.02E-03	8.44E-05	CDCA7L	-2.29E-01	1.89E-62	CINP	-2.73E-03	6.52E-04
CBFB	-1.81E-02	2.26E-06	CDK11B	-3.79E-03	8.67E-03	CISD1	-3.38E-02	4.84E-07
CBR1	-2.53E-02	1.31E-07	CDK12	-1.05E-02	1.13E-06	CISD2	-1.04E-01	1.37E-16
CBWD1	-7.65E-02	1.89E-11	CDK13	-1.20E-02	8.01E-04	CISD3	-4.10E-02	1.35E-06
CBWD5	-2.97E-02	8.61E-05	CDK2	-1.44E-01	5.81E-53	CKAP2	-6.60E-02	3.11E-16
CBX1	-1.63E-01	2.17E-34	CDK2AP1	-5.07E-02	7.93E-08	CKB	-2.44E-02	1.94E-12
CBX2	-1.79E-02	2.06E-07	CDK2AP2	-8.81E-02	7.22E-19	CKLF	-2.16E-01	7.64E-54
CBX3	-3.32E-01	4.25E-81	CDK4	-4.36E-01	1.37E-162	CKS1B	-4.48E-01	3.18E-171
CBX5	-3.03E-01	6.01E-86	CDK5RAP3	-3.19E-02	7.19E-08	CKS2	-1.79E-01	2.43E-45
CBX6	-9.27E-02	5.46E-12	CDK6	-3.53E-01	3.80E-62	CLASRP	-1.36E-02	1.18E-09
CCAR1	-2.75E-02	1.06E-04	CDKN2AIPNL	-5.38E-02	3.06E-11	CLDN10	-3.44E-02	1.86E-10
CCAR2	-1.83E-03	1.09E-05	CEBPG	-5.45E-02	1.00E-10	CLEC11A	-1.00E-01	1.24E-22
CCDC124	-6.00E-02	3.33E-13	CEBPZ	-2.38E-02	1.61E-05	CLNS1A	-8.10E-02	8.94E-09
CCDC14	-1.75E-01	4.50E-35	CELF1	-1.14E-02	1.29E-03	CLPP	-7.99E-02	1.51E-16
CCDC167	-1.58E-01	1.10E-53	CENPH	-4.86E-01	1.80E-217	CLPTM1	-1.82E-02	4.22E-09
CCDC18	-8.05E-02	9.12E-16	CENPT	-9.32E-03	7.86E-06	CLPX	-4.84E-03	4.29E-03
CCDC25	-1.08E-02	1.51E-03	CENPV	-1.16E-01	2.78E-33	CLTA	-2.66E-02	4.11E-08
CCDC28B	-5.04E-02	9.08E-14	CENPW	-1.79E-01	2.58E-65	CLTB	-3.22E-02	1.24E-06
CCDC34	-1.39E-01	1.93E-36	CENPX	-1.60E-01	2.63E-38	CLTC	-1.34E-02	1.07E-04
CCDC43	-9.83E-03	5.63E-06	CEP135	-2.70E-02	4.99E-05	CMAS	-1.72E-02	9.36E-07
CCDC47	-3.88E-02	1.22E-04	CEP170	-2.89E-02	1.50E-04	CMC1	-3.62E-02	6.35E-07
CCDC58	-3.84E-02	1.78E-06	CEP290	-4.46E-02	3.77E-05	CMC2	-5.42E-02	1.58E-12

Gene	logFC	FDR	Gene	logFC	FDR	Gene	logFC	FDR
CMSS1	-1.17E-01	5.54E-19	COX20	-1.82E-02	5.40E-09	CWC15	-1.50E-02	1.93E-07
CMTM3	-1.49E-02	1.11E-06	COX5A	-3.36E-01	9.65E-76	CWC27	-1.24E-02	2.38E-04
CMTM7	-1.62E-02	8.30E-06	COX5B	-1.62E-01	2.87E-30	CXXC1	-4.44E-02	2.09E-11
CNBP	-1.54E-01	1.25E-18	COX6A1	-2.59E-01	3.74E-56	CXXC5	-1.22E-02	3.28E-02
CNDP2	-3.63E-03	4.66E-05	COX6B1	-1.30E-01	1.10E-12	CYB561A3	-4.41E-02	2.61E-10
CNN2	-1.16E-02	1.25E-05	COX6C	-2.62E-01	2.47E-58	CYB5A	-5.10E-02	6.18E-11
CNN3	-4.52E-02	2.34E-10	COX7A2	-9.25E-02	1.60E-16	CYB5B	-5.00E-02	4.60E-12
CNOT1	-5.35E-03	1.38E-05	COX7B	-3.30E-01	1.20E-88	CYB5R3	-1.36E-02	2.62E-13
CNOT10	-1.68E-02	1.40E-09	COX8A	-2.62E-01	3.28E-72	CYB5R4	-1.70E-02	3.60E-06
CNOT2	-3.35E-03	1.79E-04	CPNE1	-8.86E-04	1.67E-03	CYBA	-3.17E-01	4.39E-82
CNOT6L	-2.33E-02	3.63E-07	CPSF1	-9.29E-03	9.03E-06	CYBC1	-2.62E-02	1.47E-05
CNOT7	-4.37E-02	2.37E-09	CPSF3	-6.45E-02	3.49E-18	CYC1	-1.98E-01	2.74E-41
CNOT8	-1.62E-02	4.85E-08	CPSF6	-1.37E-01	1.37E-19	CYCS	-8.43E-02	1.85E-09
CNOT9	-1.23E-01	2.98E-28	CPSF7	-1.02E-02	3.66E-05	CYFIP2	-1.99E-02	8.91E-03
CNP	-8.32E-02	1.31E-17	CPT1A	-4.78E-02	3.14E-07	CYP20A1	-1.38E-02	7.41E-04
CNPPD1	-5.55E-03	1.86E-04	CPXM1	-4.48E-02	5.87E-12	CYREN	-5.59E-03	2.68E-03
CNPY2	-1.54E-01	1.24E-21	CRCP	-2.77E-02	2.65E-05	CYSTM1	-6.56E-04	4.75E-04
CNPY3	-4.85E-02	3.97E-16	CREB3L2	-4.41E-03	6.57E-04	DAD1	-9.42E-02	1.17E-23
CNTLN	-7.01E-02	1.71E-10	CREBZF	-6.77E-03	3.23E-06	DAP	-3.86E-02	1.07E-11
CNTRL	-5.09E-02	2.67E-09	CRELD2	-3.88E-02	2.04E-09	DAXX	-4.34E-02	1.63E-13
COA1	-1.39E-02	1.81E-08	CRIPT	-4.02E-02	2.00E-10	DAZAP1	-1.54E-01	5.70E-38
COA3	-3.16E-02	5.15E-08	CRLS1	-5.18E-02	1.98E-10	DBF4	-2.34E-02	4.40E-06
COA4	-2.94E-02	6.29E-10	CRTAP	-2.08E-02	1.39E-07	DBI	-1.69E-01	7.96E-19
COA6	-1.59E-03	1.39E-04	CS	-4.33E-02	3.04E-08	DBNL	-1.89E-03	2.21E-08
COG4	-2.20E-03	6.23E-05	CSK	-1.95E-03	1.33E-03	DCAF10	-4.38E-03	6.19E-05
COMMD1	-1.59E-02	2.49E-05	CSKMT	-2.11E-02	3.99E-06	DCAF13	-2.02E-02	7.02E-06
COMMD3	-3.30E-02	1.25E-05	CSNK1A1	-4.40E-02	1.55E-10	DCAF16	-2.51E-02	1.05E-06
COMMD4	-1.22E-01	3.27E-31	CSNK2A1	-6.11E-02	2.31E-11	DCAF7	-2.92E-02	1.39E-07
COMMD7	-6.88E-02	9.00E-10	CSNK2A2	-3.77E-03	7.22E-05	DCAKD	-8.40E-02	1.88E-26
COMMD9	-2.02E-02	7.67E-08	CSNK2B	-7.53E-02	2.46E-11	DCK	-7.89E-02	5.87E-13
COP1	-1.53E-02	5.99E-03	CSRP1	-9.97E-03	1.91E-08	DCLRE1C	-3.71E-02	6.22E-07
COPE	-1.89E-01	5.40E-33	CSTB	-1.96E-03	2.94E-08	DCTD	-2.34E-03	4.13E-06
COPS3	-1.27E-01	2.00E-30	CSTF3	-5.95E-02	8.30E-11	DCTN1	-1.38E-02	9.41E-05
COPS4	-9.54E-03	6.03E-06	CTBP1	-1.03E-01	2.43E-25	DCTN5	-1.23E-02	2.39E-05
COPS5	-3.02E-02	4.15E-07	CTBP2	-7.48E-03	3.02E-05	DCTPP1	-3.36E-01	1.95E-106
COPS6	-6.83E-02	7.11E-16	CTCF	-7.17E-02	1.53E-15	DCUN1D1	-2.58E-02	3.41E-07
COPS7B	-1.97E-02	6.23E-06	CTDNEP1	-2.08E-02	3.88E-03	DCUN1D5	-6.72E-02	4.61E-13
COPS8	-3.10E-02	3.45E-07	CTDSPL2	-8.47E-02	1.25E-18	DCXR	-8.03E-02	1.55E-12
COPS9	-7.45E-02	2.01E-11	CTNNB1	-1.76E-01	1.05E-26	DDA1	-1.99E-02	5.43E-09
COQ2	-7.46E-02	1.75E-15	CTNNBIP1	-3.61E-02	1.84E-10	DDB1	-5.88E-02	4.42E-12
COQ4	-4.33E-02	2.75E-07	CTNND1	-7.67E-03	2.13E-04	DDB2	-1.11E-01	2.29E-28
COQ7	-1.27E-02	1.44E-02	CTSA	-1.08E-02	9.09E-05	DDOST	-4.23E-02	1.96E-07
COQ9	-1.43E-02	4.64E-05	CTSB	-4.31E-03	3.48E-07	DDT	-1.58E-01	2.09E-28
CORO1A	-1.89E-01	8.92E-26	CTSC	-3.77E-02	2.31E-07	DDX1	-4.28E-02	1.41E-07
CORO1C	-1.19E-02	2.92E-08	CUEDC2	-7.38E-02	2.69E-11	DDX18	-8.46E-03	8.13E-04
CORO7	-3.21E-02	1.67E-05	CUL1	-2.58E-02	9.23E-12	DDX19A	-2.08E-02	4.59E-04
COTL1	-1.50E-01	2.35E-42	CUL3	-3.55E-03	1.71E-07	DDX19B	-2.00E-02	6.52E-05
COX14	-6.04E-02	3.12E-10	CUL5	-6.60E-03	2.27E-04	DDX21	-1.19E-01	3.58E-13
COX16	-4.99E-02	2.61E-09	CUTA	-1.45E-01	2.71E-20	DDX39A	-1.48E-01	4.40E-36
COX17	-7.08E-02	1.99E-22	CUX1	-3.20E-02	4.04E-05	DDX39B	-1.43E-02	1.70E-06

Gene	logFC	FDR	Gene	logFC	FDR	Gene	logFC	FDR
DDX41	-3.22E-03	9.08E-05	DNMT3A	-4.54E-02	1.60E-10	EIF2S3	-5.70E-02	6.01E-03
DDX42	-7.18E-03	1.95E-06	DNPEP	-1.15E-02	1.35E-08	EIF3A	-1.54E-01	6.28E-21
DDX46	-1.77E-01	8.70E-32	DNPH1	-1.69E-01	1.28E-51	EIF3B	-6.60E-02	5.72E-09
DDX49	-3.27E-02	1.27E-05	DOCK2	-4.68E-03	1.30E-06	EIF3I	-3.32E-02	2.67E-08
DDX50	-4.20E-02	9.58E-07	DOCK5	-4.31E-02	8.08E-12	EIF3J	-7.15E-02	2.19E-09
DDX52	-4.32E-02	3.14E-05	DONSON	-5.04E-02	1.49E-04	EIF4A3	-8.55E-02	8.59E-24
DDX54	-1.67E-02	7.18E-07	DPH7	-1.05E-02	5.06E-06	EIF4E	-8.07E-02	8.89E-15
DDX6	-8.66E-02	3.27E-17	DPM2	-7.90E-02	1.86E-16	EIF4E2	-4.74E-03	3.56E-05
DECR1	-1.51E-02	6.88E-06	DPM3	-7.88E-02	5.63E-09	EIF4EBP1	-2.56E-01	2.08E-61
DEK	-7.25E-01	0.00E+00	DPP7	-1.57E-01	3.15E-28	EIF4EBP2	-5.28E-02	3.12E-10
DENR	-8.86E-02	5.56E-13	DPP8	-1.16E-03	4.80E-05	EIF4G1	-4.21E-02	1.51E-07
DERA	-6.07E-02	1.29E-13	DPY30	-8.59E-02	4.23E-26	EIF4G2	-2.30E-03	1.40E-07
DESI2	-1.18E-02	1.09E-05	DPYSL2	-2.09E-02	1.39E-05	EIF5	-2.94E-02	9.08E-09
DFFA	-2.83E-02	1.18E-08	DR1	-3.27E-02	7.09E-11	EIF5A	-6.48E-01	1.74E-239
DGCR6L	-1.49E-01	2.18E-41	DRAP1	-1.18E-01	1.95E-18	EIF5B	-1.94E-01	1.82E-34
DGUOK	-5.95E-02	5.06E-12	DRG1	-3.11E-02	4.56E-08	EIF6	-7.61E-02	6.84E-11
DHRS12	-1.78E-03	3.67E-07	DRG2	-3.92E-03	7.26E-05	EIPR1	-5.21E-02	3.96E-10
DHRS4	-2.89E-02	9.19E-07	DSTN	-5.59E-02	1.02E-07	ELAC2	-2.01E-03	1.40E-03
DHX15	-8.22E-02	5.58E-16	DTNBP1	-3.54E-03	6.43E-04	ELAVL1	-1.53E-01	1.22E-24
DHX29	-5.21E-03	1.37E-06	DTYMK	-2.06E-01	2.67E-70	ELF2	-1.08E-02	2.61E-04
DHX30	-2.53E-02	1.25E-09	DUS3L	-1.29E-03	2.22E-02	ELMSAN1	-5.72E-02	2.69E-07
DHX36	-1.34E-02	6.73E-04	DUSP10	-5.09E-02	8.51E-08	ELOB	-1.93E-01	1.21E-37
DHX40	-6.82E-03	1.35E-02	DUSP12	-2.50E-02	1.44E-07	ELOC	-5.79E-02	2.61E-20
DHX9	-1.08E-01	3.46E-23	DUSP23	-6.45E-02	1.20E-13	ELOF1	-8.28E-03	1.48E-05
DIAPH1	-3.91E-02	1.02E-05	DUT	-7.22E-01	0.00E+00	ELOVL5	-4.33E-02	2.28E-07
DIAPH2	-1.32E-02	4.36E-05	DVL2	-1.02E-02	1.71E-07	ELP5	-4.66E-02	6.65E-13
DIS3	-4.87E-03	3.01E-02	DYNC1H1	-7.53E-02	7.74E-10	ELP6	-3.45E-02	7.08E-09
DIS3L	-2.33E-02	2.51E-07	DYNLL1	-1.12E-01	1.09E-19	EMC10	-1.34E-02	2.73E-09
DKC1	-1.37E-01	1.05E-26	DYRK1A	-9.28E-03	6.08E-06	EMC4	-1.50E-02	3.11E-05
DLD	-1.60E-03	3.96E-07	E2F3	-1.57E-02	5.81E-10	EMC6	-3.61E-02	1.51E-07
DLG1	-2.44E-02	2.67E-08	E2F4	-3.24E-02	6.91E-08	EMC8	-6.08E-02	3.18E-15
DLST	-2.31E-02	2.37E-06	EBNA1BP2	-1.44E-01	1.79E-26	EMD	-2.49E-02	1.38E-03
DMAC1	-3.73E-03	1.80E-07	EBP	-1.76E-01	1.86E-43	EML4	-4.53E-02	2.18E-10
DMAC2	-4.97E-03	4.87E-03	ECD	-1.27E-02	5.22E-05	ENO1	-3.33E-01	1.24E-104
DMTF1	-3.61E-03	2.85E-05	ECH1	-4.66E-02	4.04E-14	ENOPH1	-8.08E-02	6.04E-17
DNAH14	-1.03E-02	1.45E-06	ECHDC1	-3.78E-02	1.29E-09	ENOSF1	-3.85E-02	8.37E-10
DNAJA1	-5.10E-02	8.39E-16	ECHS1	-2.38E-02	4.29E-08	ENSA	-9.92E-02	1.31E-16
DNAJA2	-1.06E-02	1.93E-05	ECI2	-4.49E-03	5.39E-06	ENY2	-1.36E-01	8.94E-22
DNAJB11	-6.75E-02	7.25E-12	EEF1B2	-1.57E-01	4.23E-44	EP300	-3.48E-03	4.38E-04
DNAJC1	-7.69E-03	5.34E-03	EEF1E1	-1.15E-01	3.60E-29	EPB41	-3.14E-02	1.60E-06
DNAJC15	-4.06E-02	1.69E-07	EFTUD2	-4.80E-02	1.19E-11	EPN1	-4.62E-02	5.07E-07
DNAJC19	-4.52E-02	1.25E-06	EI24	-8.12E-02	6.27E-18	EPS15L1	-1.11E-02	3.05E-04
DNAJC2	-2.55E-02	8.20E-13	EIF1AX	-1.56E-01	2.67E-27	ERAL1	-2.56E-02	4.99E-08
DNAJC21	-2.69E-02	8.12E-04	EIF1AY	-4.31E-02	1.88E-11	ERAP2	-1.38E-02	2.10E-04
DNAJC3	-7.35E-02	3.00E-17	EIF2AK1	-1.11E-01	1.85E-22	ERBIN	-2.26E-03	7.75E-04
DNAJC7	-6.72E-02	1.33E-13	EIF2AK2	-1.24E-01	6.09E-19	ERG28	-2.37E-02	4.43E-10
DNAJC8	-1.31E-01	2.22E-22	EIF2AK4	-1.73E-02	2.69E-04	ERGIC2	-3.11E-02	7.16E-10
DNAJC9	-2.97E-01	1.73E-100	EIF2B5	-2.45E-02	7.73E-05	ERGIC3	-2.89E-02	4.75E-03
DNM1L	-1.01E-01	1.05E-15	EIF2S1	-8.75E-02	2.60E-19	ERH	-4.18E-01	8.82E-150
DNMT1	-4.26E-01	7.93E-165	EIF2S2	-1.56E-01	5.73E-27	ERI3	-5.94E-02	1.71E-08

Gene	logFC	FDR	Gene	logFC	FDR	Gene	logFC	FDR
ERLIN1	-3.07E-03	1.94E-04	FAM50A	-3.11E-02	4.25E-07	GALK1	-8.09E-02	6.49E-19
ERO1A	-4.62E-02	3.31E-13	FAM76A	-2.90E-02	1.37E-08	GALNT1	-5.68E-02	1.69E-06
ERP29	-5.06E-02	3.33E-07	FAM76B	-2.44E-02	1.62E-05	GALNT11	-6.80E-03	6.50E-04
ERV3-1	-6.33E-03	2.88E-09	FAM91A1	-1.21E-02	5.31E-03	GALNT7	-2.08E-02	7.18E-04
ESYT2	-1.81E-02	2.68E-06	FAM92A	-2.60E-02	4.85E-12	GAMT	-8.12E-02	8.68E-17
ETF1	-9.36E-02	8.60E-17	FAM96A	-1.36E-01	6.57E-33	GANAB	-1.12E-02	1.67E-09
ETFA	-8.88E-02	3.29E-14	FAM98B	-1.56E-03	5.60E-06	GAPDH	-5.32E-01	0.00E+00
ETFB	-1.60E-01	8.81E-36	FANCL	-4.12E-02	1.03E-10	GAPVD1	-5.79E-03	1.33E-06
ETNK1	-3.19E-03	4.78E-06	FARSA	-4.78E-02	1.62E-10	GAR1	-2.37E-02	1.53E-07
ETV6	-2.76E-02	5.74E-05	FARSB	-4.26E-02	1.67E-09	GARS	-5.07E-02	3.45E-09
EWSR1	-7.56E-02	6.13E-16	FASTK	-3.66E-03	1.60E-04	GART	-6.56E-02	3.86E-13
EXOC5	-3.00E-02	1.54E-06	FBL	-1.35E-01	2.17E-16	GBE1	-1.36E-02	1.52E-06
EXOC6	-1.68E-02	1.45E-03	FBXO11	-2.85E-03	6.50E-05	GCAT	-6.64E-02	1.68E-15
EXOSC1	-2.20E-02	7.80E-05	FBXO21	-2.01E-02	4.98E-06	GCDH	-9.70E-03	6.70E-05
EXOSC10	-1.57E-02	8.40E-05	FBXO22	-2.42E-02	3.35E-04	GCFC2	-1.67E-02	3.86E-03
EXOSC5	-6.81E-02	3.90E-14	FBXO4	-7.90E-02	7.69E-19	GCHFR	-9.29E-02	4.47E-18
EXOSC6	-6.52E-02	6.73E-10	FBXO9	-1.04E-02	3.46E-03	GCSH	-1.70E-01	2.17E-42
EXOSC8	-1.47E-01	1.47E-29	FBXW5	-6.46E-03	7.55E-05	GDE1	-2.93E-02	1.64E-05
EXOSC9	-9.05E-02	7.45E-25	FCF1	-3.10E-02	2.26E-08	GDI2	-4.39E-02	1.60E-05
EXTL2	-2.21E-02	3.03E-05	FDFT1	-4.13E-02	1.16E-07	GFER	-8.23E-03	3.17E-05
EZH2	-1.53E-01	2.62E-53	FDPS	-2.22E-01	4.55E-53	GGCT	-3.20E-01	2.04E-89
EZR	-8.47E-02	5.43E-13	FDX1	-5.75E-02	2.02E-08	GGCX	-1.46E-02	2.97E-05
F8A1	-6.16E-02	5.81E-13	FECH	-1.49E-02	2.03E-03	GGH	-3.55E-01	1.22E-162
FAAP20	-4.50E-02	2.29E-12	FEM1A	-3.96E-02	1.19E-07	GHITM	-5.11E-03	8.71E-04
FABP5	-6.44E-01	3.91E-229	FGD5-AS1	-7.56E-02	4.27E-14	GIGYF1	-6.66E-02	5.86E-14
FADS1	-9.67E-02	1.05E-21	FH	-6.80E-02	1.49E-13	GIGYF2	-6.67E-03	1.13E-02
FAH	-2.66E-02	2.97E-08	FIBP	-1.76E-01	2.32E-31	GLIPR2	-2.15E-02	7.48E-04
FAHD2B	-3.73E-03	2.03E-03	FIP1L1	-1.35E-02	4.41E-03	GLO1	-2.23E-01	6.82E-54
FAM104B	-2.75E-02	9.79E-05	FKBP11	-6.41E-02	2.38E-07	GLOD4	-4.29E-02	1.38E-09
FAM111A	-2.32E-02	1.17E-19	FKBP1A	-1.63E-01	1.24E-29	GLRX3	-5.74E-02	9.63E-12
FAM120A	-3.78E-02	6.77E-11	FKBP2	-2.44E-02	7.09E-10	GLRX5	-7.96E-02	9.40E-23
FAM120AOS	-1.69E-02	6.72E-08	FKBP3	-1.99E-01	8.40E-41	GLTP	-5.42E-03	5.87E-07
FAM122B	-3.90E-02	2.61E-10	FKBP4	-7.77E-02	1.88E-12	GLUD1	-6.01E-02	7.56E-10
FAM133B	-4.06E-02	3.77E-11	FKBP5	-6.83E-02	3.68E-13	GLUL	-3.11E-02	1.10E-06
FAM136A	-9.09E-02	2.38E-16	FKBP8	-3.40E-02	1.90E-06	GLYR1	-2.56E-02	1.05E-06
FAM13A	-5.31E-04	2.83E-02	FLYWCH2	-2.44E-02	8.03E-07	GMCL1	-9.05E-02	6.24E-17
FAM13B	-2.91E-02	8.22E-07	FN3KRP	-1.08E-01	3.35E-28	GMDS	-2.44E-02	5.98E-03
FAM173A	-9.58E-04	3.04E-03	FNIP2	-1.93E-02	1.39E-02	GMEB1	-1.24E-02	4.32E-05
FAM192A	-8.42E-02	1.69E-12	FRG1	-6.18E-02	3.71E-07	GMPS	-1.50E-01	8.87E-35
FAM204A	-8.51E-03	1.65E-05	FSCN1	-7.53E-02	1.86E-16	GNA12	-7.70E-03	1.73E-04
FAM207A	-1.89E-02	9.02E-04	FUBP1	-8.08E-02	1.21E-14	GNAI2	-3.94E-02	3.71E-09
FAM208A	-3.70E-03	3.16E-02	FUNDC1	-3.95E-03	5.19E-06	GNAI3	-1.62E-02	7.78E-06
FAM210A	-3.29E-02	2.91E-07	FUNDC2	-1.32E-02	3.63E-06	GNAQ	-6.27E-02	1.63E-08
FAM213A	-7.62E-02	6.95E-16	FUS	-2.99E-01	1.99E-69	GNAS	-1.77E-01	2.55E-28
FAM216A	-3.31E-02	3.05E-05	FXN	-3.08E-02	1.08E-04	GNB1	-9.97E-02	5.41E-17
FAM229B	-3.36E-03	1.72E-04	FYTTD1	-4.28E-02	5.73E-10	GNB2	-5.12E-02	2.19E-17
FAM32A	-3.66E-02	1.17E-06	G3BP1	-1.02E-01	1.19E-14	GNB4	-2.83E-02	5.60E-07
FAM3A	-1.92E-02	1.48E-05	G6PC3	-4.54E-02	3.74E-10	GNB5	-4.57E-03	5.65E-03
FAM45A	-2.56E-02	1.18E-09	GABPB1	-1.09E-02	3.93E-11	GNG5	-1.59E-01	8.12E-29
FAM49B	-8.91E-02	6.38E-25	GADD45GIP1	-1.58E-01	4.52E-30	GNL1	-3.75E-02	2.73E-08

Gene	logFC	FDR	Gene	logFC	FDR	Gene	logFC	FDR
GNL2	-1.50E-02	2.22E-07	H3F3A	-1.51E-01	1.41E-31	HNRNPA2B1	-4.10E-01	1.57E-137
GNL3	-8.34E-02	6.86E-13	HACD1	-8.45E-02	8.48E-12	HNRNPA3	-2.46E-01	3.05E-47
GNPAT	-2.58E-02	1.77E-05	HACD3	-1.59E-01	4.86E-45	HNRNPAB	-3.17E-01	1.77E-91
GNPTG	-8.49E-03	1.03E-10	HADH	-1.55E-01	3.19E-39	HNRNPC	-7.25E-02	2.37E-04
GOLGA4	-6.42E-03	2.45E-02	HAT1	-1.44E-01	7.23E-33	HNRNPD	-1.80E-01	2.86E-38
GOLGA7	-5.22E-03	3.21E-11	HAUS1	-1.45E-01	1.27E-37	HNRNPDL	-1.13E-01	9.04E-14
GOLIM4	-9.99E-02	7.17E-17	HAUS2	-3.33E-02	5.35E-07	HNRNPF	-3.20E-01	4.32E-91
GOLPH3	-8.29E-03	1.80E-07	HAUS3	-1.32E-02	5.50E-04	HNRNPH1	-5.19E-01	4.12E-108
GORASP2	-4.21E-02	4.82E-06	HBS1L	-3.78E-02	4.17E-10	HNRNPH3	-1.17E-01	2.16E-22
GOT2	-4.37E-02	2.69E-08	HCFC1	-5.69E-02	1.68E-12	HNRNPK	-1.31E-01	8.31E-18
GPAA1	-1.96E-01	1.67E-54	HCST	-5.76E-02	3.10E-08	HNRNPL	-1.54E-01	4.11E-45
GPALPP1	-2.93E-02	3.09E-05	HDAC1	-3.44E-02	7.99E-18	HNRNPLL	-3.67E-03	9.95E-10
GPANK1	-2.76E-02	1.89E-07	HDAC10	-1.12E-03	3.70E-03	HNRNPM	-2.74E-01	2.10E-61
GPATCH11	-7.42E-03	1.30E-03	HDAC2	-2.18E-01	1.31E-47	HNRNPR	-3.25E-01	8.21E-81
GPATCH2L	-3.83E-03	4.42E-06	HDAC3	-3.22E-02	3.34E-06	HNRNPU	-1.58E-01	4.17E-25
GPATCH4	-2.59E-02	6.08E-05	HDDC2	-2.39E-02	8.96E-09	HNRNPUL1	-7.08E-02	3.84E-11
GPBP1	-5.90E-02	8.50E-13	HDGF	-8.81E-02	9.94E-26	HP1BP3	-1.27E-01	1.89E-25
GPI	-1.86E-02	1.20E-09	HDGFL3	-4.32E-02	1.20E-09	HPF1	-1.01E-01	5.64E-18
GPN1	-3.48E-02	4.88E-08	HDHD2	-1.10E-04	5.85E-07	HPRT1	-2.75E-01	2.30E-81
GPN3	-4.09E-02	5.17E-10	HDHD5	-2.09E-02	8.36E-05	HPS4	-4.14E-03	9.35E-05
GPS1	-3.89E-02	6.15E-07	HDLBP	-4.29E-02	9.31E-10	HSBP1	-1.88E-01	2.81E-33
GPSM2	-1.12E-02	4.77E-07	HELLS	-4.70E-01	6.48E-207	HSD17B10	-1.10E-01	3.97E-22
GPX4	-3.05E-01	1.25E-85	HENMT1	-5.59E-02	6.92E-15	HSD17B4	-1.35E-02	2.05E-05
GPX7	-3.03E-02	8.93E-04	HERPUD1	-9.95E-03	3.86E-05	HSD17B8	-1.63E-02	4.25E-04
GRB2	-1.88E-02	6.43E-06	HGS	-1.02E-02	1.51E-03	HSDL2	-1.55E-02	3.58E-05
GRHPR	-5.84E-03	4.75E-06	HIBADH	-1.35E-02	1.15E-06	HSH2D	-2.29E-03	1.31E-06
GRK6	-1.44E-02	1.58E-05	HIGD1A	-3.06E-03	1.47E-05	HSP90AA1	-3.53E-01	7.21E-109
GSK3B	-1.25E-02	2.40E-04	HIGD2A	-7.20E-03	9.36E-03	HSP90B1	-2.03E-01	1.94E-29
GSPT1	-5.65E-02	6.04E-10	HIKESHI	-3.30E-02	1.02E-11	HSPA4	-6.46E-02	4.11E-13
GSS	-3.97E-02	4.25E-09	HINT2	-1.13E-01	1.82E-21	HSPA8	-4.08E-01	2.10E-103
GSTO1	-4.57E-02	1.00E-09	HIPK1	-1.85E-02	2.34E-06	HSPA9	-4.61E-02	3.49E-17
GSTP1	-3.94E-01	4.46E-142	HIST1H4C	-9.13E-02	9.67E-33	HSPB1	-2.16E-01	2.99E-32
GTF2A2	-9.77E-02	1.79E-24	HIST2H2AC	-5.39E-03	7.31E-10	HSPB11	-2.05E-01	2.25E-59
GTF2H1	-2.43E-02	7.19E-09	HLTF	-3.18E-02	2.68E-04	HSPBP1	-1.41E-02	2.31E-04
GTF2H2	-8.41E-03	1.11E-02	HM13	-2.71E-02	1.31E-06	HSPD1	-3.99E-01	7.05E-90
GTF2H3	-8.86E-03	1.86E-05	HMCES	-1.77E-02	3.67E-06	HSPE1	-3.27E-01	4.88E-90
GTF2I	-3.46E-02	1.14E-03	HMG20B	-5.66E-02	2.16E-12	HSPH1	-6.73E-02	2.02E-16
GTF3A	-2.55E-01	2.63E-45	HMGA1	-6.83E-01	6.93E-301	HTATSF1	-9.30E-02	1.03E-19
GTF3C5	-3.00E-02	2.36E-07	HMGB1	-5.46E-01	1.84E-287	HTRA2	-1.99E-02	1.73E-05
GTF3C6	-9.82E-02	2.46E-21	HMGB2	-4.06E-01	1.38E-146	HUWE1	-1.71E-02	8.24E-03
GTPBP3	-2.02E-02	1.84E-05	HMGB3	-2.27E-01	6.39E-59	HYI	-3.21E-02	1.52E-08
GTPBP4	-4.24E-02	8.22E-11	HMGN1	-4.26E-01	2.11E-151	IAH1	-1.05E-01	1.82E-22
GTPBP8	-1.35E-03	1.92E-04	HMGN2	-1.05E+00	0.00E+00	IARS	-1.05E-01	1.18E-22
GUCD1	-6.99E-02	2.41E-14	HMGN3	-2.49E-01	5.53E-51	IARS2	-3.94E-02	4.99E-12
GUK1	-8.20E-02	1.81E-15	HMGN5	-2.05E-01	1.12E-44	IBTK	-2.32E-03	1.85E-02
GUSB	-1.56E-01	2.31E-44	HMGXB4	-9.84E-02	2.22E-18	ICE2	-3.83E-02	8.49E-05
GYPC	-2.19E-01	3.72E-24	HMOX2	-3.80E-02	7.92E-06	IDH2	-5.16E-01	8.38E-195
H2AFV	-2.30E-01	6.45E-35	HNRNPA0	-1.75E-01	4.00E-29	IDH3A	-2.12E-02	1.49E-08
H2AFY	-1.47E-01	7.04E-17	HNRNPA1	-3.22E-01	1.84E-143	IER3IP1	-1.91E-01	1.89E-53
H2AFZ	-1.18E+00	0.00E+00	HNRNPA1P4	-1.07E-01	2.19E-13	IFI27L1	-9.00E-02	1.07E-27

Gene	logFC	FDR	Gene	logFC	FDR	Gene	logFC	FDR
IFI6	-4.31E-02	6.14E-07	IWS1	-7.09E-03	5.71E-03	LARP1B	-1.89E-02	6.10E-04
IFNAR2	-2.89E-02	2.94E-06	JADE1	-1.79E-02	3.88E-11	LARS	-9.26E-02	2.56E-10
IFNGR2	-1.30E-02	7.31E-05	JAK3	-1.56E-02	2.10E-04	LAS1L	-1.53E-02	3.32E-07
IFRD2	-8.09E-02	1.39E-14	JARID2	-1.19E-02	2.13E-05	LASP1	-2.65E-03	4.79E-05
IFT52	-7.54E-03	5.05E-05	JOSD1	-9.55E-03	1.46E-05	LAT2	-2.87E-03	2.41E-03
IFT57	-2.35E-02	3.21E-08	JPT1	-1.03E-01	4.12E-30	LBR	-4.13E-02	1.61E-17
IGFBP7	-1.67E-01	2.87E-30	JPX	-5.79E-03	6.73E-06	LCMT1	-1.91E-02	4.85E-04
IGHM	-1.01E-01	9.53E-08	JTB	-1.32E-01	4.06E-18	LCOR	-4.16E-03	1.19E-04
IGLL1	-2.46E-01	6.35E-91	KANSL1	-1.53E-02	1.12E-03	LCP1	-5.48E-02	2.54E-12
IKBKB	-2.40E-03	1.06E-03	KANSL2	-4.34E-03	3.61E-05	LDHA	-1.95E-01	1.96E-32
ILF2	-1.97E-01	2.36E-37	KAT2A	-1.22E-02	1.34E-07	LDHB	-2.77E-01	3.00E-73
ILF3	-2.42E-01	9.78E-54	KAT6B	-5.53E-04	4.02E-05	LDLR	-1.79E-02	4.96E-03
ILK	-3.16E-03	6.05E-05	KAT7	-1.53E-02	7.16E-05	LETM1	-5.89E-02	5.54E-13
ILKAP	-3.17E-02	2.01E-06	KATNB1	-5.55E-02	8.20E-11	LINC02001	-1.26E-02	4.86E-06
ILVBL	-1.92E-03	7.01E-06	KATNBL1	-3.48E-02	9.50E-06	LKAAEAR1	-1.44E-01	5.35E-37
IMMP1L	-7.45E-02	5.65E-14	KCNAB2	-1.72E-02	2.78E-12	LLPH	-9.21E-03	5.69E-05
IMMT	-6.00E-02	1.32E-14	KDELR2	-1.10E-01	5.33E-20	LMAN1	-3.53E-02	2.30E-08
IMP4	-4.93E-02	1.30E-09	KDM1A	-1.26E-02	2.71E-04	LMAN2	-4.03E-02	2.78E-16
IMPDH1	-1.01E-02	5.06E-04	KDM5A	-2.07E-02	1.59E-03	LMF2	-4.35E-02	1.92E-13
IMPDH2	-1.89E-01	2.19E-22	KDSR	-2.92E-02	3.50E-06	LPCAT3	-7.85E-03	5.84E-08
ING2	-7.55E-02	2.39E-14	KEAP1	-1.54E-02	2.42E-06	LRIF1	-8.80E-03	1.75E-02
ING3	-6.13E-03	5.64E-06	KHDRBS1	-7.63E-02	7.33E-08	LRPAP1	-8.47E-03	4.68E-08
ING5	-2.23E-02	3.33E-05	KHSRP	-1.19E-01	4.28E-24	LRPPRC	-3.18E-02	3.39E-05
INKA1	-1.44E-02	6.68E-05	KIAA1143	-2.03E-02	1.12E-04	LRRC37B	-1.84E-04	5.09E-03
INO80C	-2.37E-02	4.67E-04	KIF20B	-1.13E-01	1.53E-25	LRRC57	-6.90E-04	5.92E-03
INO80D	-5.27E-03	2.30E-07	KIF22	-1.14E-01	9.61E-31	LRRC58	-3.31E-02	2.20E-04
INO80E	-1.34E-02	1.10E-08	KIF2A	-3.67E-02	2.40E-07	LRRC59	-1.12E-01	6.13E-22
INSR	-7.35E-02	1.98E-13	KIF9	-5.49E-03	3.82E-06	LRRC75A	-1.31E-01	5.29E-23
INTS10	-1.80E-02	1.56E-10	KLF11	-2.27E-02	8.57E-05	LRRCC1	-1.00E-01	1.57E-22
INTS13	-2.18E-02	2.91E-06	KLHDC3	-1.08E-01	2.67E-24	LSM1	-2.51E-02	6.67E-08
IPO5	-1.48E-01	2.08E-36	KLHL12	-1.02E-02	4.14E-07	LSM12	-7.96E-02	1.47E-13
IPO7	-8.84E-02	1.86E-17	KLHL23	-1.04E-01	3.41E-29	LSM14A	-8.17E-02	1.23E-14
IPO9	-5.53E-02	5.47E-12	KLHL42	-1.70E-02	1.30E-05	LSM2	-3.46E-02	4.96E-05
IQCB1	-7.57E-03	7.47E-07	KNOP1	-7.64E-02	2.32E-20	LSM3	-3.03E-01	4.25E-91
IQGAP2	-2.50E-03	2.85E-02	KPNA2	-8.38E-03	1.18E-04	LSM4	-6.39E-01	1.23E-270
ISG15	-2.08E-02	8.45E-03	KPNA3	-3.78E-02	4.96E-06	LSM5	-3.63E-01	1.31E-100
ISG20L2	-1.13E-02	9.20E-05	KPNA4	-2.17E-02	6.82E-07	LSM6	-6.40E-02	6.15E-16
ISOC1	-2.06E-02	9.88E-11	KPNA6	-9.21E-03	9.24E-04	LSM7	-2.39E-01	6.61E-39
ISOC2	-4.31E-02	8.58E-11	KPNB1	-2.54E-01	1.23E-54	LSM8	-4.68E-02	2.69E-05
ISYNA1	-2.17E-01	3.05E-51	KRAS	-2.38E-02	1.72E-05	LUC7L2	-8.47E-02	2.41E-13
ITFG1	-5.63E-03	7.09E-07	KRR1	-2.14E-02	1.08E-07	LUZP1	-8.80E-03	2.75E-07
ITGAE	-6.42E-02	1.02E-14	KRT10	-1.41E-02	8.44E-06	LY6E	-1.00E-01	6.52E-10
ITGB1	-5.41E-02	1.77E-07	KRTCAP2	-1.16E-01	1.77E-20	LYAR	-5.60E-02	3.87E-11
ITGB1BP1	-1.60E-01	1.65E-35	KTN1	-1.71E-01	2.21E-21	LYPLA1	-1.13E-01	2.89E-17
ITGB2	-5.80E-02	2.59E-09	KXD1	-2.65E-02	8.84E-06	LYPLA2	-1.34E-02	4.72E-03
ITGB3BP	-2.11E-01	1.09E-58	LAGE3	-2.41E-01	8.98E-64	LYPLAL1	-2.50E-03	8.14E-03
ITM2A	-8.03E-02	7.62E-15	LAMTOR2	-7.44E-02	1.37E-09	LYRM2	-2.70E-02	1.94E-07
ITPA	-6.74E-03	1.27E-08	LAMTOR5	-9.06E-02	2.40E-10	LYRM4	-1.51E-02	6.02E-07
ITPR2	-8.36E-03	1.70E-03	LAP3	-2.97E-02	1.42E-05	LZIC	-1.79E-02	8.98E-04
IVNS1ABP	-2.29E-02	3.42E-04	LARP1	-3.65E-02	6.00E-07	MAD2L1	-2.04E-01	1.49E-73

Gene	logFC	FDR	Gene	logFC	FDR	Gene	logFC	FDR
MAD2L2	-1.24E-01	1.46E-31	MED17	-3.68E-02	1.04E-08	MRPL1	-1.41E-02	1.90E-02
MAGED1	-1.26E-02	1.82E-05	MED23	-2.50E-02	2.52E-06	MRPL11	-2.50E-01	1.87E-57
MAGEH1	-1.96E-02	5.99E-08	MED30	-5.13E-02	1.58E-16	MRPL12	-1.12E-01	7.46E-26
MAGOH	-9.92E-02	3.68E-20	MED4	-1.05E-01	2.96E-18	MRPL13	-6.57E-02	3.12E-18
MAGOHB	-1.36E-01	6.83E-38	MESD	-2.57E-02	1.07E-05	MRPL14	-9.58E-02	4.83E-17
MAGT1	-2.62E-02	2.89E-04	MEST	-4.61E-02	2.21E-09	MRPL15	-3.70E-02	3.22E-12
MALSU1	-4.03E-03	2.50E-05	METAP1	-1.57E-02	7.46E-03	MRPL18	-1.21E-01	3.13E-28
MANBA	-1.02E-03	1.77E-03	METAP2	-5.30E-02	1.19E-06	MRPL19	-1.89E-02	3.18E-06
MANF	-6.39E-02	1.57E-08	METTL16	-5.17E-03	4.12E-03	MRPL2	-6.87E-03	3.52E-04
MAP3K13	-1.93E-02	8.04E-03	METTL21A	-5.12E-02	8.87E-13	MRPL20	-1.10E-01	6.29E-17
MAP3K2	-1.45E-02	1.77E-04	METTL26	-1.68E-01	1.95E-32	MRPL21	-3.23E-02	5.57E-08
MAP3K20	-7.98E-02	6.58E-17	METTL5	-7.70E-03	1.17E-08	MRPL22	-2.66E-02	6.95E-14
MAP3K7	-2.11E-02	1.06E-03	METTL9	-7.24E-02	2.05E-12	MRPL23	-1.22E-01	6.32E-21
MAP4	-2.51E-02	1.85E-06	MFGE8	-1.25E-01	3.00E-41	MRPL24	-4.47E-02	5.31E-09
MAP4K1	-7.34E-03	3.02E-07	MFNG	-7.20E-03	4.08E-05	MRPL27	-5.12E-02	9.16E-10
MAP4K5	-3.46E-02	7.98E-07	MFSD14C	-3.35E-02	6.91E-07	MRPL28	-2.09E-03	6.61E-07
MAP7D3	-1.41E-02	1.23E-03	MGAT1	-2.09E-03	3.73E-05	MRPL3	-8.47E-02	1.48E-12
MAPK14	-1.32E-02	4.00E-08	MGAT2	-5.37E-03	5.18E-08	MRPL33	-6.32E-03	2.55E-04
MAPK8	-1.58E-02	5.78E-06	MGAT4A	-1.02E-02	6.57E-05	MRPL34	-1.61E-02	1.10E-11
MAPKAP1	-2.74E-02	3.94E-06	MGME1	-1.75E-02	8.43E-06	MRPL36	-6.44E-02	7.67E-11
MAPKAPK3	-4.85E-02	2.03E-05	MGST1	-2.76E-01	2.93E-69	MRPL37	-7.07E-02	1.52E-12
MAPKAPK5	-4.04E-02	2.90E-06	MGST2	-1.15E-03	1.93E-02	MRPL4	-8.39E-02	1.45E-14
MAPRE2	-6.98E-03	2.71E-05	MGST3	-2.36E-02	4.29E-10	MRPL41	-7.78E-02	1.01E-12
MARCKSL1	-1.34E-01	1.98E-17	MICU1	-1.85E-02	3.04E-04	MRPL42	-5.56E-02	7.22E-07
MARK3	-2.02E-02	4.68E-06	MICU2	-6.14E-03	2.17E-05	MRPL47	-7.62E-02	4.48E-22
MARS	-2.41E-02	9.62E-05	MIER1	-3.16E-02	8.07E-05	MRPL48	-5.48E-02	6.79E-12
MATK	-1.26E-01	6.65E-28	MIF	-6.09E-01	1.14E-271	MRPL49	-2.18E-02	4.90E-08
MAZ	-6.80E-02	5.76E-17	MINOS1	-1.64E-01	2.00E-33	MRPL50	-8.02E-03	4.65E-02
MBD4	-3.15E-02	5.89E-07	MIR4435-2H	-1.09E-02	1.50E-04	MRPL51	-1.99E-01	1.48E-40
MBIP	-5.57E-03	5.37E-06	MIS18BP1	-1.88E-01	1.86E-42	MRPL52	-5.59E-02	1.26E-08
MCAT	-8.13E-03	1.53E-06	MKKS	-7.44E-03	2.82E-07	MRPL54	-3.91E-03	1.98E-07
MCCC2	-2.08E-02	1.33E-04	MLEC	-1.53E-01	9.30E-32	MRPL55	-4.25E-02	4.40E-09
MCFD2	-2.15E-02	8.08E-07	MLH1	-3.85E-02	1.13E-14	MRPL57	-7.78E-02	1.55E-11
MCM3	-5.29E-01	9.87E-224	MLST8	-2.23E-02	4.16E-10	MRPL9	-7.85E-02	5.42E-12
MCM5	-4.13E-01	1.11E-168	MMAB	-4.87E-02	1.83E-09	MRPS10	-2.16E-02	2.87E-03
MCM7	-6.43E-01	7.63E-275	MNAT1	-1.08E-02	1.04E-06	MRPS11	-6.42E-02	1.47E-12
MCMBP	-8.25E-02	1.25E-19	MOB1A	-5.95E-02	2.15E-13	MRPS12	-1.01E-01	1.35E-22
MCRIP1	-4.39E-02	1.97E-10	MORF4L1	-9.65E-02	2.19E-10	MRPS14	-4.07E-02	6.76E-10
MCRIP2	-2.40E-02	2.41E-03	MORF4L2	-5.80E-02	6.49E-19	MRPS15	-8.24E-02	4.38E-13
MCRS1	-1.52E-02	1.33E-04	MPC1	-4.08E-02	1.14E-09	MRPS16	-1.29E-01	4.71E-28
MCTS1	-1.65E-02	2.72E-05	MPC2	-1.27E-01	1.48E-34	MRPS17	-2.77E-02	2.99E-07
MCUB	-1.23E-01	1.12E-24	MPDU1	-3.39E-02	1.50E-04	MRPS18A	-1.19E-03	2.78E-03
MCUR1	-7.32E-02	1.22E-13	MPHOSPH6	-6.75E-02	5.51E-16	MRPS18B	-9.13E-04	3.60E-04
MDH1	-1.45E-01	5.75E-27	MPHOSPH9	-4.12E-02	1.77E-09	MRPS18C	-6.65E-02	1.49E-10
MDH2	-1.18E-01	1.20E-11	MPLKIP	-7.05E-02	6.67E-08	MRPS2	-2.15E-02	5.54E-09
MDK	-1.77E-01	1.29E-40	MPP6	-3.71E-02	2.04E-06	MRPS22	-7.84E-03	1.10E-04
MDM4	-1.74E-01	8.12E-22	MPPE1	-1.01E-02	1.06E-03	MRPS23	-4.18E-02	3.11E-11
ME2	-3.52E-02	7.01E-09	MPST	-7.53E-02	5.49E-13	MRPS25	-1.40E-02	1.77E-10
MEA1	-7.56E-02	5.13E-15	MRE11	-6.62E-02	1.52E-17	MRPS26	-1.65E-01	4.28E-41
MED13L	-1.17E-02	1.02E-04	MRI1	-8.78E-04	3.13E-04	MRPS34	-1.27E-01	7.91E-27

Gene	logFC	FDR	Gene	logFC	FDR	Gene	logFC	FDR
MRPS35	-3.53E-02	5.71E-06	NAA10	-1.03E-01	5.92E-15	NDUFB8	-1.15E-01	5.79E-20
MRPS6	-1.10E-01	6.01E-23	NAA15	-4.72E-02	3.30E-12	NDUFB9	-1.34E-01	6.72E-19
MRPS7	-4.54E-02	6.82E-07	NAA16	-3.12E-02	1.42E-05	NDUFC2	-2.10E-01	3.48E-46
MRTO4	-7.27E-02	8.87E-14	NAA20	-1.05E-01	2.32E-17	NDUFS1	-2.36E-02	4.28E-07
MSH2	-9.99E-02	1.16E-24	NAA25	-2.11E-02	6.58E-06	NDUFS3	-7.63E-02	5.64E-15
MSH3	-6.28E-03	1.23E-06	NAA38	-4.24E-01	7.50E-118	NDUFS5	-2.06E-01	3.46E-34
MSH6	-1.50E-01	1.68E-43	NAA50	-1.59E-01	1.87E-36	NDUFS6	-3.05E-01	1.97E-83
MSI2	-2.35E-02	3.68E-06	NABP2	-5.27E-02	1.72E-15	NDUFS7	-1.25E-03	1.23E-10
MSL3	-2.46E-02	2.58E-04	NAE1	-1.21E-01	3.88E-21	NDUFS8	-2.35E-01	1.92E-57
MSRA	-2.63E-02	3.16E-06	NAP1L1	-2.63E-01	8.69E-71	NDUFV1	-7.81E-02	4.47E-18
MSRB2	-1.77E-02	3.66E-05	NAP1L4	-1.37E-01	1.14E-26	NDUFV2	-2.23E-02	4.30E-06
MT-ATP6	-9.46E-02	1.70E-10	NAPA	-4.03E-02	1.49E-07	NDUFV3	-6.24E-04	2.94E-06
MT-CO1	-2.25E-01	7.47E-60	NARF	-7.76E-03	5.01E-08	NEDD8	-1.59E-01	9.77E-34
MT-CO2	-1.82E-01	1.54E-48	NARS	-4.86E-02	6.59E-13	NELFCD	-4.67E-02	7.77E-11
MT-CO3	-3.61E-02	1.07E-03	NARS2	-2.28E-02	1.40E-03	NELFE	-4.62E-02	1.50E-10
MT-ND4	-1.15E-01	2.08E-18	NASP	-6.15E-01	1.48E-225	NENF	-1.06E-01	1.37E-13
MT-ND4L	-7.55E-02	6.82E-10	NAT10	-1.44E-02	8.34E-03	NET1	-1.83E-02	3.01E-02
MT-ND5	-2.05E-01	7.43E-40	NAXE	-1.46E-01	1.30E-40	NF1	-3.02E-03	9.55E-07
MT-ND6	-7.48E-02	1.71E-13	NBN	-1.00E-02	8.53E-05	NFATC2IP	-7.88E-02	9.58E-17
MT2A	-2.50E-01	2.95E-57	NCBP2	-4.41E-02	1.74E-08	NFATC3	-2.07E-02	1.10E-05
MTA1	-2.43E-02	5.49E-09	NCBP2-AS2	-1.05E-02	2.19E-08	NFIC	-7.98E-02	5.67E-15
MTCH1	-5.67E-02	4.25E-08	NCBP3	-3.57E-02	1.42E-06	NFKBIB	-5.86E-03	3.34E-07
MTCH2	-1.11E-01	2.78E-22	NCF4	-1.55E-02	5.42E-04	NFYB	-4.10E-02	4.90E-13
MTDH	-9.31E-02	3.58E-15	NCL	-3.88E-01	1.99E-99	NFYC	-6.12E-03	3.91E-03
MTF2	-8.61E-02	5.67E-11	NDE1	-4.85E-03	1.14E-04	NGLY1	-4.59E-02	1.99E-07
MTHFD1	-1.56E-01	5.17E-43	NDUFA1	-1.21E-01	3.60E-25	NHLRC3	-4.10E-03	2.28E-03
MTHFD2	-1.90E-01	2.78E-50	NDUFA11	-1.85E-01	2.10E-37	NHP2	-2.47E-01	1.70E-54
MTHFD2L	-3.26E-02	1.52E-05	NDUFA12	-1.30E-01	6.76E-34	NIN	-5.92E-02	5.52E-12
MTIF2	-9.68E-03	1.31E-03	NDUFA13	-1.99E-01	3.71E-41	NINJ1	-2.72E-02	3.99E-04
MTPAP	-3.04E-02	1.84E-10	NDUFA2	-1.56E-01	6.76E-35	NIP7	-1.56E-02	5.86E-10
MTPN	-1.94E-02	1.27E-02	NDUFA3	-1.71E-01	2.36E-39	NIPA2	-4.01E-02	4.59E-12
MTR	-2.11E-02	2.15E-05	NDUFA4	-2.07E-01	3.95E-39	NIPBL	-2.89E-02	2.58E-06
MTREX	-3.39E-03	1.72E-03	NDUFA5	-1.65E-02	3.63E-05	NIPSNAP2	-1.83E-02	7.41E-05
MUL1	-2.09E-03	7.56E-05	NDUFA6	-1.49E-01	1.16E-32	NIPSNAP3A	-2.22E-02	6.50E-06
MUM1	-4.60E-03	3.16E-06	NDUFA7	-3.51E-02	1.03E-08	NIT2	-3.34E-03	6.58E-04
MVB12A	-2.34E-02	3.59E-06	NDUFA8	-4.46E-02	3.65E-10	NKAP	-1.65E-03	7.37E-04
MXD1	-6.58E-03	4.68E-06	NDUFA9	-5.73E-02	4.40E-09	NKAPD1	-1.43E-02	1.14E-04
MYCBP	-9.49E-02	1.30E-25	NDUFAB1	-1.58E-01	1.06E-30	NKIRAS2	-1.39E-03	1.68E-07
MYDGF	-8.52E-02	3.47E-22	NDUFAF2	-4.85E-02	3.33E-05	NME1	-3.72E-01	1.42E-116
MYEF2	-1.08E-03	5.70E-05	NDUFAF4	-6.31E-03	1.30E-06	NME2	-5.64E-02	7.50E-11
MYH10	-1.71E-02	9.84E-05	NDUFAF6	-7.39E-02	1.54E-15	NME4	-3.81E-01	3.77E-107
MYH9	-1.43E-02	1.17E-05	NDUFAF8	-2.08E-01	2.03E-47	NME6	-6.95E-04	3.77E-02
MYL6	-1.62E-01	1.57E-28	NDUFB1	-2.20E-01	5.17E-38	NMI	-2.31E-02	1.78E-05
MYL6B	-4.03E-02	8.74E-10	NDUFB10	-4.93E-02	1.51E-11	NMRAL1	-1.29E-01	8.75E-27
MYO5C	-3.14E-02	1.86E-06	NDUFB11	-3.23E-01	2.74E-88	NMT1	-9.27E-03	7.40E-05
MZB1	-1.50E-01	3.54E-32	NDUFB2	-2.61E-01	1.35E-71	NNT	-5.40E-02	2.69E-12
MZT1	-1.05E-01	1.09E-28	NDUFB3	-1.06E-01	4.27E-25	NNT-AS1	-1.74E-02	4.91E-05
MZT2A	-2.22E-01	1.67E-43	NDUFB4	-2.26E-03	3.51E-04	NOC2L	-1.60E-02	2.65E-03
MZT2B	-2.86E-01	7.04E-53	NDUFB6	-1.90E-01	5.00E-41	NOC4L	-2.32E-02	1.49E-04
N4BP2	-2.50E-02	3.23E-06	NDUFB7	-1.49E-01	3.26E-28	NOL10	-3.38E-02	2.59E-09

Gene	logFC	FDR	Gene	logFC	FDR	Gene	logFC	FDR
NOL11	-3.72E-02	5.20E-07	NUS1	-9.13E-03	1.46E-05	PDAP1	-1.57E-01	2.01E-25
NOL12	-5.78E-03	1.00E-03	NUTF2	-2.58E-01	8.60E-56	PDCD10	-4.02E-02	1.43E-07
NOL8	-1.78E-02	8.76E-03	NUTM2A-AS	-1.44E-02	8.60E-10	PDCD11	-3.40E-02	9.96E-06
NOLC1	-1.23E-01	1.55E-24	NUTM2B-AS	-1.24E-02	7.47E-03	PDCD2	-3.31E-03	6.73E-05
NONO	-1.65E-01	6.70E-29	NXT1	-4.92E-02	4.67E-08	PDCD5	-2.26E-01	2.72E-53
NOP10	-9.38E-02	6.43E-14	OAZ1	-1.43E-01	4.47E-20	PDCD6	-5.58E-02	1.20E-07
NOP14	-3.03E-02	3.02E-05	OAZ2	-8.81E-03	2.72E-09	PDCD7	-1.05E-02	4.81E-07
NOP16	-6.79E-02	3.91E-13	OCIAD2	-4.65E-02	5.26E-12	PDHA1	-6.61E-02	4.00E-11
NOP56	-1.50E-01	1.21E-25	ODC1	-1.06E-01	1.22E-14	PDHB	-9.89E-03	3.91E-05
NOP58	-2.59E-01	2.15E-61	ODF2	-4.49E-02	2.31E-14	PDIA3	-1.24E-01	2.43E-24
NOSIP	-1.49E-02	1.53E-03	OGFOD3	-2.65E-02	1.92E-08	PDIA4	-4.18E-02	3.47E-09
NPM3	-1.21E-01	3.83E-19	OLA1	-9.65E-02	2.35E-12	PDIA6	-3.27E-01	1.43E-68
NPRL2	-7.67E-03	4.75E-04	OPA1	-2.33E-02	1.01E-04	PDK2	-6.59E-03	1.78E-04
NQO2	-3.91E-02	7.34E-07	OSBPL1A	-3.88E-03	8.09E-07	PDLIM1	-8.32E-02	1.50E-16
NRAS	-2.38E-02	1.02E-05	OSBPL8	-6.51E-02	1.05E-08	PDLIM7	-4.80E-03	2.33E-04
NRDC	-1.79E-03	1.65E-07	OSBPL9	-1.90E-02	2.33E-04	PDRG1	-2.98E-02	9.80E-07
NREP	-1.04E-01	1.30E-17	OSGEP	-5.46E-02	1.17E-09	PDS5A	-6.25E-02	5.95E-14
NSD1	-1.51E-02	5.81E-07	OSTC	-1.95E-01	5.46E-37	PDS5B	-4.51E-02	9.37E-15
NSD3	-6.40E-02	6.70E-14	OXCT1	-8.55E-02	1.81E-13	PDZD8	-7.16E-02	2.47E-11
NSL1	-3.48E-02	1.61E-11	P4HB	-2.68E-01	8.23E-61	PEA15	-4.47E-02	8.16E-08
NSMCE4A	-5.59E-02	4.73E-15	PA2G4	-3.74E-01	9.58E-97	PEBP1	-1.60E-01	4.24E-25
NSUN4	-5.06E-03	6.10E-03	PABPC4	-1.11E-01	5.09E-26	PELP1	-1.95E-02	3.75E-06
NSUN6	-3.09E-02	5.56E-05	PABPN1	-1.09E-01	2.57E-14	PES1	-9.99E-03	2.43E-07
NT5C3B	-2.43E-03	1.18E-07	PAFAH1B1	-4.57E-03	7.56E-04	PET100	-8.01E-02	5.05E-20
NT5DC1	-5.81E-03	2.09E-03	PAFAH1B2	-3.50E-02	2.00E-05	PET117	-2.20E-02	1.80E-03
NTMT1	-1.97E-02	8.72E-03	PAFAH1B3	-1.16E-01	3.95E-23	PEX10	-2.07E-02	1.42E-06
NTPCR	-9.46E-03	1.94E-03	PAICS	-2.68E-01	7.44E-70	PFDN1	-1.01E-02	2.20E-08
NUBP2	-8.51E-02	2.71E-22	PAIP1	-2.45E-02	8.61E-07	PFDN2	-6.64E-03	7.47E-10
NUCB2	-4.11E-01	7.63E-100	PAIP2	-1.11E-01	2.40E-13	PFDN6	-6.55E-02	7.84E-10
NUCKS1	-6.06E-01	5.66E-224	PAK1	-4.47E-02	9.01E-09	PFKL	-8.28E-02	1.65E-13
NUDC	-2.02E-01	3.30E-43	PAK1IP1	-4.60E-02	3.87E-07	PFKP	-1.99E-02	5.91E-05
NUDCD2	-1.06E-01	9.76E-21	PAK2	-6.19E-02	2.44E-06	PFN1	-4.74E-01	7.18E-202
NUDT1	-2.81E-01	6.07E-91	PAN3	-3.99E-02	2.13E-07	PGAM1	-2.94E-01	1.42E-86
NUDT15	-7.40E-02	1.88E-12	PAPOLA	-3.81E-02	2.92E-10	PGAP2	-1.54E-02	1.83E-08
NUDT21	-1.40E-01	4.51E-30	PARK7	-2.28E-01	1.33E-46	PGD	-4.16E-02	1.48E-08
NUDT22	-2.93E-03	4.77E-07	PARN	-2.97E-02	1.68E-05	PGK1	-1.24E-01	8.56E-32
NUDT5	-5.20E-02	8.62E-15	PARP1	-2.42E-01	1.33E-40	PGLS	-4.88E-02	1.97E-07
NUDT8	-1.19E-01	1.72E-35	PARP14	-2.24E-02	6.38E-03	PGM1	-1.62E-02	3.54E-06
NUFIP2	-2.54E-02	8.36E-05	PARVB	-4.33E-02	2.26E-06	PGM2	-3.23E-02	4.41E-07
NUP107	-9.83E-02	1.05E-19	PAWR	-2.10E-02	1.58E-04	PGRMC1	-1.03E-01	6.38E-25
NUP160	-4.23E-02	2.78E-07	PAXX	-1.97E-01	5.63E-57	PHACTR4	-2.36E-02	1.37E-02
NUP214	-2.20E-02	8.67E-04	PBDC1	-2.67E-02	1.78E-06	PHAX	-6.85E-03	2.12E-04
NUP37	-1.56E-02	5.00E-10	PBRM1	-5.09E-02	3.69E-10	PHB	-1.60E-01	1.06E-27
NUP54	-3.55E-02	2.74E-09	PCBP1	-1.16E-01	1.33E-11	PHB2	-4.79E-02	1.69E-09
NUP58	-6.95E-02	8.08E-14	PCBP2	-7.27E-02	1.23E-08	PHF14	-4.10E-02	1.39E-07
NUP62	-7.12E-02	4.47E-18	PCLAF	-8.32E-01	0.00E+00	PHF20L1	-3.03E-02	8.61E-04
NUP88	-3.33E-04	1.99E-03	PCM1	-3.69E-02	1.09E-05	PHF3	-1.71E-02	6.37E-05
NUP93	-3.67E-02	2.37E-06	PCMT1	-8.36E-02	1.68E-18	PHF5A	-8.29E-02	9.59E-22
NUP98	-1.19E-02	8.46E-09	PCNA	-5.43E-01	1.32E-229	PHF6	-2.80E-02	3.89E-04
NUPL2	-3.16E-03	3.70E-07	PCNX4	-1.72E-02	2.42E-05	PHGDH	-4.40E-01	9.47E-154

Gene	logFC	FDR	Gene	logFC	FDR	Gene	logFC	FDR
PHIP	-6.53E-02	3.81E-10	POLK	-2.03E-02	4.46E-06	PRDM2	-6.35E-03	2.66E-02
PHKB	-2.46E-02	1.45E-03	POLR2A	-2.87E-02	1.39E-06	PRDX1	-1.87E-01	7.59E-30
PHKG1	-1.60E-01	1.50E-48	POLR2B	-6.36E-03	3.38E-05	PRDX2	-2.07E-01	6.46E-45
PHKG2	-2.06E-02	4.47E-04	POLR2D	-1.52E-01	5.89E-37	PRDX3	-2.19E-01	5.85E-42
PHPT1	-1.97E-01	2.71E-39	POLR2E	-1.48E-01	1.48E-27	PRDX4	-2.47E-01	8.20E-64
PIAS2	-2.39E-02	2.15E-03	POLR2F	-1.19E-01	1.74E-31	PRDX5	-1.37E-01	2.68E-18
PIGC	-3.28E-02	1.65E-07	POLR2G	-4.08E-02	7.32E-11	PRDX6	-2.74E-02	1.67E-03
PIGF	-2.14E-02	7.31E-06	POLR2H	-7.86E-02	3.70E-15	PRELID1	-9.36E-02	2.27E-17
PIGH	-2.60E-03	1.43E-03	POLR2I	-2.06E-01	8.82E-38	PRELID3B	-9.64E-03	9.69E-06
PIGS	-7.52E-03	2.74E-06	POLR2J	-1.91E-01	9.68E-39	PRIM1	-2.80E-01	1.85E-97
PIGT	-3.45E-02	1.68E-07	POLR2J3.1	-7.88E-02	2.19E-10	PRKAR2A	-6.76E-03	4.27E-03
PIGX	-1.41E-01	2.66E-35	POLR2K	-9.15E-02	1.94E-18	PRKCSH	-7.66E-03	3.43E-08
PIH1D1	-9.76E-02	2.63E-21	POLR2L	-3.66E-01	4.88E-106	PRKD3	-2.14E-02	1.25E-08
PIK3R1	-3.23E-02	4.19E-03	POLR3K	-8.44E-02	3.27E-28	PRKDC	-2.91E-01	5.23E-85
PIM1	-1.80E-02	7.55E-04	POMP	-1.77E-01	1.05E-34	PRKRA	-7.64E-02	1.43E-11
PIM2	-1.28E-02	3.89E-03	POP4	-5.62E-03	2.59E-07	PRMT1	-1.11E-01	2.38E-25
PIN1	-1.59E-01	4.49E-40	POP5	-3.39E-02	2.27E-05	PRMT5	-3.14E-02	1.08E-07
PIN4	-8.58E-02	3.85E-18	POP7	-1.30E-01	8.76E-40	PRPF19	-1.20E-01	9.36E-26
PIP4K2A	-5.82E-02	8.99E-11	PPA1	-2.59E-01	2.05E-45	PRPF31	-3.09E-02	4.29E-08
PITHD1	-8.26E-02	4.20E-21	PPA2	-7.65E-02	2.64E-09	PRPF38B	-3.67E-02	7.44E-05
PITPNB	-6.74E-03	5.52E-06	PPDPF	-1.50E-01	1.52E-22	PRPF4	-4.81E-02	1.23E-09
PKIG	-1.36E-02	9.83E-08	PPHLN1	-3.05E-02	2.59E-07	PRPF40A	-9.00E-02	1.79E-10
PKM	-4.79E-01	2.50E-161	PPIA	-4.97E-01	5.13E-188	PRPF4B	-5.47E-02	2.78E-09
PKN2	-5.26E-03	6.20E-05	PPIB	-1.29E-01	1.12E-24	PRPF8	-2.22E-02	1.70E-08
PLAC8	-5.32E-02	3.18E-05	PPID	-2.68E-02	2.60E-06	PRPS1	-6.25E-02	1.82E-11
PLAGL1	-2.05E-02	2.18E-04	PPIE	-1.32E-02	3.58E-09	PRPS2	-1.50E-01	3.44E-37
PLAUR	-9.16E-03	1.38E-03	PPIG	-9.98E-02	1.74E-11	PRPSAP1	-2.60E-02	8.97E-10
PLEK	-5.09E-02	1.18E-05	PPIH	-1.27E-01	6.94E-27	PRR34-AS1	-1.94E-02	3.11E-03
PLEKHB2	-2.35E-03	1.39E-04	PPIP5K2	-3.98E-03	1.39E-02	PRRC2A	-2.31E-02	2.41E-07
PLEKHJ1	-8.53E-02	8.89E-18	PPM1A	-2.17E-02	2.08E-06	PRRC2B	-3.61E-02	1.17E-04
PLGRKT	-1.44E-02	1.22E-03	PPM1G	-2.73E-01	3.17E-73	PRRC2C	-9.91E-02	8.36E-16
PLOD2	-1.05E-02	1.48E-05	PPP1CA	-1.74E-01	2.95E-36	PRSS2	-1.30E-01	1.59E-36
PLP2	-9.84E-02	5.62E-16	PPP1CB	-3.35E-02	3.85E-06	PRSS57	-9.60E-02	4.30E-12
PLPBP	-1.51E-02	1.78E-07	PPP1CC	-1.48E-01	9.71E-29	PSENEN	-2.01E-03	8.25E-04
PM20D2	-8.87E-02	2.27E-17	PPP1R14B	-6.54E-02	6.68E-18	PSIP1	-3.47E-01	2.11E-91
PMF1	-2.10E-02	2.48E-08	PPP1R7	-9.81E-03	2.57E-06	PSMA1	-9.12E-02	3.34E-12
PMPCA	-3.40E-02	1.32E-05	PPP1R8	-2.09E-02	3.02E-04	PSMA2	-1.35E-01	2.56E-28
PMVK	-3.17E-02	1.06E-08	PPP2CA	-1.04E-01	1.16E-17	PSMA3	-3.39E-02	8.76E-09
PNKD	-7.68E-02	9.53E-14	PPP2R3C	-3.83E-02	4.56E-08	PSMA3-AS1	-2.02E-03	6.38E-08
PNKP	-2.83E-02	5.92E-13	PPP2R5C	-1.08E-02	7.51E-05	PSMA4	-2.82E-01	1.58E-59
PNN	-7.47E-02	7.81E-07	PPP2R5E	-1.19E-02	3.76E-06	PSMA5	-1.11E-01	3.89E-22
PNO1	-1.31E-03	1.66E-06	PPP3CA	-8.57E-02	3.13E-14	PSMA6	-4.97E-02	2.57E-12
PNPT1	-3.72E-02	2.63E-08	PPP3R1	-1.71E-02	4.14E-10	PSMA7	-3.42E-01	4.07E-88
POGK	-8.35E-03	1.21E-02	PPP4C	-6.28E-02	4.78E-15	PSMB10	-7.20E-03	1.07E-06
POGZ	-8.00E-03	2.69E-03	PPP4R2	-2.98E-02	1.36E-05	PSMB2	-1.76E-01	6.52E-40
POLD2	-2.72E-01	1.04E-72	PPP4R3A	-1.38E-02	6.39E-10	PSMB3	-1.81E-01	6.00E-36
POLDIP2	-5.79E-02	1.83E-10	PPP4R3B	-1.15E-02	2.04E-06	PSMB4	-5.35E-02	5.20E-12
POLDIP3	-1.63E-02	6.54E-05	PPP6R1	-2.76E-02	1.03E-05	PSMB5	-9.19E-02	2.01E-17
POLE3	-1.94E-01	9.09E-50	PPT1	-5.61E-02	4.57E-18	PSMB6	-1.69E-01	1.76E-37
POLE4	-8.63E-02	1.01E-19	PRCC	-2.15E-02	1.56E-06	PSMB7	-8.87E-02	1.07E-11

Gene	logFC	FDR	Gene	logFC	FDR	Gene	logFC	FDR
PSMB8	-3.33E-02	7.79E-12	PUM2	-1.86E-02	3.07E-08	RANGRF	-9.79E-03	2.41E-02
PSMB9	-8.79E-02	1.95E-14	PUM3	-4.60E-02	9.31E-06	RAP1A	-1.45E-03	1.20E-06
PSMC1	-2.62E-02	4.25E-07	PUS7L	-4.01E-02	9.57E-06	RAP1B	-2.07E-02	4.17E-04
PSMC2	-2.94E-02	5.35E-06	PWP1	-8.23E-03	1.08E-04	RAP1GDS1	-3.83E-02	7.71E-11
PSMC3	-2.70E-01	3.98E-78	PXMP2	-2.52E-01	3.69E-110	RARS	-6.38E-03	2.02E-06
PSMC4	-3.89E-02	1.26E-05	PYCR1	-7.26E-02	8.52E-15	RASA4	-3.12E-02	4.28E-05
PSMC5	-7.72E-02	2.81E-19	PYCR2	-6.49E-02	3.24E-12	RASGEF1B	-2.59E-02	1.89E-05
PSMC6	-3.94E-02	1.85E-10	PYM1	-1.77E-02	1.12E-07	RASGRP2	-1.47E-02	4.01E-05
PSMD1	-6.69E-02	1.15E-11	PYURF	-2.05E-01	1.36E-40	RBBP4	-2.85E-01	2.79E-65
PSMD10	-2.43E-02	1.29E-04	QARS	-8.14E-02	9.64E-06	RBBP6	-2.38E-02	6.98E-06
PSMD11	-4.30E-02	1.07E-09	QDPR	-3.81E-02	2.61E-09	RBBP7	-3.07E-01	3.80E-93
PSMD12	-5.96E-02	8.02E-08	QKI	-1.69E-02	2.27E-06	RBFA	-4.36E-02	2.40E-08
PSMD13	-6.31E-03	3.16E-10	QRSL1	-1.89E-02	5.08E-07	RBM10	-9.14E-03	1.13E-05
PSMD14	-1.55E-01	6.52E-39	R3HDM1	-3.33E-02	5.36E-07	RBM14	-9.32E-02	1.65E-18
PSMD2	-9.51E-02	1.90E-16	R3HDM2	-2.05E-02	7.32E-09	RBM15B	-4.56E-03	7.46E-05
PSMD3	-2.04E-02	2.14E-12	RAB10	-2.27E-02	4.74E-08	RBM17	-1.48E-01	2.17E-28
PSMD4	-1.15E-02	2.77E-06	RAB11A	-2.72E-02	1.70E-10	RBM18	-4.03E-03	3.88E-07
PSMD6	-1.91E-02	9.72E-08	RAB14	-1.07E-02	1.33E-03	RBM25	-6.43E-02	7.49E-10
PSMD7	-4.95E-02	2.44E-14	RAB1B	-4.94E-03	3.26E-11	RBM26	-3.32E-03	4.66E-05
PSMD8	-8.38E-02	4.50E-21	RAB27A	-4.57E-02	1.77E-08	RBM28	-4.01E-02	5.70E-10
PSMD9	-1.03E-02	1.03E-04	RAB28	-1.43E-02	1.82E-05	RBM3	-1.74E-01	2.46E-20
PSME1	-3.54E-02	1.90E-02	RAB2A	-1.26E-02	1.65E-04	RBM42	-1.94E-02	4.55E-06
PSME2	-3.07E-01	3.01E-83	RAB32	-2.63E-02	3.26E-05	RBM6	-4.56E-03	3.35E-04
PSME3	-2.39E-02	4.68E-06	RAB38	-9.25E-03	2.34E-04	RBM8A	-4.06E-03	2.78E-06
PSME4	-5.26E-02	2.03E-09	RAB3GAP2	-1.05E-02	4.31E-06	RBMX	-2.01E-01	1.49E-30
PSMG1	-1.39E-01	4.60E-42	RAB4A	-1.40E-02	1.02E-04	RBX1	-2.78E-01	3.73E-61
PSMG3	-7.00E-02	6.61E-19	RAB5A	-1.68E-03	1.27E-05	RCC1	-5.85E-02	4.49E-16
PSMG4	-5.27E-02	2.95E-08	RAB5C	-6.67E-02	1.37E-14	RCC2	-7.70E-02	1.04E-14
PSPC1	-4.15E-02	3.62E-10	RAB5IF	-8.62E-02	2.40E-17	RCN1	-7.13E-02	3.92E-16
PTBP1	-1.23E-01	3.95E-23	RAB6A	-2.00E-02	1.00E-02	RCN2	-7.99E-02	9.13E-20
PTCD3	-7.62E-03	5.53E-05	RAB8A	-3.89E-02	2.67E-09	RCOR3	-7.87E-03	1.10E-04
PTDSS1	-2.97E-02	3.33E-04	RABEP1	-1.11E-02	1.85E-07	RDX	-8.39E-02	7.52E-12
PTGES2	-4.39E-03	7.26E-03	RABGGTB	-1.99E-02	6.93E-08	REC8	-3.56E-02	1.40E-02
PTGES3	-1.84E-01	5.93E-36	RAC1	-1.01E-01	6.90E-14	RECQL	-8.74E-02	1.41E-16
PTMS	-6.99E-02	3.78E-56	RAD1	-6.25E-02	7.40E-14	RER1	-4.13E-02	1.53E-13
PTOV1	-3.42E-02	4.26E-10	RAD21	-2.28E-01	1.74E-61	RETREG2	-1.25E-02	3.68E-10
PTP4A2	-1.26E-01	7.54E-12	RAD23A	-1.41E-01	1.25E-27	REV1	-1.55E-02	1.82E-06
PTPA	-3.20E-02	4.27E-07	RAD23B	-6.63E-02	7.89E-07	REV3L	-4.01E-02	2.52E-04
PTPMT1	-1.25E-01	1.19E-24	RAD51C	-8.55E-02	1.75E-19	REX1BD	-1.56E-02	4.15E-07
PTPN1	-2.53E-03	4.26E-04	RAE1	-8.37E-03	9.39E-10	RFC1	-1.83E-01	2.64E-55
PTPN11	-2.72E-02	8.26E-08	RAF1	-3.80E-02	1.31E-14	RFC2	-1.48E-01	7.51E-50
PTPN18	-5.22E-03	1.93E-05	RALA	-1.09E-02	5.80E-04	RFK	-5.46E-03	2.42E-04
PTPN4	-1.20E-02	4.88E-05	RALBP1	-4.19E-02	6.46E-07	RFLNB	-2.51E-02	2.26E-04
PTPN7	-4.85E-03	2.21E-05	RALY	-2.34E-01	1.11E-51	RFX2	-3.34E-02	4.67E-03
PTPRE	-7.83E-03	1.97E-02	RAMMET	-3.00E-03	3.69E-06	RFXANK	-1.73E-02	4.90E-06
PTRHD1	-2.90E-02	4.61E-06	RAMP1	-2.19E-02	7.92E-03	RGS1	-5.11E-02	1.02E-07
PTTG1	-2.07E-01	1.05E-80	RAN	-4.36E-01	6.44E-149	RHBDD2	-1.34E-02	3.69E-03
PTTG1IP	-3.22E-02	2.31E-07	RANBP1	-8.71E-01	0.00E+00	RHEB	-1.55E-01	2.32E-47
PUF60	-1.43E-02	5.23E-07	RANBP2	-1.18E-02	1.81E-10	RHNO1	-3.79E-02	2.47E-11
PUM1	-2.90E-02	6.82E-10	RANBP6	-9.49E-03	6.11E-06	RHOA	-2.13E-01	2.24E-35

Gene	logFC	FDR	Gene	logFC	FDR	Gene	logFC	FDR
RHOT1	-3.85E-03	1.61E-05	RPN1	-1.28E-01	9.81E-34	SCAI	-2.03E-02	7.93E-04
RHOT2	-2.29E-03	1.17E-05	RPN2	-1.13E-01	2.47E-23	SCAMP3	-1.48E-02	6.77E-05
RIC8A	-8.17E-03	6.82E-09	RPP30	-4.75E-02	1.12E-07	SCAPER	-9.99E-03	3.63E-02
RIF1	-1.55E-01	2.89E-34	RPP38	-2.27E-02	4.42E-06	SCCPDH	-1.18E-01	2.09E-28
RING1	-1.23E-02	8.86E-05	RPP40	-1.52E-02	9.71E-03	SCNM1	-4.60E-02	1.24E-06
RIOK1	-2.15E-02	8.46E-04	RPRD1A	-8.81E-03	5.45E-06	SCO1	-3.11E-02	1.41E-07
RIOK3	-3.22E-03	3.51E-07	RPRD2	-2.22E-02	1.01E-04	SCOC	-3.56E-02	2.04E-11
RIOX1	-5.01E-03	4.31E-07	RPS16	-1.26E-01	3.07E-34	SCYL1	-1.43E-02	8.33E-05
RIT1	-3.87E-02	1.40E-08	RPS17	-7.67E-02	6.59E-14	SDF2	-4.64E-03	1.01E-08
RLF	-1.19E-02	7.56E-04	RPS19BP1	-6.73E-02	1.00E-11	SDF2L1	-4.79E-02	2.24E-09
RMDN1	-7.73E-03	3.01E-06	RPS21	-1.31E-01	1.46E-48	SDF4	-1.95E-02	1.21E-11
RMND5A	-1.60E-02	1.11E-06	RPS26	-9.81E-02	5.64E-18	SDHAF3	-9.89E-02	4.94E-16
RNASEH1	-4.08E-02	6.77E-08	RPS27L	-9.62E-02	1.88E-09	SDHB	-3.72E-02	3.02E-10
RNASEH2B	-2.55E-01	6.48E-53	RPS3	-1.99E-02	1.72E-03	SDHC	-1.03E-02	1.01E-04
RNASEH2C	-2.48E-01	5.25E-63	RPS3A	-8.18E-02	1.21E-40	SDHD	-1.31E-02	3.01E-11
RNF10	-1.69E-02	5.39E-09	RPS5	-7.63E-02	5.40E-22	SEC11A	-4.07E-02	1.47E-09
RNF126	-4.95E-02	9.00E-12	RPS6KA4	-8.89E-03	1.21E-04	SEC11C	-4.67E-02	1.21E-10
RNF13	-8.40E-03	1.65E-07	RPS6KA5	-2.40E-02	2.38E-06	SEC13	-4.15E-02	3.80E-13
RNF130	-7.86E-02	1.27E-12	RPS7	-6.84E-02	6.83E-17	SEC22B	-5.84E-02	4.41E-08
RNF135	-3.07E-02	9.23E-07	RPS8	-5.82E-02	1.33E-20	SEC22C	-8.30E-03	1.42E-04
RNF138	-7.81E-02	1.68E-08	RPSA	-1.12E-01	1.04E-33	SEC61A1	-3.08E-02	1.42E-06
RNF168	-7.14E-02	2.72E-15	RPUSD1	-2.77E-02	2.52E-09	SEC61B	-1.43E-01	1.23E-18
RNF181	-1.11E-02	2.43E-06	RPUSD3	-2.71E-02	5.07E-06	SEC61G	-1.38E-01	5.27E-31
RNF187	-5.51E-02	8.51E-10	RRM1	-2.01E-01	6.21E-84	SEC63	-9.99E-03	2.16E-05
RNF2	-3.72E-02	8.26E-11	RRP1	-1.25E-02	3.74E-04	SEH1L	-3.72E-02	3.59E-08
RNF26	-1.42E-03	4.05E-08	RRP15	-3.00E-02	1.81E-03	SELENOF	-9.07E-02	8.69E-12
RNF40	-1.29E-02	4.57E-05	RRP1B	-2.21E-02	1.08E-05	SELENOH	-1.75E-01	6.32E-26
RNF5	-7.34E-02	5.31E-13	RRP7A	-7.39E-02	9.46E-11	SELENOW	-9.45E-02	1.00E-12
RNF8	-6.45E-03	6.14E-03	RRP9	-1.49E-03	7.99E-06	SEM1	-2.20E-01	4.24E-39
RNPEP	-3.21E-03	1.27E-05	RSRC1	-7.80E-02	7.67E-15	SENP2	-1.28E-02	9.55E-06
RNPS1	-2.69E-01	1.33E-50	RSRC2	-1.72E-02	3.29E-07	SENP5	-4.51E-02	1.29E-12
ROCK1	-2.93E-02	1.15E-04	RSU1	-3.94E-02	3.43E-06	SEPT1	-3.57E-02	4.30E-06
ROMO1	-1.82E-01	4.09E-29	RTF1	-1.41E-01	4.53E-20	SEPT11	-2.32E-02	1.32E-03
RPA1	-1.42E-01	4.95E-31	RTL8A	-5.44E-03	2.62E-04	SEPT2	-5.18E-02	1.10E-19
RPA2	-1.50E-01	1.95E-43	RTN3	-2.73E-02	1.68E-11	SEPT7	-1.22E-01	1.79E-26
RPA3	-3.93E-01	4.21E-152	RTN4	-2.77E-02	2.62E-02	SERBP1	-2.90E-01	6.71E-50
RPAIN	-3.05E-02	9.90E-07	RUNX1	-4.65E-02	1.68E-07	SERF2	-2.43E-01	5.74E-64
RPAP3	-7.10E-03	1.38E-02	RUVBL1	-6.61E-02	2.92E-16	SERPINB9	-1.35E-02	8.59E-06
RPIA	-8.85E-02	2.90E-13	RUVBL2	-8.13E-02	1.44E-15	SERPINE2	-6.53E-02	1.83E-07
RPL14	-2.59E-02	5.67E-03	RWDD1	-1.33E-02	8.26E-04	SERTAD2	-1.65E-02	3.03E-03
RPL18A	-3.65E-02	3.46E-08	RWDD4	-6.56E-02	1.25E-12	SET	-5.91E-01	2.23E-177
RPL22L1	-4.01E-01	3.04E-105	SAE1	-1.37E-01	1.06E-41	SETD2	-9.74E-03	3.31E-02
RPL26L1	-8.80E-02	2.19E-23	SAFB	-3.09E-02	1.40E-05	SETD5	-7.86E-02	1.75E-15
RPL27	-9.14E-02	1.07E-18	SAMM50	-1.83E-02	2.36E-07	SETD7	-4.59E-03	8.79E-04
RPL35	-6.45E-02	2.75E-17	SAP18	-3.31E-02	5.43E-05	SETD9	-8.68E-03	1.53E-06
RPL37A	-6.89E-02	9.11E-21	SAR1A	-8.85E-02	6.03E-18	SF3A1	-4.50E-02	2.34E-06
RPL4	-7.31E-02	1.13E-11	SAR1B	-1.48E-02	8.98E-03	SF3A2	-7.97E-02	3.30E-14
RPL6	-1.38E-01	5.22E-54	SASH3	-3.76E-02	1.11E-06	SF3A3	-1.04E-01	1.25E-22
RPLP0	-5.74E-02	4.30E-10	SBNO1	-2.97E-02	8.48E-15	SF3B2	-5.23E-02	6.57E-10
RPLP1	-8.03E-02	1.40E-38	SCAF11	-4.56E-02	9.56E-08	SF3B3	-6.19E-02	2.11E-18

Gene	logFC	FDR	Gene	logFC	FDR	Gene	logFC	FDR
SF3B4	-6.32E-02	8.45E-15	SLMAP	-1.30E-02	3.40E-07	SNU13	-6.33E-02	9.19E-16
SF3B5	-5.81E-02	8.16E-11	SLTM	-2.50E-02	4.19E-05	SNX10	-4.65E-02	3.90E-05
SF3B6	-1.74E-01	4.29E-28	SMAD2	-2.55E-02	6.10E-08	SNX3	-4.07E-02	5.36E-04
SFPQ	-1.92E-01	4.59E-24	SMAD5	-2.22E-02	2.38E-05	SNX5	-2.74E-02	3.71E-07
SFSWAP	-3.26E-04	6.34E-05	SMAP1	-8.19E-03	4.33E-03	SOD1	-1.38E-01	6.64E-21
SFT2D1	-1.44E-02	7.32E-04	SMARCA4	-8.77E-02	6.18E-17	SORBS3	-4.77E-03	4.87E-05
SFXN1	-1.44E-01	3.49E-33	SMARCA5	-7.96E-02	1.92E-11	SORD	-1.53E-02	3.51E-04
SGTA	-1.64E-02	3.27E-03	SMARCB1	-1.96E-01	4.06E-46	SOX4	-7.90E-02	1.65E-02
SHARPIN	-8.07E-03	2.07E-07	SMARCC1	-1.29E-01	9.16E-22	SP140L	-4.62E-03	1.25E-05
SHLD3	-4.68E-03	9.79E-04	SMARCD1	-2.78E-02	9.18E-07	SP3	-4.20E-03	1.28E-06
SHMT2	-1.12E-01	1.24E-22	SMARCE1	-3.27E-02	2.41E-08	SPAG16	-8.04E-03	4.00E-08
SIAH1	-1.57E-02	2.71E-04	SMC1A	-2.06E-01	5.36E-65	SPATS2	-1.77E-02	1.02E-05
SIGMAR1	-4.82E-02	6.05E-15	SMC2	-2.39E-01	4.25E-81	SPATS2L	-3.52E-02	4.36E-07
SIKE1	-1.45E-02	2.01E-03	SMC3	-2.40E-01	1.50E-62	SPCS2	-2.20E-01	5.55E-52
SIN3A	-3.65E-02	7.39E-05	SMC4	-1.80E-01	8.25E-45	SPCS3	-1.04E-01	9.32E-22
SINHCAF	-3.48E-02	3.50E-06	SMC5	-7.89E-02	6.46E-17	SPEN	-4.44E-02	1.01E-08
SIVA1	-3.88E-01	3.51E-135	SMCHD1	-6.73E-02	1.13E-11	SPIN1	-2.01E-02	1.69E-07
SKA2	-1.03E-01	5.10E-30	SMG1	-2.69E-02	1.97E-03	SPINK2	-1.63E-01	1.00E-28
SKP1	-1.82E-02	2.78E-04	SMIM10	-1.40E-02	5.57E-06	SPN	-5.38E-02	1.80E-07
SLBP	-2.53E-01	6.95E-81	SMIM12	-2.85E-02	2.76E-08	SPNS1	-1.18E-02	1.83E-05
SLC1A5	-5.74E-02	1.37E-10	SMIM15	-9.11E-03	8.40E-05	SPNS3	-9.06E-02	5.09E-24
SLC20A1	-8.27E-02	3.43E-22	SMIM19	-8.44E-02	2.46E-15	SPRY1	-5.19E-03	1.91E-05
SLC25A1	-6.48E-02	4.67E-19	SMIM24	-1.80E-01	1.53E-19	SPTLC1	-3.47E-03	1.13E-06
SLC25A11	-6.68E-02	7.93E-16	SMIM4	-4.54E-02	7.24E-08	SPTSSA	-9.42E-02	1.87E-20
SLC25A3	-1.43E-01	1.17E-19	SMS	-3.08E-01	5.15E-83	SQLE	-4.34E-02	1.15E-10
SLC25A37	-1.45E-02	4.86E-03	SMU1	-2.27E-02	4.84E-07	SRA1	-4.01E-03	1.41E-04
SLC25A39	-1.70E-01	5.49E-48	SMYD3	-1.11E-02	4.12E-03	SRD5A3	-8.04E-02	9.82E-21
SLC25A46	-1.24E-02	1.54E-04	SNAP29	-1.89E-03	1.88E-04	SREBF2	-1.12E-02	5.68E-07
SLC25A5	-6.69E-01	5.20E-254	SNAP47	-7.27E-03	4.16E-04	SREK1	-1.04E-01	1.87E-10
SLC25A6	-1.94E-01	1.98E-37	SND1	-8.57E-03	5.73E-05	SRM	-1.58E-01	1.28E-44
SLC27A5	-2.06E-02	1.54E-02	SNF8	-4.20E-02	1.63E-13	SRP14	-1.20E-01	8.95E-18
SLC30A5	-5.15E-02	1.17E-08	SNHG15	-4.31E-02	2.62E-07	SRP19	-4.25E-02	2.28E-06
SLC30A7	-9.90E-04	5.32E-07	SNHG21	-3.39E-02	3.54E-06	SRP54	-1.65E-02	1.14E-06
SLC35A3	-1.83E-02	1.15E-04	SNHG9	-1.15E-02	5.08E-05	SRP72	-7.28E-02	2.54E-14
SLC35A4	-2.73E-02	2.40E-07	SNRNP200	-6.29E-03	4.95E-04	SRP9	-3.91E-01	3.75E-107
SLC35B1	-2.03E-02	1.03E-05	SNRNP25	-2.06E-01	3.49E-72	SRPK1	-6.90E-02	2.54E-14
SLC35B2	-9.47E-03	1.07E-05	SNRNP27	-2.95E-02	7.92E-08	SRPK2	-1.16E-02	1.49E-04
SLC35E1	-7.15E-03	3.64E-02	SNRNP40	-1.17E-01	9.12E-31	SRPRB	-5.37E-02	2.22E-15
SLC38A1	-4.93E-02	1.52E-08	SNRNP70	-1.20E-01	2.82E-23	SRRM1	-1.35E-01	1.78E-20
SLC38A2	-4.90E-03	5.38E-04	SNRPA	-1.33E-01	6.23E-24	SRRM2	-3.63E-02	2.97E-06
SLC38A5	-2.30E-02	5.31E-06	SNRPA1	-1.23E-01	1.95E-27	SRRT	-1.18E-01	1.49E-26
SLC39A3	-9.83E-02	2.88E-20	SNRPB	-6.79E-01	2.99E-281	SRSF1	-1.46E-01	2.90E-28
SLC39A4	-4.38E-02	4.88E-09	SNRPB2	-5.76E-03	7.05E-07	SRSF10	-2.60E-01	2.53E-66
SLC39A8	-4.08E-02	8.57E-11	SNRPC	-1.99E-01	7.60E-40	SRSF11	-1.38E-01	3.43E-17
SLC43A1	-1.26E-03	1.88E-03	SNRPD1	-4.85E-01	2.23E-163	SRSF2	-5.25E-01	6.72E-172
SLC48A1	-8.86E-03	4.89E-04	SNRPD2	-8.45E-02	9.80E-08	SRSF3	-2.81E-01	1.07E-67
SLC52A2	-1.35E-02	3.33E-05	SNRPD3	-1.87E-01	1.65E-36	SRSF4	-1.15E-01	7.83E-20
SLC9A3R1	-1.63E-02	1.47E-04	SNRPE	-3.91E-01	2.68E-105	SRSF6	-1.28E-01	1.69E-14
SLIRP	-2.48E-01	1.93E-49	SNRPF	-3.54E-01	5.49E-94	SRSF7	-1.69E-01	5.73E-29
SLK	-2.54E-02	6.03E-06	SNRPG	-2.97E-01	6.76E-83	SRSF9	-2.14E-01	3.70E-35

Gene	logFC	FDR	Gene	logFC	FDR	Gene	logFC	FDR
SS18L2	-2.73E-03	6.23E-12	SYNCRIP	-1.01E-01	6.32E-15	THOC3	-9.20E-02	1.56E-25
SSB	-7.22E-02	6.95E-13	SYNGR1	-4.41E-03	3.89E-05	THOC6	-8.33E-02	3.92E-21
SSBP1	-1.39E-01	7.17E-18	SYNGR2	-1.56E-02	3.21E-05	THOC7	-8.51E-02	6.95E-15
SSFA2	-1.14E-02	3.59E-05	SYNJ2	-3.20E-02	9.11E-06	THOP1	-7.55E-02	1.73E-23
SSH2	-6.94E-03	5.83E-04	SZRD1	-8.81E-03	1.39E-04	THRAP3	-1.31E-01	1.78E-24
SSNA1	-7.34E-02	3.94E-16	TACC3	-4.51E-03	3.52E-24	THUMPD2	-1.31E-02	1.28E-05
SSR1	-6.24E-02	1.30E-10	TADA3	-2.83E-02	1.95E-07	THUMPD3	-2.53E-02	1.85E-04
SSR3	-1.10E-01	6.50E-20	TAF12	-3.05E-04	8.13E-07	THUMPD3-A	-3.80E-02	5.08E-06
SSR4	-8.46E-02	9.47E-10	TAF15	-5.51E-02	4.35E-08	THYN1	-6.29E-02	1.43E-11
SSRP1	-2.61E-01	1.61E-69	TAF3	-2.78E-02	2.96E-05	TIA1	-4.83E-02	6.52E-08
SSSCA1	-3.10E-02	8.14E-09	TAF6	-5.11E-02	5.15E-12	TIAL1	-2.78E-02	2.56E-07
SSU72	-1.14E-01	1.02E-17	TAF9	-6.09E-02	9.24E-11	TIFA	-1.75E-02	7.72E-04
ST3GAL3	-8.27E-03	7.45E-06	TAF9B	-2.58E-02	5.89E-09	TIMM10	-4.89E-02	2.88E-09
ST3GAL4	-2.71E-02	1.71E-06	TAGLN2	-1.21E-01	2.03E-14	TIMM13	-1.11E-01	7.23E-09
STAG1	-3.52E-02	2.23E-09	TAP1	-1.80E-02	2.17E-04	TIMM17A	-3.85E-02	1.67E-07
STAG2	-7.56E-02	2.73E-13	TARDBP	-3.81E-02	3.22E-08	TIMM17B	-1.40E-02	3.56E-05
STARD4-AS1	-1.35E-03	7.47E-04	TARS	-5.51E-02	4.21E-07	TIMM22	-1.77E-03	2.42E-04
STARD7	-1.08E-01	9.72E-30	TBC1D5	-1.93E-02	3.17E-08	TIMM44	-2.06E-02	1.80E-05
STARD9	-1.41E-02	1.20E-03	TBCA	-7.60E-02	3.49E-06	TIMM50	-4.88E-02	2.14E-12
STAT1	-2.70E-03	2.11E-02	TBCB	-4.54E-02	3.28E-10	TIMM8B	-1.40E-01	5.94E-26
STAU1	-4.50E-02	5.15E-10	TBL1XR1	-5.98E-03	1.46E-03	TLE3	-4.13E-02	1.15E-06
STIP1	-4.35E-02	1.30E-14	TBPL1	-1.78E-02	1.32E-06	TLK1	-1.14E-01	8.78E-13
STK32C	-2.26E-02	2.85E-04	TCAF1	-1.55E-02	7.69E-06	TM2D1	-5.67E-03	7.70E-05
STMN1	-1.37E+00	0.00E+00	TCEA1	-1.68E-01	5.06E-32	TM7SF3	-6.77E-02	4.19E-08
STMP1	-1.60E-02	7.98E-04	TCEA2	-1.10E-02	7.51E-04	TM9SF3	-1.06E-02	1.69E-09
STOML2	-2.05E-01	7.41E-47	TCEAL9	-7.34E-02	1.01E-15	TMA16	-6.11E-02	1.34E-06
STRAP	-1.59E-01	1.24E-37	TCERG1	-1.10E-01	1.87E-21	TMA7	-2.94E-01	8.93E-79
STRBP	-2.91E-02	8.57E-08	TCF12	-1.39E-02	3.69E-04	TMBIM6	-4.21E-03	2.73E-12
STT3A	-5.54E-02	2.80E-14	TCF4	-2.80E-02	1.95E-06	TMCO1	-3.27E-02	3.90E-08
STT3B	-6.06E-02	9.58E-11	TCP1	-1.97E-01	2.30E-38	TMED2	-2.77E-01	4.93E-63
STUB1	-5.22E-02	6.87E-10	TDG	-2.71E-02	4.27E-05	TMED4	-7.67E-02	1.40E-10
STX10	-2.57E-02	3.39E-07	TECR	-1.72E-01	3.44E-39	TMED9	-1.35E-01	4.60E-32
STX12	-4.68E-03	1.54E-02	TES	-1.59E-03	8.42E-07	TMEM106C	-4.03E-01	1.89E-162
SUB1	-1.42E-01	1.98E-20	TEX30	-1.06E-01	5.48E-29	TMEM107	-3.98E-02	4.56E-08
SUCLA2	-5.28E-02	4.05E-13	TFAM	-6.03E-02	6.19E-12	TMEM109	-1.70E-01	7.67E-44
SUCLG1	-4.37E-02	1.31E-04	TFAP4	-2.20E-02	2.98E-04	TMEM11	-3.16E-02	5.69E-08
SUDS3	-4.96E-02	1.69E-12	TFB2M	-4.18E-03	1.50E-02	TMEM123	-4.21E-02	6.01E-06
SUGP2	-2.55E-02	6.53E-11	TFDP1	-2.61E-01	2.91E-88	TMEM126B	-5.27E-02	1.96E-07
SUMF2	-1.76E-01	1.70E-36	TFDP2	-1.71E-02	6.22E-09	TMEM138	-1.87E-03	8.44E-06
SUMO1	-2.40E-01	3.30E-50	TFG	-2.63E-02	2.16E-04	TMEM141	-1.53E-02	2.63E-07
SUMO2	-1.92E-01	6.53E-36	TFRC	-3.71E-02	7.39E-08	TMEM147	-1.12E-01	2.24E-22
SUMO3	-2.56E-01	1.23E-47	TGFB1	-2.63E-02	2.74E-05	TMEM14A	-1.79E-02	8.70E-15
SUPT16H	-1.73E-01	1.37E-41	TGIF2	-5.78E-04	1.51E-05	TMEM14B	-2.18E-01	3.14E-41
SURF2	-8.86E-03	1.16E-03	TGS1	-6.34E-02	2.42E-09	TMEM14C	-1.81E-01	1.65E-44
SURF4	-5.43E-02	1.22E-16	THAP12	-5.45E-03	9.65E-05	TMEM159	-4.30E-02	1.92E-07
SUZ12	-1.16E-01	1.16E-31	THAP5	-3.11E-02	2.51E-08	TMEM160	-1.47E-01	3.21E-31
SVIP	-2.21E-01	6.79E-47	THAP7	-3.15E-02	1.14E-08	TMEM165	-6.49E-02	1.11E-11
SYCE1L	-1.06E-01	1.21E-33	THAP9-AS1	-4.53E-02	2.54E-09	TMEM167A	-3.41E-02	8.11E-09
SYK	-2.42E-02	1.22E-11	THOC1	-1.44E-02	1.61E-03	TMEM18	-4.12E-02	6.89E-07
SYNC	-1.07E-01	7.95E-30	THOC2	-2.06E-02	7.10E-05	TMEM183A	-4.83E-02	4.32E-13

Gene	logFC	FDR	Gene	logFC	FDR	Gene	logFC	FDR
TMEM189	-1.18E-02	2.76E-06	TPM4	-2.96E-01	3.77E-53	TUFM	-1.86E-01	3.01E-38
TMEM208	-3.47E-02	3.69E-06	TPP2	-7.16E-03	4.67E-04	TUSC2	-8.33E-03	2.85E-05
TMEM218	-1.14E-02	1.80E-07	TPR	-1.09E-01	1.30E-20	TUT4	-3.16E-03	5.36E-04
TMEM220	-8.14E-03	3.43E-05	TPRKB	-8.28E-02	8.21E-14	TWISTNB	-4.90E-02	4.39E-06
TMEM223	-5.49E-03	3.90E-04	TRA2A	-1.41E-01	2.30E-19	TWSG1	-1.93E-02	1.83E-07
TMEM230	-1.28E-01	4.20E-21	TRA2B	-1.23E-01	8.83E-13	TXN	-2.88E-01	4.90E-65
TMEM242	-3.15E-02	6.65E-06	TRABD	-1.81E-02	1.17E-05	TXNDC12	-5.69E-02	3.70E-13
TMEM258	-9.26E-02	4.42E-21	TRAF7	-4.25E-02	1.71E-12	TXNDC17	-7.04E-02	7.42E-13
TMEM33	-6.47E-02	1.87E-16	TRAM1	-6.23E-02	8.98E-10	TXNDC9	-1.48E-02	1.66E-04
TMEM39B	-4.80E-03	2.53E-05	TRAP1	-4.16E-02	3.28E-09	TXNL1	-5.23E-02	2.19E-10
TMEM41A	-3.22E-03	2.08E-03	TRAPPC1	-1.06E-01	4.49E-19	TXNL4A	-8.56E-02	1.03E-22
TMEM41B	-1.87E-02	2.18E-06	TRAPPC2L	-5.17E-02	6.98E-07	TXNRD1	-4.61E-02	1.30E-08
TMEM50A	-8.39E-02	1.43E-16	TRIAP1	-5.01E-02	4.30E-10	TYMP	-2.47E-02	3.36E-09
TMEM70	-4.28E-03	6.28E-03	TRIM24	-3.46E-02	3.56E-05	TYMS	-8.41E-01	0.00E+00
TMEM87A	-1.22E-02	3.27E-04	TRIM27	-1.19E-02	4.91E-05	U2AF2	-4.72E-02	5.38E-11
TMEM97	-1.75E-01	1.45E-58	TRIM28	-1.14E-01	4.07E-24	U2SURP	-1.01E-01	6.38E-20
TMEM98	-2.09E-02	1.65E-06	TRIM33	-9.81E-03	4.87E-03	UAP1	-5.00E-03	1.74E-02
TMIGD2	-5.77E-02	8.04E-10	TRIM44	-1.51E-02	1.35E-03	UBA2	-2.16E-01	4.04E-48
TMOD3	-2.33E-02	5.42E-05	TRIP12	-9.91E-03	2.22E-05	UBA3	-1.45E-02	4.45E-04
TMPO	-2.36E-01	2.73E-67	TRIR	-1.20E-03	1.54E-08	UBA52	-2.27E-02	2.36E-02
TMSB10	-4.34E-02	4.07E-03	TRMT112	-7.64E-02	1.13E-10	UBA6	-1.89E-02	8.65E-05
TMSB4X	-2.54E-01	1.96E-69	TRMT61B	-1.15E-02	3.40E-05	UBAC1	-4.43E-02	7.00E-11
TMUB1	-5.79E-02	2.25E-13	TRNT1	-3.99E-03	1.11E-03	UBALD2	-2.12E-03	2.24E-04
TMX1	-1.93E-01	2.84E-53	TRUB2	-2.45E-02	1.16E-07	UBAP2	-2.69E-02	1.01E-08
TMX2	-4.94E-02	1.52E-11	TSC22D4	-2.87E-02	2.53E-04	UBAP2L	-3.31E-02	5.34E-08
TNFSF13B	-5.60E-02	2.33E-07	TSEN15	-4.87E-02	6.81E-11	UBE2A	-6.63E-02	1.57E-13
TNIP2	-3.97E-03	1.18E-02	TSEN54	-5.28E-02	9.68E-11	UBE2D2	-8.54E-02	7.11E-10
TNPO1	-5.24E-02	4.45E-09	TSFM	-1.18E-02	6.99E-03	UBE2D3	-8.97E-02	7.87E-11
TNPO3	-4.30E-03	1.37E-06	TSN	-7.45E-02	9.21E-13	UBE2E3	-8.78E-02	1.60E-14
TOMM20	-3.16E-04	2.14E-03	TSPAN13	-7.68E-02	1.00E-25	UBE2G1	-3.58E-02	2.55E-06
TOMM22	-1.72E-01	4.05E-28	TSPAN3	-1.18E-01	1.34E-27	UBE2G2	-3.51E-02	5.72E-04
TOMM34	-2.63E-03	1.96E-03	TSPAN4	-2.10E-02	5.62E-07	UBE2I	-1.86E-01	6.86E-36
TOMM40	-1.61E-01	4.60E-39	TSPYL4	-1.18E-03	1.50E-03	UBE2J1	-4.73E-03	1.67E-05
TOMM5	-1.49E-01	2.48E-27	TSR1	-4.22E-02	1.62E-07	UBE2J2	-8.00E-04	1.60E-05
TOP1	-2.20E-02	2.41E-11	TSR2	-1.28E-02	1.16E-05	UBE2K	-2.90E-02	1.15E-08
TOP2B	-4.66E-02	6.14E-07	TSTA3	-5.12E-02	3.11E-13	UBE2L3	-9.27E-02	1.52E-17
TOPORS	-9.37E-03	1.91E-06	TSTD1	-6.13E-02	4.71E-12	UBE2L6	-2.03E-02	4.39E-06
TOR1A	-4.14E-02	1.84E-07	TTC1	-1.87E-02	1.87E-03	UBE2N	-9.73E-02	3.08E-27
TOR1AIP2	-9.75E-02	6.01E-19	TTC19	-3.55E-03	1.58E-05	UBE2Q2	-8.22E-03	2.04E-05
TOR2A	-1.28E-02	9.90E-07	TTC3	-5.14E-02	2.61E-09	UBE2S	-4.80E-04	4.09E-06
TOR3A	-1.01E-01	1.67E-32	TTC37	-5.82E-03	4.80E-07	UBE2V2	-1.01E-01	8.51E-18
TP53	-1.88E-01	3.78E-55	TTF1	-5.27E-02	1.50E-08	UBE2Z	-6.86E-03	2.87E-05
TP53BP1	-1.31E-02	1.14E-02	TUBA1B	-1.48E+00	0.00E+00	UBE3A	-4.13E-02	5.71E-10
TP53I13	-6.63E-02	3.57E-14	TUBA1C	-2.82E-02	5.11E-17	UBL5	-2.71E-01	9.36E-56
TP53TG1	-7.44E-03	9.26E-03	TUBA4A	-4.04E-02	6.30E-11	UBN1	-1.96E-02	5.46E-04
TPD52	-7.10E-03	2.08E-08	TUBB	-1.12E+00	0.00E+00	UBQLN1	-2.87E-03	4.00E-05
TPD52L2	-1.71E-02	3.92E-07	TUBB4B	-1.14E-01	9.42E-28	UBR5	-1.99E-02	1.20E-04
TPGS2	-1.46E-01	1.09E-35	TUBGCP2	-4.33E-03	2.56E-02	UBTF	-7.15E-02	1.03E-07
TPI1	-4.65E-01	2.90E-163	TUBGCP3	-3.44E-02	2.09E-07	UBXN2A	-3.01E-02	3.11E-06
TPM3	-2.77E-01	6.57E-53	TUBGCP4	-6.67E-03	2.52E-05	UBXN4	-2.25E-02	3.70E-11

Gene	logFC	FDR	Gene	logFC	FDR	Gene	logFC	FDR	Gene	logFC	FDR
UBXN7	-4.67E-03	1.29E-04	VPS25	-2.75E-02	7.20E-05	YTHDF2	-2.42E-02	2.91E-05	ZNF667	-1.26E-03	6.82E-03
UCHL3	-1.40E-02	3.53E-07	VPS26A	-1.87E-03	5.87E-10	YWHAB	-1.23E-01	9.78E-12	ZNF667-AS1	-3.05E-02	3.34E-07
UCHL5	-5.88E-02	1.57E-10	VPS29	-8.85E-02	1.50E-11	YWHAE	-3.91E-01	3.01E-93	ZNF672	-2.30E-02	5.55E-05
UCKL1	-1.73E-02	5.58E-04	VPS35	-2.35E-02	9.67E-09	YWHAH	-1.95E-01	1.21E-53	ZNF711	-4.74E-03	1.79E-02
UFD1	-1.17E-01	7.36E-28	VPS4A	-1.41E-02	2.41E-05	YWHAQ	-3.77E-01	2.14E-100	ZNF770	-1.78E-02	9.63E-04
UHMK1	-1.33E-02	9.89E-06	VRK1	-1.53E-01	6.62E-42	YY1	-7.81E-02	5.46E-11	ZNF814	-5.89E-03	9.64E-03
UNG	-3.56E-01	1.40E-159	VRK2	-2.40E-02	6.53E-03	ZBED1	-1.61E-03	2.82E-06	ZNHIT1	-4.77E-02	9.31E-07
UNK	-2.33E-03	2.39E-05	VSIG10	-4.88E-02	3.37E-13	ZBTB8OS	-1.64E-02	1.82E-11	ZNRF1	-3.37E-03	1.37E-04
UPF3A	-3.52E-02	8.67E-06	WAC	-1.39E-02	1.44E-07	ZC3H13	-1.25E-02	1.05E-06	ZPR1	-2.54E-02	3.25E-07
UPF3B	-4.08E-02	3.11E-08	WAPL	-1.62E-02	4.32E-03	ZC3H14	-4.47E-03	8.95E-06	ZSCAN16-AS	-9.05E-02	7.17E-19
UQCC2	-2.30E-01	3.92E-53	WASHC5	-9.99E-03	1.45E-03	ZC3H15	-9.17E-03	3.33E-07			
UQCC3	-6.37E-02	2.68E-14	WBP11	-6.13E-02	4.82E-15	ZC3H18	-2.86E-02	7.22E-09			
UQCR10	-2.26E-01	6.57E-62	WBP4	-3.28E-02	5.37E-08	ZC3H8	-8.05E-03	1.14E-07			
UQCR11	-1.17E-01	1.56E-26	WDR1	-2.79E-02	1.17E-05	ZC3HAV1	-3.50E-02	6.90E-10			
UQCRC1	-1.47E-01	7.45E-28	WDR11	-1.68E-02	2.64E-04	ZCCHC17	-1.65E-02	1.33E-05			
UQCRFS1	-3.79E-02	1.15E-04	WDR18	-3.74E-02	2.12E-08	ZCCHC9	-2.00E-02	2.18E-05			
UQCRH	-1.83E-01	2.81E-30	WDR41	-4.19E-02	3.20E-10	ZCRB1	-7.17E-02	4.42E-08			
UQCRQ	-4.17E-01	3.76E-128	WDR43	-9.84E-02	8.80E-14	ZDHHC12	-8.38E-02	2.94E-23			
URI1	-5.14E-02	7.51E-08	WDR48	-4.71E-03	3.58E-05	ZDHHC3	-1.81E-02	8.86E-08			
URM1	-2.44E-04	4.10E-06	WDR54	-1.13E-01	5.13E-29	ZDHHC4	-1.97E-02	1.77E-04			
UROD	-7.09E-02	1.10E-16	WDR60	-1.21E-02	6.44E-05	ZDHHC6	-2.71E-02	5.06E-07			
UROS	-4.92E-02	1.50E-09	WDR61	-3.04E-02	1.61E-07	ZFAND2B	-3.91E-03	2.79E-04			
USB1	-2.58E-02	7.84E-07	WDR70	-4.70E-03	6.82E-05	ZFP36L1	-6.72E-03	2.09E-03			
USP1	-3.96E-01	1.11E-152	WDR73	-8.40E-03	3.44E-04	ZFP91	-1.64E-02	7.68E-06			
USP10	-5.85E-02	1.57E-08	WDR74	-2.69E-03	1.88E-06	ZFX	-2.77E-02	2.62E-05			
USP14	-1.49E-03	1.89E-08	WDR77	-1.56E-02	5.38E-08	ZFY	-1.40E-02	5.32E-03			
USP16	-1.67E-02	9.41E-05	WHAMM	-2.58E-02	1.33E-03	ZHX1	-8.31E-03	1.33E-03			
USP22	-8.83E-03	3.79E-05	WIPI2	-2.80E-02	1.37E-08	ZMAT2	-2.49E-03	6.79E-03			
USP36	-1.63E-02	2.39E-03	WNK1	-2.25E-02	9.13E-06	ZMYND11	-1.08E-02	4.02E-05			
USP39	-4.77E-02	5.36E-13	WRB	-4.46E-02	3.20E-11	ZNF121	-3.98E-02	4.14E-07			
USP48	-8.18E-02	1.63E-15	WTAP	-1.76E-01	1.05E-34	ZNF146	-4.31E-03	3.45E-05			
USP5	-3.29E-03	3.17E-02	XPNPEP1	-2.22E-02	1.36E-04	ZNF207	-6.72E-02	3.23E-09			
USP6NL	-4.88E-03	6.74E-04	XPO1	-8.76E-02	6.40E-13	ZNF22	-2.64E-02	7.78E-09			
USP7	-2.88E-02	3.70E-04	XPO4	-7.79E-03	6.95E-05	ZNF292	-5.71E-02	5.04E-06			
UTP11	-5.06E-02	1.98E-09	XPOT	-2.48E-02	4.76E-08	ZNF3	-9.01E-03	1.91E-08			
UTP18	-1.60E-02	3.49E-04	XRCC1	-3.18E-02	2.34E-07	ZNF326	-6.57E-02	2.38E-10			
UTP23	-2.64E-02	5.47E-05	XRCC5	-1.86E-01	3.30E-37	ZNF37A	-6.11E-03	4.44E-03			
UXS1	-3.65E-02	4.55E-11	XRCC6	-1.93E-01	1.55E-37	ZNF414	-1.18E-02	8.74E-07			
VAMP7	-1.99E-04	6.88E-08	XRN1	-5.18E-03	1.01E-05	ZNF428	-7.38E-02	2.85E-14			
VAMP8	-1.11E-01	2.01E-13	XRN2	-4.36E-02	8.00E-07	ZNF43	-4.27E-02	3.33E-09			
VARS	-2.25E-03	1.96E-05	YAF2	-7.00E-03	4.30E-05	ZNF451	-3.18E-03	1.89E-02			
VBP1	-1.61E-01	7.68E-45	YARS	-1.95E-02	1.11E-07	ZNF493	-4.78E-04	3.47E-02			
VDAC1	-2.61E-01	5.59E-62	YARS2	-8.70E-03	5.84E-03	ZNF511	-5.17E-02	2.69E-07			
VDAC2	-1.88E-02	1.71E-04	YBX1	-5.00E-01	1.32E-273	ZNF512	-9.73E-03	9.26E-03			
VDAC3	-4.88E-02	4.77E-09	YDJC	-2.52E-02	4.81E-07	ZNF544	-1.48E-02	4.58E-08			
VEZT	-1.07E-02	1.31E-06	YEATS4	-2.21E-01	9.88E-60	ZNF562	-2.28E-02	4.42E-06			
VKORC1	-1.75E-01	5.24E-42	YIF1A	-3.74E-02	2.36E-06	ZNF580	-2.96E-02	1.71E-08			
VMA21	-7.87E-02	1.16E-10	YIF1B	-4.04E-02	2.55E-07	ZNF639	-1.18E-02	6.40E-04			
VPS13A	-2.13E-02	1.07E-04	YIPF5	-9.81E-04	2.69E-03	ZNF644	-8.75E-04	1.10E-05			
VPS16	-6.91E-03	2.91E-02	YLPM1	-3.57E-02	2.45E-07	ZNF652	-1.14E-02	3.79E-04			

Appendix table 4

Genes that identified as having their variability along the HSC activation state transition trajectory influenced significantly (FDR <0.05) by age in the context of the integrative analysis of the HSC dataset. waldStat – Wald test statistic acts as a metric of signal-to-noise ratio, meaning in this setting that higher values equate to higher differences of expression between aged vs young donor cells along the trajectory.

Gene	waldStat	FDR	Gene	waldStat	FDR	Gene	waldStat	FDR
FTH1	6.23E+02	0.00E+00	SMOX	1.12E+02	0.00E+00	PLAC8	7.54E+01	8.28E-13
RPL34	5.53E+02	0.00E+00	MCL1	1.12E+02	0.00E+00	ARRDC3	7.37E+01	1.85E-12
RPS3A	4.20E+02	0.00E+00	KLF6	1.12E+02	0.00E+00	MAFF	7.36E+01	1.89E-12
RPL7	3.95E+02	0.00E+00	SPINK2	1.11E+02	0.00E+00	MT-ND2	7.34E+01	2.05E-12
ID2	3.56E+02	0.00E+00	SOX4	1.11E+02	0.00E+00	SDF2L1	7.34E+01	2.10E-12
RPS18	2.97E+02	0.00E+00	HSPA1A	1.10E+02	0.00E+00	NINJ1	7.32E+01	2.21E-12
AREG	2.94E+02	0.00E+00	H3F3B	1.10E+02	0.00E+00	CDK6	7.28E+01	2.63E-12
PTMA	2.89E+02	0.00E+00	TUBA1B	1.10E+02	0.00E+00	SELL	7.28E+01	2.63E-12
FOS	2.45E+02	0.00E+00	MT-CO2	1.10E+02	0.00E+00	AMD1	7.25E+01	3.08E-12
CXCL8	2.23E+02	0.00E+00	IER2	1.05E+02	0.00E+00	RILPL2	7.22E+01	3.45E-12
RPL26	2.03E+02	0.00E+00	RPL21	1.05E+02	0.00E+00	NR4A2	7.21E+01	3.57E-12
RPL39	1.99E+02	0.00E+00	RPL11	1.04E+02	0.00E+00	JUNB	7.19E+01	3.89E-12
SAT1	1.95E+02	0.00E+00	UBC	1.03E+02	0.00E+00	ACTB	7.19E+01	3.96E-12
DUSP1	1.93E+02	0.00E+00	KLF2	1.03E+02	0.00E+00	LDHA	7.07E+01	6.87E-12
AC103591.3	1.80E+02	0.00E+00	ZFP36	1.02E+02	0.00E+00	LYZ	7.05E+01	7.42E-12
FOSB	1.77E+02	0.00E+00	JUND	1.02E+02	0.00E+00	MARCKSL1	7.02E+01	8.39E-12
HSPA5	1.74E+02	0.00E+00	RPL12	1.00E+02	0.00E+00	HSPE1	6.99E+01	9.77E-12
PRDX1	1.70E+02	0.00E+00	HOPX	9.98E+01	0.00E+00	PDE4B	6.84E+01	1.93E-11
RPL3	1.68E+02	0.00E+00	PPP1R15A	9.91E+01	0.00E+00	ARPC5L	6.82E+01	2.16E-11
TSC22D1	1.67E+02	0.00E+00	PELI1	9.83E+01	0.00E+00	HMGA1	6.73E+01	3.26E-11
SH3BGRL3	1.64E+02	0.00E+00	ARF6	9.67E+01	0.00E+00	GNA15	6.57E+01	6.91E-11
RPS19	1.64E+02	0.00E+00	CD164	9.64E+01	0.00E+00	RHOB	6.54E+01	7.65E-11
MT-ND5	1.63E+02	0.00E+00	SERPINB1	9.63E+01	0.00E+00	FABP5	6.54E+01	7.75E-11
RPLP1	1.60E+02	0.00E+00	PFN1	9.26E+01	0.00E+00	EZR	6.50E+01	9.41E-11
JUN	1.58E+02	0.00E+00	RPS27	9.11E+01	0.00E+00	PFKFB3	6.47E+01	1.05E-10
RPS6	1.54E+02	0.00E+00	NFKBIA	8.93E+01	0.00E+00	MT2A	6.34E+01	1.88E-10
CXCL3	1.50E+02	0.00E+00	HNRNPA1	8.80E+01	3.81E-15	SRSF5	6.30E+01	2.32E-10
IGHM	1.47E+02	0.00E+00	RPL41	8.59E+01	7.33E-15	EIF4A3	6.30E+01	2.32E-10
RPS15A	1.44E+02	0.00E+00	EGR1	8.57E+01	7.33E-15	AL118516.1	6.28E+01	2.43E-10
NPM1	1.43E+02	0.00E+00	MDK	8.54E+01	7.33E-15	ZNF331	6.25E+01	2.79E-10
NEAT1	1.43E+02	0.00E+00	TCOF1	8.48E+01	1.07E-14	HIST1H2BC	6.24E+01	2.96E-10
DNAJB6	1.40E+02	0.00E+00	ID1	8.47E+01	1.07E-14	SLC7A5	6.22E+01	3.25E-10
TMSB4X	1.40E+02	0.00E+00	SKIL	8.39E+01	1.75E-14	YPEL5	6.19E+01	3.70E-10
RPS4X	1.40E+02	0.00E+00	CAVIN2	8.37E+01	1.75E-14	IFIT1	6.18E+01	3.87E-10
CXCL2	1.37E+02	0.00E+00	STMN1	8.29E+01	2.73E-14	B2M	6.08E+01	6.00E-10
EIF1	1.36E+02	0.00E+00	BHLHE40	8.28E+01	2.73E-14	RPL31	6.04E+01	7.14E-10
RPS2	1.34E+02	0.00E+00	PTGER2	8.20E+01	4.05E-14	MAP3K8	6.03E+01	7.69E-10
LMNA	1.33E+02	0.00E+00	ANXA2	8.18E+01	4.33E-14	XBP1	5.87E+01	1.56E-09
AVP	1.32E+02	0.00E+00	IFIT2	8.18E+01	4.61E-14	NAMPT	5.85E+01	1.68E-09
VIM	1.31E+02	0.00E+00	CKS2	8.14E+01	5.21E-14	PIM3	5.85E+01	1.68E-09
RPL13	1.31E+02	0.00E+00	EEF1A1	8.14E+01	5.42E-14	SARAF	5.83E+01	1.85E-09
RPL10	1.28E+02	0.00E+00	IDS	8.13E+01	5.42E-14	ATF3	5.82E+01	1.92E-09
PLAUR	1.28E+02	0.00E+00	PTGER4	8.08E+01	6.94E-14	EIF4A2	5.80E+01	2.15E-09
HIST1H1C	1.28E+02	0.00E+00	SRGN	8.02E+01	9.05E-14	GADD45A	5.79E+01	2.16E-09
HMGB2	1.28E+02	0.00E+00	MIDN	8.00E+01	9.88E-14	ISG15	5.69E+01	3.52E-09
ENO1	1.26E+02	0.00E+00	CTNNB1	7.95E+01	1.24E-13	IFIT3	5.65E+01	4.12E-09
ARID5A	1.23E+02	0.00E+00	TSC22D3	7.95E+01	1.24E-13	MT-CYB	5.63E+01	4.51E-09
INSIG1	1.21E+02	0.00E+00	DDX5	7.80E+01	2.48E-13	MT-CO3	5.59E+01	5.33E-09
PMAIP1	1.20E+02	0.00E+00	GADD45B	7.77E+01	2.87E-13	ZFP36L2	5.57E+01	5.83E-09
ANKRD28	1.14E+02	0.00E+00	MZB1	7.71E+01	3.81E-13	NR4A1	5.57E+01	5.91E-09

Gene	waldStat	FDR	Gene	waldStat	FDR	Gene	waldStat	FDR
GYPC	5.56E+01	6.24E-09	FOSL1	4.07E+01	4.41E-06	NR4A3	3.32E+01	1.00E-04
SET	5.54E+01	6.66E-09	IGHD	4.06E+01	4.56E-06	AC020916.1	3.32E+01	1.02E-04
FAM30A	5.52E+01	7.14E-09	TMEM107	4.03E+01	5.14E-06	HSP90B1	3.30E+01	1.07E-04
SMIM24	5.51E+01	7.63E-09	AC011139.1	4.02E+01	5.45E-06	AC245014.3	3.29E+01	1.13E-04
RARA	5.49E+01	8.25E-09	TFPI	3.94E+01	7.81E-06	RANBP2	3.25E+01	1.34E-04
STX11	5.46E+01	9.29E-09	TM4SF1	3.94E+01	7.81E-06	CD52	3.25E+01	1.37E-04
CSF3R	5.45E+01	9.92E-09	SLBP	3.90E+01	9.00E-06	LAT2	3.21E+01	1.57E-04
HERPUD1	5.44E+01	1.01E-08	MT-ND4	3.89E+01	9.49E-06	CLU	3.21E+01	1.59E-04
EMP3	5.44E+01	1.01E-08	CDKN1A	3.83E+01	1.23E-05	S100A6	3.21E+01	1.59E-04
SPRY1	5.35E+01	1.54E-08	TUBA1A	3.83E+01	1.25E-05	BST2	3.20E+01	1.64E-04
HIST2H2AC	5.31E+01	1.85E-08	MT-ND1	3.82E+01	1.30E-05	ADAMTS1	3.17E+01	1.85E-04
BIRC2	5.29E+01	1.99E-08	CALR	3.81E+01	1.36E-05	C19orf48	3.17E+01	1.85E-04
SOCS2	5.29E+01	2.01E-08	CSKMT	3.73E+01	1.91E-05	AC007952.4	3.16E+01	1.92E-04
CCNH	5.19E+01	3.22E-08	ELMSAN1	3.71E+01	2.06E-05	TXNIP	3.15E+01	2.04E-04
ALDH1A1	5.14E+01	3.99E-08	DNAJB1	3.69E+01	2.29E-05	S100A11	3.13E+01	2.23E-04
GSTP1	5.12E+01	4.32E-08	IGLL1	3.68E+01	2.37E-05	MT1X	3.12E+01	2.35E-04
CXCR4	5.12E+01	4.32E-08	HIF1A	3.68E+01	2.38E-05	IFI16	3.03E+01	3.37E-04
RPL35A	5.10E+01	4.67E-08	FUS	3.67E+01	2.38E-05	HMGN2	3.03E+01	3.39E-04
CD69	5.08E+01	5.17E-08	MT-CO1	3.67E+01	2.45E-05	SNRK	3.02E+01	3.58E-04
TUBB	5.07E+01	5.24E-08	EVL	3.66E+01	2.47E-05	PTGS2	3.01E+01	3.76E-04
HSP90AA1	5.04E+01	6.17E-08	SNRPB	3.66E+01	2.49E-05	MSMO1	3.00E+01	3.79E-04
PIM1	5.02E+01	6.57E-08	DDIT4	3.66E+01	2.49E-05	IGSF10	3.00E+01	3.81E-04
USP12	4.97E+01	8.23E-08	ARL4A	3.66E+01	2.50E-05	WTAP	2.99E+01	3.91E-04
DDIT3	4.94E+01	9.38E-08	HIST1H2AE	3.66E+01	2.51E-05	TAGLN2	2.99E+01	4.00E-04
HIST1H2BG	4.91E+01	1.06E-07	MYC	3.64E+01	2.74E-05	PFDN4	2.98E+01	4.10E-04
CYTL1	4.86E+01	1.33E-07	IER3	3.63E+01	2.83E-05	KLF3	2.98E+01	4.13E-04
LUC7L3	4.83E+01	1.57E-07	MALAT1	3.63E+01	2.83E-05	HHEX	2.97E+01	4.22E-04
VEGFA	4.75E+01	2.24E-07	NUCB2	3.62E+01	2.95E-05	DLK1	2.97E+01	4.28E-04
TNFSF13B	4.73E+01	2.38E-07	DUSP6	3.54E+01	4.05E-05	RPS4Y1	2.96E+01	4.38E-04
C16orf54	4.69E+01	2.86E-07	EIF5	3.52E+01	4.44E-05	RPL22L1	2.95E+01	4.68E-04
TUBB4B	4.62E+01	4.01E-07	SH3BP5	3.52E+01	1.71E-05	YBX1	2.93E+01	5.10E-04
CITED2	4.52E+01	6.10E-07	TAOK3	3.51E+01	4.60E-05	HSPD1	2.93E+01	5.10E-04
MYADM	4.47E+01	7.80E-07	HLA-DRB1	3.51E+01	4.67E-05	FAM133B	2.90E+01	5.70E-04
PPP1CB	4.46E+01	8.03E-07	UBB	3.51E+01	4.68E-05	HIST1H2BD	2.89E+01	6.03E-04
H1FX	4.44E+01	8.64E-07	ATP2B1-AS1	3.50E+01	4.86E-05	HIST1H2AC	2.88E+01	6.09E-04
TPI1	4.41E+01	1.01E-06	WDR74	3.49E+01	5.09E-05	S100A4	2.86E+01	6.70E-04
RPS12	4.41E+01	1.01E-06	AC026979.2	3.49E+01	5.09E-05	EIF5A	2.84E+01	7.33E-04
FTL	4.35E+01	1.33E-06	HSPA1B	3.48E+01	5.32E-05	RASGEF1B	2.83E+01	7.56E-04
RAN	4.34E+01	1.35E-06	SRP9	3.47E+01	5.39E-05	IGFBP7	2.82E+01	7.72E-04
HLA-C	4.33E+01	1.43E-06	GAPDH	3.45E+01	5.83E-05	SELENOM	2.80E+01	8.51E-04
IFNGR1	4.21E+01	2.45E-06	RANBP1	3.44E+01	6.04E-05	PPIA	2.73E+01	1.15E-03
MYCT1	4.19E+01	2.69E-06	SRSF7	3.44E+01	6.26E-05	ORAI2	2.72E+01	1.21E-03
ACTG1	4.16E+01	3.07E-06	HNRNPA2B1	3.41E+01	6.85E-05	RFX2	2.72E+01	1.22E-03
CA2	4.13E+01	3.47E-06	IL1B	3.41E+01	7.11E-05	PER2	2.69E+01	1.38E-03
STK17A	4.11E+01	3.68E-06	HLA-DQA1	3.39E+01	7.56E-05	CRHBP	2.68E+01	1.39E-03
MRPL16	4.11E+01	3.74E-06	KLF4	3.39E+01	7.56E-05	WEE1	2.67E+01	1.44E-03
CDC42SE1	4.11E+01	3.74E-06	FAM177A1	3.38E+01	7.82E-05	CREM	2.66E+01	1.50E-03
PROM1	4.10E+01	3.83E-06	SQSTM1	3.36E+01	8.66E-05	AHR	2.66E+01	1.50E-03
TRBC2	4.08E+01	4.24E-06	CALM1	3.36E+01	8.66E-05	RNF125	2.63E+01	1.74E-03
HLA-A	4.07E+01	4.41E-06	LSP1	3.33E+01	9.75E-05	HMGB1	2.62E+01	1.80E-03

Gene	waldStat	FDR	Gene	waldStat	FDR	Gene	waldStat	FDR
HNRNPH1	2.59E+01	2.00E-03	H2AFZ	2.16E+01	1.06E-02	COCH	1.85E+01	3.30E-02
MT-ND3	2.59E+01	2.02E-03	TOB1	2.16E+01	1.08E-02	AC005921.2	1.84E+01	3.46E-02
GLUL	2.57E+01	2.24E-03	AC074327.1	2.15E+01	1.09E-02	CREBRF	1.84E+01	3.48E-02
PSMD12	2.56E+01	2.31E-03	ANP32B	2.15E+01	1.11E-02	C3orf14	1.83E+01	3.58E-02
LRRFIP1	2.55E+01	2.35E-03	PPP1R3B	2.14E+01	1.14E-02	NLRP3	1.83E+01	3.61E-02
DUT	2.51E+01	2.83E-03	KLF10	2.14E+01	1.15E-02	ANP32E	1.83E+01	3.63E-02
SBDS	2.50E+01	2.98E-03	SNHG19	2.13E+01	1.18E-02	UCP2	1.82E+01	3.70E-02
RGS2	2.49E+01	2.98E-03	RFC4	2.13E+01	1.19E-02	SEMA7A	1.81E+01	3.91E-02
HIST1H4C	2.49E+01	2.98E-03	H1F0	2.13E+01	1.20E-02	RSBN1	1.80E+01	3.94E-02
SKI	2.48E+01	3.11E-03	BTG1	2.12E+01	1.23E-02	HLA-DRA	1.80E+01	4.07E-02
NFKBIZ	2.45E+01	3.63E-03	PRMT9	2.11E+01	1.29E-02	SRSF3	1.78E+01	4.31E-02
NEU1	2.44E+01	3.69E-03	PTTG1IP	2.10E+01	1.32E-02	PYM1	1.78E+01	4.32E-02
CALM2	2.41E+01	4.25E-03	EMP1	2.09E+01	1.41E-02	REL	1.78E+01	4.36E-02
AC114760.2	2.41E+01	4.25E-03	SEC14L1	2.08E+01	1.41E-02	MEX3B	1.77E+01	4.49E-02
TCF4	2.40E+01	4.45E-03	TPM4	2.08E+01	1.45E-02	MGST1	1.77E+01	4.50E-02
ZFAND5	2.38E+01	4.73E-03	SCN1B	2.07E+01	1.46E-02	NOG	1.77E+01	4.50E-02
HLA-B	2.36E+01	5.15E-03	MIR181A1HG	2.07E+01	1.47E-02	SVIP	1.76E+01	4.53E-02
NCL	2.36E+01	5.17E-03	PTS	2.07E+01	1.50E-02	TIPARP	1.76E+01	4.54E-02
CST3	2.35E+01	5.36E-03	HIST1H2BF	2.06E+01	1.53E-02	PHKG1	1.76E+01	4.66E-02
HEMGN	2.34E+01	5.52E-03	AC095055.1	2.06E+01	1.55E-02	AL157938.3	1.75E+01	4.76E-02
PPP1R16B	2.34E+01	5.56E-03	HNRNPA3	2.05E+01	1.56E-02	CYTOR	1.75E+01	4.82E-02
CLEC11A	2.33E+01	5.84E-03	RAB31	2.04E+01	8.03E-03	PRKDC	1.74E+01	4.84E-02
EIF4A1	2.32E+01	6.01E-03	HLA-DPB1	2.03E+01	1.71E-02	HNRNPM	1.74E+01	4.90E-02
GLIPR1	2.31E+01	6.25E-03	PPP3CA	2.03E+01	1.72E-02	EGFL7	1.74E+01	4.91E-02
CDK4	2.30E+01	6.42E-03	C1QTNF4	2.02E+01	1.76E-02	PKM	1.74E+01	4.97E-02
YWHAH	2.30E+01	6.45E-03	BIRC3	2.02E+01	1.37E-03	ADGRE5	1.48E+01	3.30E-02
TRA2B	2.29E+01	6.64E-03	B3GNT2	2.02E+01	1.77E-02	PLEC	1.44E+01	3.94E-02
SLC25A5	2.28E+01	6.84E-03	AC002454.1	2.02E+01	1.81E-02	KLHL28	9.82E+00	4.63E-02
MCM3	2.28E+01	6.86E-03	HSPA8	2.01E+01	1.81E-02			
PDE4D	2.28E+01	6.91E-03	TNFRSF12A	2.00E+01	1.88E-02			
EVI2B	2.27E+01	7.30E-03	DHFR	2.00E+01	1.88E-02			
EMCN	2.26E+01	7.34E-03	RPGR	2.00E+01	1.93E-02			
SUMF2	2.25E+01	7.66E-03	EIF2S3	2.00E+01	1.94E-02			
SYAP1	2.25E+01	7.67E-03	TMPO	1.99E+01	1.99E-02			
BCL3	2.25E+01	7.70E-03	GABPB1-AS1	1.99E+01	1.99E-02			
MCM5	2.25E+01	7.82E-03	ATP1B1	1.98E+01	2.07E-02			
LAPTM4A	2.24E+01	8.04E-03	FOSL2	1.97E+01	2.09E-02			
DNAJB9	2.23E+01	8.37E-03	QPCT	1.97E+01	2.14E-02			
GNAI1	2.20E+01	9.19E-03	AC087239.1	1.96E+01	2.21E-02			
ESF1	2.20E+01	9.21E-03	AC103724.4	1.96E+01	2.22E-02			
CFL1	2.20E+01	9.47E-03	CXCL6	1.96E+01	2.22E-02			
TRA2A	2.19E+01	9.47E-03	SORL1	1.94E+01	2.34E-02			
MMRN1	2.19E+01	9.47E-03	RELB	1.94E+01	5.40E-03			
MRPL1	2.19E+01	9.51E-03	CDC20	1.94E+01	2.42E-02			
ATF7IP2	2.19E+01	9.63E-03	ANXA1	1.90E+01	2.75E-02			
MLF1	2.19E+01	9.71E-03	MIR22HG	1.90E+01	2.81E-02			
PHF20	2.18E+01	9.80E-03	NPW	1.89E+01	2.88E-02			
BEX1	2.18E+01	9.94E-03	TRMT6	1.88E+01	2.97E-02			
S100A10	2.18E+01	1.01E-02	EIF2S2	1.88E+01	2.99E-02			
HLA-DQB1	2.17E+01	1.02E-02	OSM	1.87E+01	3.16E-02			

Appendix table 5

Breakdown of the normalised enrichment scores, FDR values and leading-edge genes highlighted for the GSEA results visualised in Figure 41

Gene set	NES - recovery COVID-19 hospitalisation	FDR - recovery COVID-19 hospitalisation	leadingEdge genes - recovery COVID-19 hospitalisation	NES - ageing healthy cohort	FDR - ageing healthy cohort	leadingEdge genes - ageing healthy cohort
Adaptive Immune System	1.80E+00	1.17E-06	HLA-DPB1, HLA-DPA1, HLA-DRB1, CD99, TAP1, RBX1, HLA-DRA, ELOB, SKP1, PSMA5, ITGB2, PSMB9, PRKCB, SEC61G, HCST, CD74, HLA-DRB5, CTSC, PSMB8, PSMD9, YWHAZ, PSME1, ZAP70, PPP2CA, SEC61B, DYNLL1, ITGAL, VAMP8, CAPZA1, TRAC, PSMA7, SEM1, PPIA, ITGB1, PSMB3, CD8B, PSMB10, YWHAB, PPP2R5C, RAP1B, PSME2, CD8A, PSMB2, CLEC2B, CSK, LCK, CAPZB, LAG3, CD3D, ITGB7, KLRD1, RNF213, FBXW5, PSMB6, CALR, AP2S1, SH2D1A, PSMA4, UBE2A, B2M, UBB, TAPBP, TNFRSF14, NFATC3, UBE2L6, KLRG1, SLAMF6, BTN3A2, CYBA, HLA-B, PSMD2	1.47E+00	3.40E-03	IGKC, IGLV2-23, IGHV3-33, PILRA, IGLV3-21, IGLV4-69, LILRA5, S100A9, IGLC3, HLA-DQA2, NCF2, LILRB2, CYBB, CTLA4, IGHV4-34, IGLC2, IGLV2-8, IGKV1-17, S100A8, HLA-DQA1, IGHV3-11, IGLV1-40, RAC1, IGLV3-19, TRPC1, FBXL14, SPSB1, HLA-DQB2, SPSB2, MAPKAP1, IGLV1-44, PTEN, PPP3R1, CD300E, STUB1, ERAP2, PPP3CB, HLA-DQB1, IGLV6-57, OSCAR, DYNC1I1, SIAH2, RNF144B, IGHV3-7, HRAS, RNF220, TRAT1, CTSK, KIF3C, FBXL15, IGHV1-2, SOS1, KLHL5, IGKV1-5, LILRA2, ITGB1, CDC34, TRBV7-9, LYN, ORAI1, PPP2R5A, FBXL8, TRAV19, TAB2, BTBD1, KLRF1, UBE2Z, TLR6, BTBD6, TLR1, IGHV4-39, CD81, FBXL16, CD4, ASB2, NFKB1, CAPZA1, CSK, RBX1, RASGRP1, RBBP6, ASB13, CYBA, SLAMF6, LY96, ICOSLG, CUL3, UBE2M, LILRB4, MKRN1, CTSB, UBE2E2
Cell surface interactions at the vascular wall	1.59E+00	1.04E-01	CD99, CD2, ITGB2, CD74, ITGAL, PPIA, DOK2, ITGB1, LCK, TGFB1, SELPLG, ATP1B3, SPN, BSG	1.81E+00	6.61E-04	IGKC, IGLV2-23, IGHV3-33, IGLV3-21, IGLV4-69, IGLC3, SLC7A7, IGHV4-34, IGLC2, IGLV2-8, IGKV1-17, IGHA2, IGHV3-11, IGLV1-40, IGLV3-19, IGLV1-44, IGLV6-57, ITGA3, IGHV3-7, HRAS, IGHV1-2, SOS1, IGKV1-5, ITGB1, CD2, LYN

Disease	1.30E+00	5.67E-02	RPS10, RPL36A, RPL26, RPS4Y1, ARPC2, RBX1, CDC25B, ELOB, ACTR3, MYH9, SKP1, TXN, PSMA5, BRK1, PSMB9, PSMB8, PSMD9, YWHAZ, PSME1, PPP2CA, DYNLL1, MSN, PRDX1, POLR2L, ARPC3, CYFIP2, PSMA7, ATP1A1, SEM1, PPIA, CAPN2, VAMP2, YWHAQ, HSP90AA1, ITGB1, PSMB3, CD8B, PYCARD, PSMB10, TUBB, YWHAB, NCKAP1L, PPP2R5C, RAP1B, PSME2, PSMB2, CASP1, TPST2, GYG1, CSK, LCK, CORO1A, SND1, ARPC5, APOBEC3G, SNRPB, IQGAP1, SNRPG, RHOG, SUPT4H1, PRKAR1A, TGFB1, RPS27L, RNF213, RPS17, PSMB6, RBBP4, KPNB1, GNG5, CAPN1, ENO1, PARP1, ATP1B3, CALR, AP2S1, PSMA4, BSG, B2M, UBB, TPM4, RAC2, TPM3, FGR, CYBA, HLA-B, PSMD2, SNRPE, POLR2K, IKBKG, MGAT1, PTGER2, MYD88, CAPNS1, YWHAH, RPS15A, IMPDH1, HNRNPK, ACTB, ACTR2, ACTG1, MIB2, HMGB1, PSMB1, FYN, POLR2G, HK1, GNAI2	1.26E+00	9.93E-02	IGKC, IGLV2-23, IGHV3-33, RPS4Y1, IGLV3-21, IGLV4-69, GPR27, S100A9, YWHAH, IGLC3, SLC7A7, NOD2, C1GALT1C1, VCAN, IGHV4-34, IGLC2, MGAT4B, IGLV2-8, E2F2, IGKV1-17, S100A8, IGHV3-11, SLC40A1, IGLV1-40, PTGER2, RAC1, IGLV3-19, PIM1, CEBPB, MAPK14, ABCC9, TFDP1, CHMP7, SAP30, MAPKAP1, MYC, EREG, IGLV1-44, PTEN, ADAMTSL3, GNB2, RCOR1, GALNT12, TAF10, CDKN1C, UNC93B1, GPR15, MAML1, IGLV6-57, FNTA, KANK1, HCK, DVL3, DYNC1I1, MAP2K1, DBP, RPS27L, MAPK1, GSK3A, IGHV3-7, HRAS, ANTXR2, FRS3, CAMK2B, TRAT1, SNF8, RPS2, MAP2K2, IGHV1-2, SOS1, GPR150, B3GALT6, IGKV1-5, HMOX1, ADCY3, ITGB1, MTA1, TGFBR1, CD163, MYO1C, LYN, CTBP1, PPP2R5A, GNG11, MAPK3, TAB2, POM121, LRAT, TBL1XR1, STAT1, CHST14, RAD9B, CHD3, GCLM, CYSLTR1, HRH2, NAGLU, STRN, IL1B, TLR6, SRPK1, PRDX1, TLR1, PRKAR2B, POMGNT1, IGHV4-39, SLC9A9, GAB2, CD4, NFKB1, ABCA3, CSK, MARK3, ZDHHC2, CDKN2A, XRCC2, GCLC, RBX1, LFNG, CPSF4, MAP2K4, CYBA, SLC4A4, LY96, CUL3, EPS15, MGAT5, SLC4A1, TSHR, ETV6, COMT, NUP50
FCERI mediated NF-kB activation	1.56E+00	8.87E-02	SKP1, PSMA5, PSMB9, PSMB8, PSMD9, PSME1, PSMA7, SEM1, PSMB3,	1.80E+00	1.21E-03	IGKC, IGLV2-23, IGHV3-33, IGLV3-21, IGLV4-69, IGLC3, IGHV4-34, IGLC2, IGLV2-8, IGKV1-17, IGHV3-11, IGLV1-40, IGLV3-

			PSMB10, PSME2, PSMB2, PSMB6, PSMA4, UBB, PSMD2, IKBKG, PSMB1, PSMC4			19, IGLV1-44, IGLV6-57, IGHV3-7, IGHV1-2, IGKV1-5, CDC34, LYN, TAB2, IGHV4-39, NFKB1, RASGRP1
Fcgamma receptor (FCGR) dependent phagocytosis	1.47E+00	2.29E-01	ARPC2, ACTR3, MYH9, BRK1, CFL1, ARPC3, CYFIP2, HSP90AA1, NCKAP1L, ARPC5, FGR, ACTB, ACTR2, ACTG1, FYN	1.87E+00	5.59E-05	IGKC, IGLV2-23, IGHV3-33, IGLV3-21, IGLV4-69, IGLC3, IGHV4-34, IGLC2, IGLV2-8, IGKV1-17, IGHV3-11, IGLV1-40, RAC1, IGLV3-19, PRKCD, IGLV1-44, IGLV6-57, HCK, MAPK1, IGHV3-7, IGHV1-2, IGKV1-5, MYO1C, LYN, MAPK3
FCGR3A-mediated phagocytosis	1.48E+00	2.06E-01	ARPC2, ACTR3, MYH9, BRK1, ARPC3, CYFIP2, NCKAP1L, ARPC5, FGR, ACTB, ACTR2, ACTG1, FYN	1.90E+00	3.99E-05	IGKC, IGLV2-23, IGHV3-33, IGLV3-21, IGLV4-69, IGLC3, IGHV4-34, IGLC2, IGLV2-8, IGKV1-17, IGHV3-11, IGLV1-40, RAC1, IGLV3-19, IGLV1-44, IGLV6-57, HCK, MAPK1, IGHV3-7, IGHV1-2, IGKV1-5, MYO1C, LYN, MAPK3
Hemostasis	1.80E+00	4.22E-04	CAP1, FLNA, CD99, WDR1, PLEK, CD2, ACTN4, ITGB2, ANXA2, PRKCB, PFN1, CD74, YWHAZ, PPP2CA, ANXA5, S100A10, CFL1, ITGAL, CAPZA1, PRKCH, PPIA, DOK2, ITGB1, PPP2R5C, RAP1B, MANF, CSK, LCK, CAPZB, RHOA, FERMT3, RHOG, TAGLN2, PRKAR1A, TGFB1, GNG5, SRGN, SELPLG, ATP1B3, SPN, ATP2B4, BSG, SRI, PSAP, RAC2, FGR	1.70E+00	3.50E-05	IGKC, IGLV2-23, IGHV3-33, RARRES2, IGLV3-21, IGLV4-69, IGLC3, SERPINA1, SLC7A7, HBD, IGHV4-34, IGLC2, IGLV2-8, IGKV1-17, IGHA2, CABLES2, DOCK3, HBB, IGHV3-11, IGLV1-40, PRKG2, RAC1, IGLV3-19, TFPI, MAPK14, PRKCD, PRKCA, IGLV1-44, GNB2, RCOR1, AKAP1, IGLV6-57, KIF6, ITGA3, MAPK1, IGHV3-7, HRAS, ATP2A3, KIF3C, F5, PDE5A, IGHV1-2, SOS1, ZFPM1, IGKV1-5, KIFC2, ITGB1, CD2, LYN, KIF21B, ORAI1, PPP2R5A, GNG11, MAPK3, DOCK11, PRKAR2B, IGHV4-39, CAPZA1, CSK, RASGRP1, EHD3, CFD, CLU, PF4, DGKZ, JCHAIN, SERPINB6, RACGAP1, ABHD6, TLN1

Immune System	1.64E+00	2.08E-08	HLA-DPB1, HLA-DPA1, HLA-DRB1, S100A11, ARPC2, CAP1, TRAPPC1, FLNA, CD99, IFITM2, ATP6V0E1, TAP1, RBX1, IL10RA, HLA-DRA, ELOB, ACTR3, MYH9, SKP1, TXN, PSMA5, ITGB2, BRK1, PSMB9, ANXA2, PGAM1, CCL5, PRKCB, SEC61G, HCST, CD74, HLA-DRB5, CTSC, PSMB8, PSMD9, YWHAZ, RPS6KA1, PSME1, ZAP70, PPP2CA, SEC61B, DYNLL1, MSN, CFL1, STOM, POLR2L, IFITM3, ITGAL, VAMP8, TBC1D10C, ADAM8, CAPZA1, ARPC3, TRAC, HNRNPF, CYFIP2, PSMA7, SEM1, PPIA, VAMP2, HSP90AA1, OSTF1, ITGB1, PSMB3, CD8B, PYCARD, PSMB10, TUBB, MVP, YWHAB, GBP5, NCKAP1L, PPP2R5C, RAP1B, PSME2, CD8A, PSMB2, RHOF, CASP1, CLEC2B, ATP6V0B, IL32, TMEM179B, GZMM, GYG1, CSK, RAB27A, LCK, CAPZB, IL12RB1, RHOA, LAG3, CD3D, ARPC5, ANXA1, IQGAP1, RHOG, GSTP1, ITGB7, TGFB1, CSTB, KLRD1, RNF213, NLRC5, PTPN7, FBXW5, PSMB6, KPNB1, CAPN1, ATP6V0D1, KCNAB2, DIAPH1, CALR, AP2S1, SH2D1A, PSMA4, UBE2A, HMOX2, GPI, B2M,	1.51E+00	1.33E-06	IGKC, IGLV2-23, IGHV3-33, S100A12, PILRA, CLEC12A, IGLV3-21, CDA, MNDA, IGLV4-69, LILRA5, LYZ, S100A9, IGLC3, SERPINA1, HLA-DQA2, NCF2, NOD2, LILRB2, EDA, FCN1, CYBB, CTLA4, IGHV4-34, IGLC2, IGLV2-8, BCL2, LPCAT1, IGKV1-17, S100A8, HLA-DQA1, FPR1, HBB, IGHV3-11, IGLV1-40, DSC1, IL2RA, CAB39, CISH, IL10RA, ALOX5, LY86, MAPK10, IFIT1, GSN, EIF4E3, HTN1, RAC1, IGLV3-19, TRPC1, PIM1, FCER2, CFH, FBXL14, CD68, MAPK14, MGST1, SPSB1, HLA-DQB2, PRKCD, MEF2C, SPSB2, RNASE6, CA1, MAPKAP1, S100A11, MYC, RSAD2, CST3, IGLV1-44, PTEN, PTPN9, FRK, ATP6V1E2, PPP3R1, CD300E, STUB1, ERAP2, PPP3CB, PTPN18, IFIT3, IRAK3, UNC93B1, HLA-DQB1, COTL1, IGLV6-57, OSCAR, CSF1, HCK, CLEC7A, DYNC1I1, MAP2K1, SIAH2, GCA, MAPK1, RNF144B, MAPK11, TRIM3, IGHV3-7, HRAS, BRI3, DCD, RNF220, CAMK2B, MX1, TRAT1, DNAJC5, CTSK, TRIM22, CTSZ, KIF3C, FBXL15, CRISPLD2, IGHV1-2, SOS1, KLHL5, IGKV1-5, TNFRSF11A, PTPN20, SAMHD1, LILRA2, DGAT1, HMOX1, ATF1, DHX58, ITGB1, CDC34, TMEM30A, RAB31, TRBV7-9, IQGAP2, MYO1C, LYN, SOCS2, ORAI1, PPP2R5A, C5AR1, FBXL8, TRAV19, MAPK3, TAB2, POM121, BTBD1, STAT1, DNAJC13, CRKL, RAB3D, KLRF1, UBE2Z, PDXK, IL1B, TLR6, IFITM3, ACLY, BTBD6, NLRX1, TLR1, IGHV4-39, CD81, FBXL16, OAS1, GAB2, CD4, RHOU, ASB2, NFKB1, TNFRSF4, CAPZA1, CSK, RBX1, RASGRP1, TIMP2, RBBP6, MAP2K4, ASB13, CXCL2, ATP11A, CYBA, OAS3, SLAMF6, IRF5, LY96, ICOSLG,

			UBB, TAPBP, TNFRSF14, NFATC3, MT2A, BATF, CCL4, PSAP, SLC44A2, IQGAP2, UBE2L6, RAC2, CASP4, TNFRSF1B, KLRG1, SLAMF6, RAB37, FGR, GNLY, BTN3A2, CYBA, HLA-B, PSMD2			CUL3, UBE2M, TRIM46, AGL, CD70, CFD, MAP3K1, LILRB4, CLU, MKRN1, NUP50, CTSB, CYLD, UBE2E2
Immunoregulatory interactions between a Lymphoid and a non-Lymphoid cell	1.75E+00	6.34E-03	CD99, ITGB2, HCST, ITGAL, TRAC, ITGB1, CD8B, CD8A, CLEC2B, CD3D, ITGB7, KLRD1, SH2D1A, B2M, KLRG1, SLAMF6, HLA-B	1.76E+00	1.86E-03	IGKC, IGLV2-23, IGHV3-33, PILRA, IGLV3-21, IGLV4-69, LILRA5, IGLC3, LILRB2, IGHV4-34, IGLC2, IGLV2-8, IGKV1-17, IGHV3-11, IGLV1-40, IGLV3-19, IGLV1-44, CD300E, IGLV6-57, OSCAR, IGHV3-7, IGHV1-2, IGKV1-5, LILRA2, ITGB1, TRBV7-9, TRAV19, KLRF1, IGHV4-39, CD81
Infectious disease	1.45E+00	6.34E-03	RPS10, RPL36A, RPL26, RPS4Y1, ARPC2, RBX1, ELOB, ACTR3, MYH9, SKP1, TXN, PSMA5, BRK1, PSMB9, PSMB8, PSMD9, YWHAZ, PSME1, DYNLL1, POLR2L, ARPC3, CYFIP2, PSMA7, ATP1A1, SEM1, PPIA, VAMP2, YWHAQ, HSP90AA1, ITGB1, PSMB3, CD8B, PYCARD, PSMB10, TUBB, YWHAB, NCKAP1L, PSME2, PSMB2, CASP1, LCK, CORO1A, ARPC5, APOBEC3G, SNRPB, SNRPG, SUPT4H1, PRKAR1A, TGFB1, RPS27L, RNF213, RPS17, PSMB6, RBBP4, KPNB1, GNG5, ENO1, PARP1, ATP1B3, CALR, AP2S1, PSMA4, B2M, UBB, FGR, CYBA, HLA-B, PSMD2, SNRPE,	1.34E+00	5.82E-02	IGKC, IGLV2-23, IGHV3-33, RPS4Y1, IGLV3-21, IGLV4-69, GPR27, YWHAH, IGLC3, NOD2, IGHV4-34, IGLC2, MGAT4B, IGLV2-8, IGKV1-17, IGHV3-11, IGLV1-40, PTGER2, RAC1, IGLV3-19, MAPK14, CHMP7, SAP30, IGLV1-44, GNB2, RCOR1, TAF10, GPR15, IGLV6-57, FNTA, HCK, DVL3, DYNC1I1, MAP2K1, DBP, RPS27L, MAPK1, GSK3A, IGHV3-7, ANTXR2, SNF8, RPS2, MAP2K2, IGHV1-2, GPR150, IGKV1-5, HMOX1, ADCY3, ITGB1, MTA1, CD163, MYO1C, LYN, GNG11, MAPK3, TAB2, POM121, TBL1XR1, STAT1, CHD3, CYSLTR1, HRH2, IL1B, SRPK1, TLR1, PRKAR2B, IGHV4-39, CD4, NFKB1, ZDHHC2, RBX1, CPSF4, MAP2K4, CYBA, CUL3, EPS15, MGAT5, TSHR, COMT, NUP50

			POLR2K, IKBKG, MGAT1, PTGER2, YWHAH, RPS15A, IMPDH1, HNRNPK, ACTB, ACTR2, ACTG1, PSMB1, FYN, POLR2G, GNAI2, PSMC4, CALM1, POLR2J			
Innate Immune System	1.60E+00	2.96E-04	S100A11, ARPC2, CAP1, TRAPPC1, ATP6V0E1, ACTR3, MYH9, SKP1, TXN, PSMA5, ITGB2, BRK1, PSMB9, ANXA2, PGAM1, CTSC, PSMB8, PSMD9, RPS6KA1, PSME1, PPP2CA, DYNLL1, CFL1, STOM, POLR2L, ITGAL, VAMP8, TBC1D10C, ADAM8, CAPZA1, ARPC3, CYFIP2, PSMA7, SEM1, PPIA, HSP90AA1, OSTF1, PSMB3, PYCARD, PSMB10, TUBB, MVP, NCKAP1L, RAP1B, PSME2, PSMB2, RHOF, CASP1, ATP6V0B, TMEM179B, GZMM, GYG1, RAB27A, LCK, RHOA, ARPC5, IQGAP1, RHOG, GSTP1, CSTB, KLRD1, NLRC5, PSMB6, KPNB1, CAPN1, ATP6V0D1, KCNAB2, DIAPH1, PSMA4, HMOX2, GPI, B2M, UBB, NFATC3, PSAP, SLC44A2, IQGAP2, UBE2L6, RAC2, CASP4, TNFRSF1B, RAB37, FGR, GNLY, CYBA, HLA-B, PSMD2, CD53, POLR2K, IKBKG, ADGRE5, MYD88, GDI2, IMPDH1, CD63,	1.75E+00	2.28E-09	IGKC, IGLV2-23, IGHV3-33, S100A12, CLEC12A, IGLV3-21, CDA, MNDA, IGLV4-69, LYZ, S100A9, IGLC3, SERPINA1, NCF2, NOD2, LILRB2, FCN1, CYBB, IGHV4-34, IGLC2, IGLV2-8, BCL2, LPCAT1, IGKV1-17, S100A8, FPR1, HBB, IGHV3-11, IGLV1-40, DSC1, CAB39, ALOX5, LY86, MAPK10, GSN, HTN1, RAC1, IGLV3-19, CFH, CD68, MAPK14, MGST1, PRKCD, MEF2C, RNASE6, S100A11, CST3, IGLV1-44, FRK, ATP6V1E2, PPP3R1, CD300E, PPP3CB, IRAK3, UNC93B1, COTL1, IGLV6-57, OSCAR, HCK, CLEC7A, MAP2K1, GCA, MAPK1, MAPK11, IGHV3-7, HRAS, BRI3, DCD, DNAJC5, CTSK, CTSZ, CRISPLD2, IGHV1-2, SOS1, IGKV1-5, DGAT1, HMOX1, ATF1, DHX58, CDC34, TMEM30A, RAB31, IQGAP2, MYO1C, LYN, C5AR1, MAPK3, TAB2, DNAJC13, RAB3D, PDXK, IL1B, TLR6, ACLY, NLRX1, TLR1, IGHV4-39, CD81, GAB2, CD4, NFKB1, CAPZA1, RASGRP1, TIMP2, MAP2K4, ATP11A, CYBA, LY96, UBE2M, AGL, CFD, MAP3K1, CLU, CTSB, CYLD

			RAB6A, TCIRG1, ACTB, ACTR2, ACTG1, HMGB1, PSMB1, FYN, PSMC4, CALM1, SRP14, LAT, MAP2K3, IFI16, GRAP2, LCP2, ROCK1, LAMTOR2, GLIPR1			
Leishmania infection	1.50E+00	1.27E-01	ARPC2, ACTR3, MYH9, TXN, BRK1, ARPC3, CYFIP2, PYCARD, NCKAP1L, CASP1, ARPC5, PRKAR1A, GNG5, FGR, CYBA, PTGER2, ACTB, ACTR2, ACTG1, FYN, GNAI2, CALM1	1.85E+00	3.99E-05	IGKC, IGLV2-23, IGHV3-33, IGLV3-21, IGLV4-69, GPR27, IGLC3, IGHV4-34, IGLC2, IGLV2-8, IGKV1-17, IGHV3-11, IGLV1-40, PTGER2, RAC1, IGLV3-19, MAPK14, IGLV1-44, GNB2, GPR15, IGLV6-57, HCK, DVL3, MAPK1, IGHV3-7, IGHV1-2, GPR150, IGKV1-5, HMOX1, ADCY3, CD163, MYO1C, LYN, GNG11, MAPK3, CYSLTR1, HRH2, IL1B, PRKAR2B, IGHV4-39, NFKB1
Leishmania phagocytosis	1.48E+00	2.06E-01	ARPC2, ACTR3, MYH9, BRK1, ARPC3, CYFIP2, NCKAP1L, ARPC5, FGR, ACTB, ACTR2, ACTG1, FYN	1.90E+00	3.99E-05	IGKC, IGLV2-23, IGHV3-33, IGLV3-21, IGLV4-69, IGLC3, IGHV4-34, IGLC2, IGLV2-8, IGKV1-17, IGHV3-11, IGLV1-40, RAC1, IGLV3-19, IGLV1-44, IGLV6-57, HCK, MAPK1, IGHV3-7, IGHV1-2, IGKV1-5, MYO1C, LYN, MAPK3
Neutrophil degranulation	1.67E+00	1.78E-03	S100A11, CAP1, TRAPPC1, PSMA5, ITGB2, ANXA2, PGAM1, CTSC, DYNLL1, STOM, ITGAL, VAMP8, TBC1D10C, ADAM8, PPIA, HSP90AA1, OSTF1, PYCARD, TUBB, MVP, NCKAP1L, RAP1B, RHOF, TMEM179B, GYG1, RAB27A, RHOA, ARPC5, IQGAP1, RHOG, GSTP1, CSTB, KPNB1, CAPN1, KCNAB2, DIAPH1, HMOX2, GPI, B2M, PSAP, SLC44A2, IQGAP2, TNFRSF1B, RAB37, FGR, CYBA, HLA-B, PSMD2, CD53, ADGRE5, GDI2,	1.68E+00	1.08E-04	S100A12, CLEC12A, CDA, MNDA, LYZ, S100A9, SERPINA1, LILRB2, FCN1, CYBB, LPCAT1, S100A8, FPR1, HBB, DSC1, CAB39, ALOX5, GSN, RAC1, CD68, MAPK14, MGST1, PRKCD, S100A11, CST3, FRK, COTL1, OSCAR, GCA, MAPK1, BRI3, DNAJC5, CTSZ, CRISPLD2, DGAT1, TMEM30A, RAB31, IQGAP2, C5AR1, DNAJC13, RAB3D, PDXK, ACLY, NFKB1, TIMP2, ATP11A, CYBA, AGL, CFD, CTSB, SERPINB6, PTGES2, PYGL, MLEC, IGF2R, LAMP1, HMOX2, PRDX4, GSDMD, PTPRJ, FCER1G, METTL7A, SIGLEC9

			IMPDH1, CD63, RAB6A, TCIRG1, ACTR2, HMGB1, PSMB1			
Parasite infection	1.48E+00	2.06E-01	ARPC2, ACTR3, MYH9, BRK1, ARPC3, CYFIP2, NCKAP1L, ARPC5, FGR, ACTB, ACTR2, ACTG1, FYN	1.90E+00	3.99E-05	IGKC, IGLV2-23, IGHV3-33, IGLV3-21, IGLV4-69, IGLC3, IGHV4-34, IGLC2, IGLV2-8, IGKV1-17, IGHV3-11, IGLV1-40, RAC1, IGLV3-19, IGLV1-44, IGLV6-57, HCK, MAPK1, IGHV3-7, IGHV1-2, IGKV1-5, MYO1C, LYN, MAPK3
Regulation of actin dynamics for phagocytic cup formation	1.53E+00	1.59E-01	ARPC2, ACTR3, MYH9, BRK1, CFL1, ARPC3, CYFIP2, HSP90AA1, NCKAP1L, ARPC5	1.91E+00	5.22E-05	IGKC, IGLV2-23, IGHV3-33, IGLV3-21, IGLV4-69, IGLC3, IGHV4-34, IGLC2, IGLV2-8, IGKV1-17, IGHV3-11, IGLV1-40, RAC1, IGLV3-19, IGLV1-44, IGLV6-57, MAPK1, IGHV3-7, IGHV1-2, IGKV1-5, MYO1C, MAPK3
Respiratory electron transport	1.87E+00	2.43E-04	UQCR11, COX6A1, NDUFA11, NDUFB3, COX6C, UQCR10, UQCRH, NDUFA13, COX7B, NDUFB2, NDUFA1, COX8A, NDUFA6, NDUFB7, UQCRQ, NDUFA4, NDUFB10, MT-ND6, NDUFA3, COX5A, NDUFS6, NDUFB4, NDUFB6, COX6B1, SDHC, COX5B, NDUFS7, ETFA	-1.53E+00	1.49E-01	COA1, NDUFA7, NDUFA9, NDUFA13, CYCS, NDUFB8, COQ10B, ETFDH, NDUFC2, NDUFAF4, ETFB, COX19, COQ10A, NDUFA10
Signaling by the B Cell Receptor (BCR)	1.53E+00	5.75E-02	SKP1, PSMA5, PSMB9, PRKCB, PSMB8, PSMD9, PSME1, PSMA7, SEM1, PPIA, PSMB3, PSMB10, PSME2, PSMB2, PSMB6, PSMA4, UBB, NFATC3, PSMD2, IKBKG, PSMB1, FYN, PSMC4, CALM1	1.75E+00	8.72E-04	IGKC, IGLV2-23, IGHV3-33, IGLV3-21, IGLC3, IGHV4-34, IGLC2, IGLV2-8, IGKV1-17, IGHV3-11, IGLV1-40, IGLV3-19, TRPC1, IGLV1-44, PPP3R1, PPP3CB, IGLV6-57, IGHV3-7, HRAS, IGHV1-2, SOS1, IGKV1-5, LYN, ORAI1

Vesicle-mediated transport	1.40E+00	9.52E-02	NEDD8, ARPC2, TRAPPC1, ACTR3, MYH9, CTSC, YWHAZ, NAA38, DYNLL1, VAMP8, TBC1D10C, CAPZA1, ARPC3, ARF6, VAMP2, YWHAQ, HSP90AA1, YWHAB, RAB11A, ARF5, RAB27A, CAPZB, CD3D, ARPC5, RAB1B, CYTH4, CALR, AP2S1, TRAPPC4, UBB	1.46E+00	8.66E-03	IGKC, IGLV2-23, IGHV3-33, IGLV3-21, IGLV4-69, YWHAH, IGLC3, SERPINA1, IGHV4-34, IGLC2, IGLV2-8, IGKV1-17, IGHA2, HBB, IGHV3-11, IGLV1-40, HBA1, RAC1, IGLV3-19, BLOC1S4, ARF6, CHMP7, EREG, IGLV1-44, IGLV6-57, KIF6, DYNC1I1, IGHV3-7, PIP5K1C, SNF8, CTSZ, KIF3C, F5, IGHV1-2, TRIP10, SNX18, IGKV1-5, KIFC2, TRAPPC12, TBC1D10B, RAB31, CD163, TBC1D14, MYO1C, KIF21B, TRAPPC8, TBC1D2, REPS1, CLTB, IGHV4-39, UBQLN2, CD4, CAPZA1, LRP1, TBC1D20, C2CD5, EPS15, SBF2, AGPAT3, COPG2, JCHAIN, ZW10, PICALM, TBC1D4, RACGAP1, AKT3

Appendix table 6

A. Lists of differentially expressed genes with age in the memory T cell compartment of the healthy cohort. Only genes with a FDR <0.05 are listed. Positive logFC values are representative of genes that are upregulated with the age of the donor. The base of the logFC is 2.

Gene	logFC	FDR
GTSCR1	6.10E-02	2.28E-02
AL121748.1	5.32E-02	2.28E-02
S100A12	4.51E-02	4.75E-02
CLEC12A	4.15E-02	4.75E-02
TMEM200A	4.06E-02	4.75E-02
PILRA	3.96E-02	3.54E-02
MNDA	3.52E-02	3.61E-02
LYZ	3.42E-02	4.79E-02
AARS	3.24E-02	4.75E-02
TRAV6	3.04E-02	2.28E-02
KCTD1	2.92E-02	2.28E-02
SEPT11	2.66E-02	2.28E-02
NOD2	2.49E-02	4.75E-02
CTLA4	2.32E-02	4.75E-02
SLAIN1	2.30E-02	4.75E-02
TRAV12-3	2.22E-02	3.39E-02
MEGF9	1.81E-02	4.75E-02
MGAT4B	1.68E-02	2.37E-02
IL10RA	1.24E-02	3.09E-02
BAX	1.08E-02	4.00E-02
COA1	-1.12E-02	4.75E-02
CD7	-1.16E-02	4.59E-02
NUCB2	-1.18E-02	4.75E-02
RRM1	-1.46E-02	4.75E-02
AP002387.2	-3.31E-02	3.61E-02
RAMMET	-3.33E-02	4.20E-02
ZBTB16	-3.49E-02	2.28E-02
AC104986.2	-4.11E-02	3.78E-02
TWISTNB	-4.30E-02	2.28E-02
AL121658.1	-4.39E-02	4.75E-02
POMZP3	-4.45E-02	4.75E-02
IL4I1	-4.49E-02	3.61E-02
AC004922.1	-4.49E-02	2.28E-02
AL590764.2	-5.09E-02	4.00E-02
ATP1B2	-5.11E-02	4.75E-02
AC025159.1	-5.13E-02	3.41E-02
FLT1	-6.29E-02	3.41E-02
HIST2H2AA4	-9.13E-02	3.61E-02

B. Lists of differentially expressed genes between the memory T cells of all the convalescent patients recovering from a COVID-19 hospitalisation during the acute phase of the disease versus all the convalescent COVID-19 patients that did not require hospitalisation. Only genes with a FDR <0.05 are listed. Positive logFC values are representative of genes that are upregulated in patients recovering from a COVID-19 hospitalisation during the acute phase of the disease. The base of the logFC is Euler's number.

B1 – upregulated in patients recovering from a COVID-19 hospitalisation during the acute phase of the disease

Gene	logFC	FDR	Gene	logFC	FDR	Gene	logFC	FDR
RPS4Y1	1.86E+00	1.57E-04	CD74	4.12E-01	1.82E-06	SEC61G	2.99E-01	4.74E-09
GZMH	1.11E+00	3.79E-05	CTSC	4.11E-01	1.91E-06	CALM2	2.97E-01	2.33E-10
NKG7	1.06E+00	3.27E-05	HLA-DRA	4.06E-01	1.50E-08	DYNLL1	2.97E-01	1.18E-07
LGALS1	9.14E-01	1.99E-10	PSMB9	4.01E-01	1.26E-07	RBX1	2.96E-01	4.01E-12
CST7	9.02E-01	8.46E-05	TRAPPC1	3.83E-01	4.01E-12	MINOS1	2.96E-01	1.99E-10
HLA-DPB1	8.59E-01	2.95E-09	ADGRG1	3.83E-01	4.01E-06	TPST2	2.94E-01	3.84E-05
CCL5	8.36E-01	2.96E-04	CD2	3.82E-01	2.72E-08	CIB1	2.93E-01	8.91E-10
RPS10	8.24E-01	1.87E-11	IL10RA	3.81E-01	1.12E-09	SEC61B	2.91E-01	7.22E-08
GZMA	8.23E-01	3.04E-06	ANXA2	3.79E-01	6.01E-08	GSTP1	2.90E-01	1.48E-04
RPL36A	8.20E-01	7.74E-11	SNRPN	3.78E-01	3.15E-09	S100A10	2.85E-01	1.01E-07
HLA-DRB1	7.64E-01	4.33E-09	ATP6V0E1	3.74E-01	6.44E-11	ATP5F1E	2.85E-01	9.30E-10
HLA-DPA1	7.28E-01	8.91E-10	OAZ1	3.69E-01	1.97E-14	PSMB8	2.85E-01	1.40E-08
RPL26	7.06E-01	3.10E-10	WDR1	3.68E-01	2.77E-10	PGAM1	2.85E-01	7.27E-10
UQCR11	6.86E-01	1.10E-14	ACTR3	3.57E-01	5.28E-09	IL32	2.85E-01	2.89E-05
IFITM3	6.85E-01	7.16E-04	ITGB1	3.57E-01	2.22E-05	SCP2	2.84E-01	1.54E-09
PRF1	6.68E-01	2.65E-04	ATP5MD	3.57E-01	9.05E-11	PSMA5	2.82E-01	2.28E-10
PLEK	6.22E-01	2.73E-06	GZMM	3.54E-01	1.73E-04	TMEM258	2.81E-01	3.96E-09
FGFBP2	6.07E-01	3.17E-03	ANXA6	3.54E-01	6.50E-08	YWHAZ	2.80E-01	1.60E-08
C12orf75	5.95E-01	3.50E-09	TAP1	3.54E-01	2.06E-11	KLRG1	2.77E-01	1.63E-03
COX6A1	5.90E-01	2.02E-12	HCST	3.53E-01	1.75E-07	UQCR10	2.77E-01	1.60E-08
S100A11	5.65E-01	6.72E-10	DDT	3.48E-01	3.58E-09	CAPN2	2.76E-01	1.03E-06
CLIC1	5.65E-01	2.89E-09	SKP1	3.47E-01	6.47E-09	PSME1	2.75E-01	1.53E-08
IFITM2	5.59E-01	6.45E-08	ARHGEF1	3.38E-01	2.81E-08	ANXA5	2.75E-01	1.97E-08
GNLY	5.53E-01	4.04E-02	AL138963.3	3.36E-01	1.83E-08	POMP	2.74E-01	1.09E-09
NEDD8	5.46E-01	1.31E-10	CDC25B	3.35E-01	1.93E-10	SASH3	2.73E-01	5.46E-09
GZMB	5.44E-01	5.32E-03	ACTN4	3.34E-01	2.89E-09	APOBEC3G	2.73E-01	5.80E-05
NDUFA11	5.36E-01	1.39E-11	SUB1	3.33E-01	1.54E-08	ZAP70	2.70E-01	1.27E-08
SUN2	4.98E-01	1.48E-09	CCL4	3.29E-01	2.94E-03	DOK2	2.69E-01	7.69E-07
ITGB2	4.94E-01	1.66E-06	MYL6	3.25E-01	1.26E-10	PPP2CA	2.68E-01	1.28E-08
MYO1G	4.94E-01	3.03E-12	RARRES3	3.22E-01	1.54E-06	NOP10	2.68E-01	3.50E-09
CD8A	4.84E-01	7.02E-04	TXN	3.22E-01	1.74E-09	LITAF	2.66E-01	5.06E-05
HLA-DRB5	4.75E-01	8.57E-06	EMP3	3.22E-01	1.15E-09	PSMB10	2.65E-01	1.15E-06
FLNA	4.75E-01	3.42E-09	BRK1	3.20E-01	2.87E-09	PSME2	2.65E-01	3.85E-06
TRBC2	4.69E-01	2.87E-10	YWHAQ	3.20E-01	5.90E-06	ATP5MPL	2.62E-01	8.91E-10
CD99	4.68E-01	3.31E-09	S100A6	3.20E-01	6.32E-15	RABAC1	2.62E-01	4.38E-09
KLRD1	4.60E-01	4.33E-03	MSN	3.18E-01	5.09E-07	PRDX1	2.62E-01	4.54E-08
CYTOR	4.58E-01	5.43E-10	RAP1B	3.18E-01	1.88E-05	PPP2R5C	2.61E-01	2.62E-06
PPP1R18	4.57E-01	4.20E-11	SRGN	3.18E-01	8.62E-04	PSMD9	2.61E-01	4.18E-09
PPP1CA	4.54E-01	1.66E-09	ANXA1	3.18E-01	2.08E-04	CRIP1	2.61E-01	8.01E-08
S100A4	4.53E-01	2.55E-12	SAMD3	3.17E-01	9.26E-08	ATP5MC3	2.61E-01	1.15E-08
AHNAK	4.46E-01	1.77E-07	ATP5MF	3.17E-01	1.38E-10	ATP1A1	2.60E-01	2.87E-07
SLC9A3R1	4.44E-01	1.77E-07	APMAP	3.16E-01	8.17E-06	VAMP8	2.58E-01	6.02E-08
MYL12B	4.44E-01	1.87E-14	GUK1	3.14E-01	5.47E-09	FCRL6	2.57E-01	2.79E-03
UBL5	4.34E-01	1.11E-12	CDK2AP2	3.14E-01	4.21E-08	GBP5	2.57E-01	1.91E-06
CKLF	4.33E-01	2.43E-13	LYAR	3.10E-01	3.79E-06	PTP4A2	2.56E-01	3.50E-09
CD8B	4.30E-01	1.05E-04	VAMP2	3.10E-01	3.98E-06	HSPE1	2.56E-01	8.91E-10
DBI	4.14E-01	1.70E-11	MYH9	3.08E-01	6.74E-10	STOM	2.54E-01	2.84E-08
CAP1	4.14E-01	2.17E-11	CARD16	3.03E-01	8.73E-11	CLEC2B	2.53E-01	8.80E-06
MTRNR2L12	4.14E-01	2.14E-05	ELOB	3.01E-01	6.44E-11	PSMA7	2.53E-01	1.93E-07
ARPC2	4.13E-01	1.11E-12	PAXX	2.99E-01	2.14E-08	PARK7	2.52E-01	7.94E-09

Gene	logFC	FDR	Gene	logFC	FDR	Gene	logFC	FDR
COX7B	2.52E-01	2.10E-08	RNF167	2.19E-01	3.99E-08	CFL1	1.84E-01	5.92E-11
RASAL3	2.52E-01	3.71E-08	REEP5	2.19E-01	3.03E-07	CHST12	1.84E-01	4.50E-05
ARPC5L	2.51E-01	2.00E-05	CAPZA1	2.18E-01	6.91E-09	BAG6	1.84E-01	3.32E-08
EIF4EBP2	2.49E-01	6.08E-09	C4orf48	2.18E-01	5.15E-09	TWF2	1.83E-01	2.62E-08
POLR2L	2.49E-01	2.27E-08	CLIC3	2.15E-01	3.47E-03	LCK	1.83E-01	4.85E-07
ARF6	2.49E-01	8.52E-08	TGFBR3	2.15E-01	1.09E-05	PSMB2	1.83E-01	4.79E-08
NDUFB2	2.48E-01	3.12E-07	TUBB	2.14E-01	8.36E-08	PPIA	1.83E-01	1.17E-09
LIME1	2.48E-01	8.99E-08	PSMB3	2.13E-01	5.04E-08	UBB	1.82E-01	3.90E-05
TRAC	2.46E-01	7.08E-08	LAG3	2.12E-01	4.54E-06	TMBIM6	1.82E-01	1.27E-06
ADAM8	2.46E-01	4.21E-08	ARPC5	2.11E-01	5.51E-06	IDH2	1.81E-01	1.63E-06
MYO1F	2.45E-01	1.24E-05	CD63	2.10E-01	1.26E-03	UCP2	1.81E-01	9.57E-05
PRKCB	2.43E-01	7.56E-11	NAA38	2.08E-01	2.40E-10	AKNA	1.80E-01	9.26E-08
CYBA	2.43E-01	8.21E-04	ARL6IP5	2.07E-01	9.05E-06	CD53	1.79E-01	1.24E-04
TMA7	2.43E-01	3.31E-07	NEAT1	2.07E-01	1.11E-06	HLA-B	1.79E-01	9.21E-05
TAGLN2	2.43E-01	5.01E-05	FMNL1	2.06E-01	2.87E-10	ATP6V0B	1.78E-01	1.28E-07
HSP90AA1	2.43E-01	2.12E-07	PFN1	2.06E-01	5.08E-12	RHOG	1.78E-01	1.55E-06
NDUFB3	2.42E-01	6.73E-12	NDUFB7	2.06E-01	5.34E-07	RHOF	1.78E-01	3.58E-08
SH3BGRL3	2.42E-01	9.05E-11	CD3D	2.05E-01	3.56E-06	CD6	1.78E-01	1.89E-05
ITGAL	2.42E-01	1.87E-08	ATP5F1B	2.05E-01	1.70E-06	SERF2	1.76E-01	9.99E-10
SPON2	2.42E-01	2.74E-02	RHOA	2.03E-01	2.55E-06	CISD3	1.75E-01	2.96E-06
COX6C	2.41E-01	7.40E-10	NDUFA6	2.03E-01	9.32E-08	PSMB6	1.75E-01	4.02E-06
MT2A	2.41E-01	3.69E-04	CYFIP2	2.02E-01	5.25E-09	ZYX	1.74E-01	9.62E-08
ARHGAP45	2.40E-01	5.81E-07	MT-ND6	2.02E-01	5.05E-06	DSTN	1.74E-01	3.78E-05
NDUFA1	2.38E-01	1.89E-07	FGR	2.02E-01	2.03E-04	MFSD10	1.74E-01	1.03E-06
UQCRH	2.38E-01	3.96E-09	SELPLG	2.02E-01	2.93E-05	UBE2L6	1.74E-01	4.11E-05
OSTF1	2.38E-01	2.20E-07	SH2D2A	2.01E-01	4.89E-06	SNRPG	1.73E-01	1.03E-06
ZEB2	2.37E-01	4.08E-03	ABI3	1.99E-01	4.91E-05	SNRPB	1.72E-01	5.83E-07
YWHAB	2.37E-01	4.72E-07	IQGAP1	1.99E-01	4.61E-06	ARHGAP4	1.72E-01	8.85E-08
ARPC3	2.36E-01	3.46E-08	MVP	1.99E-01	2.81E-08	TAPBP	1.71E-01	2.41E-05
PYCARD	2.36E-01	2.45E-07	TBX21	1.98E-01	9.89E-04	NDUFA3	1.71E-01	2.70E-06
LSP1	2.35E-01	5.56E-05	CHCHD2	1.97E-01	1.11E-06	TPI1	1.71E-01	3.42E-05
PRKCH	2.35E-01	5.21E-08	RNF213	1.97E-01	9.55E-06	MT-ATP6	1.70E-01	2.66E-02
EFHD2	2.35E-01	1.92E-03	ITGB7	1.96E-01	6.28E-06	UQCRQ	1.70E-01	2.20E-07
TBC1D10C	2.34E-01	1.97E-08	ROMO1	1.96E-01	4.67E-08	RPS27L	1.69E-01	1.82E-06
CALR	2.32E-01	1.38E-04	BAX	1.96E-01	9.30E-10	NDUFA4	1.69E-01	4.75E-07
PXN	2.32E-01	2.81E-08	ATP5PB	1.93E-01	7.60E-07	TMEM59	1.69E-01	5.03E-06
NDUFA13	2.32E-01	3.50E-09	ADGRE5	1.93E-01	3.55E-04	CSTB	1.69E-01	1.77E-06
SYNE1	2.32E-01	5.80E-04	FAM96B	1.92E-01	1.75E-07	TSPO	1.67E-01	1.09E-05
CD164	2.32E-01	1.83E-06	MATK	1.90E-01	1.84E-02	CCNDBP1	1.67E-01	3.07E-07
RPS6KA1	2.31E-01	5.21E-10	DDX3Y	1.90E-01	9.03E-04	TPM3	1.66E-01	3.35E-05
WDR83OS	2.31E-01	3.03E-07	GAPDH	1.88E-01	1.12E-09	S1PR5	1.66E-01	1.80E-03
CMC1	2.29E-01	2.50E-03	CAPZB	1.88E-01	8.45E-07	TPM4	1.66E-01	3.02E-05
TBCB	2.27E-01	9.61E-09	VAMP5	1.87E-01	5.77E-07	ARF5	1.65E-01	6.86E-08
HNRNPF	2.25E-01	3.13E-08	SUMO2	1.87E-01	2.17E-07	CASP1	1.65E-01	1.33E-08
TBCA	2.24E-01	3.46E-08	SPN	1.86E-01	3.33E-05	COX5A	1.65E-01	1.24E-05
MYL12A	2.23E-01	1.70E-11	GNG5	1.86E-01	1.12E-05	GYG1	1.65E-01	7.22E-08
MIEN1	2.21E-01	8.69E-08	CORO1A	1.86E-01	9.13E-07	RAB5IF	1.64E-01	1.77E-07
COX8A	2.20E-01	2.12E-07	COX7A2	1.85E-01	3.81E-08	SLC25A3	1.63E-01	2.96E-07
SEM1	2.19E-01	2.62E-08	SIT1	1.85E-01	3.68E-08	GHITM	1.63E-01	8.89E-08
JPT1	2.19E-01	5.17E-08	PPP4C	1.84E-01	2.50E-08	IFI27L2	1.62E-01	1.38E-07

Gene	logFC	FDR	Gene	logFC	FDR	Gene	logFC	FDR
ENO1	1.62E-01	3.67E-06	FBXW5	1.46E-01	4.55E-07	LASP1	1.29E-01	9.27E-08
COMMD6	1.61E-01	5.48E-08	IL2RB	1.45E-01	3.12E-04	FAM49B	1.28E-01	3.43E-05
NDUFB10	1.61E-01	2.64E-07	CYTH4	1.44E-01	5.20E-07	SRI	1.28E-01	1.68E-06
RAB29	1.60E-01	3.79E-06	H3F3A	1.43E-01	1.34E-05	TMSB10	1.27E-01	4.38E-05
RAC2	1.60E-01	2.37E-05	TRG-AS1	1.43E-01	2.25E-05	GTF3C6	1.27E-01	3.14E-09
SRSF9	1.59E-01	3.83E-10	RASSF5	1.43E-01	2.03E-07	TRBC1	1.27E-01	6.20E-03
TMEM179B	1.59E-01	3.32E-08	ESYT1	1.42E-01	1.27E-08	G6PD	1.26E-01	1.09E-05
BSG	1.59E-01	8.35E-06	COPS9	1.42E-01	1.27E-06	SPCS2	1.25E-01	3.54E-06
LCP1	1.59E-01	1.21E-02	DCK	1.42E-01	3.89E-07	TUBA1C	1.25E-01	7.71E-07
KCNAB2	1.58E-01	2.82E-06	CDC42SE1	1.41E-01	8.98E-07	TRPV2	1.25E-01	2.18E-07
CDC42EP3	1.58E-01	2.10E-04	RNF181	1.41E-01	3.56E-08	KPNB1	1.25E-01	9.26E-08
RAB1B	1.57E-01	2.39E-07	PTPN7	1.40E-01	2.37E-07	SYNGR2	1.25E-01	2.27E-06
CSK	1.57E-01	4.09E-08	RPS17	1.40E-01	1.75E-07	TIGIT	1.25E-01	1.18E-04
H2AFZ	1.56E-01	8.93E-07	ITM2A	1.40E-01	1.30E-03	OST4	1.25E-01	6.53E-08
DDX39A	1.56E-01	3.22E-07	GPI	1.40E-01	2.98E-06	PYHIN1	1.24E-01	1.59E-03
GLUL	1.56E-01	1.69E-08	LPXN	1.40E-01	8.01E-08	PPP1R12A	1.24E-01	1.96E-06
TSEN54	1.56E-01	5.37E-06	ATP2B4	1.39E-01	1.96E-06	MED15	1.23E-01	3.03E-07
ACTB	1.55E-01	1.75E-04	CISH	1.39E-01	1.06E-03	CCDC167	1.23E-01	1.87E-06
TGFB1	1.55E-01	5.44E-07	DIAPH1	1.39E-01	1.11E-06	ELOVL1	1.23E-01	4.55E-07
LAMTOR5	1.55E-01	1.02E-06	PRKAR1A	1.38E-01	1.07E-07	ABHD17A	1.23E-01	1.42E-05
RAB27A	1.54E-01	3.96E-08	HLA-C	1.38E-01	1.80E-03	UBE2A	1.23E-01	5.06E-07
MANF	1.54E-01	9.58E-10	CD5	1.38E-01	1.13E-05	ALOX5AP	1.22E-01	2.08E-05
LY6E	1.53E-01	3.58E-02	TNFRSF14	1.38E-01	2.84E-06	TMC8	1.22E-01	2.13E-06
ATP5ME	1.53E-01	9.63E-06	PPIB	1.38E-01	4.43E-05	GIMAP7	1.21E-01	2.57E-03
MRPL51	1.53E-01	2.20E-07	ACTR2	1.37E-01	9.83E-05	NDUFB4	1.21E-01	8.98E-07
B2M	1.53E-01	7.89E-06	PARP1	1.37E-01	8.30E-07	LINC00623	1.20E-01	6.03E-06
HLA-DQB1	1.53E-01	3.12E-03	RPS15A	1.37E-01	5.02E-05	PCSK7	1.20E-01	3.89E-07
RER1	1.53E-01	4.52E-08	CHURC1	1.37E-01	8.42E-07	PSMB1	1.20E-01	4.81E-05
TMEM50A	1.53E-01	1.33E-05	YWHAH	1.37E-01	3.42E-05	OGT	1.20E-01	1.56E-07
PET100	1.52E-01	9.32E-08	FAM129A	1.36E-01	5.85E-08	NFATC3	1.20E-01	5.92E-07
SH2D1A	1.52E-01	3.96E-06	PTGER2	1.36E-01	2.49E-05	CAPN1	1.20E-01	5.26E-08
SUPT4H1	1.52E-01	2.60E-07	ZBTB38	1.36E-01	3.16E-05	C1orf21	1.20E-01	2.67E-02
RAB11A	1.52E-01	3.00E-09	IQGAP2	1.35E-01	3.96E-06	ATP6V0D1	1.19E-01	6.39E-08
BTN3A2	1.52E-01	2.17E-05	OTUB1	1.35E-01	9.77E-06	FLI1	1.19E-01	5.71E-06
GIMAP4	1.51E-01	1.08E-04	COX17	1.34E-01	3.57E-06	SRP9	1.19E-01	1.55E-06
NCKAP1L	1.51E-01	6.99E-10	ELOVL5	1.34E-01	8.84E-06	SEC61A1	1.18E-01	4.88E-06
DNAJC1	1.51E-01	1.29E-04	RBBP4	1.34E-01	1.47E-07	TMSB4X	1.18E-01	4.20E-04
PSAP	1.50E-01	9.55E-06	CASP4	1.34E-01	4.61E-06	MRPS6	1.18E-01	3.44E-06
PHPT1	1.50E-01	3.48E-07	NLRC5	1.33E-01	9.27E-08	TRIR	1.17E-01	3.66E-04
ACTG1	1.50E-01	2.26E-04	SLC44A2	1.33E-01	3.22E-06	COX6B1	1.17E-01	8.23E-06
FERMT3	1.50E-01	1.41E-07	ATP5PF	1.33E-01	7.34E-07	ATP1B3	1.17E-01	8.91E-08
GOLPH3	1.49E-01	4.74E-09	ITGB1BP1	1.33E-01	2.06E-06	PSMA4	1.16E-01	1.49E-07
PRELID1	1.48E-01	3.24E-05	IL12RB1	1.31E-01	4.90E-09	HMGB1	1.16E-01	3.37E-05
BATF	1.48E-01	7.53E-06	RNPEPL1	1.31E-01	7.70E-06	RALY	1.16E-01	1.86E-05
TNFRSF1B	1.48E-01	1.48E-05	LSM7	1.31E-01	2.14E-07	CD300A	1.16E-01	6.31E-03
ERH	1.47E-01	3.91E-05	NDUFS6	1.30E-01	1.80E-06	SSNA1	1.15E-01	1.12E-06
MAP4K1	1.47E-01	4.67E-09	MRPL33	1.30E-01	5.70E-08	SS18L2	1.14E-01	4.82E-08
SND1	1.47E-01	3.46E-08	RAB37	1.30E-01	4.62E-06	COX5B	1.14E-01	1.58E-05
HCLS1	1.46E-01	1.22E-05	SSBP4	1.30E-01	4.51E-06	AGTRAP	1.14E-01	8.64E-04
RASSF1	1.46E-01	8.58E-04	AP2S1	1.29E-01	5.34E-07	MDH1	1.14E-01	4.92E-06

Gene	logFC	FDR	Gene	logFC	FDR	Gene	logFC	FDR
VPS26B	1.14E-01	1.25E-07	PRNP	1.03E-01	1.09E-05	SNAPIN	9.17E-02	7.08E-08
CD3E	1.14E-01	2.67E-03	MRPS12	1.02E-01	1.55E-06	RSU1	9.17E-02	2.45E-06
MAT2B	1.13E-01	3.13E-06	EBP	1.02E-01	1.33E-05	FDFT1	9.12E-02	2.51E-05
CCDC107	1.13E-01	1.06E-05	TRAPPC4	1.02E-01	5.16E-08	LAPTM4A	9.03E-02	1.99E-05
KRTCAP2	1.13E-01	2.81E-06	ANXA11	1.02E-01	4.69E-06	ATP5F1C	9.02E-02	9.34E-06
GNAI2	1.13E-01	4.04E-05	SNRPE	1.01E-01	3.65E-07	SARS	8.99E-02	5.10E-07
LDHA	1.12E-01	5.67E-03	TMEM173	1.01E-01	3.37E-05	P4HB	8.98E-02	1.45E-04
ILK	1.12E-01	1.93E-06	SYTL1	1.01E-01	2.04E-05	FYN	8.95E-02	4.54E-06
ARHGDIA	1.12E-01	9.63E-05	AKAP13	1.01E-01	1.92E-04	PRDX5	8.94E-02	4.55E-04
DRAP1	1.11E-01	3.43E-04	DGKZ	1.01E-01	5.37E-06	LIPA	8.94E-02	6.77E-08
HMOX2	1.11E-01	1.62E-07	GBP1	1.01E-01	7.08E-06	AURKAIP1	8.85E-02	1.99E-06
ADRM1	1.11E-01	3.63E-06	HSPA8	1.00E-01	8.97E-04	ACADVL	8.81E-02	9.01E-06
GLIPR1	1.11E-01	1.53E-04	COPZ1	1.00E-01	1.12E-05	TAOK3	8.69E-02	1.77E-04
C4orf3	1.11E-01	3.65E-06	POLR2G	9.98E-02	1.34E-05	IFI16	8.67E-02	1.24E-05
SEC11C	1.10E-01	1.13E-05	CAPNS1	9.97E-02	1.36E-06	ANAPC11	8.66E-02	1.09E-05
POLR2K	1.10E-01	1.84E-06	SERPINB1	9.96E-02	1.39E-03	LAT	8.64E-02	9.32E-06
TCIRG1	1.10E-01	8.95E-06	GIMAP6	9.90E-02	7.36E-06	SMIM37	8.62E-02	4.41E-06
TMED2	1.10E-01	2.80E-05	CFLAR	9.87E-02	4.23E-05	ATP6V1F	8.61E-02	2.78E-05
EZR	1.09E-01	1.00E-03	ETFA	9.79E-02	4.27E-06	TALDO1	8.61E-02	1.23E-05
TPP1	1.09E-01	1.98E-06	SSR4	9.77E-02	3.21E-04	VPS29	8.60E-02	1.03E-05
GDI2	1.09E-01	6.41E-06	IKBKG	9.74E-02	5.94E-07	CD247	8.59E-02	1.05E-02
HSPB11	1.08E-01	1.05E-06	GNB2	9.69E-02	1.08E-04	TMCO1	8.58E-02	3.57E-06
DECR1	1.08E-01	1.11E-06	PSMC4	9.66E-02	1.35E-05	RNF44	8.53E-02	1.22E-05
RUNX3	1.08E-01	1.76E-05	SNHG9	9.66E-02	2.59E-05	COA3	8.52E-02	1.47E-07
RABGAP1L	1.08E-01	1.30E-06	TSC22D4	9.64E-02	5.67E-05	SLBP	8.47E-02	5.97E-06
EID1	1.07E-01	1.51E-05	DHRS7	9.59E-02	1.48E-03	STARD7	8.46E-02	6.23E-06
EIF6	1.07E-01	4.70E-06	RAB6A	9.58E-02	1.99E-06	STK10	8.45E-02	6.79E-05
MRPL41	1.07E-01	9.28E-06	DYNLRB1	9.57E-02	1.20E-05	CD52	8.43E-02	1.50E-02
PDLIM2	1.07E-01	3.96E-06	MYD88	9.56E-02	7.67E-07	ARHGDIB	8.43E-02	9.30E-03
CCDC88C	1.07E-01	2.81E-06	PDIA6	9.55E-02	2.12E-05	HLA-A	8.43E-02	6.70E-03
ASNA1	1.07E-01	3.73E-06	H2AFV	9.51E-02	1.63E-04	CDC37	8.43E-02	3.22E-05
PQLC3	1.07E-01	1.44E-06	S1PR4	9.51E-02	2.89E-06	CTDSP1	8.42E-02	4.14E-05
CYB561D2	1.06E-01	1.34E-06	SNRPB2	9.48E-02	4.92E-06	ZNHIT1	8.36E-02	1.93E-05
TUBA1B	1.06E-01	4.26E-04	SEC11A	9.48E-02	2.85E-06	LSM3	8.35E-02	1.51E-05
PSMD2	1.06E-01	5.77E-07	PDIA3	9.44E-02	9.52E-03	TADA3	8.34E-02	3.53E-05
VDAC3	1.06E-01	9.27E-08	SDF2L1	9.44E-02	3.66E-05	TRIM22	8.32E-02	2.79E-05
VDAC1	1.06E-01	5.69E-06	NONO	9.42E-02	1.41E-05	MACF1	8.32E-02	9.55E-06
NDUFB6	1.05E-01	5.48E-07	LRP10	9.41E-02	5.01E-05	HACD4	8.30E-02	4.68E-06
SLAMF6	1.05E-01	3.45E-07	CD320	9.36E-02	7.44E-03	GSTK1	8.28E-02	8.16E-05
MGAT1	1.05E-01	1.84E-06	MGST3	9.35E-02	4.30E-04	DGUOK	8.26E-02	3.36E-05
NDUFS7	1.05E-01	7.37E-06	TMEM9B	9.33E-02	2.09E-05	RANGRF	8.25E-02	2.29E-06
SRP14	1.05E-01	4.85E-05	SHKBP1	9.32E-02	7.08E-06	STARD3NL	8.23E-02	6.59E-05
SH3BGRL	1.05E-01	1.03E-04	SELENOT	9.22E-02	1.35E-05	DAD1	8.22E-02	7.94E-06
CXCR3	1.05E-01	3.04E-04	TRMT112	9.22E-02	6.28E-05	DNAJC15	8.21E-02	2.22E-04
HMGN4	1.04E-01	3.03E-07	IMPDH1	9.22E-02	1.11E-06	PTBP1	8.18E-02	1.71E-05
HLA-F	1.04E-01	2.66E-04	HK1	9.20E-02	6.05E-06	POLR2J	8.18E-02	4.11E-06
PKN1	1.04E-01	4.97E-07	IL2RG	9.19E-02	1.67E-05	COMMD8	8.17E-02	1.67E-06
HNRNPK	1.04E-01	4.32E-06	NDUFA2	9.19E-02	1.88E-05	ROCK1	8.16E-02	1.02E-05
SDHC	1.03E-01	4.34E-06	PTRHD1	9.19E-02	1.27E-06	LCP2	8.15E-02	9.63E-06
CALM1	1.03E-01	3.44E-05	MIB2	9.18E-02	3.36E-06	MAP1LC3B	8.14E-02	5.11E-04

Gene	logFC	FDR	Gene	logFC	FDR	Gene	logFC	FDR
MCRIP1	8.13E-02	3.33E-05	ATP2A3	7.26E-02	2.36E-05	MEAF6	6.61E-02	2.59E-04
TMEM256	8.12E-02	2.36E-05	COPS6	7.26E-02	3.43E-05	ENY2	6.58E-02	7.75E-06
TXNL4A	8.10E-02	4.15E-08	HDAC1	7.23E-02	2.82E-06	VPS28	6.58E-02	6.42E-05
MAD2L2	8.08E-02	7.69E-06	NCOA4	7.19E-02	1.56E-05	NARF	6.56E-02	5.58E-05
SNRPF	8.06E-02	4.67E-05	PSTPIP1	7.16E-02	1.83E-04	ARHGAP25	6.56E-02	3.75E-05
MRFAP1L1	8.06E-02	3.96E-06	SELENOS	7.15E-02	4.11E-05	ELOC	6.53E-02	5.19E-06
GLIPR2	8.05E-02	2.25E-03	SUMO1	7.15E-02	8.18E-05	CHMP2A	6.48E-02	4.94E-05
AOAH	8.05E-02	1.40E-02	MRPS18C	7.12E-02	1.15E-05	C8orf59	6.45E-02	8.20E-06
OPTN	8.02E-02	5.30E-04	RGS19	7.12E-02	2.42E-05	MCRS1	6.44E-02	4.46E-06
LAMTOR4	8.01E-02	8.91E-05	MZT2A	7.12E-02	2.12E-05	USP34	6.44E-02	1.26E-05
SDF2	7.99E-02	1.11E-06	ATP5F1D	7.09E-02	2.07E-04	RBM42	6.44E-02	6.56E-06
SPSB3	7.98E-02	7.60E-07	NUDT5	7.07E-02	1.51E-07	GRAP2	6.43E-02	4.58E-07
FKBP8	7.95E-02	4.18E-05	RALBP1	7.06E-02	3.09E-07	MT1X	6.42E-02	1.56E-05
NDUFAB1	7.94E-02	1.39E-05	CEBPB	7.05E-02	2.60E-04	UQCRB	6.42E-02	2.92E-05
MAP2K3	7.88E-02	4.16E-06	GNG2	7.04E-02	5.50E-03	DERL1	6.38E-02	6.90E-05
PCMT1	7.88E-02	4.93E-05	VOPP1	7.01E-02	8.88E-06	GBP2	6.37E-02	1.85E-05
LRRFIP1	7.86E-02	6.55E-04	CORO1B	7.00E-02	3.16E-04	ZFAND6	6.34E-02	7.09E-06
DPM3	7.85E-02	4.77E-06	HNRNPLL	7.00E-02	9.62E-07	CUEDC2	6.33E-02	5.96E-05
RPN1	7.81E-02	1.60E-05	ZBTB8OS	7.00E-02	1.11E-06	RIC8A	6.28E-02	1.60E-05
SNRPD2	7.80E-02	1.86E-04	MT1F	6.99E-02	1.06E-04	NUTF2	6.26E-02	3.68E-06
PARVG	7.80E-02	1.75E-06	UBE2L3	6.98E-02	1.22E-04	TMEM230	6.23E-02	3.12E-05
GRK6	7.77E-02	6.44E-06	DOCK8	6.98E-02	3.55E-05	FIS1	6.18E-02	8.87E-05
STMN1	7.74E-02	1.65E-04	ZNRD1	6.97E-02	1.81E-06	MOB1A	6.17E-02	2.60E-05
YPEL3	7.71E-02	3.77E-06	WNK1	6.95E-02	3.54E-05	SHISA5	6.17E-02	1.06E-04
ADD1	7.70E-02	2.49E-06	SMIM12	6.93E-02	1.46E-05	COMT	6.17E-02	3.82E-05
ARHGEF3	7.66E-02	1.41E-05	DCTN3	6.89E-02	1.71E-05	MAP4	6.16E-02	4.77E-05
ISG15	7.66E-02	1.88E-02	SH3KBP1	6.88E-02	6.40E-04	RASGRP1	6.14E-02	2.51E-05
SSBP1	7.66E-02	3.07E-05	CNPPD1	6.86E-02	5.15E-05	RPA3	6.14E-02	9.82E-06
RCBTB2	7.66E-02	6.13E-06	NDUFA12	6.85E-02	2.16E-04	DIP2A	6.13E-02	7.70E-05
FDPS	7.62E-02	1.09E-05	FTSJ1	6.84E-02	4.98E-06	MIF4GD	6.12E-02	1.41E-05
TIMM17B	7.60E-02	1.23E-05	SMG1	6.84E-02	5.27E-05	EDF1	6.12E-02	1.52E-04
SEPT9	7.59E-02	9.43E-06	BCAP31	6.83E-02	1.66E-04	INPP5K	6.12E-02	1.21E-05
WAS	7.58E-02	4.57E-05	ATP5MG	6.82E-02	2.92E-06	RAB18	6.12E-02	3.06E-05
PSMD8	7.57E-02	9.69E-06	CLEC2D	6.81E-02	6.26E-05	PFKL	6.11E-02	1.03E-05
AC026979.2	7.55E-02	3.98E-05	NFATC2	6.80E-02	2.51E-04	CHMP4B	6.11E-02	5.75E-06
EPS15	7.54E-02	1.11E-04	RNF166	6.80E-02	8.32E-05	FAS	6.11E-02	2.55E-03
CMC2	7.54E-02	2.06E-06	MRPS34	6.79E-02	2.54E-05	NDUFA8	6.08E-02	1.21E-05
GNPTAB	7.53E-02	1.87E-03	GNAI3	6.79E-02	1.46E-05	PIK3R5	6.08E-02	9.63E-06
IFI35	7.50E-02	9.55E-06	TEX264	6.76E-02	5.52E-05	ABI1	6.07E-02	6.77E-06
RAC1	7.49E-02	8.84E-05	GLUD1	6.74E-02	8.94E-06	PPM1M	6.06E-02	6.95E-06
PATL2	7.48E-02	4.28E-04	BTN3A3	6.74E-02	2.48E-04	PTPN6	6.05E-02	2.67E-04
SEPT1	7.46E-02	7.30E-07	SNX17	6.72E-02	3.58E-05	ETHE1	6.05E-02	3.95E-05
TSPAN32	7.46E-02	1.45E-04	SKAP1	6.72E-02	4.94E-05	EMC7	6.05E-02	3.90E-06
ATP6AP1	7.41E-02	2.46E-05	LUC7L3	6.71E-02	8.59E-05	RECQL	6.03E-02	3.41E-05
NDUFS8	7.39E-02	7.13E-06	CMPK1	6.69E-02	5.28E-06	FLOT2	6.02E-02	1.41E-05
PTPN22	7.36E-02	2.77E-04	PPP2R1A	6.68E-02	1.29E-05	MTCH2	5.99E-02	2.97E-05
DUSP23	7.33E-02	1.02E-05	TNIP1	6.67E-02	1.84E-06	UQCRC1	5.99E-02	1.30E-05
LAMTOR2	7.33E-02	3.56E-06	TLN1	6.67E-02	2.35E-03	TSEN15	5.99E-02	1.81E-05
MRPL28	7.32E-02	6.79E-06	NUDT22	6.66E-02	1.75E-07	NUCB1	5.96E-02	8.69E-05
PPM1G	7.27E-02	1.70E-04	BZW1	6.65E-02	6.13E-05	COPE	5.96E-02	8.52E-05

Gene	logFC	FDR	Gene	logFC	FDR	Gene	logFC	FDR
PDCD6	5.95E-02	1.99E-05	MOSPD3	5.37E-02	3.12E-04	HEXB	5.00E-02	3.64E-06
AP3S1	5.94E-02	4.46E-06	NDUFS3	5.36E-02	5.69E-05	ANAPC5	5.00E-02	3.87E-05
WDR45	5.94E-02	2.97E-05	METTL23	5.36E-02	2.04E-05	LSM10	4.97E-02	4.78E-05
NDUFB1	5.94E-02	1.81E-05	CYBC1	5.35E-02	1.34E-04	PUF60	4.96E-02	1.81E-05
INPP5D	5.93E-02	1.84E-05	GABARAPL2	5.35E-02	5.13E-05	SNX3	4.96E-02	8.26E-04
ZNF655	5.93E-02	7.83E-06	MAP2K1	5.34E-02	1.66E-05	XRCC6	4.96E-02	1.80E-05
MAGED2	5.92E-02	1.47E-04	RNF10	5.33E-02	2.05E-05	ERCC1	4.95E-02	4.01E-06
RNH1	5.90E-02	5.56E-05	SELENOW	5.31E-02	9.43E-05	UBR2	4.88E-02	4.91E-05
RBL2	5.87E-02	1.32E-04	CBX3	5.30E-02	7.46E-05	ORMDL1	4.88E-02	1.34E-05
LYPLA2	5.85E-02	3.83E-05	DR1	5.30E-02	2.24E-05	TM9SF2	4.88E-02	2.09E-05
RAP1GDS1	5.83E-02	4.91E-05	PSMC5	5.29E-02	2.69E-05	NPDC1	4.86E-02	3.07E-04
DCAF7	5.82E-02	1.40E-05	RPA2	5.29E-02	4.51E-05	SEPT7	4.86E-02	2.09E-02
MAN2B1	5.76E-02	1.25E-05	HSP90B1	5.28E-02	4.52E-05	CAPG	4.85E-02	5.60E-04
STUB1	5.76E-02	6.02E-05	BUB3	5.27E-02	3.54E-05	LNPEP	4.82E-02	5.47E-04
STX10	5.75E-02	4.15E-05	EHD1	5.27E-02	1.01E-04	LENG8	4.81E-02	1.03E-04
LYPLA1	5.75E-02	1.10E-05	ITGAE	5.27E-02	4.26E-05	SELENOF	4.81E-02	2.11E-06
GSDMD	5.74E-02	1.82E-05	LMAN2	5.27E-02	5.32E-05	GPAA1	4.79E-02	2.10E-05
IAH1	5.74E-02	1.09E-05	UBE2N	5.25E-02	1.41E-05	DNAJC8	4.79E-02	3.10E-04
PDCD10	5.74E-02	2.09E-04	ITPA	5.25E-02	4.11E-05	CUL4A	4.77E-02	6.64E-05
NDUFV1	5.72E-02	1.28E-05	CD3G	5.23E-02	1.35E-03	ALDH9A1	4.77E-02	1.16E-05
TRABD	5.72E-02	2.76E-05	NUP210	5.22E-02	2.41E-05	NAXE	4.77E-02	1.63E-04
PSMA3	5.70E-02	6.28E-06	APOBEC3C	5.22E-02	2.29E-04	UBE2I	4.76E-02	2.23E-05
JOSD2	5.70E-02	4.30E-04	CDK6	5.20E-02	8.80E-06	MZT1	4.74E-02	1.44E-04
SNRPD3	5.68E-02	3.10E-04	SRRT	5.19E-02	8.79E-05	PFDN4	4.74E-02	4.74E-06
LRBA	5.67E-02	3.22E-05	AC004687.1	5.19E-02	8.93E-04	PSMB7	4.73E-02	2.46E-05
STRAP	5.65E-02	4.41E-06	LSM8	5.19E-02	5.75E-06	VCP	4.71E-02	1.52E-04
TMEM165	5.64E-02	8.18E-05	DCAF11	5.18E-02	3.27E-05	C9orf16	4.71E-02	7.83E-04
PIN4	5.63E-02	8.12E-05	CCT5	5.16E-02	6.29E-05	DENND2D	4.68E-02	8.36E-05
TMEM109	5.62E-02	9.45E-04	GBP4	5.15E-02	2.92E-04	CLTB	4.68E-02	1.92E-04
SF3A1	5.61E-02	3.91E-05	MYBL1	5.15E-02	3.43E-03	PKM	4.67E-02	1.49E-05
SF3B6	5.61E-02	8.94E-06	SRSF4	5.15E-02	1.15E-04	SUCLG1	4.66E-02	3.84E-05
NMI	5.58E-02	1.97E-04	EPRS	5.13E-02	2.59E-05	THRAP3	4.66E-02	2.13E-05
OGFR	5.58E-02	5.12E-05	NDUFV2	5.13E-02	2.63E-05	SLC10A3	4.62E-02	1.51E-03
CHMP1A	5.57E-02	7.75E-05	IKZF1	5.12E-02	9.62E-05	SMIM29	4.62E-02	2.96E-04
AC116366.3	5.57E-02	4.98E-05	SH3BP5	5.10E-02	1.70E-04	RASA3	4.56E-02	7.28E-06
PSMD1	5.56E-02	1.84E-06	ZNF706	5.09E-02	3.45E-05	GDI1	4.56E-02	3.37E-05
PSMC3	5.54E-02	3.04E-05	NDUFA10	5.08E-02	5.68E-05	VASP	4.56E-02	5.67E-03
ACTR1A	5.53E-02	2.50E-05	SNX5	5.08E-02	1.04E-04	KLF12	4.55E-02	5.79E-05
FAM50A	5.49E-02	1.23E-04	ATP6V1E1	5.07E-02	4.34E-06	VCL	4.55E-02	1.49E-04
CD84	5.46E-02	7.94E-05	BIN2	5.07E-02	5.86E-03	MRPS36	4.55E-02	6.74E-06
FIBP	5.45E-02	2.08E-05	CYC1	5.07E-02	1.12E-04	NT5C	4.54E-02	5.02E-04
CAPZA2	5.45E-02	1.80E-06	PLEC	5.06E-02	2.08E-04	GLRX3	4.54E-02	1.15E-06
COX20	5.44E-02	1.11E-06	EMC6	5.06E-02	1.08E-04	TCF25	4.54E-02	9.39E-05
NDUFAF8	5.44E-02	4.96E-06	TSPAN14	5.06E-02	2.46E-05	SLC25A1	4.52E-02	3.42E-05
PIP4K2A	5.42E-02	3.81E-05	FDX1	5.05E-02	3.63E-05	MCTS1	4.51E-02	5.59E-06
CCDC124	5.41E-02	5.18E-05	NELFE	5.05E-02	6.52E-05	CASP8	4.51E-02	1.67E-05
DCTN2	5.40E-02	6.42E-05	RELA	5.03E-02	2.28E-05	UFD1	4.51E-02	3.10E-05
PSMD7	5.39E-02	3.04E-05	CCPG1	5.01E-02	2.60E-05	PIK3CD	4.50E-02	4.19E-05
SUPT5H	5.39E-02	3.76E-04	TMEM208	5.01E-02	6.96E-05	CMTM3	4.49E-02	2.11E-04
ARL5A	5.39E-02	6.02E-05	ORAI1	5.01E-02	1.07E-03	FRG1	4.49E-02	4.47E-05

Gene	logFC	FDR	Gene	logFC	FDR	Gene	logFC	FDR
MIDN	4.48E-02	5.88E-05	WDR82	3.99E-02	8.26E-06	TACC1	3.62E-02	3.27E-03
ITK	4.47E-02	3.21E-04	MCL1	3.98E-02	1.58E-03	USP4	3.61E-02	3.27E-05
GABARAPL1	4.47E-02	2.49E-03	MAP7D1	3.97E-02	1.60E-05	RAB9A	3.60E-02	1.02E-03
CHMP5	4.46E-02	2.07E-04	NDUFS2	3.96E-02	1.59E-05	ACAA1	3.60E-02	1.03E-04
ORMDL3	4.45E-02	7.53E-05	ATOX1	3.96E-02	5.72E-06	DDA1	3.59E-02	2.88E-04
SAT1	4.45E-02	8.56E-03	HSD17B10	3.95E-02	1.88E-05	CABIN1	3.59E-02	2.01E-05
ASF1A	4.44E-02	5.01E-05	DBNL	3.89E-02	7.05E-05	DDOST	3.58E-02	1.63E-04
STAT6	4.44E-02	1.84E-05	C19orf70	3.89E-02	2.70E-05	AP1G2	3.58E-02	5.50E-06
USB1	4.43E-02	1.71E-04	FGD3	3.89E-02	5.67E-04	RNF4	3.56E-02	2.53E-04
MLX	4.40E-02	9.44E-06	POLR2F	3.87E-02	1.73E-03	PYM1	3.55E-02	9.49E-06
UBQLN2	4.39E-02	5.41E-06	SIGIRR	3.87E-02	7.32E-05	ATXN10	3.53E-02	2.18E-04
NCK1	4.36E-02	1.54E-05	COPS8	3.87E-02	2.89E-05	SP140	3.53E-02	3.91E-04
SF3B2	4.35E-02	4.46E-04	RNF7	3.87E-02	1.65E-03	PSMD13	3.51E-02	3.43E-05
TSSC4	4.35E-02	4.45E-05	RBM6	3.86E-02	3.98E-05	PSMB8-AS1	3.49E-02	4.30E-04
DPY30	4.35E-02	5.27E-05	PBDC1	3.84E-02	2.02E-04	MRPL16	3.48E-02	2.65E-06
PDIA4	4.34E-02	1.15E-04	CYB5R3	3.83E-02	1.86E-04	TMEM170A	3.48E-02	8.49E-05
SCAMP2	4.33E-02	1.03E-03	MRPL37	3.83E-02	9.01E-06	MRPL18	3.48E-02	1.47E-04
STX8	4.33E-02	2.10E-03	ARID1A	3.82E-02	2.12E-04	EMC4	3.48E-02	7.88E-05
GALM	4.32E-02	2.42E-05	TMED5	3.82E-02	3.76E-04	YIF1A	3.47E-02	1.52E-03
MPLKIP	4.31E-02	5.79E-05	DNAJB11	3.80E-02	7.22E-05	CHTF8	3.47E-02	3.44E-05
CDKN2D	4.30E-02	2.15E-04	ZDHHC12	3.80E-02	4.26E-06	KMT2A	3.46E-02	5.40E-04
PCID2	4.29E-02	1.70E-06	TNFSF10	3.79E-02	1.63E-03	MOB2	3.46E-02	6.83E-05
SURF4	4.29E-02	9.17E-05	ADAR	3.79E-02	2.71E-04	INSIG1	3.46E-02	1.70E-04
HPRT1	4.29E-02	1.28E-05	GLOD4	3.78E-02	4.55E-04	AIP	3.44E-02	1.76E-04
PRKACB	4.28E-02	3.91E-05	LPP	3.78E-02	4.08E-05	IARS2	3.43E-02	3.75E-05
OS9	4.27E-02	2.30E-05	CTSB	3.78E-02	1.25E-05	PHB	3.42E-02	1.53E-03
PWP1	4.25E-02	6.76E-05	PCBP1	3.77E-02	1.89E-02	CRYBG1	3.41E-02	3.49E-06
FKBP1A	4.24E-02	9.05E-06	COPS5	3.76E-02	7.22E-05	CCT8	3.41E-02	3.44E-04
RAN	4.23E-02	4.89E-03	PDCD5	3.76E-02	1.02E-04	UBLCP1	3.40E-02	3.73E-04
PSMC1	4.23E-02	2.05E-04	HIKESHI	3.76E-02	1.98E-05	CBLB	3.40E-02	1.49E-04
HTATIP2	4.21E-02	7.44E-05	FAAP20	3.75E-02	3.49E-05	UBL3	3.39E-02	4.04E-04
RPA1	4.20E-02	8.95E-06	MLF2	3.75E-02	2.05E-05	BLOC1S2	3.39E-02	6.39E-05
PTPN4	4.19E-02	9.98E-04	CERS2	3.75E-02	1.40E-05	SPPL2A	3.37E-02	6.90E-04
HAGH	4.17E-02	2.33E-05	TMX1	3.74E-02	7.88E-05	AKR1B1	3.36E-02	6.13E-05
MLLT6	4.16E-02	6.00E-05	FKBP3	3.71E-02	6.72E-05	RPS27	3.35E-02	3.62E-02
RTCB	4.16E-02	5.40E-06	SEC31A	3.71E-02	1.06E-04	PRR13	3.35E-02	2.02E-03
FAM107B	4.16E-02	2.57E-04	TMBIM1	3.70E-02	1.42E-04	PEPD	3.35E-02	4.80E-04
UHMK1	4.14E-02	4.23E-05	NDUFAF3	3.70E-02	1.81E-04	RNF5	3.34E-02	2.03E-05
ZNFX1	4.12E-02	3.15E-05	ESD	3.70E-02	2.17E-04	HMGB2	3.33E-02	1.47E-04
NRBP1	4.12E-02	2.25E-05	TIMM13	3.69E-02	3.27E-04	COX14	3.33E-02	6.98E-05
SIRT2	4.11E-02	9.69E-04	PRMT1	3.68E-02	6.72E-05	ETNK1	3.31E-02	2.14E-04
PBRM1	4.11E-02	1.19E-04	TRAF3IP3	3.68E-02	1.07E-04	PSMD4	3.30E-02	2.47E-04
RNF149	4.09E-02	2.25E-04	CHCHD5	3.66E-02	1.03E-05	GMFG	3.29E-02	1.40E-04
G3BP1	4.09E-02	2.06E-05	FAM13B	3.65E-02	3.04E-04	TMEM167A	3.29E-02	7.98E-04
REXO2	4.08E-02	1.81E-05	MPG	3.65E-02	8.87E-04	APOL6	3.29E-02	7.51E-04
BID	4.04E-02	2.64E-05	STIP1	3.65E-02	2.34E-04	LSM1	3.28E-02	1.46E-04
FAM96A	4.03E-02	3.06E-05	PAIP2	3.63E-02	3.76E-04	CSRP1	3.28E-02	6.39E-04
GPS1	4.02E-02	5.45E-04	ISG20L2	3.63E-02	1.42E-05	CTSS	3.28E-02	3.06E-04
ARHGAP30	4.00E-02	9.49E-04	EIF4E2	3.63E-02	4.48E-05	RPL23A	3.26E-02	3.85E-02
SLIRP	3.99E-02	3.32E-04	TSTA3	3.62E-02	5.18E-04	HSPA4	3.26E-02	2.96E-04

Gene	logFC	FDR	Gene	logFC	FDR	Gene	logFC	FDR
COPS3	3.26E-02	7.41E-04	UROS	2.80E-02	6.19E-05	ARPP19	2.47E-02	2.24E-04
MAPKAPK3	3.25E-02	1.05E-03	DYNC1H1	2.80E-02	6.29E-05	TES	2.45E-02	6.07E-05
JAK3	3.25E-02	8.73E-05	KRCC1	2.79E-02	3.34E-03	RPUSD3	2.45E-02	3.36E-05
CST3	3.25E-02	9.57E-03	PPP1R7	2.79E-02	1.37E-04	HCFC1R1	2.43E-02	3.82E-04
TMEM87A	3.24E-02	2.98E-04	ZGPAT	2.79E-02	9.46E-06	SPG21	2.43E-02	6.10E-04
IGSF8	3.20E-02	1.06E-04	NDUFC1	2.79E-02	3.82E-06	APBB1IP	2.43E-02	1.87E-03
STMP1	3.20E-02	5.43E-06	GTF2H5	2.79E-02	8.18E-06	BUD31	2.39E-02	2.68E-04
VPS35	3.19E-02	2.51E-05	THOC7	2.78E-02	6.94E-05	TPGS1	2.38E-02	2.00E-04
MAZ	3.18E-02	2.62E-06	COMTD1	2.78E-02	7.81E-05	SDR39U1	2.37E-02	1.26E-04
NUDT1	3.17E-02	2.46E-05	CLPTM1	2.77E-02	1.06E-04	CARHSP1	2.37E-02	4.34E-04
RBM8A	3.16E-02	4.98E-04	PLEKHA1	2.76E-02	4.64E-04	CHTOP	2.37E-02	1.23E-04
CAT	3.16E-02	9.35E-06	PIH1D1	2.76E-02	8.28E-04	TAF10	2.36E-02	4.58E-05
CDK5RAP3	3.14E-02	4.21E-05	SF3B5	2.75E-02	8.47E-05	YARS	2.35E-02	1.34E-05
CYB5B	3.14E-02	2.44E-05	FAM32A	2.73E-02	2.80E-05	ASCC2	2.33E-02	2.34E-04
PFDN2	3.13E-02	6.53E-05	ZMAT2	2.73E-02	3.21E-04	ARFGAP3	2.33E-02	1.30E-02
S1PR1	3.13E-02	2.88E-04	SRA1	2.71E-02	2.90E-04	LYST	2.32E-02	1.79E-03
MRPL14	3.13E-02	6.93E-05	PSMD11	2.70E-02	1.71E-05	GNAS	2.31E-02	1.62E-04
SRPK1	3.12E-02	2.35E-04	TMEM160	2.70E-02	9.91E-04	BAD	2.31E-02	4.21E-05
VAV1	3.11E-02	1.91E-04	TMEM134	2.69E-02	1.30E-04	BOLA3	2.31E-02	1.15E-05
AASDHPPT	3.11E-02	3.46E-05	CDS2	2.69E-02	2.27E-04	TMEM126A	2.29E-02	1.94E-03
CNIH4	3.11E-02	3.98E-05	SLF1	2.67E-02	3.92E-05	HMGN3	2.29E-02	1.73E-04
DPP7	3.08E-02	2.62E-06	MDH2	2.67E-02	6.92E-05	PHKG2	2.28E-02	4.01E-04
RNF11	3.08E-02	3.02E-04	ULK3	2.67E-02	5.46E-05	TMEM14B	2.27E-02	1.46E-04
ADH5	3.07E-02	3.29E-04	STX4	2.67E-02	1.45E-04	SPAG7	2.25E-02	7.93E-05
ATP5IF1	3.06E-02	4.69E-06	SSR1	2.64E-02	4.66E-04	RHEB	2.25E-02	9.11E-05
ARL6IP6	3.03E-02	4.08E-04	APEH	2.64E-02	1.35E-04	TRIM69	2.25E-02	1.05E-04
NME3	3.01E-02	6.19E-05	PRDM1	2.64E-02	3.94E-03	CDIPT	2.25E-02	1.15E-04
PRPF40A	3.01E-02	1.26E-04	MAPRE1	2.62E-02	1.03E-04	PGK1	2.25E-02	6.65E-05
ATF6B	3.00E-02	3.19E-05	AP1M1	2.61E-02	9.66E-05	BANF1	2.25E-02	1.53E-03
MRPS26	2.99E-02	1.92E-04	CMTM6	2.61E-02	9.69E-04	MAGOH	2.24E-02	6.07E-05
PLEKHJ1	2.98E-02	1.34E-04	EIF2S1	2.61E-02	3.11E-05	NDUFA5	2.23E-02	1.74E-05
HM13	2.97E-02	3.49E-05	ATG3	2.61E-02	2.32E-04	IKZF3	2.23E-02	5.70E-04
GPR65	2.97E-02	1.02E-02	DAZAP1	2.60E-02	1.09E-03	TNIP2	2.22E-02	3.73E-04
MRPL52	2.95E-02	9.34E-06	FUNDC2	2.59E-02	5.33E-05	DNPEP	2.21E-02	3.53E-05
PSMC6	2.95E-02	4.67E-05	DPM2	2.58E-02	8.28E-04	CDC26	2.20E-02	6.78E-05
ZNF207	2.94E-02	4.44E-05	TUFM	2.57E-02	3.66E-04	LIX1L	2.19E-02	4.47E-06
AIMP1	2.91E-02	2.50E-03	LSM6	2.56E-02	5.75E-05	HIGD2A	2.19E-02	1.42E-04
CISD2	2.89E-02	4.84E-04	CSNK1D	2.55E-02	1.02E-04	PLCG1	2.18E-02	2.54E-03
PPID	2.89E-02	2.29E-03	SERINC3	2.55E-02	7.02E-05	TINF2	2.17E-02	1.33E-04
LMF2	2.89E-02	5.98E-05	PLD3	2.55E-02	9.65E-05	INO80E	2.15E-02	1.41E-04
RAB7A	2.89E-02	1.09E-04	BECN1	2.53E-02	5.76E-05	ATXN2L	2.15E-02	1.59E-03
ICAM3	2.87E-02	1.05E-04	FBXO7	2.52E-02	1.27E-05	SSRP1	2.15E-02	1.18E-03
STAT4	2.86E-02	1.30E-04	SNU13	2.52E-02	2.46E-05	SRP54	2.14E-02	1.82E-04
NSG1	2.85E-02	5.80E-03	POLE3	2.51E-02	3.32E-04	MRPL4	2.14E-02	5.04E-04
BTN3A1	2.84E-02	4.11E-05	PPP2R3C	2.51E-02	1.13E-04	CHD9	2.13E-02	1.79E-04
TP53TG1	2.84E-02	2.34E-05	RAB10	2.50E-02	2.53E-04	COX7C	2.13E-02	1.11E-02
STOML2	2.83E-02	3.92E-06	SLC52A2	2.49E-02	6.81E-05	MRPL43	2.09E-02	1.25E-04
RPN2	2.83E-02	1.12E-03	CDC123	2.49E-02	1.06E-04	C22orf39	2.09E-02	1.66E-04
HADHB	2.81E-02	6.14E-05	IDH3G	2.49E-02	3.82E-05	NUDCD2	2.08E-02	3.60E-03
SDHA	2.81E-02	1.19E-04	TXN2	2.49E-02	1.66E-04	DEF6	2.08E-02	2.11E-05

Gene	logFC	FDR	Gene	logFC	FDR	Gene	logFC	FDR
SNRNP40	2.07E-02	1.09E-04	ARL2BP	1.73E-02	7.10E-05	AAMP	1.39E-02	1.79E-02
PPP3CC	2.06E-02	2.72E-04	IK	1.73E-02	1.26E-04	COA6	1.39E-02	1.13E-03
MRPL20	2.05E-02	3.71E-05	SCNM1	1.73E-02	1.46E-03	NUBP2	1.39E-02	1.29E-04
PSMD6	2.05E-02	8.19E-05	RNPS1	1.73E-02	9.91E-05	THOC2	1.37E-02	3.65E-04
PSMA1	2.04E-02	3.02E-04	CAMTA1	1.72E-02	2.77E-05	UBA3	1.35E-02	2.91E-04
FNTA	2.04E-02	6.65E-05	UBL7	1.72E-02	9.21E-05	LRRFIP2	1.34E-02	4.11E-05
SCAMP3	2.04E-02	2.01E-05	TUSC2	1.72E-02	2.11E-05	BLCAP	1.34E-02	4.49E-04
EPN1	2.04E-02	6.45E-04	DHRS4	1.72E-02	1.11E-03	CYTH1	1.33E-02	1.78E-04
ARRDC1	2.03E-02	5.44E-05	FBXL15	1.71E-02	6.80E-05	DNAJC7	1.32E-02	4.41E-04
KLHDC3	2.03E-02	4.49E-04	IDH3B	1.71E-02	3.41E-05	C15orf61	1.31E-02	1.62E-04
RILPL2	2.01E-02	2.04E-05	UQCC2	1.70E-02	1.03E-04	ATP6V1H	1.30E-02	3.74E-03
DEK	1.99E-02	1.99E-04	TRADD	1.69E-02	6.20E-03	MTCH1	1.30E-02	2.54E-04
KRAS	1.98E-02	6.77E-05	PANK2	1.68E-02	1.80E-04	LAMTOR1	1.29E-02	4.84E-04
GARS	1.97E-02	2.09E-04	RFTN1	1.68E-02	1.28E-03	EWSR1	1.27E-02	6.23E-05
ERAP2	1.97E-02	5.11E-04	PRELID3B	1.66E-02	6.53E-05	GUSB	1.27E-02	3.17E-03
RHOT2	1.97E-02	2.74E-05	GSTO1	1.65E-02	2.96E-05	SH3BP1	1.26E-02	2.14E-04
DERL2	1.96E-02	5.01E-04	RNF113A	1.64E-02	4.19E-05	CCDC90B	1.24E-02	1.02E-03
ECHS1	1.96E-02	1.05E-04	PNKD	1.64E-02	5.92E-04	NFYC	1.23E-02	8.78E-04
MRPS10	1.94E-02	1.92E-03	ACD	1.63E-02	4.93E-04	UBQLN1	1.23E-02	4.78E-04
WDR46	1.94E-02	6.25E-05	MPC1	1.63E-02	6.03E-05	GADD45GIP1	1.23E-02	4.38E-05
NMRAL1	1.93E-02	2.01E-04	VPS36	1.62E-02	3.64E-04	C17orf49	1.23E-02	3.20E-04
SUMO3	1.91E-02	4.27E-04	DOCK2	1.62E-02	1.07E-04	WASHC3	1.23E-02	5.11E-05
CIAO1	1.91E-02	7.02E-06	MTIF3	1.62E-02	2.46E-05	MZT2B	1.23E-02	2.71E-05
NAA20	1.89E-02	2.97E-04	PHAX	1.60E-02	2.87E-04	AP2M1	1.22E-02	4.04E-04
YIF1B	1.88E-02	5.22E-04	LYSMD2	1.59E-02	2.25E-04	KLF10	1.21E-02	1.25E-02
AUP1	1.87E-02	3.10E-04	PIGT	1.58E-02	8.35E-05	SEPT2	1.21E-02	3.06E-04
RBCK1	1.87E-02	7.83E-05	PRPF31	1.58E-02	6.11E-05	PPP1CB	1.20E-02	2.49E-04
NADSYN1	1.86E-02	1.79E-04	C19orf24	1.56E-02	3.87E-04	YIPF3	1.20E-02	1.05E-03
DDX18	1.85E-02	4.21E-03	NLRC3	1.56E-02	3.44E-02	PSMD3	1.20E-02	5.29E-05
CD226	1.85E-02	5.68E-03	EIF2S2	1.54E-02	5.10E-04	FAM208A	1.19E-02	7.41E-05
OSTC	1.84E-02	7.75E-05	ACTR10	1.53E-02	4.67E-05	PFDN1	1.19E-02	2.14E-04
KDM5A	1.84E-02	5.57E-05	PPP6C	1.53E-02	7.54E-05	RPS6KB2	1.17E-02	8.68E-05
CCDC115	1.84E-02	2.47E-04	CENPX	1.53E-02	1.31E-04	SLC25A11	1.16E-02	1.86E-04
AMZ2	1.84E-02	2.51E-04	ATRAID	1.52E-02	6.46E-04	TRAPPC2L	1.15E-02	4.00E-05
GGA1	1.84E-02	3.64E-04	SZRD1	1.52E-02	7.42E-04	PTGES2	1.15E-02	3.58E-03
TBPL1	1.84E-02	2.62E-04	GLO1	1.51E-02	3.14E-04	SHMT2	1.14E-02	3.02E-04
HERC1	1.83E-02	9.21E-05	BRMS1	1.51E-02	1.31E-04	SNAP23	1.13E-02	1.00E-04
PPIH	1.83E-02	8.68E-05	COA4	1.50E-02	2.64E-03	UBE2J2	1.12E-02	3.19E-05
LCMT1	1.82E-02	1.92E-05	ADSL	1.49E-02	7.81E-05	CCT7	1.09E-02	8.31E-06
SNRNP200	1.80E-02	3.13E-05	CTR9	1.48E-02	2.01E-03	SHOC2	1.08E-02	1.78E-05
WIPF1	1.78E-02	2.07E-04	VPS72	1.46E-02	6.40E-05	FBXL5	1.08E-02	6.24E-03
NDUFAF4	1.77E-02	2.91E-06	STAT1	1.46E-02	5.64E-03	THEMIS	1.07E-02	1.42E-05
RFXANK	1.77E-02	3.87E-04	CDK4	1.46E-02	1.52E-04	SHARPIN	1.06E-02	1.09E-04
TAF12	1.76E-02	1.91E-04	TXNDC12	1.45E-02	2.09E-04	PHF14	1.05E-02	3.13E-05
EXOSC1	1.76E-02	2.04E-03	SNX20	1.43E-02	1.19E-03	CSDE1	1.03E-02	2.94E-04
DDX54	1.75E-02	1.03E-04	SRSF2	1.43E-02	6.70E-03	UBA2	1.02E-02	1.36E-03
POLR2I	1.75E-02	7.71E-05	ZCRB1	1.43E-02	1.93E-04	CHCHD7	1.01E-02	1.91E-04
SF3B4	1.74E-02	5.58E-04	SMIM19	1.42E-02	3.23E-04	STK25	1.01E-02	3.06E-04
ATP6AP2	1.74E-02	2.98E-04	UFC1	1.40E-02	1.65E-03	OTUD6B-AS1	1.00E-02	2.35E-04
SRPK2	1.73E-02	2.74E-04	GPRIN3	1.39E-02	9.94E-04	CAMLG	1.00E-02	4.98E-04

Gene	logFC	FDR	Gene	logFC	FDR	Gene	logFC	FDR	Gene	logFC	FDR
AAMP	1.39E-02	1.79E-02	ARFGAP2	1.00E-02	6.83E-04	RAB4A	5.78E-03	3.50E-04	MED30	2.46E-03	2.31E-03
COA6	1.39E-02	1.13E-03	ELOF1	9.96E-03	7.79E-06	OSTM1	5.71E-03	1.40E-03	ATP5PD	2.46E-03	1.68E-05
NUBP2	1.39E-02	1.29E-04	HPS1	9.89E-03	3.04E-04	USP14	5.70E-03	3.50E-04	IRF2	2.45E-03	1.72E-04
THOC2	1.37E-02	3.65E-04	CRELD2	9.86E-03	4.19E-05	PPA1	5.70E-03	6.79E-05	RPS19BP1	2.39E-03	8.72E-05
UBA3	1.35E-02	2.91E-04	PHC3	9.84E-03	4.74E-04	ARAP2	5.66E-03	3.14E-02	SYTL3	2.31E-03	9.69E-04
LRRFIP2	1.34E-02	4.11E-05	TUBA4A	9.80E-03	5.33E-03	AHSA1	5.51E-03	8.78E-04	ATP5MC1	2.29E-03	9.90E-06
BLCAP	1.34E-02	4.49E-04	MLEC	9.78E-03	2.61E-03	SLA	5.43E-03	3.36E-03	PIN1	2.24E-03	4.54E-04
CYTH1	1.33E-02	1.78E-04	EFR3A	9.77E-03	3.91E-05	ENOPH1	5.36E-03	3.37E-04	VMP1	2.19E-03	2.35E-04
DNAJC7	1.32E-02	4.41E-04	GTF2E2	9.72E-03	1.62E-04	MYDGF	5.31E-03	5.76E-04	ERP44	2.04E-03	8.75E-04
C15orf61	1.31E-02	1.62E-04	PSMD14	9.71E-03	2.31E-04	CCDC82	5.26E-03	6.84E-04	RC3H1	1.95E-03	3.81E-04
ATP6V1H	1.30E-02	3.74E-03	SLFN5	9.70E-03	1.31E-03	ADSS	5.14E-03	1.41E-04	HDDC2	1.92E-03	1.88E-04
MTCH1	1.30E-02	2.54E-04	H2AFY	9.61E-03	2.64E-05	TAF11	5.10E-03	1.16E-03	RNF187	1.84E-03	1.23E-04
LAMTOR1	1.29E-02	4.84E-04	C1D	9.28E-03	1.64E-04	LAP3	5.05E-03	5.67E-05	DALRD3	1.74E-03	5.33E-05
EWSR1	1.27E-02	6.23E-05	DENND1C	9.27E-03	6.22E-04	RTN4	4.98E-03	3.76E-04	MRPL11	1.67E-03	2.97E-04
GUSB	1.27E-02	3.17E-03	TMEM141	9.26E-03	3.44E-04	KIAA0040	4.91E-03	1.36E-04	SMARCA4	1.66E-03	2.06E-06
SH3BP1	1.26E-02	2.14E-04	GLTP	9.21E-03	3.59E-03	SERINC1	4.88E-03	7.48E-05	UBE2G1	1.60E-03	5.91E-04
CCDC90B	1.24E-02	1.02E-03	KDELR2	9.07E-03	1.50E-04	GRHPR	4.85E-03	1.00E-03	TIA1	1.56E-03	2.64E-06
NFYC	1.23E-02	8.78E-04	NDUFB5	9.02E-03	1.26E-04	RPAIN	4.84E-03	9.93E-05	LSM2	1.46E-03	3.87E-04
UBQLN1	1.23E-02	4.78E-04	PDE6D	8.80E-03	4.51E-05	UFL1	4.77E-03	1.88E-04	SNRPC	1.29E-03	1.20E-05
GADD45GIP1	1.23E-02	4.38E-05	MRPS18B	8.78E-03	1.28E-04	ZMYM5	4.77E-03	4.57E-05	CPNE3	1.27E-03	1.91E-04
C17orf49	1.23E-02	3.20E-04	UPP1	8.72E-03	1.66E-03	STT3B	4.73E-03	7.77E-06	AKR7A2	1.18E-03	2.99E-04
WASHC3	1.23E-02	5.11E-05	MKRN1	8.63E-03	9.80E-04	UBE2K	4.69E-03	1.55E-04	HMG20B	1.01E-03	3.57E-06
MZT2B	1.23E-02	2.71E-05	SIRT7	8.54E-03	7.51E-04	SBNO1	4.69E-03	1.40E-04	XRCC5	1.00E-03	4.33E-04
AP2M1	1.22E-02	4.04E-04	TANK	8.49E-03	1.63E-04	GPR108	4.63E-03	8.61E-05	RNF126	9.99E-04	4.65E-04
KLF10	1.21E-02	1.25E-02	MED4	8.42E-03	1.07E-04	MEI1	4.49E-03	4.74E-05	LPIN1	7.56E-04	3.25E-03
SEPT2	1.21E-02	3.06E-04	HTATSF1	8.26E-03	1.17E-03	TIMMDC1	4.45E-03	4.81E-04	COTL1	6.85E-04	1.06E-04
PPP1CB	1.20E-02	2.49E-04	MECP2	8.22E-03	1.07E-03	EIF4G1	4.34E-03	1.90E-04	MRPS16	6.73E-04	1.69E-05
YIPF3	1.20E-02	1.05E-03	EIF2B1	8.11E-03	1.29E-04	HNRNPAB	4.33E-03	1.02E-03	GLG1	4.25E-04	1.38E-04
PSMD3	1.20E-02	5.29E-05	ATG4B	7.95E-03	3.05E-04	METTL26	4.21E-03	8.61E-05	PRPF19	3.74E-04	1.55E-03
FAM208A	1.19E-02	7.41E-05	SORL1	7.84E-03	1.52E-05	LARP7	4.02E-03	5.01E-03	MRPL55	3.08E-04	2.35E-03
PFDN1	1.19E-02	2.14E-04	NUCKS1	7.73E-03	1.14E-04	JTB	3.90E-03	3.09E-05	MEA1	2.71E-04	2.46E-05
RPS6KB2	1.17E-02	8.68E-05	NSL1	7.69E-03	1.93E-04	EIF4A1	3.89E-03	1.12E-05	PIAS1	2.58E-04	5.79E-04
SLC25A11	1.16E-02	1.86E-04	WDR61	7.69E-03	2.71E-05	CDC42SE2	3.68E-03	6.14E-05	STAT3	2.41E-04	6.55E-03
TRAPPC2L	1.15E-02	4.00E-05	DAZAP2	7.47E-03	7.19E-03	RGS14	3.59E-03	1.22E-05	PGLS	1.11E-04	7.47E-04
PTGES2	1.15E-02	3.58E-03	TMED3	7.37E-03	1.93E-05	POLR2B	3.56E-03	4.96E-06	CARD8	7.78E-05	9.98E-05
SHMT2	1.14E-02	3.02E-04	PLPBP	7.33E-03	1.22E-03	PITPNB	3.56E-03	3.21E-04	SLC25A38	5.27E-05	8.48E-04
SNAP23	1.13E-02	1.00E-04	WASHC1	7.01E-03	1.03E-04	PPP4R3A	3.51E-03	3.90E-03	UCHL5	3.61E-05	4.12E-04
UBE2J2	1.12E-02	3.19E-05	ARFRP1	7.01E-03	5.55E-05	SMPD1	3.44E-03	8.38E-05	SURF2	7.92E-06	9.54E-04
CCT7	1.09E-02	8.31E-06	VBP1	6.93E-03	4.19E-05	KCNA3	3.42E-03	5.34E-04			
SHOC2	1.08E-02	1.78E-05	SPTAN1	6.61E-03	5.01E-05	PEF1	3.39E-03	8.05E-04			
FBXL5	1.08E-02	6.24E-03	SEC13	6.60E-03	1.29E-04	SF3A3	3.35E-03	7.81E-05			
THEMIS	1.07E-02	1.42E-05	MGMT	6.60E-03	8.71E-05	PPM1B	3.22E-03	1.60E-04			
SHARPIN	1.06E-02	1.09E-04	U2AF1L4	6.47E-03	2.59E-06	TOR1AIP1	3.19E-03	9.27E-05			
PHF14	1.05E-02	3.13E-05	RASSF7	6.33E-03	6.02E-05	PMVK	2.96E-03	5.37E-04			
CSDE1	1.03E-02	2.94E-04	ATG12	6.31E-03	8.52E-04	NOC2L	2.88E-03	6.33E-04			
UBA2	1.02E-02	1.36E-03	PPIG	6.11E-03	7.22E-05	HADHA	2.75E-03	6.42E-05			
CHCHD7	1.01E-02	1.91E-04	KIF22	5.89E-03	1.98E-05	DCXR	2.67E-03	3.06E-05			
STK25	1.01E-02	3.06E-04	TMED9	5.86E-03	6.39E-04	CCM2	2.66E-03	2.04E-05			
OTUD6B-AS1	1.00E-02	2.35E-04	SMARCB1	5.85E-03	3.27E-04	B4GALT3	2.53E-03	5.36E-05			
CAMLG	1.00E-02	4.98E-04	TROVE2	5.83E-03	3.06E-04	MMADHC	2.50E-03	3.16E-04			

B2 – downregulated in patients recovering from a COVID-19 hospitalisation during the acute phase of the disease

Gene	logFC	FDR	Gene	logFC	FDR	Gene	logFC	FDR
CD47	-7.61E-05	7.46E-05	SPNS1	-4.15E-03	3.29E-05	DRG1	-7.04E-03	1.91E-04
ANP32A	-8.58E-05	2.24E-04	ERG28	-4.17E-03	2.21E-04	CRY1	-7.07E-03	3.92E-05
ANXA7	-9.69E-05	3.04E-04	CREB1	-4.18E-03	2.04E-05	STK38	-7.13E-03	3.86E-04
BOD1L1	-1.25E-04	2.70E-04	GFER	-4.30E-03	2.11E-03	AL139246.5	-7.24E-03	3.70E-03
SAP30BP	-3.09E-04	1.86E-04	PAF1	-4.35E-03	1.82E-03	HNRNPD	-7.47E-03	4.75E-04
RRP7A	-5.02E-04	5.78E-04	C19orf25	-4.36E-03	1.42E-03	MRPS30	-7.51E-03	1.65E-04
CCNG1	-5.35E-04	1.28E-03	RAB11B	-4.42E-03	5.28E-04	SERPINB9	-7.59E-03	7.42E-05
GON4L	-5.67E-04	2.24E-04	LRRC59	-4.49E-03	7.68E-04	MRPS31	-7.72E-03	3.52E-04
C1orf123	-5.93E-04	7.75E-05	DARS	-4.54E-03	1.62E-04	UBE2E3	-7.78E-03	4.71E-03
NENF	-8.13E-04	3.18E-04	DEDD2	-4.55E-03	2.04E-03	APRT	-7.83E-03	1.28E-03
ADPGK	-8.31E-04	7.81E-05	SNX1	-4.58E-03	3.57E-04	TPGS2	-7.83E-03	6.91E-05
PREB	-9.32E-04	4.19E-05	CCT6A	-4.59E-03	8.87E-05	PPA2	-7.85E-03	2.28E-05
SVBP	-9.78E-04	6.80E-04	PHTF2	-4.66E-03	3.09E-04	TAPBPL	-7.90E-03	6.09E-04
RNASEH2B	-1.03E-03	1.48E-05	CMTM7	-4.68E-03	8.02E-05	PSMD12	-7.94E-03	8.55E-05
MRPL57	-1.04E-03	2.80E-04	BCL7B	-4.73E-03	7.25E-04	DDRGK1	-8.01E-03	3.53E-05
MRPS15	-1.15E-03	3.61E-04	PRRC2B	-4.82E-03	7.04E-05	PRKAG1	-8.02E-03	9.91E-03
PMS1	-1.21E-03	5.18E-04	NELFCD	-4.83E-03	1.30E-04	NAPA	-8.14E-03	1.04E-04
POLD4	-1.37E-03	3.38E-05	P2RY8	-4.99E-03	7.94E-05	GRSF1	-8.19E-03	3.39E-04
VTI1B	-1.37E-03	2.14E-04	KARS	-5.13E-03	1.20E-04	ASB8	-8.34E-03	2.70E-05
DNMT1	-1.52E-03	8.49E-05	SEC22B	-5.23E-03	3.06E-05	SNRPD1	-8.39E-03	2.66E-04
PFDN6	-1.54E-03	4.94E-04	PDCL3	-5.24E-03	9.70E-04	RCN2	-8.53E-03	4.95E-05
SMS	-1.58E-03	6.98E-05	PRPF8	-5.32E-03	1.71E-05	SMARCC1	-8.54E-03	8.11E-05
PNP	-1.62E-03	1.03E-03	XRN2	-5.35E-03	6.75E-04	RANBP1	-8.56E-03	9.85E-05
NUMA1	-1.65E-03	6.10E-04	WIPI2	-5.38E-03	1.40E-04	ARL8B	-8.67E-03	7.67E-04
RAB24	-1.92E-03	4.82E-05	AC008555.5	-5.48E-03	1.89E-05	CHORDC1	-8.77E-03	4.84E-05
EIF3A	-1.98E-03	1.61E-04	ZNF800	-5.81E-03	4.90E-05	UBE2D3	-8.80E-03	1.48E-04
RAB8A	-2.05E-03	6.05E-04	USP47	-5.81E-03	1.87E-04	RBPJ	-9.08E-03	4.68E-04
PDCD4	-2.12E-03	2.79E-05	UQCRC2	-5.81E-03	4.08E-05	CAPRIN1	-9.13E-03	2.63E-04
BPTF	-2.32E-03	1.88E-03	RICTOR	-5.83E-03	4.82E-05	GIT2	-9.13E-03	5.07E-04
GTF2I	-2.35E-03	5.63E-04	ILF2	-5.89E-03	2.48E-05	PHIP	-9.25E-03	1.96E-03
DYNC1LI1	-2.47E-03	3.38E-04	POLR2E	-5.97E-03	7.02E-05	CCS	-9.25E-03	4.40E-05
UFM1	-2.81E-03	1.30E-04	DHPS	-5.98E-03	1.62E-04	U2AF2	-9.25E-03	6.62E-04
SETX	-2.85E-03	3.12E-03	ACO2	-6.00E-03	7.54E-05	DMAC1	-9.26E-03	7.78E-04
CHD4	-2.88E-03	2.02E-03	ZDHHC24	-6.02E-03	8.87E-04	CCDC25	-9.32E-03	2.73E-04
PRDX6	-3.15E-03	9.29E-05	POLDIP2	-6.02E-03	1.03E-03	DPYD	-9.34E-03	1.84E-05
VMA21	-3.23E-03	4.94E-04	BRD4	-6.13E-03	8.41E-04	SON	-9.37E-03	1.64E-04
MRPL10	-3.27E-03	1.00E-03	TMUB2	-6.22E-03	3.66E-04	TNKS2	-9.61E-03	1.12E-04
IMP3	-3.31E-03	8.88E-05	PARP15	-6.25E-03	7.72E-05	GNPTG	-9.70E-03	6.52E-05
SSB	-3.45E-03	1.70E-03	XPC	-6.29E-03	2.06E-05	TRIM38	-9.74E-03	1.00E-03
SPCS1	-3.46E-03	6.46E-04	INTS11	-6.31E-03	4.44E-05	QARS	-9.85E-03	1.74E-04
MRPS21	-3.58E-03	1.71E-05	ATIC	-6.33E-03	8.48E-04	PRKAR2A	-9.87E-03	3.44E-04
AKIRIN2	-3.66E-03	1.71E-03	ELAVL1	-6.68E-03	3.62E-04	FKBP2	-9.95E-03	3.49E-04
HDAC3	-3.75E-03	3.06E-05	SNX6	-6.76E-03	1.60E-03	FRYL	-1.01E-02	9.70E-04
PRPSAP1	-3.80E-03	8.18E-05	IRF7	-6.80E-03	6.72E-03	KANSL1	-1.01E-02	3.98E-03
EIF5B	-3.84E-03	7.81E-04	GLRX	-6.83E-03	9.98E-04	ZFAND2B	-1.03E-02	7.81E-05
DDX21	-3.95E-03	2.83E-04	POLR3GL	-6.87E-03	8.31E-06	CCAR1	-1.04E-02	6.20E-04
JAGN1	-3.97E-03	1.43E-04	PARP8	-6.88E-03	3.33E-03	SAR1B	-1.05E-02	6.97E-04
GNPAT	-4.00E-03	5.17E-05	TCHP	-6.91E-03	1.54E-02	CRBN	-1.07E-02	5.15E-05
ECHDC1	-4.11E-03	4.45E-04	AKR1A1	-7.03E-03	1.41E-05	MICU2	-1.07E-02	3.59E-04
CRLF3	-4.14E-03	8.77E-05	ASAH1	-7.04E-03	1.90E-04	USP1	-1.08E-02	5.89E-05

Gene	logFC	FDR	Gene	logFC	FDR	Gene	logFC	FDR
RBBP7	-1.08E-02	9.83E-05	RB1	-1.46E-02	4.35E-04	FOXN3	-1.78E-02	7.02E-05
GMPR2	-1.09E-02	2.38E-05	SRRM2	-1.46E-02	2.39E-03	PHF11	-1.79E-02	1.33E-03
EMC3	-1.10E-02	5.05E-05	COMMD1	-1.47E-02	8.78E-05	C7orf50	-1.81E-02	1.11E-03
PRKCQ	-1.11E-02	1.56E-05	IDI1	-1.48E-02	9.15E-03	KATNBL1	-1.81E-02	4.43E-04
DCAF5	-1.12E-02	9.73E-05	CNOT8	-1.48E-02	8.01E-05	MFF	-1.82E-02	1.96E-04
GPR174	-1.12E-02	9.95E-05	TOR3A	-1.49E-02	2.22E-04	RAD21	-1.84E-02	4.84E-04
USP36	-1.12E-02	1.50E-04	SUCLG2	-1.49E-02	3.19E-05	EIF3J	-1.86E-02	3.11E-05
SCAF4	-1.13E-02	1.18E-04	MAN1B1	-1.51E-02	1.82E-05	ARID5A	-1.86E-02	4.15E-05
MPC2	-1.14E-02	8.80E-04	ERBIN	-1.52E-02	2.34E-04	RP9	-1.86E-02	2.88E-04
BST2	-1.15E-02	9.38E-03	SNX2	-1.53E-02	6.96E-05	SLC3A2	-1.87E-02	3.79E-03
SELENOK	-1.15E-02	5.37E-04	IFI6	-1.53E-02	2.61E-02	NMRK1	-1.89E-02	3.98E-05
PRDX2	-1.15E-02	1.76E-04	ANAPC15	-1.54E-02	7.10E-05	RAP2B	-1.89E-02	2.39E-04
DRG2	-1.16E-02	1.27E-03	PPP2R5E	-1.55E-02	3.52E-04	TOP1	-1.91E-02	5.18E-04
MMP24OS	-1.17E-02	2.71E-04	PAFAH1B3	-1.55E-02	2.36E-05	USP8	-1.91E-02	4.48E-03
CAMK2G	-1.17E-02	6.87E-05	PLIN2	-1.56E-02	4.33E-03	PHF20L1	-1.92E-02	2.86E-05
USO1	-1.20E-02	4.17E-05	SRP72	-1.56E-02	9.06E-04	METTL17	-1.92E-02	2.44E-05
UGP2	-1.20E-02	7.48E-05	C6orf89	-1.57E-02	3.27E-05	AP3B1	-1.93E-02	2.60E-04
ABCF1	-1.20E-02	9.55E-04	FASTK	-1.57E-02	1.28E-04	CCDC57	-1.95E-02	2.43E-05
NKAP	-1.20E-02	3.58E-03	HINT2	-1.58E-02	8.04E-04	BIRC6	-1.95E-02	3.64E-04
SREK1IP1	-1.21E-02	1.58E-03	DHX36	-1.58E-02	5.27E-04	RNF115	-1.96E-02	2.66E-04
PDCD2	-1.21E-02	2.76E-03	PPIE	-1.58E-02	8.73E-06	OARD1	-1.97E-02	9.46E-05
BSDC1	-1.21E-02	1.36E-04	LAMP1	-1.58E-02	1.01E-03	PHF5A	-1.99E-02	4.86E-04
DYM	-1.23E-02	2.30E-04	TMEM18	-1.59E-02	4.91E-05	RPS27A	-2.00E-02	1.10E-04
PPT1	-1.23E-02	9.66E-05	TAF9	-1.59E-02	1.31E-04	HBP1	-2.02E-02	6.01E-05
CLTA	-1.23E-02	8.62E-05	ZNF32	-1.59E-02	1.96E-04	KPNA3	-2.02E-02	1.66E-04
TENT2	-1.24E-02	1.01E-04	SET	-1.60E-02	2.76E-04	CDK11A	-2.02E-02	1.65E-04
COQ4	-1.24E-02	1.85E-05	FAM173A	-1.62E-02	2.29E-03	SNAPC5	-2.02E-02	1.94E-05
CCDC12	-1.25E-02	1.33E-03	NSRP1	-1.62E-02	1.38E-04	ARL6IP4	-2.02E-02	2.51E-04
MBP	-1.26E-02	2.20E-02	SECISBP2L	-1.63E-02	2.32E-04	CLNS1A	-2.02E-02	2.46E-04
SNRPA1	-1.27E-02	1.48E-03	TMOD3	-1.63E-02	7.84E-04	AK2	-2.02E-02	5.11E-04
BBX	-1.27E-02	2.88E-04	SRP19	-1.65E-02	1.44E-03	ANAPC13	-2.02E-02	2.31E-05
TRAPPC6A	-1.28E-02	1.13E-06	HDAC2	-1.66E-02	2.36E-05	PSMB4	-2.04E-02	1.41E-05
PTPRA	-1.28E-02	2.36E-03	GID8	-1.66E-02	6.89E-06	CCDC69	-2.06E-02	2.69E-04
RNASEK	-1.29E-02	7.79E-04	TMEM106B	-1.67E-02	1.86E-03	ACTR1B	-2.08E-02	3.35E-05
KRT10	-1.31E-02	1.05E-04	SAT2	-1.68E-02	3.88E-05	SREK1	-2.09E-02	2.10E-05
DNAJB14	-1.32E-02	3.36E-04	MRPL21	-1.69E-02	4.80E-04	DNAJC9	-2.09E-02	1.06E-04
MBD4	-1.32E-02	8.60E-05	CALCOCO2	-1.70E-02	2.05E-03	RSAD1	-2.10E-02	5.49E-05
TMEM183A	-1.32E-02	1.10E-03	HELZ	-1.70E-02	1.18E-02	C6orf226	-2.11E-02	3.21E-05
SLC25A5	-1.35E-02	1.69E-04	MAF1	-1.71E-02	2.39E-05	EBPL	-2.13E-02	2.00E-04
DNAJB6	-1.35E-02	3.09E-04	MITD1	-1.71E-02	6.44E-04	TMEM50B	-2.14E-02	1.75E-03
CCDC137	-1.35E-02	5.64E-04	SDAD1	-1.72E-02	4.28E-04	TMEM248	-2.14E-02	6.99E-04
TCP1	-1.36E-02	3.15E-03	RAD23B	-1.72E-02	3.77E-03	CLINT1	-2.15E-02	5.58E-05
ADIPOR1	-1.36E-02	4.15E-05	WDR54	-1.74E-02	8.42E-04	PFKP	-2.15E-02	1.95E-03
MRPS33	-1.37E-02	3.65E-04	RPL7L1	-1.74E-02	1.53E-05	PRPS1	-2.16E-02	2.98E-05
PSMG2	-1.37E-02	1.10E-04	SDCBP	-1.75E-02	3.33E-05	PMPCB	-2.16E-02	1.04E-04
LRRC47	-1.38E-02	1.16E-04	TPP2	-1.76E-02	1.01E-04	PDCD6IP	-2.17E-02	1.45E-05
AATF	-1.42E-02	5.26E-04	ISG20	-1.76E-02	6.06E-04	NOP56	-2.18E-02	6.18E-04
METTL9	-1.45E-02	2.77E-04	THYN1	-1.76E-02	1.74E-05	BRD2	-2.19E-02	1.05E-02
IL16	-1.45E-02	4.02E-05	DRAM2	-1.77E-02	1.94E-04	ATRX	-2.19E-02	8.19E-05
FLOT1	-1.45E-02	5.31E-03	API5	-1.77E-02	1.44E-04	ABTB1	-2.19E-02	6.83E-04

Gene	logFC	FDR	Gene	logFC	FDR	Gene	logFC	FDR
EIF3I	-2.20E-02	3.62E-05	NDEL1	-2.54E-02	3.37E-04	SIGMAR1	-2.94E-02	2.52E-05
PIGC	-2.20E-02	3.10E-04	H2AFJ	-2.55E-02	1.25E-03	ANKRD10	-2.95E-02	1.21E-05
MESD	-2.20E-02	3.10E-04	ENSA	-2.57E-02	4.74E-06	N4BP2L2	-2.96E-02	1.31E-05
MAP4K5	-2.23E-02	1.16E-03	WAC	-2.59E-02	4.28E-04	FKBP11	-2.96E-02	3.12E-03
LTA4H	-2.24E-02	7.58E-05	GSPT1	-2.59E-02	5.95E-04	LRPAP1	-2.96E-02	1.95E-05
CFAP298	-2.25E-02	1.56E-05	PSMA3-AS1	-2.61E-02	4.05E-05	DELE1	-2.96E-02	3.43E-05
RPLP1	-2.25E-02	4.65E-02	STARD3	-2.62E-02	7.53E-05	HARS	-2.99E-02	3.88E-05
RNASEH2C	-2.25E-02	5.24E-04	SDHB	-2.63E-02	6.79E-05	RPS15	-2.99E-02	2.13E-02
ME2	-2.27E-02	7.90E-04	RTF1	-2.65E-02	3.06E-04	YIPF5	-2.99E-02	4.00E-04
SLC4A7	-2.27E-02	4.05E-04	NR1H2	-2.66E-02	1.80E-03	MTF2	-3.00E-02	1.19E-05
RNF13	-2.27E-02	1.17E-04	SGF29	-2.66E-02	1.70E-04	CD37	-3.00E-02	2.33E-02
MRPS2	-2.28E-02	3.06E-05	ACAP1	-2.68E-02	3.33E-05	LSM5	-3.01E-02	1.81E-05
MIS18BP1	-2.29E-02	6.46E-04	SRSF1	-2.69E-02	6.05E-05	ARRB2	-3.02E-02	9.85E-05
ARIH2	-2.30E-02	1.17E-03	MRPL9	-2.69E-02	4.12E-06	XBP1	-3.02E-02	1.53E-02
COX19	-2.32E-02	7.22E-05	AP002387.2	-2.70E-02	1.19E-04	NUTM2B-AS1	-3.05E-02	2.27E-04
TMEM147	-2.32E-02	1.14E-04	ACP1	-2.70E-02	7.10E-05	NCF1	-3.06E-02	3.15E-05
C20orf27	-2.34E-02	2.79E-05	SEPHS2	-2.70E-02	1.39E-04	BAG1	-3.06E-02	1.46E-04
MTMR14	-2.35E-02	3.08E-04	ANKRD36C	-2.71E-02	1.55E-04	FAU	-3.07E-02	2.71E-02
KDELR1	-2.35E-02	3.87E-04	GOLGA7	-2.72E-02	7.06E-05	SMIM20	-3.07E-02	1.00E-05
GNL1	-2.36E-02	5.95E-05	LSM4	-2.73E-02	2.00E-04	SSR3	-3.08E-02	8.28E-04
ATG16L2	-2.36E-02	2.06E-03	GMCL1	-2.74E-02	4.96E-06	DDX27	-3.11E-02	1.43E-04
PEX16	-2.37E-02	2.42E-05	STN1	-2.74E-02	2.74E-05	RAP1A	-3.12E-02	4.35E-04
PSPC1	-2.37E-02	7.57E-04	TRAPPC3	-2.75E-02	1.39E-05	NDUFB11	-3.13E-02	1.16E-03
PUM1	-2.38E-02	1.10E-03	ZNHIT3	-2.75E-02	2.49E-05	RORA	-3.13E-02	3.33E-03
DNAJC4	-2.39E-02	1.06E-04	YY1	-2.76E-02	4.34E-04	ZNF292	-3.14E-02	9.89E-06
CHCHD3	-2.39E-02	3.78E-05	ZNF106	-2.76E-02	8.33E-04	IMMT	-3.14E-02	3.53E-05
BIN1	-2.39E-02	3.58E-04	TSPYL1	-2.76E-02	5.82E-04	SRSF8	-3.15E-02	3.27E-05
GTF2A2	-2.40E-02	1.62E-03	FGFR1OP2	-2.77E-02	1.14E-04	CNOT6L	-3.15E-02	4.18E-04
PSMF1	-2.40E-02	1.51E-04	TERF2IP	-2.77E-02	6.74E-04	NGDN	-3.17E-02	5.96E-05
ZFAND2A	-2.40E-02	3.42E-04	MAP4K2	-2.78E-02	2.87E-04	ASXL1	-3.19E-02	3.67E-05
RTRAF	-2.42E-02	4.99E-05	PTPN2	-2.79E-02	6.73E-04	TIPRL	-3.20E-02	4.83E-06
RNF145	-2.43E-02	7.58E-05	CLIP1	-2.80E-02	1.36E-03	BTF3L4	-3.20E-02	1.27E-05
HUWE1	-2.43E-02	2.66E-04	SMC3	-2.80E-02	6.53E-04	UBE2Q2	-3.21E-02	1.18E-04
MRPL54	-2.43E-02	8.65E-04	OCIAD2	-2.81E-02	1.05E-05	TOMM40	-3.22E-02	1.06E-05
NCOA7	-2.43E-02	4.30E-04	HAX1	-2.81E-02	4.42E-05	MRPL34	-3.23E-02	5.98E-04
SAMHD1	-2.44E-02	2.97E-05	C6orf62	-2.81E-02	4.59E-05	UQCRFS1	-3.23E-02	5.47E-04
RBBP6	-2.44E-02	1.49E-04	RPL18A	-2.83E-02	7.38E-03	ZNF524	-3.24E-02	1.50E-04
B3GAT3	-2.44E-02	8.18E-05	UBN1	-2.83E-02	4.55E-04	NME4	-3.25E-02	5.94E-05
STX5	-2.44E-02	2.60E-04	PDAP1	-2.84E-02	2.04E-05	ITFG2	-3.26E-02	5.92E-07
KDSR	-2.45E-02	9.40E-05	PSMA6	-2.88E-02	1.09E-04	SUGT1	-3.27E-02	2.48E-04
EIF3G	-2.45E-02	2.94E-03	FAM102A	-2.88E-02	1.68E-04	CNIH1	-3.28E-02	1.47E-05
BFAR	-2.46E-02	7.94E-05	NAE1	-2.88E-02	2.20E-05	DNAJC2	-3.29E-02	1.82E-04
HNRNPL	-2.47E-02	1.73E-04	SHISAL2A	-2.89E-02	4.49E-05	TGOLN2	-3.29E-02	1.44E-03
CCT2	-2.47E-02	1.71E-05	YTHDF2	-2.90E-02	5.26E-05	CWC27	-3.29E-02	4.60E-04
EXOC4	-2.51E-02	5.36E-05	SMU1	-2.91E-02	2.59E-04	PPHLN1	-3.30E-02	2.85E-04
TMEM222	-2.51E-02	1.79E-05	APH1A	-2.91E-02	3.04E-05	EFCAB14	-3.32E-02	2.43E-04
GORASP2	-2.51E-02	1.08E-05	SLC25A39	-2.92E-02	2.55E-04	RGL4	-3.32E-02	6.72E-05
ZNF22	-2.52E-02	1.81E-03	BCL11B	-2.93E-02	6.83E-04	KRI1	-3.33E-02	3.01E-04
CNOT7	-2.53E-02	1.92E-05	AC243960.1	-2.93E-02	7.29E-05	CAND1	-3.33E-02	2.12E-06
PPP2R2A	-2.54E-02	1.15E-04	ILKAP	-2.94E-02	5.55E-05	VDAC2	-3.33E-02	6.37E-05

Gene	logFC	FDR	Gene	logFC	FDR	Gene	logFC	FDR
MRPS7	-3.34E-02	1.19E-04	TTC1	-3.74E-02	2.84E-05	MAPKAPK5-AS	-4.14E-02	3.25E-05
NSFL1C	-3.34E-02	2.46E-05	ZFAND3	-3.75E-02	5.56E-05	SMARCE1	-4.18E-02	4.02E-04
PLGRKT	-3.35E-02	7.10E-05	CPSF6	-3.76E-02	1.24E-04	EXOSC8	-4.20E-02	1.14E-05
BET1L	-3.35E-02	3.47E-04	ARL16	-3.77E-02	4.99E-05	XRN1	-4.21E-02	4.26E-04
TFDP2	-3.35E-02	5.29E-03	RAD23A	-3.77E-02	5.37E-05	CHMP2B	-4.22E-02	4.05E-04
ARF1	-3.36E-02	1.80E-03	RBM22	-3.77E-02	3.84E-05	CUL1	-4.22E-02	1.51E-05
TECR	-3.36E-02	1.96E-04	SAMD9	-3.79E-02	5.06E-04	VHL	-4.23E-02	1.66E-04
KAT8	-3.36E-02	2.92E-05	MRPS5	-3.80E-02	3.38E-04	NUDC	-4.24E-02	1.18E-04
TTC19	-3.37E-02	9.88E-04	SLC35C2	-3.80E-02	9.92E-06	POU2F2	-4.25E-02	4.00E-04
UBE2J1	-3.37E-02	1.77E-04	RASGRP2	-3.81E-02	4.13E-05	CCDC174	-4.26E-02	6.53E-04
RPL8	-3.38E-02	2.68E-02	INTS10	-3.81E-02	9.44E-06	TAGAP	-4.27E-02	2.12E-04
CRTAP	-3.38E-02	4.28E-05	AP1S2	-3.82E-02	7.41E-05	TPRKB	-4.27E-02	5.44E-05
DNAJC19	-3.38E-02	7.89E-06	COMMD2	-3.83E-02	6.85E-05	NIPSNAP2	-4.28E-02	2.12E-05
CIR1	-3.39E-02	7.88E-05	ISCU	-3.84E-02	1.50E-03	HSPH1	-4.28E-02	7.54E-05
KDM4C	-3.39E-02	1.30E-04	UBE2E1	-3.84E-02	4.15E-05	VEZF1	-4.31E-02	4.43E-04
COX7A2L	-3.40E-02	1.28E-04	USP11	-3.89E-02	9.46E-05	TXNL1	-4.31E-02	1.46E-04
MON2	-3.41E-02	3.67E-04	XPO1	-3.89E-02	9.14E-05	C15orf40	-4.33E-02	6.05E-04
UNC119	-3.41E-02	1.23E-03	URM1	-3.90E-02	1.34E-05	TTC14	-4.33E-02	8.31E-05
CCT3	-3.43E-02	1.73E-04	CEBPZ	-3.91E-02	6.71E-04	SMIM26	-4.36E-02	2.60E-05
ZNF511	-3.44E-02	1.07E-04	NAAA	-3.92E-02	1.77E-05	SPG7	-4.38E-02	3.59E-06
MRPL24	-3.44E-02	2.24E-04	URI1	-3.92E-02	1.55E-05	RPIA	-4.39E-02	1.70E-04
MUC20-OT1	-3.44E-02	5.44E-05	MAN1A2	-3.93E-02	2.86E-05	CANX	-4.39E-02	1.02E-02
USP16	-3.47E-02	4.21E-05	ERCC5	-3.95E-02	1.03E-05	DAP	-4.42E-02	2.37E-05
NOLC1	-3.48E-02	3.59E-04	ANKRD11	-3.96E-02	6.83E-05	IWS1	-4.43E-02	3.44E-05
GPATCH8	-3.50E-02	3.94E-05	PBXIP1	-3.96E-02	1.65E-04	UBASH3A	-4.44E-02	1.38E-05
FOXN2	-3.50E-02	5.03E-05	POLR1D	-3.96E-02	2.73E-04	CNOT2	-4.45E-02	1.71E-05
ERGIC2	-3.51E-02	1.20E-04	PHYKPL	-3.97E-02	1.50E-04	SH2B1	-4.45E-02	1.03E-05
RAB8B	-3.52E-02	5.65E-03	TIMM9	-3.98E-02	9.75E-05	VSIR	-4.47E-02	1.03E-04
CDK13	-3.52E-02	7.38E-03	POP5	-3.99E-02	1.12E-05	CTSA	-4.47E-02	5.26E-03
CDC5L	-3.52E-02	9.73E-05	FAM120AOS	-3.99E-02	2.16E-06	CRIP2	-4.48E-02	4.95E-04
RTF2	-3.54E-02	1.85E-04	SDF4	-4.00E-02	2.29E-03	ATP2B1	-4.48E-02	7.45E-04
PITPNC1	-3.55E-02	8.78E-04	DEGS1	-4.00E-02	6.10E-05	PA2G4	-4.49E-02	1.95E-03
GOLGA4	-3.56E-02	4.79E-03	AGGF1	-4.02E-02	3.55E-04	RALGAPA1	-4.51E-02	3.85E-04
SP110	-3.57E-02	1.23E-04	NIFK	-4.04E-02	2.82E-05	RNF168	-4.51E-02	9.56E-05
VPS4B	-3.62E-02	1.82E-04	BAZ2A	-4.05E-02	1.29E-04	RNASEH1	-4.52E-02	1.12E-05
PQBP1	-3.63E-02	7.42E-05	EIF3D	-4.06E-02	3.41E-06	EVL	-4.52E-02	4.14E-03
HNRNPH3	-3.63E-02	2.61E-04	DDX46	-4.06E-02	7.41E-05	HNRNPH1	-4.52E-02	2.27E-05
NHP2	-3.63E-02	1.57E-04	GMPS	-4.06E-02	1.35E-05	SMIM27	-4.52E-02	7.53E-05
SYPL1	-3.64E-02	1.03E-04	MED10	-4.07E-02	2.53E-04	SSU72	-4.53E-02	3.85E-04
POLE4	-3.64E-02	7.61E-05	NRDC	-4.09E-02	4.09E-04	CELF2	-4.53E-02	2.79E-05
ARMC10	-3.65E-02	6.12E-05	KHDRBS1	-4.09E-02	8.54E-05	SMARCA2	-4.54E-02	8.88E-06
EAPP	-3.66E-02	2.49E-05	ZNF622	-4.10E-02	8.77E-05	NCBP2	-4.54E-02	5.35E-07
CCDC66	-3.66E-02	8.27E-05	MRPL40	-4.10E-02	3.29E-05	UPF3A	-4.54E-02	3.32E-03
UBE2V2	-3.67E-02	4.64E-06	UBAP1	-4.11E-02	5.92E-07	ARHGAP9	-4.55E-02	3.00E-04
KRIT1	-3.68E-02	2.36E-05	YWHAE	-4.11E-02	8.82E-06	TMEM63A	-4.56E-02	4.22E-05
HECTD1	-3.68E-02	2.07E-04	NOB1	-4.11E-02	3.06E-05	DCTD	-4.57E-02	1.31E-06
SH3GLB1	-3.69E-02	3.48E-04	RPL28	-4.11E-02	2.00E-02	FPGS	-4.57E-02	1.58E-05
USP33	-3.72E-02	1.43E-03	LIMD2	-4.12E-02	2.03E-02	RSBN1L	-4.58E-02	5.97E-04
PCIF1	-3.73E-02	7.88E-04	TMUB1	-4.13E-02	6.52E-05	RPS7	-4.59E-02	1.26E-02
ZMYM2	-3.74E-02	5.93E-06	LMBRD1	-4.14E-02	9.99E-04	CWC15	-4.60E-02	3.98E-05

Gene	logFC	FDR	Gene	logFC	FDR	Gene	logFC	FDR
C12orf10	-4.62E-02	2.70E-05	RPL17	-5.12E-02	3.14E-03	RPL7A	-5.59E-02	6.08E-04
COQ7	-4.62E-02	1.42E-04	SPEN	-5.12E-02	3.58E-04	NFE2L2	-5.59E-02	2.33E-05
CLPP	-4.64E-02	7.18E-05	TBCC	-5.14E-02	3.22E-04	PPP3CA	-5.63E-02	2.36E-04
DCP1A	-4.65E-02	1.15E-05	FBXO21	-5.16E-02	2.42E-05	HOOK3	-5.65E-02	6.83E-05
RPS3	-4.66E-02	2.92E-05	FUBP1	-5.16E-02	4.22E-05	POLD2	-5.65E-02	1.01E-05
SOD1	-4.66E-02	8.13E-04	PYURF	-5.18E-02	2.46E-05	SUPT16H	-5.67E-02	2.34E-04
PRKCSH	-4.67E-02	2.20E-04	RAB1A	-5.19E-02	9.16E-06	STX17	-5.67E-02	1.02E-06
C18orf32	-4.68E-02	1.59E-04	TAZ	-5.19E-02	6.95E-06	HNRNPA3	-5.67E-02	7.98E-03
UPF2	-4.68E-02	8.01E-05	EIF3M	-5.19E-02	4.02E-05	MTPN	-5.68E-02	1.11E-03
UBR5	-4.69E-02	1.47E-04	TBC1D10A	-5.21E-02	4.08E-05	SSR2	-5.68E-02	3.12E-02
SMNDC1	-4.69E-02	3.94E-04	NUB1	-5.22E-02	1.89E-04	AGTPBP1	-5.69E-02	3.17E-05
NDUFB9	-4.70E-02	7.37E-05	FAM162A	-5.23E-02	5.03E-06	FAM200B	-5.69E-02	2.34E-05
PSMG4	-4.70E-02	9.07E-05	RAB14	-5.23E-02	7.15E-06	CDV3	-5.70E-02	7.04E-03
ZNF428	-4.70E-02	2.46E-05	DHX29	-5.23E-02	2.05E-05	SFXN1	-5.71E-02	5.34E-06
NASP	-4.71E-02	3.19E-05	TMED10	-5.24E-02	2.35E-03	PIM3	-5.73E-02	2.72E-04
SMARCC2	-4.72E-02	6.65E-05	HERC2	-5.24E-02	3.27E-05	ELP5	-5.73E-02	2.28E-05
BAZ1B	-4.72E-02	1.02E-04	MPHOSPH10	-5.25E-02	2.03E-05	ZC3H13	-5.74E-02	2.38E-03
METAP2	-4.73E-02	3.67E-05	TC2N	-5.25E-02	3.33E-05	KLF13	-5.74E-02	8.41E-05
SMC1A	-4.73E-02	3.10E-04	RSRC1	-5.25E-02	9.63E-05	STAU1	-5.76E-02	7.17E-05
TMEM219	-4.73E-02	2.96E-05	ADAM10	-5.26E-02	1.25E-04	TCF12	-5.77E-02	1.19E-04
B4GALT1	-4.74E-02	3.11E-03	TAF7	-5.26E-02	3.10E-04	SPOP	-5.78E-02	2.52E-07
REST	-4.79E-02	1.16E-04	OSGEP	-5.26E-02	4.70E-06	EIF1B	-5.80E-02	3.91E-05
EP400	-4.80E-02	3.96E-06	DNAJA2	-5.27E-02	6.80E-04	PNKP	-5.81E-02	1.38E-06
SRPRA	-4.80E-02	9.89E-04	UTP23	-5.28E-02	1.56E-04	RANBP2	-5.82E-02	9.57E-07
MTR	-4.81E-02	1.57E-04	PTDSS1	-5.28E-02	1.66E-06	KTN1	-5.82E-02	7.07E-04
IRF3	-4.81E-02	5.35E-04	PTOV1	-5.30E-02	6.14E-04	CHRAC1	-5.82E-02	3.01E-05
CPNE1	-4.83E-02	4.85E-05	IL17RA	-5.31E-02	4.82E-05	OFD1	-5.82E-02	2.05E-04
RRP1B	-4.84E-02	8.05E-05	ERICH1	-5.31E-02	5.44E-04	RIOK3	-5.87E-02	3.45E-03
CCNK	-4.85E-02	2.53E-04	WAPL	-5.32E-02	7.46E-06	CCDC91	-5.87E-02	3.01E-06
RB1CC1	-4.86E-02	2.86E-05	YDJC	-5.35E-02	8.42E-05	SFSWAP	-5.89E-02	7.58E-05
FAM136A	-4.88E-02	8.94E-06	C19orf66	-5.37E-02	7.63E-06	STK4	-5.89E-02	6.12E-04
MAD1L1	-4.90E-02	4.07E-05	PPP4R2	-5.37E-02	3.36E-05	SLFN12L	-5.89E-02	7.22E-05
PRDM2	-4.90E-02	7.21E-05	RPL35A	-5.38E-02	4.69E-02	PRKX	-5.90E-02	1.94E-02
ARHGEF6	-4.92E-02	3.19E-04	ZDHHC6	-5.38E-02	1.28E-06	PTP4A1	-5.90E-02	1.18E-04
MTG1	-4.93E-02	2.05E-05	SNHG15	-5.39E-02	6.85E-05	RTN3	-5.91E-02	2.35E-04
ANXA2R	-4.93E-02	2.97E-04	KIF5B	-5.39E-02	2.33E-04	BUD23	-5.92E-02	4.27E-06
SUPT20H	-4.93E-02	6.96E-05	ZBTB20	-5.40E-02	2.46E-04	CCNL2	-5.93E-02	1.64E-05
SLC16A7	-4.93E-02	7.01E-05	SCAND1	-5.41E-02	2.58E-03	GOLGB1	-5.94E-02	5.27E-03
TBC1D22A	-4.94E-02	2.46E-05	BNIP3	-5.43E-02	2.42E-05	TMEM35B	-5.94E-02	3.06E-05
BRIX1	-5.00E-02	3.25E-05	RSL24D1	-5.46E-02	2.66E-05	DYNLT3	-5.94E-02	2.46E-05
BLOC1S4	-5.02E-02	3.76E-05	SNW1	-5.49E-02	9.24E-06	ECHDC2	-5.96E-02	4.66E-06
NDUFS5	-5.03E-02	2.81E-04	GRAMD1A	-5.49E-02	2.62E-05	FBXO32	-5.97E-02	6.44E-05
SLC39A10	-5.04E-02	2.96E-05	HNRNPUL1	-5.52E-02	6.87E-05	BORCS5	-5.97E-02	1.48E-06
CEP57	-5.04E-02	2.96E-06	PRKDC	-5.52E-02	5.67E-05	IMP4	-5.97E-02	6.91E-06
SETD5	-5.05E-02	1.52E-05	BCCIP	-5.53E-02	2.06E-06	LMAN1	-5.99E-02	2.19E-05
MED28	-5.08E-02	3.73E-06	NUDT21	-5.55E-02	6.34E-05	TMC6	-6.00E-02	3.76E-04
AAK1	-5.09E-02	2.65E-04	OGA	-5.55E-02	2.37E-04	KLHDC2	-6.01E-02	1.81E-07
KAT6B	-5.09E-02	1.28E-04	ZC3H15	-5.57E-02	1.58E-03	ADK	-6.03E-02	1.41E-05
LAGE3	-5.10E-02	1.30E-04	WTAP	-5.57E-02	4.02E-05	ANKRD44	-6.03E-02	1.03E-04
S100A8	-5.12E-02	8.95E-04	PCED1B	-5.58E-02	6.80E-04	ATG5	-6.03E-02	1.37E-07

Gene	logFC	FDR	Gene	logFC	FDR	Gene	logFC	FDR
HNRNPU	-6.04E-02	7.25E-03	RALA	-6.48E-02	1.24E-05	STAG2	-6.97E-02	3.14E-04
EIF2AK2	-6.04E-02	2.50E-03	PPM1K	-6.49E-02	8.55E-05	GATAD2B	-6.99E-02	9.32E-08
ANAPC16	-6.04E-02	1.25E-05	TBC1D1	-6.49E-02	2.52E-07	PPP1R11	-6.99E-02	2.46E-05
LUC7L	-6.05E-02	2.73E-05	ERGIC3	-6.49E-02	4.34E-06	CEP350	-6.99E-02	9.20E-03
PDE4B	-6.06E-02	1.32E-03	ERLEC1	-6.50E-02	1.18E-04	CEMIP2	-6.99E-02	5.01E-05
RBMS1	-6.07E-02	4.89E-05	TUBGCP2	-6.51E-02	8.62E-06	ZNF131	-7.02E-02	1.53E-07
CNPY3	-6.11E-02	5.62E-05	IGBP1	-6.51E-02	8.66E-05	RNF214	-7.02E-02	1.66E-04
C9orf78	-6.12E-02	9.48E-05	ZNF148	-6.54E-02	1.57E-05	OLA1	-7.03E-02	1.19E-05
ZNF580	-6.13E-02	7.46E-06	DNPH1	-6.55E-02	7.39E-07	TTC17	-7.04E-02	9.55E-06
TRPM7	-6.13E-02	5.93E-06	RIN3	-6.56E-02	3.16E-05	SURF1	-7.04E-02	2.42E-05
WDR33	-6.14E-02	7.46E-05	NECAP2	-6.60E-02	4.79E-05	GCHFR	-7.05E-02	2.97E-05
RNF19A	-6.18E-02	3.83E-03	RNPC3	-6.62E-02	4.20E-06	ABCE1	-7.06E-02	4.45E-06
COQ10B	-6.19E-02	7.36E-06	FXR1	-6.62E-02	6.45E-06	ZCCHC7	-7.06E-02	1.09E-05
AFF4	-6.19E-02	4.21E-05	SMAP1	-6.62E-02	6.94E-04	BNIP3L	-7.06E-02	3.05E-06
ICAM2	-6.19E-02	4.25E-04	ZNF644	-6.62E-02	1.98E-05	NPC2	-7.06E-02	1.24E-05
CCDC130	-6.19E-02	5.36E-06	RPL6	-6.63E-02	9.00E-03	ADI1	-7.07E-02	1.72E-05
EIF4A2	-6.20E-02	6.29E-03	DENR	-6.64E-02	1.12E-05	RING1	-7.09E-02	3.12E-07
UBTF	-6.20E-02	8.33E-05	VPS13A	-6.64E-02	1.59E-05	DNAAF2	-7.10E-02	8.76E-04
ATF4	-6.20E-02	1.96E-05	PPP1CC	-6.65E-02	9.73E-05	HERPUD2	-7.11E-02	4.78E-04
PARP14	-6.21E-02	5.03E-04	LRPPRC	-6.66E-02	1.13E-05	HNRNPC	-7.11E-02	1.16E-03
CDC40	-6.21E-02	6.18E-06	RPS23	-6.66E-02	3.94E-03	NT5C3A	-7.13E-02	2.82E-05
RPS16	-6.22E-02	3.28E-02	CACYBP	-6.67E-02	1.23E-05	KANSL1-AS1	-7.13E-02	1.47E-03
HMGN1	-6.23E-02	1.66E-04	CDC73	-6.68E-02	1.01E-04	LINC00667	-7.15E-02	3.05E-06
ADD3	-6.25E-02	1.65E-04	PRMT2	-6.69E-02	3.06E-02	RUNX1	-7.16E-02	3.34E-05
CD4	-6.27E-02	3.27E-05	NKTR	-6.70E-02	1.34E-04	ENOSF1	-7.18E-02	1.98E-05
MRPL3	-6.28E-02	1.47E-05	VPS51	-6.70E-02	2.24E-04	TRNT1	-7.18E-02	4.69E-06
CEBPZOS	-6.28E-02	3.99E-06	MSL3	-6.71E-02	8.38E-05	NUDT16L1	-7.22E-02	8.64E-07
KXD1	-6.30E-02	1.03E-05	LUC7L2	-6.73E-02	6.52E-04	ANKRD12	-7.22E-02	1.02E-03
RNF114	-6.30E-02	1.85E-06	CCT4	-6.73E-02	9.22E-05	SLTM	-7.22E-02	3.43E-05
KRR1	-6.30E-02	1.38E-05	M6PR	-6.75E-02	3.87E-04	RPS14	-7.22E-02	2.13E-02
SUSD3	-6.31E-02	9.80E-05	SMIM10L1	-6.76E-02	1.11E-05	TMX4	-7.27E-02	9.08E-04
EBAG9	-6.33E-02	1.11E-06	TOX4	-6.78E-02	2.03E-05	SPCS3	-7.27E-02	1.03E-04
METTL5	-6.34E-02	2.70E-05	MAPRE2	-6.81E-02	1.48E-02	TOMM5	-7.27E-02	6.98E-05
REX1BD	-6.35E-02	4.88E-03	COX16	-6.82E-02	6.37E-05	KAT6A	-7.28E-02	2.51E-04
TMF1	-6.35E-02	1.57E-05	SYF2	-6.83E-02	1.49E-04	NIN	-7.30E-02	4.53E-03
TOMM22	-6.36E-02	3.88E-04	PJA2	-6.84E-02	8.75E-05	ODC1	-7.32E-02	7.93E-04
ZBTB25	-6.37E-02	2.61E-04	CNTRL	-6.84E-02	9.35E-05	C1orf52	-7.33E-02	8.83E-08
IRAK4	-6.38E-02	1.94E-05	ITSN2	-6.84E-02	7.48E-05	WBP1	-7.33E-02	1.89E-07
TCERG1	-6.39E-02	1.41E-05	MLLT10	-6.88E-02	9.60E-08	APEX1	-7.34E-02	2.22E-05
MOAP1	-6.39E-02	1.20E-06	PRPF6	-6.88E-02	3.95E-05	TSR2	-7.35E-02	4.94E-07
C1orf43	-6.40E-02	1.03E-05	HSF1	-6.89E-02	1.13E-04	PRR7	-7.35E-02	1.38E-04
CFDP1	-6.40E-02	9.61E-05	ITGB2-AS1	-6.90E-02	8.53E-04	ST3GAL1	-7.35E-02	2.64E-05
EIF2AK1	-6.41E-02	6.19E-05	BNIP2	-6.92E-02	1.08E-05	RFC1	-7.36E-02	3.07E-05
PPCS	-6.41E-02	1.08E-04	HAUS3	-6.94E-02	1.03E-04	FAM204A	-7.36E-02	1.84E-06
PTBP3	-6.42E-02	3.38E-05	EMD	-6.95E-02	4.02E-05	RPLP2	-7.38E-02	3.91E-03
NGLY1	-6.43E-02	1.32E-05	GOPC	-6.95E-02	1.29E-08	GSK3B	-7.38E-02	2.95E-04
CSKMT	-6.44E-02	2.03E-05	OXLD1	-6.96E-02	6.76E-06	NUDCD3	-7.39E-02	1.75E-07
EEF1A1	-6.45E-02	2.81E-02	SAE1	-6.96E-02	1.95E-06	ANKRD36B	-7.40E-02	7.41E-05
PUM3	-6.46E-02	3.91E-05	NIPSNAP1	-6.96E-02	6.98E-06	POLR2C	-7.41E-02	2.44E-07
HNRNPA2B1	-6.46E-02	2.58E-03	EIF1	-6.96E-02	2.48E-02	ICE1	-7.42E-02	2.28E-05

Gene	logFC	FDR	Gene	logFC	FDR	Gene	logFC	FDR
ZNF24	-7.42E-02	4.53E-05	MAPKAP1	-7.97E-02	1.55E-05	KANSL2	-8.62E-02	2.29E-06
RPL12	-7.43E-02	1.00E-02	ZNF394	-7.97E-02	2.11E-06	UBE2B	-8.70E-02	1.40E-05
SORBS3	-7.44E-02	2.59E-05	UBXN2A	-7.98E-02	9.53E-07	KIAA1109	-8.71E-02	5.94E-04
APPL1	-7.46E-02	1.70E-04	TGS1	-7.99E-02	1.99E-06	RSBN1	-8.72E-02	2.99E-06
CWC25	-7.46E-02	1.29E-05	ZFR	-8.00E-02	8.02E-05	FTH1	-8.76E-02	4.01E-05
CUL5	-7.46E-02	1.80E-06	TRIP11	-8.00E-02	1.52E-05	NCOR1	-8.78E-02	9.64E-05
H3F3B	-7.48E-02	4.81E-02	HSPB1	-8.01E-02	5.64E-05	SNRNP70	-8.79E-02	2.18E-06
NUTM2A-AS1	-7.50E-02	1.15E-04	NUP153	-8.02E-02	2.05E-06	SNRPA	-8.79E-02	2.73E-05
THOC3	-7.50E-02	2.35E-04	FAM111A	-8.02E-02	5.93E-06	MRPS35	-8.79E-02	1.93E-06
DGCR6L	-7.51E-02	1.04E-05	ZNF721	-8.02E-02	9.23E-06	CTBS	-8.79E-02	5.29E-07
RBM3	-7.51E-02	4.06E-02	TRA2A	-8.03E-02	4.01E-04	CD40LG	-8.79E-02	1.06E-03
ARID4A	-7.51E-02	4.56E-05	EHMT1	-8.04E-02	5.41E-06	SEC63	-8.82E-02	1.19E-05
A1BG	-7.53E-02	1.15E-03	SIVA1	-8.05E-02	1.83E-05	ARL14EP	-8.83E-02	7.72E-06
BRWD1	-7.53E-02	2.89E-06	CREBRF	-8.05E-02	7.43E-05	NAP1L4	-8.83E-02	9.63E-06
TMED4	-7.53E-02	1.02E-05	RPAP2	-8.06E-02	2.35E-05	ATP6V0E2	-8.83E-02	3.06E-05
RPS5	-7.54E-02	4.83E-02	RPL29	-8.06E-02	3.53E-03	GRPEL1	-8.84E-02	2.49E-08
UBXN1	-7.55E-02	1.33E-03	LENG1	-8.07E-02	1.24E-06	TKT	-8.85E-02	3.39E-06
ASH1L	-7.57E-02	1.67E-05	SUDS3	-8.08E-02	4.57E-06	RPL22L1	-8.88E-02	4.11E-05
KMT2C	-7.57E-02	2.07E-04	PIP4P1	-8.11E-02	1.38E-08	SLC38A1	-8.89E-02	4.09E-04
AMD1	-7.58E-02	2.76E-05	ATP5F1A	-8.12E-02	2.07E-04	NXT1	-8.90E-02	9.94E-04
LARS	-7.60E-02	1.46E-05	FAM172A	-8.14E-02	7.93E-06	ELMO1	-8.91E-02	2.33E-06
ARIH1	-7.61E-02	5.34E-04	SLC25A45	-8.14E-02	6.77E-06	BDP1	-8.92E-02	7.46E-05
NSMCE1	-7.62E-02	1.11E-05	CFAP97	-8.15E-02	7.46E-05	NCBP2-AS2	-8.94E-02	5.14E-05
ERN1	-7.66E-02	1.47E-03	FYTTD1	-8.17E-02	9.38E-04	IER5	-8.94E-02	3.64E-03
NINJ1	-7.69E-02	2.25E-05	BAZ1A	-8.18E-02	5.50E-06	LETMD1	-8.95E-02	3.70E-07
TMEM204	-7.69E-02	2.04E-05	USP48	-8.18E-02	1.35E-05	CYCS	-8.95E-02	2.97E-04
SLC25A6	-7.69E-02	2.72E-02	HELB	-8.18E-02	9.01E-06	HNRNPR	-8.97E-02	2.01E-05
LONP2	-7.70E-02	1.03E-06	CD82	-8.22E-02	3.96E-06	PCMTD1	-8.98E-02	6.42E-06
CCND3	-7.71E-02	2.17E-02	TRIM4	-8.23E-02	4.82E-07	MX1	-8.99E-02	2.04E-02
FYB1	-7.71E-02	1.21E-02	BEX4	-8.24E-02	3.88E-05	YBX1	-9.00E-02	1.15E-03
RNF216	-7.72E-02	1.88E-05	CCDC85B	-8.24E-02	6.02E-05	OCIAD1	-9.01E-02	1.91E-06
HSPA9	-7.72E-02	5.44E-06	ASCC3	-8.25E-02	5.49E-05	HDLBP	-9.01E-02	1.02E-06
CALM3	-7.74E-02	4.61E-05	XAF1	-8.25E-02	3.38E-02	ITM2B	-9.02E-02	9.14E-03
DMTF1	-7.75E-02	2.91E-06	SYNRG	-8.25E-02	2.23E-05	IL27RA	-9.02E-02	8.13E-05
ING5	-7.78E-02	9.87E-07	RPL10	-8.26E-02	1.14E-03	ILF3	-9.06E-02	2.49E-05
TCEA1	-7.78E-02	1.32E-03	SAFB	-8.28E-02	2.05E-06	FAM133B	-9.06E-02	4.32E-06
KAT7	-7.79E-02	3.68E-06	DNAJC3	-8.28E-02	3.57E-06	AKAP9	-9.07E-02	5.16E-03
CBLL1	-7.80E-02	2.22E-05	WDR43	-8.31E-02	1.20E-07	LEMD3	-9.07E-02	1.84E-06
DNTTIP2	-7.82E-02	4.66E-05	HSD17B11	-8.32E-02	1.96E-05	MARCH7	-9.13E-02	8.02E-04
LY9	-7.83E-02	4.49E-04	FGD5-AS1	-8.33E-02	4.34E-06	NFKBIB	-9.14E-02	4.28E-04
SYNCRIP	-7.84E-02	9.40E-05	EMC10	-8.35E-02	4.15E-07	RPS6	-9.14E-02	1.59E-02
RPL3	-7.85E-02	4.62E-02	LYRM2	-8.36E-02	7.20E-07	ARID5B	-9.16E-02	1.92E-02
UBXN4	-7.85E-02	1.24E-05	NEMF	-8.41E-02	1.67E-05	TFAM	-9.16E-02	6.01E-08
BAG5	-7.85E-02	1.72E-06	RPL32	-8.42E-02	2.66E-03	GPSM3	-9.16E-02	5.15E-04
RHBDD2	-7.89E-02	1.47E-05	UTRN	-8.44E-02	1.40E-02	PHB2	-9.17E-02	6.13E-06
WWP1	-7.90E-02	6.75E-06	ISCA1	-8.45E-02	1.67E-06	DDX50	-9.17E-02	1.00E-07
CREBZF	-7.90E-02	1.29E-07	EDEM3	-8.48E-02	6.39E-08	TNIK	-9.19E-02	3.56E-06
NACA	-7.91E-02	2.64E-04	C12orf65	-8.50E-02	1.19E-06	CASC4	-9.25E-02	1.07E-04
CDK12	-7.94E-02	2.95E-05	PTMA	-8.59E-02	2.37E-08	EIF4H	-9.30E-02	4.24E-05
UBE2G2	-7.95E-02	1.84E-06	MIA2	-8.61E-02	2.31E-05	HNRNPM	-9.30E-02	4.99E-06

Gene	logFC	FDR	Gene	logFC	FDR	Gene	logFC	FDR
ACAP2	-9.31E-02	4.41E-04	NPEPPS	-9.95E-02	3.44E-03	SNRK	-1.08E-01	6.39E-08
GRINA	-9.32E-02	1.08E-06	SAP18	-9.95E-02	1.13E-02	VAPA	-1.08E-01	1.48E-06
MAX	-9.34E-02	3.07E-07	AES	-9.95E-02	4.87E-04	UBE2D2	-1.09E-01	4.54E-05
ZNF638	-9.34E-02	1.59E-05	FBXO9	-9.97E-02	3.54E-05	S100A9	-1.09E-01	7.65E-03
PNISR	-9.37E-02	3.81E-04	HMGN2	-9.98E-02	6.46E-04	TRA2B	-1.09E-01	1.08E-03
U2SURP	-9.38E-02	2.71E-04	CASP8AP2	-1.00E-01	1.35E-06	ZFP36L1	-1.09E-01	5.40E-03
FIP1L1	-9.38E-02	7.64E-08	IVNS1ABP	-1.00E-01	2.50E-05	SF3A2	-1.09E-01	1.54E-05
GIMAP2	-9.40E-02	1.23E-05	DUT	-1.00E-01	2.60E-05	C1QBP	-1.10E-01	1.58E-05
USP10	-9.42E-02	1.24E-02	ZRSR2	-1.01E-01	1.06E-04	NBEAL1	-1.10E-01	1.03E-05
NBDY	-9.48E-02	6.13E-05	CAPN7	-1.01E-01	8.09E-06	MTERF4	-1.10E-01	3.65E-08
DDX6	-9.49E-02	2.66E-05	HCG18	-1.01E-01	1.18E-06	SENP7	-1.10E-01	1.40E-06
CD96	-9.50E-02	3.53E-04	SYAP1	-1.01E-01	5.36E-06	R3HDM4	-1.11E-01	3.27E-05
CCNT1	-9.50E-02	2.13E-08	CNN2	-1.01E-01	1.21E-03	CCNI	-1.12E-01	4.43E-02
CCNH	-9.51E-02	2.33E-02	NLRP1	-1.01E-01	2.41E-06	UBAC2	-1.12E-01	5.34E-07
CYP20A1	-9.52E-02	5.83E-07	RAB2A	-1.01E-01	9.66E-06	EIF5A	-1.12E-01	3.83E-02
DHX9	-9.56E-02	6.80E-05	CCDC186	-1.01E-01	4.21E-05	HIST1H1C	-1.12E-01	3.17E-03
WBP2	-9.57E-02	1.07E-06	RPS13	-1.01E-01	2.36E-03	CHIC2	-1.12E-01	5.36E-06
RPL13	-9.57E-02	9.16E-03	RPL24	-1.01E-01	1.55E-06	FAM177A1	-1.13E-01	9.04E-06
SCAF11	-9.58E-02	8.66E-05	RPL22	-1.02E-01	5.08E-03	PABPC4	-1.13E-01	1.11E-03
RPS25	-9.58E-02	1.08E-03	ANKLE2	-1.02E-01	9.65E-07	TPT1	-1.13E-01	2.80E-03
RPL5	-9.59E-02	9.16E-03	KDM6A	-1.02E-01	5.57E-05	GPR183	-1.13E-01	7.81E-05
OXA1L	-9.64E-02	3.32E-06	CGGBP1	-1.02E-01	8.95E-06	RPL7	-1.13E-01	1.17E-02
CDK17	-9.69E-02	3.64E-04	GTF2B	-1.03E-01	2.05E-06	NIPBL	-1.13E-01	8.37E-06
RPL18	-9.69E-02	5.34E-04	ALDOA	-1.03E-01	4.80E-04	SP100	-1.13E-01	2.62E-04
SATB1	-9.70E-02	9.27E-04	DAP3	-1.03E-01	7.78E-06	IFNAR1	-1.14E-01	2.10E-06
PDE3B	-9.71E-02	2.54E-05	RAB5A	-1.03E-01	2.47E-06	NAA16	-1.14E-01	6.82E-08
NT5DC1	-9.71E-02	1.11E-06	NGRN	-1.03E-01	8.09E-06	C11orf58	-1.14E-01	8.07E-05
GTF2F1	-9.71E-02	2.19E-06	RPL11	-1.03E-01	1.20E-04	RPL9	-1.14E-01	1.76E-04
RACK1	-9.72E-02	6.29E-04	MRFAP1	-1.03E-01	7.40E-07	NSD1	-1.15E-01	5.99E-07
OSBPL8	-9.72E-02	3.94E-05	RCSD1	-1.03E-01	2.59E-05	CHD3	-1.15E-01	1.10E-04
ATM	-9.76E-02	1.17E-03	RPL14	-1.04E-01	9.05E-06	TXNIP	-1.15E-01	3.87E-02
ATF7IP2	-9.77E-02	2.13E-05	WARS2	-1.04E-01	1.72E-05	CXorf38	-1.15E-01	1.92E-07
UVRAG	-9.78E-02	1.13E-06	PHF20	-1.05E-01	1.09E-06	IPCEF1	-1.16E-01	7.71E-07
ZFAND1	-9.79E-02	6.62E-07	CCSER2	-1.05E-01	2.52E-04	RPS8	-1.16E-01	2.22E-04
GABPB1-AS1	-9.80E-02	4.41E-05	TPR	-1.05E-01	1.19E-04	JPX	-1.16E-01	2.72E-06
RPL19	-9.81E-02	6.81E-05	ACBD6	-1.06E-01	3.07E-07	SOCS3	-1.16E-01	2.48E-02
TRAF5	-9.82E-02	1.10E-04	H1FX	-1.06E-01	3.48E-06	HPCAL1	-1.17E-01	5.03E-06
CNOT4	-9.82E-02	7.09E-06	SUCO	-1.06E-01	3.26E-07	SETD2	-1.17E-01	1.60E-04
NR3C1	-9.83E-02	7.58E-05	MALT1	-1.06E-01	1.13E-06	TRAM1	-1.18E-01	7.22E-05
SINHCAF	-9.83E-02	8.87E-07	TARSL2	-1.06E-01	6.12E-07	ALG13	-1.18E-01	2.64E-07
PITHD1	-9.83E-02	2.49E-07	C1GALT1	-1.06E-01	5.77E-07	MYCBP2	-1.18E-01	1.65E-05
RWDD1	-9.83E-02	4.80E-05	XPA	-1.07E-01	8.57E-09	VPS4A	-1.19E-01	9.48E-07
WBP11	-9.85E-02	2.34E-05	SMAP2	-1.07E-01	5.52E-05	SLC25A36	-1.19E-01	1.83E-09
ZBTB1	-9.86E-02	4.27E-04	PCM1	-1.07E-01	8.55E-05	NFKB2	-1.19E-01	8.92E-05
KDM2A	-9.89E-02	1.06E-03	ABRACL	-1.07E-01	8.53E-05	ACIN1	-1.19E-01	1.03E-04
MBNL1	-9.90E-02	3.12E-03	BEX2	-1.08E-01	7.93E-05	ARPC1B	-1.19E-01	1.65E-03
C19orf53	-9.90E-02	2.21E-05	TMPO	-1.08E-01	1.71E-05	HEXIM1	-1.20E-01	8.17E-05
RPS12	-9.91E-02	4.52E-04	TAF15	-1.08E-01	7.81E-05	DCP2	-1.21E-01	3.71E-06
EIF2A	-9.93E-02	1.19E-04	PAG1	-1.08E-01	3.42E-05	PPP4R3B	-1.21E-01	1.33E-06
PLAC8	-9.94E-02	1.01E-03	CFAP36	-1.08E-01	5.98E-06	COPS2	-1.21E-01	4.19E-05

Gene	logFC	FDR	Gene	logFC	FDR	Gene	logFC	FDR
RSRP1	-1.21E-01	6.40E-03	CNBP	-1.39E-01	1.02E-03	SECISBP2	-1.55E-01	1.70E-07
LINC01550	-1.21E-01	2.05E-06	HNRNPA1	-1.39E-01	2.94E-04	KIAA1551	-1.55E-01	4.92E-02
PTPN11	-1.21E-01	4.11E-05	SVIP	-1.39E-01	2.17E-06	MDM4	-1.57E-01	6.01E-08
TLE4	-1.21E-01	6.01E-05	PCGF5	-1.39E-01	4.83E-05	CD28	-1.57E-01	8.93E-06
FKBP5	-1.22E-01	3.22E-05	LBR	-1.40E-01	5.15E-06	STMN3	-1.57E-01	6.07E-07
DBF4	-1.22E-01	5.97E-07	SIRPG	-1.40E-01	6.30E-06	PAFAH1B1	-1.57E-01	1.51E-05
CLK1	-1.22E-01	1.90E-03	ANP32E	-1.40E-01	3.49E-05	TIAL1	-1.58E-01	1.19E-05
BLOC1S6	-1.22E-01	5.99E-07	MIA3	-1.40E-01	2.21E-05	PAPOLA	-1.59E-01	5.19E-06
ELF2	-1.22E-01	4.32E-08	FXYD5	-1.40E-01	3.88E-03	HIF1A	-1.59E-01	5.94E-07
EIF5	-1.22E-01	6.14E-03	NELL2	-1.41E-01	6.01E-04	EIF3E	-1.60E-01	2.53E-02
RPL4	-1.23E-01	2.04E-02	PLP2	-1.41E-01	1.33E-03	RBM33	-1.60E-01	5.92E-07
DNAJB9	-1.23E-01	1.98E-06	EBLN3P	-1.41E-01	5.09E-09	CHCHD10	-1.60E-01	2.62E-06
LSM14A	-1.24E-01	1.15E-05	CCND2	-1.42E-01	9.44E-06	RBM17	-1.61E-01	1.99E-06
RGS1	-1.24E-01	1.77E-02	TMEM131L	-1.43E-01	2.27E-07	TGFBR2	-1.61E-01	3.07E-07
TAF3	-1.24E-01	8.01E-08	ERP29	-1.44E-01	5.77E-04	DDX24	-1.61E-01	1.21E-05
AC087239.1	-1.24E-01	8.53E-04	TCTA	-1.44E-01	1.76E-09	SNHG7	-1.62E-01	2.31E-02
ZRANB2	-1.24E-01	2.49E-05	RNMT	-1.44E-01	7.42E-05	UXT	-1.62E-01	1.38E-04
MTDH	-1.25E-01	6.40E-06	PIBF1	-1.45E-01	5.06E-07	RPL13A	-1.62E-01	6.87E-05
TSPYL4	-1.27E-01	2.41E-06	FNBP1	-1.45E-01	1.71E-05	SERBP1	-1.62E-01	1.08E-04
ZC3H7A	-1.27E-01	4.30E-07	LINC00861	-1.45E-01	5.68E-05	ZNF331	-1.63E-01	3.81E-07
IL6R	-1.27E-01	5.37E-05	SPOCK2	-1.45E-01	1.21E-03	USP3	-1.64E-01	1.03E-06
SUMF2	-1.27E-01	1.16E-08	RPS3A	-1.46E-01	2.70E-03	YTHDC1	-1.64E-01	6.98E-05
ETFB	-1.28E-01	7.60E-07	CSNK1A1	-1.47E-01	5.99E-07	NDE1	-1.65E-01	5.36E-06
PCF11	-1.29E-01	6.79E-07	SOD2	-1.47E-01	6.84E-08	C1orf162	-1.66E-01	6.86E-03
CYLD	-1.29E-01	7.35E-05	UBE3A	-1.47E-01	5.89E-06	BCAS2	-1.67E-01	3.54E-06
SENP6	-1.29E-01	2.01E-04	SEC62	-1.48E-01	9.07E-05	SSH2	-1.67E-01	7.52E-08
IMPDH2	-1.29E-01	1.44E-05	CCDC59	-1.48E-01	1.48E-06	MORF4L1	-1.68E-01	5.39E-06
GGNBP2	-1.31E-01	4.26E-07	CD46	-1.49E-01	2.18E-04	WASF2	-1.68E-01	3.94E-08
LIMS1	-1.31E-01	6.89E-07	NUP58	-1.49E-01	6.83E-06	MFNG	-1.68E-01	1.75E-07
ARCN1	-1.31E-01	6.40E-06	EPB41L4A-AS1	-1.49E-01	1.86E-06	SNHG12	-1.69E-01	4.17E-05
SPTBN1	-1.32E-01	8.95E-07	ATP6V0C	-1.49E-01	2.87E-04	DUSP1	-1.69E-01	3.87E-02
SP140L	-1.32E-01	8.79E-06	CNST	-1.49E-01	5.52E-07	MAPK1IP1L	-1.69E-01	8.18E-05
RNF138	-1.32E-01	4.61E-06	PNPLA2	-1.49E-01	6.83E-07	HP1BP3	-1.70E-01	1.38E-03
SMARCA5	-1.32E-01	1.76E-04	TBRG1	-1.50E-01	1.25E-06	MIER1	-1.71E-01	5.53E-07
TMEM14C	-1.33E-01	7.16E-05	RELB	-1.51E-01	4.70E-06	PNRC2	-1.71E-01	5.25E-07
CEP85L	-1.33E-01	9.23E-08	EEF1B2	-1.51E-01	9.61E-05	MATR3-1	-1.71E-01	3.42E-09
SEMA4D	-1.34E-01	1.06E-04	MORC3	-1.52E-01	1.48E-06	NOL7	-1.71E-01	4.70E-08
KLF9	-1.34E-01	2.50E-06	SAFB2	-1.52E-01	1.47E-07	VPS13C	-1.72E-01	1.67E-03
TAX1BP1	-1.34E-01	1.25E-03	PTGES3	-1.53E-01	6.61E-05	FBL	-1.73E-01	4.96E-06
RPL31	-1.35E-01	7.28E-05	SERTAD1	-1.53E-01	4.56E-02	AL121944.1	-1.73E-01	2.36E-05
RLF	-1.35E-01	1.87E-08	CD48	-1.53E-01	1.04E-02	CD55	-1.73E-01	5.14E-05
PDXDC1	-1.35E-01	2.59E-06	RSF1	-1.53E-01	3.81E-08	MYC	-1.73E-01	7.86E-04
SELENOH	-1.35E-01	1.91E-04	AC025164.1	-1.53E-01	3.27E-04	SMC5	-1.74E-01	6.71E-07
CUTA	-1.36E-01	2.82E-06	ATP2B1-AS1	-1.53E-01	2.49E-04	RBMX	-1.75E-01	6.71E-07
PRPF38B	-1.36E-01	5.89E-07	REL	-1.54E-01	3.49E-05	MALAT1	-1.75E-01	2.50E-03
LSM12	-1.36E-01	9.61E-09	EEA1	-1.54E-01	8.45E-07	MPHOSPH8	-1.75E-01	2.79E-05
RPS4X	-1.37E-01	9.25E-03	TNFRSF25	-1.54E-01	3.94E-06	STK17A	-1.75E-01	1.06E-03
LPIN2	-1.38E-01	2.34E-06	AKIRIN1	-1.54E-01	4.12E-07	HMGA1	-1.75E-01	4.93E-07
RNASET2	-1.38E-01	4.27E-03	NFKBIZ	-1.55E-01	7.87E-03	ODF2L	-1.75E-01	5.44E-05
TESPA1	-1.39E-01	6.37E-05	CENPC	-1.55E-01	3.06E-05	IFRD1	-1.75E-01	6.44E-04

Gene	logFC	FDR	Gene	logFC	FDR	Gene	logFC	FDR
MLLT3	-1.76E-01	9.84E-08	PCNP	-1.99E-01	4.30E-10	ZC3HAV1	-2.34E-01	5.33E-06
GTF3A	-1.76E-01	4.11E-05	PTGER4	-1.99E-01	2.38E-03	TENT5C	-2.35E-01	3.16E-03
GPX4	-1.77E-01	1.56E-03	HSPD1	-1.99E-01	1.68E-06	TSTD1	-2.35E-01	1.17E-05
PTPN1	-1.77E-01	2.80E-07	BCL2	-1.99E-01	3.75E-04	HSP90AB1	-2.36E-01	2.34E-05
RPL23	-1.77E-01	3.60E-02	ETS1	-2.01E-01	3.10E-03	PAK2	-2.36E-01	7.89E-06
TTC3	-1.77E-01	1.15E-07	TMEM243	-2.01E-01	5.53E-07	ATF7IP	-2.37E-01	2.65E-04
SQSTM1	-1.79E-01	3.67E-03	LINC02273	-2.01E-01	9.51E-04	PRRC2C	-2.37E-01	3.81E-04
EFCAB2	-1.79E-01	1.03E-04	DOCK10	-2.01E-01	1.09E-05	DGKA	-2.38E-01	1.68E-06
MAML2	-1.80E-01	9.61E-09	PDE4D	-2.01E-01	2.73E-04	SLC38A2	-2.38E-01	2.65E-04
TNF	-1.80E-01	9.16E-03	PIM2	-2.03E-01	8.17E-04	TNFAIP8	-2.39E-01	2.97E-05
SLAIN2	-1.81E-01	1.47E-07	SRRM1	-2.03E-01	7.89E-06	NOP58	-2.40E-01	2.45E-07
RHOH	-1.81E-01	8.18E-05	PRPF4B	-2.03E-01	1.08E-05	GCC2	-2.41E-01	3.36E-05
SGTB	-1.83E-01	1.75E-09	IRF1	-2.04E-01	2.43E-02	AL118516.1	-2.41E-01	6.32E-05
ZFC3H1	-1.83E-01	1.39E-06	PHF1	-2.04E-01	1.94E-07	MYLIP	-2.44E-01	1.56E-05
PEBP1	-1.83E-01	3.42E-04	EIF4A3	-2.05E-01	4.39E-04	EPC1	-2.44E-01	1.44E-05
NAP1L1	-1.83E-01	6.65E-05	TRABD2A	-2.09E-01	2.60E-05	NSD3	-2.45E-01	2.75E-06
NUCB2	-1.84E-01	3.70E-04	NUFIP2	-2.09E-01	1.66E-05	FCMR	-2.45E-01	3.34E-05
STX16	-1.85E-01	2.95E-07	TAF1D	-2.10E-01	3.15E-05	CDC14A	-2.46E-01	1.92E-06
IRF2BP2	-1.86E-01	1.97E-05	H2AFX	-2.11E-01	2.57E-03	EIF4G2	-2.46E-01	9.01E-03
SRSF11	-1.86E-01	7.63E-07	RASA2	-2.11E-01	3.32E-08	NPM1	-2.47E-01	2.11E-06
SF1	-1.86E-01	1.07E-02	WDR74	-2.13E-01	2.00E-02	FLT3LG	-2.48E-01	4.75E-03
TNRC6B	-1.86E-01	1.49E-05	AC016831.7	-2.13E-01	9.01E-05	EIF1AX	-2.48E-01	1.26E-04
THUMPD1	-1.87E-01	4.54E-06	AC016405.3	-2.13E-01	8.55E-05	ZFAND5	-2.51E-01	2.11E-06
PABPC1	-1.87E-01	4.72E-04	CA5B	-2.13E-01	8.97E-05	RGS10	-2.51E-01	3.08E-03
CIRBP	-1.87E-01	2.26E-03	C12orf57	-2.14E-01	4.62E-04	YME1L1	-2.52E-01	1.60E-04
ARL4A	-1.88E-01	3.18E-03	CD44	-2.15E-01	4.30E-04	RSRC2	-2.52E-01	8.83E-07
SOCS1	-1.88E-01	1.16E-04	ELF1	-2.16E-01	2.76E-06	USP15	-2.53E-01	7.33E-07
INPP4B	-1.88E-01	1.20E-04	LDLRAP1	-2.16E-01	1.33E-05	KIF2A	-2.54E-01	3.74E-04
GYPC	-1.89E-01	2.88E-03	WHAMM	-2.17E-01	3.98E-07	TTC39C	-2.55E-01	1.20E-04
POLR2A	-1.89E-01	3.45E-05	SPINT2	-2.17E-01	7.09E-06	DDX17	-2.60E-01	5.67E-04
SCML4	-1.89E-01	1.86E-06	TUBB4B	-2.17E-01	3.47E-02	SRSF3	-2.61E-01	8.68E-05
ARID4B	-1.90E-01	1.88E-06	JMJD1C	-2.17E-01	1.98E-05	NCL	-2.62E-01	4.30E-04
GATA3	-1.90E-01	6.84E-04	BCLAF1	-2.18E-01	9.91E-05	MGAT4A	-2.62E-01	3.34E-05
TIMP1	-1.90E-01	2.15E-03	IL6ST	-2.19E-01	2.45E-07	NSA2	-2.63E-01	3.65E-03
PKN2	-1.90E-01	5.55E-09	C6orf48	-2.20E-01	2.27E-05	SRSF10	-2.63E-01	4.52E-08
ABHD14B	-1.90E-01	6.52E-06	TUT4	-2.21E-01	2.96E-07	SFPQ	-2.63E-01	6.36E-05
NORAD	-1.91E-01	8.71E-07	ATP6V1G1	-2.21E-01	5.30E-05	BIRC3	-2.64E-01	1.39E-05
CHMP1B	-1.92E-01	1.36E-04	CSRNP1	-2.22E-01	2.76E-02	NME2	-2.66E-01	8.31E-05
AC119396.1	-1.92E-01	1.22E-05	KLF2	-2.22E-01	2.05E-02	MCUB	-2.66E-01	1.10E-04
HNRNPDL	-1.92E-01	1.10E-04	HERPUD1	-2.23E-01	1.71E-03	SERP1	-2.67E-01	4.44E-04
GRB2	-1.92E-01	2.13E-05	WSB1	-2.24E-01	3.38E-04	TOMM20	-2.68E-01	3.85E-06
SH3YL1	-1.94E-01	1.98E-03	SERINC5	-2.25E-01	1.03E-06	RNF125	-2.69E-01	5.76E-06
ARF4	-1.95E-01	8.62E-05	ATXN7L3B	-2.26E-01	9.15E-07	KMT2E	-2.70E-01	1.22E-06
C16orf54	-1.95E-01	8.45E-06	THEM4	-2.26E-01	2.38E-06	TOB1	-2.70E-01	8.59E-03
MIF	-1.95E-01	2.04E-02	HSPA5	-2.26E-01	1.83E-02	JUNB	-2.71E-01	1.78E-04
G3BP2	-1.96E-01	4.22E-05	PPP1R15B	-2.28E-01	3.99E-06	EGR1	-2.72E-01	3.47E-03
GABARAP	-1.96E-01	3.58E-04	EIF3L	-2.28E-01	8.39E-03	PHF3	-2.72E-01	1.08E-06
GPBP1	-1.97E-01	1.10E-07	PNN	-2.30E-01	1.82E-06	ZFAS1	-2.74E-01	2.05E-04
PPP1R10	-1.97E-01	1.24E-04	SELENOM	-2.30E-01	2.20E-07	PTPRCAP	-2.79E-01	1.44E-03
ALKBH7	-1.99E-01	3.49E-05	HIST1H1D	-2.33E-01	1.75E-02	ARHGAP15	-2.79E-01	1.02E-02

Gene	logFC	FDR	Gene	logFC	FDR
FNBP4	-2.80E-01	1.58E-06	RPS20	-3.83E-01	6.29E-05
TRAT1	-2.83E-01	5.53E-05	FOXP1	-3.84E-01	1.27E-05
CHD1	-2.84E-01	5.37E-07	PNRC1	-3.89E-01	6.07E-10
SRSF5	-2.84E-01	1.66E-06	ABLIM1	-3.93E-01	7.22E-08
HNRNPA0	-2.84E-01	2.13E-05	SARAF	-3.93E-01	8.91E-10
ST13	-2.85E-01	4.98E-06	ZFP36	-3.99E-01	8.33E-05
CDKN2AIP	-2.88E-01	1.88E-09	Z93241.1	-4.03E-01	1.57E-05
DNAJA1	-2.88E-01	1.31E-04	FOS	-4.06E-01	2.49E-06
MYADM	-2.89E-01	1.60E-03	FUS	-4.07E-01	2.24E-07
IDS	-2.90E-01	3.47E-03	DDX3X	-4.15E-01	1.24E-05
RPL27A	-2.91E-01	2.33E-03	CCR7	-4.19E-01	1.93E-05
RIPOR2	-2.92E-01	9.16E-04	ILF3-DT	-4.21E-01	3.81E-08
NDFIP1	-2.93E-01	1.26E-04	SBDS	-4.22E-01	4.93E-07
MT-ND4L	-2.94E-01	4.59E-05	YPEL5	-4.25E-01	6.06E-04
NOP53	-2.94E-01	3.64E-03	ZFP36L2	-4.26E-01	2.02E-11
JAK1	-2.96E-01	5.93E-05	TSC22D3	-4.30E-01	1.08E-06
PPP1R2	-3.01E-01	7.34E-07	EIF4B	-4.30E-01	1.33E-03
SNHG8	-3.02E-01	2.97E-05	EPB41	-4.36E-01	4.14E-06
RBM25	-3.02E-01	3.37E-07	LEF1	-4.40E-01	8.19E-05
EIF3H	-3.04E-01	1.63E-05	DDIT4	-4.41E-01	8.33E-04
PIK3R1	-3.04E-01	1.06E-03	LBH	-4.57E-01	7.07E-07
LYZ	-3.07E-01	6.62E-03	NFKBIA	-4.59E-01	7.92E-06
JUN	-3.08E-01	7.23E-05	RCAN3	-4.71E-01	2.05E-05
SF3B1	-3.14E-01	5.41E-03	CCNL1	-4.76E-01	9.08E-05
SELL	-3.14E-01	1.15E-02	PIK3IP1	-4.84E-01	2.24E-06
CHD2	-3.14E-01	1.51E-07	CITED2	-4.88E-01	5.93E-06
MARCKSL1	-3.17E-01	2.63E-05	MAL	-5.03E-01	1.51E-04
PPP1R15A	-3.18E-01	6.53E-04	SLC2A3	-5.06E-01	5.95E-04
ANP32B	-3.18E-01	3.42E-05	CAMK4	-5.12E-01	3.08E-06
EIF2S3	-3.19E-01	2.42E-04	BTG2	-5.20E-01	4.38E-05
RBM39	-3.22E-01	2.07E-06	GADD45B	-5.36E-01	3.53E-05
IER2	-3.23E-01	4.21E-05	DNAJB1	-5.38E-01	9.53E-06
OXNAD1	-3.24E-01	8.38E-06	TMEM123	-5.56E-01	3.74E-05
RSL1D1	-3.24E-01	5.52E-07	TSPYL2	-5.59E-01	3.18E-08
SEPT6	-3.28E-01	3.91E-05	TCF7	-5.96E-01	2.79E-05
BTG1	-3.34E-01	2.68E-10	NOSIP	-6.11E-01	1.61E-05
CYTIP	-3.34E-01	1.03E-05	HIST1H1E	-6.17E-01	8.75E-03
EML4	-3.36E-01	1.84E-06	IL7R	-6.19E-01	1.45E-04
LEPROTL1	-3.41E-01	5.18E-04	TNFAIP3	-6.66E-01	1.90E-06
HIST1H4C	-3.44E-01	2.22E-02	STK17B	-6.79E-01	1.71E-09
CD27	-3.49E-01	5.76E-05	RGCC	-7.21E-01	1.90E-11
TLK1	-3.51E-01	9.06E-09	LTB	-7.84E-01	2.75E-04
DUSP2	-3.54E-01	9.44E-03	CXCR4	-7.94E-01	3.07E-07
AQP3	-3.56E-01	6.48E-04	MT-ATP8	-1.95E+00	2.20E-07
KLF3	-3.58E-01	5.09E-07			
SMCHD1	-3.62E-01	5.06E-07			
PSIP1	-3.67E-01	1.23E-06			
NR4A2	-3.73E-01	1.87E-03			
CDKN1B	-3.74E-01	2.10E-05			
ARGLU1	-3.74E-01	6.25E-06			

Appendix table 7

Performance metrics of the 4 types of classification models aiming to predict the acute severity label of each donor following the evaluation using the repeated cross-validated methodology.

ROC AUC						
Model	**Min.**	**1st quartile**	**Median**	**Mean**	**3rd quartile**	**Max.**
LDA	0.399	0.568	0.601	0.601	0.654	0.748
KNN	0.553	0.702	0.752	0.751	0.802	0.895
svmRadial	0.508	0.731	0.788	0.781	0.842	0.958
Random forest	0.652	0.773	0.833	0.826	0.881	1.000

Sensitivity						
Model	**Min.**	**1st quartile**	**Median**	**Mean**	**3rd quartile**	**Max.**
LDA	0.364	0.545	0.636	0.603	0.652	0.909
KNN	0.455	0.623	0.727	0.691	0.767	0.917
svmRadial	0.364	0.614	0.652	0.670	0.750	0.917
Random forest	0.455	0.636	0.667	0.693	0.733	1.000

Specificity						
Model	**Min.**	**1st quartile**	**Median**	**Mean**	**3rd quartile**	**Max.**
LDA	0.250	0.500	0.538	0.567	0.615	0.833
KNN	0.500	0.583	0.667	0.673	0.750	0.923
svmRadial	0.500	0.750	0.769	0.779	0.846	1.000
Random forest	0.667	0.769	0.846	0.839	0.917	0.923

Appendix methods table 1

Gene lists that were used for the computation of AUCell scores in the integrative analysis of the HSC datasets

Gene set	Component genes
Tirosh_2016_G2M_phase	HMGB2,CDK1,NUSAP1,UBE2C,BIRC5,TPX2,TOP2A,NDC80,CKS2,NUF2,CKS1B,MKI67,TMPO,CENPF,TACC3,PIMREG,SMC4,CCNB2,CKAP2L,CKAP2,AURKB,BUB1,KIF11,ANP32E,TUBB4B,GTSE1,KIF20B,HJURP,CDCA3,JPT1,CDC20,TTK,CDC25C,KIF2C,RANGAP1,NCAPD2,DLGAP5,CDCA2,CDCA8,ECT2,KIF23,HMMR,AURKA,PSRC1,ANLN,LBR,CKAP5,CENPE,CTCF,NEK2,G2E3,GAS2L3,CBX5,CENPA
Tirosh_2016_S_phase	MCM5,PCNA,TYMS,FEN1,MCM7,MCM4,RRM1,UNG,GINS2,MCM6,CDCA7,DTL,PRIM1,UHRF1,CENPU,HELLS,RFC2,POLR1B,NASP,RAD51AP1,GMNN,WDR76,SLBP,CCNE2,UBR7,POLD3,MSH2,ATAD2,RAD51,RRM2,CDC45,CDC6,EXO1,TIPIN,DSCC1,BLM,CASP8AP2,USP1,CLSPN,POLA1,CHAF1B,MRPL36,E2F8
Rodriguez-Fraticelli_2020_Platelet_bias_HSC	MT-CO3,MT-ND5,TBL1Y,TGM2,JADE3,MAGEE1,MAGED2,YWHAB,FOS,EVC,EYA2,UCHL1,WDR44,AGPAT3,TSC22D1,SLC37A1,RHOJ,ITSN1,SLC39A6,SPATA13,CYTH4,CXADR,RPS21,KLF6,FUT8,PDXK,ADGRA3,JAM2,MAFF,RPS4X,SAMSN1,APP,CLEC14A,FUNDC2,BMP4,TTC39B,SOX18,SLC35E4,PDGFB,PDE9A,BEX1,ITM2A,PIGP,SDC4,TWSG1,SMARCA2,BEX4,SOGA1,RPL3,CDC42BPB,ORMDL3,CORO2A,RPL36A,PDLIM1,TIMP3,PML,WT1,EVC2,TPST2,INVS,NF2,CLU,SMIM14,FKBP1A,FKBP1C,ZFAND5,RIN2,PLXDC2,KLHL7,RAB40C,BEX2,RND2,PANX2,MAMDC2,TLN1,PALLD,ZDHHC9,SREBF2,PABPC4L,GOLGA5,REEP3,ATP6V1B2,IRF2,IL2RG,FOXK1,MARCKS,C2CD4C,TSPAN14,ZFAND3,PIM1,AKAP10,SEMA7A,PTPRM,ADGRG6,P2RX1,PNPLA8,PHYHIPL,SERPINA3,RNF24,EHD4,NEO1,FNBP1,MAGED1,KCNK5,FERMT1,CPNE8,KATNAL2,DLG5,LCP1,TMEM38B,PSME1,HOXB9,ARMC3,IL22RA2,GRB10,TLR8,R3HDM4,NCOA7,HSPA12B,MANSC1,TAS2R13,APH1B,KIZ,POFUT1,CBX6,RFXAP,TCF15,CAMKK1,RAB38,CNN2,BDH2,TES,GSPT2,MARVELD1,IGHV3-15,IGHV3OR15-7,ERG,RPL39,ARHGAP28,LIN54,CTDSP2,FAM210B,PRNP,ETV6,TSHZ1,PDLIM5,NEFH,COL4A1,STX7,H3-5,C18orf32,ALDH1A1,GDA,LPIN2,GABARAPL1,MYOF,SRXN1,SMAD4,MMRN1,HABP4,SERINC3,SKAP2,GNG11,ENPP5,STK24,PROCR,MLLT3,PRAF2,COL4A2,PBX3,EPSTI1,RPS29,SMCR8,CLEC1A,TRPC6,CD2AP,DHRS11,TBL1X,CARD19,SLC18A2,DUSP18,PRR5L,SMAGP,LAMP2,MFNG,DNAJC3,SLC9A8,FUT10,ITM2B,LHX3,GDF3,CLDN10,RGP1,BBS1,CX3CL1,RPS19,KLF2,PTK2,ARMCX6,SBSPON,SORBS2,H1-0,ITGB1,AK1,HLA-E,RBP1,RPL30,ADTRP,FZD8,SKI,ST3GAL1,GRINA,RPLP1,ZFP2,RAB11FIP3,FAM110C,NTRK2,FHDC1,EPB41L4B,DNAJB4,TMEM158,ECSCR,FAAP20,SPR,ABCG2,SLC25A4,SLC48A1,RUNX1T1,PRKCA,B4GALT4,PODXL,TREML2,NLGN2,ZMYND8,PIK3R1,NR1D2,ZNF467,FRMD4B,PTPRCAP,RMND5B,MBD6,SPRY1,RBPMS2,PLXNC1,TNS2,PRCP,DDIT4,ZNF324B,KCNV2,GLRX,CSRP2,TFPI,CALCRL,MKLN1,ITM2C,SLC25A22,CD38,FCHSD1,RNF185,SERPINB6,RAB11A,TNFSF10,LBH,TNFSF12,TM4SF1,SDCBP,EML4,CHCHD7,CYTIP,ADAD1,RPL31,ZBP1,PTGER4,FMNL2,MPDZ,RHBDF1,ELF4,INSIG1,CCNDBP1,ALDH2,NEURL3,ADGRL4,PRRC2B,LYS

	MD2,ROBO4,EXOSC4,RFTN1,WDPCP,ZFP36,CDIPT,KIFC3,EYA1,LAPTM4A,PADI4,BBX,NCKAP1,HOXB7,RPL34,ESAM,CD302,RBMS3,LHCGR,FSCN1,GPRASP2,TRAV26-2,SGMS1,TAGLN,GPX8,PDE1B,ATP11A,KLHDC10,HSD17B10,GAS2L3,TMEM64,NFKBIA,NFIC,BASP1,P3H3,INSR,EID1,ABCB1,ITGB3,SOCS2,SARAF,IGF1,TERF2IP,HK2,GPR157,APRT,CEBPB,FADS1,GIMAP1-GIMAP5,MAP3K9,ALDH7A1,MMD2,CLDN12,IGHV3-72,IGHV3-73,ARMC12,BICD1,FSTL1,CDCP1,LST1,ARHGEF26,NCOR2,NPDC1,MICB,CRIM1,RCN1,NKX2-8,RPL22L1,DCUN1D1,VASP,IFIT1B,ASB13,CTSF,IGF2R,PPP1R15A,RPL37A,UBE2L6,HDAC11,FKRP,AKT1,NUB1,TNKS1BP1,RPL37,HDC,GIMAP1,EHD3,FAM219B,ZMYND11,TMEM130,GLIS2,LTB,ANXA5,TNFAIP8,SPTBN1,ARF3,JAZF1,TMEM134,IL18BP,HLF,GYS1,SOCS5,ADGRD1,LMO2,MATN4,CCND2,IRF2BPL,RBM18,MEIS1,SMO,LY6E,RBFOX2,VPREB1,FZD1,CBFA2T3,MROH7,MROH7-TTC4,NPR2,COX7A2L,ALDH3A2,HMGN3,SDC2,TIE1,GIMAP6,ZBTB25,HACD4,RGMB,RPS16,NDN,AIG1,CLSTN1,YPEL3,ZFP36L2,TSPAN3,TMEM176A,SCX,TMTC2,PPP1R11,UBE2E2,CD177,TGFBI,DDX58,C9orf152,PPP1R18,FGD5,CITED2,HOXB6,EID2,LPAR6,PEX11A,C16orf90,CRTAP,ATP6V1D,SFRP1,TMEM176B,PTGS1,ACTN3,VMP1,SNAP29,SIAE,RPL7,CRACR2B,GIMAP4,IGF1R,TBXAS1,PPIC,TOX,C1R,CECR2,RAVER2,PIM2,TRIP10,CXXC5,KLF9,PTPN18,GNAI2,THRA,BBS10,SHROOM4,TRIP6,HOXB8,RDH10,RPS7,CLSTN3,MYL10,MSMO1,PTK2B,PKIA,NEURL1,PCBD1,NISCH,MSANTD4,C11orf96,ASAP3,SLC15A2,MBOAT2,SH3BP5,KRT32,AIP,CDKN1B,NKX2-3,ERGIC1,CREBRF,NMUR1,S100A6,CHPF2,NT5C3A,CCND1,PBX1,WBP2,FAM171B,GLIPR1L1,RPL28,TMEM9,CYP26B1,APOE,RHBDD2,PLXNA1,IRGM,RACK1,LDHB,TRAPPC9,RPS8,LGALS3BP,AGO3,GABARAP,ALDH6A1,PCOLCE2,GIMAP8,DEF8,HID1,ARHGEF3,EMC1,NSA2,RPS14,TSPAN4,LIMD2,ABI2,NKAIN3,CTSB,GATA2,UNC45B,NPR1,PLSCR4,VAMP5,JUND,RAB7A,SYT11,GIMAP5,CASP12,NRXN1,CRTC2,CAPNS1,RPS15,TMBIM4,RGS18,RPS9,TMEM237,TRIM47,CADPS2,MINK1,JUNB,CLTB,RGS1,UTRN,FAM43A,CYP4V2,UBA7,CNOT6L,DIO1,HOXA3,LRRC56,PCDHB9,PCDHB10,KRT18,CCDC181,TGFBR3,ZBTB20,MTMR14,AMOTL2,NUPR1,EFCAB14,PLD1,TCF25,SLC66A3,ITGA6,SLC6A15,OST4,RORC,TEDDM1,DENND2D,PIANP,RYBP,PDZK1IP1,ZBTB4,CHIA,SHISA5,SFT2D2,PDE6H,PEA15,RPS28,STAT1,RASGEF1B,TMEM37,ZNF700,ZNF878,SORD,MLLT6,H3-3B,KLHDC1,TRAIP,NAB1,CD74,PKP4,MEF2D,SRGAP3,NOS1AP,VDR,SLAMF1,ASCL4,NFE2,S100A4,MECOM,SPINT2,RYK,DLG2,IER2,DNM3,IPO11,MYLK,ZNF324,S100A8,DIAPH1,TMEM94,GOLGB1,RPL8,BMPR2,EXD2,UBA52,RPL35A,MCTP1,AMACR,PCSK4,RPS11,QSOX1,CISH,CPNE3,ACOX1,SCARF1,HNRNPH3,PRSS54,SEC14L1,GSTM1,MPL,TPD52,PCGF2,RPS6,SLFN12,SLFN12L,JAM3,PXN,PRL,F11R,PHACTR1,CREBL2,AMIGO3,CCDC126,ALDOC,TIMP2,EEF2,CSGALNACT1,ART4,RPS20,LIMA1,LTF,CAMK2N1,GATA3,MIER1,EBI3,APLP2,SNX17,HMGA2,TXNIP,IKZF4,POR,SELP,GKN3P,BAK1,RPL32,AMPD2,PDLIM7,MT1G,VWF,EVA1B,WDR89,CD63,GBP2,IFI44,NCEH1,TMEM140,TINAGL1,GBP5,POLB,CFAP36,MAST4,CLEC2D,FAM187B,HOXB3,PEAR1,GCNT2,B2M,RELL2,RPL24,PTPRN,FPGT,NAT8,NAT8B,MEF2C,ID2,TERF2,PLCG2,CSNK1D,STAT3,COL16A1,GBP6,C1RL,SLC6A6,RTP4,ATP13A4,NR4A2,PAQR7,SLC24A5,ANKRD13D,JUN,GRN,LUZP1,PEF1,CD9,PRDX6,ANGPT1,SMTNL1,MAP2K1,GNS,RIT1,OBSL1,GLUL,RPL13,DTX3L,DUSP1,WDR77,GBP4,CDKN1C,NFIX,RRAS,CHST2,CSAD,MSI2,CDC34,RHOF,SSBP3,IL16,DR1,POMGNT2,OXR1,CFL2,PLSCR1,MICA,PRKACB,ZNF579,RPL26,PSAP,CLPB,NICN1,UBE2G1,TMCO4,FKBP7,ADGRG1,METTL7A,RPS13,SYF2,EF

	NA1,ENSA,TTC14,CAPG,SPINK6,MTMR10,TJP1,AFF1,UPP2,ITPKB,ATP2C1,ORAI1,ST7L,NEDD4,INPPL1,CLEC4G,TICAM1,PGR,CLIP3,PITPNA,MYCT1,BHLHE40
Rodriguez-Fraticelli_2020_Multilineage_HSC	MT-ND1,MAFIP,PCDH11Y,AKAP6,GART,EIF4ENIF1,LGALS1,U2AF1,BORA,CDC123,PSMC6,EIF2S2,RBX1,RBL1,GINS1,HDHD2,POLE2,BIK,RBM3,RFC3,WNT7B,RCL1,HMGB3,GTSE1,RRP1B,MIS18A,KRTAP13-1,KRTAP13-2,TRMT6,SPATA2,DHX15,KLHL34,ATP6AP2,DRG1,SLC25A5,SLX4IP,BEX4,PSMD10,NOP56,ACSS1,SLC25A21,PSMA7,JAKMIP1,HSPH1,ATP5ME,C21orf58,PARVG,ZBED4,GLRX5,P2RY10,HMGN5,CST7,CDKL5,SKA1,SNRPB2,IPO5,ATP5F1C,EGLN3,ATP5F1A,MIS18BP1,IL17RA,PIN4,ENTPD6,GID8,SUMO3,SEC11C,MTHFD1,ZNRF2,CKS2,POLA2,CENPM,INIP,C1QBP,BCLAF1,WDR24,PLAA,PHF5A,RB1,BCOR,DCTN6,NAT2,FRAT2,CYCS,MCM3,ARHGAP19-SLIT1,ARHGAP19,SNRPD3,GTPBP1,CCNB2,UBE2A,SIVA1,EEF1E1,SEMA5A,DEK,MS4A3,ARHGEF39,PDSS1,INCENP,NRP1,SHC4,PCNA,XYLT1,SUZ12,PSMD3,CDC45,GOLM1,MCM5,ITPA,U2AF1L5,EVL,TEX30,E2F1,SLIRP,NPC2,CDCA2,SERPINB5,OSTC,MAPKAP1,REC114,E2F8,CPLX3,POLR2F,HNRNPD,FBXW4,COX5A,FLT3,MRPL36,SYK,PRMT3,RAB44,S1PR3,NRBF2,MYBL2,UTP14A,SLC29A1,ALDH1A1,NARS1,ITGA8,DNM1,ELOVL5,ARL11,CENPQ,SLPI,ANKRD10,GTF2E2,IL10RB,SHMT2,PRIM2,FECH,ZNHIT3,PC,SDCBP2,TRPM5,SRSF6,RGS10,MAGOHB,SCIN,BUB1B-PAK6,BAG1,TTC17,PALM,EFCAB11,RPS24,RANGAP1,TFAP2B,SWI5,CCL23,CCL15,CCL15-CCL14,OLR1,USP14,ENDOD1,EWSR1,HSP90AA1,ZNF22,DNAH8,STX3,SNRPD1,GPR26,SMARCA5,TBRG4,SCLT1,ATP7B,BCCIP,GYPE,GYPB,GYPA,YBX3,TPX2,MAD2L1,ARPC5L,SDF2L1,CISD1,ANLN,SMC2,RIMS4,DSN1,RAD51,RANBP1,WSB1,BMX,CLEC4D,CSTF2,FAM133B,UPF3A,RNASEH2B,ANP32B,UBE2C,DNTT,SLC26A1,MED21,TYMS,UCHL3,PSMB5,SLTM,PLK4,CTSA,CCNG2,BID,SPIRE1,ADD3,RIN3,CDC5L,NDUFA4,SRPK1,HDAC2,CLEC4E,COL5A1,MNS1,TSPO2,FASTKD3,KREMEN1,PGAM1,PRPS1,RPS27L,WBP4,UBE2K,EMILIN2,CCDC178,DOCK11,ABCB4,GADD45A,CHTF18,COTL1,NKRF,CCNF,RASGEF1A,ATP6V0C,MRPL18,SDHD,AARS1,TBC1D31,AGO2,MSANTD2,PHF10,SLA,APOOL,MCM7,SUCLG1,UHRF1,NUP107,CLDN34,PATE3,SLF1,ARMCX4,PAICS,EIF3J,NUP93,F13A1,NT5C2,EIF5AL1,MMP19,KIF11,HAAO,HLA-DOB,TPM4,UNC5C,CRY1,RPA1,FABP5,CEBPA,NOLC1,FSBP,LMNB1,LUC7L3,FOXK2,CENPW,BLVRB,TAOK3,NOA1,ADD2,FAM117A,CCZ1B,CCZ1,CNOT6,CKAP2L,HSPA8,PCDH11X,PPID,FIS1,TMEM258,MBTD1,GDPD5,IGFALS,NUTF2,ANAPC5,AMMECR1,AKIRIN2,RFC5,UQCR11,HNRNPDL,RRS1,RASA4B,TMEM147,HNRNPA2B1,SCGB3A2,CLEC5A,HELLS,MCM4,DLX6,NCAPH,ZAN,TCTN3,ANXA3,SMS,STEAP3,RRM1,DTX4,UBN1,IRF8,TMEM14C,ZRANB3,FRG1,CASP6,TUBGCP4,HGH1,CFDP1,CENPI,SRGN,PTGR1,PTGES2,NPM3,PSMD14,MAP2K6,CHCHD1,SRSF7,CCNE1,MUC6,MRGPRD,EED,DDX39B,PAPSS2,ALAD,EFR3B,UHRF1BP1L,SOD2,DNAJC6,SMN2,LRP8,DYNLL1,RCC2,CXCR4,NUDT7,GP6,SPDL1,SIGMAR1,DMKN,ACTR3,CDK6,HK3,PPAT,METAP2,RNF5,CIAPIN1,ATP5IF1,EIF1AD,RAD54B,AVPR1A,ZBTB45,ZNF277,WDR18,CA1,PGAM4,IDH3A,SLC22A3,GINS2,POP1,SLC39A8,KIF15,ATP1B2,MPEG1,CFAP20,ARMC1,DTYMK,TMBIM6,DRAM1,LPCAT2,IFNGR1,CRIP1,ADAM17,B4GALNT1,GTF3C6,MTHFD1L,NAA15,HNF4A,NAT1,IGHM,GTPBP10,SLCO3A1,MED30,GATM,CPOX,METTL17,GNPTAB,TCP1,CHCHD2,CMTM7,BARD1,DBR1,NUDCD2,C6orf136,COX4I1,MYC,GPC4,AGA,IGHE,ATP1B3,SKA3,NT5DC2,TOP2A,SERPINB1,OIP5,NDUFB4,OAZ1,GMNN,GRM1,PSMB2,ATAD5,USP1,MAPK10,CSGALNACT2,VRK1,CDCA8,RGCC,GATA1,CCNB1,FARSB,FBXO5,PLK1,MGAT5,RPF2,SNRNP40

	,INHBB,NDUFAB1,KEL,NAP1L1,SIM1,UTP14C,LGALS16,LGALS14,PRC1,PLEK,PABPC3,CPSF2,PAOX,DHFR,DAZAP2,LIG1,DNAJB6,COX7C,EPHX2,DOCK8,GEMIN6,ITGBL1,GARS1,PIEZO1,CDT1,GNA11,CTSG,FEN1,TESPA1,PLAC8,CSF2RB,BANF1,LSM8,MCM6,ICE2,CBX3,SARS2,RGS9BP,FREM1,ELANE,CDK4,CENPH,RHEB,PI4K2B,HYPK,MPO,DDX28,HNRNPAB,PROM1,ANK1,DEPDC1B,DNAJC8,NAA40,NUBP1,AQP1,NEBL,PPP1R37,NSMCE4A,GAPDHS,PIN1,TUBA1B,SCN2B,LTV1,TSHR,SF3A3,THOC6,SF3B6,EMB,CD37,ANKRD44,PECR,TUBB,RFC2,TMEM97,HLA-E,ZNF740,HBA2,HBA1,ACSL5,CCNA2,SUV39H1,DSCC1,CYC1,HSPA14,CENPA,PPP2CA,SYMPK,AP3S1,SERP1,HMGB2,SLBP,TALDO1,WEE1,FSCN3,ANKRD34B,SUDS3,MARS2,NXPE2,TEKT4,PSMA1,SSRP1,TP53,SLC38A5,PTBP3,ACOT9,ALG5,SIGLEC6,CD33,HNRNPC,HNRNPCL1,HNRNPCL2,HNRNPCL4,HNRNPCL3,WDR43,MYO15B,HINT1,ACTL6A,OR7G2,YBX1,EZH2,EEF1B2,CUTA,PDHX,DENND5B,TMED2,NEK10,METTL8,HNRNPL,SGMS2,ARAP2,RPSAP58,RPSA,CENPL,POLR3C,PMF1-BGLAP,PMF1,PCDHGB2,DCTPP1,LHX5,ECT2,STX2,MRPS5,PTCD3,CDC25A,IVNS1ABP,PARP1,LY86,SRSF10,TAMM41,KIF22,MATR3,UBE2I,RNASEH2A,LGALS13,SERBP1,ENY2,PABPC1,DHFR2,SSR2,NDUFS5,MDH2,POLR2D,PPP1CC,C8orf76,ZHX1-C8orf76,SH2D5,RHAG,SLC11A2,ASPM,DBF4,CCDC12,C1orf112,KIF14,SLC16A11,RAD21,ABCA9,HNRNPU,RCC1,NASP,DHRS13,DCP2,UBE2S,PSENEN,NUP43,PRSS57,SPTA1,ALYREF,CDK1,MCM2,ESPL1,HARS1,BDP1,PPM1G,ASF1A,VRK2,AUNIP,NDC1,PTBP1,MUC4,LRPPRC,OR8K3,LYST,AGTR1,PCNX3,NOBOX,NOL6,WDR74,RAB7B,PPIL3,NUCKS1,MMS22L,FARSA,CHDH,FOXE3,TTC13,SF3B1,CD44,PRSS50,BRIP1,CENPN,BRI3BP,IL6R,NCAPD2,PSMD13,SMC3,NEK2,NKG7,HNRNPM,CALR,ERMAP,WDSUB1,TDG,DNAJC9,MPHOSPH9,COX6C,PRMT7,CD34,CLDN16,ZNF700,ZNF878,BTF3,TRIM65,G3BP1,MFSD6L,STIL,DHX9,PANX1,DOT1L,SYNC,TIFAB,HNRNPH1,DPYSL4,CPA3,ZEB2,TRNP1,PCMT1,SNRNP70,CLEC12A,GCLM,MYOCD,EMC10,EXOSC5,GPRIN1,IGKC,PSMG3,POC1A,DUT,MTHFD2,SRM,METRN,DLAT,PAQR9,GAS2L2,SETSIP,ATP5MC3,RPL4,MSRB1,RHD,RHCE,TRA2B,PLEKHF1,UMPS,ANP32E,NR1I2,FBL,SRSF1,PPTC7,HDGF,INTS7,SELL,GPX1,C1orf56,NHEJ1,NME1,ZNF605,RRM2,SSB,POLR3K,ITPRIPL1,LRRC59,CD47,TIPIN,TOP2B,COX5B,RABGAP1L,HYOU1,PAMR1,SLC16A1,DMPK,GAPDH,SYCE2,MUTYH,TCOF1,ODC1,MFSD2B,SF3B4,CCDC125,SELPLG,MED8,SLC26A9,SPHK1,UCHL5,IL12A,SLC16A6,BIN1,GPR87,HSPE1,MYB,NDUFC2-KCTD14,NDUFC2,TOPBP1,SNRPF,FCGR2A,FCGR2C,FCGR2B,TAF9,SH3BGRL3,PITPNC1,ARHGAP11A,ARHGAP11B,NUDT21,SATB1,ST3GAL5,RFX6,WDR46,SF1,PCBP2,CD69,CITED4,NPEPPS,CLP1,PHGDH,CNN3,COX17,NDUFS6,MRPL55,CCDC124,CACYBP,TMEM92,NRM,ADGRG3,CCSAP,ARL6IP6,ORC2,GINS4,ACSM3,ASF1B,TAF2,PDF,KLKB1,EVI2B,PSME3,GAPT,TMEM119,DAZAP1,EPHA4,U2AF1L4,DTL,VDAC2,EIF3H,G0S2,VIM,WDR83,MRPL3,MRPS14,FGF18,KLF1,H3-3A,LAX1,PSMB6,CCNE2,TACC3,SH2D4B,GSR,UQCRC1,SFPQ,FAM111A,IRF2BP2,RAD54L,CTXND2,MICAL2,MLEC,CTSE,EIF5A,PCBP1,HSD11B1,GTF2IRD1,KCNAB2,FCHO1,FASN,FFAR2,G6PC2,E2F4,ZCWPW1,PDCD4,SKP2,BSN,NCF1,BCAS2,CLEC10A,ADAMTS17,C1orf131,PTPN11,SPCS2,TFRC,PA2G4,RECQL4,HJURP,KMT5A,ARL6IP4,ARHGAP44,TM6SF1,ABAT,GALK1,METTL18,OR2Y1,NAA50,CKS1B,UNG,SRSF2,GPN3,RBBP4,SNX14,CD48,RASA4,ARL2BP,COMMD5,PABPC4,BZW1,ITGAL,BIRC5,RPN1,UBE2M,KNSTRN,LSM6,ST3GAL3,WDR12,FIGNL1,MRPS35,TK1,HNRNPF,DCUN1D5,STMN1,KLHL12,ICA1L,IL1R1,EFCC1,ATXN7L1,MAPT,SMN1,RPA2,UBC,CAB39,DNMT1,CD53,AGPAT5,HPN,LYAR,TRIP13,PSMB4,MTUS1,OR10P1,UCK2,TCF3,PGD,ABCB10,POLR2J3,POLR2J,SMC4

Rodriguez-Fraticelli_2020_Low_output_HSC	MT-ND4L,MT-ND2,MT-ND3,MT-ND5,MT-CO3,MT-ATP8,TBL1Y,LRRN4,AGPAT3,TSC22D1,TCEAL5,SNX6,PGRMC1,ITSN1,C20orf173,CYTH4,CHST7,SPATA13,SRSF5,RHOJ,XPNPEP3,TRDC,MAGED2,TGM2,EVC,TOMM34,EYA2,YWHAB,IDH3B,FOS,SAMSN1,INSM1,RPS4X,APP,PHYH,HUNK,TCEAL8,MAGEH1,NCAM2,RHOXF1,PKDREJ,RPS21,KLF6,ZBTB14,PI4KA,TRMT2B,JAM2,PDXK,ADGRA3,MAFF,ARHGEF6,FUT8,TTC3,FGD1,CDH4,IMPACT,RBBP9,RNF4,BEX1,PDE9A,FAM3B,ADGRG2,BMP4,TTC39B,PELI2,KLHL4,INSL6,SOX18,ZNF521,TCF4,SDC4,SLC16A2,SMARCA2,BEX4,TRIOBP,RPL3,SOGA1,CDC42BPB,SPO11,DCAF12L2,PTPN21,SLC19A1,MORC3,JAG1,C4orf50,XK,IFNA16,IFNA2,IFNA6,IFNA13,IFNA7,IFNA17,SERPINB8,TBC1D4,PIGP,PIK3IP1,NOL12,IL1RAPL2,NCOA7,UGT2A3,PLEKHO2,ELMOD1,CBX6,DBNDD2,MANSC1,CYB5A,SERPINA3,TRMT11,UPP1,IRF9,MARVELD1,GSPT2,FLYWCH2,RAB38,PNP,ARHGAP28,ASPHD2,COL4A1,FAM210B,PRNP,GDA,FAM234A,PRICKLE1,ANG,RRAS2,PKD1,MMRN1,SGCG,ENPP5,ATRNL1,PRAF2,PROCR,AHR,MIB1,SNX15,SLC46A3,ETV4,SEC14L2,CLEC1A,SMCR8,P3H4,CARD19,GPR180,UBQLN2,GNAZ,RAB20,GOLGA1,VPS41,ITM2B,SLC9A8,DNAJC3,FUT10,WARS1,GAS6,CYP11A1,FKBP1A,FKBP1C,CLU,AQP5,PSMA8,VAT1,MAMDC2,BEX2,MAPK12,SREBF2,ZDHHC9,MORC2,MED31,COG6,GOLGA5,EBPL,MARCKS,PDGFRA,SMPDL3A,LAMA3,IL2RG,IRF2,B4GALT6,ZFAND3,AKAP10,SEMA7A,POM121L12,PIM1,P2RX1,MAGED1,CPD,PLPP2,EHD4,PSME1,TPST1,LCP1,TMEM38B,CPNE8,RFK,TRAF6,PDE2A,GRB10,HSPA12B,AVPI1,FOXJ2,MORF4L2,GALNT12,TNIP3,KIZ,IFT88,EMCN,TCF15,RPS3A,PDGFD,NMT2,PCMTD1,BDH2,ABCA3,CAMKK1,TRAPPC8,ERG,SLA2,PRPSAP2,NEFH,TSHZ1,ZBTB43,ALDH1A1,GALC,UBOX5,PDE3B,MYOF,EEPD1,GABARAPL1,B3GAT2,GNG11,AR,PBX3,FHIP2A,COL4A2,TM9SF3,MLLT3,TSPAN9,TRPC6,UBA6,SLC18A2,TBL1X,DHRS11,DLGAP4,GLRA3,MFNG,LAMP2,PRR5L,SMAGP,WFDC2,RGP1,PPP1R9A,CORO2B,PPDPF,PDLIM1,RPL36A,ORMDL3,SEC31A,ITGAE,WT1,EVC2,TIMP3,GKAP1,MSRB2,TPST2,SMIM14,KLF4,IFNA1,IFNA14,IFNA10,IFNA4,IFNA8,FAM184A,TRIM44,PLXDC2,ZFAND5,PANX2,N4BP2,ZNFX1,RND2,WIPF2,FJX1,NHLRC4,ENPP4,PALLD,TNKS2,REEP3,ZNF287,FOXK1,RASL11A,SCML4,RGS3,DYDC2,TSPAN14,RTCB,NOX4,PACRGL,RBBP7,RNF24,ZNF395,CDKAL1,PNPLA8,TRIB3,KLRB1,TSPAN13,ANKS6,TCEAL3,FNBP1,NEO1,FRMD6,FKBP10,ZNF407,KCNK5,HOXB9,NDNF,GRID1,TECPR1,CBFA2T3,ALDH3A2,COX7A2L,SDC2,TIE1,GIMAP6,CALML3,LY6E,ABHD5,ADGRD1,LMO2,MATN4,IRF2BPL,AVEN,MTHFSD,ANKRD33B,ARF3,PLOD2,ANXA5,HSPBP1,TNFAIP8,ZMYND11,GYPC,GLIS2,TNKS1BP1,GIMAP1,GDPD3,EHD3,AKT1,CYP4F8,PPP1R15A,VASP,CRIM1,TIFA,ARHGEF25,ZFAND6,IFT43,LRRC55,NFIA,NCOR2,NPDC1,STXBP4,GPR34,PNMA8A,JRK,ATXN7L3B,PRDX4,IFIT3,CTSC,LST1,FADS3,CLDN12,MMD2,GAL3ST3,CCL27,IFNB1,NTRK3,RIPK1,NBEA,EIF4E,SALL2,RAVER2,DOCK9,TBXAS1,PZP,MED28,CTNNAL1,FRS3,EBAG9,TCEAL6,GIMAP4,FBXO10,NDFIP1,TTLL7,ITGA2,OLIG3,SLC12A2,ATN1,FAM219A,RAB2A,SFRP1,TLE2,DDX17,MS4A13,IFNA5,IFNA21,ST7,ENG,TRIM6,WFDC1,FGD5,HOXB6,NOC3L,EID2,ARID1B,MTMR1,ALDH4A1,TGFBI,TUBB4B,OSGIN1,C9orf152,ATP8A1,ZNF449,PPP1R18,ZFP36L2,TSPAN3,NAB2,PPP1R11,YLPM1,CLSTN1,SPCS3,TNFSF10,AFAP1L1,RNF185,SUGP1,RAB11A,TFPI,AGPAT4,CALCRL,APOH,PRDM16,OR5K3,GLRX,EPM2A,TNS2,RMND5B,PTPRCAP,RGS7BP,SPRY1,BBC3,PLXNC1,SCRN1,ARPIN-AP3S2,ARPIN,TCF20,NLGN2,NR1D2,FRMD4B,B4GALT4,ADM,ASB5,SLC25A4,ABCG2,SLC48A1,SHANK3,COPS8,FAAP20,VCPKMT,SCFD1,DENND2A,DNAJB4,EPB41L4B,TMEM158,RBM38,ENOX2,PLIN3,IL21R,VPS26A,SKI,RPLP1,RAB11FIP3,STX4,AK1,LPCAT3,RBP1,HSPA5,ARHGEF12,CDK17,LPAR4,METTL25,G2E3,TRIM6-TRIM34,TRIM34,CX3CL1,CEBPB,EIF1B,FADS1,GIMAP1-GIMAP5,HCFC1R1,TERF2IP,HK2,PKD2,OR8K5,SOCS2,ZBTB3,LMCD1,KAZALD1,CD82,NFIC,CEP57,LYPD5,NFAT5,ZFP28,SI,GEM,

	VWA5A,FAM107A,SERPINF1,RBMS3,FOSB,HLA-E,BBX,VPS37D,PPA1,OTUD6B,HOXB7,PDZD2,RIN1,MMP16,NEURL3,DBNL,ROBO4,OR10Q1,NDST1,ZBP1,PTGER4,TAS1R3,IFIT2,NFE2L1,RHOBTB3,MSANTD1,E2F5,IP6K1,PLPP3,IFIT1B,HMGN3,MEIS1,LRFN5,SMO,VPREB1,SOCS5,CA2,CCND2,GPT2,DEXI,TMEM134,GYS1,HLF,VIPR2,ZCCHC24,ANXA6,PRKAG2,SPTBN1,XBP1,LTB,MAP4K2,MAG,RPL37,ADGRE5,RPL37A,UBE2L6,FKRP,FLI1,SMAD5,ASB13,ARL3,IGF2R,RPL22L1,DCUN1D1,MICB,TMEM109,PHF11,FSTL1,CC2D2A,EXOC1L,CALCOCO1,JAK1,CMAS,MYL10,CLSTN3,PTK2B,SHROOM4,TRIP6,RDH10,HOXB8,RPS7,PPT2,PPT2-EGFL8,PTPN18,SLC38A9,CENPT,CXXC5,MCFD2,STARD4,KLF9,TOX,PYGM,C1R,FOXRED2,SLC25A14,LIPN,IGSF11,PPIC,RPL7,SLC25A36,CRACR2B,VMP1,FAM174B,ACTN3,KIF23,MICALL1,TMEM176B,LPAR6,PEX11A,CRTAP,ATP6V1D,CITED2,FBXO16,GAA,UBE2E2,UQCRHL,UQCRH,PGM2,STK3,SYDE1,TMEM176A,PGAP2,PARP16,PFKP,NDN,AIG1,IFT57,HACD4,ANKRD55,LONP2,RGMB,TNFSF12,TM4SF1,DMXL2,FAM181B,CD38,FCHSD1,IL27,TMOD3,NETO2,SERPINB6,DZIP3,TSC22D3,DENND1C,ZNF195,FTL,ATP6V1A,ABCA5,NRAP,CPT1A,SRPRA,RIC8B,CSRP2,PARP14,DDIT4,PRCP,CD81,MBD6,EEF2KMT,VEGFC,ANKH,PIK3R1,TFEC,ZNF467,PODXL,CHRM5,WTIP,C16orf74,GALNT7,NET1,LATS2,IL4,LAMP1,ECSCR,ARRDC4,UACA,DCTD,PLCG1,WDR41,ST3GAL1,APOL3,APOL4,APOL2,APOL1,GRINA,FAM110C,FAM107B,ALCAM,RPL30,DNALI1,FOXN3,H1-0,BATF2,CD276,ITGB1,KLF2,STAU2,SBSPON,EID2B,CRTC1,APRT,OSBPL9,TCF7L1,OTUB2,TLCD2,GPRASP1,NRARP,DLX4,CRISPLD1,ABCB1,ITGB3,CFAP77,PCOLCE,SLC31A1,TMTC3,FCHO2,DNAJB9,GAS2L3,BASP1,CDK14,P3H3,INSR,EID1,VKORC1,SH3BGRL2,CSRNP3,PDE1B,PGGT1B,KLHDC10,HSD17B10,KBTBD6,KBTBD7,SGMS1,LHCGR,FSCN1,OR8G2P,OR8G3P,JSRP1,ESAM,CD164L2,FAM3C,CD302,PRKCE,PADI4,LAPTM4A,NCKAP1,SFXN5,CLDN34,UNC5A,ALDOA,EXOSC4,RFTN1,ACO1,HELQ,DKKL1,ADGRL4,PRRC2B,KDR,LYSMD2,INSIG1,SYCP3,GINM1,WFIKKN2,FMNL2,MPDZ,CPQ,USP46,TRIML1,TJP2,TNP1,ACTR3B,CHCHD7,PTOV1,EXOC3,UAP1,CHPF,LGALS3BP,ECI2,NTS,DEF8,GIMAP8,CTSH,ACTR3C,SELENBP1,WBP2,SRR,OR5P2,CHPF2,MSTN,PLXNA1,RHBDD2,GLIPR1L1,KMT2A,NISCH,SACM1L,COA7,CYP2J2,MFN2,MBOAT2,PWP1,PHF1,FASTK,UTRN,GRAMD1C,MTMR11,LPP,CLTB,SASH1,FAS,FAM43A,RPS15,MINK1,TMEM237,DSTYK,PHACTR2,TNR,RND3,SIKE1,PLEKHM1,UNC13D,CTSB,JUND,MYH10,MRFAP1L1,MRFAP1,CDC23,MLLT6,NFKBIZ,MYL6,GBP6,NOS1AP,APOBR,ANKRD63,SFT2D2,CFTR,SHISA5,ZBTB4,PDZK1IP1,STAT1,TNFRSF1A,EFCAB14,PLD1,ABCC1,CAPN5,NUPR1,SLC6A15,RORC,SLC66A3,TCF25,CLEC2D,ACY3,SLC6A20,DIO1,PLEKHA5,PCDHB9,PCDHB10,KRT18,CDC42BPA,LRRC56,WNT2B,GAB1,JAM3,SLC50A1,TMEM52,OR5AN1,CCDC126,FAM86B1,FAM86B2,TMEM9B,RHOB,CISH,EAF1,SLFN12,SLFN12L,TPD52,GSTM1,HNRNPH3,SCARF1,ACOX1,ACOT1,ACOT2,DIAPH1,KLHL21,MTUS1,TMEM106B,MCTP1,IRGM,RCN3,CCDC74B,CCDC74A,VN1R5,SPINT2,ZNF429,NUMA1,S100A4,SLAMF1,VDR,CTF1,MYLK,CCDC17,IPO11,AGT,RMDN1,EIF1,ZNF653,GBP2,FBXO11,LRPAP1,GRIK5,PLEKHB2,WDR89,MRPL4,CD63,ERP27,TOE1,POR,SMG7,DYNC2LI1,IKZF4,PAFAH1B1,EBI3,UBR3,PLEKHO1,CAMK2N1,CMTM4,TXNIP,FUZ,HMGA2,RAB29,CSF1,ART4,SMIM7,EEF2,TIMP2,DST,LRRC47,AP4B1,TMEM120B,C16orf72,FASLG,EXT2,HRK,ADPRH,RTP4,IL27RA,C1RL,ARF4,SLC24A5,CACNA1D,ELMO1,JADE2,SUPT6H,FPGT,RELL2,WLS,APOBEC4,PDE4DIP,MEF2C,MAST4,ZNF32,POLB,RAB11B,B2M,EVI5,OR5H8,OR5H1,OR5H14,OR5H6,OR5H2,OR5H15,TMEM40,CHIA,MICA,PLSCR1,TXNDC15,ECE1,POMGNT2,ZDHHC17,FPR1,MSI2,IRAK3,ALDH1L1,TMUB2,RHOF,GNS,DYNC1I2,TM2D2,MAP2K1,RPL13,VN1R4,S1PR1,LDLRAD2,LUZP1,SMTNL1,DDX20,POU2F2,PITPNA,XPO7,BHLHE40,STK11IP,MYCT1,SIGLECL1,GFI1,HMGB4,PLCH1,NCDN,RARB,LGALS8,ABCB9,CAPG,ENSA,RPL6,PRKD2,RAMP2,ACP6,

	PTPRJ,PSAP,RPL26,GORAB,METTL7A,B3GNT8,FCGRT,HPCAL1,ADGRG1,ISG20,MPZL1,HID1,TSPAN4,SYCP1,RPS14,NSA2,HBEGF,NBEAL2,TRAPPC9,LDHB,CBARP,LCP2,PCOLCE2,CALML4,ALDH6A1,GABARAP,FAM171B,PBX1,CCND1,NT5C3A,S100A6,SDHAF2,APOE,KMO,CYP26B1,TMEM9,RSAD2,MCL1,PLEKHG6,PCBD1,TPRG1,NKX2-3,BMP1,TPP1,SH3BP5,ASAP3,C11orf96,HS2ST1,RCHY1,DIMT1,GBP4,RGS1,CYP4V2,UBXN6,RGS18,POGLUT1,HMGCL,PFDN5,LAMB2,CADPS2,TRIM47,RPS9,CASP12,GIMAP5,PRPF40B,PNRC2,CAPNS1,QRICH2,EIF4B,ATF2,OR5B3,DAG1,RGL1,GATA2,SPINK14,BHLHE41,TRIM5,LIMD2,RNASEL,RAB7A,S100A11,PLSCR4,NPR1,SEMA4B,UNC45B,TBKBP1,SORD,TMEM37,OR6F1,RNF26,TRAIP,NAB1,RHOQ,CD74,RYBP,DENND2D,TRNP1,KDELR1,RPS28,KISS1,METTL24,TGFBR3,ZBTB20,AMOTL2,OST4,ITGA6,TMEM181,PITPNM1,IFI44L,UBA7,AMPD3,HDAC9,NCOA1,EPB41,SH3GL1,AMIGO3,PHACTR1,TNPO2,F11R,GPR108,PCF11,MYADM,AMACR,RPS6,CERS4,MPL,SEC14L1,FAF1,TAPBPL,EXD2,ST3GAL6,BMPR2,MECOM,GOLT1A,SLC25A20,FANCD2OS,ROM1,FLOT2,RYK,DLG2,SFXN3,CISD3,LURAP1,VWF,MT1G,PDLIM7,ANXA7,EVA1B,RHOC,SELP,APBA2,AMPD2,TMEM150A,TAPBP,CTNND1,NR4A1,GATA3,MOBP,LIMA1,ADRB2,APLP2,CFAP70,PNMA8C,CSGALNACT1,PKD1L3,EVX2,SLC4A9,PLA2G4A,RPS20,FOXL2,PRKD3,NR4A2,PRRG2,LPGAT1,SLC6A6,CPAMD8,CEPT1,PAQR7,OR2T1,CDH1,GUK1,COL16A1,HOXA5,FMO5,STAT3,CYP8B1,TAF7,C6orf141,RPL24,GP2,EXOC3L1,VAMP4,PCSK7,GBP5,TINAGL1,NCEH1,GCNT2,ATPAF1,HOXB3,MYO3B,CDC42SE2,CFL2,OXR1,ZNF148,RPL38,ESR1,HES1,CSAD,CHST2,RRAS,NFIX,CDKN1C,PLK2,TGOLN2,EXOC6B,CAMK2A,GLUL,OBSL1,ARHGEF5,DUSP1,DTX3L,PRDX6,FOXD2,ATF7IP,ZMPSTE24,PIK3CD,ANGPT1,CCDC190,PGR,NEDD4,NSG1,ORAI1,AKAP8,VCPIP1,UPP2,PEX12,FKBP9,CCL20,OR2Y1,RPS13,TTC14,EFNA1,CSDE1,CLPB,PAX6,UBB,PURA,PKM,FKBP7,HEBP1

Rodriguez-Fraticelli_2020_High_output_HSC	RBL1,EIF4ENIF1,LTBP2,LGALS1,U2AF1,BORA,GLUD2,SH3KBP1,RBM3,HMGB3,CCDC68,GINS1,HDHD2,GATA5,BIK,POLE2,ATP6AP2,ELF1,DRG1,IL13RA2,ERCC6L,MIS18A,F8,SEH1L,GGT7,BEX4,TMPRSS3,MXD4,SLC25A5,TFAP2C,PARVG,ATP5ME,ZBED4,TST,NOP56,ME2,TEC,ACSS1,RELL1,SMOX,ZNF518B,CEP128,DEFB127,DEFB121,JAKMIP1,CNDP2,SNRPB2,GLRX5,PMAIP1,TP53INP2,CST7,HMGN5,EGLN3,MIS18BP1,TSPO,PSPC1,IL17RA,RBM25,SLC2A9,ATP5F1E,SLC35C2,PIN4,PSMG2,SH3BGRL,REM1,ATP5F1C,IPO5,USP11,TPTE,SEC11C,MTHFD1,RALY,SLIT2,MAPRE2,NOX1,PGM3,SRSF3,GOT1,TDRD3,MRPS26,IL10RB,TMEM123,ANK3,POLR1E,ZMYM3,HIRA,TEX30,PRPS2,ZMYND19,NPC2,IGHV2-26,CDCA2,PES1,SYK,FGF3,MRPL36,AIMP2,E2F8,HNRNPD,GALNT1,FLT3,CCNB2,EEF1E1,SIVA1,HACD3,DPH7,ZC2HC1C,ARHGEF39,INCENP,INPP5F,PCNA,XYLT1,RPS19BP1,CYP2D6,EVL,HSCB,ITPA,CENPM,ZNRF2,CKS2,GPR65,C1QBP,OR4C45,NAA10,BCOR,PHF5A,SNRPD3,CYCS,MCM3,RNF182,CFP,MAPRE1,PIGA,PRPS1,OR4L1,PDAP1,STARD3,MMP24,CCDC178,ESCO1,CCNG2,RBMX,ST8SIA6,BMP15,CDS2,SAMD4A,HDAC2,WNT8B,MRPL1,SRPK1,MAP1A,NDUFA1,RNASE13,TUBA8,RANBP1,NANOS1,YBX3,TPX2,OGN,RNPS1,LRCH1,TSPAN18,ZDHHC13,DHRS4,RNASEH2B,UBE2C,IGFBP4,BUB1B-PAK6,SUSD1,TMEM151B,SNX5,ASRGL1,TFAP2B,PALM,RANGAP1,TADA2B,STX3,ENDOD1,EWSR1,DNAH8,ZNF22,NRBF2,AP1G2,RAB44,SLC29A1,ALKBH1,ARL11,ELOVL5,CENPQ,LRRN3,OR52B4,RAD21L1,CPB2,SHMT2,PRIM2,TMEM217,SOD1,CSRP3,UBE2L3,EMID1,E2F1,CENPP,SPNS3,PFN1,PCID2,ZNF217,REC114,SEL1L2,PARVB,YPEL1,COX5A,FBXW4,UBE2A,GTPBP1,RPN2,PDSS1,NRP1,MS4A3,DEK,CDC45,GOLM1,MCM5,CDCA5,MGAT3,SUZ12,U2AF1L5,ABCA7,COX19,HSP90AB1,POLA2,RASL10A,INIP,COL15A1,BCLAF1,CWC15,PHIP,DCTN6,CCL3,CCL18,CCL3L3,CCL3L1,FRAT2,C7orf26,CAAP1,TOMM22,VSTM4,TSPO2,MNS1,CLEC4E,PGAM1,NDUFS8,RPS27L,DEFB132,DEFB104B,DEFB104A,TXN,EMILIN2,DOCK11,NOP9,TPTE2,SMAP1,STOM,RBFA,ADD3,RIN3,CDC5L,UBL4A,NDUFA4,TBRG4,TEAD4,ABRACL,PBK,AGTR2,SDF2L1,SOX4,SMC2,DSN1,RAD51,MAD2L1,MIF,CAPRIN1,CLEC4D,MED21,ATP8B4,ISCA1,GPC6,PSMB5,ANP32B,DNTT,NONO,SCIN,BAG1,RGS10,CCL23,CCL15,CCL15-CCL14,SWI5,ATP4B,SNRPD1,APCDD1,FOXK2,CENPW,BLVRB,CEBPA,LMNB1,UCK1,HLA-E,CKAP2L,HSPA1A,HSPA1B,HIRIP3,SGTB,EXOSC8,GDPD5,PDP2,RTN4IP1,CASP3,EIF2S1,POLR1D,ATF6B,HNRNPDL,FAM78A,UQCR11,CEACAM21,KIAA1143,MCM4,TMEM147,MFSD10,RRS1,IDH3G,COTL1,SCNN1G,CARD14,CHTF18,GADD45A,CASP7,KCNN2,ARHGEF1,MED9,SLA,KCNJ5,RTN3,SLF1,PATE3,UHRF1,NUP107,ASS1,XKR4,CSF3,TMED9,EIF3J,KIF11,CUX1,OR56B4,UNC5C,RPL27,COX8A,SLC12A6,HLA-DOB,TUBD1,CHERP,MYLK3,CXCR4,DYNLL1,DNAJC6,RHCG,EIF4EBP2,PKD1L2,GP6,FANCI,HYAL2,CDK6,ALPK3,SAE1,HACD2,DMKN,ACTR3,ATP5IF1,CIAPIN1,EIF1AD,HK3,SLC22A3,GNB2,GINS2,PGAM4,TYK2,KDM4A,ATP1B2,POP1,SLC12A9,CHRNA6,IL33,CXCR2,DEFB108B,SYTL1,UBN1,TMEM14C,FAM227A,TTC7A,SMS,SPINK9,ZRANB3,GALNT10,NAT9,CEL,NR2C2AP,TIMM17B,SRGN,CENPI,SRSF7,CHCHD1,PQBP1,PIF1,UCP2,UBE2E3,EFR3B,ALAD,OS9,ATP1B3,IGHV2OR16-5,IGHV2-5,IGHV2-70D,IGHV2-70,GMNN,OIP5,VRK1,DOHH,FBXO5,COA3,CDCA8,RPF2,SLC1A5,SNRNP40,NAP1L1,LRWD1,ATP13A1,PLEK,LGALS16,LGALS14,EDIL3,DHFR,RNF214,LIG1,PABPC3,CPSF2,ADAM17,PRKDC,TMEM129,PTPRE,VARS1,GTF3C6,TP53RK,IGHM,SLCO3A1,CHCHD2,GNPTAB,KLHL31,MACROD1,GNG12,CMTM7,MRPS18C,MOB3A,TUBA1B,HPGD,SF3B6,SF3A3,FNDC3B,PSCA,TUBB,TRAV8-1,TRAV8-3,CD37,TOMT,RFC2,MICAL1,KNDC1,PKMYT1,SPI1,SYMPK,CP,SIX3,PPP4C,HBA2,HBA1,SLBP,RMI2,HADHB,HEY1,SPACA1,ADA

	MTS13,SSRP1,PTBP3,LYVE1,DOCK8,WASF2,HSPA12A,NDUFB2,COX6A1,INSM2,CDT1,GPR3,FLOT1,BANF1,TESPA1,PNO1,CDK4,EIF4A1,CBX3,HNRNPAB,PI4K2B,HYPK,MPO,CENPH,AQP1,SAPCD1,TECTB,DHRS4L2,SYCP3,NOLC1,LUC7L3,MTF1,FABP5,CTLA4,CCZ1B,CCZ1,HACD1,FAM117A,NUBP2,CLEC4F,CD180,GXYLT1,TAOK3,RASGRP2,PPP2R5B,CNOT6,LAT2,GNG10,MBTD1,IGFALS,MAP3K6,LILRB4,HAUS3,LPAR2,CLEC5A,CAPZB,RASA4B,HNRNPA2B1,FUS,CCNF,ABCB4,SDHD,MRPL18,ZNF76,NECAP2,ADM2,MCM7,SNRPB,COX6B1,PSMA2,ADAM8,GM2A,EIF5AL1,PAICS,HAAO,BRD2,FXN,ZSCAN10,CACNA1G,RPA1,PDX1,TRAPPC12,GLUD1,RCC2,NDUFB6,MRPL19,MRPS36,CCT2,NUDT7,GMFG,EFNB3,WDR31,NDUFB8,CDCA7,AVPR1A,TICRR,CA1,UGCG,NDE1,ZNF277,OR10G2,KIF15,LPCAT2,IFNGR1,SAP30,ATP8A2,POLE4,B4GALT1,USF2,INPP5B,MTPN,ARMC1,MRPL13,DTYMK,NCAPH,FBLL1,IRF8,PRAMEF18,PRAMEF2,PRAMEF4,PRAMEF13,PRAMEF10,PRAMEF11,PRAMEF1,PRAMEF6,PRAMEF5,PRAMEF33,PRAMEF7,PRAMEF8,STEAP3,RRM1,DTX4,JPH1,PRIMPOL,UGDH,RPS19,ARL6IP1,CASP6,NPM3,LMO4,PPRC1,PURB,SFXN1,PPP1CA,DDX39B,CRX,PLCZ1,OAZ1,GRM6,BTNL9,TOP2A,SERPINB1,CSGALNACT2,USP1,ATAD5,MGAT5,CACNG5,B4GALT7,NUP210,GATA1,HNRNPLL,CYP2A6,CYP2A13,CDKL3,FITM1,PPP1CB,RAD51C,PAOX,GAR1,CNTRL,NUP188,ADAM33,CRIP1,ITGAV,BMPR1B,SPN,MFSD9,HNF4A,MRPS28,SCRIB,MTHFD1L,SIGLEC11,B4GALNT1,CMKLR1,MSH3,XRCC1,AQP9,CALCA,TCP1,TMEM125,TMEM256-PLSCR3,TMEM256,CORO1A,ENO4,MYC,NCAPG,COX4I1,RAD18,BARD1,MAL,CLDN6,FBXL6,CLIC1,ELMOD2,PIN1,TSC22D4,ANKRD44,DYNLT1,EMB,UBA2,TPRN,FAM151B,CYC1,CENPA,TALDO1,HMGB2,OXGR1,AP3S1,OR4E1,PPP6R3,CFB,SUDS3,PABPN1L,CCP110,SLC38A5,CALM3,LETM1,PSMA1,MARS2,ATP5MGL,GSE1,PTRH2,EPHX2,LRP1B,COX7C,CLTA,TNFAIP1,SIPA1L1,FEN1,MDGA1,FUT7,CTSG,LSM8,MCM6,PLAC8,CSF2RB,ELANE,ACTB,RAB37,NDRG1,DDX28,CA6,IGLV9-49,PARK7,PRPH2,SDHB,MYB,HSPE1,UBXN1,CLEC4A,ATXN7L3,FCGR2A,FCGR2C,FCGR2B,TOPBP1,SNRPF,CENPO,KIRREL2,ALPP,ALPG,ALPI,DMXL1,TAF9,SH3BGRL3,DDX21,FAM78B,HDAC4,CYP2A7,SPAG5,PITPNC1,NUDT21,RUNX3,SATB1,ISYNA1,RUFY4,COX5B,RABGAP1L,SYCE2,UBE2QL1,ARHGAP22,GAPDH,SIGLEC10,MBD3,OR1R1P,PRR22,SERPINC1,LARS2,SELPLG,SF3B4,SVBP,CCDC125,CDK5RAP2,MFSD2B,TRIM59,CSRP1,METTL6,CEP350,LTF,JMJD4,C1orf54,MED8,UCHL5,ASCL5,RNF144A,NADK,IL1RL1,DDX49,BIN1,ABCA8,TUBA4A,HES6,NAA25,THOP1,STMN4,ACAP2,IL12A,FAM189B,G6PC3,TSHB,OR51E2,UNK,PIP5K1A,CYB561D1,ORC2,ASF1B,IKZF2,DHX57,PSME3,GAPT,EVI2B,CFAP74,CD52,ATXN2L,COX7A2,DTL,TRIM42,RPS2,EPHA4,DAZAP1,HNRNPUL1,SCAMP3,EIF3H,CCDC32,MARK2,PLCD1,WDR83,ACADS,ATP5MG,BMP10,VIM,CD69,PHGDH,NPEPPS,TRIM16,TPCN1,NHP2,SYT6,OR4C15,OR14C36,ALDH9A1,NDUFS6,IQGAP3,GPSM2,POLD1,CCDC124,NRM,HNRNPA0,ARHGAP33,ADGRG3,ATP5F1B,BSN,PDCD4,ANO5,TOMM40,CHEK1,DOCK10,ZNF513,GRHL1,MTF2,PA2G4,CDCA3,NMNAT2,KDM2B,DHPS,HJURP,GRB2,KMT5A,CKS1B,SLC45A3,ARID1A,UNG,TM6SF1,GALK1,MIF4GD,SRSF2,SCRN3,OGDH,KCNIP1,ACVR1B,LILRA6,LILRB5,LILRB3,LILRA5,LILRA4,AATK,COMMD5,CD48,RASA4,GPBP1L1,RBBP4,PSMB3,SNX14,EPHA6,CXCR5,KLF1,FGF18,FES,HCST,INPP5D,IKZF1,AURKB,PLPPR3,ITGA2B,PSMB6,TACC3,STK11,BLM,ALOX5,H3-3A,SFPQ,COX6B2,PRDX2,IRF2BP2,FAM111A,UQCRC1,XPC,C17orf50,DPP4,RAD54L,MKRN2,EIF5A,ARPC4-TTLL3,TTLL3,MLEC,CNP,CD7,LITAF,B3GNT2,PSMD7,HSD11B1,SCAP,MYO1B,CDC42SE1,DBN1,FCHO1,SMPD4,HNRNPA1,GTF2IRD1,LLPH,KCNAB2,ARRB2,E2F4,FFAR2,RPA2,ABCG5,DNMT1,TBX21,WDR48,CD53,AGPAT5,ETFB,LYAR,NAPSA,MSLNL,CARHSP1,CSNK1G2,ATP5PD,PGD,TCF3,LSM4,MSH6,TYROBP,ABCB10,SMC4,PABPC4,TMEM205,NFYA,PRAMEF12,PRAMEF15,PRAM

	EF14,PRAMEF19,PRAMEF17,PRAMEF20,PRAMEF27,PRAMEF25,PRAMEF9,PRAMEF26,ZYX,BIRC5,IFNLR1,RPN1,ITGAL,TKT,DBT,LSM6,CLEC11A,KNSTRN,UBE2M,FIGNL1,MRPS35,PRRT2,PSMD8,SNRNP25,LAMTOR4,TK1,STMN1,BAZ1B,CEACAM18,AFF3,NDUFB7,LSM7,HNRNPF,IQGAP1,TOMM20,B9D2,ATXN7L1,TRAK1,HYAL3,IL1R1,PGLS,PMF1-BGLAP,PMF1,POLR2I,DCTPP1,PCDHGB2,PRG4,ECT2,SRPK2,SPC24,LY86,RGS2,BAZ1A,TAMM41,CCDC47,SNRNP48,CMIP,SNAPC4,RXFP4,MTA3,KIF22,NFYB,SPATA22,SERBP1,LGALS13,RNASEH2A,UBE2I,MATR3,MFSD11,CD5L,DHFR2,ICAM4,PABPC1,HDAC7,HNRNPC,HNRNPCL1,HNRNPCL2,HNRNPCL4,HNRNPCL3,SIGLEC6,CD33,ACTL6A,HINT1,MED25,CFAP126,YBX1,UQCRQ,PDHX,CUTA,MRPL12,OR5AP2,EZH2,EEF1B2,FCRL1,NEK10,TMED2,ATOX1,CA11,HNRNPL,MRPL51,RPSAP58,RPSA,EZR,RBMXL1,LIN9,PFDN6,MDC1,CCR2,SNRPD2,CCHCR1,LRRC8C,CNST,CDK1,MCM2,SAMD14,C3orf38,ALYREF,NKTR,MARCKSL1,CEP83,TAP2,SIPA1L2,AUNIP,ASF1A,VRK2,LRTOMT,ARHGEF18,PPM1G,HP1BP3,ALG3,FANCD2,MAP4K1,TRIM28,MUC4,DHRS9,TWF2,PTBP1,NDC1,METTL7A,LRRC10B,EME1,NMRAL1,CAPZA1,PCNX3,FCER1G,VAMP8,SCARB1,ACTG1,CDV3,NCL,CDC34,PSMC4,SH2D5,PPP1CC,CCDC174,NDUFS5,BCL10,MDH2,ASPM,DBF4,CCDC12,ACSBG2,SLC16A11,PHF23,CGNL1,HEATR6,TAF1C,NASP,SLIT3,GPRC6A,RCC1,HNRNPU,UBE2S,CACNG3,FAM221A,IL31RA,STPG3,BOLA1,PRSS57,TGFB1,TDG,LAMTOR2,TNFAIP8L2,POLE,DNAJC9,COX6C,F13B,PRMT7,CD34,FMO4,SMIM5,BTF3,DCLRE1B,CCDC62,CSK,ARHGAP30,DHX9,PANX1,FHL5,STIL,KCNK12,REXO1,WDR74,REEP5,HNRNPA3,CYP2S1,FARSA,WNT2,MMS22L,NUCKS1,GAK,CHDH,NCAPD3,PSMA6,SF3B1,PRSS50,ARPC3,CHIA,RAMP1,CENPN,RPL28,HRAS,SMC3,STK16,NCAPD2,PSMD13,MCOLN3,BRI3BP,DHX37,CALR,MRPL34,ERMAP,ALS2,HNRNPM,NKG7,NEK2,APAF1,EXO1,CSRNP2,MSRB1,PTP4A3,RPL4,ATP5MC3,PLEKHF1,UMPS,TRA2B,TMEM275,OR5B3,MAST3,ANP32E,OR5H8,OR5H1,OR5H14,OR5H6,OR5H2,OR5H15,HDGF,FBL,GPX1,C1orf56,SENP8,SELL,RPL8,SPAG9,GP5,ADGRL2,RRM2,SSB,NME1,TOP2B,TIPIN,CD47,TMEM208,LRRC59,DEFB134,PTPN23,FOXJ1,APOC1,CWC25,MFAP4,HNRNPH1,LAT,BTG2,NDUFV1,S100A10,CPA3,NEXN,PEG3,TIMM13,SNRNP70,CLEC12A,FBXO25,DPYD,COX10,EXOSC5,MTIF2,BANP,RPL18,B3GNT5,SRM,ERP29,DUT,C2orf78,POC1A,TBC1D2B,RASSF1,HNRNPUL2-BSCL2,HNRNPUL2,SETSIP,ORC1,RAD51AP1,METRN,AMBN

Rodriguez-Fraticelli_2020_serial_engraftment_HSC	MT-ND5,DDX3Y,XK,ARHGEF6,FUT8,ATRN,NCAM2,PHF21B,APP,SMARCA2,BEX4,EIF2S2,SERPINB10,GLUD2,APBB2,SAMSN1,TNIP2,SDC4,TGIF1,NUDT11,RNF128,THBD,BMP4,TGM2,SLC25A17,HS3ST1,FAM217B,RHOJ,BEX1,TSC22D1,RP2,PDGFB,CARD10,RPAP3,ENPP5,SERINC3,GNG11,AR,MSL1,TSPAN14,THNSL1,SLPI,OGT,KLRB1,PTPRM,SPIN1,MFHAS1,TRMT2A,PIM1,PROCR,MLLT3,HOOK3,COL4A2,ALG10B,SEMA7A,SAMHD1,DLC1,DRG2,TGFBR1,FRMD6,CLEC1A,FNBP1,TSPAN13,ITM2B,GRB10,GDF3,HOXB9,PRR5L,MFNG,ACADSB,SEC31A,ZNF143,SDAD1,RAB11FIP2,GALNT12,RPL12,PDLIM1,CORO2A,RPL36A,RCAN1,INTS10,HSPA12B,INVS,FAM184A,CLU,CCDC86,FKBP1A,FKBP1C,MARVELD1,CPXM1,TCF15,ERLIN2,SDHAF4,BEX2,DUSP4,PANX2,COL4A1,CCL23,CCL15,CCL15-CCL14,TIAM1,FRAT1,ERG,PNP,LIN54,C9orf85,GABARAPL1,MYOF,ZNF287,LPL,IGFBP4,ARHGAP23,PALLD,ENPP4,ZDHHC9,CHCHD10,ALDH1A1,GDA,APBA3,IL6ST,MAX,ZNF195,SPATS2,GIMAP1,PEPD,EHD3,CTSC,LST1,CDCP1,STXBP4,PYURF,PNPLA1,CLDN12,GALNT11,JAK1,IFT43,NFIA,MATN4,NUMB,KCMF1,CCND2,ADGRD1,LMO2,SH3GL3,HLF,HMGN3,CBFA2T3,LY6E,FZD1,MAT2B,CPA6,PLOD2,LTB,IFT80,SESN2,SF3B6,CHRNB1,ACIN1,SMC5,TRIM6,THSD1,LPAR6,SETD7,FNBP4,EID2,HOXB6,SAT1,TMEM176B,MTUS2,REXO2,RGMB,HACD4,C9orf152,POLR3B,PTPRK,DDX58,TMTC2,ZFP36L2,ZNF706,PRTN3,MCFD2,NBEA,CACNA2D1,KLF9,PTK2B,EDAR,FLCN,PHYHD1,ACBD5,HOXB8,RDH10,SEPSECS,IL4R,GIMAP4,CTNNAL1,UTP6,VMP1,TOX,LRRC49,HOXB4,C1R,PYGM,EPB41L4B,TMEM158,GPR4,ST3GAL1,PDPR,WDR41,FZD8,DUSP2,DENND2A,SRGN,SBSPON,GPR45,USP3,HSPA5,FAM107B,SH3YL1,TACSTD2,NRAP,AGPAT4,SLC12A9,TFPI,CMSS1,JMJD8,DIO2,ZNF324B,TM4SF1,TNFSF10,L3MBTL3,CD38,FCHSD1,GUCA1A,ZNF467,FEZ1,MGAM,PIK3R1,TFEC,TREML2,PODXL,TNS2,TSPYL1,GLUD1,RFTN1,KDR,ADGRL4,N4BP2L2,RBM27,TMEM263,SLC9A1,MTERF4,UNC5A,OXSR1,UBE2H,LRRC57,CYTIP,NAT8L,DNAJA2,EIF4G2,MBNL2,MPDZ,PTGER4,ZBTB3,FBXL12,ITGB3,RPS6KA2,SOCS2,INTS8,INSR,SH3BGRL2,NFIC,ALG10,GPRASP1,GIMAP1-GIMAP5,CEBPB,NCAM1,GNG10,FSCN1,CD302,CABLES2,ESAM,CEBPD,PNRC1,CEP131,KIAA0319L,ZRSR2,CDKN1A,SGMS1,CBL,CSGALNACT1,ART4,TRAPPC4,RASAL2,CNPY3,CAMK2N1,ADORA2B,GATA3,ATP1A1,GFPT1,ACAD8,C4orf48,SENP2,CYP20A1,LDHD,SELP,PHF21A,GIT1,C3orf70,NSF,KLHDC2,PDLIM7,FGF12,MT1G,GAPDH,VWF,CIC,KIT,CD63,HNRNPC,HNRNPCL1,HNRNPCL2,HNRNPCL4,HNRNPCL3,ADD1,NCEH1,RAD9A,GCNT2,PFDN2,PTPRN,PPFIA4,EXOC3L1,CTBS,ID2,PLCG2,STX2,SMIM8,CCDC51,HOXA5,COL16A1,FN1,DCTN1,OXSM,AKT1S1,C1RL,MARVELD2,RTP4,AHCTF1,NR4A2,SLC24A5,LYPLAL1,MTMR4,KCNAB1,FNIP1,GRN,FOXD2,MEN1,ZNF7,ZNF429,POU2F2,SRD5A1,ANGPT1,CCDC92,MAP2K1,SNAPC3,PUM1,OBSL1,GLUL,NDEL1,CDKN1C,DYNC2H1,LLGL2,CHST2,MAN2C1,CNN3,RBKS,MAT2A,ORC4,SNX7,TGOLN2,DR1,OXR1,FBXO21,ACKR1,CDC42,NICN1,CLPB,PKM,BEND5,ADGRG1,EFNA1,PSME3,MBD5,TJP1,NSUN2,GFI1,BSG,MDH1,HAGHL,NEDD4,ZG16,PGR,GNAT2,MTFR1L,CX3CR1,SLC35F5,NEURL1,LINS1,MBOAT2,CDKN1B,S100A6,NT5C3A,CCND1,BRDT,U2AF2,CAMLG,ALDH6A1,DEF8,LRCH3,PLPPR3,DOCK2,NKAIN3,BHLHE41,C4orf47,UNC45B,CDC23,PLSCR4,STXBP6,VPS54,ANKRD13A,GIMAP5,CASP12,NACA,YIPF2,PLEKHM1,EIF4B,ZNF689,SESN1,PHACTR2,SPCS2,TRIM46,TRIM47,RASIP1,POGZ,JUNB,GPR35,FAM43A,UBXN6,RGS14,ANKRD39,UBA7,RBM4B,STARD7,GIGYF2,AMPD3,IRAK2,AMOTL2,NUPR1,KHSRP,EFHD2,ITGA6,RORC,GCLM,CFTR,PDE6H,SFT2D2,ALS2CL,MYLPF,HGS,TRAIP,RHOQ,SSBP2,SRGAP3,GSTM1,SLAMF1,VDR,MECOM,SLFN13,TSNAX-

	DISC1,DLG2,RYK,MYLK,ZNF324,CALM1,C2CD2L,AMACR,PCSK4,EAF1,PCYT1A,MPL,SEC14L1,SMTNL2,PID1,JAM3,FOXP2,F11R,ZNF436,DHX34,KCND3

Pietras_2015_HSC	TBL1Y,CBR3,PTPN21,ITIH5,NRK,RPS6KA6,REPS2,RNF4,RBBP9,PPM1A,TCEA2,IL15RA,RHOJ,ITSN1,TCEAL5,NUDT11,EYA2,MAGED2,SMARCA2,N6AMT1,SLC16A2,FAM110A,ITM2A,BEX1,WDR19,ZNF521,KLHL4,TTC39B,MTAP,JAM2,MAFF,TXNL1,SMU1,TGM2,MAGEE1,BEX4,XK,ARHGAP6,DYNLT3,IMPACT,SEH1L,CDKL5,HDAC8,TBC1D19,EFHC2,AKR1E2,SNX6,ACSS2,BTG3,SPO11,CAB39L,SLC14A1,CLOCK,LDB2,LRCH2,ADAMTS1,TSR2,MAGEH1,TCEAL8,LRRC9,ARHGEF6,PI4KA,PKDREJ,RAB27B,NAP1L3,PGRMC1,NDRG3,PCMTD2,SYTL5,CLEC1A,HSPA4L,DHX32,NXF2,NXF2B,TMEM135,FUT10,THTPA,MMRN1,GCNT1,ADARB1,ENPP5,PROCR,ACSS3,HTR2A,TSPAN6,DUSP4,HMG20A,RRAS2,MORN4,SRXN1,SPART,TM9SF4,MANSC1,FGFBP3,SERPINA3,TCEAL3,UPP1,ME1,SFXN4,RAB38,AUH,MAGED1,OSBPL1A,TGFB3,TCEAL1,SGCE,PCYT1B,NSFL1C,DTD1,GRB10,ZC3H7B,WDR45,TMEM98,IRAK1BP1,P2RX1,BIVM-ERCC5,BIVM,LIN7C,PFKM,RNF113A,MAMDC2,BEX2,SREBF2,TTC8,PABPC4L,COG6,ARHGEF9,EBPL,COPS4,CASD1,TRIM21,RBMS2,MYOM1,TRPC6,PEX3,SLC18A2,MYO1D,TBL1X,SPIRE1,LRRC1,MFNG,WFDC2,SLC35F2,PPP1R13B,GNG11,PBX3,ZNF711,PRPS1,MLLT3,PON3,STAU1,MFHAS1,RHOBTB1,ALDH1A1,GALC,GJA1,DSEL,IFT52,GABARAPL1,MYOF,EEPD1,RCN2,MSMP,HSPA12B,MORF4L2,ASCC1,TNIP3,EMCN,ARHGAP12,MID2,PDGFD,CPXM1,NMT2,METTL4,CAMKK1,GATAD1,BDH2,OPHN1,ISLR,KCNK5,RRAGB,IL22RA2,PRRG4,FECH,ZC3H14,RBBP7,PSMF1,CAT,PLXDC2,MED23,UBL7,RIC3,PIK3C3,PALLD,ENPP4,EFNB2,RAB12,PDLIM1,HSCB,CA5B,GKAP1,TIMP3,PJA1,ENKUR,ARL4A,INVS,FAM184A,CMAS,JAK1,FADS3,CLDN12,STXBP4,CC2D2A,CDCP1,FSTL1,BICD1,SERINC1,FAM135A,POMT2,GALM,NFIA,BCO2,MTRF1,TOM1L1,PHLDB2,KLF12,PARN,RAI14,RUFY2,NSDHL,CTSF,ARL3,STXBP1,ZNF195,ATAD1,RBM22,ZNF462,GALNT5,GNL3L,FBXO32,CCDC28A,TAF9B,ZMYND11,CTSO,ANPEP,LTB,OR11G2,CA13,PLOD2,ANXA5,PHLDA2,RCOR2,PRKAG2,ETFDH,PRPF8,FZD6,VIPR2,PUS3,C11orf54,PARP12,MYO5C,DOCK1,HLF,GNAI1,HEY1,CA2,LMO2,PDK3,CD99L2,MAT2B,MEIS1,RNF14,ARSK,COX7A2L,NPR2,TMEM60,SLC16A9,E2F5,XRCC5,TIE1,GIMAP6,HMGN3,SDC2,METTL3,LONP2,UBE3C,ANAPC4,PLS3,SLC30A4,ETNK1,PSMD12,ARPP19,AIG1,TNFRSF18,TMEM176A,THUMPD2,ABCC3,TMTC2,PKHD1L1,PRPF6,PRKCH,ELL2,DDX58,ACAT1,PGM2,SYDE1,ATP8A1,C9orf152,EI24,FBXO16,EID2,PREX2,IL7,RBM43,ACYP2,PRDM5,CCDC112,TMEM176B,ENG,PTGS1,STOX1,CCT4,CCL19,GFPT2,TNFSF9,AASDH,TTLL7,POLR2B,BAG2,POT1,ACAT2,NDST2,SIAE,SLC12A2,CTNNAL1,RPL7,TTC23,SQLE,TCEAL6,TBXAS1,LAMA4,PPIC,SLC17A8,DCTN5,PYGM,TOX,TFB1M,LRRC49,RAVER2,PTN,MCOLN2,PIM2,STARD4,NBEA,CTSW,ADIPOR2,UBE3D,ANXA4,PLCB4,SERPINB6,ARHGAP5,SHROOM4,CCL27,C11orf1,EHD2,ZNF827,ZKSCAN5,CLSTN3,ZNF45,HMOX2,SLC36A4,CHIC1,TBRG1,PKIA,ZC3H12B,ALDH18A1,ST6GALNAC3,PTK2,STAU2,KHDRBS3,ALG11,BATF2,H1-0,ARHGEF12,CCDC122,ZMYM6,RBP1,CYP4F8,DPY19L3,ENOX2,FAM110C,STX4,CAV2,PHC1,COPB1,SPA17,PPME1,DNAJB4,SCFD1,CFDP1,ARMCX1,ARRDC4,NET1,PTER,BPGM,EPCAM,ABL1,ABCG2,SLC25A4,DOCK7,SLC48A1,TREML2,PIK3R1,FRMD4B,ZNF248,PLXNC1,RBPMS2,CD81,SCRN1,VEGFC,CAPSL,C12orf29,PHKB,PRCP,TSBP1,BBS12,CCDC60,KBTBD4,CPT1A,SLC16A12,CAPN3,DDX19A,TFPI,GPRC5B,PLAG1,NRAP,PRDM16,ABCA5,TMOD3,PAK1,AFAP1L1,RAB11A,TARS3,TTPA,BATF,TEK,TJP2,APOOL,PCCB,CA8,CHCHD7,PJA2,SERHL2,HLA-E,RHOBTB3,TCF12,ERCC5,RIPK2,MPDZ,FMNL2,CLIC4,ITGB6,COPZ2,N4BP2L2,MMP16,ROBO4,VPS39,RABEPK,ZFP37,ZMYM4,CTNNA1,ADAM10,PPA1,NCKAP1,PAIP1,PAFAH1B2,STK39,VSIG2,DPF2,PLEKHA8,ESAM,ZNF420,RAPGEF4,SERPINF1,CHURC1-FNTB,FNTB,GHR,DDX50,CROT,FSCN1,LHCGR,VWA5A,TRPC4AP,SGMS1,GNPDA2,DNAJC16,ZRSR2,RANBP17,CYP7B1,GPX8,AH

	I1,MRAS,RORA,PSTK,DECR1,HSD17B10,SPRED2,EID1,SOCS2,CRISPLD1,MAOA,NIPAL2,KIAA2012,GALNT6,GIMAP1-GIMAP5,FADS1,OR5B21,SLC25A3,FPGT,C6orf141,RELL2,GCNT2,AP3B1,TMEM40,ZNF32,ASPA,CHST14,GBP5,IFI44,TMEM140,MAP3K12,LYPLAL1,SLC24A5,AKT3,PAM,MARVELD2,MAPRE3,MAPK9,LPIN1,WDR47,HOXA5,ZNF551,PDXDC1,MMP23B,FNBP1L,SAMD12,CRYZ,RAB13,GOLPH3L,DNAJC7,TXNIP,APLP2,PRKCQ,GATA3,CTNND1,GFPT1,CLN6,ACSL3,KDM3A,FN3K,KPTN,PLA2G4A,ART4,CSGALNACT1,LAMC1,ALDOC,EFR3A,EEF2,DST,GBP2,SLC27A6,ZNF410,FAM114A2,GRIK5,ERP27,KIT,GSTM3,VWF,ZNF286A,ZNF286A-TBC1D26,TMEM67,UBE2O,ADAMTS6,USP54,CYP51A1,DYNC2LI1,POR,SELP,ACADM,XRCC4,ZNF700,ZNF878,ACVR1,TMEM218,IFIH1,RAD9B,IFT81,RWDD3,LGALS8,NTMT2,STX12,MITD1,CUL1,IK,RNF139,RARB,ADAM22,SNX25,METTL7A,GORAB,MUC13,FKBP7,ISG20,NICN1,ACP6,PPT1,FADS2,ARL15,MYNN,SBF2,NSG1,MYCT1,GNAT2,CLIP3,AS3MT,NEDD4,FKBP9,TXNRD3,TJP1,STAT4,ADSS2,OBSL1,GLUL,ZNF34,KIF3A,GNS,ARHGEF5,ECHDC1,S1PR1,TTC21B,PRDX6,OR8D1,AIDA,RBAK,ZNF429,SUCLG2,SLC3A2,FBXO21,GTF2I,PTGER3,ZDHHC17,TAF1B,PLSCR1,CFL2,PRKACB,IRF6,PLK2,EXOC6B,GBP6,DAND5,EIF5A2,AHCYL1,MBTPS1,RHOF,IRAK3,TOM1L2,GHITM,ALDH1L1,OAS1,SOX6,PAIP2,ELMO3,SORBS1,CASP12,HSBP1,CCDC62,GIMAP5,PDCD6,AHCYL2,IFT172,ZIK1,PLSCR4,MYH10,C4orf47,F2R,SEMA4B,SLC41A1,CEBPZ,ABI2,KLHL6,TNFSF4,CYP4V2,ZC3H8,EHBP1,GRAMD1C,MTMR11,LRP12,ZSCAN18,TMEM59,MINK1,CADPS2,TRIM47,DHX58,BBS4,HACL1,RGS18,SESN1,GNB5,CPNE2,NOMO3,NOMO2,NOMO1,ZNF667,ETV3,TBC1D17,GULP1,ZNF487,ZNF778,CAPRIN2,IFT122,APOE,RCOR3,RSAD2,PBX1,SRR,FAM171B,NT5C3A,CCND1,DNAJC18,ARHGAP29,CYP2J2,IGF2BP2,MBOAT2,DUSP16,STX6,TSPAN4,FAM110B,MAP4K3,GSTM4,IQCB1,RBL2,GIMAP8,ZNF345,DEF8,KIF21A,ZNF512,ST14,ZNF239,IRGM,LDHB,TMEM38A,VEZF1,SMYD3,RCN3,EPHX1,ZNF121,TDRKH,VPS45,MYLK,RYK,CCDC91,DLG2,ISOC1,ZBTB38,SLC25A20,VDR,SLAMF1,WDR5B,CREBL2,FZD3,F11R,AKAP7,DYRK3,JAM3,FAP,ETV5,TMBIM1,MPL,ACOX1,CISH,EXTL3,PTPN14,F2RL3,SLC6A15,FBXO25,ITGA6,BCS1L,ZNF317,GTPBP8,C5orf63,NUPR1,LRRC66,HDAC1,PPP2R2B,TGFBR3,KRT18,CDC42BPA,LMBR1,HDAC9,ACY3,SIRT2,PLEKHA5,RNF208,LIX1L,SRGAP3,PKP4,KLHDC1,SORD,IFT20,LAT,RASGEF1B,DCTN4,DENND2D
Giladi_2018_StemScore	CD274,GABARAPL1,MLLT3,WFDC2,ZFAND5,OSBPL1A,TNIP3,DAPP1,ZNF831,PROCR,BGN,C11orf54,GIMAP6,LMO2,STXBP4,GIMAP1,TBXAS1,PTPRCAP,RBP1,SRGN,CA2,HLF,HLA-E,UBE2L6,MYL10,PTPN18,TMEM176A,TMEM176B,CD81,PNRC1,LHCGR,BASP1,DKKL1,RTP4,ALDOC,TXNIP,PDE4B,MYCT1,HOXB2,ACOT1,ACOT2,CISH,KRT18,SHISA5,PDZK1IP1,GCNT2,CLIP3,RGS1,PCP4L1,LDHB,CD27,MECOM,NFE2,MPL,CD74
Wilson_2015_MolO	SOX18,UBL3,NEO1,PROCR,MLLT3,CLDN10,LTB,NEIL2,CD82,FADS3,GIMAP6,GIMAP1,CTSF,PDE1B,FGFR3,METTL7A,TRIM47,SMTNL1,PTPN14,RAMP2,VWF,PDZK1IP1,LIMD2,CDKN1C,GSTM1
Wilson_2015_SuMO	NDNF,PROCR,MLLT3,WFDC2,MAPK12,INHBA,RALGAPA1,LY6E,ST8SIA4,GBP6,RAMP2,CD74,CYP27A1,ABLIM1

Lauridsen_2018_RAdim_HSC	MT-CO1,CBX7,ITSN1,PIK3IP1,LGALS1,RNF125,CYTH4,LBP,TSC22D1,SLC35C2,PCMTD2,LRRN4,SMAD7,APH1B,TEF,SAMHD1,ISLR,TECPR1,FGD2,POLI,UBL7,UNC93B1,MBOAT4,MLLT3,COL4A2,RPL35,DLGAP4,UBL3,GBA2,AHNAK,RPS3A,BDH2,CCL4,CCL4L2,GABARAPL1,MYOF,IL2RG,SMPDL3A,B4GALT6,PIM1,SEMA7A,SASH3,PSME1,ARMC3,PPCDC,FAM53B,PLCB2,CASD1,GAS6,FAU,MAMDC2,VAT1,PTGES,PNPLA7,TCF7L2,PROCR,S1PR4,SH3BP1,UPP1,SOX4,ITGB7,POLD4,CCND2,GABBR1,HLF,PKP3,DDX31,COX7A2L,NPR2,E2F5,GIMAP6,TIE1,ODF3B,SPI1,PAFAH2,CD37,ENO2,LTB,ZFP1,P2RX7,ANXA6,CHRNB1,AGPAT2,CTSF,CYP4F8,DYNC1H1,IFIT1B,GIMAP1,HDAC11,MRPL23,FLOT1,STXBP4,EEF1A1,LST1,CSF2RB,ERMARD,TCP11L2,PRTN3,SEMA4G,PIM2,MCFD2,KLC4,PTK2B,RPS7,PRDX5,PSTPIP1,CCDC88B,TBC1D10C,DCXR,ATP6V1D,HOXB6,TMEM176B,TSPYL2,TLE2,HBP1,NDN,RPS16,PTPRE,TMEM176A,YPEL3,FTL,ZNF618,TMEM63B,DENND1C,PARP14,TNFSF12,TRAV12-1,TRAV12-2,TRAV12-3,GUCA1A,MAPK1IP1L,SERPINB6,HK3,ZNF467,ERGIC3,XAF1,PTPRCAP,RABAC1,ST3GAL1,DUSP2,ATP6V1G2-DDX39B,ABCG2,CNRIP1,ECSCR,SYTL1,RPGRIP1,LDLRAP1,CD82,KAZALD1,SNN,EID1,PVR,SIDT2,GALNT6,GPRASP1,GIMAP1-GIMAP5,IL18,LAT2,FIS1,LAPTM5,LSP1,PTK7,PDE1B,PNRC1,DUSP5,DKKL1,NEURL3,ROBO4,PADI4,HLA-E,PTGER1,TMEM132A,ARID4A,B4GALNT4,TMUB1,RPL18A,ENTPD1,PCCB,SRSF12,RHBDF1,CLCF1,RASGEF1A,FMNL2,EVA1B,GAPDH,SNX20,LFNG,ARHGDIB,HYI,CAMK1,APLP2,EBI3,KDM6B,MVP,GSTM2,PDLIM2,CA11,ART4,ANKRD13D,GBP6,C1RL,PRRG2,LPIN1,HOXA9,AIM2,SH3BGRL3,LENG8,LYL1,CLIP1,DNAH1,COPG1,TINAGL1,IFI44,CLEC2D,SGIP1,GRAMD1B,TXNDC15,IL16,TOM1L2,PBXIP1,GBP4,VAMP2,POU2F2,RNF25,CLIP3,MAP3K14,IKBKE,ORAI1,ITPKB,RPS23,RPL27A,PARP3,METTL7A,C1orf109,HOXA7,CTSS,WDR83,TSPAN4,RPS14,CD27,ACER2,HID1,RPS27,LAX1,CTSH,DOK3,LDHB,IRGM,RPL28,RAMP1,SGPL1,CYP2J2,RPL19,TMEM53,TNFAIP8L2,TRIM47,RPS15,TBC1D17,SESN1,ELMO3,RGL1,CHD3,BCL9L,GIMAP5,ACAP1,TBKBP1,SDSL,LIMD2,RNASEL,ARID5A,CARNS1,OAS1,CLN3,CD74,P2RX4,TMEM37,ARID3B,ZBTB4,PDZK1IP1,SFT2D2,SHISA5,RAP1GAP,TCF25,MIB2,ZBTB20,LTBP3,EFCC1,UBA7,ADCY7,SLC50A1,TNS1,RAB6B,LTBR,SLFN12,SLFN12L,PSD4,NAPSA,DDIT3,ACOT1,ACOT2,VAMP1,MYLK,CUEDC1,MPND,USE1,GSTM1,SLFN13,MECOM
Cabezas_Wallscheid_2017_sc_dHSC	TMSB4Y,PI4KA,RPL3,RPS4X,PAN3,SON,RBM25,YWHAB,RPS21,ARGLU1,RPL39,TPT1,RPS29,ITM2B,RPL23,PIM1,SOD1,NT5DC1,COX14,SRSF3,RPL12,H3-5,RPS24,OGT,AP2B1,FTH1,HSP90AB1,FAU,RBM39,ALOX5AP,PABPC4L,MADD,RPS3A,ENTPD7,SERINC3,RPL35,MRPL50,PRPS1,DDTL,ZNF318,RPL36A,PPP2R2A,PSAT1,HSPA8,HNRNPA2B1,UBE2B,MYH9,BCL11A,EID1,FCHO2,INSIG1,NBR1,GM2A,RPS3,RPS5,TSC22D3,FTL,ARL6IP1,RPS19,TRAPPC1,RPL30,HLA-E,NOP14,EED,LSM2,RPL7,VMP1,OAZ1,SERPINB1,PTPN18,RPS7,UQCRHL,UQCRH,ZNF706,TMEM176B,EMB,STT3B,GMPS,CCND2,PTRH2,CA2,HLF,EEF1A1,UBAP2,JAK1,RPL37,FLI1,RPL10A,RPL37A,ACTB,RPL34,GIMAP1-GIMAP5,RPL18A,EML4,RPL31,YWHAZ,RPL27,RPL22,DDX18,ANKLE2,RPGRIP1,TMEM30A,RPLP1,SRGN,TIMM10,BLOC1S6,CBX1,PABPC3,WTAP,SEC24C,RPS16,ARID1B,SMARCC1,SPTAN1,DDX17,TNFAIP8,DDT,TUBB,CD37,C8orf33,LMO2,LY6E,WDR76,COX6A1,SCMH1,NFIA,RHEB,CBX3,RPL14,MBIP,SENP1,RPS15,PDCD4,PET100,CLK1,YIF1B,PRRC2C,PRPF31,HNRNPA1,CDKN1B,CALM2,PCBP1,FUBP1,RPS11,CUL3,KMT2C,CAB39,GSTM1,RPL35A,NDUFA3,RPL23A,PDZK1IP1,TAGLN2,IQGAP1,KHSRP,PTGES3,OPA1,B2M,RSRP1,SYCE2,EIF1,RNF144A,EEF2,TXNIP,PTP4A2,DNAJC10,ICAM2,RPS23,RPL27A,RPL29,ADGRG1,RPL26,RPL6,

	RPS2,ARPC2,MSI2,ZNF207,RPL13,RPS9,RGS18,CWF19L2,RPL19,GIMAP5,SLC35A1,RPS8,GNB1,RPS26,RPS14,FARSA,RPS27,RPL28,RPS6,RPS25,PTP4A3,RPL4,CS,TMA7,TRA2B,WWP2,ISOC1,CD47,GPX1,UBA52,RPL8,SPAG9,RPS28,H3-3B,HNRNPH1,CELF2,RPL18,SETSIP,GIGYF2,UBA7,MPP7,ZBTB20,SSR3,TLCD1,PTPRC,PABPC1,CNOT8,SNRNP48,RPL24,RPL32,ACTR2,DDX5,RPS20,HNRNPL,RPL15,RPSAP58,RPSA,CLN6,RAP2B,DNAJC19,SMIM20,UBB,ARHGAP17,RPS13,LRRC58,SNX27,NOTCH2,RBM15,RPL38,ANGPT1,ABCC5,CLASP2,DTX3L
Cabezas_Wallscheid_2017_bulk_dHSC	CYTH4,JAM2,PPARGC1A,PPP1R16B,SPATA13,ACAA2,RBBP9,CYBB,PHYH,BTBD3,PRPF39,IMPACT,SIRPG,ANKRD12,TGM2,PAN3,PELI2,VPREB3,IL13RA1,SDC4,ITSN1,NOVA1,USPL1,EYA2,BRWD1,NRK,CLCN5,CCDC171,SPRY2,DDHD1,USP27X,RBM47,JAG1,TSC22D1,MN1,SYN3,LBP,IRF9,KLRD1,CBX6,CYB5A,ATP8B4,YAP1,TRPM5,ARGLU1,PNP,PNCK,PROCR,TULP3,CD2AP,SPON1,TGFBR1,CCL23,CCL15,CCL15-CCL14,NRP1,MS4A3,GLIPR2,RAB44,TXNDC17,B4GALT6,BGN,ATP6V1B2,IL2RG,PDE2A,LGR4,GATAD1,GYPE,GYPB,GYPA,TNIP3,TCN2,RAC2,SLC44A1,ALKBH5,MTURN,CLEC7A,ARAF,AP1S2,MEDAG,TUBB6,ZNF831,CD24,UPB1,DPH7,CREB3,GLCCI1,EFNB2,NIPA1,ZNFX1,UBL7,TNFRSF19,PYGL,ISCA1,RIN2,GCHFR,TSPAN14,TECPR1,CAMK2B,NPC2,ISLR,SAMHD1,EXPH5,TRAF1,SRXN1,PPM1H,PRNP,PORCN,IL15,ROR2,ENPP5,PNPLA7,TAX1BP3,GPR183,GRIA3,RNF167,NR6A1,MAPK12,ANXA1,SIRPB1,SIRPA,SASH3,CCSER2,SFRP2,BACH2,SGSM1,SMPDL3A,MARCKS,SLPI,IRF2,CHMP5,LCN2,TCEAL1,TBC1D20,ZCCHC18,CPNE8,MAGED1,OSBPL1A,RPS3A,ELAC1,APOBEC1,PLD4,AHNAK,MYOF,NACC2,CD83,CCL4,CCL4L2,ERG,MFHAS1,MLLT3,TMEM154,HDAC10,TLR4,CCNT1,MFNG,ZNF318,PML,LZTS1,RENBP,DCAF11,ZNF287,MMP9,PLXDC2,TRIB3,MGST1,PKIB,KAT6B,MPEG1,LGALS3,AGPAT4,PLAG1,TULP4,PAK1,ATG10,MAP3K1,PHPT1,RNF216,FRMD4B,HK3,QPRT,MARF1,SMIM24,PHKB,PLIN3,BST1,RAB11FIP3,CD200R1,CSF2RB,ZHX2,BTG1,RUNX1T1,TRIM6-TRIM34,TRIM34,XDH,SLC31A2,HIVEP3,RPGRIP1,CD82,KAZALD1,SOCS2,FAM118B,C6orf47,IGF1,GIMAP1-GIMAP5,KIAA2012,PHF8,ZCCHC12,GPRASP2,ITGA9,DUSP5,TRIB1,NEIL1,ADD2,PGLYRP1,MMP16,TPM4,FGFR3,ARID4A,NHSL2,HLA-E,AGO4,LPXN,CLCF1,SQSTM1,ZFP82,TRPS1,IRF7,CLDN5,ZC2HC1A,CCNDBP1,RHBDF1,MATN4,WASF1,NPR2,COX7A2L,GIMAP6,CEBPE,ANXA5,HBA2,HBA1,SCAPER,TNFAIP8,DUS2,ARL6IP5,NDRG2,MAP3K5,CTSF,DDX60,CYP4F8,MPO,RABEP2,DPM2,LST1,ZC3H12D,NFIA,GALM,TIFA,NBEA,FBXO44,EBF1,RNF214,RELB,EHD2,MS4A4A,CATSPERG,KLC4,WTAP,ZEB1,ATP1A3,IGF1R,TBXAS1,MCOLN2,CYBA,ZCCHC7,ST7,HBP1,C9orf131,SLC22A18,HSPA2,ARHGAP26,DMTF1,FOXO3,TSPAN31,CNBD2,OSGIN1,C9orf152,ZCCHC10,PARP14,FTL,TSC22D3,IFNGR1,DENND1C,OSBPL5,UGCG,GALNT7,PIK3R1,LY6D,PDE7A,RAB3IL1,NOTCH1,IL4,ECSCR,IGSF6,NET1,DUSP2,KLF2,DSE,TULP1,ALCAM,DTX4,CPM,FAM107B,IRF8,LILRB4,FCHO2,SLC31A1,ETS1,SARAF,NIPBL,TMEM141,LSP1,ZNF354C,CD302,PRUNE2,FSCN1,ZMAT1,FIS1,SGMS1,CLMP,RORA,HSD17B10,SNX18,ARID5B,TRIP4,SERPINB9

	,DKKL1,ZFP36,FAM102A,F13A1,GM2A,ALDOA,B4GALNT4,ABHD2,CYTIP,ST8SIA4,GINM1,PTAFR,NR1D1,CPQ,INSIG1,PROM2,PTPRU,HLF,USB1,SORL1,RBM18,IP6K1,ENO2,LTB,EMB,XBP1,RFX3,TCF7,IFITM1,ANXA6,PLA2G15,SLC26A11,IGF2R,ACTB,ELANE,ACSL1,LETM2,MAP4K2,HDC,CTSG,TNFAIP1,EEF1A1,PLAC8,TCP11L2,ARHGEF26,MICB,MAF,FMC1-LUC7L2,LUC7L2,GZMA,SNRPN,SLC25A36,RPL7,PYGM,TOX,CDC26,MTM1,TMEM176B,SAT1,CD79A,PGLYRP2,GFPT2,NDN,TMEM176A,ELL2,CTNS,NUDT12,PTPRC,CCRL2,ABCG4,PRRG2,PAQR7,LY86,APBB1,CD2,ZNF780A,C6orf141,TAF7,VAMP4,MS4A4E,POU6F1,ID2,TINAGL1,NCEH1,PFKFB2,HOXB3,SLC25A44,FOXP1,SCPEP1,LURAP1,SIGLEC6,CD33,TP53INP1,SH2D2A,ARHGDIB,FABP4,LIMA1,FN3K,GATA3,CCR2,IRF1,GPR171,POU2F1,PECAM1,CLIP3,AFF1,ELMOD3,M1AP,EFNA1,FCER1G,ARHGAP17,LYST,CTSS,NOTCH2,CDC42SE2,SP140,ABLIM1,IVD,AGTRAP,C1orf116,CSAD,CHST2,PLK2,GBP6,EXOC6B,GLUL,CCNL2,CD209,TNIP1,PIK3CD,CD84,UBE2F-SCLY,UBE2F,MED11,SESN1,PRKCB,TRIM41,TRIM52,MCEMP1,SHROOM1,SPARC,BAZ2B,GIMAP5,SYNE1,RGL1,BLNK,TRIM65,ARID5A,TRIM5,SMAP2,MPZL1,HID1,AMZ2,IDH1,LDHB,SLC4A3,OTUB1,ABHD14B,RBL2,CYB561A3,S100A6,SMURF2,ACBD4,CYP26B1,BIN3,KMT2D,PCBD1,INPP4A,RRM2B,FCRLA,TPP1,SH3BP5,AKAP7,TNS1,BLK,CREBL2,EPS8L2,MYADM,PTPN14,PID1,CERS4,VPS45,ERLEC1,ECI2,SELL,TMC4,TMEM50A,ROCK2,SLFN13,MECOM,SSH3,KLRC1,MEIS3,TIFAB,CLN3,CLEC12A,TRAF3IP3,CHIA,ZBTB20,HHAT,ACOT1,ACOT2,BLZF1,UBA7,CD200R1L,PAM,C1RL,SLC39A1,PARD3B,SFMBT2,ELK4,LPIN1,TBC1D8,HOXB5,IFI44,EZH1,SATB1,B2M,ALAS1,GSTM3,CD1D,MROH1,POR,KDM5B,CCR1,NAV2,CAMK2N1,EBI3,TXNIP,EEF2,ART4,KDM6B,C16orf72,PGPEP1,IFITM3,IFITM2,RNF39,FYCO1,GBA,GFI1,IKZF2,SLFN5,MDH1,IKBKE,CD52,ICAM1,PRKAA2,PSAP,VIPAS39,METTL7A,R3HDM1,FCGRT,MXD1,NPEPPS,GPRC5C,MICA,TBCE,ZSCAN26,ABHD14A,DOK1,DPH5,IL16,NADK2,MS4A6A,MS4A6E,MILR1,XRN1,RIT1,LONRF2,HPR,HP,BTD,MZB1,SMTNL1,LPP,DOCK10,NCF1,BOC,GPR35,UTRN,CSF1R,ATP1B1,PPOX,DNHD1,COL1A1,GPX3,KIF1B,LY9,FGD4,HGFAC,CTSB,RIC1,LILRA6,LILRB5,LILRB3,LILRA5,LILRA4,TAF8,DPP4,SEMA4A,SELENBP1,CTSH,GIMAP8,COPZ1,CD247,CREBRF,HSD11B1,CD7,PDE8B,CTSE,STAMBP,KMT2A,CYP2J2,CDKN1B,SLC50A1,GPN1,LCK,GPR141,KCND3,CISH,CIRBP,CD53,SLFN12,SLFN12L,OBSCN,ZNF121,MXRA8,EPHX1,ZNF329,USE1,VDR,GSTM1,PIK3R6,TYROBP,CCPG1,EVI2A,NCF2,ZBTB4,PDZK1IP1,SHISA5,STAT2,TNFRSF1A,COL8A2,ACE,TMEM161B,SLC66A3,BIRC6,MB21D2,NOTCH3,ZNF23,IQGAP1,ICA1L
Platelet_bias_lineageTraced_HSC	HLA-DRB6,HLA-DQB2,PTGR1,ENO1,PAX8-AS1,TMEM230,STK3,LOC729218,ANKRD34A,CLEC3B,SOCS2,TTPAL,NFE2L2,HLA-A,GPC5,LOC100132215,XYLT2,SCHIP1,RPL19P12,LAPTM4A,LIMCH1,PA2G4P4,ALKBH2,STAP1,CD74,USP53,SCN9A,HLA-F,TM4SF1,FAM45A,HLF,LYRM9,MLLT3,SELM,ANXA5,ACTG1P20,RAB29,LOC653653,EIF2S3,CXorf40B,GUCY1A3,TMEM182,RSU1,APBB2,HLA-DQA2,BEX1,HSPH1,APOL3,METTL12,LOC101929295,AES,AP2B1,CDC37,HNMT,TSC22D3,HEIH,ERMP1,CHRAC1,DDX10,HLA-DRA,ENOPH1,HSP90B2P

Multilineage_lineageTraced_HSC	GSTM1,CRYBB2,H3F3C,FBLN2,WTH3DI,SKP1P2,GATM,CTSG,CSMD3,PRSS57,LINC00987,GSTM2P1,BCAN,MIR3654,PABPC3,MIR4426,SPATA22,POLR2J2,HNRNPA1L2,LOC101928663,SNHG10,RPS26,SLC25A37,LOC100507642,FTH1P3,ZCCHC11,CYP4V2,UBE2E4P,MTRNR2L2,LILRA1,MMP8,DNMT3A,RNVU1-8,MIR6723,MAZ,HERC2P10,LOC440311,ATP5EP2,INTS6-AS1,ZNF98,ZDHHC11,MYCBP,SCML1,NBPF15,AUTS2,NACA2,FLJ44635,EIF5AL1,SNORD57,WDR72,GSTM5,PYROXD2,CBWD5,SNORA84,ALMS1,NPIPB11,AKR1C1,FAM26F,NCK2,SLC7A5P2,ACTG2,LOC100129216,GBP7,CSNK1A1P1,APOBEC3A,TNRC6B,DERA,YBX3P1,PIPSL
Pang_2011_elderlyHSC	ANXA3,SELP,MICAL3,PTGS1,F2RL1,USP46,CCDC88A,FUT1,HOXA9,AURKA,MYC,FOS
Montecino-Rodriguez_2019_My_biased_mHSC	IL17RA,SH3KBP1,RGS19,CHAF1B,UPF3B,SOX4,RUNX2,STK38,NONO,TNS3,SNX5,DNAH8,FLNA,MSL1,SYK,FLT3,ARRDC1,CLIP2,PLCG1,POLG,SRRT,BTK,DGKZ,GMFG,DTX3,ANTXR2,ARID4A,RINL,ARHGEF1,ITPR2,HLA-E,NDRG1,HNRNPAB,PBX4,SYMPK,CD37,MPRIP,BMP2K,RASAL3,CMTM7,MYC,FNBP4,BOP1,PPP6R1,ADAMTS10,SUPT20H,PLEK,PUM3,PHF14,USP1,VIM,MUC13,ITGA4,ZNF608,ARHGEF18,BDP1,TAP2,IQGAP2,ZC3H18,PTPN7,GRAMD1B,WDR46,RUNX3,IFFO1,RGS2,HOXA9,CCDC125,CD1D,GPS2,ESYT1,GRAMD1A,TET3,MAST3,SPNS2,EEF2K,APOBR,ANKRD13A,ACAP1,ARHGAP30,SOX6,PPOX,CD34,RGS1,DOCK10,GRK2,FCHO1,KCNAB2,MLEC,RAMP1,IRF2BP2,BAG6,ITGA2B,CD27,CCNT2
Montecino-Rodriguez_2019_Ly_biased_mHSC	CDC42BPB,SOGA1,EVC2,TRPC6,CLU,MYOM1,MMRN1,CLEC1A,MLLT3,MYOF,RLIM,LRBA,SNAP23,GDA,SGMS1,ITGB3,ARHGAP31,GPRASP1,STT3A,NCKAP1,ITGB1,ST3GAL1,NET1,MAP9,HACD4,PLCL1,CCDC136,CCND2,DOCK1,CLTC,FLI1,TNS2,PLXNC1,CALCRL,CTNNAL1,NBEA,ATP8A1,FGD5,LNPEP,CHD7,TNKS1BP1,ANKRD17,AMPD3,AMOTL2,ITGA6,EPB41,DLG2,PBX1,EXOC6B,PLK2,SBF2,VWF,APLP2,RPN1,CISH,SLAMF1,LPP,NADK2,MED12L,ECE1,PTPRJ,UNC13B,ART4,FNBP1L
Belluschi_2018_My/Ery_biased_CD49f+HSCs	RP11-676M6.1,HLA-DRB1,RP11-264I13.2,CXCR4,HSP90AB1,GABPB1,HLA-E,AC097523.3,RP11-43D4.2,U2,SNX9,SKI,RP11-325P15.1,RNVU1-19,FTH1P23,RNU12,WDR45B,RANBP2,FTH1P2,RGPD5,EIF5,NFKBIA,DDX6,DNAJB1,SBDS,ETF1,EIF1P3,NFIA,FOSL2,SNORD3A,PHTF1,RPS26P3,AC007319.1,RNU5F-1,ZFP36L2,HSP90AA2P,RNVU1-15,FXYD5,MYH9,CSNK1D,FOSB,RP11-144L1.8,NKTR,MECOM,HIF1AP1,HLA-DRB5,NFIB,PTPRC,CD74,RPS3AP26,RP11-386I14.4,OSER1,RP3-323K23.3,TSPYL1,PABPC1P3,RBM39,FTLP3,RNU2-38P,HIF1A,PELI1,YTHDC1,DUSP1,ANKRD28,ELF1,FTL,YWHAZ,RNF144B,TP53INP1,JUND,MTRNR2L1,LAPTM4A,PPP2R5C,UBC,GRASP,NAMPT,MEIS1,EIF1,RPS27,DDX5,NAMPTP1,TSC22D3,RPS4XP22,TXNIP,NEAT1,CTD-3014M21.1,HSPA1A,FTH1P8,JUN,HSPA1B,SMCHD1,MALAT1,HSP90AA1,PPP1CB,FTH1,MLLT3,SRGN
Belluschi_2018_My/Ly_biased_CD49f+HSCs	B9D2,PRSS2,C3orf17,TFDP1,MT-CO3,KIAA0125,CASK,MIR4435-2HG,MT-CO1,MT-RNR1,HCST,RPLP1,PURA,RBMXL1,CDK6,TRBV25-1,DYNLL1P1,RPLP0P6,AC016739.2,CALM2,NDUFAB1,RPL6P27,JCHAIN,GART,MT-TT,RP5-857K21.11,ATP5A1P2,CALM2P2,RPLP0P2,RPL6P21,RPL6,HAUS6,MT-CO2,ATP5E,RPLP0

Anjos-Afonso_2022 EPCR+ HSC	EFEMP1,TGM2,SULF1,NAPSB,PID1,MGP,HMOX1,HK3,IL1RN,HDC,CPE,LILRB4,ARHGEF10L,Lnc-SGSH-1,CD300E,VCAN,SASH1,SERPINA1,C5AR1,ITGB3,COL4A1,MAFB,CD36,SEMA6B,CD1D,TJP1,HCAR2,MPO,THBS1,MPEG1,SLC15A3,CCN2,PHOSPHO1,MYOF,PPBP,CD300LB,CCR1,MTMR11,CRISPLD2,LOC107984360,CXCL16,PADI2,IFI30,SHE,ACVRL1,CDH5,KCNQ2,SLC26A11,SPTB,LYZ,FCGR2C,TBC1D30,CSF1R,TBC1D9,P2RY2,STX1A,COL4A2,CDA,CEBPD,F5,CDH4,FN1,ABI3BP,SEMA3F,GLI2,FGD2,CD226,LRRC32,CD68,ALOX5,PTPRJ,RAB20,NCF1,VDR,GP9,VWF,RTN1,ARHGAP24,ERC2,AQP1,THBD,CLEC7A,HCK,KIAA0513,SPAG17,IGF2,SLC24A4,RBFOX1P,IRF4,SPTBN5,NR3C2,CCND1,HPSE,LRP1,SLC7A7,COL9A3,SULF2,SLC24A3,LRRK2,FLT4,NCF2,EMP2,CUEDC1,PLVAP,KIAA1671,AHRR,LYNX1,HRNR,ABI3,LTBP2,AIRE,SLC11A1,CFD,lnc-IGLL1-1,LONRF3,SORBS2,SYT15,NIBAN3,TYMP,SAMD11,NOD2,PROCR,H19,SIGLEC14,CLEC3B,ADM,NFIB,ARAP3,UPP1,NAMPTP1,CLMN,TIMP2-AS,PLAUR,ITGAM,SIRPB2,LGALSL,ID3,SOX8,SAMHD1,STAB1,SECTM1,GPC5,ARFGEF3,CELSR1,VEGFA,BCL2L11,CLEC14A,IL13RA1,CRB2,ENSG00000268903,ITGAX,SSTR1,F12,FGFR3,TUBB1,HES1,ENSG00000281741,RNF39,KCNJ2-AS1,FAM20C,LINC00877,MRPL37P1,ID1,CTSH,GPBAR1,C1orf115,GAS6,EPAS1,DMPK,UBE2QL1,FGL2,DMWD,LRP3,FBN2,Lnc-FAM78A-1,PDGFA,NFAM1,PDE10A,KAZALD1,HYDIN2P,NCKAP1,COLQ,IL21R,Lnc-RIOK1-2,HRH2,EHD4,FAM198B-AS1,CPVL,VIPR1,LILRB2,OR2A9P,Lnc-GATA5-9,RPS2P53,NAMPT,TNFRSF12A,Lnc-CYS1-1,BTBD19,PELI1,GASK1B,NCR3LG1,SLC2A3,RASAL2,CCDC149,Lnc-HOXB4-1,KCTD12,CD4,LAMB1,CR1,TNFRSF1B,SRGAP1,ECE1,KBTBD8,RBMS1P1,ALOX15B,NR4A2,VWA7,JAG1,TLE1,KIF1C,MIR22HG,CAMSAP2,MYO1E,EPPK1,ANXA2,PLK3,S100A11,CNTNAP1,PTGS1,TMEM8B,TGFBR3,SPEG,Lnc-PARVG-5,HLA-L,MIR29B2CHG,IGF2BP2P,MYL9,TAMALIN,PCLO,NRIP3,PRDX3P1,NRGN,GPRC5C,PHLDB1,ANK3,DDN,CEROX1,CNKSR3,MAN1C1,DOK2,PRKCD,ITGB2-AS1,ENSG00000278918,PEG3,ZFPM2,ZNF423,TTC34,ZNF331,SH2B3,MRS2P2,IER3,IRAG1,DLGAP2,ACE,HLA-DMB,LINC01122,ADA2,ZC3H12A,EMCN,IQCA1,CST3,CHD7,PLB1,PER3,TCOF1,PLEC,SNED1,SYNE2,ENSG00000234290,MYORG,SSPOP,FYB1,MIDN,SDCBP2-AS1,KCTD7,PIK3R5,NPIPA9P,AHNAK2,ACOT11,SIRPA,SENCR,PITPNM1,PARD3B,LIMCH1,TUBA4A,APOBR,NBEAL2,CPED1,RELT,MCC,FOSL2,COL9A2,NAV1,CDC42BPB,CDC25B,Lnc-OR4F29-3,STARD4,ARRDC2,ETV3,ZNF467,KCNC4,ENSG00000280138,LINC00963,IGF2BP2-AS1,TTC28,MFAP4,NIBAN2,NR4A3,MPIG6B,CRYBG3,TNFAIP2,MTSS1,NOTCH4,IL6R,TREML2,CASZ1,MCF2L,EHBP1L1,KLHL3,CCDC85C,EPN2,ABCA13,PER2,FXYD6,MAST3,DENND3,ITPRIP,CAMK2D,PER1,TUBB4B,TOB1,ARHGEF12,SYNE3,NDEL1,PIK3C2B,HLF,Lnc-TTC21A-76,Lnc-ANKRD36B-3,ACAP3,KSR1,RNF213,BTBD6,TCIRG1,PSTPIP1,ZFHX3,LMTK2,ARHGEF40,PREX2,TIE1,SORT1,AMPD2,ARID3B,TBKBP1,C15orf39,CCDC88B,BIN3,WDR1,ARHGAP31,FOXO1,ARMCX4,RASSF2,CCNL1,HOXB3,GABBR1,MECOM,FOXP4,TACC1,PLEKHO2,NLRP1,CBX6,RANBP2

Anjos-Afonso_2022 EPCR- HSC	RPS2,RPL5,STT3B,RPL37A,ESYT2,APEX1,RPL18A,RPS6,MDH1,VRK1,CPSF3,TOP2B,SEC11A,CDIPT,MYB,CCNB1IP1,SNRPD1,SLC4A1AP,RPS13,PELI2,MTIF2,SMO,EEF1B2,PPIH,COX7C,CALM2,RPL31,PTPRCAP,RPS29,RPS5,VPS72,HSBP1,RPL29,RPL36A,MRPL45,IFI16,RPL39,ENSG00000223509,RPS3A,RPL37,NKAPD1,DRAM2,LDHB,MZT2B,DOK1,RPS17,ATP5MF,MATK,SCARNA9,GAS5,GUCY1B1,PRKACB,TAF1D,RPS21,IMPA1,RPL18AP3,RPS7,ABRACL,ZNF277,TESPA1,NOSIP,RFC2,RN7SK,WASF1,RBMX2,SNRPE,POLR2G,PCYT1B,KIAA1586,PSMA6,AP4M1,FH,CD244,ABRAXAS1,CKS2,H4C9,CIAO2A,CDK6,GPX7,ARMH1,ZSCAN2,ZNF521,LAT2,TAP1,ITM2A,RPL9P8,F2R,ZAP70,ZBTB41,C12orf76,H2AC11,SLC4A7,ACADM,MRFAP1L1,SERPINB1,MRPS31,RNF130,FRG1CP,TSEN54,ITGA9,ING4,ZNF555,H4C14,SNORA73B,Lnc-GAPDH-2,TADA2A,SLAIN1,CSTF3,PTPRD,SNORA73A,METTL5,TBC1D31,TRBC2,TTC4,SNORD17,H3C7,SMIM24,RAB33A,QPRT,FAM117A,SDHAF1,CARD8-AS1,ENSG00000274267,MICAL2,GIHCG,MRPL46,PTPN14,ANKRD36BP2,ARHGAP11A,H3C12,MYC,NOG,ZNF675,B4GALNT4,PRR11,CD69,SLC40A1,DEPDC1B,MED12L,TMOD1,MYCN,ZNF625,SLCO5A1,IGFBP7,WDCP,IGLL1,SLC18A2,DMC1,PLXNB1,PCBP3,RIMS1,PGAP4,CA2,KIF15,HPGDS,KCNMB4,FREM1,CGNL1,CPA3,KCNK5,NEIL3,CDK6-AS1,CYP26B1,C2orf66,IL1RL1,TBC1D3,SPECC1L-ADORA2A

Platelet_bias_computational_HSC	AAED1,ABHD14B,AC011139.1,AC020916.1,AC026369.3,AC090204.1,AC093673.1,AC100810.1,AC103591.3,AC114760.2,ACOT11,ACSM3,ACTR1A,ACTR1B,ADAM28,ADAM8,ADAR,ADD1,ADGRE5,AES,AFF4,AFTPH,AGPS,AHNAK,AIDA,AIF1,AIMP1,AJ009632.2,AKAP13,AKAP17A,AKIRIN1,AKIRIN2,AKR1C3,AL031777.3,AL118516.1,AL121944.1,ALCAM,ALDH1A1,ALG13,ALKBH5,AMPD2,AMZ2,ANAPC16,ANKRD12,ANKRD28,ANKRD54,ANXA1,ANXA6,ANXA7,AP1G2,AP2B1,AP3M2,APH1A,APMAP,APOBEC3G,APOL3,APP,AREG,ARF4,ARID5A,ARL2BP,ARL4A,ARMCX1,ARRDC2,ASAH1,ASB8,ASCC2,ASNSD1,ATF3,ATG101,ATG16L2,ATP2B1-AS1,ATP6AP1,ATP8B4,ATRAID,AUP1,AVP,B3GNT5,BABAM2,BAG5,BAG6,BCAS2,BCL2A1,BCL2L13,BCL7B,BEX1,BEX2,BEX4,BEX5,BIRC2,BIRC3,BLOC1S4,BLVRA,BMI1,BNIP2,BNIP3,BNIP3L,BORCS7,BRMS1,BST2,BTG1,BUD23,C11orf21,C16orf45,C16orf72,C18orf32,C19orf38,C19orf53,C2orf69,C7orf50,C8orf59,CA5B,CABIN1,CALCOCO2,CALN1,CANX,CAPN2,CAPN7,CAPZA2,CARD19,CASC4,CAST,CAVIN1,CAVIN2,CCDC115,CCDC59,CCDC69,CCDC85B,CCND3,CCNH,CCNL1,CCSER2,CD109,CD151,CD164,CD300A,CD37,CD44,CD46,CD52,CD53,CD55,CD63,CD74,CD82,CD83,CD9,CDADC1,CDC42BPA,CDC73,CDH7,CDKN1A,CEBPB,CEBPZOS,CENPC,CEP70,CFAP20,CFH,CGGBP1,CGRRF1,CHCHD7,CHD9,CHIC2,CHMP1B,CHMP2B,CHPF2,CHPT1,CHST11,CHST13,CIRBP,CITED2,CLDN15,CLEC9A,CLIC2,CLINT1,CLIP1,CLK1,CLK3,CLU,CMPK1,CMTM6,CNOT2,CNOT4,CNPPD1,CNST,COMMD10,COMMD6,COPA,COPS2,COQ10B,CORO1B,CORO1C,COX19,COX20,CPED1,CPNE3,CPQ,CREM,CRHBP,CRYGD,CRYL1,CSNK1D,CSNK1E,CSRNP1,CSRP1,CST3,CTBS,CTDSP2,CTNNA1,CTNND1,CTR9,CTSB,CTSD,CTSF,CTSO,CTSS,CTSW,CWC25,CWF19L2,CXCL2,CXCL3,CXCL8,CXCR4,CYBRD1,CYSLTR1,CYTH1,CYTH2,CYTIP,CYTOR,DAP,DAZAP2,DBNL,DCAF8,DCP1A,DDIT3,DDX18,DDX24,DDX3X,DDX3Y,DDX5,DEDD2,DEGS1,DERL1,DHRS4L2,DHRS7,DIMT1,DLK1,DNAJB1,DNAJB14,DNAJB6,DNAJB9,DPH3,DPM1,DRAM1,DST,DUSP1,DUSP11,DUSP2,DUSP22,DUSP3,DYNC1LI1,DYNLRB1,DYNLT3,EBLN3P,EDF1,EEF1A1,EEF1AKMT2,EGR1,EID1,EIF1,EIF1B,EIF2B1,EIF4A2,EIF4B,EIF4G2,EIF4H,ELF1,ELK4,ELMO1,EMC3,EMC7,EMCN,EMP1,EMP3,EPB41L4A-AS1,EPC1,EPHA1-AS1,ERICH1,ERLEC1,ERP44,ETV3,EVI2B,EXOC7,F2R,FAHD2B,FAM104A,FAM118A,FAM124B,FAM162A,FAM177A1,FAM19A2,FAM3C,FAM96B,FASTK,FAU,FBXL15,FBXL5,FBXO25,FCER1A,FCGRT,FERMT3,FEZ2,FHL1,FIS1,FLII,FLOT1,FLOT2,FOS,FOSB,FOSL2,FRMD8,FTH1,FTL,FXYD5,G3BP2,GABARAP,GABARAPL2,GADD45A,GADD45B,GALNT2,GATA2,GATA3,GBP4,GCLM,GFM1,GFOD1,GGA1,GGNBP2,GGPS1,GIMAP2,GLB1,GLMP,GLTP,GMPR2,GNA15,GOLGA4,GOSR1,GPAT3,GPATCH8,GPBP1L1,GPR108,GPR146,GRINA,GSN,GSTM3,GSTM5,GSTO2,GTF2F1,GTF2IRD2,GUCY1A1,HARS,HAX1,HBP1,HDAC10,HERPUD2,HEXB,HGSNAT,HINT1,HIST1H1C,HIST1H2AE,HIST1H2BC,HIST1H2BG,HIST2H2AC,HIST2H2BE,HLA-A,HLA-B,HLA-C,HLA-DMA,HLA-DMB,HLA-DOA,HLA-DPA1,HLA-DPB1,HLA-DQA1,HLA-DQA2,HLA-DQB1,HLA-DRA,HLA-DRB1,HLA-DRB5,HLA-E,HLA-F,HLF,HMGA2,HNRNPH2,HOXA5,HOXB-AS3,HSBP1L1,HSD17B12,HSF1,HSP90AB1,HSPA1A,ICAM2,ICAM3,ICAM4,ID1,ID2,IDI1,IDS,IER2,IFI27L2,IFI35,IFI44L,IFI6,IFITM2,IFITM3,IFNGR1,IFRD1,IK,IL12A-AS1,IL27RA,ILF3-DT,ILVBL,IMMP2L,IMP3,INO80E,INSIG1,INTS6,IRAK3,IRF3,ISCA1,ISCU,IST1,ITM2B,ITSN2,JAK1,JAML,JKAMP,JMJD1C,JMJD6,JUN,JUNB,JUND,KANSL2,KAT5,KAT6A,KDELR1,KDM2A,KDM6B,KLC1,KLF10,KLF13,KLF2,KLF3,KLF4,KLF5,KLF6,KLF7,KLHDC2,KLHL6,KMT2E,KPNA4,KRCC1,KTI12,LAIR1,LAMP2,LAMTOR1,LAMTOR3,LAMTOR4,LAPTM4A,LAPTM5,LDLR,LENG1,LEPROT,LEP

	ROTL1,LETMD1,LIMCH1,LINC00623,LINC01122,LIPA,LITAF,LMBRD1,LMNA,LPCAT2,LPIN1,LPP,LRCH4,LRP10,LRRFIP2,LST1,LTBP4,LTC4S,LUC7L,LXN,LYRM1,LYRM9,LYZ,M6PR,MAF1,MAFF,MAFG,MAGED2,MAGEF1,MAN1B1,MAN2A2,MAP1LC3B,MAP3K8,MAP4K2,MAP7D1,MAP9,MAPK1IP1L,MAPK6,MAPRE1,MARCH7,MAT2B,MAX,MBTPS1,MCL1,MECOM,MECP2,MED19,MED21,MEF2C,MEG3,MEIS1,METTL15,MFNG,MGAT1,MID1IP1,MIDN,MIER1,MIR155HG,MKRN1,MLF1,MLF2,MLLT3,MLLT6,MMGT1,MMRN1,MOAP1,MOB2,MOB4,MOCS2,MPHOSPH8,MPV17,MRPL33,MRPL53,MSN,MSRB3,MT-ND1,MT-ND2,MT-ND3,MTFR1L,MTIF3,MX1,MYADM,MYCT1,MYEF2,MYLIP,NAAA,NAF1,NAMPT,NANS,NAP1L3,NAPRT,NARFL,NBL1,NDFIP1,NDRG2,NDUFAF3,NDUFC1,NDUFS7,NEAT1,NEIL2,NEU1,NFAT5,NFATC1,NFE2L2,NFIA,NFKBIA,NFKBIL1,NFKBIZ,NKTR,NME3,NOL7,NOP53,NORAD,NPC2,NPDC1,NPRL3,NR1H2,NR3C1,NR4A1,NR4A2,NRBP1,NSFL1C,NSMCE1,NSRP1,NT5C3B,NTHL1,NUCB1,NUDT14,NUDT16,NUDT4,NUMB,NXF1,OAT,OGFR,OPTN,OS9,OST4,OTUB1,OTUD6B-AS1,OXA1L,P4HTM,PARP10,PCBD1,PCDH9,PCGF5,PCID2,PDE4B,PER1,PEX16,PFDN5,PGGT1B,PHACTR1,PHF1,PHF11,PHF20,PHF3,PHLDB2,PHTF1,PHYKPL,PI4KB,PIGBOS1,PIK3IP1,PIM3,PIP4P1,PIP4P2,PIP5K1B,PJA2,PLAUR,PLD3,PLD4,PLEKHA2,PLEKHA3,PLEKHO1,PLK3,PLPBP,PLPP5,PLSCR1,PLXDC2,PML,PNMA1,PNPLA8,PNRC1,POLR2C,PPIL4,PPP1CB,PPP1R10,PPP1R11,PPP1R15A,PPP1R2,PPP3CC,PPP6C,PRAF2,PRDM2,PRKACB,PRKAR1A,PRKCH,PRMT2,PRNP,PRPF38A,PRR14,PRR7,PSAP,PSENEN,PSTPIP2,PTGER4,PTGS1,PTGS2,PTP4A1,PTPN2,PURB,R3HDM4,RAB18,RAB1A,RAB21,RAB34,RAB37,RAB3GAP1,RAB5A,RAB7A,RAB9A,RABAC1,RAD54L2,RAPGEF2,RARA,RARRES3,RASSF1,RASSF5,RBCK1,RBM23,RBM33,RBM39,RBM7,RBMS1,RBMX2,RBPJ,RBPMS,RC3H2,RCHY1,RELA,RENBP,REPIN1,REX1BD,RFTN1,RGL2,RGL4,RGP1,RGS14,RGS19,RHOC,RHOH,RIC3,RILPL2,RIMKLB,RIPK2,RNASET2,RNF11,RNF114,RNF125,RNF145,RNF26,RNF6,RNH1,ROBO3,ROBO4,RPL11,RPL13,RPL23A,RPL24,RPL30,RPL31,RPL34,RPL35A,RPL36,RPL36A,RPL36AL,RPL38,RPL41,RPL8,RPL9,RPLP2,RPS12,RPS20,RPS23,RPS27,RPS27A,RPS4Y1,RPS6KB2,RPS9,RRAGA,RRBP1,RSBN1,RSBN1L,RSRC2,RTF2,RTN4,RYBP,S100A10,S100A11,S100A4,S100A6,S1PR4,SAFB2,SAMD9L,SAMSN1,SARAF,SARNP,SAT1,SAT2,SBDS,SC5D,SCAMP2,SCN9A,SDE2,SDF4,SDHAF2,SDR39U1,SEC14L1,SEC22C,SEC23A,SEC62,SELENOK,SELENOM,SELENOP,SELENOS,SELENOT,SERINC1,SERINC3,SETD3,SF1,SH3BGRL3,SHOC2,SIL1,SIRT2,SKAP1,SKIL,SLC16A7,SLC25A24,SLC25A38,SLC2A3,SLC37A1,SLC3A2,SLC44A1,SLU7,SMIM10L1,SMIM26,SMIM29,SMIM3,SMIM37,SNAP23,SNAPC1,SNHG12,SNHG8,SNRK,SNRPN,SNW1,SNX9,SOCS2,SOCS3,SOD2,SON,SORBS3,SP100,SP3,SPART,SPIN2B,SPINT2,SPOP,SPRTN,SPRY1,SQOR,SQSTM1,SREK1IP1,SRGN,SRP68,SRPRA,SRRM2,SRSF5,SS18,SSBP3,ST3GAL1,STARD3,STARD3NL,STAT6,STK17A,STK17B,STK4,STN1,STOM,STX16,STX3,STX4,STX5,SUCLG2,SUGT1,SUN2,SWAP70,SYAP1,SYF2,SYPL1,SYTL4,TACC1,TAF11,TAGAP,TANK,TAPBPL,TARSL2,TBC1D5,TBCC,TBRG1,TCEAL2,TCEAL3,TCF25,TCF7,TCOF1,TCTEX1D1,TENT2,TENT5A,TENT5C,TERF2IP,TFEC,TFPI,TFPT,TGFB1,TGIF1,THEMIS2,THUMPD1,TIE1,TINF2,TIPARP,TLE4,TM2D3,TM9SF2,TMBIM4,TMC6,TMC8,TMED1,TMED5,TMED7,TMEM134,TMEM167B,TMEM170A,TMEM173,TMEM219,TMEM220,TMEM222,TMEM243,TMEM248,TMEM30A,TMEM38B,TMEM43,TMEM50B,TMEM59,TMEM91,TMEM9B,TMF1,TMX4,TNFAIP3,TNFRSF14,TNFSF10,TOB1,TOB2,TOE1,TOMM7,TOR1AIP1,TP53TG1,TPST2,TPT1,TRAPPC2B,TRAPPC3,TRIM13,TRIM22,TRIM4,TRIM56,TRIM8,TRIR,TRPV2,TSC22D1,TSC22D2,TSC22D3,TSEN34,TSG101,TSPAN32,TSPO,TSPYL2,TSSC4,TUBA1A,TUBA1C,TXNIP,UBA5,UBA7,UBB,UBC,UBE2B,UBE2D1,UBE2E1,UBE2S,UBL3,UBQLN2,UBXN1,UCHL1,UFM1,UNC45A,UNC50,UNK,USP11,USP12,USP14,VAMP2,VAMP5,VAPA,VCP,VEZF1,VIM,VPS26C,VPS37B,VPS4A,VPS51,VSIR,WASHC1,WBP2,WDR13,WDR45,WDR45B,WDR83OS,WS

	B1,XBP1,XPA,XPC,YBX3,YIPF5,YME1L1,YPEL5,YTHDC1,YWHAZ,ZBED5,ZEB1,ZFAND1,ZFAND3,ZFAND5,ZFP36,ZFYVE21,ZMAT1 ,ZMAT2,ZNF136,ZNF148,ZNF274,ZNF3,ZNF32,ZNF331,ZNF350,ZNF394,ZNF426,ZNF644,ZNF706,ZNF83,ZNF830,ZSCAN18,

Multilineage_computational_HSC	AAMP,AATF,ABCE1,ABCF1,ABHD14A,ABI2,ABRACL,ABT1,AC010642.2,AC026979.2,AC245014.3,ACAA2,ACADM,ACADVL,ACAT1,ACAT2,ACBD6,ACD,ACIN1,ACO2,ACP1,ACTB,ACTL6A,ACTN1,ACTN4,ACTR10,ACTR2,ACTR3,ACYP1,ADAM10,ADAM15,ADAM17,ADD3,ADI1,ADIPOR1,ADK,ADNP,ADPGK,ADRM1,ADSL,ADSS,AFG3L2,AGO2,AGPAT2,AGPAT5,AGTRAP,AHCY,AHCYL1,AHI1,AHSA1,AIG1,AK2,AK3,AK6,AKIP1,AKR1A1,AKR1B1,AKR7A2,AKT2,AL157938.3,ALDH18A1,ALDOA,ALG3,ALG5,ALG8,ALKBH2,ANAPC11,ANAPC13,ANAPC15,ANAPC5,ANAPC7,ANKLE2,ANKRD10,ANKRD11,ANKRD36,ANKRD36C,ANP32A,ANP32B,ANP32E,ANXA5,AP002360.1,AP1M1,AP1S1,AP1S2,AP2M1,AP2S1,AP3B1,AP3S1,API5,APIP,APOPT1,APPL1,ARAF,ARF3,ARF5,ARF6,ARHGAP4,ARHGDIA,ARIH2,ARL1,ARL16,ARL2,ARL5A,ARL6IP1,ARL6IP4,ARL6IP6,ARL8B,ARMC1,ARMC10,ARMC8,ARPC1A,ARPC1B,ARPC2,ARPC4,ARPC5,ARPC5L,ARPP19,ARRB2,ASNA1,ASPH,ATAD2,ATG12,ATG3,ATG5,ATIC,ATOX1,ATP1A1,ATP1B3,ATP2A3,ATP2B1,ATP5F1A,ATP5F1B,ATP5F1C,ATP5F1E,ATP5IF1,ATP5MC1,ATP5MC3,ATP5MD,ATP5ME,ATP5MF,ATP5MPL,ATP5PB,ATP5PD,ATP5PF,ATP5PO,ATP6AP2,ATP6V0B,ATP6V0D1,ATP6V0E1,ATP6V0E2,ATP6V1D,ATP6V1H,ATXN10,ATXN2L,AURKAIP1,AZIN1,B2M,B3GAT3,BAALC,BABAM1,BAD,BAG1,BAG2,BANF1,BAX,BAZ1A,BAZ1B,BCAP29,BCAP31,BCCIP,BCKDK,BCL7A,BCLAF1,BDP1,BECN1,BEX3,BID,BIRC6,BLMH,BLOC1S1,BLOC1S2,BLVRB,BMS1,BOD1L1,BOLA3,BOP1,BRD2,BRD3,BRD4,BRD7,BRIX1,BSG,BST1,BTG3,BUB3,BUD31,BZW1,C11orf58,C12orf45,C12orf57,C12orf75,C15orf61,C19orf24,C19orf48,C19orf70,C1D,C1GALT1,C1QBP,C1orf123,C1orf131,C1orf35,C1orf43,C1orf52,C20orf27,C22orf39,C3orf14,C3orf38,C4orf48,C5orf24,C6orf62,C8orf33,C9orf16,C9orf78,CACYBP,CALM1,CALM2,CALM3,CALR,CALU,CAMTA1,CAND1,CAP1,CAPG,CAPNS1,CAPZA1,CARHSP1,CASP2,CBFB,CBR1,CBWD1,CBWD5,CBX1,CBX2,CBX3,CBX5,CBX6,CCAR1,CCDC124,CCDC14,CCDC167,CCDC34,CCDC47,CCDC66,CCDC82,CCDC88A,CCNC,CCNK,CCNY,CCT2,CCT3,CCT4,CCT5,CCT6A,CCT7,CCZ1,CD2AP,CD2BP2,CD47,CD59,CD69,CD81,CD99,CDC123,CDC26,CDC37,CDC42,CDC5L,CDCA7L,CDK2AP1,CDK2AP2,CDK4,CDK5RAP3,CDK6,CDKN2AIPNL,CEBPG,CEBPZ,CELF1,CENPH,CENPV,CENPW,CENPX,CEP135,CEP170,CEP290,CEP350,CEP57,CEP63,CERS2,CERS6,CETN2,CETN3,CFAP298,CFAP97,CFDP1,CFL1,CHCHD1,CHCHD10,CHCHD2,CHCHD3,CHD1,CHD1L,CHD4,CHID1,CHMP1A,CHMP4B,CHRAC1,CHTF8,CIAPIN1,CIB1,CISD1,CISD2,CISD3,CKAP2,CKB,CKLF,CKS1B,CKS2,CLEC11A,CLNS1A,CLPP,CLPTM1,CLTB,CMAS,CMC1,CMC2,CMSS1,CNBP,CNDP2,CNN3,CNOT1,CNOT10,CNOT6L,CNOT7,CNOT9,CNP,CNPY2,CNPY3,CNTLN,CNTRL,COA1,COA3,COA4,COMMD1,COMMD4,COMMD7,COMMD8,COMMD9,COP1,COPE,COPS3,COPS5,COPS6,COPS7B,COPS8,COPS9,COQ4,COQ9,CORO1A,COTL1,COX14,COX16,COX17,COX5A,COX5B,COX6A1,COX6B1,COX6C,COX7A2,COX7B,COX8A,CPSF3,CPSF6,CPSF7,CRCP,CREBZF,CRELD2,CRIPT,CRLS1,CRTAP,CSKMT,CSNK2A1,CSNK2B,CSTB,CSTF3,CTBP1,CTCF,CTDSPL2,CTNNB1,CTNNBIP1,CTSA,CTSC,CUEDC2,CUL1,CUTA,CWC15,CWC27,CXXC1,CYB561A3,CYB5A,CYB5B,CYB5R3,CYBA,CYBC1,CYC1,CYCS,DAD1,DAXX,DAZAP1,DBF4,DBI,DCAF13,DCAF16,DCAF7,DCK,DCTD,DCTN1,DCTPP1,DCUN1D1,DCUN1D5,DCXR,DDA1,DDB1,DDB2,DDOST,DDT,DDX1,DDX19B,DDX21,DDX39A,DDX41,DDX46,DDX50,DDX52,DDX6,DECR1,DEK,DENR,DERA,DERL2,DFFA,DGCR6L,DGUOK,DHRS4,DHX15,DHX30,DHX9,DIAPH1,DIS3,DIS3L,DKC1,DLD,DLST,DNAJA1,DNAJA2,DNAJB11,DNAJC15,DNAJC19,DNAJC2,DNAJC21,DNAJC3,DNAJC8,DNAJC9,DNM1L,DNMT1,DNPH1,DNTTIP2,DOCK2,DONSON,DPM2,DPM3,DPP7,DPY30,DPYSL2,DR1,DRAP1,DRG1,DRG2,DSG2,DSTN,DTNBP1,DTYMK,DUS3L,DUSP12,DUSP23,DUT,DVL2,DYNC1H1,DYNLL1,DYNLT1,E2F4,EBAG9,EBNA1BP2,EBP,ECD,ECH1,ECHDC1,ECHS1,EEF1B2,EEF1E1,EI24,EIF1AX,EIF1AY,EIF2AK1,EIF2AK2,EIF2B5,EIF2S1,EIF2S2,EIF3A,EIF3B,EIF3I,EIF3J,EIF4A3,EIF4E,EIF4EBP1,EIF4EBP2,EIF4G1,EIF5,EIF5A,EIF5B,EIF6,EIPR1,ELAC2,ELAVL1,ELMSAN1,ELOB,ELO

	C,ELOVL5,ELP5,ELP6,EMC10,EMC4,EMC6,EMC8,EMD,EMG1,ENO1,ENOPH1,ENOSF1,ENSA,ENY2,EPB41,EPN1,ERAP2,ERG28, ERGIC2,ERH,ERI3,ESF1,ETF1,ETFA,ETFB,EWSR1,EXOC5,EXOSC1,EXOSC4,EXOSC5,EXOSC6,EXOSC8,EXOSC9,EXTL2,EZR,F8A1,F AAP20,FABP5,FADS1,FAF1,FAH,FAIM,FAM111A,FAM120A,FAM120AOS,FAM122B,FAM133B,FAM136A,FAM192A,FAM213A ,FAM216A,FAM32A,FAM3A,FAM45A,FAM49B,FAM50A,FAM92A,FAM96A,FARSA,FARSB,FBL,FBXO11,FBXO21,FBXO4,FDFT1, FDPS,FDX1,FGD5- AS1,FH,FIBP,FKBP11,FKBP1A,FKBP2,FKBP3,FKBP4,FKBP5,FLYWCH2,FN3KRP,FRG1,FSCN1,FUBP1,FUNDC1,FUNDC2,FUS,FXN, FYTTD1,G3BP1,G6PC3,GABPB1,GADD45GIP1,GALK1,GALNT1,GALNT11,GAMT,GANAB,GAPDH,GAR1,GARS,GART,GBE1,GCA T,GCFC2,GCHFR,GCSH,GGCT,GGH,GHITM,GLIPR2,GLO1,GLOD4,GLRX3,GLRX5,GLUD1,GLUL,GLYR1,GMCL1,GMPS,GNAI2,GN AI3,GNAQ,GNAS,GNB1,GNB2,GNB4,GNB5,GNG5,GNL1,GNL2,GNL3,GNPAT,GOLGA7,GOLIM4,GORASP2,GOT2,GPAA1,GPAN K1,GPATCH4,GPBP1,GPI,GPN1,GPN3,GPS1,GPX4,GRK6,GSPT1,GSS,GSTO1,GSTP1,GTF2A2,GTF2H1,GTF2H2,GTF3A,GTF3C5,G TF3C6,GTPBP4,GUK1,GUSB,H2AFV,H2AFY,H2AFZ,H3F3A,HACD1,HACD3,HACL1,HADH,HAT1,HAUS1,HAUS4,HBS1L,HDAC1,H DAC2,HDAC3,HDDC2,HDGF,HDGFL3,HDHD2,HDHD5,HDLBP,HELLS,HENMT1,HERPUD1,HIBADH,HIGD1A,HIKESHI,HINT2,HIST 1H4C,HLTF,HM13,HMG20B,HMGA1,HMGB1,HMGB2,HMGB3,HMGCS1,HMGN1,HMGN2,HMGN3,HMGN5,HMGXB4,HNRNP A0,HNRNPA1,HNRNPA1P48,HNRNPA2B1,HNRNPA3,HNRNPAB,HNRNPC,HNRNPD,HNRNPDL,HNRNPF,HNRNPH1,HNRNPH3, HNRNPK,HNRNPL,HNRNPLL,HNRNPM,HNRNPR,HNRNPU,HNRNPUL1,HP1BP3,HPF1,HPRT1,HSBP1,HSD17B10,HSD17B8,HSP 90AA1,HSP90B1,HSPA4,HSPA5,HSPA8,HSPA9,HSPB1,HSPB11,HSPBP1,HSPD1,HSPE1,HSPH1,HTATIP2,HTATSF1,HTRA2,IAH1,I ARS,IARS2,ICE2,IDH2,IER3IP1,IFNGR2,IFRD2,IFT27,IFT52,IFT57,IGFBP7,IL2RG,ILF2,ILF3,ILKAP,IMMP1L,IMMT,IMP4,IMPDH2,I NG2,ING3,ING5,INTS10,INTS13,IPO5,IPO7,IPO9,IQCB1,IQGAP1,ISCA2,ISG20L2,ISOC1,ISOC2,ISYNA1,ITFG1,ITGAE,ITGB1,ITGB 1BP1,ITGB2,ITGB3BP,ITM2A,IVNS1ABP,JADE1,JOSD1,JPT1,JTB,KATNB1,KATNBL1,KDELR2,KDM1A,KDSR,KEAP1,KHSRP,KIAA1 143,KIF20B,KIF22,KIF2A,KLHDC3,KPNA2,KPNA3,KPNB1,KRAS,KRR1,KRT10,KRTCAP2,KTN1,KXD1,LAGE3,LAMP1,LAMTOR2,LA MTOR5,LAP3,LARP7,LARS,LAS1L,LBR,LCP1,LDHA,LDHB,LGALS3BP,LINC02001,LKAAEAR1,LLPH,LMAN1,LMAN2,LPCAT3,LRPA P1,LRPPRC,LRRC47,LRRC57,LRRC58,LRRC59,LRRC75A,LSM1,LSM12,LSM14A,LSM3,LSM4,LSM5,LSM6,LSM7,LSM8,LUC7L2,LY 6E,LYAR,LYPLA1,LYPLA2,LYRM2,LYRM7,MAD2L1,MAD2L2,MAGOH,MAGOHB,MAGT1,MALSU1,MANF,MAP3K13,MAP3K2,M AP3K20,MAP3K7,MAP4,MAP4K1,MAP4K5,MAPK8,MAPKAP1,MAPKAPK5,MAPRE2,MARCKSL1,MATK,MAZ,MBD4,MBIP,MCF D2,MCM3,MCM5,MCM7,MCRIP1,MCRIP2,MCRS1,MCUB,MCUR1,MDH1,MDH2,MDK,ME2,MEA1,MEAF6,MED10,MED17,M ED30,MED4,MESD,MEST,METTL21A,METTL26,METTL5,METTL9,MFGE8,MFSD14C,MGAT2,MGAT4A,MGST1,MGST2,MGST3, MIF,MINOS1,MIR4435- 2HG,MIR4458HG,MIS18BP1,MLEC,MLST8,MMAB,MOB1A,MORF4L1,MORF4L2,MPC1,MPC2,MPDU1,MPHOSPH6,MPHOSPH 9,MPLKIP,MRE11,MRPL1,MRPL11,MRPL12,MRPL13,MRPL14,MRPL15,MRPL18,MRPL19,MRPL2,MRPL20,MRPL21,MRPL22, MRPL23,MRPL24,MRPL27,MRPL3,MRPL34,MRPL36,MRPL37,MRPL4,MRPL41,MRPL42,MRPL47,MRPL48,MRPL49,MRPL50, MRPL51,MRPL52,MRPL55,MRPL57,MRPL9,MRPS10,MRPS11,MRPS12,MRPS14,MRPS15,MRPS16,MRPS18A,MRPS18C,MRPS 2,MRPS23,MRPS25,MRPS26,MRPS34,MRPS35,MRPS6,MRPS7,MRTO4,MSH2,MSH3,MSH6,MSRA,MSRB2,MT-ATP6,MT- CO1,MT-CO2,MT-CYB,MT-ND4,MT-ND4L,MT-ND5,MT-

	ND6,MT2A,MTCH1,MTCH2,MTDH,MTF2,MTHFD1,MTHFD2,MTPAP,MTRF1L,MYCBP,MYDGF,MYL6,MYL6B,MZT1,MZT2A,MZT2B,NAA10,NAA15,NAA20,NAA25,NAA38,NAA50,NABP2,NAE1,NAP1L1,NAP1L4,NAPA,NARF,NARS,NARS2,NASP,NAXE,NCBP2,NCBP2-AS2,NCBP3,NCF4,NCL,NDUFA1,NDUFA11,NDUFA12,NDUFA13,NDUFA2,NDUFA3,NDUFA4,NDUFA5,NDUFA6,NDUFA7,NDUFA8,NDUFA9,NDUFAB1,NDUFAF2,NDUFAF4,NDUFAF6,NDUFAF8,NDUFB1,NDUFB10,NDUFB11,NDUFB2,NDUFB3,NDUFB6,NDUFB7,NDUFB8,NDUFB9,NDUFC2,NDUFS1,NDUFS3,NDUFS5,NDUFS6,NDUFS8,NDUFV1,NDUFV2,NEDD8,NELFCD,NELFE,NENF,NFATC2IP,NFATC3,NFIC,NFKBIB,NGDN,NGLY1,NHP2,NIN,NINJ1,NIP7,NIPA2,NIPBL,NIPSNAP2,NIT2,NME1,NME2,NME4,NMI,NMRAL1,NNT,NOC2L,NOL10,NOL11,NOL8,NOLC1,NONO,NOP10,NOP56,NOP58,NOSIP,NPM3,NQO2,NRAS,NREP,NSD3,NSL1,NSMCE4A,NSUN2,NSUN6,NTMT1,NTPCR,NUBP2,NUCB2,NUCKS1,NUDC,NUDCD2,NUDT1,NUDT15,NUDT21,NUDT5,NUFIP2,NUP107,NUP160,NUP37,NUP54,NUP58,NUP62,NUP93,NUS1,NUTF2,NXT1,OAZ1,OCIAD1,OCIAD2,ODC1,ODF2,ODR4,OLA1,OPA1,OSBPL8,OSBPL9,OSER1,OSGEP,OSTC,OXCT1,P4HB,PA2G4,PABPC4,PABPN1,PAFAH1B3,PAICS,PAIP1,PAIP2,PAK1IP1,PAK2,PAPOLA,PARK7,PARL,PARP1,PARP14,PARVB,PAXX,PBDC1,PBRM1,PCBP1,PCLAF,PCM1,PCMT1,PCNA,PCNP,PDAP1,PDCD10,PDCD11,PDCD5,PDCD6,PDCL3,PDHA1,PDIA3,PDIA4,PDIA6,PDLIM1,PDRG1,PDS5A,PDS5B,PEA15,PEBP1,PET100,PET117,PEX10,PFDN2,PFDN6,PFKL,PFKP,PFN1,PGAM1,PGAP2,PGK1,PGM1,PGM2,PGRMC1,PHAX,PHB,PHF20L1,PHF5A,PHF6,PHGDH,PHIP,PHPT1,PIAS2,PIGC,PIGF,PIGH,PIGT,PIGX,PIH1D1,PIN1,PIN4,PITHD1,PITPNB,PKIG,PKM,PLEK,PLEKHJ1,PLGRKT,PLOD2,PLP2,PLRG1,PM20D2,PMAIP1,PMF1,PMPCA,PMVK,PNKD,PNKP,PNO1,PNPT1,POLD2,POLDIP2,POLDIP3,POLE3,POLE4,POLK,POLR2A,POLR2D,POLR2E,POLR2F,POLR2G,POLR2H,POLR2I,POLR2J,POLR2J3.1,POLR2K,POLR2L,POMP,POP5,POP7,PPA1,PPA2,PPDPF,PPHLN1,PPIA,PPIB,PPID,PPIE,PPIG,PPIH,PPM1A,PPM1G,PPP1CA,PPP1CC,PPP1R14B,PPP1R7,PPP1R8,PPP2CA,PPP2R3C,PPP3R1,PPP4C,PPP4R2,PPP4R3A,PPP4R3B,PPP6R1,PPT1,PRCC,PRDX1,PRDX2,PRDX3,PRDX4,PRDX5,PRDX6,PRELID1,PRELID3B,PRIM1,PRKD3,PRKDC,PRKRA,PRMT1,PRMT5,PRPF19,PRPF31,PRPF38B,PRPF4,PRPF40A,PRPF4B,PRPF8,PRPS1,PRPS2,PRPSAP1,PRRC2A,PRRC2B,PRRC2C,PSIP1,PSMA1,PSMA2,PSMA3,PSMA4,PSMA5,PSMA6,PSMA7,PSMB1,PSMB10,PSMB2,PSMB3,PSMB5,PSMB6,PSMB7,PSMB8,PSMB9,PSMC1,PSMC2,PSMC3,PSMC4,PSMC5,PSMC6,PSMD1,PSMD11,PSMD12,PSMD13,PSMD14,PSMD2,PSMD3,PSMD6,PSMD7,PSMD8,PSMD9,PSME1,PSME2,PSME3,PSME4,PSMG1,PSMG3,PSMG4,PSPC1,PTBP1,PTCD3,PTDSS1,PTGES3,PTMA,PTMS,PTOV1,PTP4A2,PTPMT1,PTPN7,PTS,PTTG1,PUF60,PUM1,PUM3,PUS7L,PXMP2,PYCR1,PYCR2,PYURF,QDPR,QKI,QPRT,RAB10,RAB11A,RAB1B,RAB27A,RAB28,RAB2A,RAB32,RAB38,RAB5C,RAB5IF,RAB6A,RAB8A,RABGGTB,RAC1,RAD1,RAD21,RAD23A,RAD23B,RAD51C,RAF1,RALA,RALY,RAN,RANBP1,RANBP2,RANGRF,RAP1A,RAP1B,RARS,RASGEF1B,RBBP4,RBBP6,RBBP7,RBFA,RBM14,RBM17,RBM25,RBM28,RBM3,RBM42,RBM8A,RBMX,RBX1,RCC2,RCN1,RCN2,RDH11,RDX,RECQL,RER1,REV1,REV3L,REXO2,RFC1,RFC2,RFLNB,RFX2,RGCC,RHBDD2,RHEB,RHNO1,RHOA,RHOT2,RIC8A,RIF1,RIOK1,RIT1,RNASEH1,RNASEH2B,RNASEH2C,RNF126,RNF138,RNF168,RNF187,RNF2,RNF5,RNPS1,ROMO1,RPA1,RPA2,RPA3,RPAIN,RPAP3,RPIA,RPL21,RPL22L1,RPL26L1,RPL6,RPL7,RPN1,RPN2,RPP30,RPP40,RPS17,RPS19BP1,RPS21,RPS26,RPS27L,RPS3A,RPS6KA5,RRM1,RRP1,RRP7A,RSRC1,RSU1,RTF1,RTN3,RUNX1,RUVBL1,RUVBL2,RWDD4,SAE1,SAFB,SAMM50,SAP18,SAP30BP,SAR1A,SAR1B,SBNO1,SCAF11,SCAMP3,SCAPER,SCCPDH,SCNM1,SCOC,SDAD1,SDF2,SDF2L1,SDHA,SDHAF3,SDHB,SDHD,SEC11A,SEC11C,SEC13,SEC22B,SEC61A1,SEC61B,SEC61G,SEC63,SEH1L,SELENOF,SELENOH,SELENOW,SEM1,SENP5,SEP

	T1,SEPT11,SEPT2,SEPT7,SERBP1,SERF2,SERPINE2,SET,SETD2,SETD5,SETD9,SF3A1,SF3A2,SF3A3,SF3B2,SF3B3,SF3B4,SF3B5,SF3B6,SFPQ,SFR1,SFT2D1,SFXN1,SGTA,SHMT2,SIKE1,SIN3A,SINHCAF,SIVA1,SKA2,SKP1,SLBP,SLC1A5,SLC20A1,SLC25A11,SLC25A3,SLC25A39,SLC25A5,SLC25A6,SLC30A5,SLC30A9,SLC35A3,SLC35A4,SLC35B1,SLC38A1,SLC38A2,SLC39A1,SLC39A3,SLC39A8,SLC9A3R1,SLIRP,SMAD2,SMARCA4,SMARCA5,SMARCB1,SMARCC1,SMARCE1,SMC1A,SMC2,SMC3,SMC4,SMC5,SMCHD1,SMIM10,SMIM12,SMIM15,SMIM19,SMIM4,SMS,SMU1,SNCA,SNF8,SNHG10,SNHG15,SNHG21,SNHG9,SNRNP25,SNRNP27,SNRNP40,SNRNP70,SNRPA,SNRPA1,SNRPB,SNRPB2,SNRPC,SNRPD1,SNRPD2,SNRPD3,SNRPE,SNRPF,SNRPG,SNU13,SNX10,SNX3,SNX5,SOD1,SP140L,SPAG16,SPATS2,SPCS1,SPCS2,SPCS3,SPEN,SPIN1,SPINK2,SPTLC1,SPTSSA,SQLE,SRD5A3,SREK1,SRFBP1,SRI,SRM,SRP14,SRP19,SRP54,SRP72,SRP9,SRPK1,SRPRB,SRRM1,SRRT,SRSF1,SRSF10,SRSF11,SRSF2,SRSF3,SRSF4,SRSF7,SRSF9,SS18L2,SSB,SSBP1,SSNA1,SSR1,SSR3,SSR4,SSRP1,SSSCA1,SSU72,ST3GAL4,STAG1,STAG2,STARD7,STAU1,STIP1,STMN1,STOML2,STRAP,STUB1,STX10,SUB1,SUCLA2,SUCLG1,SUDS3,SUGP2,SUMF2,SUMO1,SUMO2,SUMO3,SUPT16H,SURF4,SUZ12,SVIP,SYNCRIP,SYNGR2,SZRD1,TAF12,TAF15,TAF3,TAF6,TAF9,TAF9B,TAGLN2,TARDBP,TARS,TBC1D15,TBCB,TBPL1,TCEA1,TCEAL9,TCERG1,TCF12,TCP1,TCTN3,TDG,TECR,TEX264,TEX30,TFAM,TFDP1,TFG,TGS1,THAP9-AS1,THOC1,THOC2,THOC3,THOC6,THOC7,THRAP3,THUMPD3,THUMPD3-AS1,THYN1,TIA1,TIMM10,TIMM10B,TIMM17A,TIMM17B,TIMM50,TIMM8B,TIMMDC1,TIMP1,TLE3,TLK1,TM7SF3,TMA16,TMA7,TMBIM6,TMCO1,TMED10,TMED2,TMED4,TMED9,TMEM106C,TMEM107,TMEM109,TMEM11,TMEM123,TMEM126B,TMEM141,TMEM147,TMEM14A,TMEM14B,TMEM14C,TMEM160,TMEM165,TMEM167A,TMEM18,TMEM183A,TMEM208,TMEM218,TMEM230,TMEM242,TMEM258,TMEM33,TMEM50A,TMEM70,TMEM87A,TMEM9,TMEM97,TMEM98,TMOD3,TMPO,TMSB10,TMSB4X,TMUB1,TMX1,TMX2,TNPO1,TNPO3,TOMM22,TOMM34,TOMM40,TOMM5,TOP1,TOP2B,TOPORS,TOR1A,TOR1AIP2,TOR3A,TP53,TP53BP1,TP53I13,TPD52,TPD52L2,TPGS2,TPI1,TPM3,TPM4,TPR,TPRKB,TRA2A,TRA2B,TRAF7,TRAM1,TRAP1,TRAPPC1,TRAPPC2L,TRAPPC4,TRIAP1,TRIM24,TRIM28,TRMT10C,TRMT112,TRMT61B,TRUB2,TSEN15,TSEN54,TSN,TSPAN13,TSPAN3,TSPAN4,TSPYL4,TSR1,TSR2,TSTA3,TSTD1,TTC1,TTC3,TTF1,TUBA1B,TUBB,TUBB4B,TUFM,TWISTNB,TWSG1,TXN,TXNDC12,TXNDC17,TXNDC9,TXNL4A,TXNRD1,TYMP,TYMS,U2AF2,U2SURP,UBA2,UBA3,UBAP2L,UBE2A,UBE2D2,UBE2D3,UBE2E3,UBE2G1,UBE2G2,UBE2I,UBE2J2,UBE2K,UBE2L3,UBE2L6,UBE2N,UBE2V2,UBE3A,UBL5,UBTF,UBXN2A,UBXN4,UCHL3,UCHL5,UFD1,UHMK1,UNG,UPF3A,UPF3B,UQCC2,UQCC3,UQCR10,UQCR11,UQCRC1,UQCRFS1,UQCRH,UQCRQ,URI1,UROD,UROS,USP1,USP10,USP39,USP4,USP48,USP5,UTP11,UTP18,UTP23,UXS1,VAMP8,VBP1,VDAC1,VDAC2,VDAC3,VKORC1,VMA21,VPS13A,VPS25,VPS26A,VPS29,VPS35,VRK1,VRK2,VSIG10,WBP11,WBP4,WDR1,WDR11,WDR18,WDR43,WDR54,WDR61,WHAMM,WIPI2,WNK1,WRB,WTAP,XPNPEP1,XPO1,XPOT,XRCC1,XRCC5,XRCC6,XRN1,YAF2,YARS,YBX1,YDJC,YEATS4,YIF1A,YTHDF2,YWHAB,YWHAE,YWHAH,YWHAQ,YY1,ZBTB8OS,ZC3H14,ZC3H18,ZC3HAV1,ZCCHC17,ZCCHC9,ZCRB1,ZDHHC12,ZDHHC3,ZDHHC4,ZDHHC6,ZFP91,ZMYND11,ZNF121,ZNF207,ZNF22,ZNF292,ZNF326,ZNF37A,ZNF428,ZNF451,ZNF511,ZNF544,ZNF667-AS1,ZNF770,ZNF800,ZNHIT1,ZPR1,

Appendix methods table 2

Gene lists that were used for the cell type annotation of the clusters rich in T cells in the healthy donor and convalescent cohort datasets

T cell type	Genes
CD8_naive	MXRA8,TTC34,RP3-477M7.5,CA6,LINC01355,TCEA3,MDS2,RCAN3,RP4-594I10.3,LDLRAP1,MAN1C1,AZIN2,ZFP69B,RP5-997D24.3,HOOK1,CYP2J2,CACHD1,AK5,CNN3,AMY2B,AMIGO1,GSTM2,GSTM3,PHGDH,REG4,BCL9,RP11-350G8.5,EFNA1,TTC24,PRDX6,CAMSAP2,MFSD4A,C1orf147,C4BPB,GTF2IP20,OBSCN,CHRM3-AS2,ZNF496,LINC00954,KLHL29,DNMT3A,AC016907.3,LCLAT1,MTA3,AC093609.1,PLEKHH2,PREPL,AC007386.4,RP11-287D1.3,DNAH6,TRABD2A,CD8A,CD8B,ANAPC1P1,MAL,AC103563.9,TSGA10,REV1,NPAS2,CD8BP,EDAR,SH3RF3,RP11-77A13.1,EPB41L5,ARHGEF4,CCNT2-AS1,RBM43,ACVR1C,CERS6-AS1,UBR3,METAP1D,ITGA6,PDK1,SCRN3,DFNB59,TTN,CCDC141,FSIP2,FAM117B,CARF,FN1,SPEG,SERPINE2,SLC19A3,FBXO36,LINC01891,IQCA1,COL6A3,PASK,AC093642.4,TSEN2,FBLN2,OXNAD1,RP11-415F23.2,RP11-415F23.3,RP11-415F23.4,RP11-158G18.1,SATB1-AS1,ZNF662,SNRK,ZKSCAN7,PRKAR2A-AS1,DOCK3,WDR82,CACNA1D,DENND6A,FLNB,FLNB-AS1,SUCLG2-AS1,RP11-298C2.1,FOXP1-AS1,ROBO1,FILIP1L,ZBED2,CFAP44,TXNRD3,TMCC1-AS1,TMEM108,BFSP2-AS1,PXYLP1,LMLN,RP11-1191J2.5,RNF212,LINC01259,ATP8A1,TXK,SULT1B1,LEF1,LEF1-AS1,RPL34-AS1,PLA2G12A,ZGRF1,USP53,RP11-33B1.1,PRDM5,PGRMC2,NR3C2,DKFZP434I0714,CTD-2228K2.7,SDHAP3,FAM134B,RP11-53O19.3,CTD-2366F13.1,IL6ST,ADAMTS6,ANKRD31,MTX3,THBS4,SERINC5,CTC-458I2.2,RASGRF2,CKMT2-AS1,TMEM161B-AS1,CTD-2587M2.1,AC010468.2,RAPGEF6,CTC-432M15.3,AC034220.3,TCF7,KLHL3,LINC01024,NDFIP1,CTC-463A16.1,TIMD4,HAVCR1,FNDC9,FAM153B,ARL10,DBN1,FAM153A,FAM153C,HIVEP1,CARMIL1,ZNF204P,ZNF391,PRRT1,PPT2,EGFL8,COL11A2,PPARD,MOCS1,PTK7,CUL9,KCNQ5,SH3BGRL2,NT5E,BACH2,RP3-512E2.2,RN7SKP110,RP1-45N11.1,PNISR,SLC16A10,FAM229B,FAM184A,HSF2,RNF217-AS1,THEMIS,PTPRK,EPM2A,GTF2H5,LINC01624,DLL1,AC093627.9,PRKAR1B,LSM5,YAE1D1,SUGCT,COA1,TPST1,MAGI2-AS3,SEMA3A,GAL3ST4,NRCAM,LRRN3,POT1-AS1,CEP41,MEST,AGBL3,UBN2,TRBV2,TRBV4-1,TRBV6-2,TRBV9,TRBV11-2,TRBV6-5,TRBV7-6,TRBV5-6,TRBV7-9,TRBV13,TRBV12-4,TRBV14,TRBV15,TRBV19,TRBV23-1,TRBV27,TRBV29-1,EPHA1,EPHA1-AS1,RP4-800G7.2,ATP6V0E2-AS1,BET1P1,ATG9B,AC145124.2,MICU3,RP11-468H14.2,MTUS1,NKX3-1,EPHX2,SARAF,PLAG1,PDE7A,LACTB2-AS1,PKIA-AS1,RP11-267M23.1,ANKRD46,GAPDHP62,AF230666.2,RHPN1,WDR97,GLIS3,SPATA6L,CDC37L1,RP11-70L8.4,RP11-70L8.5,C9orf131,NPR2,PCSK5,RP11-575L7.4,SEMA4D,LINC00476,ERCC6L2,ZNF883,STXBP1,RP11-228B15.4,RP11-203J24.8,SLC25A25-AS1,PRKCQ-AS1,RP11-554I8.1,CDNF,CUBN,SLC39A12-AS1,THNSL1,ANKRD26,ZNF37A,H2AFY2,CFAP70,CFL1P1,PLCE1,SFRP5,OLMALINC,MFSD13A,SFXN2,RBM20,RP11-317F20.3,RGS10,IKZF5,BNIP3,PGGHG,RP11-326C3.11,RP11-326C3.12,RP11-326C3.15,TNNT3,DNHD1,DCHS1,TMEM41B,DKK3,PDE3B,NUCB2,DEPDC7,RP11-484D2.3,AGBL2,RP11-655C2.3,CD248,SLC29A2,CARNS1,PLEKHB1,CAPN5,DLG2,MAML2,ATM,C11orf65,EXPH5,LAYN,C11orf1,DIXDC1,TMEM25,AP002954.4,OAF,CRTAM,ROBO3,CDON,MIR4697HG,THYN1,IQSEC3,NRIP2,RP11-277P12.20,KLRK1,KLRC4-KLRK1,KLRC4,RP11-291B21.2,MAGOHB,C12orf60,ETFRF1,ABCD2,NELL2,AMIGO2,PCED1B,FAM186B,ASIC1,KRT72,KRT73-AS1,KRT73,RP11-983P16.2,SOAT2,TMEM198B,PMEL,ERBB3,KIF5A,GLIPR1L2,LINC01619,USP44,RP11-181C3.1,FAM216A,LINC01089,RP11-

	347I19.8,MLXIP,MPHOSPH9,ATP8A2,SHISA2,LINC00598,MTRF1,NAA16,LINC00562,LINC00282,LINC00402,TBC1D4,LMO7,RBM26,RBM26-AS1,CCR12P,MCF2L,LINC00565,SALL2,TRAV1-1,TRAV1-2,TRAV3,TRAV4,TRAV5,TRAV12-1,TRAV12-2,TRAV14DV4,TRAV12-3,TRAV17,TRAV19,TRAV20,TRAV21,TRAV24,TRAV25,TRAV27,TRAV35,TRAV38-1,TRAV38-2DV8,TRAV41,SLC7A8,PPP1R3E,SLC22A17,NUBPL,TMEM30B,ACTN1,PTGR2,YLPM1,FBLN5,DICER1-AS1,LINC01550,RP11-61O1.2,BCL11B,AL109767.1,WHAMMP3,MKRN3,NPAP1,PWAR5,PWAR6,WHAMMP2,APBA2,ADAL,STRCP1,TLN2,ZNF609,CPEB1,ADAMTS17,RP11-526I2.5,PRKXP1,PCSK6,DNM1P47,RP11-161M6.2,IFT140,LA16c-380F5.3,CLUAP1,LINC01569,TFAP4,NAGPA-AS1,CTA-276F8.1,CTA-481E9.4,CTD-3203P2.1,NKD1,RP11-44F14.9,RP11-44F14.10,RP11-44F14.7,RP11-44F14.6,AKTIP,PLLP,LINC00920,SLC9A5,PLEKHG4,RP11-96D1.8,DHODH,RP11-486L19.2,RP11-517C16.2,SNAI3-AS1,RP11-104N10.2,SMG6,SGSM2,PELP1,CLDN7,TNK1,ADPRM,TMEM220,TMEM220-AS1,RP11-214O1.3,KRT17P1,SREBF1,TOM1L2,KRT17P2,TRIM16L,LYRM9,CRLF3,NLE1,RP11-799D4.4,MMP28,PLXDC1,MPP2,CTD-2020K17.1,MAP3K14-AS1,MRPL45P2,B4GALNT2,NOG,PRKCA,PRKCA-AS1,FOXJ1,RNF157-AS1,RNF157,CTD-2357A8.2,RP11-334C17.5,RP11-21J18.1,RP11-411B10.7,DSC1,RNF138,GAREM1,RP11-158H5.7,DSEL,CTD-2541J13.2,CCDC102B,HSBP1L1,ADNP2,CTD-3113P16.11,CTB-31O20.2,TBXA2R,TMIGD2,ARRDC5,ACER1,ADAMTS10,ZNF559-ZNF177,ZNF491,ZNF69,ZNF563,LINC00663,CTC-559E9.5,GRAMD1A,TMEM147-AS1,CTC-360G5.9,FCGBP,AC006129.3,LYPD3,ZNF229,PPM1N,ZNF667,ZNF667-AS1,ZNF471,ZSCAN18,A1BG,CTD-2619J13.8,ZNF497,CTD-2619J13.9,SNPH,SIRPG,SIRPG-AS1,MCTS2P,RP5-1184F4.7,UQCC1,DLGAP4-AS1,ZHX3,FITM2,STX16,GID8,bP-21264C1.2,RBM11,N6AMT1,PAXBP1-AS1,SLC5A3,PDE9A,COL18A1,COL6A1,S100B,PRMT2,DSTNP1,DGCR6,P2RX6,AP000347.2,SEC14L2,RP4-539M6.21,PIK3IP1-AS1,PATZ1,SFI1,C1QTNF6,SSTR3,CBY1,RP3-370M22.8,MSL3,SCML1,CNKSR2,USP11,RP11-348F1.3,ZC3H12B,SLC7A3,ITGB1BP2,NAP1L3,TSPAN6,XKRX,ARMCX1,ARMCX2,GPRASP1,GPRASP2,BEX3,MORF4L2-AS1,NKAP,RHOXF1P3,RHOXF1-AS1,SMARCA1

CD4_naive	CA6,AGMAT,TCEA3,MDS2,RCAN3,LDLRAP1,MAN1C1,RP1-187B23.1,MATN1-AS1,ZFYVE9,HOOK1,CACHD1,AK5,SYDE2,FLJ27354,CNN3,AMIGO1,GSTM2,GSTM3,CHI3L2,BCL9,EFNA1,GPA33,CAMSAP2,MFSD4A,SUSD4,OBSCN,CHRM3-AS2,RP11-1086F11.1,RNF144A,LINC00954,DNMT3A,LCLAT1,PLEKHH2,TRABD2A,ANKRD36BP2,MAL,AC103563.9,NPAS2,EDAR,SH3RF3,FBLN7,TMEM177,ARHGEF4,RBM43,ACVR1C,CERS6-AS1,AC093818.1,PDK1,COL5A2,PLCL1,SPEG,SERPINE2,LINC01891,AC093642.4,CAND2,WNT7A,OXNAD1,RP11-415F23.2,RP11-415F23.3,RP11-415F23.4,RP11-158G18.1,SATB1-AS1,VIPR1,ALS2CL,TMIE,FHIT,SUCLG2-AS1,RP11-298C2.1,B4GALT4,RAB43,PXYLP1,AC069513.4,LINC01259,SULT1B1,LEF1,LEF1-AS1,RPL34-AS1,RP11-223C24.1,RNF175,FAM134B,IL6ST,FLJ31104,ANKRD55,GCNT4,SERINC5,CTC-458I2.2,RFESD,RGMB,NUDT12,CAMK4,AC010468.2,RAPGEF6,ACSL6,TCF7,NDFIP1,TIMD4,HAVCR1,CTB-4E7.1,RP11-91H12.1,FAM153B,FAM153A,SLC22A23,ADTRP,CARMIL1,ZNF204P,ZNF391,LINC00243,PRRT1,BACH2,RP3-512E2.2,RN7SKP110,MANEA-AS1,KLHL32,SLC16A10,FAM184A,GTF2H5,PARK2,ZNF815P,LINC00957,TECPR1,GAL3ST4,FAM185A,NRCAM,LRRN3,TRBV1,TRBV2,TRBV3-1,TRBV4-1,TRBV5-1,TRBV6-1,TRBV6-2,TRBV7-2,TRBV7-3,TRBV11-2,TRBV6-5,TRBV5-4,TRBV6-6,TRBV5-5,TRBV5-6,TRBV7-9,TRBV13,TRBV10-3,TRBV11-3,TRBV12-3,TRBV12-4,TRBV12-5,TRBV15,TRBV18,TRBV19,TRBV20-1,TRBV21-1,TRBV23-1,TRBV24-1,TRBV25-1,TRBV30,EPHB6,EPHA1,EPHA1-AS1,ATP6V0E2-AS1,GIMAP3P,AC145124.2,MTUS1,TNFRSF10D,CHMP7,EPHX2,SARAF,PLAG1,AC022182.3,PKIA,GAPDHP62,PCAT1,RHPN1,EPPK1,CYHR1,PLPP6,PCSK5,RP11-203J24.8,LAMC3,DBH-AS1,SARDH,AKR1E2,NET1,PRKCQ-AS1,RP11-554I8.1,ANK3,ARL4AP1,HKDC1,C10orf35,SFXN2,SORCS3,RP11-313D6.3,PDCD4-AS1,BNIP3,DCHS1,TMEM41B,LTBP3,CD248,PLEKHB1,ME3,MAML2,RP11-110I1.12,RP11-730K11.1,TMEM45B,RP11-664D1.1,LRP6,NELL2,RP11-493L12.4,KRT72,KRT73-AS1,KRT73,KRT18,PMEL,LINC01619,EEA1,SLC8B1,LINC01089,RP11-347I19.8,PITPNM2,LINC00282,LINC00402,TBC1D4,LMO7,RBM26-AS1,CCR12P,MCF2L-AS1,TRAV1-1,TRAV2,TRAV4,TRAV6,TRAV8-1,TRAV10,TRAV12-1,TRAV8-2,TRAV8-3,TRAV13-1,TRAV8-4,TRAV13-2,TRAV9-2,TRAV12-3,TRAV8-6,TRAV16,TRAV17,TRAV20,TRAV23DV6,TRAV25,TRAV26-1,TRAV27,TRAV29DV5,TRAV26-2,TRAV35,TRAV38-1,TRAV41,SLC22A17,ACTN1,FBLN5,C14orf132,LINC01550,RP11-61O1.2,AL109767.1,WHAMMP2,APBA2,ITGA11,HYKK,IGF1R,ADAMTS17,RP11-526I2.5,TMEM8A,RP11-161M6.2,TMEM204,LA16c-380F5.3,CLUAP1,LINC01569,GPRC5B,RP11-401P9.7,RP11-44F14.9,PLLP,LINC00920,RP11-297D21.4,SLC7A6,RP11-96D1.8,TNK1,ADPRM,TOM1L2,RP11-799D4.4,MMP28,PLXDC1,MAP3K14-AS1,NOG,AXIN2,PRKCA,PRKCA-AS1,RNF157-AS1,RNF157,RP11-28G8.1,DSC1,HSBP1L1,TLE2,TMIGD2,SH2D3A,ADGRE4P,CTD-2666L21.1,ZNF563,ZNF506,ZNF599,LGALS17A,AC007191.4,CTB-12A17.2,NOSIP,ZNF582-AS1,RP5-1184F4.7,TSHZ2,RP11-15M15.1,CTD-3184A7.4,RBM11,N6AMT1,PAXBP1-AS1,PDE9A,SEC14L2,PIK3IP1-AS1,SSTR3,SCML1,CNKSR2,KLHL34,LINC01281,RP11-348F1.3,WNK3,ZC4H2,TSPAN6,XKRX,GPRASP1,BEX3,MID2,VSIG1,SMARCA1,CD40LG

CD8_TCM	RP3-477M7.5,ZNF683,CD8A,CD8B,ANAPC1P1,ARHGEF4,CCR8,ITGA1,GZMK,LRRN3,TRBV4-2,WDR86-AS1,LINC00824,STXBP1,DKK3,CD248,RP11-277P12.20,KLRC4-KLRK1,KLRC4,RP11-291B21.2,NELL2,SOAT2,IFNG-AS1,HNRNPA1P70,FGF9,LINC00402,TRAV24,TRAV27,TRAV38-1,MEOX1
CD8_TEM	MIB2,DRAXIN,ZNF683,SESN2,PODN,SLC1A7,LEXM,TGFBR3,EPHX4,FTH1P22,CD160,FCRL6,XCL2,XCL1,FASLG,COLGALT2,C1orf21,GS1-115G20.1,LGR6,LINC01871,TOGARAM2,RAB11FIP5,GNLY,CD8A,CD8B,ANAPC1P1,TFCP2L1,FAR2P2,MYO3B,NMUR1,LINC02084,EOMES,CMC1,CX3CR1,PROK2,PHLDB2,TIGIT,TPRG1,TM4SF19-AS1,TM4SF19,DGKQ,SPON2,RP11-20I20.4,JAKMIP1,RP11-539L10.2,FGFBP2,DTHD1,HOPX,SLC4A4,GZMA,ARHGEF28,ENC1,F2R,SLCO4C1,EFNA5,SH3RF2,PPP2R2B,KRT8P48,JAKMIP2,PDGFRB,SGCD,ENPP4,ENPP5,RCAN2,MYO6,RP11-73O6.3,GPR141,TRGC2,TRGJP2,TRGC1,TRGJP,TRGJP1,TRGV10,TRGV9,TRGV8,TRGV7,TRG-AS1,TRGV4,TRGV3,TRGV2,TRBV9,TRBV28,MYBL1,MSC-AS1,MSC,BNC2,CEP78,RP11-305L7.1,PTRH1,TTC16,C8G,CLIC3,ZNF365,FUT11,RP13-39P12.3,OSBPL5,CTSW,PRSS23,PDGFD,NCAM1,CRTAM,FEZ1,GLB1L2,B3GAT1,RP11-627G23.1,LAG3,VDAC2P2,BTG1P1,RP11-705C15.5,KLRF1,KLRD1,RP11-277P12.20,KLRC4-KLRK1,KLRC4,KLRC3,RP11-277P12.6,KLRC2,RP11-291B21.2,KLRA1P,STYK1,KIF21A,SCN8A,IFNG,RP11-81H14.2,RP11-81H14.1,CMKLR1,LINC00943,LINC00944,RAP2A,TRAV1-2,TRAV5,TRAV12-2,TRAV19,TRAV24,TRAV34,GZMH,GZMB,PTGDR,BATF,GPR68,IFI27L2,RP11-204N11.1,PATL2,PIF1,PRSS30P,GTF3C1,HMGB3P32,ADGRG1,HEATR9,ERBB2,TBX21,LINC02086,TSPOAP1,RGS9,KIF19,LLGL2,MXRA7,RPTOR,PTPRM,SMAD7,GZMM,ABHD17A,MATK,S1PR5,SERTAD1,SERTAD3,ATP1A3,SIGLEC17P,NKG7,CTD-2616J11.2,KIR3DX1,KIR2DL3,KIR2DL1,KIR3DL1,KIR2DS4,KIR3DL2,NCR1,CST7,APMAP,IGLV3-13,KIAA1671,TPST2,APOBEC3G,RP4-742C19.12,APOBEC3H,SYNGR1,TTC38,LANCL3,FRMPD3,F8
CD4_TEM	HDAC11,SH3RF2,SGCD,GLB1L2,TRAV14DV4,KIF19
Treg	TNFRSF18,TNFRSF4,MEGF6,TCEA3,ID3,MDS2,HPCAL4,CH17-472G23.4,RP4-791M13.3,TUFT1,PMF1-BGLAP,GPA33,F5,SELP,HMCN1,PRG4,TPR,RP11-21J7.1,KIF14,RRM2,RGPD1,RP11-1399P15.1,RGPD2,MAL,EDAR,FBLN7,RP11-399B17.1,PKP4,AC093818.1,TTN,CCDC141,PLCL1,CTLA4,ICOS,IKZF2,TMEM169,SGPP2,LINC01891,LMCD1,RP11-669C19.1,RBMS3,CCR4,CCR8,HNRNPA1P21,LRRC2,SEMA3G,CHDH,IL17RB,TIGIT,KALRN,LAMP3,MCF2L2,LEF1-AS1,RP11-223C24.1,RNF175,NEIL3,IL6ST,GCNT4,RGMB,GRPEL2,TIMD4,HAVCR1,MIR3142HG,FAM153B,FAM153A,ADTRP,PI16,SLC16A10,FAM184A,GPR146,ZNF815P,ICA1,CCM2,GAL3ST4,STRIP2,TRBV1,TRBV2,TRBV3-1,TRBV4-1,TRBV5-1,TRBV6-1,TRBV6-2,TRBV7-2,TRBV7-3,TRBV11-2,TRBV6-5,TRBV5-4,TRBV6-6,TRBV5-5,TRBV7-6,TRBV5-6,TRBV13,TRBV10-3,TRBV12-3,TRBV12-4,TRBV12-5,TRBV18,TRBV19,TRBV20-1,TRBV21-1,TRBV23-1,TRBV25-1,TRBV30,ATG9B,NEFL,CDCA2,PBK,DUSP4,PKIA,LAMC3,SARDH,IL2RA,RP11-428L9.2,MCM10,HACD1,STAM,RP11-342D11.3,RP11-521C22.2,ZWINT,RTKN2,FANK1,GLYATL1,LRRC32,SESN3,CASP1P2,CARD17,RNF214,TMPRSS13,DUSP16,IKZF4,LINC01619,PITPNM2,LINC00544,LINC00402,TBC1D4,TRAV1-1,TRAV2,TRAV3,TRAV4,TRAV6,TRAV8-1,TRAV10,TRAV12-1,TRAV8-2,TRAV8-3,TRAV13-1,TRAV12-2,TRAV8-4,TRAV13-2,TRAV9-2,TRAV12-3,TRAV8-6,TRAV16,TRAV17,TRAV20,TRAV22,TRAV23DV6,TRAV24,TRAV25,TRAV26-1,TRAV27,TRAV29DV5,TRAV26-2,TRAV34,TRAV35,TRAV36DV7,TRAV38-1,TRAV38-2DV8,TRAV41,TSHR,RP11-61O1.2,CRIP2,RP11-603B24.1,C15orf53,MYZAP,ACAN,HAPLN3,ZCCHC14,TRIM16,RP11-799D4.4,GSDMA,TOP2A,HAP1,CCR10,MEOX1,NOG,RNF157-AS1,TK1,LDLRAD4-AS1,TJP3,CEACAM4,LINC01727,BCAS1,PDE9A,PIK3IP1-AS1,SSTR3,RP11-265P11.1,LINC01281,FOXP3,PPP1R3F,FAAH2,LINC00891,BEX3,VSIG1

Tfh	TNFRSF4,TCEA3,MDS2,HPCAL4,KCNA2,CH17-472G23.4,GPA33,PRG4,TPR,MAL,LIMS1,LIMS1-AS1,LIMS3,FBLN7,ACVR1,NAB1,CD28,CTLA4,ICOS,TMEM256P2,PASK,PDCD1,AC093642.4,WNT7A,CMTM8,CCR4,ALS2CL,GPR15,TIGIT,MCF2L2,AC069513.4,RP11-223C24.1,ANKRD55,GCNT4,SERINC5,FAM153A,ADTRP,HIVEP2,ESR1,ICA1,TRBV1,TRBV2,TRBV3-1,TRBV5-1,TRBV6-1,TRBV4-2,TRBV6-2,TRBV7-2,TRBV7-3,TRBV11-2,TRBV6-5,TRBV5-4,TRBV6-6,TRBV5-5,TRBV7-6,TRBV5-6,TRBV13,TRBV10-3,TRBV11-3,TRBV12-3,TRBV12-4,TRBV14,TRBV15,TRBV18,TRBV19,TRBV20-1,TRBV24-1,TRBV25-1,TRBV30,GIMAP3P,MTUS1,AP3M2,FAM95C,ZNF483,SARDH,RP11-342D11.3,ARL4AP1,GOLGA7B,RP11-106M7.1,CARD17,CXCR5,TMEM45B,DUSP16,ST8SIA1,MORN3,RP3-446N13.3,LINC00544,LINC00402,TBC1D4,TRAV2,TRAV3,TRAV4,TRAV6,TRAV8-1,TRAV10,TRAV12-1,TRAV8-2,TRAV13-1,TRAV12-2,TRAV8-4,TRAV9-2,TRAV12-3,TRAV8-6,TRAV16,TRAV17,TRAV20,TRAV22,TRAV23DV6,TRAV25,TRAV26-1,TRAV27,TRAV30,TRAV26-2,TRAV35,TRAV38-1,TRAV38-2DV8,TRAV41,C14orf132,RP11-554D20.1,FBXL8,MAF,CDK5R1,RP5-1028K7.2,DNAI2,LDLRAD4-AS1,ISM1,LINC01727,TSHZ2,RP11-15M15.1,CACNA1I,RP5-1158E12.3,RP11-348F1.3,FAAH2,LINC00891,BEX3,VSIG1,CD40LG,
Th1/Th17	TNFRSF4,FAAHP1,DAB1,IL12RB2,SLC44A3-AS1,EMBP1,RORC,AL450992.2,B3GALT2,RP11-21J7.1,CFH,HSD11B1,GREM2,RP11-1399P15.1,FBLN7,KIF5C,SLC4A10,DPP4,CHN1,ADAM23,MB21D2,PTPN13,ZDHHC11B,AC138517.6,SLC17A3,CLIC5,ELOVL4,SOGA3,CCR6,TRBV2,TRBV18,WDR86-AS1,LZTS1,LINC00824,ZNF462,RP11-342D11.3,TSPAN15,ADAM12,PARVA,TSPAN18,DUSP16,METTL21B,TRAV8-1,TRAV8-4,TRAV9-2,TRAV16,TRAV20,TRAV23DV6,TRAV26-1,TRAV35,TRAV38-1,TRAV41,RP11-554D20.1,FBXL8,ACE,PLPP2,IL4I1,LINC01644,LINC00892,CD40LG
Th2	TNFRSF4,RNF207,TCEA3,RP1-187B23.1,HYI,FAAHP1,NBPF13P,PDE4DIP,SUSD4,CFAP36,MAL,FBLN7,RP11-399B17.1,ACVR2A,AC020571.3,ICOS,ADAM23,SNED1,WNT7A,CCR4,CCR8,HNRNPA1P21,ALS2CL,CHDH,IL17RB,FHIT,KALRN,RPL5P13,RP11-223C24.1,RP11-18H21.1,TRIM2,TPPP,ZDHHC11B,ZDHHC11,SEMA5A,ANKRD55,GCNT4,THBS4,CDO1,PI16,KIAA0408,GPR146,ZNF815P,INMT,EEPD1,TRBV4-1,TRBV5-1,TRBV7-2,TRBV11-2,TRBV5-4,TRBV6-6,TRBV5-5,TRBV5-6,TRBV13,TRBV10-3,TRBV12-3,TRBV18,TRBV19,TRBV25-1,NOS3,ATG9B,WDR86-AS1,MFHAS1,NEFM,NEFL,PKIA,SIGMAR1,GALT,IL11RA,FAM95C,ZNF462,ZNF483,SARDH,RP11-428L9.2,RP11-342D11.3,RTKN2,ZNF365,ZMIZ1-AS1,FANK1,NRIP3,TSPAN18,PTGDR2,RP11-356J5.12,RNF214,RP11-730K11.1,ARHGAP32,MIR4697HG,RP11-664D1.1,PKP2,KRT1,LINC00402,MYO16,TRAV6,TRAV8-1,TRAV10,TRAV8-2,TRAV8-4,TRAV9-2,TRAV12-3,TRAV8-6,TRAV16,TRAV17,TRAV23DV6,TRAV25,TRAV26-1,TRAV30,TRAV26-2,TRAV41,C14orf132,CRIP2,HAPLN3,RP11-161M6.2,PLLP,TRADD,FBXL8,CCR10,MEOX1,AXIN2,PRKCA,LINC00511,ST6GALNAC1,TNFRSF11A,AC092566.1,LSR,LGALS17A,LINC01727,EDN3,TIAM1,CBR3,RFPL2,CACNA1I,CRLF2,RP5-1158E12.3,FAAH2,LINC00892,CD40LG,MAMLD1,IL9R

CD8_TEMRA	CMC1,NKG7,CCL5,GZMH,CST7,GZMA,B2M,CD8A,GZMM,HCST,CD8B,PFN1,KLRD1,HLA-B,CTSW,HLA-A,C12orf75,CD3D,PRF1,KLRG1,CD160,IL32,LYAR,CD99,SH2D1A,PLEK,SH3BGRL3,CCL4,KLRF1,TMSB4X,FGFBP2,HLA-C,FCRL6,HLA-DPB1,LAG3,MT-CO1,PTP4A2,PTPRC,MYO1F,PTPRCAP,ARPC5L,MATK,SLAMF7,RARRES3,CLIC1,CYBA,CFL1,CTSC,PYHIN1,PSMB9,EOMES,GUK1,EFHD2,RAB27A,ARPC2,APMAP,MYL6,PPP2R5C,SAMD3,CHST12,PTMS,ACTB,CD3E,C1orf21,MALAT1,ITGB2,IFITM2,CD2,MYL12B,MYL12A,PPP1R18,ITGAL,C9orf142,RAP1B,STOM,MIAT,PPP1CA,RHOC,CRTAM,LCK,CORO1A,ABHD17A,CALM1,ABI3,FYN,CD3G,PSME2,MT-CO2,SYNE1,FLNA,TSEN54,MT-CYB,LITAF,AOAH,ZBTB38,RASAL3,MT-ATP6,TMA7,IFNG,RNF213,GSTP1,APOBEC3G,SSBP4,JAKMIP1,HOPX,MYO1G,IDH2,TIGIT,PSME1,SRGN,MT-ND5,SERF2,SLC9A3R1,LPCAT1,RNF166,RAC2,RASSF1,MBP,BIN2,S100A4,UBL5,ARHGAP30,MT-ND2,PPP2R2B,LSP1,PRKCH,OAZ1,MFSD10,ANXA6,FCGR3A,XCL2,ARPC1B,FAM49B,ZAP70,KLRB1,EMP3,LCP1,AKNA,STK17A,MAPK1,HLA-E,ZEB2,CALR,IFI6,MSN,SYNE2,PDGFD,ISG15,MT2A,C5orf56,COL6A2,GAPDH,TPST2,WIPF1,SHISA5,PITPNC1,SASH3,GNG2,S1PR5,HLA-F,LY6E,CAPZB,CD53,CD244,SRP14,FMNL1,GAB3,DTHD1,PARK7,SH2D2A,TAP1,CHI3L2,MYBL1,P4HB,MT-ND1,SRSF9,ACTN4,TSC22D4,COX8A,NEDD8,SEPT7,CD81,PTPN7,ARPC4,PPIB,CLIC3,CAPN2,RAB37,PLA2G16,RNF167,ARF6,NDUFA1,SUN2,RHOF,DBI,MT-ND4,MSC,CD63,C19orf43,GRAP2,RUNX3,HENMT1,ARHGDIB,SRPK2,PATL2,CLEC2B,TAPBP,PSMC4,SRI,RPS6KA1,GNLY,PPP4C,YWHAQ,PTPN22,PDIA3,PSMB8,APOBEC3C,IL2RG,CHCHD2,EBP,CAP1,GABARAPL1,SIPA1,CDKN2D,GPR56,IL10RA,PSMA7,PTPN4,ACTG1,BATF,RORA,ID2,GFI1,CD52,MAZ,RNF126,DGKZ,MT-CO3,TCEB2,BTN3A2,ITGB1BP1,DNAJC1,THEMIS,PPDPF,OPTN,CX3CR1,CISD3,MYEOV2,MOSPD3,BSG,LMAN2,PPIA,PDCD1,TMEM160,TAOK3,RAP2B,TNFSF14,HSP90B1,CCDC88C,FKBP11,FBXW5,TLN1,TBCB,MRPL43,DDX46,AKAP13,TGFBR3,MYO6,HSPB11,DENND2D,RER1,NDUFA6,RBCK1,PTGDR,ARAP2,NDUFA3,CDK2AP2,SPON2,CIB1,CD97,ARL4C,USP28,SCP2,PTPRA,ACAP1,RALGDS,PDLIM2,ARF1,GIMAP7,ARRB2,CBLB,USMG5,SHARPIN,NDUFS6,LAT,RABAC1,F2R,SUB1,MT1X,NFATC3,SERPINB6,FAM96B,REEP5,VIMP,TBX21,TC2N,IFI35,SH3BP1,GLCCI1,GGA1,ARPC3,RAB9A,POMP,SSNA1,CFLAR,WNK1,IL12RB1,B3GAT2,C6orf1,NDUFB8,STK10,ITGB1,MRPL10,POLR2G,BTBD6,ARHGDIA,ACADVL,DOK2,CD84,ANKRD32,GBP5,TBC1D10C,PCSK7,ATP5B,MRPS7,ATP5E,CCDC107,TSPAN17,CCR5,DRAP1,CARD8,DPM3,TXN,FKBP8,ROCK1,DIAPH1,DEK,TNIP2,GIMAP4,NMRAL1,ARL5A,ECH1,SH3KBP1,SEC61G,MAP2K2,KIF19,PLEKHF1,MCOLN2,STAT4,MFSD11,C9orf16,GATAD2A,RNF187,RNPEPL1,TTC38,YARS,ZNF655,NLRC5,YPEL1,NDUFB10,COPE,NCK1,PARP8,TRAPPC1,ATP5J2,SHFM1,ATXN1,TMED2,PIN1,AKR1B1,CCDC85B,PRELID1,TPRG1,PRR5L,SYTL3,RAB5C,EIF5B,CDKN2A,MAP4K1,ADRB2,PYURF,JAKMIP2,TOX,TRAPPC4,RNF7,VPS53,AHNAK,PSTPIP1,ADRM1,BAX,JTB,DNAJC8,SNRNP200,RAB6A,PIP4K2A,NDUFS8,NDUFB7,CD247,HMBOX1,SH3BGRL,ITPA,FLOT1,TPM3,IRF3,SLC25A24,SPN,KIAA1671,SUPT4H1,COPS6,RABL6,NPDC1,PARP10,UBE2N,RBBP7,RALY,RAB1B,MLLT6,GPR65,FEZ1,EPS15,UBXN4,ARHGAP25,LCNL1,CASC4,LPXN,ZBTB7A,RNF4,CKLF,CLDND1,CDC37,DPP7,C19orf24,EML4,SIT1,PSMA5,FAM160A2,APBB1IP,BCL7C,PKN1,BZRAP1,TRIM69,DERL2,ANKRD36C,DHX29,CDC42,TTC28,WDR1,PROSER1,C21orf59,SPCS2,RSU1,CANX,TMEM258,CYTH4,PIF1,FAM217B,PSMB3,AP2B1,ZNRD1,PPP3CC,CD320,S100A10,CMTM3,OST4,ZNF428,TBC1D9B,SIGIRR,HN1,ACTR3,PSMB2,EMB,SSR4,ENSA,SNRPB,USF2,UQCR11,TTC16,MVD,SLC27A3,C19orf66,FAM219B,INPP4A,FAM173A,UQCR10,ITGB7,RASSF5,PILRB,CNOT6L,ATP2B4,DDX58,LSM12,ATG2A,FBXW2,MRPL41,NFAT5,RASGRP1,EMD,NFATC2,DERL1,FBXO6,SNRPD1,PTTG1,PRKCB,MXD4,DHRS7,NSG1,ZRSR2,GLS,ZSWIM8,MYH9,KIAA1109,TNF,MECP2,KDM5B,ORMDL3,CCND3,STK4,BCL9L,EML3,TMBIM6,ARIH2,STK38,SRRT,RNF168,TMEM181,HSD17B10,TCEA1,ABHD14A,CHN2,CALM2,ERLEC1,APOBEC3H,NUCB1,PSMB6,AFF4,COPZ1,XIST,VDAC3,CABIN1,MIEN1,BTN3A1,ATP5G3,FAM107B,WDR83OS,RHOA,BCAP29,NCALD,SUPT16H,KIF21A,SMKR1,NAPA,LAGE3,AP2M1,PTPMT1,PTPRE,PTRH1,SLFN12L,PRR13,M6PR,DGKQ,LRRFIP1,UPF2,ITGA4,BUB3,TMED9,CHMP1A,ISOC1,RTF1,PHF1,ARL6IP5,HNRNPA3,GPS1,TMEM203,SEC11C,BIN1,PEF1,MAF1,VGLL4,SLAMF1,MAGED2,FAM134A,KRAS,CLTB,RECQL,STUB1,TRPV2,SRSF4,TMEM59,SIVA1,ZDHHC24,C1

	6orf13,NAA10,CYB561D2,FDPS,TBKBP1,CIZ1,SDF2L1,CD300A,POLR2L,BROX,TGFB1,TAF8,FCRL3,TUFM,ERAP1,ATP11B,PYCARD,PTRHD1,ST6GALNAC6,EIF5A,NEK7,MESDC2,ZNF276,ISG20L2,MYCBP,CHD8,PTPN18,ARHGEF1,PSMA3,TSG101,B3GAT3,PDS5A,ICAM3,ORAI1,C11orf21,HIGD1A,PHF11,SAMHD1,FERMT3,MAPKAPK2,RFTN1,PSMD4,BZW1,POP4,CCSER2,ABI2,CD2BP2,TMEM109,UBE2E3,GLTSCR1L,PQLC3,EID1,RGS3,HNRNPA2B1,BAZ1B,CASP1,SF3B2,SMARCE1,SRPR,C19orf10,ASCC3,MICU2,PPM1A,EIF6,CALM3,SELT,TMEM147,SEC61B,RAD9A,WBSCR22,BLOC1S1,MAP3K8,ENC1,PSMC1,PGP,VPS28,ISCU,NTAN1,TCF25,HSPA5,GPI,TXNDC15,UBE2L3,VPS26B,DHX38,PMVK,SYT11,TBPL1,ZFAND6,CLASP1,FAM126B,U2SURP,PDRG1,TMEM126B,CLEC2D,ERH,ASXL1,DNM2,FBXO7,RPA2,NCL,BAZ2A,EZR,EWSR1,HMGN3,RBM15B,ASNSD1,MT-ND3,CALHM2,TXNIP,CDC25B,SIRT2,D2HGDH,CNOT4,EMC4,GTDC1,RAB7L1,CDC42EP3,MAP4,TIMM22,GSDMD,SNAPC2,GTF3A,GPKOW,TAGLN2,ADAR,QDPR,UBE2M,C19orf70,ZBP1,ANAPC11,MGA,C6orf47,NUB1,CDV3,FTSJ1,RELA,RNF169,ARL1,PINK1,SNF8,CRLS1,CARNS1,MED15,LMAN1,RNF34,TRAPPC3,NUDT19,CC2D1A,LSMD1,PPP2R5A,TMEM165,GLTP,LPP,VPS4A,CLN3,URI1,AURKAIP1,ZNF420,TERF2IP,CCDC124,TEX264,NME6,GTF2E2,FUS,SLA,DGCR6L,ADSS,MTCH1,HIVEP3,SEP15,C19orf12,KXD1,MAP1LC3A,MACF1,NCOR1,WDR45,CEP78,PSMD8,SCOC,EID2,IGFBP3,TMX1,TPD52,GPAA1,PSMA1,MGAT2,POLR2F,TMUB2,UBAP2,DTD1,SRM,SURF4,NUDCD2,RCN1,AAED1,COPB1,SLC25A3,RNF115,DNAJB11,FAM179A,CYB561D1,ARL6IP1,KLRC2,MRPS23,SNX5,C11orf58,RBM25,KLC1,LSM1,GPR108,MIF4GD,CNPY2,SLC39A3,PSME3,RXRB,SRRM2,SPSB3,ADAM8,RFXANK,GOSR2,MRPL36,DCAF5,PEPD,AGO3,ATP6V0E1,EXOG,CNPY4,MRPS6,CCDC53,ANXA1,RALBP1,S1PR1,NAGPA,HNRNPL,HCLS1,ACBD5,SLC35A4,ATP8A1,PSMD11,ATG12,TXNL4A,ATXN2,ARHGAP9,CMC2,CBX4,PURA,UTRN,SEPW1,PRKACB,DECR1,CFDP1,NIPSNAP1,YEATS2,ABHD12,HAUS6,CCDC102A,PHAX,PRKAG1,SEPT2,RBX1,IFIH1,ATP2A3,VAMP5,PTCD1,SNX17,TADA3,CHPF2,TCEB1,BCL7B,VTI1B,COA1,CCZ1B,GBP2,TMEM120B,GXYLT1,TMEM128,PTBP1,ATP5I,GNL1,ABCD4,PSMA4,RPN2,DCAF8,MIB2,METRN,UBR5,MT-ND4L,LYST,CDC5L,CYTH1,NDUFS3,DAPK3,PDZD4,THAP4,IRF2BP1,ITGAM,OASL,RNF8,TMEM259,PWP1,KCNAB2,G6PD,SGCD,ZMAT5,LGR6,ZC3H18,NDUFB9,CCDC22,ZNF827,GYG1,DUSP23,NDUFA13,SAMD9L,PABPN1,XRCC5,C6orf226,SSR2,PTGER2,KLHDC2,COX16,GOLGA4,MXRA7,SCAMP3,BCL2L1,LIX1L,INPP5D,PHF14,GFM1,ASCC2,NSMAF,CXXC11,PRDX2,CARHSP1,BMI1,MANF,CDC42SE1,PAK2,HPS1,GLO1,USP25,SIAH2,CUL3,PLEKHA1,IKBKB,MAD2L2,DNAJC5,KPNB1,CHD6,MRPL51,CUL2,NUDT21,PNKP,DDX23,TNFSF12,C1orf61,TMX4,GLOD4,ZCCHC6,KMT2A,MMAB,SLA2,SMUG1,KAT7,UBE2V2,DDX39B,COMT,PGAM1,CLINT1,BRD2,ARHGAP18,CHMP4A,CEP164,PDCD6,RNF6,TAX1BP1,RANGRF,PIGH,GRK6,HSD17B7,CAPZA1,IQGAP2,SPATA13,ABHD2,RMND5A,ACO2,ROMO1,DCTN2,TRPM7,MRPL16,KANSL3,AIP,CASZ1,SEC13,VPS13A,PRR14,DENR,DR1,PRMT2,MMP23B,TMUB1,HDDC2,PDIA4,CSK,ATPIF1,APOL1,SLFN5,FIBP,YWHAB,CRELD2,UPF3A,ADAMTS6,PLEKHJ1,KPNA1,HEXDC,GPR137B,FAM8A1,ANAPC7,R3HCC1,YIPF3,HMBS,CDK5RAP3,SLC25A36,TTC13,AIFM1,TMEM50A,SMG6,SNX11,C19orf48,CHMP2A,ARL3,DCAF11,CADM1,STARD3NL,PICALM,UTS2,PUF60,MARCH2,ANXA2,SNRPC,KLF3,C2orf76,ELOF1,YPEL3,C22orf39,AGPAT1,RBL2,RAB11B,SCML4,C7orf49,LMNB2,PRMT1,NCOA1,CTDSP1,NDUFA12,RRP1B,ISY1,DAZAP1,MPST,FIS1,TMEM9B,TAP2,EPG5,RCBTB2,DPM2,PHB2,COQ9,LRBA,FAM53B,ARHGAP26,CYC1,FBXL6,NDUFS7,C14orf142,VEZF1,HDAC10,CMTM7,VOPP1,SMYD3,DCTN3,UPF3B,ATG4D,NRD1,MRPL11,MARK3,KIF1B,RPN1,SLAMF6,PPP2CA,CAPNS1,AGA,ASNA1,UBE2I,SVIL,GNPTG,PPP5C,WAS,SSU72,PRR5,ATP6V1F,LAMTOR2,CLPTM1,BAZ2B,FAM89B,YIPF4,STK24,TMCO1,KRTCAP2,LY9,LAMTOR5,ABCF1,UCHL5,MKLN1,C11orf30,TAPSAR1,WSB2,MRPS16,NAA50,NDUFB4,OTUB1,FASLG,KLHDC3,RNF220,SEC24C,GHITM,APOBR,TBCD,PHB,GLRX3,CEP85L,PSMD7,MARK4,VAMP2,PARL,SERGEF,COPS8,PPP1R12A,GOLPH3,ANXA2R,EFHC1,PCBP4,FAM98B,TOR2A,ZNF384,HAGH,TMEM222,TANK,PXN,FGFR1OP2,CMIP,GFER,ELOVL1,PELP1,MEAF6,NELFCD,ZDHHC7,YKT6,GPR114,USP1,RNF216,RNF5,OFD1,YIF1A,APOL6,CINP,ADIPOR1,TUBA4A,SULF2,DONSON,ARPC5,POLR2J,EGLN2,THOC1,SEPT1,UROS,ARRDC1,CCNDBP1,BPTF,MAEA,DCTN5,CRYZ,RPS6KB2,PLCB2,EDF1,DYRK1B,LAMTOR1,HSPA6,SLC20A1,STX18,UPP1,KIR3DL2,RBM3,BLOC1S4,TNIP1,MAP1LC3B,HDDC3,DPP8,SMARCC2,RBM4,DKC1,ELAC2,BCR,FNIP1,MLF2,CALCOCO2,PDLIM1,POLR3GL,CEP44,TRAPPC2,PPP1R8,GNAO1,DBN1,NPRL3,GADD45GIP1,PIK3CG,TMEM50B,BOD1L1,MAP4K5,CAMK2G,TRIM8,COQ4,GSTK1,SRP9,DHX30,ATE1,DDB1,BIRC6,RRP9,CCND2,PSMD13,VPS26A,CROCC,USO1,CACNA2D2,RABGAP1,DNAJB6,SYNRG,VASP,EEF1E1,POLR2C,LLGL2,POLR2I,IMMP1L,LAP3,SHKBP1,ARID1A,ADA,VW

	A9,TAOK1,FAM160B2,ABCA2,TIMM17A,ARPP19,MEF2D,PNKD,HIGD2A,XRCC6,CELF2,RPA1,ERBB2IP,HEXA,CTNNBIP1,HMGB1,SAR1A,SYMPK ,DIP2A,NHP2,SGK3,MAGIX,SLC7A5,LRP10,TRAPPC10,FNBP4,NDUFB2,SLC25A39,MLEC,SKIV2L2,VAV1,GNGT2,PHKG2,GALNT1,RGS19,SKA2,N ME3,SLC25A4,IFI16,GIPC1,PSMC5,TEN1,TMEM39A,EXOSC9,PSENEN,CCSAP,SRP54,RHOT2,CHD3,ATG5,TNIK,ZDHHC18,CBX7,BRMS1,DYNLRB 1,ABI1,TMC6,CD58,NHLRC3,CDC42SE2,EIF2B2,GLT8D1,NMI,TM2D1,CNOT11,TSR3,PRPF18,CDK5,EMC7,GNB2,MGST3,HP1BP3,SLC52A2,CAS P8,MEA1,NPRL2,COX7A2,SCD5,TNFRSF1B,CEBPZ,DPH7,MRPL37,USP48,SP4,SCAPER,HDAC11,RAB4B,DENND4C,RGS9,RSAD1,ADRBK1,MTER FD2,C22orf34,TBCC,RPS19BP1,AAK1,APOA1BP,TMED10,PHIP,SLC2A4RG,RNF19A,EDRF1,NCOA7,ACTR10,HERPUD2,ATG16L1,ITCH,ODF2,TCE RG1,SDHC,OS9,RAB11A,BAZ1A,POR,RAB22A,PKD1,IER3IP1,GLUL,SDHA,MCUR1,B4GALT4,ING4,ARGLU1,NDUFAF4,ST3GAL4,CAPN1,PCCB,AP H1A,MT1E,PEX16,SLC35C2,TSPAN31,SIRT7,PRSS23,GSK3B,PDCD10,HMHA1,MFNG,PPP1R35,LAX1,NSD1,MARCH5,SUDS3,ACIN1,DDX6,SLC3 9A6,MNT,USB1,CCDC69,COX17,SKAP1,GRSF1,SEC23B,AGTPBP1,WEE1,PTBP3,PRKCI,LASP1,MRPS10,PRPSAP1,NCKAP1L,GABARAPL2,IRAK1, GRIPAP1,VKORC1,MGEA5,KEAP1,C17orf62,C15orf40,KDM1A,RAPGEF2,PDIA6,CREB3L2,MUS81,HSPA13,MRFAP1L1,FN3KRP,LBR,ILK,CIAO1, ARHGEF3,CCDC82,FAS,PRDM1,EIF3A,TRAPPC12,ELP3,CDADC1,SRA1,ALKBH5,SLC4A4,OTUD5,MRPL20,GNAI2,UBXN7,RAPGEF1,MVB12B,ZBT B44,NARFL,COMMD7,PPIH,AP2S1,CHTOP,NDRG1,NDUFB3,IFI27L2,SCNM1,RCN2,UHMK1,GALNT11,SLC7A6OS,UBA7,PIGT,PSMD6,MESDC1,F YTTD1,CRYZL1,TMBIM1,PSMD9,CSNK1G2,ACTA2,CLIP4,ANKRD39,NDUFAF6,PAFAH2,ALDOA,POLR2K,ELMOD3,YWHAZ,CD46,DSTN,RAP1A,T BRG1,BCAT2,RNF149,MAPK13,KIAA1143,SCAMP2,DDX52,MKNK1,NIPBL,FCF1,GALNS,TGIF1,CPQ,TMEM138,MED17,PSMA6,WDR83,MRPS9, SYTL1,TBC1D19,SMARCC1,USP9X,RUVBL1,RBL1,SLTM,USP8,NIT2,MRPS15,NDUFA4,TXN2,TMEM30A,CD6,UQCRQ,TYK2,CCDC97,ZFPL1,TME M230,MAGOH,MRPS11,MRPL14,GDE1,AAGAB,TAF12,CASC3,GSK3A,UNC13D,PIK3R2,KIF22,PNPLA6,EIF3J,PLEKHA5,SNRNP70,FAM208B,CCN L2,ZFYVE16,LPIN1,KLHL20,COMMD1,TESC,C1orf216,PPP2R5E,BCKDK,ANAPC5,TP53TG1,WIPI2,CLK3,PLCD1,GTPBP6,IKZF1,PCNX,PSMC3,GE MIN7,C21orf2,TSPAN5,MAP7D1,PPP2R2A,MAP2K1,DNAJC7,IARS2,ADAP1,SYTL2,AZI2,C14orf1,TSSC4,RRAS2,CYB5B,H2AFV,PITHD1,SUMO1, CHIC2,GNG5,POLR2M,PITPNM1,CDIPT,ACSL5,RBBP4,UBE2A,PPARA,METTL13,TRPT1,MRPL22,TRMU,FDX1,AKR7A2,EI24,SNRPD2,EIF4ENIF1, RBM8A,FAM120AOS,ARHGAP35,HSPA9,ZNHIT1,GIT2,FAM58A,TMEM237,PCBD1,GNB1,TMEM106C,MEX3C,MTFP1,GANAB,UBA3,MAT2B,B RI3BP,EIF2AK2,PFDN6,COX5A,PHTF1,YAF2,SPATS2L,PRRC2A,RPAIN,CDK11A,SF3B4,TM9SF3,GPANK1,HLCS,DDX24,SMAD3,GAK,TSSC1,TWF2, SPNS1,RBM22,TNFSF9,TMEM11,ZNF28,HNRNPC,THOC7,ISOC2,DDHD1,LYPLA2,CCDC88B,ATP6AP1,RBM34,TTC17,ATP5J,LAIR2,ZBTB8OS,NK TR,TOX4,BRD9,MDH1,RBM33,EIF4G3,ADD1,CCNK,OSBPL9,TPP1,ZMPSTE24,RMDN3,SH3GLB2,ACAD8,IDH3B,SF3B14,LRRC45,TMEM223,DOC K11,STK39,TPI1,AKT1,LTBP4,TGFBR1,MCTP2,DHCR7,LAMP1,PRKAR2A,RAB8B,SLC12A9,SPATS2,AHSA2,PARP15,MRPL19,ZNF746,SLFN11,DN AJB14,EDEM2,MAD1L1,SLC38A10,MEI1,RPL26L1,RNPS1,GALNT3,STAG2,UBE2G1,OAS2,IBA57,PDAP1,ITGAE,CISD2,GART,CDKN2AIPNL,RELL2 ,SGMS1,UBA5,FZR1,TAF7,GTF2A2,MRPL24,CPSF3L,CCDC28A,IFITM1,SMG1,SNAP47,TMEM199,ENOPH1,SARS,DNAJC9,MPHOSPH10,DYNLL1 ,MADD,SNRNP27,CASP7,MRPL28,RITA1,CHCHD3,C6orf89,RNF145,C17orf59,RICTOR,HARS,NENF,TINF2,ATPAF1,CGGBP1,PTGES3,TAF15,POP 7,ST8SIA4,YY1,BRD3,SAP30BP,SETD2,HUWE1,ARL8A,WDR46,WWP2,NDUFA8,PSPC1,DEF6,MRPL47,NEDD9,PSD4,FAM204A,CBR4,DYNC1I2, NAGLU,HDAC3,ABHD6,LYRM9,SPRTN,RPUSD3,DHCR24,ZFYVE21,USP14,DBT,OGFR,NAA40,CSRP1,SLC25A29,DUT,NSRP1,C20orf24,COPS7A, MFSD6,SETD1B,AKIRIN2,MOB1A,SNTB1,ARHGAP27,FAR1,GLG1,NCOA2,ATHL1,SNX14,ASH1L,GPN1,CASP4,MBNL3,RPL36AL,LYRM1,EXOSC1, ZC3H15,RAB3GAP2,SIK3,GPS2,FGFR1OP,AGO4,KDM5A,SH3GLB1,SERINC1,GPR132,HNRNPUL2,MED11,CUL1,RCE1,KLRC4,ANKRA2,USP33,T MEM189,DDX17,C15orf61,AP3S1,TBC1D20,SMAD7,NOL11,PPP1R7,RBM42,ATRX,SLU7,C7orf50,TPGS2,WASH4P,TUBA1B,RHOG,SBK1,STOM L2,DDX39A,C1orf122,DDX41,FEZ2,RHBDF2,NCR1,ZDHHC4,LSM7,LAIR1,MRPS17,ACP1,ENY2,AKAP8L,TMEM248,TAPBPL,ZNF362,ST3GAL2,IK, CHFR,NDUFA11,KIAA1430,MGRN1,CDS2,MAF,CTU2,SPCS1,GPM6B,ARSG,ANKRD44,GIGYF2,NCOR2,R3HDM1,PAPOLA,C11orf73,HUS1,CREB L2,TRMT112,RBM28,PRRG2,IMP4,SS18L2,SP100,GTF2H2,OGFOD3,ENO1,C11orf48,ZCCHC17,OSTC,KMT2D,SRSF11,IL2RB,PTK2B,FOSL2,PARP 4,NAA15,MOGS,REL,SDHAF2,CTR9,TXLNA,TMEM179B,ZCCHC10,DYNC1LI1,IKBKG,DCTPP1,TOP1,TSTA3,PTGES2,STRN,PET100,CYB5R3,RALA, RAP1GDS1,LRRC58,GALC,SDHD,LLGL1,UTP3,KLRC1,MRGBP,TERF1,ACAA1,UBE3C,CPNE1,ARF3,DOHH,GBP3,MED10,FECH,ZFYVE27,ADH5,CC

	DC12,BTN3A3,AGGF1,C6orf62,UNC45A,PHF23,FAM127A,MRPS5,COMMD2,KIAA2026,ZMYM1,ARL6IP6,PIN4,CYB5R4,CMAS,UBE2F,PBDC1,JPX,KIAA0319L,NUS1,CERS4,C1orf174,PSMD14,CAMK2N1,P2RY8,ARFGAP3,AGPAT4,C12orf29,HNRNPR,SF3B1,RSRC1,DDX10,C14orf119,C1orf123,CAST,UCP2,PRKRIR,JMJD6,MED4,STRA13,HDAC1,RIC8A,NIP7,GALK2,RAP2A,MUL1,RSBN1L,SNTB2,TMEM184B,ZADH2,PAIP2,SLC4A7,CNBP,LRIF1,C9orf69,PPP3R1,NFATC2IP,HRASLS2,CDCA4,YTHDF2,ATF6B,ZCRB1,EMC3,RPL39L,NINJ1,N4BP2L1,NLRP1,STK25,ATG4B,PHPT1,HPS3,RTFDC1,SLC37A3,GTPBP3,NBEAL2,RPIA,SAP30,HDGFRP2,FBXO3,GALNT10,MFAP1,HOTAIRM1,MTOR,TRPC4AP,EXOSC6,CCPG1,DDX60,TTC19,KLHDC4,RHBDD3,OSBPL8,ZBTB22,ZFAND3,PRPF38B,POLL,SMARCA2,SNX18,UBAC1,USP24,ETHE1,PLEKHA3,HERC2,ACTR6,MRPL48,ANXA11,SLC39A7,PRDX1,MST4,EXOC1,ERLIN2,DLG3,MSI2,TMED3,LTN1,PSMA2,OSBPL3,SP140,MAPK3,CCNH,CCDC47,RHBDD2,ING3,ZFP36L2,TUBB,MCRS1,RPL7L1,POC1B,ANKRD11,ABAT,TRAPPC2L,ARSA,TOP2B,SFXN3,COX6A1,EMG1,DDX19B,PRADC1,ASB15,SHPRH,TFDP1,SNX6,INSIG1,ZNF559,TRERF1,VRK3,PTPN6,CLPP,LTB4R,NAA38,PPIE,MRPL34,KATNB1,ZNF683,TOR1A,MAN1A1,SLC25A11,MRPL23,TSHZ1,TPGS1,AAMP,PRPF31,OSTM1,SH3BP2,RTN4,FNBP1,ATP5D,KIAA0040,DBNL,TMEM19,PRKCQ,ZFP64,MSRA,NUCKS1,VPS4B,ZCCHC2,ARPC1A,ATXN7,DPY19L1,ATP5S,MTMR2,APBA3,NDUFC2,SLC14A1,NQO2,IAH1,DPP9,LRRFIP2,CD164,SRPK1,NSUN2,RNF11,PRDX5,SPAG9,C1GALT1,LCOR,ARFGEF1,YDJC,HSPBP1,MORC3,ITPR2,PSMB1,MTERFD1,SLC38A1,CENPT,TRANK1,TSPAN32,CLIP1,SUCLG1,SCFD1,DNAJC3,TGOLN2,TNFRSF14,HNRNPF,ARNTL,CLSTN3,SFT2D2,HPGD,ELF2,EIF4E3,TBC1D31,PPP4R2,NUDT18,MCMBP,MRPS21,PPP6R2,TMEM2,NBN,GMEB2,NHP2L1,DDX19A,TAF11,PDZD11,KIAA1551,ARHGEF9,

GammaDelta	IL12RB2,EPHX4,CD160,XCL2,XCL1,FASLG,C1orf21,GS1-115G20.1,LGR6,IL18RAP,AC007278.2,AC007278.3,TFCP2L1,LINC02084,EOMES,CXCR6,CACNA2D2,SPTSSB,C4orf50,JAKMIP1,FGFBP2,DTHD1,TNIP3,GZMK,ENPP5,TRGJP2,TRGC1,TRGJP,TRGV9,RP11-121A8.1,TRGV8,TRGV7,TRGV2,MYBL1,CLIC3,NPDC1,RP13-39P12.3,CDHR1,PDGFD,ZBTB16,FEZ1,LAG3,HNRNPA1P34,VDAC2P2,LINC00612,A2M-AS1,BTG1P1,PZP,TPT1P12,A2MP1,LINC00987,RP11-118B22.4,KLRB1,KLRD1,KLRC4-KLRK1,KLRC4,KLRC2,KLRC1,AE000661.37,TRDV2,TRDJ1,TRDC,TRDV3,RP11-382A20.3,SYNM,PRSS30P,BOLA2B,UNC45B,TBX21,CYB561,KIF19,PLPP2,MATK,S1PR5,NFKBIB,SERTAD1,SIGLEC17P,KIR3DL1,RP11-445H22.3,AF131217.1,COL6A2,S100B,RP4-742C19.12,MIB2,GPR153,ERRFI1,DRAXIN,RUNX3,ZNF683,SESN2,PIK3R3,PODN,SLC1A7,LEXM,DHCR24,WDR63,TGFBR3,SYT11,FCRL6,SH2D1B,LINC01871,AC092580.1,TOGARAM2,VIT,GNLY,FAR2P2,AC009495.2,IKZF2,AC017104.6,NMUR1,CMC1,CX3CR1,TIGIT,MLF1,EIF5A2,TPRG1,TM4SF19-AS1,TM4SF19,DGKQ,RP11-20I20.4,SLC4A4,TLR3,GZMA,ARHGEF28,ENC1,F2R,SLCO4C1,EFNA5,EPB41L4A,PCDH1,PPP2R2B,KRT8P48,JAKMIP2,PDGFRB,SGCD,NCR3,SCUBE3,ENPP4,RCAN2,MYO6,AOAH-IT1,GPR141,TRGC2,TRGJP1,TRGV10,TRG-AS1,TRGV5,TRGV4,TRGV3,SRRT,BPGM,PGBD4P1,VIPR2,MYOM2,TOX,RDH10,KB-1396H2.2,BNC2,CEP78,RP11-305L7.1,PTCH1,LINC00092,RGS3,TTC16,RALGDS,C8G,IDI1,ZNF365,FUT11,DLG5,OSBPL5,CLP1,PLA2G16,CTSW,PRSS23,NCAM1,USP28,CADM1,CRTAM,GLB1L2,B3GAT1,RP11-705C15.5,KLRF1,RP11-277P12.20,KLRC3,RP11-277P12.6,RP11-291B21.2,KLRA1P,STYK1,KIF21A,IFNG,GNPTAB,NUAK1,CMKLR1,LINC00943,LINC00944,RP11-21K12.2,RAP2A,TRDV1,GZMH,GZMB,ATL1,PTGDR,GPR68,RP11-204N11.1,PAK6,PIF1,ADCY9,GTF3C1,ITGAD,HMGB3P32,ADGRG1,MVD,CHRNE,SLC47A1,SLFN13,HEATR9,AC069363.1,AC131056.3,ERBB2,ARL4D,TBKBP1,LINC02086,GNGT2,TSPOAP1,RGS9,LLGL2,MXRA7,ABHD17A,TUBB4A,PDE4A,SERTAD3,ATP1A3,NKG7,KIR3DX1,KIR2DL3,KIR2DP1,KIR2DL1,KIR2DL4,KIR2DS4,KIR3DL2,NCR1,CTC-550B14.7,CST7,APMAP,SCAND1,CNBD2,CYP24A1,RP4-800J21.3,IGLV3-13,SGSM1,KIAA1671,TPST2,SYNGR1,TTC38,MLC1,DGKK,ARHGEF9,KLHL4

MAIT	RP3-395M20.8,UBXN10,PIK3R3,FAAHP1,MKNK1,DAB1,IL23R,IL12RB2,ODF2L,SLC44A3-AS1,EMBP1,TDRKH,LINGO4,RORC,AL450992.2,THEM5,FASLG,B3GALT2,RP11-21J7.1,RP11-98G13.1,EEF1A1P14,CFH,NEK7,SIPA1L2,GREM2,LINC01871,AC092580.1,LINC00299,AC006369.2,CD8A,IL18R1,IL18RAP,AC007278.2,AC007278.3,GTDC1,KIF5C,TANC1,SLC4A10,DPP4,IKZF2,AGAP1,IL17RE,EAF1-AS1,COLQ,LINC02084,EOMES,FYCO1,CXCR6,CCR5,CACNA2D2,PLXND1,RAB6B,GYG1,ERICH6-AS1,GPR171,P2RY14,LINC00880,SPTSSB,PLD1,USP13,MAEA,RP11-539L10.2,ABCG2,DKK2,ELOVL6,ARSJ,SPRY1,ARHGAP10,HPGD,CTD-2313F11.1,GZMK,TMEM171,RASGRF2,CTC-505O3.3,PPP2R2B,ADRB2,GALNT10,DBN1,GFPT2,FLT4,RBM24,SLC17A3,NCR3,CLIC5,ENPP5,ELOVL4,TPBG,ME1,PRSS35,SESN1,RP11-787I22.3,PHACTR2,PHACTR2-AS1,CCR6,CYTH3,TRGJP2,TRGC1,TRGJP,TRGJP1,TRGV10,TRGV9,TRGV8,TRGV7,TRGV5,TRGV4,TRGV2,ABCB1,PCOLCE,TRBV6-1,TRBV4-2,TRBV6-2,TRBV6-4,TRBV15,TRBV21-1,WDR86,WDR86-AS1,ENPP7P1,BLK,RPS3AP34,MYBL1,CA2,FSBP,MATN2,TBC1D31,CASC8,VLDLR,ARHGEF39,TLE1,ROR2,WHRN,DAB2IP,MVB12B,DOLPP1,COL5A1,ABCA2,KIAA1217,RAB18,VSTM4,TSPAN15,CDHR1,SCD,ADAM12,SCART1,CYP2E1,DKK3,SPON1,PLEKHA7,NCR3LG1,MPPED2,DOC2GP,SYTL2,RP11-693N9.2,ZBTB16,MCAM,FEZ1,CACNA2D4,LAG3,KLRG1,HNRNPA1P34,VDAC2P2,LINC00612,A2M-AS1,A2M,KRT17P8,BTG1P1,PZP,TPT1P12,A2MP1,LINC00987,RP11-118B22.4,RP13-735L24.1,KLRB1,DUSP16,WNT10B,SOAT2,RARG,CYP27B1,METTL21B,PHLDA1,NTN4,ELK3,BTBD11,DLEU1,TRAV1-1,TRAV1-2,TRAV2,TRAJ33,PTGDR,GALC,GPR65,LINC01146,GPR68,CTD-2547L24.3,RP11-747H7.3,LPCAT4,LTK,RORA-AS1,CTD-2501E16.2,NEO1,AXIN1,ADCY9,GTF3C1,CPNE2,ZCCHC14,SLC7A5,CPNE7,ATP1B2,NR1D1,IGFBP4,TANC2,PRR29-AS1,CYB5A,PLPP2,MATK,TMIGD2,FSD1,TNFSF14,COL5A3,S1PR5,CYP4F22,ELL,RP11-678G14.3,CAPN12,B3GNT8,IL4I1,PLCB1,RP4-568C11.4,EDEM2,PROCR,MMP24,CH507-9B2.9,NRIP1,AF127577.11,CHODL,AF131217.1,EVA1C,TRAPPC10,COL6A2,AC000068.9,RTN4R,RBFOX2,PDGFB,PRR5,CERK,LINC01644,LONRF3,CD40LG,F8

References

1. de Magalhães JP. The biology of ageing. In: Stuart-Hamilton I, editor. An Introduction to Gerontology. Cambridge: Cambridge University Press; 2011. p. 21–47.
2. López-Otín C, Blasco MA, Partridge L, Serrano M, Kroemer G. The hallmarks of aging. Cell. 2013;153(6):1194.
3. Ahadi S, Zhou W, Schüssler-Fiorenza Rose SM, Sailani MR, Contrepois K, Avina M, et al. Personal aging markers and ageotypes revealed by deep longitudinal profiling. Nat Med. 2020;26(1):83–90.
4. Aunan JR, Cho WC, Søreide K. The biology of aging and cancer: A brief overview of shared and divergent molecular hallmarks. Aging Dis. 2017;8(5):628–42.
5. Hung CW, Chen YC, Hsieh WL, Chiou SH, Kao CL. Ageing and neurodegenerative diseases. Ageing Res Rev. 2010;9(SUPPL.):S36–46.
6. Kalyani RR, Egan JM. Diabetes and Altered Glucose Metabolism with Aging. Endocrinol Metab Clin North Am. 2013;42(2):333–47.
7. Steenman M, Lande G. Cardiac aging and heart disease in humans. Biophys Rev. 2017;9(2):131–7.
8. Finch CE, Pike MC, Witten M. Slow mortality rate accelerations during aging in some animals approximate that of humans. Science (80-). 1990;249(4971):902–5.
9. Oeppen J VJW. Broken Limits to Life Expectancy. Science (80-). 2002;296(5570):1029–31.
10. Kontis V, Bennett JE, Mathers CD, Li G, Foreman K, Ezzati M. Future life expectancy in 35 industrialised countries: projections with a Bayesian model ensemble. Lancet. 2017;389(10076):1323–35.
11. Partridge L, Deelen J, Slagboom PE. Facing up to the global challenges of ageing. Nature. 2018;561(7721):45–56.
12. Most J, Tosti V, Redman LM, Fontana L. Calorie restriction in humans: An update. Ageing Res Rev. 2017;39:36–45.
13. Wei M, Brandhorst S, Shelehchi M, Mirzaei H, Cheng CW, Budniak J, et al. Fasting-mimicking diet and markers/risk factors for aging, diabetes, cancer, and cardiovascular disease. Sci Transl Med. 2017;9(377).
14. Springmann M, Clark MA, Rayner M, Scarborough P, Webb P. The global and regional costs of healthy and sustainable dietary patterns: a modelling study. Lancet Planet Heal. 2021;5(11):e797–807.
15. Harris A, Sharma A. Estimating the future health and aged care expenditure in Australia with changes in morbidity. PLoS One. 2018;13(8):1–10.
16. Wang L, Lankhorst L, Bernards R. Exploiting senescence for the treatment of cancer. Nat Rev Cancer. 2022;21.
17. Bartleson JM, Radenkovic D, Covarrubias AJ, Furman D, Winer DA, Verdin E. SARS-CoV-2, COVID-19 and the aging immune system. Nat Aging. 2021;1(9):769–82.

18. De-Carvalho DP, Jacinto A, Saúde L. The right time for senescence. Elife. 2021;10:1–21.
19. Halazonetis TD, Gorgoulis VG, Bartek J. An oncogene-induced DNA damage model for cancer development. Science (80-). 2008;319(5868):1352–5.
20. Coppé JP, Patil CK, Rodier F, Sun Y, Muñoz DP, Goldstein J, et al. Senescence-associated secretory phenotypes reveal cell-nonautonomous functions of oncogenic RAS and the p53 tumor suppressor. PLoS Biol. 2008;6(12).
21. Ruhland MK, Loza AJ, Capietto AH, Luo X, Knolhoff BL, Flanagan KC, et al. Stromal senescence establishes an immunosuppressive microenvironment that drives tumorigenesis. Nat Commun. 2016;7.
22. Akbar AN, Gilroy DW. Aging immunity may exacerbate COVID-19. Science (80-). 2020;369(6501):256–7.
23. Kadambari S, Klenerman P, Pollard AJ. Why the elderly appear to be more severely affected by COVID-19: The potential role of immunosenescence and CMV. Rev Med Virol. 2020;30(5):1–5.
24. Rydyznski Moderbacher C, Ramirez SI, Dan JM, Grifoni A, Hastie KM, Weiskopf D, et al. Antigen-Specific Adaptive Immunity to SARS-CoV-2 in Acute COVID-19 and Associations with Age and Disease Severity. Cell. 2020;183(4):996-1012.e19.
25. Mittelbrunn M, Kroemer G. Hallmarks of T cell aging. Nat Immunol. 2021;22(June).
26. Zhu Y, Tchkonia T, Fuhrmann-Stroissnigg H, Dai HM, Ling YY, Stout MB, et al. Identification of a novel senolytic agent, navitoclax, targeting the Bcl-2 family of anti-apoptotic factors. Aging Cell. 2016;15(3):428–35.
27. Däbritz JHM, Yu Y, Milanovic M, Schönlein M, Rosenfeldt MT, Dörr JR, et al. CD20-targeting immunotherapy promotes cellular senescence in B-cell lymphoma. Mol Cancer Ther. 2016;15(5):1074–81.
28. Kipps TJ, Eradat H, Grosicki S, Catalano J, Cosolo W, Dyagil IS, et al. A phase 2 study of the BH3 mimetic BCL2 inhibitor navitoclax (ABT-263) with or without rituximab, in previously untreated B-cell chronic lymphocytic leukemia. Leuk \& Lymphoma. 2015;56(10):2826–33.
29. Kirkland JL, Tchkonia T. Senolytic drugs: from discovery to translation. J Intern Med. 2020;288(5):518–36.
30. Camell CD, Yousefzadeh MJ, Zhu Y, Langhi Prata LGP, Huggins MA, Pierson M, et al. Senolytics reduce coronavirus-related mortality in old mice. Science (80-). 2021;373(6552).
31. Fisher RA. The genetical theory of natural selection. Oxford: at the Clarendon Press; 1930.
32. Flatt T, Partridge L. Horizons in the evolution of aging. BMC Biol. 2018;16(1):93.
33. Rando TA, Wyss-Coray T. Asynchronous, contagious and digital aging. Nat Aging. 2021;1(1):29–35.
34. Medawar PB. An Unsolved problem of biology : an inaugural lecture delivered at University College, London, 6 December, 1951. London: H.K. Lewis and Co.; 1952. (Inaugural lecture (University College, London) ; 1951).

35. Williams GC. Pleiotropy , Natural Selection , and the Evolution of Senescence. Evolution (N Y). 1957;11(4):398–411.
36. Kirkwood TBL. Evolution of ageing. Nature. 1977;270(November):301–4.
37. Hayflick L. Entropy explains aging, genetic determinism explains longevity, and undefined terminology explains misunderstanding both. PLoS Genet. 2007;3(12):2351–4.
38. Márquez EJ, Chung C han, Marches R, Rossi RJ, Nehar-Belaid D, Eroglu A, et al. Sexual-dimorphism in human immune system aging. Nat Commun. 2020;11(1).
39. Holzscheck N, Söhle J, Kristof B, Grönniger E, Gallinat S, Wenck H, et al. Multi-omics network analysis reveals distinct stages in the human aging progression in epidermal tissue. Aging (Albany NY). 2020;12(12):12393–409.
40. Gladyshev VN. Aging: progressive decline in fitness due to the rising deleteriome adjusted by genetic, environmental, and stochastic processes. Aging Cell. 2016;15(4):594–602.
41. Gladyshev VN, Kritchevsky SB, Clarke SG, Cuervo AM, Fiehn O, de Magalhães JP, et al. Molecular damage in aging. Nat Aging. 2021;1(12):1096–106.
42. Stamatoyannopoulos JA, Adzhubei I, Thurman RE, Kryukov G V., Mirkin SM, Sunyaev SR. Human mutation rate associated with DNA replication timing. Nat Genet. 2009;41(4):393–5.
43. Lodato MA, Woodworth MB, Lee S, Evrony GD, Mehta BK, Karger A, et al. Somatic mutation in single human neurons tracks developmental and transcriptional history. Science (80-). 2015;350(6256):94–8.
44. Carelli V, Chan DC. Mitochondrial DNA: Impacting central and peripheral nervous systems. Urology. 2014;84(6):1126–42.
45. Lodato MA, Walsh CA. Genome aging: somatic mutation in the brain links age-related decline with disease and nominates pathogenic mechanisms. Hum Mol Genet. 2019;28(R2):R197–206.
46. Niedernhofer LJ, Gurkar AU, Wang Y, Vijg J, Hoeijmakers JHJ, Robbins PD. Nuclear Genomic Instability and Aging. Annu Rev Biochem. 2018;87:295–322.
47. Baker DJ, Childs BG, Durik M, Wijers ME, Sieben CJ, Zhong J, et al. Naturally occurring p16 Ink4a-positive cells shorten healthy lifespan. Nature. 2016;530(7589):184–9.
48. Beerman I. Accumulation of DNA damage in the aged hematopoietic stem cell compartment. Semin Hematol. 2017;54(1):12–8.
49. Wang J, Clauson CL, Robbins PD, Niedernhofer LJ, Wang Y. The oxidative DNA lesions 8,5′-cyclopurines accumulate with aging in a tissue-specific manner. Aging Cell. 2012;11(4):714–6.
50. Tranah GJ, Katzman SM, Lauterjung K, Yaffe K, Manini TM, Kritchevsky S, et al. Mitochondrial DNA m.3243A > G heteroplasmy affects multiple aging phenotypes and risk of mortality. Sci Rep. 2018;8(1):1–9.
51. Martin-Herranz DE, Aref-Eshghi E, Bonder MJ, Stubbs TM, Choufani S, Weksberg R, et al. Screening for genes that accelerate the epigenetic aging clock in humans reveals a role for the H3K36 methyltransferase NSD1. Genome Biol. 2019;20(1):1–19.

52. Sziráki A, Tyshkovskiy A, Gladyshev VN. Global remodeling of the mouse DNA methylome during aging and in response to calorie restriction. Aging Cell. 2018;17(3).
53. Horvath S. DNA methylation age of human tissues and cell types. Genome Biol. 2013 Dec 13;14(10):R115.
54. Horvath S, Raj K. DNA methylation-based biomarkers and the epigenetic clock theory of ageing. Nat Rev Genet. 2018;19(6):371–84.
55. Lu AT, Quach A, Wilson JG, Reiner AP, Aviv A, Raj K, et al. DNA methylation GrimAge strongly predicts lifespan and healthspan. Aging (Albany NY). 2019;11(2):303–27.
56. Levine ME, Lu AT, Quach A, Chen BH, Assimes TL, Bandinelli S, et al. An epigenetic biomarker of aging for lifespan and healthspan. Aging (Albany NY). 2018 Apr 18;10(4):573–91.
57. Kurosaki T, Popp MW, Maquat LE. Quality and quantity control of gene expression by nonsense-mediated mRNA decay. Nat Rev Mol Cell Biol. 2019;20(7):406–20.
58. Wu CCC, Peterson A, Zinshteyn B, Regot S, Green R. Ribosome Collisions Trigger General Stress Responses to Regulate Cell Fate. Cell. 2020;182(2):404-416.e14.
59. Heintz C, Doktor TK, Lanjuin A, Escoubas CC, Zhang Y, Weir HJ, et al. Splicing factor 1 modulates dietary restriction and TORC1 pathway longevity in C. elegans. Nature. 2017;541(7635):102–6.
60. Wang K, Wu D, Zhang H, Das A, Basu M, Malin J, et al. Comprehensive map of age-associated splicing changes across human tissues and their contributions to age-associated diseases. Sci Rep. 2018;8(1):1–12.
61. de Magalhães JP, Curado J, Church GM. Meta-analysis of age-related gene expression profiles identifies common signatures of aging. Bioinformatics. 2009;25(7):875–81.
62. Palmer D, Fabris F, Doherty A, Freitas AA, de Magalhães JP. Ageing transcriptome meta-analysis reveals similarities and differences between key mammalian tissues. Aging (Albany NY). 2021;13(3):3313–41.
63. Levine RL, Stadtman ER. Oxidative modification of proteins during aging. Exp Gerontol. 2001 Sep;36(9):1495–502.
64. Golubev A, Hanson AD, Gladyshev VN, Banerjee R. Non-enzymatic molecular damage as a prototypic driver of aging. J Biol Chem. 2017;292(15):6029–38.
65. Gorisse L, Pietrement C, Vuiblet V, Schmelzer CEH, Köhler M, Duca L, et al. Protein carbamylation is a hallmark of aging. Proc Natl Acad Sci U S A. 2016;113(5):1191–6.
66. Khare S, Linster CL, Clarke SG. The interplay between protein L-isoaspartyl methyltransferase activity and insulin-like signaling to extend lifespan in Caenorhabditis elegans. PLoS One. 2011;6(6).
67. Kim E, Lowenson JD, Maclaren DC, Clarke S, Young SG. Deficiency of a protein-repair enzyme results in the accumulation of altered proteins, retardation of growth, and fatal seizures in mice. Proc Natl Acad Sci U S A. 1997;94(12):6132–7.
68. Sabath N, Levy-Adam F, Younis A, Rozales K, Meller A, Hadar S, et al. Cellular

proteostasis decline in human senescence. Proc Natl Acad Sci U S A. 2020;117(50):31902–13.
69. Raz Y, Guerrero-Ros I, Maier A, Slagboom PE, Atzmon G, Barzilai N, et al. Activation-Induced Autophagy Is Preserved in CD4+ T-Cells in Familial Longevity. J Gerontol A Biol Sci Med Sci. 2017;72(9):1201–6.
70. Piedrafita G, Keller MA, Ralser M. The impact of non-enzymatic reactions and enzyme promiscuity on cellular metabolism during (Oxidative) stress conditions. Biomolecules. 2015;5(3):2101–22.
71. Sitte N, Merker K, Grune T, Von Zglinicki T. Lipofuscin accumulation in proliferating fibroblasts in vitro: An indicator of oxidative stress. Exp Gerontol. 2001;36(3):475–86.
72. Gentile F, Arcaro A, Pizzimenti S, Daga M, Cetrangolo GP, Dianzani C, et al. DNA damage by lipid peroxidation products: implications in cancer, inflammation and autoimmunity. AIMS Genet. 2017;04(02):103–37.
73. Höhn A, Jung T, Grimm S, Catalgol B, Weber D, Grune T. Lipofuscin inhibits the proteasome by binding to surface motifs. Free Radic Biol Med. 2011;50(5):585–91.
74. Terman A, Dalen H, Brunk UT. Ceroid/lipofuscin-loaded human fibroblasts show decreased survival time and diminished autophagocytosis during amino acid starvation. Exp Gerontol. 1999;34(8):943–57.
75. Kakimoto Y, Okada C, Kawabe N, Sasaki A, Tsukamoto H, Nagao R, et al. Myocardial lipofuscin accumulation in ageing and sudden cardiac death. Sci Rep. 2019;9(1):1–8.
76. Slack JMW. What is a stem cell? Wiley Interdiscip Rev Dev Biol. 2018;7(5):e323.
77. Laurenti E, Göttgens B. From haematopoietic stem cells to complex differentiation landscapes. Nature. 2018;553(7689):418–26.
78. Laurenti E, Frelin C, Xie S, Ferrari R, Dunant CF, Zandi S, et al. CDK6 levels regulate quiescence exit in human hematopoietic stem cells. Cell Stem Cell. 2015;16(3):302–13.
79. Shyh-Chang N, Ng HH. The metabolic programming of stem cells. Genes Dev. 2017;31(4):336–46.
80. Signer RAJ, Magee JA, Salic A, Morrison SJ. Haematopoietic stem cells require a highly regulated protein synthesis rate. Nature. 2014;508(7498):49–54.
81. Majeti R, Park CY, Weissman IL. Identification of a Hierarchy of Multipotent Hematopoietic Progenitors in Human Cord Blood. Cell Stem Cell. 2007;1(6):635–45.
82. Kiel MJ, Yilmaz ÖH, Iwashita T, Yilmaz OH, Terhorst C, Morrison SJ. SLAM family receptors distinguish hematopoietic stem and progenitor cells and reveal endothelial niches for stem cells. Cell. 2005;121(7):1109–21.
83. Wolf NS, Priestley G V, Averill LE. Depletion of reserve in the hemopoietic system: III. Factors affecting the serial transplantation of bone marrow. Exp Hematol. 1983 Sep;11(8):762–71.
84. Dykstra B, Olthof S, Schreuder J, Ritsema M, Haan G De. Clonal analysis reveals multiple functional defects of aged murine hematopoietic stem cells. J

Exp Med. 2011;208(13):2691–703.
85. Van Zant G, Holland BP, Eldridge PW, Chen JJ. Genotype-restricted growth and aging patterns in hematopoietic stem cell populations of allophenic mice. J Exp Med. 1990 May 1;171(5):1547–65.
86. De Haan G, Lazare SS. Aging of hematopoietic stem cells. Blood. 2018;131(5):479–87.
87. Yang D, de Haan G. Inflammation and aging of hematopoietic stem cells in their niche. Cells. 2021;10(8):1–13.
88. Lu R, Czechowicz A, Seita J, Jiang D, Weissman IL. Clonal-level lineage commitment pathways of hematopoietic stem cells in vivo. Proc Natl Acad Sci U S A. 2019;116(4):1447–56.
89. Rodriguez-Fraticelli AE, Weinreb C, Wang SW, Migueles RP, Jankovic M, Usart M, et al. Single-cell lineage tracing unveils a role for TCF15 in haematopoiesis. Nature. 2020;583(7817):585–9.
90. Rodriguez-Fraticelli AE, Camargo F. Systems analysis of hematopoiesis using single-cell lineage tracing. Curr Opin Hematol. 2021;28(1):18–27.
91. Weinreb C, Rodriguez-Fraticelli A, Camargo FD, Klein AM. Lineage tracing on transcriptional landscapes links state to fate during differentiation. Science (80-). 2020 Feb 14;367(6479):755.
92. Bowling S, Sritharan D, Osorio FG, Nguyen M, Cheung P, Rodriguez-Fraticelli A, et al. An Engineered CRISPR-Cas9 Mouse Line for Simultaneous Readout of Lineage Histories and Gene Expression Profiles in Single Cells. Cell. 2020;181(6):1410-1422.e27.
93. Ludwig LS, Lareau CA, Ulirsch JC, Christian E, Muus C, Li LH, et al. Lineage Tracing in Humans Enabled by Mitochondrial Mutations and Single-Cell Genomics. Cell. 2019;176(6):1325-1339.e22.
94. Rodriguez-Fraticelli AE, Wolock SL, Weinreb CS, Panero R, Patel SH, Jankovic M, et al. Clonal analysis of lineage fate in native haematopoiesis. Nature. 2018;553(7687):212–6.
95. Dorshkind K, Höfer T, Montecino-Rodriguez E, Pioli PD, Rodewald HR. Do haematopoietic stem cells age? Nat Rev Immunol. 2020;20(3):196–202.
96. Bernitz JM, Kim HS, MacArthur B, Sieburg H, Moore K. Hematopoietic Stem Cells Count and Remember Self-Renewal Divisions. Cell. 2016;167(5):1296-1309.e10.
97. Pietras EM, Warr MR, Passegué E. Cell cycle regulation in hematopoietic stem cells. J Cell Biol. 2011;195(5):709–20.
98. Walter D, Lier A, Geiselhart A, Thalheimer FB, Huntscha S, Sobotta MC, et al. Exit from dormancy provokes DNA-damage-induced attrition in haematopoietic stem cells. Nature. 2015;520(7548):549–52.
99. Jaiswal S, Ebert BL. Clonal hematopoiesis in human aging and disease. Science (80-). 2019;366(6465).
100. Attema JL, Pronk CJH, Norddahl GL, Nygren JM, Bryder D. Hematopoietic stem cell ageing is uncoupled from p16 INK4A -mediated senescence. Oncogene. 2009;28(22):2238–43.
101. Janzen V, Forkert R, Fleming HE, Saito Y, Waring MT, Dombkowski DM, et al. Stem-cell ageing modified by the cyclin-dependent kinase inhibitor p16 INK4a.

Nature. 2006;443(7110):421–6.
102. Mejia-Ramirez E, Florian MC. Understanding intrinsic hematopoietic stem cell aging. Haematologica. 2020;105(1):22–37.
103. Florian MC, Klose M, Sacma M, Jablanovic J, Knudson L, Nattamai KJ, et al. Aging alters the epigenetic asymmetry of HSC division. Vol. 16, PLoS Biology. 2018. 1–35 p.
104. Florian MC, Dörr K, Niebel A, Daria D, Schrezenmeier H, Rojewski M, et al. Cdc42 activity regulates hematopoietic stem cell aging and rejuvenation. Cell Stem Cell. 2012;10(5):520–30.
105. Amoah A, Keller A, Emini R, Hoenicka M, Liebold A, Vollmer A, et al. Aging of human hematopoietic stem cells is linked to changes in Cdc42 activity. Haematologica. 2022;107(2):393–402.
106. Verovskaya E V., Dellorusso P V., Passegué E. Losing Sense of Self and Surroundings: Hematopoietic Stem Cell Aging and Leukemic Transformation. Trends Mol Med. 2019;25(6):494–515.
107. Chandel NS, Jasper H, Ho TT, Passegué E. Metabolic regulation of stem cell function in tissue homeostasis and organismal ageing. Nat Cell Biol. 2016;18(8):823–32.
108. Ho TT, Warr MR, Adelman ER, Lansinger OM, Flach J, Verovskaya E V., et al. Autophagy maintains the metabolism and function of young and old stem cells. Nature. 2017;543(7644):205–10.
109. Dong S, Wang Q, Kao YR, Diaz A, Tasset I, Kaushik S, et al. Chaperone-mediated autophagy sustains haematopoietic stem-cell function. Nature. 2021;591(7848):117–23.
110. Anguiano J, Garner TP, Mahalingam M, Das BC, Gavathiotis E, Cuervo AM. Chemical modulation of chaperone-mediated autophagy by retinoic acid derivatives. Nat Chem Biol. 2013;9(6):374–82.
111. Taiwo O, Wilson GA, Emmett W, Morris T, Bonnet D, Schuster E, et al. DNA methylation analysis of murine hematopoietic side population cells during aging. Epigenetics. 2013;8(10):1114–22.
112. Oshima M, Iwama A. Epigenetics of hematopoietic stem cell aging and disease. Int J Hematol. 2014;326–34.
113. Park IK, Qian D, Kiel M, Becker MW, Pihalja M, Weissman IL, et al. Bmi-1 is required for maintenance of adult self-renewing haematopoietic stem cells. Nature. 2003;423(6937):302–5.
114. Xie H, Xu J, Hsu JH, Nguyen M, Fujiwara Y, Peng C, et al. Polycomb repressive complex 2 regulates normal hematopoietic stem cell function in a developmental-stage-specific manner. Cell Stem Cell. 2014;14(1):68–80.
115. Benayoun BA, Pollina EA, Singh PP, Mahmoudi S, Harel I, Casey KM, et al. Remodeling of epigenome and transcriptome landscapes with aging in mice reveals widespread induction of inflammatory responses. Genome Res. 2019;29(4):697–709.
116. Beerman I, Bock C, Garrison BS, Smith ZD, Gu H, Meissner A, et al. Proliferation-dependent alterations of the DNA methylation landscape underlie hematopoietic stem cell aging. Cell Stem Cell. 2013;12(4):413–25.
117. Yu VWC, Yusuf RZ, Oki T, Wu J, Saez B, Wang X, et al. Epigenetic Memory

Underlies Cell-Autonomous Heterogeneous Behavior of Hematopoietic Stem Cells. Cell. 2016;167(5):1310-1322.e17.
118. Izzo F, Lee SC, Poran A, Chaligne R, Gaiti F, Gross B, et al. DNA methylation disruption reshapes the hematopoietic differentiation landscape. Nat Genet. 2020;52(4):378–87.
119. Saçma M, Pospiech J, Bogeska R, de Back W, Mallm JP, Sakk V, et al. Haematopoietic stem cells in perisinusoidal niches are protected from ageing. Nat Cell Biol. 2019;21(11):1309–20.
120. Maryanovich M, Zahalka AH, Pierce H, Pinho S, Nakahara F, Asada N, et al. Adrenergic nerve degeneration in bone marrow drives aging of the hematopoietic stem cell niche. Nat Med. 2018;24(6):782–91.
121. Frisch BJ, Hoffman CM, Latchney SE, LaMere MW, Myers J, Ashton J, et al. Aged marrow macrophages expand platelet-biased hematopoietic stem cells via interleukin-1B. JCI Insight. 2019;4(10).
122. Guidi N, Sacma M, Ständker L, Soller K, Marka G, Eiwen K, et al. Osteopontin attenuates aging-associated phenotypes of hematopoietic stem cells. EMBO J. 2017;36(7):840–53.
123. Ho YH, del Toro R, Rivera-Torres J, Rak J, Korn C, García-García A, et al. Remodeling of Bone Marrow Hematopoietic Stem Cell Niches Promotes Myeloid Cell Expansion during Premature or Physiological Aging. Cell Stem Cell. 2019;25(3):407-418.e6.
124. Zhao M, Perry JM, Marshall H, Venkatraman A, Qian P, He XC, et al. Megakaryocytes maintain homeostatic quiescence and promote post-injury regeneration of hematopoietic stem cells. Nat Med. 2014;20(11):1321–6.
125. Bruns I, Lucas D, Pinho S, Ahmed J, Lambert MP, Kunisaki Y, et al. Megakaryocytes regulate hematopoietic stem cell quiescence through CXCL4 secretion. Nat Med. 2014;20(11):1315–20.
126. Pinho S, Marchand T, Yang E, Wei Q, Nerlov C, Frenette PS. Lineage-Biased Hematopoietic Stem Cells Are Regulated by Distinct Niches. Dev Cell. 2018;44(5):634-641.e4.
127. Valletta S, Thomas A, Meng Y, Ren X, Drissen R, Sengül H, et al. Micro-environmental sensing by bone marrow stroma identifies IL-6 and TGFβ1 as regulators of hematopoietic ageing. Nat Commun. 2020;11(1).
128. Fulop T, Witkowski JM, Olivieri F, Larbi A. The integration of inflammaging in age-related diseases. Semin Immunol. 2018;40(June):17–35.
129. Helbling PM, Piñeiro-Yáñez E, Gerosa R, Boettcher S, Al-Shahrour F, Manz MG, et al. Global Transcriptomic Profiling of the Bone Marrow Stromal Microenvironment during Postnatal Development, Aging, and Inflammation. Cell Rep. 2019;29(10):3313-3330.e4.
130. Chavez JS, Rabe JL, Loeffler D, Higa KC, Hernandez G, Mills TS, et al. PU.1 enforces quiescence and limits hematopoietic stem cell expansion during inflammatory stress. J Exp Med. 2021;218(6).
131. Pietras EM, Mirantes-Barbeito C, Fong S, Loeffler D, Kovtonyuk L V., Zhang S, et al. Chronic interleukin-1 exposure drives haematopoietic stem cells towards precocious myeloid differentiation at the expense of self-renewal. Nat Cell Biol. 2016;18(6):607–18.

132. Pietras EM, Lakshminarasimhan R, Techner JM, Fong S, Flach J, Binnewies M, et al. Re-entry into quiescence protects hematopoietic stem cells from the killing effect of chronic exposure to type I interferons. J Exp Med. 2014;211(2):245–62.
133. Yamashita M, Passegué E. TNF-α Coordinates Hematopoietic Stem Cell Survival and Myeloid Regeneration. Cell Stem Cell. 2019;25(3):357-372.e7.
134. Haas S, Hansson J, Klimmeck D, Loeffler D, Velten L, Uckelmann H, et al. Inflammation-Induced Emergency Megakaryopoiesis Driven by Hematopoietic Stem Cell-like Megakaryocyte Progenitors. Cell Stem Cell. 2015;17(4):422–34.
135. Mann M, Mehta A, de Boer CG, Kowalczyk MS, Lee K, Haldeman P, et al. Heterogeneous Responses of Hematopoietic Stem Cells to Inflammatory Stimuli Are Altered with Age. Cell Rep. 2018;25(11):2992-3005.e5.
136. Pang WW, Price EA, Sahoo D, Beerman I, Maloney WJ, Rossi DJ, et al. Human bone marrow hematopoietic stem cells are increased in frequency and myeloid-biased with age. Proc Natl Acad Sci U S A. 2011;108(50):20012–7.
137. Knapp DJHF, Hammond CA, Hui T, Van Loenhout MTJ, Wang F, Aghaeepour N, et al. Single-cell analysis identifies a CD33+subset of human cord blood cells with high regenerative potential. Nat Cell Biol. 2018;20(6):710–20.
138. Biasco L, Pellin D, Scala S, Dionisio F, Basso-Ricci L, Leonardelli L, et al. In Vivo Tracking of Human Hematopoiesis Reveals Patterns of Clonal Dynamics during Early and Steady-State Reconstitution Phases. Cell Stem Cell. 2015;19(1):107–19.
139. Aiuti A, Biasco L, Scaramuzza S, Ferrua F, Cicalese MP, Baricordi C, et al. Lentiviral hematopoietic stem cell gene therapy in patients with wiskott-aldrich syndrome. Science (80-). 2013;341(6148).
140. Belluschi S, Calderbank EF, Ciaurro V, Pijuan-Sala B, Santoro A, Mende N, et al. Myelo-lymphoid lineage restriction occurs in the human haematopoietic stem cell compartment before lymphoid-primed multipotent progenitors. Nat Commun. 2018;9(1).
141. Notta F, Doulatov S, Laurenti E, Poeppl A, Jurisica I, Dick JE. Isolation of Single Human Hematopoietic Stem Cells Capable of Long-Term Multilineage Engraftment. Science (80-). 2011 Jul 8;333(6039):218–21.
142. Anjos-Afonso F, Buettner F, Mian SA, Rhys H, Perez-Lloret J, Garcia-Albornoz M, et al. Single cell analyses identify a highly regenerative and homogenous human CD34+ hematopoietic stem cell population. Nat Commun. 2022;13(1):1–13.
143. Pyrkov T V., Avchaciov K, Tarkhov AE, Menshikov LI, Gudkov A V., Fedichev PO. Longitudinal analysis of blood markers reveals progressive loss of resilience and predicts human lifespan limit. Nat Commun. 2021;12(1):1–10.
144. Nilsson AR, Soneji S, Adolfsson S, Bryder D, Pronk CJ. Human and murine hematopoietic stem cell aging is associated with functional impairments and intrinsic megakaryocytic/erythroid bias. PLoS One. 2016;11(7):1–20.
145. Serre-Miranda C, Roque S, Barreira-Silva P, Nobrega C, Vieira N, Costa P, et al. Age-Related Sexual Dimorphism on the Longitudinal Progression of Blood Immune Cells in BALB/cByJ Mice. Journals Gerontol Ser A. 2021;77(5):883–91.

146. Chang J, Wang Y, Shao L, Laberge RM, Demaria M, Campisi J, et al. Clearance of senescent cells by ABT263 rejuvenates aged hematopoietic stem cells in mice. Nat Med. 2016;22(1):78–83.
147. Caiado F, Pietras EM, Manz MG. Inflammation as a regulator of hematopoietic stem cell function in disease, aging, and clonal selection. J Exp Med. 2021;218(7):1–19.
148. Pawelec G, Bronikowski A, Cunnane SC, Ferrucci L, Franceschi C, Fülöp T, et al. The conundrum of human immune system "senescence." Mech Ageing Dev. 2020;192(August).
149. Urlacher SS, Ellison PT, Sugiyama LS, Pontzer H, Eick G, Liebert MA, et al. Tradeoffs between immune function and childhood growth among Amazonian forager-horticulturalists. Proc Natl Acad Sci U S A. 2018;115(17):E3914–21.
150. Kirkwood TBL. Understanding the odd science of aging. Cell. 2005;120(4):437–47.
151. Puchta A, Naidoo A, Verschoor CP, Loukov D, Thevaranjan N, Mandur TS, et al. TNF Drives Monocyte Dysfunction with Age and Results in Impaired Anti-pneumococcal Immunity. PLoS Pathog. 2016;12(1):1–23.
152. Luo OJ, Lei W, Zhu G, Ren Z, Xu Y, Xiao C, et al. Multidimensional single-cell analysis of human peripheral blood reveals characteristic features of the immune system landscape in aging and frailty. Nat Aging. 2022;2(4):348–64.
153. Krishnamurthy J, Torrice C, Ramsey MR, Kovalev GI, Al-Regaiey K, Su L, et al. Ink4a/Arf expression is a biomarker of aging. J Clin Invest. 2004;114(9):1299–307.
154. Pinti M, Appay V, Campisi J, Frasca D, Fülöp T, Sauce D, et al. Aging of the immune system: Focus on inflammation and vaccination. Eur J Immunol. 2016;46(10):2286–301.
155. Vicente R, Mausset-Bonnefont AL, Jorgensen C, Louis-Plence P, Brondello JM. Cellular senescence impact on immune cell fate and function. Aging Cell. 2016;15(3):400–6.
156. Yousefzadeh MJ, Flores RR, Zhu Y, Schmiechen ZC, Brooks RW, Trussoni CE, et al. An aged immune system drives senescence and ageing of solid organs. Vol. 594, Nature. Springer US; 2021. 100–105 p.
157. Mogilenko DA, Shchukina I, Artyomov MN. Immune ageing at single-cell resolution. Nat Rev Immunol. 2021;0123456789.
158. FRANCESCHI C, BONAFÈ M, VALENSIN S, OLIVIERI F, DE LUCA M, OTTAVIANI E, et al. Inflamm-aging: An Evolutionary Perspective on Immunosenescence. Ann N Y Acad Sci. 2006 Jan 25;908(1):244–54.
159. Shen-Orr SS, Furman D, Kidd BA, Hadad F, Lovelace P, Huang YW, et al. Defective Signaling in the JAK-STAT Pathway Tracks with Chronic Inflammation and Cardiovascular Risk in Aging Humans. Cell Syst. 2016;3(4):374-384.e4.
160. Rea IM, Gibson DS, McGilligan V, McNerlan SE, Denis Alexander H, Ross OA. Age and age-related diseases: Role of inflammation triggers and cytokines. Front Immunol. 2018;9(APR):1–28.
161. Weiskopf D, Weinberger B, Grubeck-Loebenstein B. The aging of the immune system. Transpl Int. 2009;22(11):1041–50.

162. Derhovanessian E, Solana R, Larbi A, Pawelec G. Immunity, ageing and cancer. Immun Ageing. 2008;5:1–16.
163. Fourati S, Cristescu R, Loboda A, Talla A, Filali A, Railkar R, et al. Pre-vaccination inflammation and B-cell signalling predict age-related hyporesponse to hepatitis B vaccination. Nat Commun. 2016;7:1–12.
164. Nikolich-Zugich J, Knox KS, Rios CT, Natt B, Bhattacharya D, Fain MJ. SARS-CoV-2 and COVID-19 in older adults: what we may expect regarding pathogenesis, immune responses, and outcomes. GeroScience. 2020;42(2):505–14.
165. Leng SX, Margolick JB. Aging, sex, inflammation, frailty, and CMV and HIV infections. Cell Immunol. 2020;348(November 2019).
166. Huang Z, Chen B, Liu X, Li H, Xie L, Gao Y, et al. Effects of sex and aging on the immune cell landscape as assessed by single-cell transcriptomic analysis. Proc Natl Acad Sci U S A. 2021;118(33).
167. Selmi C, Brunetta E, Raimondo MG, Meroni PL. The X chromosome and the sex ratio of autoimmunity. Autoimmun Rev. 2012;11(6–7):A531–7.
168. Jeung IC, Cheon K, Kim MR. Decreased Cytotoxicity of Peripheral and Peritoneal Natural Killer Cell in Endometriosis. Biomed Res Int. 2016;2016.
169. Yovel G, Shakhar K, Ben-Eliyahu S. The Effects of Sex, Menstrual Cycle, and Oral Contraceptives on the Number and Activity of Natural Killer Cells. Gynecol Oncol. 2001 May 1;81(2):254–62.
170. Furman D, Hejblum BP, Simon N, Jojic V, Dekker CL, Thiebaut R, et al. Systems analysis of sex differences reveals an immunosuppressive role for testosterone in the response to influenza vaccination. Proc Natl Acad Sci U S A. 2014;111(2):869–74.
171. Tedeschi V, Paldino G, Kunkl M, Paroli M, Sorrentino R, Tuosto L, et al. CD8+ T Cell Senescence: Lights and Shadows in Viral Infections, Autoimmune Disorders and Cancer. Int J Mol Sci. 2022;23(6).
172. Elyahu Y, Monsonego A. Thymus involution sets the clock of the aging T-cell landscape: Implications for declined immunity and tissue repair. Ageing Res Rev. 2021;65(July 2020):101231.
173. Seidler S, Zimmermann HW, Bartneck M, Trautwein C, Tacke F. Age-dependent alterations of monocyte subsets and monocyte-related chemokine pathways in healthy adults. BMC Immunol. 2010;11.
174. Loukov D, Naidoo A, Puchta A, Marin JLA, Bowdish DME. Tumor necrosis factor drives increased splenic monopoiesis in old mice. J Leukoc Biol. 2016;100(1):121–9.
175. Stervbo U, Meier S, Mälzer JN, Baron U, Bozzetti C, Jürchott K, et al. Effects of aging on human leukocytes (part I): immunophenotyping of innate immune cells. Age (Omaha). 2015;37(5).
176. Mogilenko DA, Shpynov O, Andhey PS, Arthur L, Swain A, Esaulova E, et al. Comprehensive Profiling of an Aging Immune System Reveals Clonal GZMK+ CD8+ T Cells as Conserved Hallmark of Inflammaging. Immunity. 2021;54(1):99-115.e12.
177. Ide S, Yahara Y, Kobayashi Y, Strausser SA, Ide K, Watwe A, et al. Yolk-Sac-derived macrophages progressively expand in the mouse kidney with age.

Elife. 2020;9:1–12.
178. Wong CP, Magnusson KR, Ho E. Aging is associated with altered dendritic cells subset distribution and impaired proinflammatory cytokine production. Exp Gerontol. 2010;45(2):163–9.
179. Angelidis I, Simon LM, Fernandez IE, Strunz M, Mayr CH, Greiffo FR, et al. An atlas of the aging lung mapped by single cell transcriptomics and deep tissue proteomics. Nat Commun. 2019;10(1):1–17.
180. Vivier E, Artis D, Colonna M, Diefenbach A, Di Santo JP, Eberl G, et al. Innate Lymphoid Cells: 10 Years On. Cell. 2018;174(5):1054–66.
181. Hazeldine J, Lord JM. The impact of ageing on natural killer cell function and potential consequences for health in older adults. Ageing Res Rev. 2013;12(4):1069–78.
182. Manser AR, Uhrberg M. Age-related changes in natural killer cell repertoires: impact on NK cell function and immune surveillance. Cancer Immunol Immunother. 2016;65(4):417–26.
183. Hazeldine J, Hampson P, Lord JM. Reduced release and binding of perforin at the immunological synapse underlies the age-related decline in natural killer cell cytotoxicity. Aging Cell. 2012;11(5):751–9.
184. Lee JS, Park S, Jeong HW, Ahn JY, Choi SJ, Lee H, et al. Immunophenotyping of covid-19 and influenza highlights the role of type i interferons in development of severe covid-19. Sci Immunol. 2020;5(49).
185. Fung ITH, Sankar P, Zhang Y, Robison LS, Zhao X, D'Souza SS, et al. Activation of group 2 innate lymphoid cells alleviates aging-associated cognitive decline. J Exp Med. 2020;217(4).
186. Rubtsov A V., Rubtsova K, Fischer A, Meehan RT, Gillis JZ, Kappler JW, et al. Toll-like receptor 7 (TLR7)-driven accumulation of a novel CD11c+ B-cell population is important for the development of autoimmunity. Blood. 2011;118(5):1305–15.
187. Hao Y, O'Neill P, Naradikian MS, Scholz JL, Cancro MP. A B-cell subset uniquely responsive to innate stimuli accumulates in aged mice. Blood. 2011;118(5):1294–304.
188. Schaum N, Lehallier B, Hahn O, Pálovics R, Hosseinzadeh S, Lee SE, et al. Ageing hallmarks exhibit organ-specific temporal signatures. Nature. 2020;583(7817):596–602.
189. Almanzar N, Antony J, Baghel AS, Bakerman I, Bansal I, Barres BA, et al. A single-cell transcriptomic atlas characterizes ageing tissues in the mouse. Nature. 2020;583(7817):590–5.
190. Kimmel JC, Penland L, Rubinstein ND, Hendrickson DG, Kelley DR, Rosenthal AZ. Murine single-cell RNA-seq reveals cell-identity- And tissue-specific trajectories of aging. Genome Res. 2019;29(12):2088–103.
191. Russell Knode LM, Naradikian MS, Myles A, Scholz JL, Hao Y, Liu D, et al. Age-Associated B Cells Express a Diverse Repertoire of V H and Vκ Genes with Somatic Hypermutation . J Immunol. 2017;198(5):1921–7.
192. Pioli PD, Casero D, Montecino-Rodriguez E, Morrison SL, Dorshkind K. Plasma Cells Are Obligate Effectors of Enhanced Myelopoiesis in Aging Bone Marrow. Immunity. 2019;51(2):351-366.e6.

193. Bodogai M, O'Connell J, Kim K, Kim Y, Moritoh K, Chen C, et al. Commensal bacteria contribute to insulin resistance in aging by activating innate B1a cells. Sci Transl Med. 2018;10(468):1–14.
194. Lee-Chang C, Bodogai M, Moritoh K, Olkhanud PB, Chan AC, Croft M, et al. Accumulation of 4-1BBL+ B cells in the elderly induces the generation of granzyme-B+ CD8+ T cells with potential antitumor activity. Blood. 2014;124(9):1450–9.
195. Lee-Chang C, Bodogai M, Moritoh K, Chen X, Wersto R, Sen R, et al. Aging Converts Innate B1a Cells into Potent CD8 + T Cell Inducers . J Immunol. 2016;196(8):3385–97.
196. Rodriguez-Zhurbenko N, Quach TD, Hopkins TJ, Rothstein TL, Hernandez AM. Human B-1 cells and B-1 cell antibodies change with advancing age. Front Immunol. 2019;10(MAR):1–15.
197. Van Den Broek T, Borghans JAM, Van Wijk F. The full spectrum of human naive T cells. Nat Rev Immunol. 2018;18(6):363–73.
198. Chambers ES, Akbar AN. Can blocking inflammation enhance immunity during aging? J Allergy Clin Immunol. 2020;145(5):1323–31.
199. Mannick JB, Del Giudice G, Lattanzi M, Valiante NM, Praestgaard J, Huang B, et al. mTOR inhibition improves immune function in the elderly. Sci Transl Med. 2014;6(268):268ra179.
200. Vukmanovic-Stejic M, Chambers ES, Suárez-Fariñas M, Sandhu D, Fuentes-Duculan J, Patel N, et al. Enhancement of cutaneous immunity during aging by blocking p38 mitogen-activated protein (MAP) kinase–induced inflammation. J Allergy Clin Immunol. 2018;142(3):844–56.
201. Xu M, Pirtskhalava T, Farr JN, Weigand BM, Palmer AK, Weivoda MM, et al. Senolytics improve physical function and increase lifespan in old age. Nat Med. 2018;24(8):1246–56.
202. Amor C, Feucht J, Leibold J, Ho YJ, Zhu C, Alonso-Curbelo D, et al. Senolytic CAR T cells reverse senescence-associated pathologies. Nature. 2020;583(7814):127–32.
203. Hickson LTJ, Langhi Prata LGP, Bobart SA, Evans TK, Giorgadze N, Hashmi SK, et al. Senolytics decrease senescent cells in humans: Preliminary report from a clinical trial of Dasatinib plus Quercetin in individuals with diabetic kidney disease. EBioMedicine. 2019;47:446–56.
204. Robbins PD, Jurk D, Khosla S, Kirkland JL, Lebrasseur NK, Miller JD, et al. Senolytic Drugs: Reducing Senescent Cell Viability to Extend Health Span. Annu Rev Pharmacol Toxicol. 2021;61:779–803.
205. Czesnikiewicz-Guzik M, Lee WW, Cui D, Hiruma Y, Lamar DL, Yang ZZ, et al. T cell subset-specific susceptibility to aging. Clin Immunol. 2008;127(1):107–18.
206. Egorov ES, Kasatskaya SA, Zubov VN, Izraelson M, Nakonechnaya TO, Staroverov DB, et al. The changing landscape of naive T cell receptor repertoire with human aging. Front Immunol. 2018;9(JUL):1–12.
207. Calder AE, Hince MN, Dudakov JA, Chidgey AP, Boyd RL. Thymic involution: Where endocrinology meets immunology. Neuroimmunomodulation. 2011;18(5):281–9.

208. Bains I, Thiébaut R, Yates AJ, Callard R. Quantifying Thymic Export: Combining Models of Naive T Cell Proliferation and TCR Excision Circle Dynamics Gives an Explicit Measure of Thymic Output. J Immunol. 2009;183(7):4329–36.
209. Howard JK, Lord GM, Matarese G, Vendetti S, Ghatei MA, Ritter MA, et al. Leptin protects mice from starvation-induced lymphoid atrophy and increases thymic cellularity in ob/ob mice. J Clin Invest. 1999;104(8):1051–9.
210. Duggal NA, Pollock RD, Lazarus NR, Harridge S, Lord JM. Major features of immunesenescence, including reduced thymic output, are ameliorated by high levels of physical activity in adulthood. Aging Cell. 2018;17(2).
211. Bektas A, Schurman SH, Gonzalez-Freire M, Dunn CA, Singh AK, Macian F, et al. Age-associated changes in human CD4+ T cells point to mitochondrial dysfunction consequent to impaired autophagy. Aging (Albany NY). 2019 Nov 9;11(21):9234–63.
212. Sanderson SL, Simon AK. In aged primary T cells, mitochondrial stress contributes to telomere attrition measured by a novel imaging flow cytometry assay. Aging Cell. 2017;16(6):1234–43.
213. Ron-Harel N, Notarangelo G, Ghergurovich JM, Paulo JA, Sage PT, Santos D, et al. Defective respiration and one-carbon metabolism contribute to impaired naïve T cell activation in aged mice. Proc Natl Acad Sci U S A. 2018;115(52):13347–52.
214. Soto-Heredero G, Gómez de las Heras MM, Gabandé-Rodríguez E, Oller J, Mittelbrunn M. Glycolysis – a key player in the inflammatory response. FEBS J. 2020;287(16):3350–69.
215. Callender LA, Carroll EC, Beal RWJ, Chambers ES, Nourshargh S, Akbar AN, et al. Human CD8+ EMRA T cells display a senescence-associated secretory phenotype regulated by p38 MAPK. Aging Cell. 2018;17(1):1–9.
216. Ramstead AG, Wallace JA, Lee SH, Bauer KM, Tang WW, Ekiz HA, et al. Mitochondrial Pyruvate Carrier 1 Promotes Peripheral T Cell Homeostasis through Metabolic Regulation of Thymic Development. Cell Rep. 2020;30(9):2889-2899.e6.
217. Baixauli F, Acín-Pérez R, Villarroya-Beltrí C, Mazzeo C, Nuñez-Andrade N, Gabandé-Rodriguez E, et al. Mitochondrial respiration controls lysosomal function during inflammatory t cell responses. Cell Metab. 2015;22(3):485–98.
218. Younes SA, Talla A, Ribeiro SP, Saidakova E V., Korolevskaya LB, Shmagel K V., et al. Cycling CD4+ T cells in HIV-infected immune nonresponders have mitochondrial dysfunction. J Clin Invest. 2018;128(11):5083–94.
219. Böhme J, Martinez N, Li S, Lee A, Marzuki M, Tizazu AM, et al. Metformin enhances anti-mycobacterial responses by educating CD8+ T-cell immunometabolic circuits. Nat Commun. 2020;11(1).
220. Terao C, Suzuki A, Momozawa Y, Akiyama M, Ishigaki K, Yamamoto K, et al. Chromosomal alterations among age-related haematopoietic clones in Japan. Nature. 2020;584(7819):130–5.
221. Fraietta JA, Nobles CL, Sammons MA, Lundh S, Carty SA, Reich TJ, et al. Disruption of TET2 promotes the therapeutic efficacy of CD19-targeted T cells. Nature. 2018;558(7709):307–12.

222. Frick M, Chan W, Arends CM, Hablesreiter R, Halik A, Heuser M, et al. Role of donor clonal hematopoiesis in allogeneic hematopoietic stem-cell transplantation. J Clin Oncol. 2019;37(5):375–85.
223. Lee-Six H, Øbro NF, Shepherd MS, Grossmann S, Dawson K, Belmonte M, et al. Population dynamics of normal human blood inferred from somatic mutations. Nature. 2018;561(7724):473–8.
224. Zhang H, Weyand CM, Goronzy JJ. Hallmarks of the aging T-cell system. FEBS J. 2021;1–20.
225. Young AL, Challen GA, Birmann BM, Druley TE. Clonal haematopoiesis harbouring AML-associated mutations is ubiquitous in healthy adults. Nat Commun. 2016;7.
226. Shao L, Fujii H, Colmegna I, Oishi H, Goronzy JJ, Weyand CM. Deficiency of the DNA repair enzyme ATM in rheumatoid arthritis. J Exp Med. 2009;206(6):1435–49.
227. Shao L, Goronzy JJ, Weyand CM. DNA-dependent protein kinase catalytic subunit mediates T-cell loss in rheumatoid arthritis. EMBO Mol Med. 2010;2(10):415–27.
228. Li Y, Shen Y, Hohensinner P, Ju J, Wen Z, Goodman SB, et al. Deficient Activity of the Nuclease MRE11A Induces T Cell Aging and Promotes Arthritogenic Effector Functions in Patients with Rheumatoid Arthritis. Immunity. 2016;45(4):903–16.
229. Kim C, Jin J, Ye Z, Jadhav RR, Gustafson CE, Hu B, et al. Histone deficiency and accelerated replication stress in T cell aging. J Clin Invest. 2021;131(11).
230. Dozmorov MG, Coit P, Maksimowicz-McKinnon K, Sawalha AH. Age-associated DNA methylation changes in naive CD4+ T cells suggest an evolving autoimmune epigenotype in aging T cells. Epigenomics. 2017;9(4):429–45.
231. Hu B, Jadhav RR, Gustafson CE, Le Saux S, Ye Z, Li X, et al. Distinct Age-Related Epigenetic Signatures in CD4 and CD8 T Cells. Front Immunol. 2020;11(November):1–13.
232. Cheung P, Vallania F, Warsinske HC, Donato M, Schaffert S, Chang SE, et al. Single-Cell Chromatin Modification Profiling Reveals Increased Epigenetic Variations with Aging. Cell. 2018;173(6):1385-1397.e14.
233. Witkowski JM, Mikosik A, Bryl E, Fulop T. Proteodynamics in aging human T cells – The need for its comprehensive study to understand the fine regulation of T lymphocyte functions. Exp Gerontol. 2018;107(July 2017):161–8.
234. Stepensky P, Rensing-Ehl A, Gather R, Revel-Vilk S, Fischer U, Nabhani S, et al. Early-onset Evans syndrome, immunodeficiency, and premature immunosenescence associated with tripeptidyl-peptidase II deficiency. Blood. 2015;125(5):753–61.
235. Clarke AJ, Simon AK. Autophagy in the renewal, differentiation and homeostasis of immune cells. Nat Rev Immunol. 2019;19(3):170–83.
236. DiToro D, Harbour SN, Bando JK, Benavides G, Witte S, Laufer VA, et al. Insulin-Like Growth Factors Are Key Regulators of T Helper 17 Regulatory T Cell Balance in Autoimmunity. Immunity. 2020;52(4):650-667.e10.
237. Akbar AN, Henson SM, Lanna A. Senescence of T Lymphocytes: Implications

for Enhancing Human Immunity. Trends Immunol. 2016;37(12):866–76.
238. Ahmed R, Miners KL, Lahoz-Beneytez J, Jones RE, Roger L, Baboonian C, et al. CD57+ Memory T Cells Proliferate In Vivo. Cell Rep. 2020;33(11).
239. Pereira BI, De Maeyer RPH, Covre LP, Nehar-Belaid D, Lanna A, Ward S, et al. Sestrins induce natural killer function in senescent-like CD8+ T cells. Nat Immunol. 2020;21(6):684–94.
240. Guo Z, Wang G, Wu B, Chou WC, Cheng L, Zhou C, et al. DCAF1 regulates Treg senescence via the ROS axis during immunological aging. J Clin Invest. 2020;130(11):5893–908.
241. Elyahu Y, Hekselman I, Eizenberg-Magar I, Berner O, Strominger I, Schiller M, et al. Aging promotes reorganization of the CD4 T cell landscape toward extreme regulatory and effector phenotypes. Sci Adv. 2019;5(8).
242. Li M, Yao D, Zeng X, Kasakovski D, Zhang Y, Chen S, et al. Age related human T cell subset evolution and senescence. Immun Ageing. 2019;16(1):1–7.
243. den Braber I, Mugwagwa T, Vrisekoop N, Westera L, Mögling R, Bregje de Boer A, et al. Maintenance of Peripheral Naive T Cells Is Sustained by Thymus Output in Mice but Not Humans. Immunity. 2012;36(2):288–97.
244. Hussain T, Quinn KM. Similar but different: virtual memory CD8 T cells as a memory-like cell population. Immunol Cell Biol. 2019;97(7):675–84.
245. White JT, Cross EW, Burchill MA, Danhorn T, McCarter MD, Rosen HR, et al. Virtual memory T cells develop and mediate bystander protective immunity in an IL-15-dependent manner. Nat Commun. 2016 Sep 21;7(1):11291.
246. Quinn KM, Fox A, Harland KL, Russ BE, Li J, Nguyen THO, et al. Age-Related Decline in Primary CD8+ T Cell Responses Is Associated with the Development of Senescence in Virtual Memory CD8+ T Cells. Cell Rep. 2018;23(12):3512–24.
247. Sun X, Nguyen T, Achour A, Ko A, Cifello J, Ling C, et al. Longitudinal analysis reveals age-related changes in the T cell receptor repertoire of human T cell subsets. J Clin Invest. 2022 Jun 16;
248. Goronzy JJ, Weyand CM. Mechanisms underlying T cell ageing. Nat Rev Immunol. 2019;19(9):573–83.
249. Krishna C, Chowell D, Gönen M, Elhanati Y, Chan TA. Genetic and environmental determinants of human TCR repertoire diversity. Immun Ageing. 2020;17(1):1–7.
250. Gil A, Yassai MB, Naumov YN, Selin LK. Narrowing of Human Influenza A Virus-Specific T Cell Receptor α and β Repertoires with Increasing Age. J Virol. 2015;89(8):4102–16.
251. Sportès C, Hakim FT, Memon SA, Zhang H, Chua KS, Brown MR, et al. Administration of rhIL-7 in humans increases in vivo TCR repertoire diversity by preferential expansion of naive T cell subsets. J Exp Med. 2008;205(7):1701–14.
252. Choutka J, Jansari V, Hornig M, Iwasaki A. Unexplained post-acute infection syndromes. Nat Med. 2022;28(5):911–23.
253. Su Y, Yuan D, Chen DG, Ng RH, Wang K, Choi J, et al. Multiple early factors anticipate post-acute COVID-19 sequelae. Cell. 2022;185(5):881-895.e20.

254. Zhou P, Yang X Lou, Wang XG, Hu B, Zhang L, Zhang W, et al. A pneumonia outbreak associated with a new coronavirus of probable bat origin. Nature. 2020;579(7798):270–3.
255. Wang Q, Zhang Y, Wu L, Niu S, Song C, Zhang Z, et al. Structural and Functional Basis of SARS-CoV-2 Entry by Using Human ACE2. Cell. 2020;181(4):894-904.e9.
256. Sungnak W, Huang N, Bécavin C, Berg M, Queen R, Litvinukova M, et al. SARS-CoV-2 entry factors are highly expressed in nasal epithelial cells together with innate immune genes. Nat Med. 2020;26(5):681–7.
257. Wu CT, Lidsky P V., Xiao Y, Lee IT, Cheng R, Nakayama T, et al. SARS-CoV-2 infects human pancreatic β cells and elicits β cell impairment. Cell Metab. 2021;33(8):1565-1576.e5.
258. Wiersinga WJ, Rhodes A, Cheng AC, Peacock SJ, Prescott HC. Pathophysiology, Transmission, Diagnosis, and Treatment of Coronavirus Disease 2019 (COVID-19): A Review. JAMA - J Am Med Assoc. 2020;324(8):782–93.
259. Zhou F, Yu T, Du R, Fan G, Liu Y, Liu Z, et al. Clinical course and risk factors for mortality of adult inpatients with COVID-19 in Wuhan, China: a retrospective cohort study. Lancet. 2020;395(10229):1054–62.
260. Chakraborty C, Sharma AR, Sharma G, Bhattacharya M, Lee SS. SARS-CoV-2 causing pneumonia-associated respiratory disorder (COVID-19): Diagnostic and proposed therapeutic options. Eur Rev Med Pharmacol Sci. 2020;24(7):4016–26.
261. Mao L, Jin H, Wang M, Hu Y, Chen S, He Q, et al. Neurologic Manifestations of Hospitalized Patients with Coronavirus Disease 2019 in Wuhan, China. JAMA Neurol. 2020;77(6):683–90.
262. Sette A, Crotty S. Adaptive immunity to SARS-CoV-2 and COVID-19. Cell. 2021;184(4):861–80.
263. Torres Acosta MA, Singer BD. Pathogenesis of COVID-19-induced ARDS: Implications for an ageing population. Eur Respir J. 2020;56(3).
264. Liu B, Jayasundara D, Pye V, Dobbins T, Dore GJ, Matthews G, et al. Whole of population-based cohort study of recovery time from COVID-19 in New South Wales Australia. Lancet Reg Heal - West Pacific. 2021;12:100193.
265. Centers for Disease Control and Prevention (CDC). COVID Data Tracker, Atlanta [Internet]. 2022 [cited 2022 Jun 20]. Available from: https://covid.cdc.gov/covid-data-tracker/#datatracker-home
266. Team C-F. Variation in the COVID-19 infection–fatality ratio by age, time, and geography during the pre-vaccine era: a systematic analysis. Lancet. 2022 Apr;399(10334):1469–88.
267. Merad M, Blish CA, Sallusto F, Iwasaki A. The immunology and immunopathology of COVID-19. Science (80-). 2022;375(6585):1122–7.
268. Podestà MA, Valli F, Galassi A, Cassia MA, Ciceri P, Barbieri L, et al. COVID-19 in Chronic Kidney Disease: The Impact of Old and Novel Cardiovascular Risk Factors. Blood Purif. 2021;50(6):740–9.
269. Sharma JR, Yadav UCS. COVID-19 severity in obese patients: Potential mechanisms and molecular targets for clinical intervention. Obes Res Clin

Pract. 2021;15(2):163–71.
270. Molony RD, Nguyen JT, Kong Y, Montgomery RR, Shaw AC, Iwasaki A. Aging impairs both primary and secondary RIG-I signaling for interferon induction in human monocytes. Sci Signal. 2017;10(509):1–12.
271. Kasuga Y, Zhu B, Jang KJ, Yoo JS. Innate immune sensing of coronavirus and viral evasion strategies. Exp Mol Med. 2021;53(5):723–36.
272. Diamond MS, Kanneganti TD. Innate immunity: the first line of defense against SARS-CoV-2. Nat Immunol. 2022;23(2):165–76.
273. Pérez-Cabezas B, Naranjo-Gómez M, Fernández MA, Grífols JR, Pujol-Borrell R, Borràs FE. Reduced numbers of plasmacytoid dendritic cells in aged blood donors. Exp Gerontol. 2007;42(10):1033–8.
274. Wong C, Goldstein DR. Impact of aging on antigen presentation cell function of dendritic cells. Curr Opin Immunol. 2013;25(4):535–41.
275. Nelde A, Bilich T, Heitmann JS, Maringer Y, Salih HR, Roerden M, et al. SARS-CoV-2-derived peptides define heterologous and COVID-19-induced T cell recognition. Nat Immunol. 2021;22(1):74–85.
276. Eaton SM, Burns EM, Kusser K, Randall TD, Haynes L. Age-related defects in CD4 T cell cognate helper function lead to reductions in humoral responses. J Exp Med. 2004;200(12):1613–22.
277. Frasca D, Diaz A, Romero M, Blomberg BB. Human peripheral late/exhausted memory B cells express a senescent-associated secretory phenotype and preferentially utilize metabolic signaling pathways. Exp Gerontol. 2017;87:113–20.
278. Giamarellos-Bourboulis EJ, Netea MG, Rovina N, Akinosoglou K, Antoniadou A, Antonakos N, et al. Complex Immune Dysregulation in COVID-19 Patients with Severe Respiratory Failure. Cell Host Microbe. 2020;27(6):992-1000.e3.
279. Montero-Escribano P, Matías-Guiu J, Gómez-Iglesias P, Porta-Etessam J, Pytel V, Matias-Guiu JA. Anti-CD20 and COVID-19 in multiple sclerosis and related disorders: A case series of 60 patients from Madrid, Spain. Mult Scler Relat Disord. 2020;42(April):102185.
280. Adamo S, Michler J, Zurbuchen Y, Cervia C, Taeschler P, Raeber ME, et al. Signature of long-lived memory CD8+ T cells in acute SARS-CoV-2 infection. Nature. 2022;602(7895):148–55.
281. Notarbartolo S, Ranzani V, Bandera A, Gruarin P, Bevilacqua V, Putignano AR, et al. Integrated longitudinal immunophenotypic, transcriptional and repertoire analyses delineate immune responses in COVID-19 patients. Sci Immunol. 2021;6(62):1–19.
282. Gil-Manso S, Miguens Blanco I, López-Esteban R, Carbonell D, López-Fernández LA, West L, et al. Comprehensive Flow Cytometry Profiling of the Immune System in COVID-19 Convalescent Individuals. Front Immunol. 2022;12(January):1–16.
283. Moldofsky H, Patcai J. Chronic widespread musculoskeletal pain, fatigue, depression and disordered sleep in chronic post-SARS syndrome; a case-controlled study. BMC Neurol. 2011;11.
284. Morroy G, Keijmel SP, Delsing CE, Bleijenberg G, Langendam M, Timen A, et al. Fatigue following acute Q-fever: A systematic literature review. PLoS One.

2016;11(5):1–21.
285. Hung TM, Wills B, Clapham HE, Yacoub S, Turner HC. The Uncertainty Surrounding the Burden of Post-acute Consequences of Dengue Infection. Trends Parasitol. 2019;35(9):673–6.
286. A Longitudinal Study of Ebola Sequelae in Liberia. N Engl J Med. 2019;380(10):924–34.
287. Centers for Disease Control and Prevention (CDC). Post-COVID conditions [Internet]. 2022. Available from: https://www.cdc.gov/coronavirus/2019-ncov/long-term-effects/
288. Organisation WH. A clinical case definition of post COVID-19 condition by a Delphi consensus data accessed :2021-12-23. WHO/2019-nCoV/Post_COVID-19_condition/Clinical_case_definition/20211. 2021;(October).
289. National Institute for Health and Care Excellence (NICE) SIGN (SIGN) and RC of GP (RCGP). Covid19-Rapid-Guideline-Managing-the-Longterm-Effects-of-Covid19-Pdf-51035515742. 114 Publ 01032022. 2022;1–106.
290. Huang C, Huang L, Wang Y, Li X, Ren L, Gu X, et al. 6-month consequences of COVID-19 in patients discharged from hospital: a cohort study. Lancet. 2021;397(10270):220–32.
291. Evans RA, McAuley H, Harrison EM, Shikotra A, Singapuri A, Sereno M, et al. Physical, cognitive, and mental health impacts of COVID-19 after hospitalisation (PHOSP-COVID): a UK multicentre, prospective cohort study. Lancet Respir Med. 2021;9(11):1275–87.
292. Nikolich-Žugich J. The twilight of immunity: Emerging concepts in aging of the immune system review-article. Nat Immunol. 2018;19(1):10–9.
293. Harari S, Tahor M, Rutsinsky N, Meijer S, Miller D, Henig O, et al. Drivers of adaptive evolution during chronic SARS-CoV-2 infections. Nat Med. 2022;28(7):1501–8.
294. Söderberg-Nauclér C. Does reactivation of cytomegalovirus contribute to severe COVID-19 disease? Immun Ageing. 2021;18(1):1–7.
295. Gaebler C, Wang Z, Lorenzi JCC, Muecksch F, Finkin S, Tokuyama M, et al. Evolution of antibody immunity to SARS-CoV-2. Nature. 2021;591(7851):639–44.
296. Lanz T V., Brewer RC, Ho PP, Moon JS, Jude KM, Fernandez D, et al. Clonally expanded B cells in multiple sclerosis bind EBV EBNA1 and GlialCAM. Nature. 2022;603(7900):321–7.
297. Wallukat G, Hohberger B, Wenzel K, Fürst J, Schulze-Rothe S, Wallukat A, et al. Functional autoantibodies against G-protein coupled receptors in patients with persistent Long-COVID-19 symptoms. J Transl Autoimmun. 2021;4(April):0–5.
298. Matthay MA, Zemans RL, Zimmerman GA, Arabi YM, Beitler JR, Mercat A, et al. Acute respiratory distress syndrome. Nat Rev Dis Prim. 2018;5(1).
299. Juan Guardela BM, Sun J, Zhang T, Xu B, Balnis J, Huang Y, et al. 50-gene risk profiles in peripheral blood predict COVID-19 outcomes: A retrospective, multicenter cohort study. EBioMedicine. 2021;69:103439.
300. Method of the Year 2013. Nat Methods. 2014;11(1):1.
301. Papalexi E, Satija R. Single-cell RNA sequencing to explore immune cell

heterogeneity. Nat Rev Immunol. 2018;18(1):35–45.
302. Strzelecka PM, Damm F. Haematopoietic ageing through the lens of single-cell technologies. DMM Dis Model Mech. 2021;14(1).
303. Wang X, He Y, Zhang Q, Ren X, Zhang Z. Direct Comparative Analyses of 10X Genomics Chromium and Smart-seq2. Genomics, Proteomics Bioinforma. 2021;19(2):253–66.
304. He X, Memczak S, Qu J, Belmonte JCI, Liu GH. Single-cell omics in ageing: a young and growing field. Nat Metab. 2020;2(4):293–302.
305. Kowalczyk MS, Tirosh I, Heckl D, Rao TN, Dixit A, Haas BJ, et al. Single-cell RNA-seq reveals changes in cell cycle and differentiation programs upon aging of hematopoietic stem cells. Genome Res. 2015;25(12):1860–72.
306. Grover A, Sanjuan-Pla A, Thongjuea S, Carrelha J, Giustacchini A, Gambardella A, et al. Single-cell RNA sequencing reveals molecular and functional platelet bias of aged haematopoietic stem cells. Nat Commun. 2016;7.
307. Efremova M, Vento-Tormo M, Teichmann SA, Vento-Tormo R. CellPhoneDB: inferring cell–cell communication from combined expression of multi-subunit ligand–receptor complexes. Nat Protoc. 2020;15(4):1484–506.
308. Jin S, Guerrero-Juarez CF, Zhang L, Chang I, Ramos R, Kuan CH, et al. Inference and analysis of cell-cell communication using CellChat. Nat Commun. 2021;12(1):1–20.
309. Van den Berge K, Roux de Bézieux H, Street K, Saelens W, Cannoodt R, Saeys Y, et al. Trajectory-based differential expression analysis for single-cell sequencing data. Nat Commun. 2020;11(1):1–13.
310. Saelens W, Cannoodt R, Todorov H, Saeys Y. A comparison of single-cell trajectory inference methods. Nat Biotechnol. 2019;37(5):547–54.
311. Le J, Park JE, Ha VL, Luong A, Branciamore S, Rodin AS, et al. Single-Cell RNA-Seq Mapping of Human Thymopoiesis Reveals Lineage Specification Trajectories and a Commitment Spectrum in T Cell Development. Immunity. 2020;52(6):1105-1118.e9.
312. Baran-Gale J, Chandra T, Kirschner K. Experimental design for single-cell RNA sequencing. Brief Funct Genomics. 2018;17(4):233–9.
313. Hagemann-Jensen M, Ziegenhain C, Chen P, Ramskold D, Hendriks G-J, Larsson AJM, et al. Single-cell RNA counting at allele- and isoform-resolution using Smart-seq3. bioRxiv. 2019;(Icmc):817924.
314. Luecken MD, Theis FJ. Current best practices in single-cell RNA-seq analysis: a tutorial. Mol Syst Biol. 2019;15(6).
315. Osorio D, Cai JJ. Systematic determination of the mitochondrial proportion in human and mice tissues for single-cell RNA-sequencing data quality control. Bioinformatics. 2021;37(7):963–7.
316. McGinnis CS, Murrow LM, Gartner ZJ. DoubletFinder: Doublet Detection in Single-Cell RNA Sequencing Data Using Artificial Nearest Neighbors. Cell Syst. 2019;8(4):329-337.e4.
317. McCarthy DJ, Campbell KR, Lun ATL, Wills QF. Scater: Pre-processing, quality control, normalization and visualization of single-cell RNA-seq data in R. Bioinformatics. 2017;33(8):1179–86.

318. Stuart T, Butler A, Hoffman P, Hafemeister C, Papalexi E, Mauck WM, et al. Comprehensive Integration of Single-Cell Data. Cell. 2019;177(7):1888-1902.e21.
319. Hafemeister C, Satija R. Normalization and variance stabilization of single-cell RNA-seq data using regularized negative binomial regression. Genome Biol. 2019;20(1):1–15.
320. Moon KR, Stanley JS, Burkhardt D, van Dijk D v., Wolf G, Krishnaswamy S. Manifold learning-based methods for analyzing single-cell RNA-sequencing data. Curr Opin Syst Biol. 2018;7:36–46.
321. Pearson K. LIII. On lines and planes of closest fit to systems of points in space . London, Edinburgh, Dublin Philos Mag J Sci. 1901;2(11):559–72.
322. McInnes L, Healy J, Melville J. UMAP: Uniform Manifold Approximation and Projection for Dimension Reduction. 2018;
323. Blondel VD, Guillaume JL, Lambiotte R, Lefebvre E. Fast unfolding of communities in large networks. J Stat Mech Theory Exp. 2008;2008(10).
324. Aran D, Looney AP, Liu L, Wu E, Fong V, Hsu A, et al. Reference-based analysis of lung single-cell sequencing reveals a transitional profibrotic macrophage. Nat Immunol. 2019;20(2):163–72.
325. Lütge A, Zyprych-Walczak J, Kunzmann UB, Crowell HL, Calini D, Malhotra D, et al. CellMixS: Quantifying and visualizing batch effects in single-cell RNA-seq data. Life Sci Alliance. 2021;4(6):1–17.
326. Tran HTN, Ang KS, Chevrier M, Zhang X, Lee NYS, Goh M, et al. A benchmark of batch-effect correction methods for single-cell RNA sequencing data. Genome Biol. 2020;21(1):1–32.
327. Chu SK, Zhao S, Shyr Y, Liu Q. Comprehensive evaluation of noise reduction methods for single-cell RNA sequencing data. Brief Bioinform. 2022;23(2):1–17.
328. Korsunsky I, Millard N, Fan J, Slowikowski K, Zhang F, Wei K, et al. Fast, sensitive and accurate integration of single-cell data with Harmony. Nat Methods. 2019;16(12):1289–96.
329. Dann E, Henderson NC, Teichmann SA, Morgan MD, Marioni JC. Differential abundance testing on single-cell data using k-nearest neighbor graphs. Nat Biotechnol. 2022;40(2):245–53.
330. Street K, Risso D, Fletcher RB, Das D, Ngai J, Yosef N, et al. Slingshot: cell lineage and pseudotime inference for single-cell transcriptomics. BMC Genomics. 2018 Dec 19;19(1):477.
331. Pullin JM, McCarthy DJ. A comparison of marker gene selection methods for single-cell RNA sequencing data. bioRxiv. 2022;2022.05.09.490241.
332. Chen Y, Lun ATL, Smyth GK. From reads to genes to pathways: Differential expression analysis of RNA-Seq experiments using Rsubread and the edgeR quasi-likelihood pipeline. F1000Research. 2016;5:1–51.
333. Squair JW, Gautier M, Kathe C, Anderson MA, James ND, Hutson TH, et al. Confronting false discoveries in single-cell differential expression. Nat Commun. 2021;12(1).
334. Subramanian A, Tamayo P, Mootha VK, Mukherjee S, Ebert BL, Gillette MA, et al. Gene set enrichment analysis: A knowledge-based approach for interpreting

genome-wide expression profiles. Proc Natl Acad Sci U S A. 2005;102(43):15545–50.
335. Korotkevich G, Sukhov V, Budin N, Shpak B, Artyomov M, Sergushichev A. Fast gene set enrichment analysis. bioRxiv. 2021;
336. Chen S, Mar JC. Evaluating methods of inferring gene regulatory networks highlights their lack of performance for single cell gene expression data. BMC Bioinformatics. 2018;19(1):1–21.
337. Aibar S, González-Blas CB, Moerman T, Huynh-Thu VA, Imrichova H, Hulselmans G, et al. SCENIC: single-cell regulatory network inference and clustering. Nat Methods. 2017 Nov 9;14(11):1083–6.
338. Kharchenko P V. The triumphs and limitations of computational methods for scRNA-seq. Nat Methods. 2021;18(7):723–32.
339. Lähnemann D, Köster J, Szczurek E, McCarthy DJ, Hicks SC, Robinson MD, et al. Eleven grand challenges in single-cell data science. Vol. 21, Genome Biology. Genome Biology; 2020. 1–35 p.
340. Andrews TS, Kiselev VY, McCarthy D, Hemberg M. Tutorial: guidelines for the computational analysis of single-cell RNA sequencing data. Nat Protoc. 2021;16(1).
341. Lun A. Overcoming systematic errors caused by log-transformation of normalized single-cell RNA sequencing data. bioRxiv. 2018;1–20.
342. Zimmerman KD, Espeland MA, Langefeld CD. A practical solution to pseudoreplication bias in single-cell studies. Nat Commun. 2021;12(1):1–9.
343. Goeman JJ, Bühlmann P. Analyzing gene expression data in terms of gene sets: Methodological issues. Bioinformatics. 2007;23(8):980–7.
344. Noureen N, Ye Z, Chen Y, Wang X, Zheng S. Signature-scoring methods developed for bulk samples are not adequate for cancer single-cell RNA sequencing data. Elife. 2022;11:1–12.
345. Burel JG, Pomaznoy M, Arlehamn CSL, Weiskopf D, da Silva Antunes R, Jung Y, et al. Circulating T cell-monocyte complexes are markers of immune perturbations. Elife. 2019;8:1–21.
346. Burel JG, Pomaznoy M, Lindestam Arlehamn CS, Seumois G, Vijayanand P, Sette A, et al. The Challenge of Distinguishing Cell–Cell Complexes from Singlet Cells in Non-Imaging Flow Cytometry and Single-Cell Sorting. Cytom Part A. 2020;97(11):1127–35.
347. Hao Y, Hao S, Andersen-Nissen E, Mauck WM, Zheng S, Butler A, et al. Integrated analysis of multimodal single-cell data. Cell. 2021;184(13):3573-3587.e29.
348. Ren X, Wen W, Fan X, Hou W, Su B, Cai P, et al. COVID-19 immune features revealed by a large-scale single-cell transcriptome atlas. Cell. 2021;1–19.
349. Stephenson E, Reynolds G, Botting RA, Calero-Nieto FJ, Morgan MD, Tuong ZK, et al. Single-cell multi-omics analysis of the immune response in COVID-19. Nat Med. 2021 May 20;27(5):904–16.
350. Bray NL, Pimentel H, Melsted P, Pachter L. Near-optimal probabilistic RNA-seq quantification. Nat Biotechnol. 2016;34(5):525–7.
351. Heaton H, Talman AM, Knights A, Imaz M, Gaffney DJ, Durbin R, et al. Souporcell: robust clustering of single-cell RNA-seq data by genotype without

reference genotypes. Nat Methods. 2020;17(6):615–20.
352. Lun ATL, Mccarthy DJ, Marioni JC. A step-by-step workflow for low-level analysis of single-cell RNA-seq data with Bioconductor [version 2 ; referees : 3 approved , 2 approved with reservations]. F1000Research. 2016;5(2122):1–69.
353. Wolock SL, Lopez R, Klein AM. Scrublet: Computational Identification of Cell Doublets in Single-Cell Transcriptomic Data. Cell Syst. 2019;8(4):281-291.e9.
354. Wolf FA, Angerer P, Theis FJ. SCANPY: large-scale single-cell gene expression data analysis. Genome Biol. 2018 Dec 6;19(1):15.
355. Macosko EZ, Basu A, Satija R, Nemesh J, Shekhar K, Goldman M, et al. Highly parallel genome-wide expression profiling of individual cells using nanoliter droplets. Cell. 2015;161(5):1202–14.
356. Hoffman P, Yuhan Hao SG. SeuratDisk. 2022.
357. Dowle M, Srinivasan A. data.table: Extension of `data.frame`. 2021.
358. Satija R, Butler A, Hoffman P, Stuart T. SeuratObject: Data Structures for Single Cell Data. 2021.
359. Hafemeister C, Satija R. Normalization and variance stabilization of single-cell RNA-seq data using regularized negative binomial regression. bioRxiv. 2019;576827.
360. Patterson-Cross RB, Levine AJ, Menon V. Selecting single cell clustering parameter values using subsampling-based robustness metrics. BMC Bioinformatics. 2021;22(1):1–13.
361. Zappia L, Oshlack A. Clustering trees: a visualization for evaluating clusterings at multiple resolutions. Gigascience. 2018;7(7):1–9.
362. Zhang Y, Ma Y, Huang Y, Zhang Y, Jiang Q, Zhou M, et al. Benchmarking algorithms for pathway activity transformation of single-cell RNA-seq data. Comput Struct Biotechnol J. 2020;18:2953–61.
363. Giladi A, Paul F, Herzog Y, Lubling Y, Weiner A, Yofe I, et al. Single-cell characterization of haematopoietic progenitors and their trajectories in homeostasis and perturbed haematopoiesis. Nat Cell Biol. 2018;20(7):836–46.
364. Lauridsen FKB, Jensen TL, Rapin N, Aslan D, Wilhelmson AS, Pundhir S, et al. Differences in Cell Cycle Status Underlie Transcriptional Heterogeneity in the HSC Compartment. Cell Rep. 2018 Jul;24(3):766–80.
365. Wilson NK, Kent DG, Buettner F, Shehata M, Macaulay IC, Calero-Nieto FJ, et al. Combined Single-Cell Functional and Gene Expression Analysis Resolves Heterogeneity within Stem Cell Populations. Cell Stem Cell. 2015;16(6):712–24.
366. Pietras EM, Reynaud D, Kang YA, Carlin D, Calero-Nieto FJ, Leavitt AD, et al. Functionally Distinct Subsets of Lineage-Biased Multipotent Progenitors Control Blood Production in Normal and Regenerative Conditions. Cell Stem Cell. 2015;17(1):35–46.
367. Cabezas-Wallscheid N, Buettner F, Sommerkamp P, Klimmeck D, Ladel L, Thalheimer FB, et al. Vitamin A-Retinoic Acid Signaling Regulates Hematopoietic Stem Cell Dormancy. Cell. 2017;169(5):807-823.e19.
368. Durinck S, Spellman PT, Birney E, Huber W. Mapping identifiers for the integration of genomic datasets with the R/ Bioconductor package biomaRt. Nat

Protoc. 2009;4(8):1184–91.
369. Maechler M, Rousseeuw P, Struyf A, Hubert M, Hornik K. cluster: Cluster Analysis Basics and Extensions. 2022.
370. Korsunsky I, Nathan A, Millard N, Raychaudhuri S. Presto scales Wilcoxon and auROC analyses to millions of observations. bioRxiv. 2019;653253.
371. Monaco G, Lee B, Xu W, Mustafah S, Hwang YY, Carré C, et al. RNA-Seq Signatures Normalized by mRNA Abundance Allow Absolute Deconvolution of Human Immune Cell Types. Cell Rep. 2019;26(6):1627-1640.e7.
372. Martos SN, Campbell MR, Lozoya OA, Wang X, Bennett BD, Thompson IJB, et al. Single-Cell Analyses Identify Dysfunctional CD16+ CD8 T Cells in Smokers. Cell Reports Med. 2020;1(4):100054.
373. Muroyama Y, Wherry EJ. Memory t-cell heterogeneity and terminology. Cold Spring Harb Perspect Med. 2021;13(10).
374. Finak G, McDavid A, Yajima M, Deng J, Gersuk V, Shalek AK, et al. MAST: A flexible statistical framework for assessing transcriptional changes and characterizing heterogeneity in single-cell RNA sequencing data. Genome Biol. 2015;16(1):1–13.
375. Robinson MD, McCarthy DJ, Smyth GK. edgeR: A Bioconductor package for differential expression analysis of digital gene expression data. Bioinformatics. 2009;26(1):139–40.
376. McCarthy DJ, Chen Y, Smyth GK. Differential expression analysis of multifactor RNA-Seq experiments with respect to biological variation. Nucleic Acids Res. 2012;40(10):4288–97.
377. Shen Li SIs. GeneOverlap: Test and visualize gene overlaps. Bioconductor version: Release (3.14); 2021.
378. Kuhn M. caret: Classification and Regression Training. 2022.
379. Andreatta M, Carmona SJ. UCell: Robust and scalable single-cell gene signature scoring. Comput Struct Biotechnol J. 2021;19:3796–8.
380. Liberzon A, Birger C, Thorvaldsdóttir H, Ghandi M, Mesirov JP, Tamayo P. The Molecular Signatures Database Hallmark Gene Set Collection. Cell Syst. 2015;1(6):417–25.
381. Montecino-Rodriguez E, Kong Y, Casero D, Rouault A, Dorshkind K, Pioli PD. Lymphoid-Biased Hematopoietic Stem Cells Are Maintained with Age and Efficiently Generate Lymphoid Progeny. Stem Cell Reports. 2019;12(3):584–96.
382. Xie SZ, Garcia-Prat L, Voisin V, Ferrari R, Gan OI, Wagenblast E, et al. Sphingolipid Modulation Activates Proteostasis Programs to Govern Human Hematopoietic Stem Cell Self-Renewal. Cell Stem Cell. 2019;25(5):639-653.e7.
383. Tirosh I, Izar B, Prakadan SM, Wadsworth MH, Treacy D, Trombetta JJ, et al. Dissecting the multicellular ecosystem of metastatic melanoma by single-cell RNA-seq. Science (80-). 2016;352(6282):189–96.
384. Kaufmann KB, Zeng AGX, Coyaud E, Garcia-Prat L, Papalexi E, Murison A, et al. A latent subset of human hematopoietic stem cells resists regenerative stress to preserve stemness. Nat Immunol. 2021;22(6):723–34.
385. Chen D, Abu Zaid MI, Reiter JL, Czader M, Wang L, McGuire P, et al. Cryopreservation Preserves Cell-Type Composition and Gene Expression

Profiles in Bone Marrow Aspirates From Multiple Myeloma Patients. Front Genet. 2021;12(April):1–10.
386. Baumgartner C, Toifl S, Farlik M, Halbritter F, Scheicher R, Fischer I, et al. An ERK-Dependent Feedback Mechanism Prevents Hematopoietic Stem Cell Exhaustion. Cell Stem Cell. 2018;22(6):879-892.e6.
387. Beerman I, Seita J, Inlay MA, Weissman IL, Rossi DJ. Quiescent hematopoietic stem cells accumulate DNA damage during aging that is repaired upon entry into cell cycle. Cell Stem Cell. 2014;15(1):37–50.
388. Biechonski S, Yassin M, Milyavsky M. DNA-damage response in hematopoietic stem cells: An evolutionary trade-off between blood regeneration and leukemia suppression. Carcinogenesis. 2017;38(4):367–77.
389. Calvanese V, Nguyen AT, Bolan TJ, Vavilina A, Su T, Lee LK, et al. MLLT3 governs human haematopoietic stem-cell self-renewal and engraftment. Nature. 2019;576(7786):281–6.
390. Lu Z, Hong CC, Kong G, Assumpção ALFV, Ong IM, Bresnick EH, et al. Polycomb Group Protein YY1 Is an Essential Regulator of Hematopoietic Stem Cell Quiescence. Cell Rep. 2018;22(6):1545–59.
391. Dai X, Yan X, Wintergerst KA, Cai L, Keller BB, Tan Y. Nrf2: Redox and Metabolic Regulator of Stem Cell State and Function. Trends Mol Med. 2020;26(2):185–200.
392. Vitali C, Bassani C, Chiodoni C, Fellini E, Guarnotta C, Miotti S, et al. SOCS2 controls proliferation and stemness of hematopoietic cells under stress conditions and its deregulation marks unfavorable acute leukemias. Cancer Res. 2015;75(11):2387–99.
393. García-Prat L, Kaufmann KB, Schneiter F, Voisin V, Murison A, Chen J, et al. TFEB-mediated endolysosomal activity controls human hematopoietic stem cell fate. Cell Stem Cell. 2021;28(10):1838-1850.e10.
394. Capone S, Connor KM, Colombo A, Li X, Triche TJ, Ramsingh G. Senescent human hematopoietic progenitors show elevated expression of transposable elements and inflammatory genes. Exp Hematol. 2018;62:33-38.e6.
395. Hernández-Malmierca P, Vonficht D, Schnell A, Uckelmann HJ, Bollhagen A, Mahmoud MAA, et al. Antigen presentation safeguards the integrity of the hematopoietic stem cell pool. Cell Stem Cell. 2022;29(5):760-775.e10.
396. Cole CB, Russler-Germain DA, Ketkar S, Verdoni AM, Smith AM, Bangert C V, et al. Haploinsufficiency for DNA methyltransferase 3A predisposes hematopoietic cells to myeloid malignancies. J Clin Invest. 2017;127(10):3657–74.
397. Khajuria RK, Munschauer M, Ulirsch JC, Fiorini C, Ludwig LS, McFarland SK, et al. Ribosome Levels Selectively Regulate Translation and Lineage Commitment in Human Hematopoiesis. Cell. 2018;173(1):90-103.e19.
398. Aksöz M, Gafencu G-A, Stoilova B, Buono M, Meng Y, Jakobsen NA, et al. Identification and Age-dependent Increase of Platelet Biased Human Hematopoietic Stem Cells. bioRxiv. 2022;2022.01.14.475546.
399. Martinez-Jimenez CP, Eling N, Chen H, Vallejos CA, Kolodziejczyk AA, Connor F, et al. Aging increases cell-to-cell transcriptional variability upon immune stimulation. Science (80-). 2017 Mar 31;355(6332):1433–6.

400. Kovtonyuk L V., Ashcroft P, Spaltro G, Tata NR, Skoda RC, Bonhoeffer S, et al. Hematopoietic Stem Cells Increase Quiescence during Aging. Blood. 2019;134(Supplement_1):2484–2484.
401. Yang X, Wang X, Lei L, Sun L, Jiao A, Zhu K, et al. Age-Related Gene Alteration in Naïve and Memory T cells Using Precise Age-Tracking Model. Front Cell Dev Biol. 2021;8(February):1–16.
402. Zanello G, Goethel A, Forster K, Geddes K, Philpott DJ, Croitoru K. Nod2 activates NF-kB in CD4+ T cells but its expression is dispensable for T cell-induced colitis. PLoS One. 2013;8(12):1–10.
403. Mirza N, Pollock K, Hoelzinger DB, Dominguez AL, Lustgarten J. Comparative kinetic analyses of gene profiles of naïve CD4 + and CD8 + T cells from young and old animals reveal novel age-related alterations. Aging Cell. 2011;10(5):853–67.
404. Almanan M, Raynor J, Ogunsulire I, Malyshkina A, Mukherjee S, Hummel SA, et al. IL-10–producing Tfh cells accumulate with age and link inflammation with age-related immune suppression. Sci Adv. 2020;6(31):1–12.
405. Smith LK, Boukhaled GM, Condotta SA, Mazouz S, Guthmiller JJ, Vijay R, et al. Interleukin-10 Directly Inhibits CD8+ T Cell Function by Enhancing N-Glycan Branching to Decrease Antigen Sensitivity. Immunity. 2018;48(2):299-312.e5.
406. Gindin Y, Gaggar A, Lok AS, Janssen HLA, Ferrari C, Subramanian GM, et al. DNA Methylation and Immune Cell Markers Demonstrate Evidence of Accelerated Aging in Patients with Chronic Hepatitis B Virus or Hepatitis C Virus, with or without Human Immunodeficienct Virus Co-infection. Clin Infect Dis. 2021;73(1):E184–90.
407. Hashimoto K, Kouno T, Ikawa T, Hayatsu N, Miyajima Y, Yabukami H, et al. Single-cell transcriptomics reveals expansion of cytotoxic CD4 T cells in supercentenarians. Proc Natl Acad Sci U S A. 2019;116(48):24242–51.
408. Szabó E, Hornung Á, Monostori É, Bocskai M, Czibula Á, Kovács L. Altered cell surface N-glycosylation of resting and activated T cells in systemic lupus erythematosus. Int J Mol Sci. 2019;20(18).
409. Zhou Z, Sun B, Yu D, Bian M. Roles of tRNA metabolism in aging and lifespan. Cell Death Dis. 2021;12(6).
410. de Almeida Chuffa LG, Freire PP, dos Santos Souza J, de Mello MC, de Oliveira Neto M, Carvalho RF. Aging whole blood transcriptome reveals candidate genes for SARS-CoV-2-related vascular and immune alterations. J Mol Med. 2022;100(2):285–301.
411. Aandahl EM, Sandberg JK, Beckerman KP, Taskén K, Moretto WJ, Nixon DF. CD7 Is a Differentiation Marker That Identifies Multiple CD8 T Cell Effector Subsets. J Immunol. 2003;170(5):2349–55.
412. Nersisyan L, Nikoghosyan M, Arakelyan A, Francioli LC, Menelaou A, Pulit SL, et al. WGS-based telomere length analysis in Dutch family trios implicates stronger maternal inheritance and a role for RRM1 gene. Sci Rep. 2019;9(1):1–9.
413. Garagnani P, Marquis J, Delledonne M, Pirazzini C, Marasco E, Kwiatkowska KM, et al. Whole-genome sequencing analysis of semi-supercentenarians. Elife. 2021;10:1–26.

414. Aminian A, Bena J, Pantalone KM, Burguera B. Association of obesity with postacute sequelae of COVID-19. Diabetes, Obes Metab. 2021;23(9):2183–8.
415. Cao X, Li W, Wang T, Ran D, Davalos V, Planas-Serra L, et al. Accelerated biological aging in COVID-19 patients. Nat Commun. 2022;13(1):1–7.
416. Sirivongrangson P, Kulvichit W, Payungporn S, Pisitkun T, Chindamporn A, Peerapornratana S, et al. Endotoxemia and circulating bacteriome in severe COVID-19 patients. Intensive Care Med Exp . 2020;8(1).
417. Islam H, Chamberlain TC, Mui AL, Little JP. Elevated Interleukin-10 Levels in COVID-19: Potentiation of Pro-Inflammatory Responses or Impaired Anti-Inflammatory Action? Front Immunol. 2021;12(June):10–4.
418. Barry JC, Shakibakho S, Durrer C, Simtchouk S, Jawanda KK, Cheung ST, et al. Hyporesponsiveness to the anti-inflammatory action of interleukin-10 in type 2 diabetes. Sci Rep. 2016;6:1–9.
419. André S, Picard M, Cezar R, Roux-Dalvai F, Alleaume-Butaux A, Soundaramourty C, et al. T cell apoptosis characterizes severe Covid-19 disease. Cell Death Differ. 2022;(January):1–14.
420. Thompson EA, Cascino K, Ordonez AA, Zhou W, Vaghasia A, Hamacher-Brady A, et al. Metabolic programs define dysfunctional immune responses in severe COVID-19 patients. Cell Rep. 2021;34(11):108863.
421. Gupta S, Young T, Yel L, Su H, Gollapudi S. Differential sensitivity of naïve and subsets of memory CD4+ and CD8+ T cells to hydrogen peroxide-induced apoptosis. Genes Immun. 2007;8(7):560–9.
422. Aggarwal S, Gupta S. Increased apoptosis of T cell subsets in aging humans: altered expression of Fas (CD95), Fas ligand, Bcl-2, and Bax. J Immunol. 1998;160(4):1627–37.
423. Crowell HL, Soneson C, Germain PL, Calini D, Collin L, Raposo C, et al. Muscat Detects Subpopulation-Specific State Transitions From Multi-Sample Multi-Condition Single-Cell Transcriptomics Data. Nat Commun. 2020;11(1):1–12.